

**UCLA**

**UCLA Electronic Theses and Dissertations**

**Title**

Palladium-Catalyzed Oxidative Couplings and Applications to the Synthesis of Macrocycles and Strained Cyclic Dienes

**Permalink**

<https://escholarship.org/uc/item/95h074r0>

**Author**

Boon, Byron

**Publication Date**

2017

Peer reviewed|Thesis/dissertation

UNIVERSITY OF CALIFORNIA

Los Angeles

Palladium-Catalyzed Oxidative Couplings and Applications to the Synthesis of Macrocycles and  
Strained Cyclic Dienes

A dissertation submitted in partial satisfaction of the  
requirements for the degree of Doctor of Philosophy  
in Chemistry

by

Byron Adrian Boon

2017

© Copyright by

Byron Adrian Boon

2017

## ABSTRACT OF THE DISSERTATION

# Palladium-Catalyzed Oxidative Couplings and Applications to the Synthesis of Macrocycles and Strained Cyclic Dienes

by

Byron Adrian Boon

Doctor of Philosophy in Chemistry

University of California, Los Angeles, 2017

Professor Craig A. Merlic, Chair

The palladium(II)-catalyzed oxidative macrocyclization of bis(vinylboronate esters) is demonstrated as an efficient method for the synthesis of macrocyclic dienes. The macrocyclization reactions feature mild conditions due to a palladium(II) catalytic cycle which obviates the need for a high energy oxidative addition step of standard palladium(0) catalytic cycles. Instead, this oxidative coupling is promoted by chloroacetone as a terminal re-oxidant in the catalytic cycle. An extension of the oxidative coupling/macrocyclization strategy is highlighted where molecular oxygen may be used in place of chloroacetone as the terminal re-oxidant. Homocoupling reactions of vinylboronate esters served as a template to screen reaction conditions for this method. From these experiments, multiple reaction conditions gave the oxidative homocoupling product in high yield. These reaction conditions were successfully applied to the oxidative macrocyclization of a bis(vinylboronate ester) using molecular oxygen as a re-oxidant.

Syntheses of strained cyclic dienes were accomplished via the palladium(II)-catalyzed oxidative cyclizations of terminal bis(vinylboronate esters). The reactions generated strained (*E,E*)-1,3-dienes that underwent spontaneous  $4\pi$ -electrocyclizations to form bicyclic cyclobutenes. Formation of the cyclobutenes is driven by strain in the medium-ring (*E,E*)-1,3-diene intermediates. Thermal ring openings of the cyclobutenes give (*Z,Z*)-1,3-diene products, again for thermodynamic reasons. These results are in contrast with typical acyclic *trans*-3,4-dialkyl cyclobutenes, which favor outward torquoselective ring-openings to give (*E,E*)-1,3-dienes. DFT calculations verified the thermodynamic versus kinetic control of the reactions and kinetic studies are in excellent agreement with the calculated energy changes.

Investigations on the transannular Pauson-Khand reaction are also highlighted. The Pauson-Khand reaction is a powerful tool for the synthesis of cyclopentenones through the efficient [2+2+1] cycloaddition of dicobalt alkyne complexes with alkenes. While intermolecular and intramolecular variants are widely known, transannular versions of this reaction are unknown and the basis of this study. Our successful transannular Pauson-Khand reaction required a cyclic enyne incorporating one short three-membered linker chain and a rigid aryl linker in the backbone of the long linker chain. This rigidity of the aryl linker is proposed to facilitate the transannular [2+2+1] cyclization. Computational studies revealed that transannular Pauson-Khand reactions are thermodynamically favored for cyclic enynes featuring a long linker of at least 5 carbons, but with smaller chains the reactions are thermodynamically disfavored. Experimental studies show that long linking chains with more than 5 members are required to prevent steric interactions between the dicobalt hexacarbonyl moiety and the linking chain to allow the reaction to be kinetically favored.

The final part of this work highlights progress towards the total synthesis of (+)-kingianin A. This natural product was isolated as a racemic mixture from the bark of *Endiandra kingiana* and is an inhibitor of antiapoptotic protein Bcl-Xl, highlighting its potential use in cancer treatments. Its structure is proposed to arise from an intermolecular Diels-Alder dimerization reaction of bicyclo[4.2.0]octadiene fragments derived from an  $8\pi/6\pi$ -electrocyclization cascade. Although two total syntheses of ( $\pm$ )-kingianin A have been reported, an enantioselective synthesis has not been achieved and is the purpose of this study. This synthetic route begins from L-(+)-dimethyl tartrate, a cheap and commercially available starting material, and aims to follow a biomimetic synthetic pathway featuring a substrate controlled diastereoselective palladium(II)-catalyzed oxidative cyclization and  $8\pi/6\pi$ -electrocyclization cascade. Although the feasibility of this cascade pathway has not yet been realized, key synthetic transformations to install the requisite carbocyclic framework of (+)-kingianin A have been discovered, paving the way for future investigations on the palladium(II)-catalyzed coupling/electrocyclization cascade and completion of the synthesis.

The dissertation of Byron Adrian Boon is approved.

Kendall N. Houk

Lily Wu

Craig A. Merlic, Committee Chair

University of California, Los Angeles

2017

## TABLE OF CONTENTS

Abstract of Dissertation .....	ii
List of Schemes .....	ix
List of Tables .....	xiii
List of Figures .....	xiv
Abbreviations .....	xv
Acknowledgements.....	xix
Vita.....	xx
Publications and Presentations.....	xxi

### ***Chapter 1. Palladium-Catalyzed Synthesis of Strained Rings: A Review***

1.1. Introduction.....	1
1.2. Palladium-Catalyzed Synthesis of Cyclopropanes .....	3
1.3. Palladium-Catalyzed Synthesis of Cyclobutanes.....	6
1.4. Palladium-Catalyzed Synthesis of Cyclobutenes.....	7
1.5. Palladium-Catalyzed Synthesis of Epoxides .....	13
1.6. Palladium-Catalyzed Synthesis of Aziridines.....	16
1.7. Palladium-Catalyzed Synthesis of Azetidines .....	19
1.8. Palladium-Catalyzed Synthesis of Strained Polycyclic Aromatic Hydrocarbons .....	21
1.9. Palladium-Catalyzed Synthesis of Strained Rings in Natural Product Synthesis.....	23
1.10. Summary and Outlook .....	25
1.11. References and Notes.....	25

### ***Chapter 2. Palladium(II)-Catalyzed Oxidative Coupling Reactions Using Molecular Oxygen as Terminal Re-oxidant***

2.1. Abstract .....	30
2.2. Introduction.....	30
2.3. Results and Discussion .....	36
2.4. Conclusions.....	42
2.5. Experimental .....	42
2.6. References and Notes.....	51



**Chapter 3. Using Ring Strain to Control 4 $\pi$ -Electrocyclization Reactions:  
Torquoselectivity in Ring-Closing of Medium-Ring Dienes and Ring-  
Opening of Bicyclic Cyclobutenes**

3.1. Abstract .....	54
3.2. Introduction.....	54
3.3. Results and Discussion .....	63
3.4. Conclusions.....	83
3.5. Experimental.....	84
3.6. Supporting Information.....	112
3.7. Copyright Information .....	112
3.8. References and Notes.....	112

**Chapter 4. The Transannular Pauson-Khand Reaction**

4.1. Abstract .....	117
4.2. Introduction.....	118
4.3. Results and Discussion .....	129
4.4. Conclusions.....	137
4.5 Experimental.....	137
4.6. Computational Methods.....	155
4.7. Supporting Information.....	155
4.8. References and Notes.....	155

**Chapter 5. Progress Towards the Total Synthesis of (+)-Kingianin A**

5.1. Abstract .....	161
5.2. Introduction.....	161
5.3. Results and Discussion .....	174
5.4. Conclusions.....	186
5.5. Experimental.....	187
5.6. References and Notes.....	197

**Appendices**

Appendix A – Spectral Data .....	202
Appendix B – Experimental Kinetic Data .....	310

Appendix C – Computational Data..... 312

## LIST OF SCHEMES

### **Chapter 1**

Scheme 1.1. Synthesis of a 3-azabicyclo[3.1.0]hexane featuring a 3- <i>exo-trig</i> cyclization .....	4
Scheme 1.2. (a) Substrate scope of the “diverted Heck” reaction. (b) “Diverted Heck” reaction pathway to form cyclopropanes .....	5
Scheme 1.3. (a) Oxidative cyclization of 1,6-enynes. (b) Mechanism of Pd(II)/Pd(IV) oxidative cyclization.....	6
Scheme 1.4. (a) Tricyclic cyclobutanes from a Heck reaction pathway of allylic acetates. (b) Mechanism of palladium-catalyzed cyclobutane formation .....	7
Scheme 1.5. Rh-catalyzed transannular [2+2+2] cycloaddition reactions.....	8
Scheme 1.6. Stable cyclobutenes from 1,7-enynes.....	8
Scheme 1.7. (a) Ring expansion of methylene cyclopropanes. (b) Mechanism of methylene cyclopropane ring expansion .....	9
Scheme 1.8. (a) Directing group-free Heck/C-H activation cascade. (b) Mechanism of spirobenzocyclobutene formation.....	11
Scheme 1.9. Aryl benzocyclobutene synthesis by <i>t</i> -butyl C-H activation.....	11
Scheme 1.10. Mechanism of aryl benzocyclobutene formation by <i>t</i> -butyl C-H activation...	12
Scheme 1.11. <i>trans</i> -Epoxides from allenic alcohols.....	13
Scheme 1.12. Mechanism of epoxide formation from allenyl alcohols .....	14
Scheme 1.13. Palladium-catalyzed synthesis of epoxides from allylic alcohols .....	15
Scheme 1.14. Mechanism of palladium-catalyzed epoxide synthesis from allylic alcohols .	16
Scheme 1.15. (a) Palladium-catalyzed synthesis of aziridines from allylic amines. (b) Mechanism of diastereoselective aziridine formation .....	17
Scheme 1.16. Aziridine synthesis by a C-H activation pathway .....	18
Scheme 1.17. (a) Scope of azetidine synthesized from amino allenes. (b) Mechanism of formation of azetidines from amino allenes.....	20
Scheme 1.18. Azetidine synthesis by a C-H activation pathway.....	21
Scheme 1.19. Synthesis of [5]CPP by a Pd(II)-catalyzed oxidative cyclization .....	22
Scheme 1.20. Strained hexabenzoparaphenylene synthesized by a palladium-catalyzed trimerization of an aryne.....	23
Scheme 1.21. Key Heck reaction in Danishefsky’s total synthesis of Taxol .....	23
Scheme 1.22. Key Stille coupling in Danishefsky’s total synthesis of Dynemicin A .....	24

## Chapter 2

Scheme 2.1. Pd(0) and Pd(II) catalytic cycles .....	31
Scheme 2.2. Oxidative homocoupling of aryl boronic acids facilitated by N,O-ligands .....	33
Scheme 2.3. Oxidative homocoupling of aryl, styryl, and alkenyl boronic acids in water ...	34
Scheme 2.4. Oxidative homocoupling of aryl boronate esters .....	35
Scheme 2.5. Oxidative macrocyclization of bis(vinylboronate esters).....	36
Scheme 2.6. Preparation of bis(vinylboronate ester) <b>2-7</b> .....	37
Scheme 2.7. Oxidative macrocyclization of bis(vinylboronate ester) <b>2-7</b> .....	38

## Chapter 3

Scheme 3.1. Electrocyclic ring opening of <i>cis</i> - and <i>trans</i> -3,4-dimethyl substituted cyclobutenes.....	55
Scheme 3.2. Preferential modes of cyclobutene ring openings .....	56
Scheme 3.3. Electrocyclic ring opening of highly substituted bicyclic cyclobutenes .....	57
Scheme 3.4. Palladium-catalyzed synthesis of unstable cyclobutenes from 1,6-enynes and their electrocyclic ring opening .....	58
Scheme 3.5. Disrotatory electrocyclic ring opening of bicyclic cyclobutenes .....	58
Scheme 3.6. Electrocyclic ring opening of bicyclic cyclobutenes with inward alkyl rotation of alkyl groups.....	59
Scheme 3.7. Electrocyclic ring closure of strained cyclic dienes to bicyclic cyclobutenes ..	60
Scheme 3.8. Electrocyclic ring closure in the biosynthesis of cyclobutenbriarein A.....	61
Scheme 3.9. Transannular Diels-Alder reactions of a strained triene and dienyne intermediates .....	63
Scheme 3.10. Synthesis of ( <i>E,E</i> )-bis(vinylboronate esters) <b>3-52</b> , <b>3-55</b> , and <b>3-59</b> .....	65
Scheme 3.11. Synthesis of ( <i>E,Z</i> )-bis(vinylboronate ester) <b>3-66</b> .....	66
Scheme 3.12. Macrocyclic and medium sized rings from cyclization of bis(vinylboronate esters) featuring <i>p</i> -anisidine linkers .....	67
Scheme 3.13. A <i>trans</i> -bicyclic cyclobutene from an oxidative cyclization/4 $\pi$ -electrocyclization pathway.....	68
Scheme 3.14. Mechanism of <i>cis</i> -cyclobutene formation by oxidative palladacycle formation and reductive elimination.....	69
Scheme 3.15. Computed free-energy surface (gas phase; 298K) for electrocyclic ring-closure of ( <i>E,E</i> )-diene <b>3-75</b> to give <i>trans</i> - <b>3-74</b> and ring-opening to yield ( <i>Z,Z</i> )-diene <b>3-76</b> .....	71

Scheme 3.16. Computed free-energy surface (gas phase; 298K) for electrocyclic ring opening of <b>3-3</b> to give either ( <i>E,E</i> ) or ( <i>Z,Z</i> )-1,3-dienes .....	73
Scheme 3.17. Electrocyclic ring opening of cyclobutene <b>3-71</b> to give ( <i>Z,Z</i> )-diene <b>3-77</b> .....	74
Scheme 3.18. Experimental activation parameters and conditions for ring opening of cyclobutene <b>3-71</b> .....	76
Scheme 3.19. Structural modifications of known substrates .....	77
Scheme 3.20. Synthesis of bis(vinylboronate esters) <b>3-75</b> and <b>3-79</b> .....	77
Scheme 3.21. Possible mechanism for the formation of ( <i>Z,Z</i> )-diene <b>3-85</b> .....	78
Scheme 3.22. Attempted palladium-catalyzed ring opening of cyclobutene <b>3-71</b> .....	79
Scheme 3.23. Formation of sulfone cyclobutene <b>3-87</b> and thermal ring opening reactions..	80
Scheme 3.24. Computed free-energy surface (gas phase; 298K) for electrocyclic ring-closure of ( <i>E,E</i> )-diene <b>3-86</b> to give the trans-cyclobutene <b>3-87</b> and ring-opening to yield ( <i>Z,Z</i> )-diene <b>3-88</b> .....	82
<b>Chapter 4</b>	
Scheme 4.1. Mechanism of the Pauson-Khand reaction.....	118
Scheme 4.2. Synthesis of fused bicyclo[3.2.1]octenone rings.....	120
Scheme 4.3. Transannular Diels-Alder reactions of macrocyclic dienynes and dienyne cobalt complexes .....	121
Scheme 4.4. Dicobalt octacarbonyl catalyzed intermolecular [2+2+2] cycloaddition reactions .....	122
Scheme 4.5. Intermolecular [2+2+1+1] cycloaddition reactions promoted by NH <sub>4</sub> OH .....	123
Scheme 4.6. Effects of tether chain length on intramolecular PK reactions.....	124
Scheme 4.7. Effects of tether chain length on intramolecular PK reactions.....	125
Scheme 4.8. First transannular Pauson-Khand reaction .....	126
Scheme 4.9. Successful intermolecular PK reactions to form medium ring fused and bridged bicyclic cyclopentenones .....	127
Scheme 4.10. Ring closing metathesis and deprotection sequence of <i>vic</i> -dibromotrienes to give cyclic enynes .....	129
Scheme 4.11. Syntheses of linchpin <b>4-60</b> and alkene <b>4-64</b> .....	130
Scheme 4.12. Synthesis of sulfonamide <b>4-69</b> .....	130
Scheme 4.13. Synthesis of macrocyclization precursor <b>4-72</b> .....	131

Scheme 4.14. Key macrocyclization and deprotection steps in the synthesis of dicobalt enyne complex <b>4-47</b> .....	132
Scheme 4.15. Successful examples of the transannular Pauson-Khand reaction .....	133
Scheme 4.16. Possible regioisomers of the transannular Pauson-Khand reaction .....	134
Scheme 4.17. Formation of TAPK products for Gibbs free-energy calculations .....	134
Scheme 4.18. Mechanism of cobalt-promoted Pauson-Khand and [4 + 2] reactions .....	136

## **Chapter 5**

Scheme 5.1. Proposed biosynthesis of kingianin A .....	164
Scheme 5.2. Proposed biosynthesis of endiandric acids A-D .....	165
Scheme 5.3. Total synthesis of ocellapyrone B by Trauner and co-workers .....	166
Scheme 5.4. Synthesis of pre-kingianin A by the Moses group .....	167
Scheme 5.5. Attempted Diels-Alder dimerizations of pre-kingianin A .....	168
Scheme 5.6. Sherburn's $8\pi/6\pi$ -electrocyclization cascade .....	169
Scheme 5.7. Sherburn's total synthesis of kingianin A, D, and F .....	170
Scheme 5.8. Suzuki coupling/electrocyclization cascade .....	171
Scheme 5.9. Tethered radical cation Diels-Alder reactions .....	172
Scheme 5.10. Parker's completion of the total synthesis of ( $\pm$ )-kingianin A .....	173
Scheme 5.11. Ni(II)-catalyzed oxidative coupling/ $8\pi$ -electrocyclization cascade .....	174
Scheme 5.12. Pd(II)-catalyzed oxidative coupling/ $8\pi$ -electrocyclization cascade .....	175
Scheme 5.13. Retrosynthesis of (+)-kingianin A featuring a desymmetrization strategy ...	177
Scheme 5.14. Retrosynthesis of electrocyclization precursor <b>5-63</b> and the diastereoselective $8\pi/6\pi$ -electrocyclization cascade .....	178
Scheme 5.15. Preparation of bis(tosylate) <b>5-65</b> and diiodide <b>5-70</b> .....	179
Scheme 5.16. Synthesis of bromoenyne <b>5-66</b> .....	180
Scheme 5.17. <i>In-situ</i> formation of a bis-epoxide <b>5-74</b> and double epoxide ring opening ...	183
Scheme 5.18. Attempted bis(epoxide) formation and nucleophilic ring opening with lithium phenylacetylene and bromoenyne <b>5-66</b> .....	184
Scheme 5.19. Addition of <b>5-66</b> to benzaldehyde .....	185

## **Appendix**

Scheme A.1. Ring opening reaction for kinetic studies .....	310
---	-----

## LIST OF TABLES

### *Chapter 2*

Table 2.1. Oxidative homocoupling reaction condition screening .....	39
Table 2.2. Effect of base on product ratios for oxidative homocoupling reactions .....	40
Table 2.3. Oxidative macrocyclization conditions with molecular oxygen as re-oxidant.....	41

### *Chapter 5*

Table 5.1. Bcl-XL binding affinity of kingianins A-F.....	163
Table 5.2. Attempted Gilman couplings with Grignard reagents .....	181
Table 5.3. Attempted Gilman couplings with organolithium reagents.....	182
Table 5.4. Reaction conditions screen for double epoxide ring opening.....	186

### *Appendix*

Table A.1. Kinetic data for conversion of cyclobutene <b>3-71</b> to diene <b>3-77</b> .....	310
Table A.2. Enyne single point energies and zero point energies .....	312
Table A.3. Enyne temperature corrections and Gibbs free energies.....	312
Table A.4. Cyclopentenone single point energies and zero point energies .....	313
Table A.5. Cyclopentenone temperature corrections and Gibbs free energies.....	313
Table A.6. Carbon monoxide single point energies and zero point energies .....	313
Table A.7. Carbon monoxide temperature corrections and Gibbs free energies .....	313
Table A.8. Gibbs free energies of reaction .....	314

## LIST OF FIGURES

### **Chapter 1**

- Figure 1.1. Rings sizes from palladium-catalyzed intramolecular cyclizations ..... 2
- Figure 1.2. Palladacycle intermediates in strained ring formation via (a) square planar complexes or (b) coordination complexes ..... 3

### **Chapter 3**

- Figure 3.1. Free-energy profiles of (a) acyclic dienes, (b) asymmetric macrocyclic (*E,Z*)-dienes, (c) symmetric strained cyclic (*E,Z*)-dienes, and (d) strained cyclic (*E,E*)-dienes ..... 62
- Figure 3.2. Predicted strain energies (kcal/mol) of cyclic dienes ..... 64
- Figure 3.3. Predicted lowest energy structures, dihedral angles and relevant coupling constants for *cis*-**3-74** and *trans*-**3-74** ..... 70
- Figure 3.4. Eyring plot for ring opening of cyclobutene **3-71** to (*Z,Z*)-diene **3-77** ..... 75
- Figure 3.5. Predicted strain energy (kcal/mol) of heterocyclic dienes ..... 83

### **Chapter 4**

- Figure 4.1. Regioselectivity of inter- and intramolecular Pauson-Khand reactions and the transannular Pauson-Khand reaction ..... 119
- Figure 4.2. Proposed TAPK reaction ..... 128
- Figure 4.3. Gibbs free-energy of the TAPK reaction ..... 135

### **Chapter 5**

- Figure 5.1. Structure of ( $\pm$ )-kingianin A ..... 162
- Figure 5.2. Structure of kingianins A-F ..... 163

### **Appendix**

- Figure A.1. Plot of temperature dependent conversion of cyclobutene **3-71** to diene **3-77** at four temperatures ..... 310
- Figure A.2. Arrhenius plot showing temperature dependent rate constant at four temperatures for thermal ring opening of cyclobutene **3-71** to diene **3-77** ..... 311
- Figure A.3. Eyring plot showing temperature dependent rate constant at four temperatures for thermal ring opening of cyclobutene **3-71** to diene **3-77** ..... 311
- Figure A.4. Computed structures and representative reaction ..... 312



## ABBREVIATIONS

~	Approximately
o	Degree
*	Star
$\alpha$	Alpha
$\beta$	Beta
$\delta$	Delta
$\mu$	Micro
$\pi$	Pi
$\sigma$	Sigma
$\omega$	Omega
Ac	Acetyl
ATR	Attenuated total reflection
aq	Aqueous
Ar	Any aryl
atm	Atmosphere
b	Broadened
Bn	Benzyl
Boc	<i>tert</i> -Butyloxycarbonyl
Bu	Butyl
C	Celsius
cal	Calorie
cm <sup>-1</sup>	Inverse centimeters
Cy	Cyclohexyl
d	Doublet
DA	Diels-Alder
DCE	1,2-Dichloroethane
DCM	Dichloromethane
DEG	Diethylene glycol

DFT	Density functional theory
DIAD	Diisopropyl azodicarboxylate
DIBAL	Diisobutylaluminum hydride
DMA	Dimethyl acetamide
DMAD	Dimethyl acetylene dicarboxylate
DMAP	4-Dimethylamino pyridine
DMF	<i>N,N</i> -Dimethylformamide
DMSO	Dimethyl sulfoxide
dppb	1,3-Bis(diphenylphosphino)butane
dppf	1,3-Bis(diphenylphosphino)ferrocene
dppp	1,3-Bis(diphenylphosphino)propane
<i>dr</i>	Diastereomeric ratio
<i>E</i>	Entgegen
$E_2$	Bimolecular elimination
EDC	1-Ethyl-3-(3-dimethylaminopropyl)carbodiimide
<i>ee</i>	Enantiomeric excess
equiv	Equivalents
Et	Ethyl
Et <sub>2</sub> O	Diethyl Ether
EtOAc	Ethyl Acetate
EtOH	Ethanol
FG	Functional group
g	Gram
<i>gem</i>	Geminal
Grubbs I	Grubbs' first generation catalyst
Grubbs II	Grubbs' second generation catalyst
h	Hour
HMPA	Hexamethylphosphoramide
HRMS	High resolution mass spectroscopy

hν	Light
Hz	Hertz
<i>i</i>	Iso
IR	Infrared
J	joule
kcal	Kilocalorie
L	Ligand
LAH	Lithium aluminum hydride
<i>m</i>	meta
m	Milli
M	Molar
mCPBA	<i>meta</i> -Chloroperoxybenzoic acid
Me	Methyl
MeOH	Methanol
MHz	Megahertz
NHC	N-heterocyclic carbene
mol	Mole
mmol	Millimole
Ms	Mesyl
NMO	<i>N</i> -Methylmorpholine- <i>N</i> -oxide
NMR	Nuclear magnetic resonance
<i>o</i>	Ortho
Ox	Oxidant
<i>p</i>	Para
p	Pentet
PA	Picolinamide
Ph	Phenyl
pin	Pinacol
PK	Pauson-Khand

ppm	Parts per million
Pr	Propyl
PTC	Phase transfer catalyst
q	Quartet
R	Any alkyl group
<i>R</i>	Rectus
rt	Room temperature
s	Singlet
<i>S</i>	Sinister
S <sub>N</sub> 2	Bimolecular substitution
t	Triplet
TADA	Transannular Diels-Alder
TAPK	Transannular Pauson-Khand
TBAB	Tetrabutylammonium bromide
TBAF	Tetrabutylammonium fluoride
TBDPS	<i>tert</i> -Butyldiphenylsilyl
TBS	<i>tert</i> -Butyldimethylsilyl
Tf	Triflate
TFA	Trifluoroacetic acid
THF	Tetrahydrofuran
TIPS	Triisopropylsilyl
TLC	Thin layer chromatography
TMTU	1,1,3,3-Tetramethylthiourea
Tol	Tolyl
Ts	Tosyl
UV	Ultraviolet
<i>vic</i>	Vicinal
Z	Zusammen

## ACKNOWLEDGEMENTS

I would like to thank my research advisor Professor Craig A. Merlic. I appreciate the freedom granted to me to develop my curiosity in chemistry and the guidance I have received to allow me to become a critical thinker and an independent scientist.

I would also like to recognize members of the Merlic Group who I have overlapped with during my time at UCLA. Thank you to Rob Tobolowsky, Brett Cory, Tioga Martin, and Sedef Karabiyikoglu for your friendship and making our work environment an enjoyable place.

I would like to thank Dr. Josef Michl, Dr. Akin Akdag, and Dr. Wade Braunecker for raising me as a scientist during my undergraduate studies at the University of Colorado and for inspiring me to pursue an advanced degree in chemistry. I am fortunate to have worked with such skilled and passionate scientists.

I am grateful to have worked alongside my collaborators Dr. Kendall Houk, Dr. Peng Liu, Dr. Aaron Green, Dr. Robert Iafe, and Dr. Sedef Karabiyikoglu on a variety of projects. I would also like to recognize Dr. Jane Strouse and Dr. Robert Taylor of UCLA for their helpful discussions related to NMR spectroscopy and Cyndi He for discussions about computational chemistry.

I would also like to thank the UCLA Department of Chemistry and Biochemistry Organic Division and Dr. Judith Smith for financial support in the form of the Christopher S. Foote Senior Graduate Fellowship.

I cannot express enough gratitude for my friends and family. Thank you for supporting me and being a part of my life. None of this would have been possible without you.

## VITA

- 2010  
B.A., Chemistry  
University of Colorado  
Boulder, Colorado
- 2013  
M.S., Chemistry  
University of California  
Los Angeles, CA
- 2011-2017  
Teaching Fellow  
University of California, Los Angeles, CA
- 2013  
Hanson-Dow Excellence in Teaching Award  
University of California, Los Angeles, CA
- 2014-2015  
Senior Foote Graduate Fellow

## PUBLICATIONS AND PRESENTATIONS

Braunecker, W. A.; Akdag, A.; Boon, B. A.; Michl, J. "Highly Branched Polypropylene via Li<sup>+</sup>-Catalyzed Radical Polymerization," *Macromolecules* **2011**, *44*, 1229.

Iafe, R. G.; Chan, D. G.; Kuo, J. L.; Boon, B. A.; Faizi, D. J.; Saga, T.; Turner, J. W.; Merlic, C. A. "Cyclization Strategies to Polyenes Using Pd(II)-Catalyzed Couplings of Pinacol Vinylboronates," *Org. Lett.* **2012**, *14*, 4282.

Boon, B. A.; Green, A. G.; Liu, P.; Merlic, C. A. "Palladium-Catalyzed Synthesis of Strained 1,3-Dienes and Cascade Cyclizations: Unusual Selectivity in 4 $\pi$ -Electrocyclizations." *248<sup>th</sup> ACS National Meeting - Metal Mediated Reactions and Syntheses Poster Presentation*, San Francisco, CA, August **2014**.

Boon, B. A.; Green, A. G.; Liu, P.; Merlic, C. A. "Using Ring Strain to Control 4 $\pi$ -Electrocyclization Reactions: Torquoselectivity in Ring Closing of Medium-Ring Dienes and Ring Opening of Bicyclic Cyclobutenes." *251<sup>st</sup> ACS National Meeting - Metal Mediated Reactions and Syntheses Poster Presentation*, San Diego, CA, March **2016**.

Boon, B. A.; Green, A. G.; Liu, P.; Houk, K. N.; Merlic, C. A. "Using Ring Strain to Control 4 $\pi$ -Electrocyclization Reactions: Torquoselectivity in Ring Closing of Medium-Ring Dienes and Ring Opening of Bicyclic Cyclobutenes," *J. Org. Chem.* **2017**, *82*, 4613.

Karabiyikoglu, S.; Boon, B. A.; Merlic, C. A. "Cycloaddition Reactions of Cobalt-Complexed Macrocylic Alkynes: The Transannular Pauson-Khand Reaction," *Accepted*.

## Chapter 1

### Palladium-Catalyzed Synthesis of Strained Rings: A Review

#### 1.1. Introduction

The discovery of palladium-catalyzed carbon-carbon and carbon-heteroatom bond forming reactions has revolutionized the fields of organic and organometallic chemistry. Palladium-catalyzed methodologies are under continual development and are used in a number of industrial processes as well as the total synthesis of natural products.<sup>1,2</sup> The ongoing development of novel palladium-catalyzed methods highlights the breadth of chemistry yet to be discovered.<sup>3</sup>

The remarkably diverse range of palladium-catalyzed carbon-bond forming reactions can be broadly classified into intermolecular and intramolecular variants. Intermolecular coupling reactions are most common, leading to linear coupling products. On the other hand, intramolecular palladium-catalyzed coupling reactions lead to cyclic structures, of which there are four types of rings formed (Figure 1.1). Large macrocyclic rings are accessible, although they are challenging synthetic targets due to the entropic penalty associated with macrocyclization.<sup>4</sup> These methods have been particularly amenable to the synthesis of macrocyclic natural products.<sup>5-9</sup> Equally synthetically challenging are palladium-catalyzed ring forming reactions leading to medium-sized rings, where transannular steric interactions are an obstacle to medium ring formation.<sup>10</sup> Considerable progress has been made towards the synthesis of 7-11 membered rings.<sup>11</sup> By far the most common intramolecular palladium-catalyzed cyclizations are related to the synthesis of 5- and 6-membered rings. On the other hand, palladium-catalyzed syntheses of 3- and 4-membered rings is much less common and are highlighted in this review.



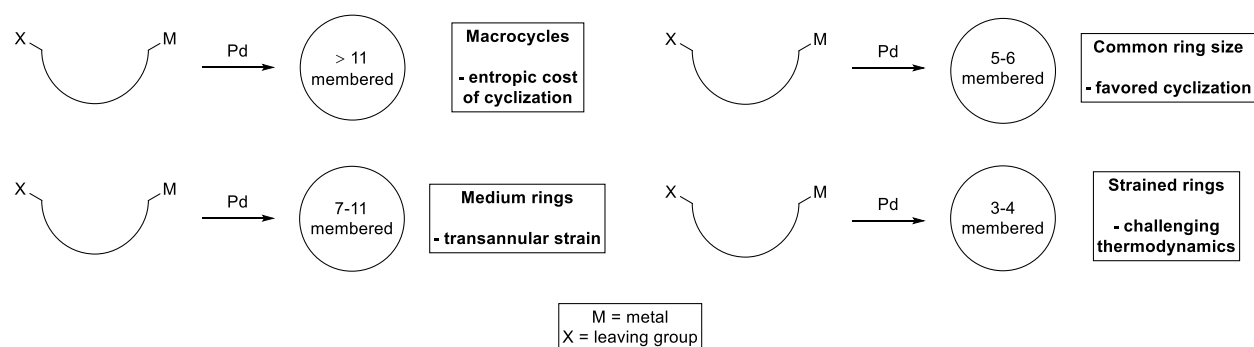


**Figure 1.1. Rings sizes from palladium-catalyzed intramolecular cyclizations.**

Palladium-catalyzed synthesis of 3- and 4-membered rings is difficult due to the challenging thermodynamics related to their formation. Typically, these rings are the result of reductive elimination from 4- or 5-membered palladacycle intermediates. The strain energies of cyclopropane (27.5 kcal/mol) and cyclobutane (26.5 kcal/mol)<sup>12</sup> rings are hardly compensated for by the formation of a new carbon-carbon bond ( $\sim 90$  kcal/mol)<sup>13</sup> with the loss of two weak carbon-palladium bonds ( $\sim 30$  kcal/mol each).<sup>14</sup> To further complicate matters, C-C bond activation via oxidative addition is typically favored for small strained 3- and 4-membered rings with transition metal catalysts, the opposite of reductive elimination.<sup>15</sup> On the other hand, formation of 4- and 5-membered palladacycle intermediates is kinetically allowed, so identification of proper reaction conditions that favor reductive elimination may allow the formation of 3- or 4-membered rings. Key to the successful formation of small strained rings is the ability to form a palladacycle intermediate (Figure 1.2). While bond lengths and internal bond angles in a cyclopropane make it strained, a four-membered palladacycle precursor will be considerably less strained due to two long Pd-C bonds (typically  $\sim 2.1$  Å for  $C_{sp^2}$ -Pd(II) bonds) and the  $\sim 90^\circ$  C-Pd-C bond angle favored for a Pd(II) square planar complex.<sup>14,16</sup> In the case of an insertion leading to a cyclopropane (Figure 1.2b), the effective Pd-C bond lengths in the  $\pi$ -complex are longer ( $\sim 2.1$  Å for a Pd(II)-propene complex) again reducing strain.<sup>14,17</sup> Despite these challenges, palladium-catalyzed syntheses of

strained 3- and 4-membered rings is a rarity in the literature of palladium catalysis with plenty of opportunity for further exploration.

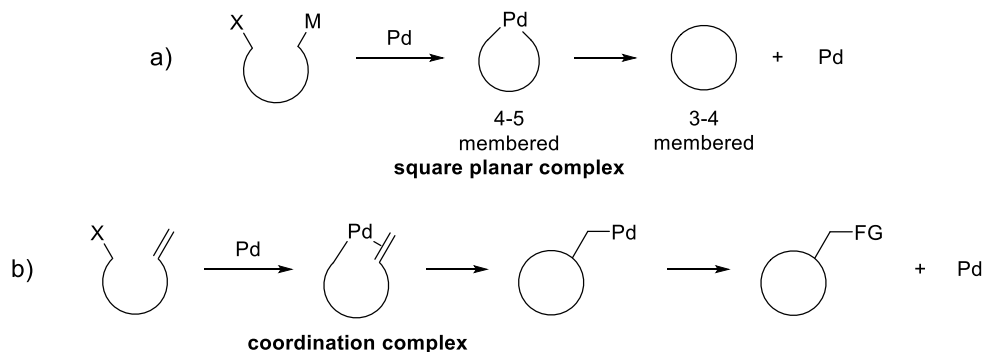


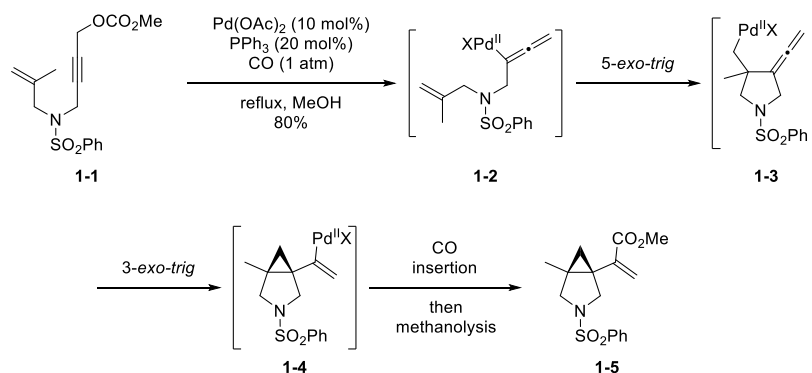
**Figure 1.2. Palladacycle intermediates in strained ring formation via (a) square planar complexes or (b) coordination complexes.**

This review will explore the palladium-catalyzed synthesis of a broad range of 3- and 4-membered rings. Intramolecular reactions and rearrangements are covered, as well as intermolecular reactions that result in cyclization to rings of these sizes. Carbocyclic rings discussed in this review include cyclopropanes, cyclobutanes, and cyclobutenes. Heterocycles discussed include epoxides, aziridines, and azirines. Palladium has also found use for the synthesis of strained polycyclic aromatic hydrocarbons and natural products, both of which are covered at the end of this review.

## 1.2. Palladium-Catalyzed Synthesis of Cyclopropanes

Synthesis of cyclopropanes in the framework of 3-azabicyclo[3.1.0]hexane structures was discovered by Grigg and coworkers in a dramatic cascade sequence featuring 1,6-enynes with propargylic carbonates. Reaction of enyne **1-1** with  $\text{Pd}(\text{OAc})_2$  in methanol under a carbon monoxide atmosphere gave the rearranged 3-azabicyclo[3.1.0]hexane methyl ester **1-5** in good yield (Scheme 1.1).<sup>18</sup> Oxidative addition of Pd(0) formed from  $\text{Pd}(\text{OAc})_2$  to **1-1** gave

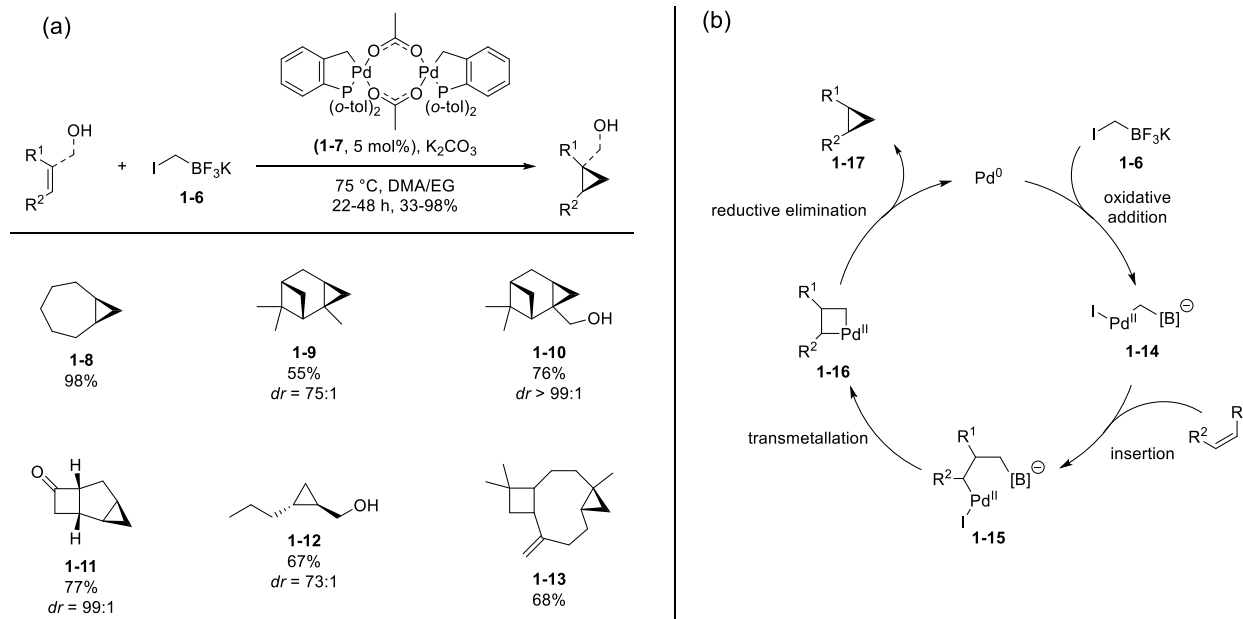
allenylpalladium(II) intermediate **1-2**, which underwent a *5-exo-trig* insertion to form allene **1-3**. A subsequent *3-exo-trig* carbopalladation gave the strained 3-azabicyclo[3.1.0]hexane ring **1-4**. Typically, organopalladium(II) intermediates add to the central carbon of allenes, but due to the rigid ring structure of **1-3**, addition occurs at the terminal carbon. Carbon monoxide insertion followed by methanolysis gave the ester product **1-5**.



**Scheme 1.1. Synthesis of a 3-azabicyclo[3.1.0]hexane featuring a *3-exo-trig* cyclization.**

Chen and coworkers reported the cyclopropanation of norbornene with potassium iodomethyltrifluoroborate **1-6** in the presence of the Herrmann-Beller palladium catalyst (**1-7**) in a “diverted Heck” reaction pathway.<sup>19</sup> The scope of the reaction was later extended to a series of unactivated olefins and the reaction conditions were tolerant of alcohols and ketones (Scheme 1.2a).<sup>20</sup> Stereospecific cyclopropanations were successful starting from 1,2-disubstituted alkenes. The reaction mechanism follows a Pd(0)/Pd(II) catalytic cycle. Oxidative addition to **1-6** gives alkyl Pd(II) intermediate **1-14** which undergoes alkene insertion to give **1-15** (Scheme 1.2b). Intermediate **1-15** follows an intramolecular transmetalation rather than a  $\beta$ -hydride elimination pathway resulting in 4-membered palladacycle intermediate **1-16**. At this point the reaction has undergone a “diverted Heck” pathway due to the fast transmetalation which prevents  $\beta$ -hydride

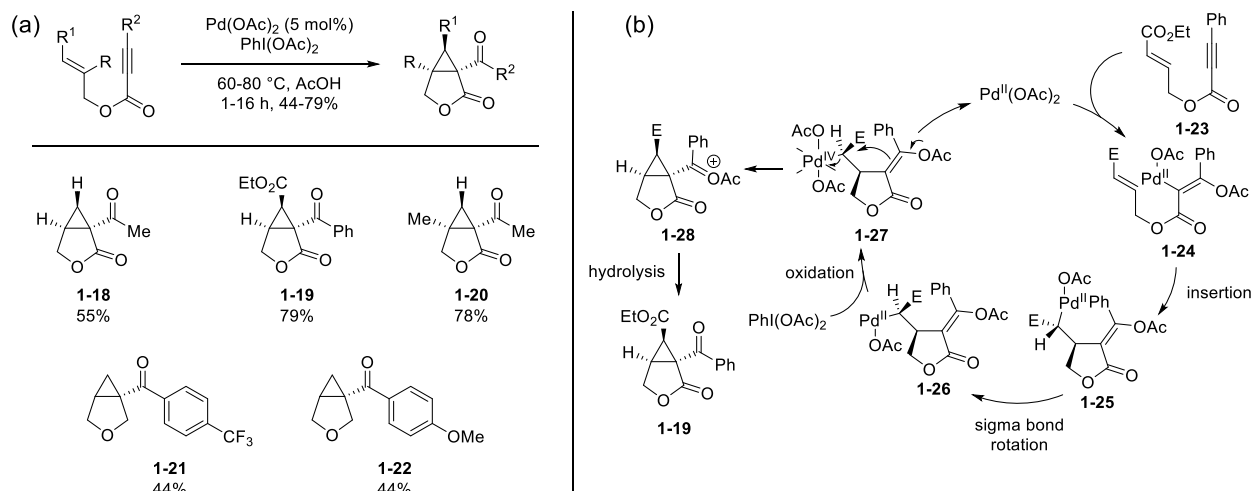
elimination of the standard Heck reaction. Reductive elimination gives the cyclopropane, completing the catalytic cycle.



**Scheme 1.2. (a) Substrate scope of the “diverted Heck” reaction. (b) “Diverted Heck” reaction pathway to form cyclopropanes.**

In 2007, the Tse group reported a palladium-catalyzed cyclization of substituted 1,6-enynes to form 3-oxobicyclo[3.1.0]hexane structures under oxidative conditions in the presence of  $PhI(OAc)_2$ .<sup>21</sup> Identical reaction conditions were reported the same year by the Sanford group, extending the scope to 1,6-enynes with alkene substituents to form substituted bicyclic products (Scheme 1.3a).<sup>22</sup> An enantioselective variation has been reported featuring chiral bis(isoxazole) ligands.<sup>23</sup> Mechanistic studies suggest a Pd(II/IV) catalytic cycle is involved and an internal  $S_N2$  displacement of Pd(IV) accounts for the stereochemistry of the product.<sup>24</sup> The proposed mechanism is shown in Scheme 1.3b. Enyne **1-23** underwent acetoxypalladation, followed by a diastereoselective alkene insertion to give intermediate **1-25**. After  $\sigma$ -bond rotation, oxidation of

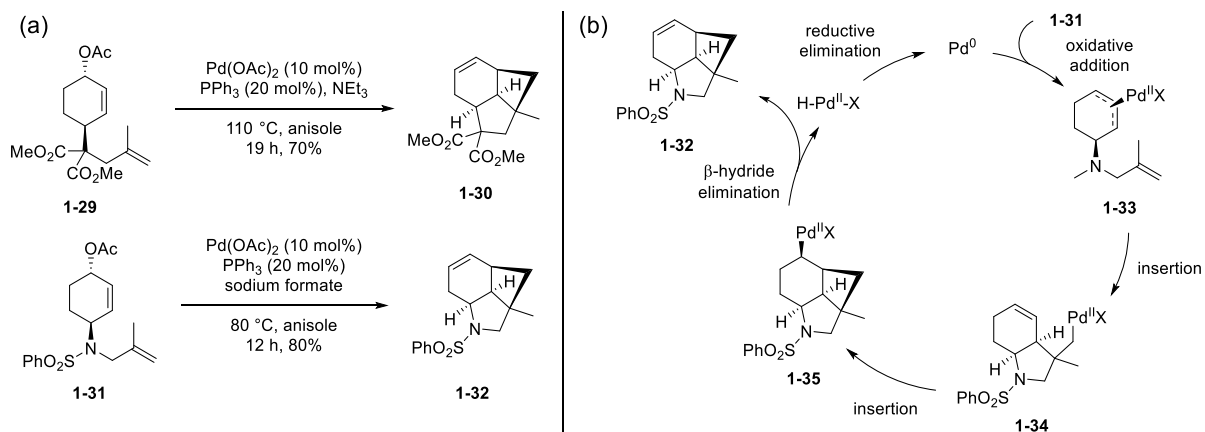
Pd(II) to Pd(IV) by  $\text{PhI}(\text{OAc})_2$  allows an internal  $\text{S}_{\text{N}}2$  displacement of Pd(IV) to establish the observed stereochemistry of the bridged cyclopropane ring. Hydrolytic removal of the acetyl group gave product **1-19**.



**Scheme 1.3. (a) Oxidative cyclization of 1,6-enynes. (b) Mechanism of Pd(II)/Pd(IV) oxidative cyclization.**

### 1.3. Palladium-Catalyzed Synthesis of Cyclobutanes

Palladium-catalyzed synthesis of cyclobutanes is an exceptionally rare process, but in an elegant example complex polycyclic structures were synthesized by a diastereoselective double Heck-insertion reaction of allylic acetates. Malonate and sulfonamide allyl acetates **1-29** and **1-31** cyclized to the strained polycyclic cyclobutanes **1-30** and **1-32** in the presence of catalytic  $\text{Pd}(\text{OAc})_2$  (Scheme 1.4a).<sup>25</sup> The proposed mechanism begins with an oxidative addition of Pd(0) to the allyl acetate to form the palladium  $\pi$ -allyl complex **1-33** (Scheme 1.4b). A diastereoselective 5-*exo-trig* alkene insertion leads to fused bicyclic intermediate **1-34**. Unable to undergo  $\beta$ -hydride elimination, **1-34** undergoes an unusual 4-*exo-trig* cyclization to form **1-35**, which upon  $\beta$ -hydride elimination yields tricyclic cyclobutane **1-32**.

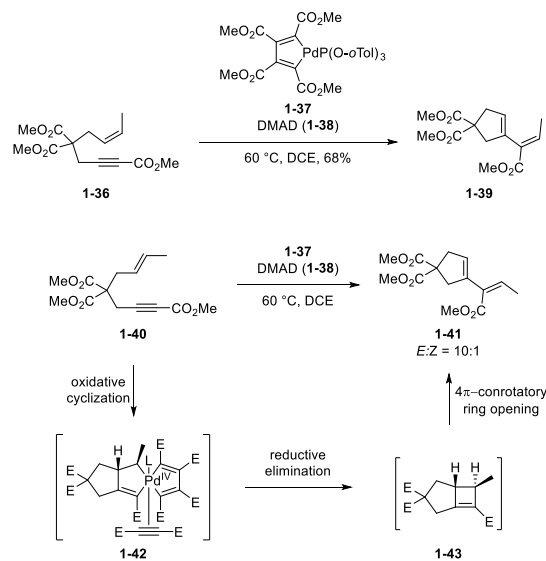


**Scheme 1.4. (a) Tricyclic cyclobutanes from a Heck reaction pathway of allylic acetates. (b)**

### **Mechanism of palladium-catalyzed cyclobutane formation.**

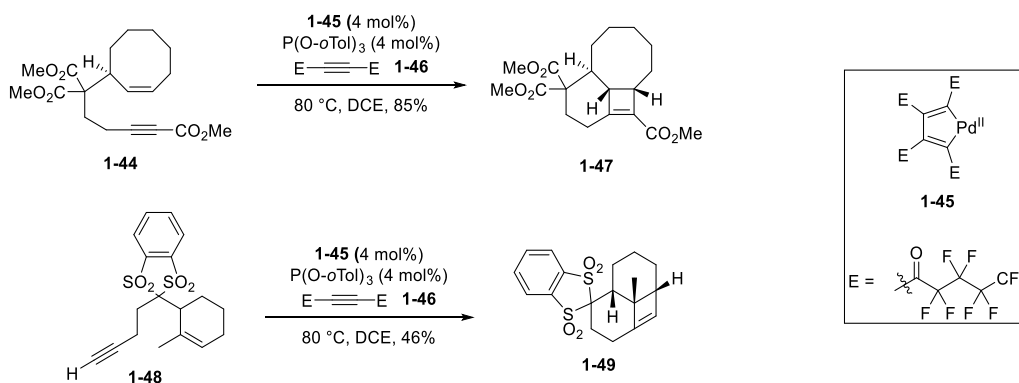
#### **1.4. Palladium-Catalyzed Synthesis of Cyclobutenes**

In contrast, palladium-catalyzed synthesis of cyclobutenes is much more common relative to cyclobutanes. The first reported cyclobutenes from a palladium-catalyzed process were unstable intermediates resulting from the oxidative cyclization of 1,6-enynes. Treatment of *cis*- and *trans*-1,6-enynes **1-36** and **1-40** with palladacyclobutadiene complex **1-37** in the presence of dimethyl acetylene dicarboxylate (**1-38**, DMAD) afforded diene products **1-39** and **1-41**, respectively (Scheme 1.5).<sup>26</sup> Diene **1-39** was obtained in a good 68% yield. Neither catalyst loading nor the yield of **1-41** was reported. Mechanistic studies suggested the unusual rearrangement starts by a  $\text{Pd}(\text{II})$ -catalyzed oxidative cyclization of **1-40** to form spirocyclic palladacycle **1-42**, which undergoes reductive elimination from  $\text{Pd}(\text{IV})$  to give bicyclic cyclobutene **1-43**. The strained anti-Bredt olefin<sup>27,28</sup> in cyclobutene **1-43** renders it unstable which causes a  $4\pi$ -conrotatory electrocyclic ring opening to occur resulting in formation of product **1-41**.



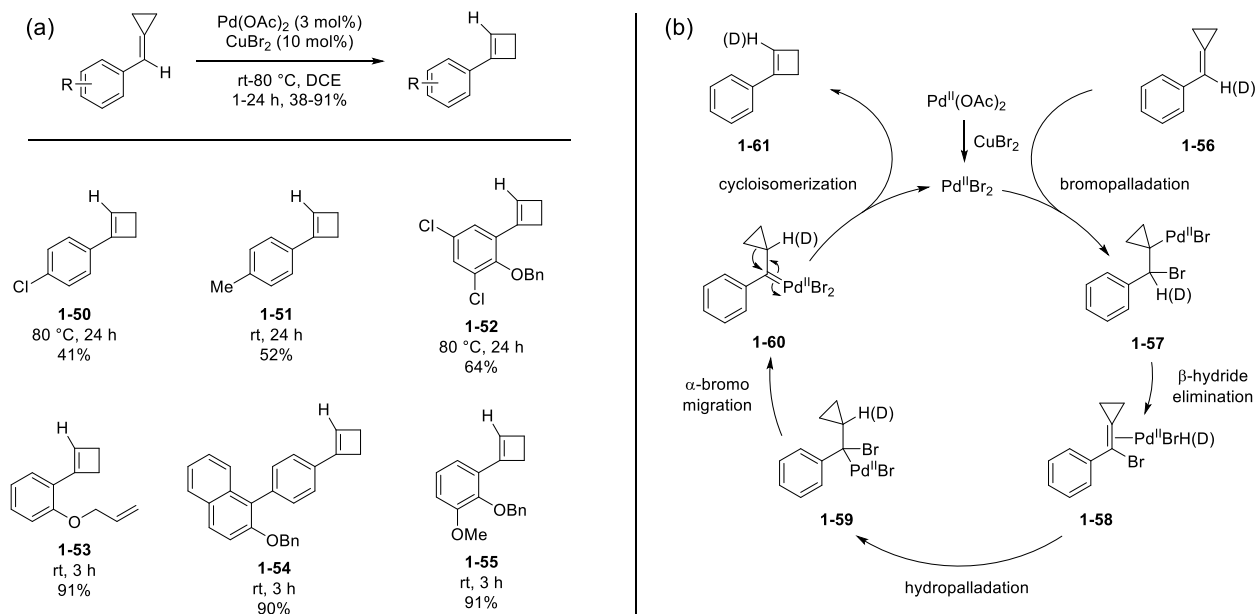
**Scheme 1.5. Unstable cyclobutenes from 1,6-enynes and their electrocyclic ring opening.**

To isolate stable cyclobutenes, the palladium-catalyzed cycloisomerization methodology was extended from 1,6- to 1,7-enynes. While anti-Bredt bridgehead olefins in bicyclo[3.2.0]pentane rings from 1,6-enynes were unstable (**1-43**, Scheme 1.5), equivalent to unstable *trans*-cycloheptene, bridgehead olefins in bicyclo[4.2.1]octane rings are stable, equivalent to stable *trans*-cyclooctene (Scheme 1.6). Treatment of 1,7-enynes with Pd(II) catalyst **1-45** gave stable cyclobutenes **1-47** and **1-49**.<sup>29</sup>



**Scheme 1.6. Stable cyclobutenes from 1,7-enynes.**

Ring expansion of methylene cyclopropanes offers convenient access to cyclobutenes. Aryl substituted methylene cyclopropanes undergo ring expansion in the presence of Pd(OAc)<sub>2</sub> with CuBr<sub>2</sub> under mild conditions in moderate to good yields (Scheme 1.7a).<sup>30</sup> Electron-donating aryl substituents allow rearrangement products **1-53**, **1-54**, and **1-55** to form at room temperature with short reaction times. Halogenated aryl substituents require elevated temperatures and longer reaction times (**1-50** and **1-52**). Highly substituted aryl rings are tolerated as well, and multiple electron withdrawing substituents are tolerated simultaneously assuming one substituent is electron-donating (**1-52**).

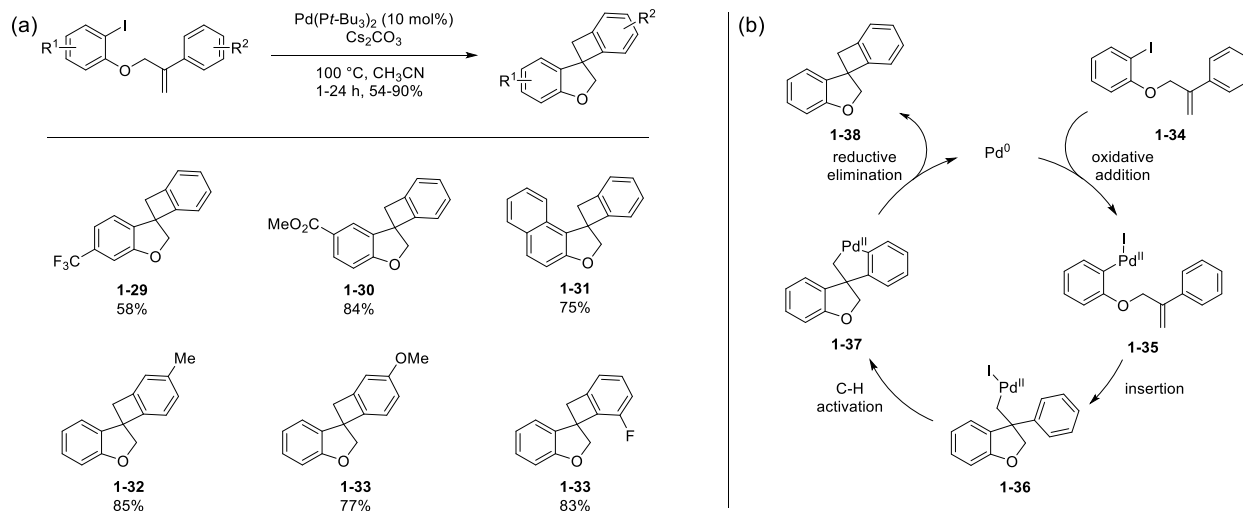


**Scheme 1.7. (a) Ring expansion of methylene cyclopropanes. (b) Mechanism of methylene cyclopropane ring expansion.**



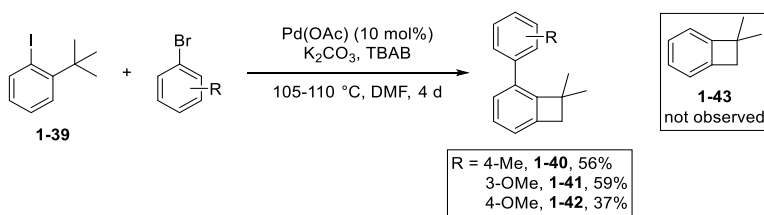
Labeling studies found deuterium migration from the methylene position of the cyclopropane to the vinyl position of the cyclobutene. The catalytic cycle commences with formation of the active catalyst, PdBr<sub>2</sub>, from ligand exchange of Pd(OAc)<sub>2</sub> in the presence of CuBr<sub>2</sub> (Scheme 1.7b). Bromopalladation of the double bond, followed by β-hydride elimination results in palladium hydride complex **1-58**, which in turn hydropalladates the newly formed bromo methylenecyclopropane **1-58**. At this point deuterium has undergone a formal 1,2-shift. To complete the isomerization, an α-bromo migration leads to Pd(II) carbene **1-60** which then cycloisomerizes to cyclobutene **1-61**.

A remote C-H activation strategy was demonstrated in an intramolecular Heck/C-H activation cascade to form spirocyclic benzocyclobutenes. Reaction of alkene-tethered aryl iodides under Pd(0)-catalysis gave the strained spirocyclic products (Scheme 1.8a).<sup>31</sup> Electron-rich and electron-poor aryl substituents on either aryl ring gave satisfactory yields of products. C-H activation typically requires an *ortho* directing group to direct palladium to the desired site of reactivity. In this example, the alkene serves as a directing group for the C-H activation step. Oxidative addition, followed by a 5-*exo-trig* alkene insertion forms organopalladium intermediate **1-36**. Unable to undergo β-hydride elimination, **1-36** undergoes a concerted metallation-deprotonation C-H activation step to give the 5-membered palladacycle **1-37**, verified by DFT calculations. Reductive elimination from Pd(II) was facilitated by electron-rich tri-*t*-butylphosphine ligand to give the strained spirocyclic cyclobutene **1-38**.



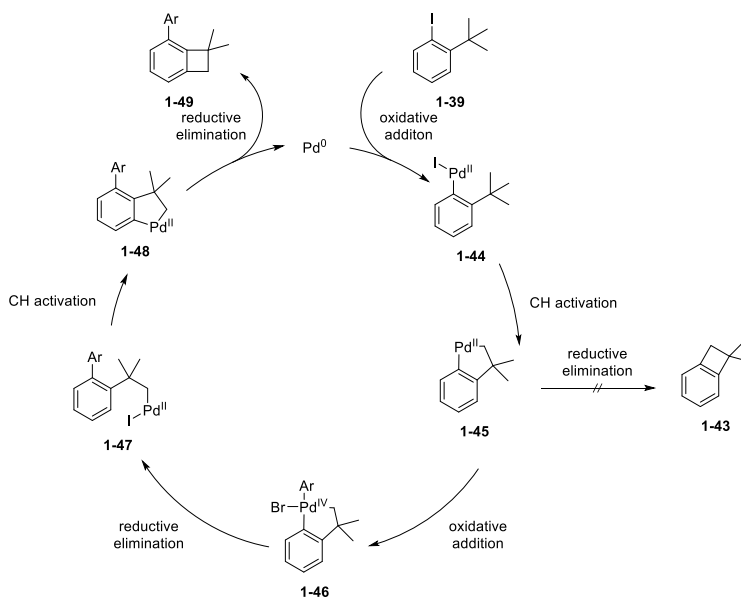
**Scheme 1.8. (a) Directing group-free Heck/C-H activation cascade. (b) Mechanism of spirobenzocyclobutene formation.**

A similar directing group-free CH activation/arylation process was reported to give arylated benzocyclobutenes. Reaction of *t*-butyl substituted aryl iodide **1-39** and aryl bromides in the presence of Pd(OAc)<sub>2</sub> gave arylated benzocyclobutenes, the result of *t*-butyl C-H activation (Scheme 1.9).<sup>32</sup> Intermolecular coupling products **1-40**, **1-41**, and **1-42** were observed rather than the direct intramolecular C-H activation product **1-43**, suggesting the possibility of a Pd(IV) intermediate.



**Scheme 1.9. Aryl benzocyclobutene synthesis by *t*-butyl C-H activation.**

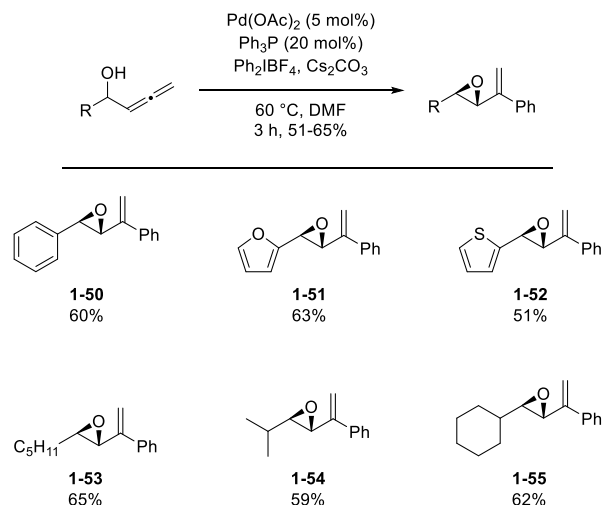
The proposed mechanism proceeds by oxidative addition to the aryl iodide bond, followed by Csp<sup>3</sup>-H activation of a *t*-butyl C-H bond to give 5-membered palladacycle **1-45** (Scheme 1.10).<sup>32</sup> Rather than undergo reductive elimination, a second oxidative addition with the aryl bromide coupling partner leads to Pd(IV) intermediate **1-46**. Reductive elimination from **1-46** leads to **1-47** with aryl-aryl C-C bond formation. Aryl C-H activation gives palladacycle intermediate **1-48**, which undergoes reductive elimination to form the observed product. Reductive elimination to form the strained 4-membered ring is proposed to occur from **1-48** rather than **1-45** due to unfavorable steric interactions between the aryl substituent and the *gem*-dimethyl group.



**Scheme 1.10. Mechanism of aryl benzocyclobutene formation by *tert*-butyl C-H activation.**

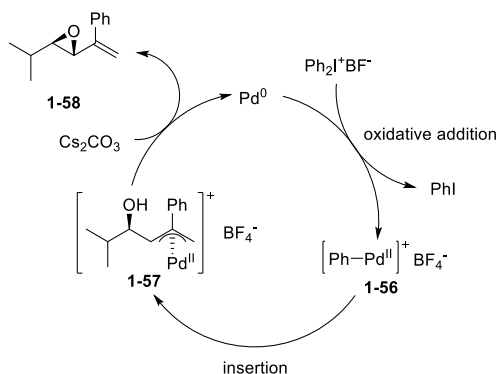
## 1.5. Palladium-Catalyzed Synthesis of Epoxides

An early palladium-catalyzed synthesis of epoxides was realized as a modification of the Tsuji-Trost arylation of allenes by nucleophilic trapping with oxygen. Treatment of allenyl alcohols with hypervalent iodonium salts in the presence of Pd(OAc)<sub>2</sub> and cesium carbonate resulted in the stereoselective formation of *trans*-1,2-disubstituted epoxides (Scheme 1.11).<sup>33</sup> Products were successfully formed from substituted allenyl alcohols with phenyl (**1-50**), furyl (**1-51**), thiophenyl (**1-52**), and alkyl substituents (**1-53**, **1-54**, and **1-55**). Unfortunately, useful reaction conditions were only demonstrated with diphenyl hypervalent iodonium salts to give phenyl substituted alkene products.



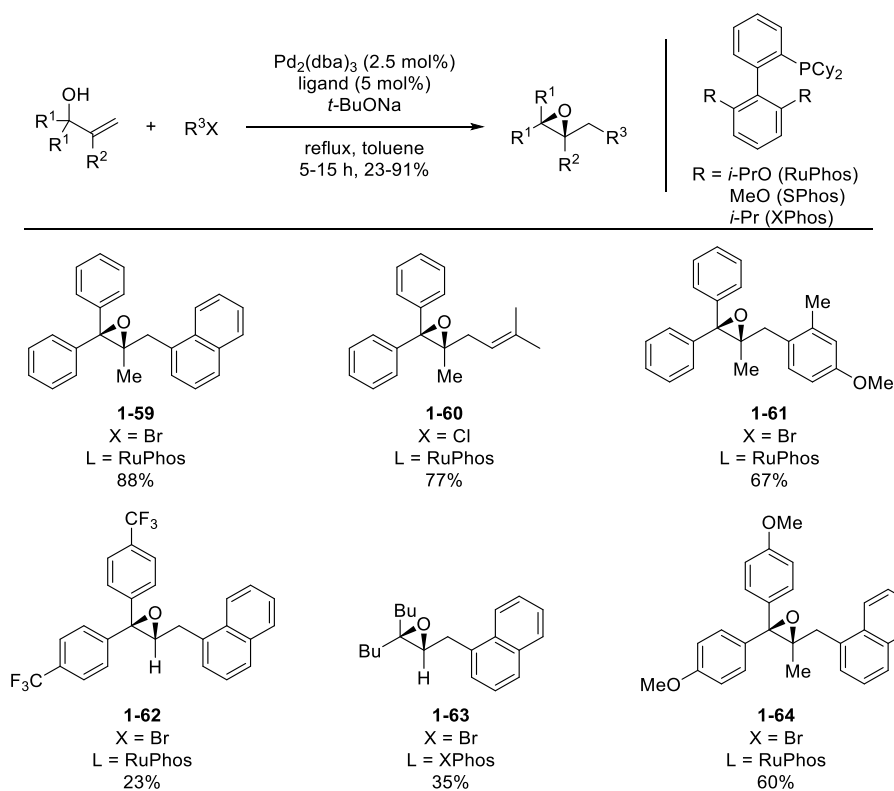
**Scheme 1.11.** *trans*-Epoxides from allenic alcohols.

The mechanism of formation is reminiscent of standard Tsuji-Trost alkylation of allenes, where nucleophilic addition of the carbon nucleophile occurs at the internal allenyl carbon to form palladium  $\pi$ -allyl intermediate **1-56** (Scheme 1.12). In the presence of tertiary nitrogen bases  $\beta$ -hydride elimination occurs, resulting in 1,3-dienes, which tautomerize to  $\alpha,\beta$ -unsaturated carbonyl products.<sup>34</sup> In this case, the stronger base  $\text{Cs}_2\text{CO}_3$  likely deprotonates oxygen and intramolecular nucleophilic attack displaces palladium in a 3-*exo-trig* cyclization to give the epoxide product.



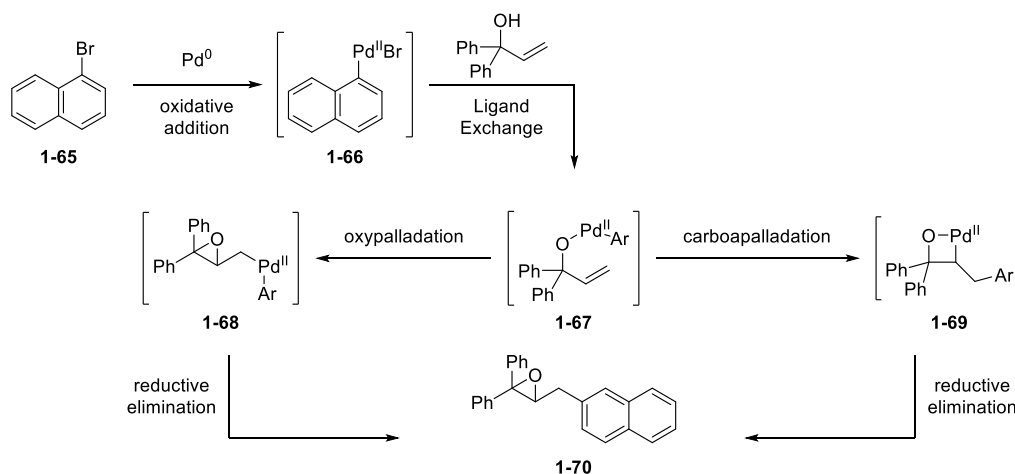
### Scheme 1.12. Mechanism of epoxide formation from allenyl alcohols.

The analogous reaction of allylic alcohols with aryl and vinyl halides gives tri- and tetrasubstituted epoxides (Scheme 1.13).<sup>35</sup> Generally 1,1-diaryl substituted epoxides are formed, although in select cases 1,1-dialkyl substituted epoxides are accessible by this method (**1-63**). Choice of ligand was critical to the success of the reaction as monodentate phosphine ligands such as  $\text{PPh}_3$ ,  $\text{dppb}$ , and  $\text{dppf}$  ligands favored Heck reaction products. On the other hand,  $\text{RuPhos}$  and  $\text{XPhos}$  favored epoxide formation over the Heck pathway, presumably due to their steric bulk and electron-rich nature.<sup>36</sup> Aryl and vinyl chlorides or bromides were acceptable coupling partners.



### Scheme 1.13. Mechanism of epoxide formation from allenyl alcohols.

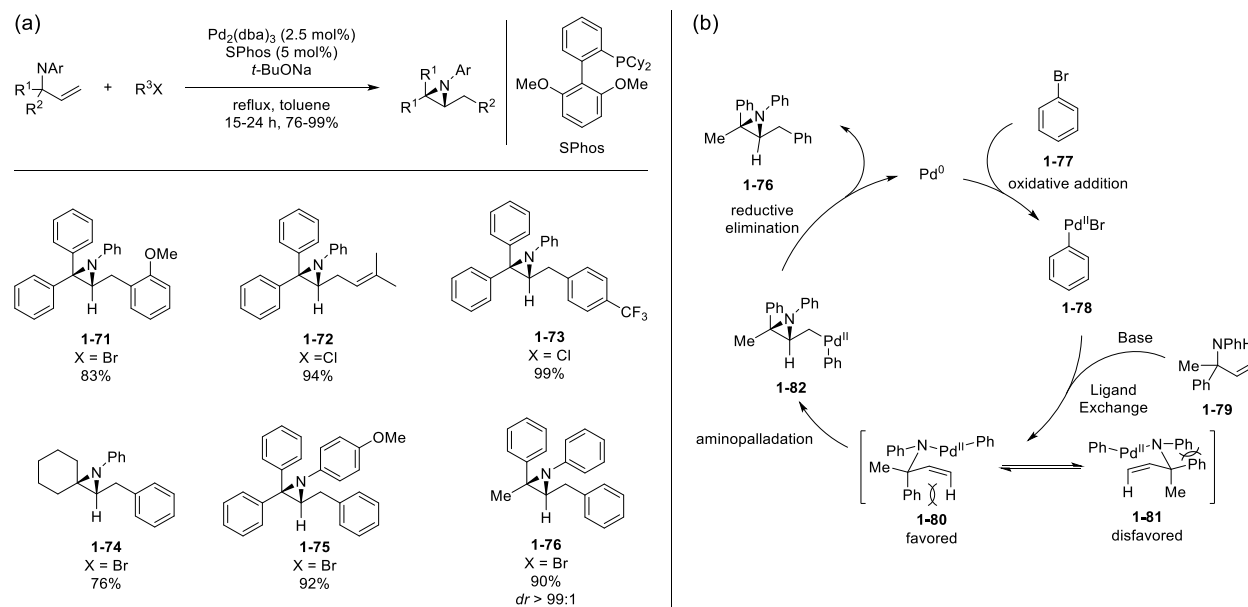
Two possible reaction pathways are possible, one of which occurs preferentially to the competing Heck reaction pathway. Oxidative addition of Pd(0) with the aryl or vinyl halide is followed by ligand exchange, likely facilitated by base, resulting in alkoxy Pd(II) intermediate **1-67** (Scheme 1.14). From here, two possible pathways can lead to product. Oxopalladation leads directly to epoxide **1-68**, which undergoes reductive elimination resulting in aryl or vinyl carbon bond formation to give product **1-70**. Alternatively, carbopalladation of the alkene results in 4-membered palladacycle **1-69** which can undergo reductive elimination to form the C-O bond of the epoxide product **1-70**. Studies were not conducted to discriminate between the two pathways.



**Scheme 1.14. Mechanism of palladium-catalyzed epoxide synthesis from allylic alcohols.**

## 1.6. Palladium-Catalyzed Synthesis of Aziridines

In an extension of the palladium-catalyzed synthesis of epoxides from allylic alcohols (Scheme 1.14), allylic amines were shown to react with aryl and vinyl halides to give trisubstituted aziridines (Scheme 1.15a).<sup>37</sup> Aryl and vinyl chlorides or bromides were all acceptable coupling partners. Typically, 1,1-diaryl substituted aziridines are formed, although there are select cases of 1,1-dialkyl substituted aziridines synthesized with this method (**1-74**). Like the previously discussed reaction of allylic alcohols, sterically hindered and electron-rich ligands were required for successful reactions to occur. Although the reaction of allylic alcohols required these ligands to prevent the Heck reaction pathway, this competing reaction pathway was not operative for the reaction of allylic amines.



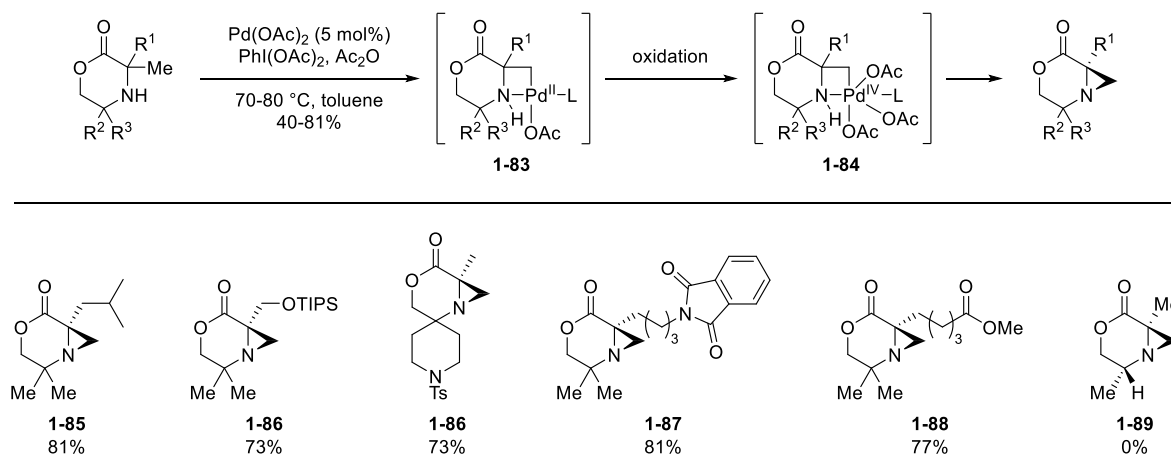
**Scheme 1.15. (a) Palladium-catalyzed synthesis of aziridines from allylic amines. (b)**

**Mechanism of diastereoselective aziridine formation.**

The reaction of allylic amines to form aziridines is diastereoselective in select cases. Product **1-76** is a representative example with excellent diastereoselectivity (Scheme 1.15b).<sup>37</sup> Diastereoselectivity originates in the aminopalladation step from intermediate **1-80** or **1-81**. Two sources of strain are in competition, a 1,3-pseudodiaxial interaction between allylic substituents with the terminal alkene hydrogen, as shown for **1-80**, and the 1,2-pseudoequatorial interaction between allylic substituents and the nitrogen phenyl group, as shown for **1-81**. The smaller phenyl-methyl 1,2-pseudoequatorial interaction in **1-80** is favored over the phenyl-phenyl 1,2-pseudoequatorial interaction in **1-81**, despite the larger phenyl-hydrogen 1,3-pseudoaxial interaction found in **1-80** when compared to the methyl-hydrogen 1,3-pseudoaxial interaction of **1-81**. Consequently, **1-80** preferentially undergoes aminopalladation to give **1-82**, which upon reductive elimination gives aziridine **1-76**.



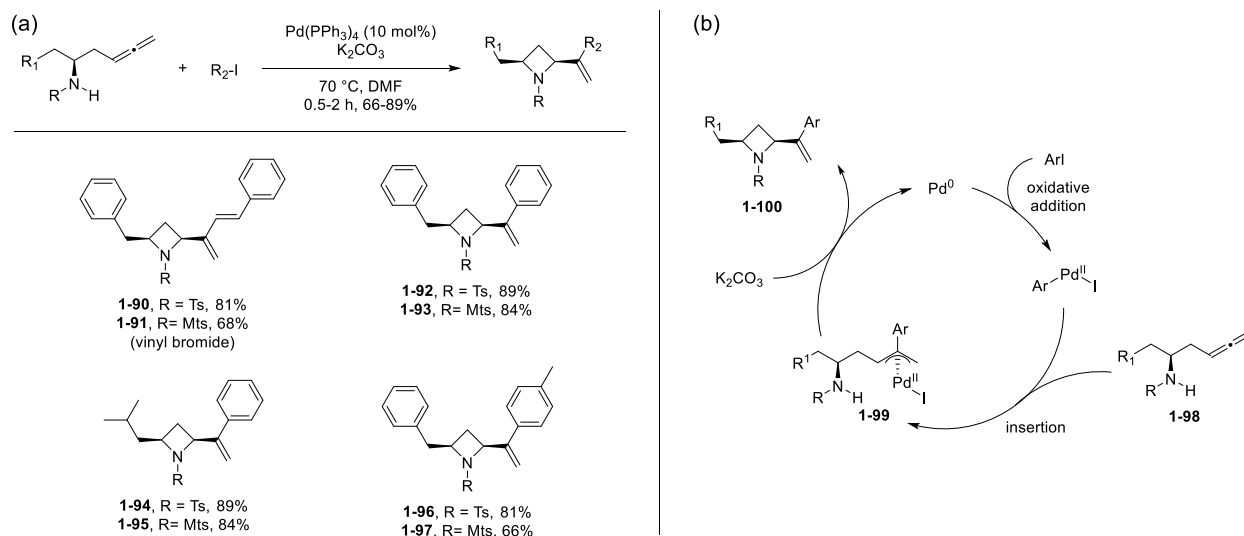
A unique C-H activation of amino lactones catalyzed by palladium under oxidative conditions gave aziridines by an unusual mechanism involving a 4-membered amino palladacycle intermediate. Amino lactones bearing  $\alpha$ -methyl substitution underwent C-H activation in the presence of Pd(OAc)<sub>2</sub> and PhI(OAc)<sub>2</sub> to give bicyclic aziridines (Scheme 1.16).<sup>38</sup> Acceptable  $\alpha$ -substituents included branched alkanes (**1-85**), silyl protected alcohols (**1-86**), halogens as well as imides and esters (**1-87** and **1-88**, respectively). Substrates lacking dialkyl substitution at the  $\gamma$ -position were unable to undergo aziridine formation (**1-89**). The mechanism likely involves formation of a 4-membered palladacycle intermediate **1-83**, the result of a methyl C-H activation. Intermediate **1-83** was isolable in the absence of PhI(OAc)<sub>2</sub> with added phosphine ligand, an unprecedented 4-membered amino palladacycle. After oxidation of **1-83** with PhI(OAc)<sub>2</sub> to give Pd(IV) intermediate **1-84**, reductive elimination likely occurs with loss of a proton to give the aziridine products.



**Scheme 1.16.** Aziridine synthesis by a C-H activation pathway.

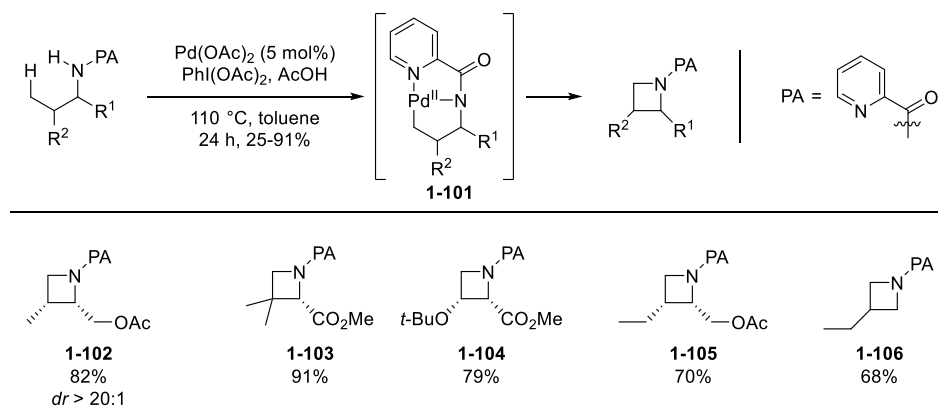
## 1.7. Palladium-Catalyzed Synthesis of Azetidines

The first reported synthesis of azetidines via palladium catalysis was a modification of the Tsuji-Trost arylation of allenes with nucleophilic trapping by nitrogen. This closely resembles the analogous reaction of allenyl alcohols to form *trans*-1,2-disubstituted epoxides (Scheme 1.11 and 1.12).<sup>33</sup> In this case, chiral homoallylic amines reacted with aryl iodides in the presence of Pd(PPh<sub>3</sub>)<sub>4</sub> and potassium carbonate in DMF to give *cis*-2,4-disubstituted azetidines in a diastereoselective cyclization (Scheme 1.17a).<sup>39</sup> Reactions performed in solvents other than DMF gave mixtures of *cis*- and *trans*-isomers. Although the substrate scope is limited to simple aryl iodides, two examples with vinyl bromides were demonstrated (**1-90** and **1-91**). Similar reaction conditions have been demonstrated on shorter chain allenyl amines to give aziridine products.<sup>40</sup> The proposed mechanism is shown in Scheme 1.17b. After oxidative addition to the aryl iodide, nucleophilic addition of the aryl component occurs at the internal carbon to give palladium  $\pi$ -allyl **1-99**. Diastereoselective C-N bond formation occurs with displacement of Pd(II) to form azetidine **1-100** and Pd(0). The mechanistic details leading to diastereoselectivity are currently unknown. One possibility is coordination of the amine to palladium provides a diastereoselective allene insertion to  $\pi$ -allyl intermediate **1-99**. Then amine addition to the  $\pi$ -allyl *anti* to palladium yields the 2,4-*cis* azetidine products.



**Scheme 1.17 (a) Scope of azetidine synthesized from amino allenes. (b) Mechanism of formation of azetidines from amino allenes.**

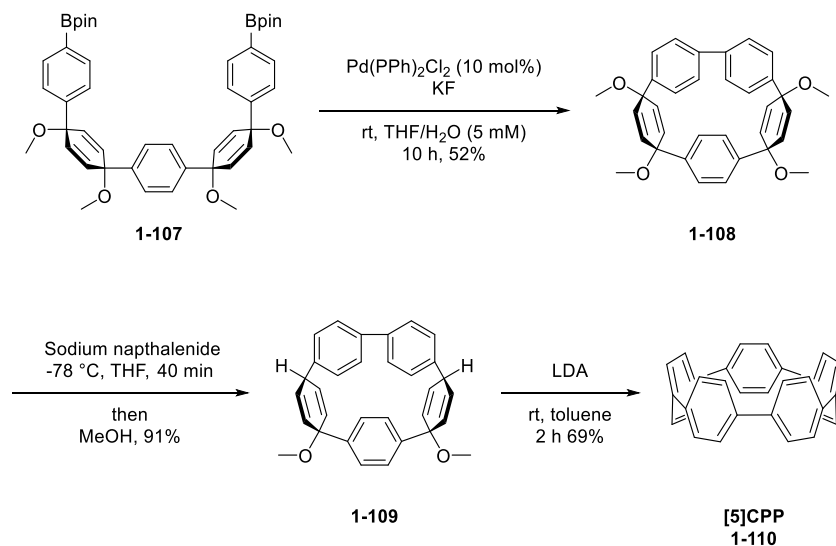
The Chen group reported synthesis of azetidines by a directed C-H activation pathway in the presence of hypervalent iodine reagents. Picolinamide (PA) substituted amines with  $\gamma$ -hydrogen  $\text{C}_{\text{sp}}^3\text{-H}$  bonds gave substituted azetidine rings upon treatment with  $\text{Pd}(\text{OAc})_2$  and  $\text{PhI}(\text{OAc})_2$  with heating (Scheme 1.18).<sup>41</sup> Similar reaction conditions were later applied to the synthesis of benzazetidine structures with PA directing groups.<sup>42</sup> The reaction pathway likely proceeds via a palladacycle intermediate **1-101**, which upon oxidation with hypervalent iodine undergoes reductive elimination to the azetidine product. Products from  $\gamma$ -arylation or  $\beta$ -hydride elimination pathways were not observed, although  $\gamma$ -acetoxylation was observed in some cases. Typically C-H activation occurred at the least substituted  $\text{C}_{\text{sp}}^3\text{-H}$  bond on the  $\gamma$ -carbon. In the case of diastereotopic methyl groups, C-H activation was diastereoselective to give azetidine **1-102** with excellent *cis*-selectivity.



**Scheme 1.18.** Azetidine synthesis by a C-H activation pathway.

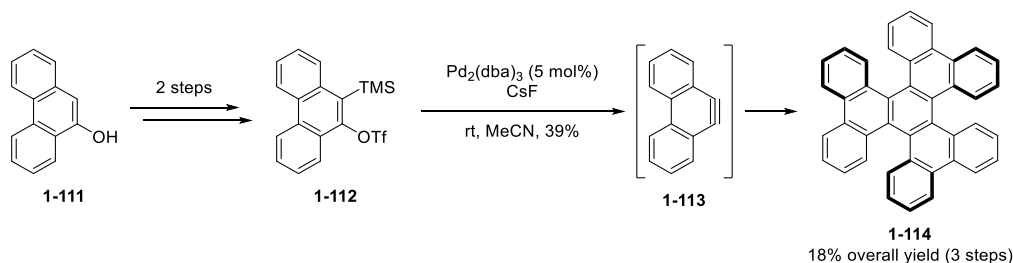
### 1.8. Palladium-Catalyzed Synthesis of Strained Polycyclic Aromatic Hydrocarbons

Geometric novelties such as carbon nano hoops have captivated the interest of physical organic chemists and material scientists alike due to their unique structures and their implications for electronic and material applications.<sup>43</sup> Aside from their potential applications, cycloparaphenylenes (CPPs) are a challenging synthetic target for chemists. Of the many CPP structures, [5]CPP is the most strained CPP synthesized to date, featuring 5 phenyl groups linked in a cyclic structure by *para*-attachments. The Jasti group reported the first successful synthesis of [5]CPP employing a Pd(II)-catalyzed oxidative cyclization as the key step (Scheme 1.19).<sup>44</sup> Cyclization of bis(aryl boronate ester) **1-107** occurred by a Pd(II/0) catalytic cycle to give highly strained product **1-108** in good yield. The reactions were performed under an ambient atmosphere where molecular oxygen serves as the terminal re-oxidant for Pd(0). Reduction of **1-108** with sodium naphthalenide and protonation resulted in **1-109**. Treatment of **1-109** with LDA gave a double E2 elimination to aromatize the remaining rings giving [5]CPP (**1-110**) in good yield. This method was later generalized for the synthesis of a variety of CPP rings.<sup>45</sup>



**Scheme 1.19. Synthesis of [5]CPP by a Pd(II)-catalyzed oxidative cyclization.**

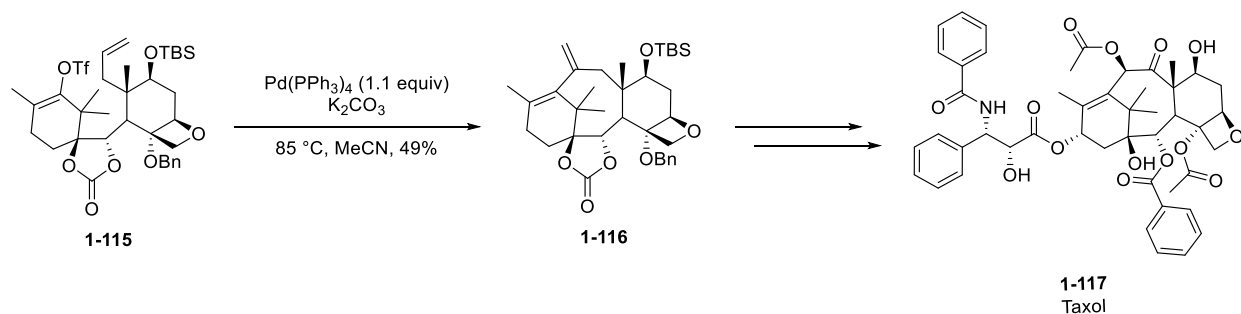
Overcrowded polycyclic aromatic hydrocarbons with significant intramolecular steric interactions undergo distortion from planarity to give saddles, twists, helicenes, or even bowl-shaped structures. Synthesis of these types of structures is challenging and is typically low yielding, requiring harsh reaction conditions for their formation. For example, hexabenzoparaphenylene **1-114** is synthesized in a low 12% yield from the pyrolysis of benzocyclobutene-1,2-dione at  $700^\circ\text{C}$ .<sup>46</sup> **1-114** exists in a propeller-type conformation due to the steric interaction of adjacent aromatic rings in the planar form.<sup>47</sup> A significantly improved yield was achieved by trimerization of the in situ generated aryne **1-113** from silyl triflate **1-112** in the presence of catalytic  $\text{Pd}_2(\text{dba})_3$  (Scheme 1.20).<sup>48</sup> The trimerization occurred in a relatively high yield of 39%, corresponding to an 18% overall yield over three steps from **1-111**. Similarly strained bowl-shaped structures have been synthesized using Buchwald-Hartwig and Stille couplings.<sup>49</sup>



**Scheme 1.20. Strained hexabenzoparaphenylene synthesized by a palladium-catalyzed trimerization of an aryne.**

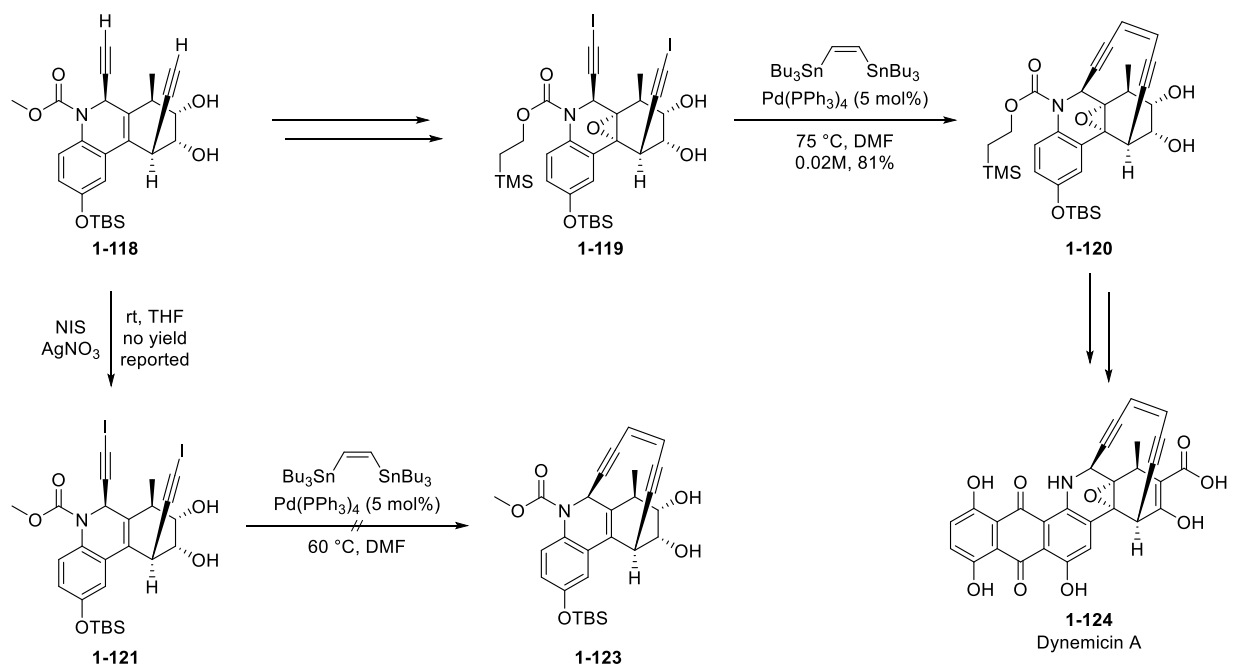
### 1.9. Palladium-Catalyzed Synthesis of Strained Rings in Natural Product Synthesis

The Danishefsky group showcased an intramolecular Heck reaction as the key ring-closing step for the strained 7-membered ring in the total synthesis of Taxol.<sup>50</sup> Although the product is technically not an anti-Bredt olefin, the bridgehead double bond in **1-116** is highly strained (Scheme 1.21). To further complicate matters, a sterically hindered quaternary center is geminal to the reacting vinyl triflate bond of **1-115**. The uncommon *7-exo-trig* ring formation is similarly disfavored. Eventually, success was realized despite these challenges by treatment with stoichiometric Pd(0) in acetonitrile where vinyl triflate **1-115** was cyclized to the key strained intermediate **1-116** in 49 % yield. This key intermediate **1-116** would successfully be converted to baccatin III, which upon subsequent reactions gave Taxol.



**Scheme 1.21. Key Heck reaction in Danishefsky's total synthesis of Taxol.**

A Stille coupling proved useful for the synthesis of the strained enediyne motif in Dynemicin A (**1-124**). From alkene **1-118**, multiple functional group transformations gave diyne **1-119**, which underwent a smooth Stille coupling to give strained dienyne **1-120** (Scheme 1.22).<sup>51</sup> On the other hand, attempted cyclization of the epoxide-free alkene **1-121** was unsuccessful. The successful reaction of **1-119** is attributed to the conformation induced by the internal epoxide, where the alkyne termini exist in closer proximity to allow the palladium-catalyzed cyclization to occur. This was also proposed to alleviate ring strain of **1-120** relative to **1-123**. With enediyne **1-120** in hand the Danishefsky group was able to successfully complete the total synthesis of Dynemicin A.



**Scheme 1.22. Key Stille coupling in Danishefsky's total synthesis of Dynemicin A.**

## 1.10. Summary and Outlook

Presented here are the small, but growing, number of palladium-catalyzed reactions for the synthesis of strained cyclic rings. This review highlighted the synthesis of 3- and 4-membered rings accessible by palladium-catalyzed methodologies. Strained rings emphasized in this work included carbocyclic rings such as cyclopropanes and cyclobutanes, as well their heterocyclic counterparts, namely aziridines, azetidines, and epoxides. This ability of palladium to catalyze the synthesis of highly strained rings was also demonstrated in applications to the synthesis of strained natural products and strained polycyclic aromatic hydrocarbons. Perhaps not surprising, the quantity of palladium-catalyzed methodologies for the synthesis of 3- and 4-membered rings is relatively rare compared to the plethora of methods to make larger rings, and is dwarfed in comparison to palladium-catalyzed methodologies geared toward intermolecular coupling reactions. Given that palladium-catalyzed methodologies have proven effective in a multitude of applications, both for the synthesis of strained and unstrained compounds alike, palladium-catalyzed synthesis of strained rings is vastly underexplored and has exciting potential for many future discoveries.

## 1.11. References and Notes

- (1) Torborg, C.; Beller, M. *Adv. Synth. Catal.* **2009**, *351*, 3027–3043.
- (2) Nicolaou, K. C.; Bulger, P. G.; Sarlah, D. *Angew. Chemie Int. Ed.* **2005**, *44*, 4442–4489.
- (3) *Handbook of Organopalladium Chemistry for Organic Synthesis*; Negishi, E., Ed.; John Wiley & Sons, Inc: New York, 2002.
- (4) Martí-Centelles, V.; Pandey, M. D.; Burguete, M. I.; Luis, S. V. *Chem. Rev.* **2015**, *115*, 8736–8834.



- (5) Chen, Q.; Schweitzer, D.; Kane, J.; Davisson, V. J.; Helquist, P. *J. Org. Chem.* **2011**, *76*, 5157–5169.
- (6) Lee, E.; Song, H. Y.; Kang, J. W.; Kim, D.-S.; Jung, C.-K.; Joo, J. M. *J. Am. Chem. Soc.* **2002**, *124*, 384–385.
- (7) Garg, N. K.; Hiebert, S.; Overman, L. E. *Angew. Chemie Int. Ed.* **2006**, *45*, 2912–2915.
- (8) Nicolaou, K. C.; Nold, A. L.; Milburn, R. R.; Schindler, C. S.; Cole, K. P.; Yamaguchi, J. *J. Am. Chem. Soc.* **2007**, *129*, 1760–1768.
- (9) Molander, G. A.; Dehmel, F. *J. Am. Chem. Soc.* **2004**, *126*, 10313–10318.
- (10) Illuminati, G.; Mandolini, L. *Acc. Chem. Res.* **1981**, *14*, 95–102.
- (11) Yet, L. *Chem. Rev.* **2000**, *100*, 2963–3008.
- (12) Wiberg, K. B. *Angew. Chemie Int. Ed. English* **1986**, *25*, 312–322.
- (13) Blanksby, S. J.; Ellison, G. B. *Acc. Chem. Res.* **2003**, *36*, 255–263.
- (14) Ananikov, V. P.; Musaev, D. G.; Morokuma, K. *Organometallics* **2005**, *24*, 715–723.
- (15) Jun, C.-H. *Chem. Soc. Rev.* **2004**, *33*, 610–618.
- (16) Canty, A. J. In *Comprehensive Organometallic Chemistry II*; Abel, E. W., Stone, F. G. A., Wilkinson, G., Eds.; Elsevier: Oxford, UK, 1995; Vol. 9, pp 225.
- (17) Espinet, P.; Albéniz, A. C. In *Comprehensive Organometallic Chemistry III*; Crabtree, R. H., Mingos, D., Michael, P., Eds.; Elsevier: Oxford, UK, 2007; Vol. 8, pp 315.
- (18) Grigg, R.; Rasul, R.; Redpath, J.; Wilson, D. *Tetrahedron Lett.* **1996**, *37*, 4609–4612.

- (19) Hartog, T. den; Toro, J. M. S.; Chen, P. *Org. Lett.* **2014**, *16*, 1100–1103.
- (20) Tchawou, A. A. S. W.; Raducan, M.; Chen, P. *Organometallics* **2017**, *36*, 180–191.
- (21) Tong, X.; Beller, M.; Tse, M. K. *J. Am. Chem. Soc.* **2007**, *129*, 4906–4907.
- (22) Welbes, L. L.; Lyons, T. W.; Cychosz, K. A.; Sanford, M. S. *J. Am. Chem. Soc.* **2007**, *129*, 5836–5837.
- (23) Tsujihara, T.; Takenaka, K.; Onitsuka, K.; Hatanaka, M.; Sasai, H. *J. Am. Chem. Soc.* **2009**, *131*, 3452–3453.
- (24) Lyons, T. W.; Sanford, M. S. *Tetrahedron* **2009**, *65*, 3211–3221.
- (25) Grigg, R.; Sridharan, V.; Sukirthalingam, S. *Tetrahedron Lett.* **1991**, *32*, 3855–3858.
- (26) Trost, B. M.; Tanoury, G. J. *J. Am. Chem. Soc.* **1988**, *110*, 1636–1638.
- (27) Brecht, J. *Justus Liebigs Ann. Chem.* **1924**, *437*, 1–13.
- (28) Shea, K. J. *Tetrahedron* **1980**, *36*, 1683–1715.
- (29) Trost, B. M.; Yanai, M.; Hoogsteen, K. *J. Am. Chem. Soc.* **1993**, *115*, 5294–5295.
- (30) Shi, M.; Liu, L.-P.; Tang, J. *J. Am. Chem. Soc.* **2006**, *128*, 7430–7431.
- (31) Ye, J.; Shi, Z.; Sperger, T.; Yasukawa, Y.; Kingston, C.; Schoenebeck, F.; Lautens, M. *Nat Chem* **2017**, *9*, 361–368.
- (32) Dyker, G. *Angew. Chemie Int. Ed. English* **1994**, *33*, 103–105.
- (33) Kang, S.-K.; Yamaguchi, T.; Pyun, S.-J.; Lee, Y.-T.; Baik, T.-G. *Tetrahedron Lett.* **1998**,

- 39, 2127–2130.
- (34) Shimizu, I.; Sugiura, T.; Tsuji, J. *J. Org. Chem.* **1985**, *50*, 537–539.
- (35) Hayashi, S.; Yorimitsu, H.; Oshima, K. *J. Am. Chem. Soc.* **2009**, *131*, 2052–2053.
- (36) Surry, D. S.; Buchwald, S. L. *Angew. Chemie Int. Ed.* **2008**, *47*, 6338–6361.
- (37) Hayashi, S.; Yorimitsu, H.; Oshima, K. *Angew. Chemie Int. Ed.* **2009**, *48*, 7224–7226.
- (38) McNally, A.; Haffemayer, B.; Collins, B. S. L.; Gaunt, M. J. *Nature* **2014**, *510*, 129–133.
- (39) Anzai, M.; Toda, A.; Ohno, H.; Takemoto, Y.; Fujii, N.; Ibuka, T. *Tetrahedron Lett.* **1999**, *40*, 7393–7397.
- (40) Ohno, H.; Toda, A.; Miwa, Y.; Taga, T.; Osawa, E.; Yamaoka, Y.; Fujii, N.; Ibuka, T. *J. Org. Chem.* **1999**, *64*, 2992–2993.
- (41) He, G.; Zhao, Y.; Zhang, S.; Lu, C.; Chen, G. *J. Am. Chem. Soc.* **2012**, *134*, 3–6.
- (42) He, G.; Lu, G.; Guo, Z.; Liu, P.; Chen, G. *Nat Chem* **2016**, *8*, 1131–1136.
- (43) Lewis, S. E. *Chem. Soc. Rev.* **2015**, *44*, 2221–2304.
- (44) Evans, P. J.; Darzi, E. R.; Jasti, R. *Nat Chem* **2014**, *6*, 404–408.
- (45) Darzi, E. R.; White, B. M.; Loventhal, L. K.; Zakharov, L. N.; Jasti, R. *J. Am. Chem. Soc.* **2017**, *139*, 3106–3114.
- (46) Hacker, N. P.; McOmie, J. F. W.; Meunier-Piret, J.; Van Meerssche, M. *J. Chem. Soc. Perkin Trans. 1* **1982**, No. 0, 19–23.

- (47) Barnett, L.; Ho, D. M.; Baldrige, K. K.; Pascal, R. A. *J. Am. Chem. Soc.* **1999**, *121*, 727–733.
- (48) Peña, D.; Pérez, D.; Guitián, E.; Castedo, L. *Org. Lett.* **1999**, *1*, 1555–1557.
- (49) Qian, H.; Yue, W.; Zhen, Y.; Di Motta, S.; Di Donato, E.; Negri, F.; Qu, J.; Xu, W.; Zhu, D.; Wang, Z. *J. Org. Chem.* **2009**, *74*, 6275–6282.
- (50) Danishefsky, S. J.; Masters, J. J.; Young, W. B.; Link, J. T.; Snyder, L. B.; Magee, T. V.; Jung, D. K.; Isaacs, R. C. A.; Bornmann, W. G.; Alaimo, C. A.; Coburn, C. A.; Di Grandi, M. J. *J. Am. Chem. Soc.* **1996**, *118*, 2843–2859.
- (51) Shair, M. D.; Yoon, T. Y.; Mosny, K. K.; Chou, T. C.; Danishefsky, S. J. *J. Am. Chem. Soc.* **1996**, *118*, 9509–9525.

## Chapter 2

### Palladium(II)-Catalyzed Oxidative Coupling Reactions Using Molecular Oxygen as the Terminal Re-oxidant

#### 2.1 Abstract

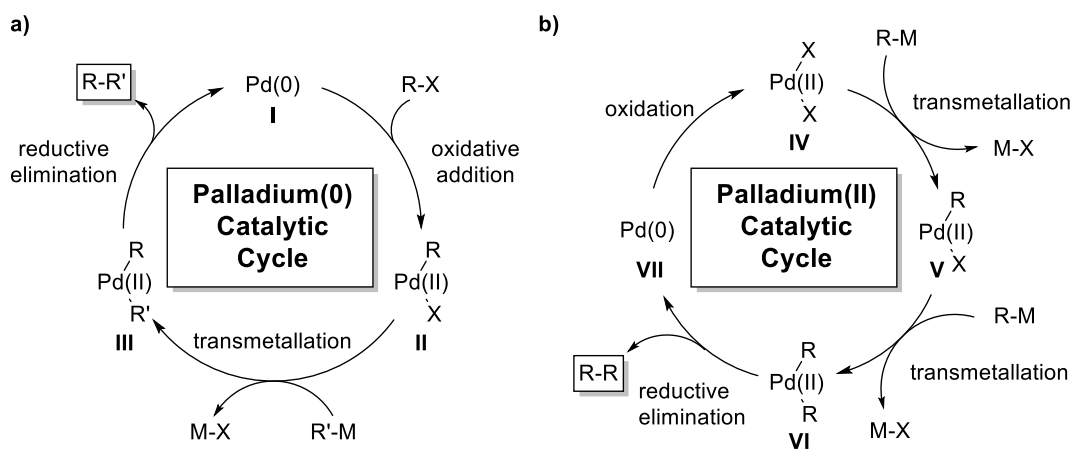
The palladium(II)-catalyzed oxidative macrocyclization of bis(vinylboronate esters) is demonstrated as an efficient method for the synthesis of macrocyclic dienes. The synthesis of long chain  $\alpha,\omega$ -bis(vinylboronate esters) is highlighted to emphasize their ease of preparation prior to macrocyclization. The macrocyclization reactions feature mild reaction conditions due to a palladium(II) catalytic cycle which obviates the need for a high energy oxidative addition step of standard palladium(0) catalytic cycles. Instead, this oxidative coupling is promoted by chloroacetone as a terminal re-oxidant in the catalytic cycle. An extension of the oxidative coupling/macrocyclization strategy is highlighted where molecular oxygen may be used in place of chloroacetone as the terminal re-oxidant. Homocoupling reactions of vinylboronate esters served as a template to screen reaction conditions for this method. From these experiments, multiple reaction conditions gave the oxidative homocoupling product in high yield. These reaction conditions were successfully applied to the oxidative macrocyclization of a bis(vinylboronate ester) using molecular oxygen as a re-oxidant.

#### 2.2 Introduction

Palladium-catalyzed carbon-carbon bond forming reactions have revolutionized the fields of organic synthesis and organometallic chemistry since the discovery of palladium-catalyzed coupling reactions.<sup>1,2</sup> Palladium-catalyzed coupling reactions may be broadly categorized into three categories: (i) coupling between carbon-based electrophiles, typically aryl/vinyl halides or

pseudohalides, and nucleophilic coupling partners, typically organometallic compounds such as organozinc, magnesium or boron reagents (ii) reductive coupling between two organic electrophiles and (iii) oxidative coupling of two organometallic nucleophiles, the subject of this study.

Cross-coupling reactions proceed by a Pd(0) catalytic cycle (Scheme 2.1a). The catalytic cycle begins with oxidative addition of Pd(0) with the organic electrophile partner giving the Pd(II) intermediate **II**, which undergoes transmetallation with the organometallic coupling partner to form diorgano-Pd(II) intermediate **III**. Reductive elimination from Pd(II) forms the new carbon-carbon bond and Pd(0), which re-enters the catalytic cycle. Typically, cross couplings reactions require high temperature reaction conditions to facilitate the high energy oxidative addition step.



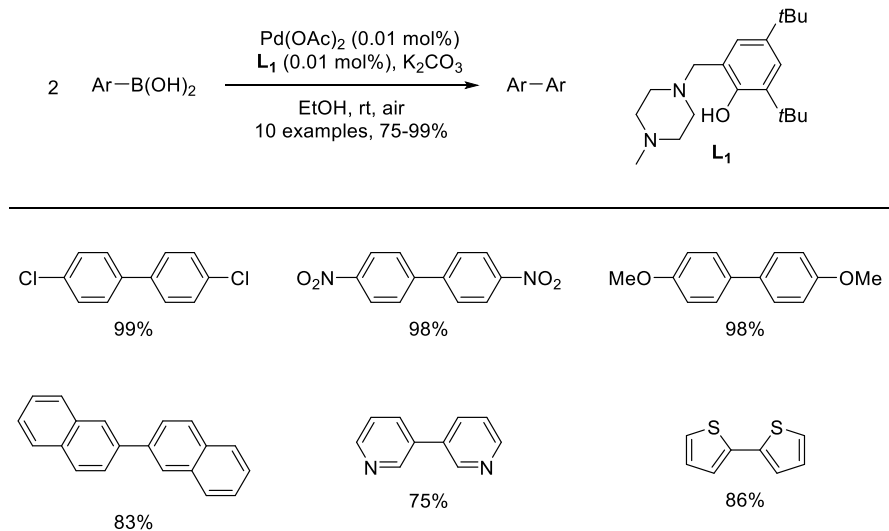
**Scheme 2.1. Pd(0) and Pd(II) catalytic cycles.**

On the other hand, Pd(II)-catalyzed coupling of two organometallic reagents under oxidative conditions results in carbon-carbon bond formation under relatively mild reaction conditions (Figure 2.1b). Starting from Pd(II) intermediate **IV**, transmetallation with one equivalent of organometallic reagent gives **V**, which undergoes a second transmetallation to give diorgano-Pd(II) intermediate **VI**. Reductive elimination generates Pd(0) with formation of a new

carbon-carbon bond. Pd(0) is oxidized to Pd(II) by an external re-oxidant to complete the catalytic cycle.

The cross-coupling between organic electrophiles (halides, triflates), and organoboron reagents, also known as the Suzuki coupling, has found tremendous popularity.<sup>3</sup> Oxidative coupling of organoboron compounds, originally identified as a side reaction of the Suzuki reaction has grown and developed into a field of its own. The remainder of this introduction will highlight homocoupling reactions of organoboron compounds under Pd(II) catalysis, as well as the oxidative cyclization of bis(organoboron) compounds.

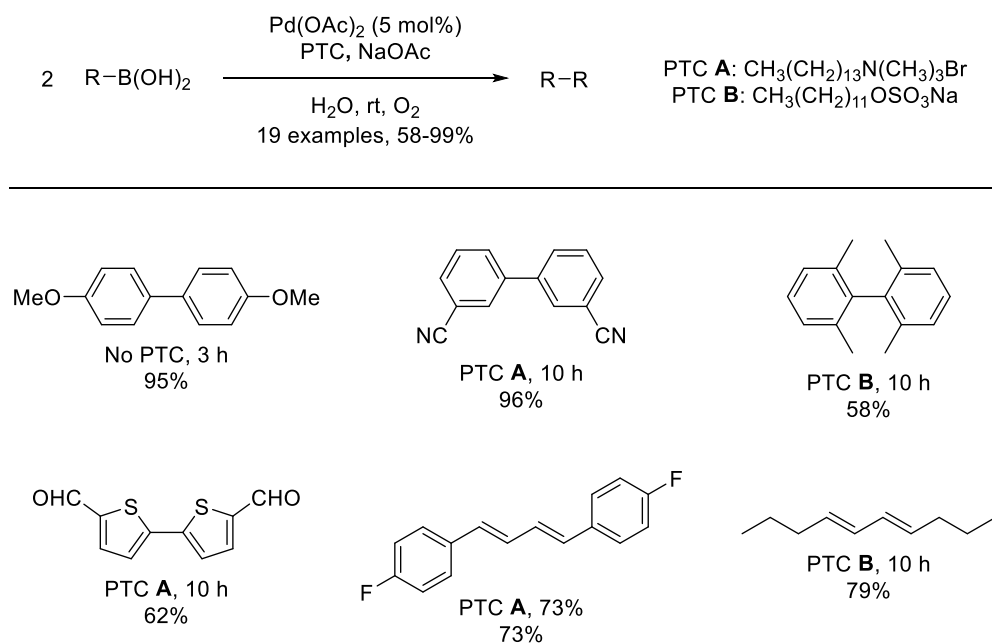
Aryl boronic acids have been demonstrated to be efficient coupling partners, with Pd(OAc)<sub>2</sub> loadings as low as 0.01 mol%, when used in conjunction with N,O-ligands such as **L1** in the presence of K<sub>2</sub>CO<sub>3</sub> employing air as the terminal oxidant (Scheme 2.2).<sup>4</sup> *para*-Substituted aryl boronic acids with electron withdrawing or donating substituents are well tolerated, as well as heterocyclic boronic acids. Ligand and base-free oxidative homocoupling reactions of boronic acids are also known, although higher catalyst loadings are typically required.<sup>5</sup> Ligands such as P(*o*-tolyl)<sub>3</sub> and P(OEt)<sub>3</sub> have also been demonstrated to be more effective relative to ligand free conditions.<sup>6</sup>



**Scheme 2.2. Oxidative homocoupling of aryl boronic acids facilitated by N,O-ligands.**

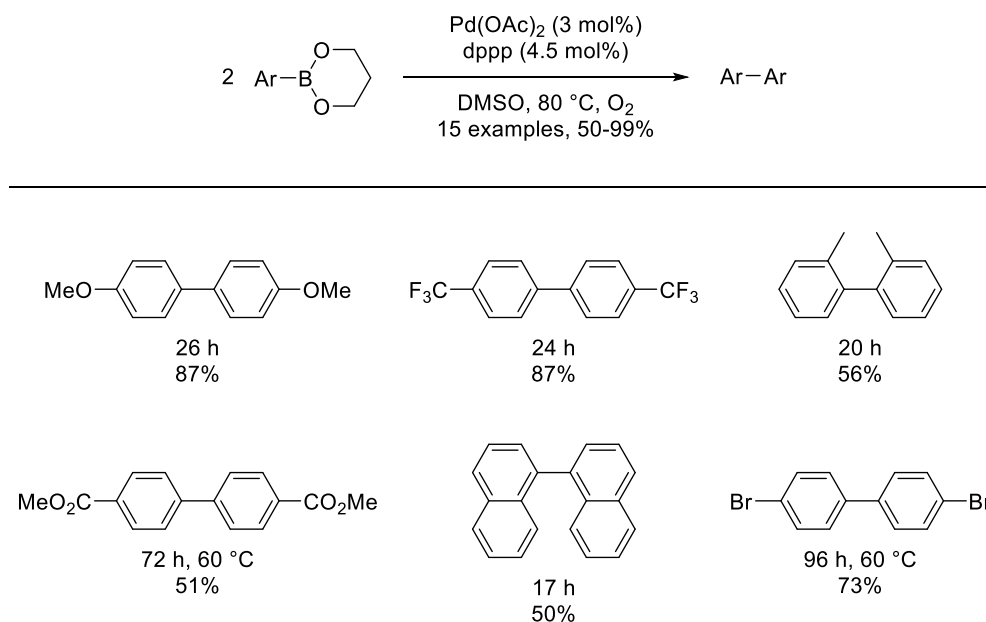
Styryl and alkenyl boronic acids have also undergone successful oxidative homocoupling reactions under Pd(II)-catalysis. In a water-based solvent system, styryl and alkenyl boronic acids were successfully coupled in the presence of catalytic Pd(OAc)<sub>2</sub> with phase transfer catalysts using molecular oxygen as the terminal re-oxidant (Scheme 2.3).<sup>7</sup> Aryl boronic acids were also successful homocoupling partners in this study. Styryl boronic acids have also been homocoupled in the presence of Pd(OAc)<sub>2</sub> complexes containing N-heterocyclic carbene ligands with *p*-benzoquinone as a terminal re-oxidant.<sup>8</sup>





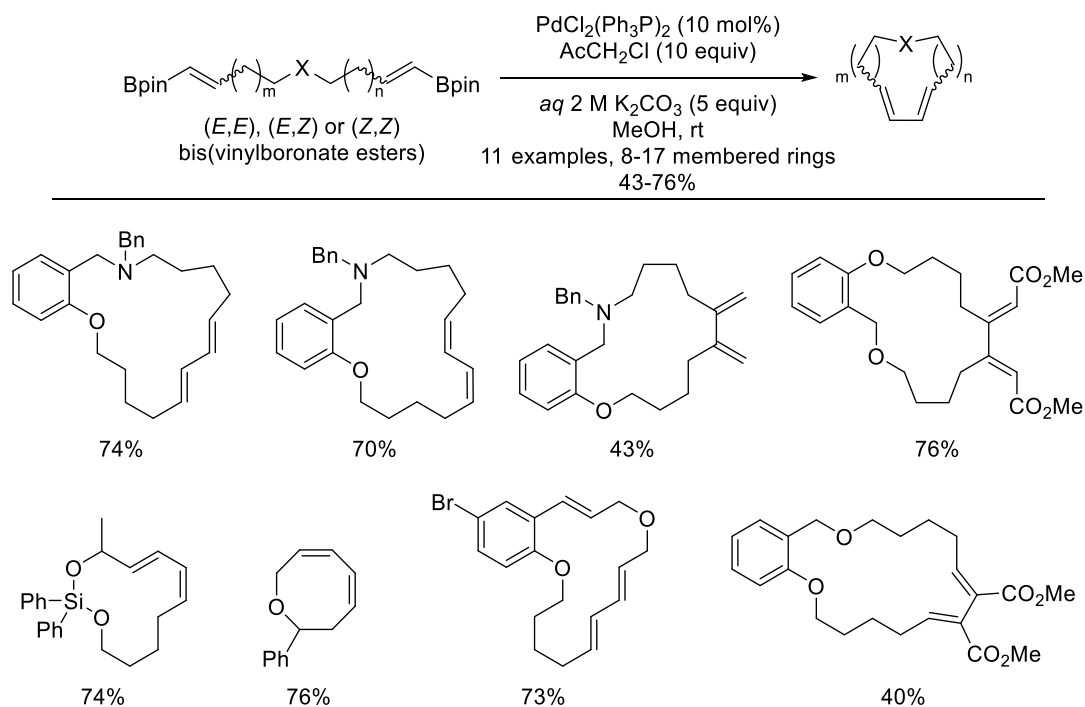
**Scheme 2.3. Oxidative homocoupling of aryl, styryl, and alkenyl boronic acids in water.**

Extension of the oxidative coupling of organoboronic acids to aryl boronate esters has been successful in isolated cases. Oxidative coupling of aryl 1,3,2-dioxaboranines catalyzed by  $\text{Pd(OAc)}_2$  under oxygen atmospheres gave a variety of biaryls with electron withdrawing or donating substituents (Scheme 2.4).<sup>9</sup> Base-free reaction conditions were tolerant of base sensitive functional groups such as esters. Aryl boronate esters have also been coupled under air atmospheres with fluoride base in the presence of  $\text{PdCl}_2(\text{PPh}_3)_2$ .<sup>10</sup>



**Scheme 2.4. Oxidative homocoupling of aryl boronate esters.**

Oxidative cyclizations of bis(organoboron) compounds is an underexplored topic where two main avenues of research dominate the field. The Jasti group pioneered the synthesis of highly strained polyparaphenylenes, featuring the oxidative cyclization of aryl bis(pinacolboronate esters), as highlighted previously (Scheme 1.19, Chapter 1).<sup>11-13</sup> The Merlic group reported a second method, the palladium-catalyzed oxidative macrocyclization of bis(vinylboronate esters), as an entry point to the synthesis of macrocyclic dienes (Scheme 2.5).<sup>14</sup> Dienes with (*E,E*)-, (*Z,Z*)-, and (*E,Z*)-double bond configurations in 8- to 17-membered rings are accessible under the mild reaction conditions. Bis(vinylboronate esters) with internal dienes gave macrocyclic products in good yields as well. The synthesis of terminal bis(vinylboronate esters) is easily achieved by a bidirectional chain synthesis strategy, where double alkyne installation, followed by double hydroboration provides the macrocyclization precursors in high yield. This contrasts with standard cross-coupling cyclization substrates that require nucleophilic and electrophilic end groups, increasing the synthetic complexity required to synthesize the cyclization precursor.

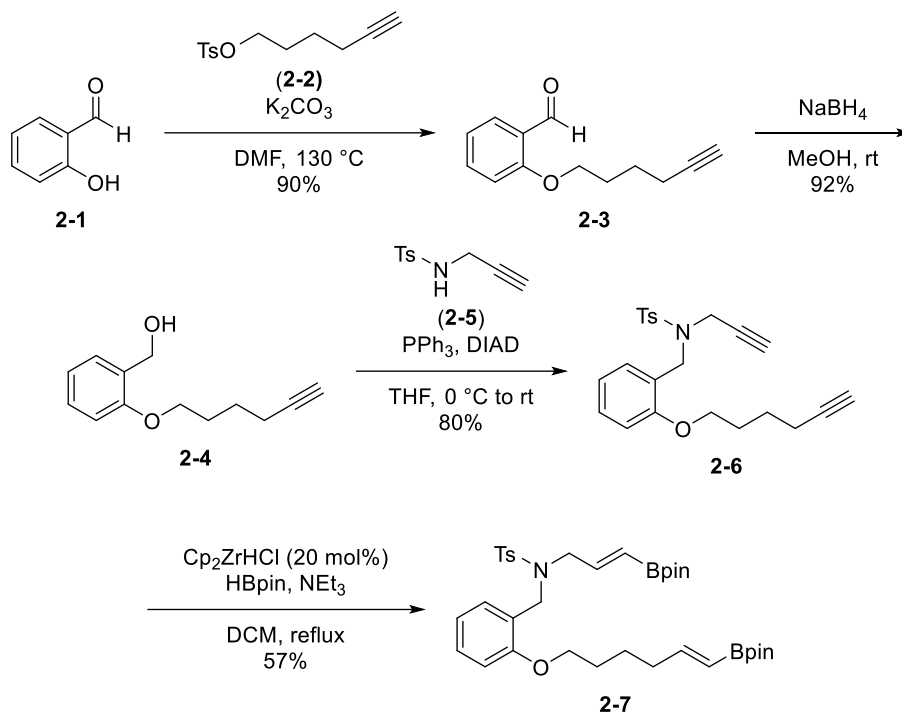


**Scheme 2.5. Oxidative macrocyclization of bis(vinylboronate esters).**

### 2.3 Results and Discussion

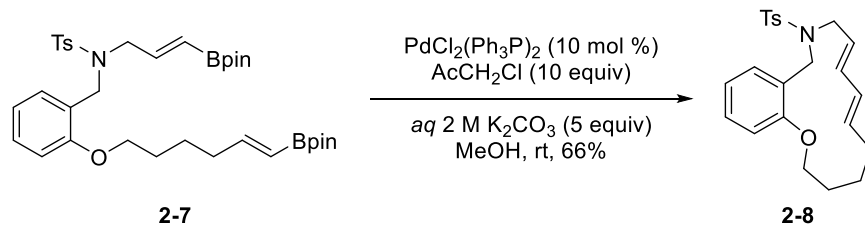
To establish the palladium-catalyzed oxidative cyclization strategy as a versatile method to synthesize complex macrocyclic dienes, we sought to diversify the established substrate scope. Simultaneously, we wished to determine an efficient palladium-catalyzed oxidative homocoupling methodology of pinacol boronate esters using molecular oxygen as a terminal re-oxidant and apply it in macrocyclization context. To increase the substrate scope of the palladium-catalyzed oxidative cyclization methodology, we embarked upon the synthesis of bis(vinylboronate ester) **2-7**, adapted from a previously established synthetic route (Scheme 2.6).<sup>15</sup> C-O bond formation between salicylaldehyde (**2-1**) and tosylate **2-2** in the presence of  $K_2CO_3$  gave aldehyde **2-3**. Sodium borohydride reduction gave alcohol **2-4**, which was converted to sulfonamide **2-6** by a Mitsunobu

reaction. Double hydroboration with pinacolborane catalyzed by Schwartz's reagent<sup>16</sup> gave the desired bis(vinylboronate ester) **2-7**.



**Scheme 2.6. Preparation of bis(vinylboronate ester) 2-7.**

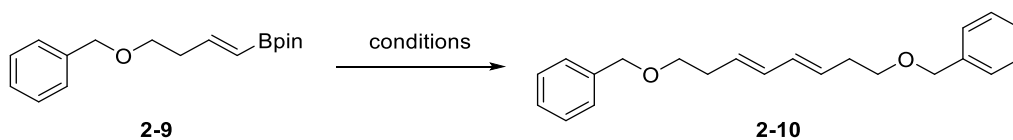
Reaction conditions for the macrocyclization of bis(vinylboronate esters) were previously developed by my colleague Dr. Robert Iafe during his graduate research.<sup>15</sup> Cyclization of bis(vinylboronate ester) **2-7** under these conditions was successful upon treatment with catalytic  $\text{Pd}(\text{PPh}_3)_2\text{Cl}_2$  in methanol using  $\text{K}_2\text{CO}_3$  base and chloroacetone as the terminal re-oxidant (Scheme 2.7). High dilution conditions of 0.002 M were required to prevent oligomerization of bis(vinylboronate ester) **2-7**. Cyclic diene **2-8** was the only cyclic diene isomer detected in this stereospecific cyclization reaction.



**Scheme 2.7. Oxidative macrocyclization of bis(vinylboronate ester) 2-7.**

We switched to explorations on whether molecular oxygen could serve as the terminal oxidant in the oxidative macrocyclization of bis(vinylboronate esters) rather than chloroacetone. Although many variants of oxidative homocoupling reactions were known at the time of these studies, oxidative homocoupling of pinacol vinylboronate using molecular oxygen as a terminal re-oxidant were not. To determine the feasibility of an oxidative macrocyclization of terminal bis(vinylboronate esters) using molecular oxygen as a terminal re-oxidant, we sought to optimize the oxidative homocoupling of alkenyl pinacol boronate esters, and later apply it to macrocyclic substrates.

Initially reaction conditions were screened for the oxidative homocoupling reaction of vinylboronate ester **2-9** based upon preliminary work by my co-worker Dr. Oscar Villalta.<sup>17</sup> High yields of diene **2-10** were observed with catalyst loadings as low as 4 mol%  $\text{PdCl}_2(\text{dppp})$  using  $\text{Cs}_2\text{CO}_3$  base open to air in DMF (Table 2.1, entry 1). Acetonitrile and THF were also suitable solvents for oxidative homocoupling (entries 2, 3). Reaction conditions similar to our oxidative macrocyclization conditions using methanol/water solvent systems surprisingly gave low yields of diene product. Reactions in methanol solvent in the absence of water had a slower rate of reaction (entry 4 vs. 5). As a comparison, our oxidative coupling conditions catalyzed by  $\text{PdCl}_2(\text{PPh}_3)_2$  with chloroacetone as a re-oxidant with aqueous  $\text{K}_2\text{CO}_3$  base in methanol gave comparable yields of diene **2-10** (entry 6).

**Table 2.1. Oxidative homocoupling reaction conditions screening.<sup>a</sup>**

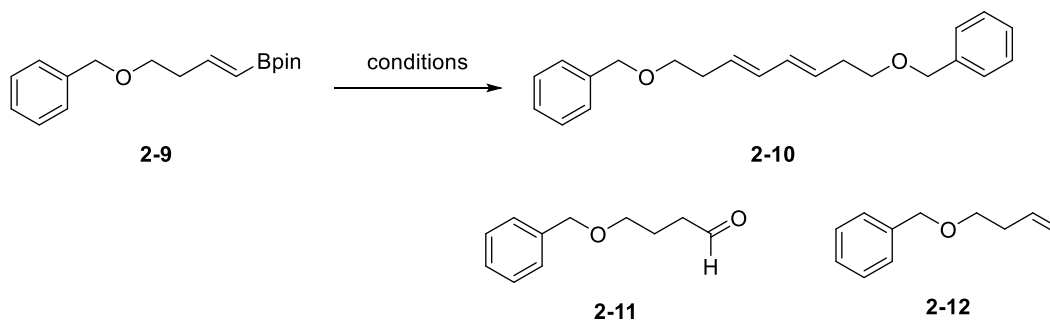
Entry	Solvent	Isolated Yield (%)
<b>1</b>	DMF	88
<b>2</b>	MeCN	84
<b>3</b>	THF	66
<b>4</b>	MeOH/H <sub>2</sub> O (10/1)	32
<b>5</b>	MeOH	N.D.
<b>6<sup>b</sup></b>	MeOH	62

<sup>a</sup>Reaction conditions: PdCl<sub>2</sub>(dppp) (4 mol%), Cs<sub>2</sub>CO<sub>3</sub> (4 equiv), **2-9** (2 equiv, 0.1 M), rt, air, overnight. <sup>b</sup>Reaction conditions: PdCl<sub>2</sub>(PPh<sub>3</sub>)<sub>2</sub> (5 mol%), K<sub>2</sub>CO<sub>3</sub> (2.6 equiv, aq 2M), chloroacetone (5.2 equiv), **2-9** (1 equiv, 0.1 M), rt, under nitrogen, 72 h. N.D. = not determined.

We determined the effect of bases by <sup>1</sup>H-NMR analysis of crude reaction mixtures. Reactions employing Cs<sub>2</sub>CO<sub>3</sub>, K<sub>2</sub>CO<sub>3</sub>, or aq K<sub>2</sub>CO<sub>3</sub> were stopped after 5 h and the ratio of unreacted starting material **2-9**, diene **2-10**, oxidation side product **2-11**, and protodeboronation side product **2-12** were measured (Table 2.2). Protodeboronation is a common side product in reactions of organoboron compounds,<sup>18</sup> but was not observed in any of these reactions. Reactions with Cs<sub>2</sub>CO<sub>3</sub> or K<sub>2</sub>CO<sub>3</sub> in the absence of water additive consumed vinylboronate **2-9** at a slower rate, but had lower ratios of oxidation byproduct **2-11**. Cs<sub>2</sub>CO<sub>3</sub> promoted the formation of product more efficiently compared to K<sub>2</sub>CO<sub>3</sub>, giving a higher percentage of product relative to side products. With the information from these results, Cs<sub>2</sub>CO<sub>3</sub> was chosen as the base for future oxidative homocoupling reactions.

Product **2-11** likely is the result of the reaction of vinylboronate ester **2-9** with hydrogen peroxide rather than water. Reaction of aryl boronic acids have been demonstrated to undergo oxidation to phenols in the presence of hydrogen peroxide.<sup>19</sup> Standard hydroboration-oxidation procedures use basic solutions of hydrogen peroxide to generate alcohols from *in-situ* generated alkyl- and alkenylboron compounds.<sup>20</sup> In oxidative homocoupling experiments oxidation of Pd(0) by molecular oxygen is proposed to give an  $\eta^2$ -Pd(II) peroxy complex which generates an equivalent of hydrogen peroxide after catalytic turnover, which is responsible for the formation of phenol side products.<sup>21,22</sup> High yielding homocoupling reactions have been successful in aqueous solutions under basic conditions<sup>7</sup> suggesting that neither water nor hydroxide couple to boronic acids at appreciable rates under Pd(II) catalysis.

**Table 2.2. Effect of base on product ratios for oxidative homocoupling reactions.<sup>a</sup>**

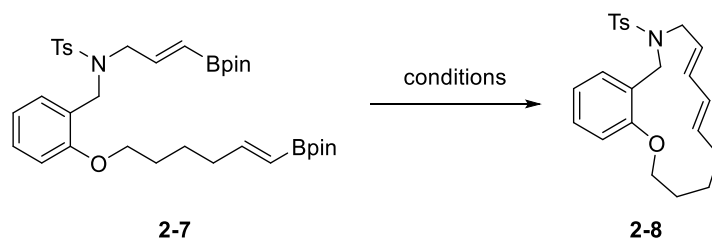


Entry	Base	Mol% <b>2-9</b>	Mol% <b>2-10</b>	Mol% <b>2-11</b>	Mol% <b>2-12</b>
<b>1</b>	CS <sub>2</sub> CO <sub>3</sub>	21	64	15	0
<b>2</b>	K <sub>2</sub> CO <sub>3</sub>	32	45	24	0
<b>3</b>	K <sub>2</sub> CO <sub>3</sub> (aq)	0	58	42	0

<sup>a</sup>Reaction conditions: PdCl<sub>2</sub> (4 mol%), dppp (4 mol%), CS<sub>2</sub>CO<sub>3</sub> (4.2 equiv), **2-9** (2 equiv, 0.1 M), DMF, rt. Ratios determined by <sup>1</sup>H-NMR analysis of crude reaction mixtures after 5 h.

With a set of oxidative homocoupling conditions in hand, we attempted the macrocyclization of bis-vinylboronate ester **2-7** with molecular oxygen as a terminal re-oxidant (Table 2.3). The oxidative macrocyclization was most successful in DMF solvent under high dilution conditions (0.002 M) with stirring open to air where a moderate 51% yield was observed (entry 1). Unfortunately, the large quantities of DMF were tedious to remove, so alternative solvents were tested. Oxidative macrocyclizations were successful in methanol and acetonitrile, but slower reaction rates were observed as evidenced by remaining starting material (entries 2-4). Using pure oxygen atmosphere with acetonitrile solvent gave similar yields, but with shorter reaction times (entry 3). With these preliminary studies, further optimization of the oxidative macrocyclization with molecular oxygen re-oxidant and extension of its substrate scope are possible.

**Table 2.3. Oxidative macrocyclization conditions with molecular oxygen as re-oxidant.<sup>a</sup>**



Entry	Atmosphere	Time (h)	Catalyst (mol%)	Solvent	Yield (%)
1	Air	24	PdCl <sub>2</sub> (dppp) (10)	DMF	51
2	Air	46	PdCl <sub>2</sub> (dppp) (10)	MeCN	34
3	O <sub>2</sub>	24	PdCl <sub>2</sub> (dppp) (10)	MeCN	33
4	Air	16	PdCl <sub>2</sub> (dppp) (10)	MeOH	22

<sup>a</sup> Reaction conditions: **2-7** (1 equiv, 0.31 mmol, 0.002M), PdCl<sub>2</sub>(dppp) (0.1 equiv, 0.031 mmol), Cs<sub>2</sub>CO<sub>3</sub> (4 equiv, 1.2 mmol), O<sub>2</sub> balloon or open to air.



## 2.4 Conclusions

The palladium(II)-catalyzed oxidative macrocyclization of bis(vinylboronate esters) has been successfully demonstrated by two different methods. Previously established reaction conditions were applied to the cyclization of a novel bis(vinylboronate ester) that gave a 15-membered macrocyclic (*E,E*)-1,3-diene. These mild palladium(II)-catalyzed macrocyclization conditions featured chloroacetone as a terminal re-oxidant. Reaction conditions were later established based on reaction condition screening for the oxidative homocoupling of vinylboronate esters using molecular oxygen as a terminal re-oxidant. These reaction conditions were successfully applied to the oxidative macrocyclization of a bis(vinylboronate ester). Further optimization of the oxidative homocoupling/macrocyclization reaction conditions and exploration of the substrate scope will generalize this method for the synthesis of linear and macrocyclic dienes.

## 2.5 Experimental

All commercial compounds were used as received. Dichloromethane, triethylamine, and acetonitrile were purified by distillation over CaH<sub>2</sub>. Methanol was distilled over Mg. Tetrahydrofuran and ether were distilled prior to use from sodium-benzophenone ketyl. All reactions were carried out in flame-dried glassware under a nitrogen atmosphere, unless otherwise stated. Bis(triphenylphosphine)palladium(II) dichloride (PdCl<sub>2</sub>(Ph<sub>3</sub>P)<sub>2</sub>, Aldrich, ≥ 99%) was used as received. Reactions were monitored using TLC and the plates were developed using vanillin, cerium ammonium molybdate, or potassium permanganate stains. Column chromatography was performed using silica gel (40-63 micron) and reagent grade solvents without deactivation, unless noted. NMR spectra were recorded at 400 or 500 MHz as noted and calibrated to the solvent signal (CDCl<sub>3</sub> δ = 7.26 ppm or C<sub>6</sub>D<sub>6</sub> δ = 7.16 ppm for <sup>1</sup>H NMR, and CDCl<sub>3</sub> δ = 77.0 ppm or C<sub>6</sub>D<sub>6</sub> δ =

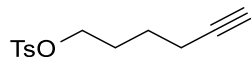
128.1 for  $^{13}\text{C}$  NMR). Multiplicities are indicated by s (singlet), d (doublet), t (triplet), q (quartet), p (pentet), m (multiplet), or b (broadened). IR spectra were recorded with an ATR attachment and selected peaks are reported in  $\text{cm}^{-1}$ . High resolution mass spectral data was recorded with an IonSense ID-CUBE DART source or an ESI LC-TOF Micromass LCT.

***General Procedure A: Oxidative homocoupling of vinylboronate 2-9.***

A flame dried 15 mL flask was charged with  $\text{PdCl}_2(\text{dppp})$  (6 mg, 0.0097 mmol). DMF (4.9 mL) was added, followed by **2-9** (140 mg, 0.486 mmol), and  $\text{Cs}_2\text{CO}_3$  (317 mg, 0.972 mmol). The reaction was stirred overnight open to air. In the case of non-volatile solvents, the reaction mixture diluted with water, extracted with  $\text{Et}_2\text{O}$ , dried with  $\text{MgSO}_4$  upon completion. In the case of volatile solvents, the reaction was diluted with EtOAc and passed through a Celite plug rather than extraction. After evaporation, chromatography with 19:1 petroleum ether/EtOAc gave 76 mg (83%) of **2-9** as a clear colorless oil.

***General Procedure B: Oxidative macrocyclization of bis(vinylboronate) 2-7.***

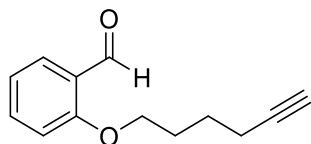
A flame dried 500 mL flask was charged with  $\text{PdCl}_2(\text{dppp})$  (18 mg, 0.031 mmol). DMF (160 mL) was added, followed by **2-7** (200 mg, 0.307 mmol), then  $\text{Cs}_2\text{CO}_3$  (400 mg, 1.23 mmol) added and the reaction was stirred overnight open to air. Upon completion, the reaction mixture diluted with water, extracted with  $\text{Et}_2\text{O}$ , dried with  $\text{MgSO}_4$ . In the case of volatile solvents, the reaction was passing through a Celite plug rather than extraction. After evaporation, chromatography with 9:1 Hex:EtOAc gave 62 mg (51%) of **2-8** as a clear colorless oil.



### hex-5-yn-1-yl 4-methylbenzenesulfonate (2-2)

To a flame dried flask was added DMAP (200 mg, 1.64 mmol). The flask was flushed with nitrogen, then DCM (23 mL) was added. After the addition of hex-5-yn-1-ol (2.1 mL, 19.0 mmol) and  $\text{NEt}_3$  (2.9 mL, 20.9 mmol), the flask was cooled to 0 °C, and *p*-TsCl (6.570 g, 34.5 mmol) was added slowly. The flask was warmed to rt and stirred 1 h. The mixture was diluted with saturated aq.  $\text{NH}_4\text{Cl}$  (60 mL), extracted with DCM (2x60mL), and dried with  $\text{MgSO}_4$ . Solvent was removed *in vacuo* and column chromatography with a 0% to 20% Hex:EtOAc gradient solvent system gave 3.860 g (80% yield) of the known<sup>23</sup> clear colorless oil.

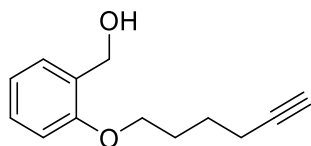
$^1\text{H NMR}$  (400 MHz,  $\text{CDCl}_3$ , ppm)  $\delta$  7.79 (d,  $J = 8.4$  Hz, 2H), 7.35 (d,  $J = 8.0$  Hz, 2H), 4.06 (t,  $J = 6.2$  Hz, 2H), 2.45 (s, 3H), 2.17 (td,  $J = 6.9, 2.7$  Hz, 2H), 1.92 (t,  $J = 2.6$  Hz, 1H), 1.82-1.75 (m, 2H), 1.56 (p,  $J = 7.2$  Hz, 2H).



### 2-(hex-5-yn-1-yloxy)benzaldehyde (2-3)

To a flame dried flask was added salicylaldehyde (**2-1**, 1.34 mL, 12.8 mmol), freshly ground  $\text{K}_2\text{CO}_3$  (2.115 g, 15.3 mmol), and **2-2** (3.859 g, 15.3 mmol). The flask was flushed with nitrogen, then DMF (110 mL) was added. The mixture was heated at 130 °C for 24 h, then cooled to rt. The mixture was diluted with water, and extracted with  $\text{Et}_2\text{O}$ . The organic layer was washed with 1M NaOH, brine, and dried with  $\text{MgSO}_4$ . Column chromatography with a 10:1 Hex:EtOAc gave 2.310 g (90% yield) of the known<sup>14</sup> clear colorless oil.

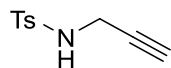
**<sup>1</sup>H NMR** (400 MHz, CDCl<sub>3</sub>, ppm) δ 10.52 (d, *J* = 0.7 Hz, 1H), 7.84 (dd, *J* = 7.7, 1.8 Hz, 1H), 7.53 (td, *J* = 7.8 Hz, 1.8 Hz, 1H), 7.02 (t, *J* = 7.5 Hz, 1H), 6.98 (d, *J* = 8.4 Hz, 1H), 4.12 (t, *J* = 6.2 Hz, 2H), 2.30 (td, *J* = 6.9, 2.7 Hz, 2H), 2.04-1.97 (m, 2H), 1.98 (t, *J* = 2.6 Hz, 1H), 1.76 (p, *J* = 7.3 Hz, 2H).



#### **(2-(hex-5-yn-1-yloxy)phenyl)methanol (2-4)**

To a flame dried flask was added **2-3** (2.400 g, 11.9 mmol). The flask was flushed with nitrogen, then MeOH (28 mL) was added. NaBH<sub>4</sub> (584 mg, 15.4 mmol) was added at rt. The reaction was stirred 15 h. The mixture was diluted with water and extracted with Et<sub>2</sub>O. The organic extracts were rinsed with water, then the solvent was removed *in vacuo*. Column chromatography with a 5:2 Hex:EtOAc gave 2.200 g (92% yield) of the known<sup>14</sup> clear colorless oil.

**<sup>1</sup>H NMR** (400 MHz, CDCl<sub>3</sub>, ppm) δ 7.29-7.24 (m, 2H), 6.94 (td, *J* = 7.4, 0.9 Hz, 1H), 6.87 (bd, *J* = 8.1 Hz, 1H), 4.70 (bd, *J* = 6.4 Hz, 2H), 4.06 (t, *J* = 6.2 Hz, 2H), 2.30 (td, *J* = 7.0, 2.7 Hz, 2H), 2.00-1.93 (m, 2H), 1.98 (t, *J* = 2.6 Hz), 1.74 (p, *J* = 7.3 Hz, 2H).

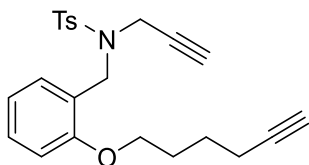


#### **4-methyl-N-(prop-2-yn-1-yl)benzenesulfonamide (2-5)**

To a flame dried flask was added propargyl amine (1.053 g, 19.1 mmol). The flask was flushed with nitrogen, then DCM (28 mL), NEt<sub>3</sub> (2.66 mL, 19.1 mmol), and DMAP (23 mg, 0.191 mmol). The mixture was cooled to 0 °C, then tosyl chloride (3.663 g, 19.1 mmol) was added

slowly. The mixture was stirred at 0 °C for 30 min, then 48 h at rt. The reaction was diluted with water and extracted with Et<sub>2</sub>O. The solvent was removed *in vacuo*. Column chromatography with a gradient elution from 100% hexanes to 5:1 Hex:EtOAc gave 3.440 g (86% yield) of the known<sup>24</sup> white solid.

<sup>1</sup>H NMR (400 MHz, CDCl<sub>3</sub>, ppm) δ 7.77 (d, *J* = 8.3 Hz, 2H), 7.32 (d, *J* = 7.9 Hz, 2H), 3.84 (dd, *J* = 6.1, 2.6 Hz, 2H), 2.44 (s, 3H), 2.11 (t, *J* = 2.6 Hz, 1H).



***N*-(2-(hex-5-yn-1-yloxy)benzyl)-4-methyl-*N*-(prop-2-yn-1-yl)benzenesulfonamide (2-6)**

To a solution of (2-(hex-5-yn-1-yloxy)phenyl)methanol **2-4** (1.281 g, 6.3 mmol), **2-5** (1.312 g, 7.4 mmol) and PPh<sub>3</sub> (1.646 g, 6.3 mmol) in THF (12.8 mL) was added DIAD (1.269 g, 6.3 mmol) at 0 °C. The mixture was stirred for 30 h at rt. Solvent was removed *in vacuo*. Chromatography with 4:1 Hex:EtOAc gave 2.001 g (80% yield) of a white solid.

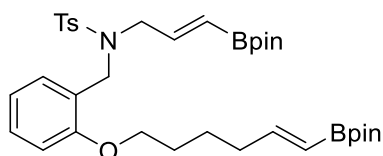
**R<sub>f</sub>** = 0.260 (4:1 Hex:EtOAc);

<sup>1</sup>H NMR (400 MHz, CDCl<sub>3</sub>, ppm) δ 7.80 (d, *J* = 8.4 Hz, 2 H), 7.40 (dd, *J* = 7.4, 1.4 Hz, 1 H), 7.31 (d, *J* = 8.0 Hz, 2 H), 7.25 (td, *J* = 7.8, 1.6 Hz, 1H), 6.93 (td, *J* = 8.0, 0.9 Hz, 1 H), 6.84 (d, *J* = 8.0 Hz, 1 H), 4.45 (s, 2 H), 4.01 (d, *J* = 2.4 Hz, 2 H), 3.98 (t, *J* = 6.0 Hz, 2 H), 2.44 (s, 3 H), 2.26 (td, *J* = 8.4, 2.7 Hz, 2 H), 2.00 (t, *J* = 2.4 Hz, 1 H), 1.95-1.88 (m, 2 H), 1.93 (t, *J* = 2.6 Hz, 1 H), 1.73 (p, *J* = 5.5 Hz);

$^{13}\text{C}$  NMR (100 MHz,  $\text{CDCl}_3$ , ppm)  $\delta$  157.1, 143.4, 136.4, 130.2, 129.5, 129.2, 127.9, 123.5, 120.6, 111.29, 84.2, 77.0, 73.7, 68.7, 67.5, 44.5, 36.3, 28.3, 25.1, 21.6, 18.2;

IR (neat, ATR): 3305, 3018, 2948, 2871, 2115, 1600, 1493, 1455, 1347, 1215, 1159, 1092, 896, 745;

HRMS (ES): calcd  $[\text{M}+\text{Na}]^+$  ( $\text{C}_{23}\text{H}_{25}\text{NO}_3\text{SNa}$ ) 418.1453, found 418.1456.



**4-methyl-N-((E)-3-(4,4,5,5-tetramethyl-1,3,2-dioxaborolan-2-yl)allyl)-N-(2-(((I)-6-(4,4,5,5-tetramethyl-1,3,2-dioxaborolan-2-yl)hex-5-en-1-yl)oxy)benzyl)benzenesulfonamide (2-7)**

A flame dried 25 mL round bottom flask was charged with **2-6** (1.322 g, 3.3 mmol), and flushed with nitrogen for 10 min. Pinacolborane (1.94 mL, 13.4 mmol),  $\text{NEt}_3$  (90  $\mu\text{L}$ , 0.7 mmol), and DCM (10 mL) were added via syringe to the flask and stirred at 0  $^\circ\text{C}$  for 5 min. The mixture was transferred via a cannula to another round bottom flask containing  $\text{Cp}_2\text{ZrHCl}$  (171 mg, 0.7 mmol). The reaction stirred for 64 h under reflux. The solvent was removed *in vacuo*. Chromatography with 5:1 petroleum ether/EtOAc afforded 1.226 g (57% yield) of a very viscous colorless oil.

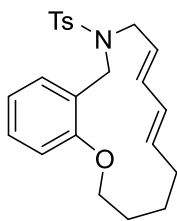
$^1\text{H}$  NMR (400 MHz,  $\text{CDCl}_3$ , ppm)  $\delta$  7.64 (d,  $J = 8.2$  Hz, 2 H), 7.31 (d,  $J = 7.6$  Hz, 1 H), 7.24 (d,  $J = 8.4$  Hz, 2 H), 7.17 (t,  $J = 7.8$  Hz, 1 H), 6.87 (t,  $J = 7.4$  Hz, 1 H), 6.73 (d,  $J = 8.1$  Hz, 1 H), 6.61 (dt,  $J = 18.0, 6.4$  Hz, 1 H), 6.33 (dt,  $J = 18.0, 5.6$  Hz, 1 H), 5.44 (d,  $J = 18.0$  Hz, 1H), 5.38 (d,  $J = 17.6$  Hz, 1 H), 4.39 (s, 2 H), 3.87-3.84 (m, 4 H), 2.40 (s, 3 H), 2.19 (dt,  $J = 6.8,$

6.8 Hz, 2 H), 1.74 (p,  $J = 7.0$  Hz, 2 H), 1.53 (p,  $J = 7.4$  Hz, 2 H), 1.26 (s, 12 H), 1.21 (s, 12 H);

$^{13}\text{C}$  NMR (100 MHz,  $\text{CDCl}_3$ , ppm)  $\delta$  156.9, 153.9, 147.3, 142.8, 137.6, 130.2, 129.5, 128.7, 127.3, 124.3, 120.4, 110.9, 83.2, 83.1, 67.6, 51.7, 45.8, 35.3, 28.7, 24.8, 24.7, 24.7, 21.5 (boron substituted carbons, absent);

IR (neat, ATR): 2978, 2929, 2867, 1638, 1494, 1359, 1321, 1266, 1241, 1142, 1092, 1142, 1092, 970, 734;

HRMS (ES): calcd  $[\text{M}+\text{Na}]^+$  ( $\text{C}_{35}\text{H}_{51}\text{B}_2\text{NO}_7\text{SNa}$ ) 674.3483, found 674.3463.



**(6E,8E)-11-tosyl-3,4,5,10,11,12-hexahydro-2H-benzo[b][1]oxa[5]azacyclotetradecine (2-8)**

A flame dried 250 mL flask was charged with  $\text{Pd}(\text{PPh}_3)_2\text{Cl}_2$  (21 mg, 0.031 mmol) and flushed with nitrogen for 10 min. Freshly distilled MeOH (160 mL), chloroacetone (0.24 mL, 3.1 mmol), **2-7** (200 mg, 0.307 mmol), and aq 2 M  $\text{K}_2\text{CO}_3$  (0.77 mL, 1.5 mmol), were subsequently added and the reaction was stirred 16 h. Upon completion, MeOH was removed *in vacuo*. The product was extracted with  $\text{Et}_2\text{O}$ , washed with water and brine, and dried over  $\text{MgSO}_4$ . Chromatography with 9:1 Hex:EtOAc afforded 81 mg (66% yield) of a clear colorless oil.

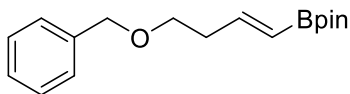
$^1\text{H}$  NMR (400 MHz,  $\text{CDCl}_3$ , ppm)  $\delta$  7.79 (d,  $J = 8.24$  Hz, 2 H), 7.48 (dd,  $J = 7.6, 1.6$  Hz, 1 H), 7.36 (d,  $J = 8.4$  Hz, 2 H), 7.20 (td,  $J = 8.6, 1.3$  Hz, 1 H), 6.97 (t,  $J = 7.4$  Hz, 1 H), 6.80 (d,  $J = 8.40$  Hz, 1 H), 5.92 (dd,  $J = 15.0, 10.6$  Hz, 1 H), 5.60 (dd,  $J = 15.0, 10.6$  Hz, 1 H), 5.41

(dt,  $J = 15.2, 7.7$  Hz, 1 H), 4.89 (dt,  $J = 15.2, 7.5$  Hz, 1 H), 4.38 (s, 2H), 3.79 (d,  $J = 10.8$  Hz, 2 H), 3.71 (t,  $J = 7.0$  Hz, 2 H), 2.47 (s, 3 H), 2.16 (dt,  $J = 7.2, 6.9$  Hz, 2 H), 1.76 (p,  $J = 6.0$  Hz, 2 H), 1.50 (p,  $J = 5.8$  Hz, 2 H);

$^{13}\text{C NMR}$  (100 MHz,  $\text{CDCl}_3$ , ppm)  $\delta$  156.7, 143.1, 137.7, 136.7, 133.0, 132.0, 129.8, 129.6, 128.2, 127.1, 123.5, 123.3, 121.0, 112.5, 69.8, 48.2, 41.4, 32.7, 25.3, 24.3, 21.6;

**IR** (neat, ATR): 2925, 2858, 1684, 1600, 1455, 1336, 1240, 1155, 1018, 753, 655;

**HRMS** (ES): calcd  $[\text{M}+\text{Na}]^+$  ( $\text{C}_{23}\text{H}_{27}\text{NO}_3\text{SNa}$ ) 420.1609, found 420.1599.

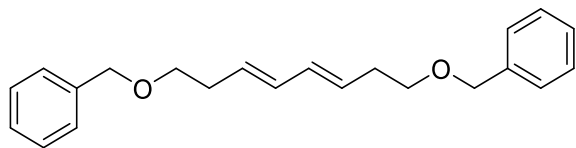


**(E)-2-(4-(benzyloxy)but-1-en-1-yl)-4,4,5,5-tetramethyl-1,3,2-dioxaborolane (2-9)**

A flame dried round bottom flask was charged with  $\text{Cp}_2\text{ZrHCl}$  (464 mg, 1.8 mmol) under a nitrogen atmosphere.  $\text{NEt}_3$  (0.34 mL, 2.4 mmol) was added, followed by **2-13** (2.000 g, 12.4 mmol), then pinacolborane (5.2 mL, 36.1 mmol). The mixture was heated at 60 °C and stirred for 60 h. The reaction was cooled to rt and passed through a silica plug with EtOAc. The solvent was removed *in vacuo*. Chromatography with 15:1 petroleum ether/EtOAc gave 1.734 g (54% yield) of the known<sup>25</sup> clear light yellow oil.

$^1\text{H NMR}$  (400 MHz,  $\text{CDCl}_3$ , ppm)  $\delta$  7.34-7.27 (m, 5H), 6.63 (dt,  $J = 18.0, 6.4$  Hz, 1H), 5.53 (dt,  $J = 18.0, 1.5$  Hz, 1H), 4.51 (s, 2H), 3.56 (t,  $J = 6.9$  Hz, 2H), 2.49 (qd,  $J = 6.7, 1.49$  Hz, 2H), 1.26 (s, 12H).





**(3E,5E)-1,8-bis(benzyloxy)octa-3,5-diene (2-10)**

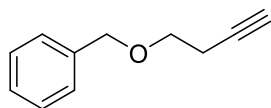
This compound was prepared according to General Procedure A. PdCl<sub>2</sub>(dppp) (6 mg, 0.0097 mmol), DMF (4.9 mL), **2-9** (140 mg, 0.486 mmol), and Cs<sub>2</sub>CO<sub>3</sub> (317 mg, 0.972 mmol) were combined to give 76 mg (88%) of the known<sup>26</sup> clear light yellow oil after column chromatography with 19:1 petroleum ether/EtOAc.

**<sup>1</sup>H NMR** (400 MHz, CDCl<sub>3</sub>, ppm) δ 7.38-7.35 (m, 8H), 7.32-7.27 (m, 2H), 6.14-6.06 (m, 2H), 5.68-5.57 (m, 2H), 4.53 (s, 4H), 3.52 (t, *J* = 6.8 Hz, 4H), 2.41 (q, *J* = 6.7 Hz, 4H);

**<sup>13</sup>C NMR** (100 MHz, CDCl<sub>3</sub>, ppm) δ 138.5, 132.0, 128.9, 128.4, 127.7, 127.6, 72.9, 69.9, 33.1;

**IR** (neat, ATR): 3063, 3027, 2928, 2855, 2789, 1652, 1496, 1454, 1363, 1204, 1100, 989, 737;

**HRMS** (DART): calcd [M+H]<sup>+</sup> (C<sub>23</sub>H<sub>27</sub>O<sub>2</sub>) 323.20056, found 323.19958.



**((but-3-yn-1-yloxy)methyl)benzene (2-13)**

To a flame dried flask was added NaH (60% dispersion on mineral oil, 0.558 g, 13.7 mmol). The flask was flushed with nitrogen, then THF (18 mL) was added and the mixture was cooled to 0 °C. But-3-yn-1-ol (0.95 mL, 12.5 mmol) was added dropwise and stirred 15 min at 0 °C. The reaction was warmed to rt, then benzyl bromide (1.63 mL, 13.7 mmol) was added dropwise. The reaction was stirred 3 days, then quenched with water. THF was removed *in vacuo*. The aqueous

layer was extracted with Et<sub>2</sub>O and dried with MgSO<sub>4</sub>. The solvent was removed *in vacuo*. Column chromatography with 30:1 Hex:EtOAc gave 1.248 g (62% yield) of the known<sup>27</sup> clear light yellow oil.

<sup>1</sup>H NMR (400 MHz, CDCl<sub>3</sub>, ppm) δ 7.36-7.28 (m, 5H), 4.57 (s, 2H), 3.61 (t, *J* = 7.0 Hz, 2H), 2.51 (td, *J* = 7.0, 2.6 Hz, 2H), 2.00 (t, *J* = 2.7 Hz, 1H).

## 2.6 References and Notes

- (1) *Cross-Coupling Reactions: A Practical Guide*; Miyaura, N., Ed.; Springer: Berlin, 2002.
- (2) *Handbook of Organopalladium Chemistry for Organic Synthesis*; Negishi, E., Ed.; John Wiley & Sons, Inc: New York, 2002.
- (3) Miyaura, N.; Suzuki, A. *Chem. Rev.* **1995**, *95*, 2457.
- (4) Zhou, Z.; Hu, Q.; Du, Z.; Xue, J.; Zhang, S.; Xie, Y. *Synth. React. Inorg. Met. -Org. Chem.* **2012**, *42*, 940.
- (5) Yamamoto, Y.; Suzuki, R.; Hattori, K.; Nishiyama, H. *Synlett* **2006**, *7*, 1027.
- (6) Wong, M. S.; Zhang, X. L. *Tetrahedron Lett.* **2001**, *42*, 4087.
- (7) Parrish, J. P.; Jung, Y. C.; Floyd, R. J.; Jung, K. W. *Tetrahedron Lett.* **2002**, *43*, 7899.
- (8) Yamamoto, Y. *Synlett* **2007**, *12*, 1913.
- (9) Yoshida, H.; Yamaro, Y.; Ohshita, J.; Kunai, A. *Tetrahedron Lett.* **2003**, *44*, 1541.
- (10) Punna, S.; Díaz, D. D.; Finn, M. G. *Synlett* **2004**, *13*.
- (11) Jasti, R.; Bhattacharjee, J.; Neaton, J. B.; Bertozzi, C. R. *J. Am. Chem. Soc.* **2008**, *130*, 17646.

- (12) Evans, P. J.; Darzi, E. R.; Jasti, R. *Nat. Chem.* **2014**, *6*, 404.
- (13) Darzi, E. R.; White, B. M.; Loventhal, L. K.; Zakharov, L. N.; Jasti, R. *J. Am. Chem. Soc.* **2017**, *139*, 3106.
- (14) Iafe, R. G.; Chan, D. G.; Kuo, J. L.; Boon, B. A.; Faizi, D. J.; Saga, T.; Turner, J. W.; Merlic, C. A. *Org. Lett.* **2012**, *14*, 4282.
- (15) Iafe, R. G. Palladium(II)-Catalyzed Reactions of Pinacol Vinylboronates: New Cyclization Strategies to Prepare Polyene Macrocycles and Transannular Diels-Alder Cycloaddition Substrates. Ph.D. Dissertation, University of California, Los Angeles, CA, 2011.
- (16) Wang, Y. D.; Kimball, G.; Prashad, A. S.; Wang, Y. *Tetrahedron Lett.* **2005**, *46*, 8777.
- (17) Villalta, O. A. Selectivity in Palladium Transmetalation Reactions and Palladium(II)-Catalyzed Reactions of Pinacol Vinylboronates with Oxygen Reoxidant. Ph.D. Dissertation, University of California, Los Angeles, CA, 2011.
- (18) Cox, P. A.; Leach, A. G.; Campbell, A. D.; Lloyd-Jones, G. C. *J. Am. Chem. Soc.* **2016**, *138*, 9145.
- (19) Ainley, A. D.; Challenger, F. *J. Chem. Soc.* **1930**, 2171.
- (20) Brown, H. C.; Zweifel, G. *J. Am. Chem. Soc.* **1959**, *81*, 247.
- (21) Adamo, C.; Amatore, C.; Ciofini, I.; Jutand, A.; Lakmini, H. *J. Am. Chem. Soc.* **2006**, *128*, 6829.
- (22) Lakmini, H.; Ciofini, I.; Jutand, A.; Amatore, C.; Adamo, C. *J. Phys. Chem. A* **2008**, *112*, 12896.

- (23) Davison, E. C.; Fox, M. E.; Holmes, A. B.; Roughley, S. D.; Smith, C. J.; Williams, G. M.; Davies, J. E.; Raithby, P. R.; Adams, J. P.; Forbes, I. T.; Press, N. J.; Thompson, M. J. *J. Chem. Soc. Perkin Trans. 1* **2002**, 1494.
- (24) Kavanagh, Y.; Chaney, C. M.; Muldoon, J.; Evans, P. *J. Org. Chem.* **2008**, *73*, 8601.
- (25) Winternheimer, D. J.; Merlic, C. A. *Org. Lett.* **2010**, *12*, 2508.
- (26) Kanemoto, S.; Matsubara, S.; Oshima, K.; Utimoto, K.; Nozaki, H. *Chem. Lett.* **1987**, *16*, 5.
- (27) Citron, C. A.; Dickschat, J. S. *Org. Biomol. Chem.* **2013**, *11*, 7447.

## Chapter 3

### Using Ring Strain to Control $4\pi$ -Electrocyclization Reactions: Torquoselectivity in Ring-Closing of Medium-Ring Dienes and Ring-Opening of Bicyclic Cyclobutenes

#### 3.1. Abstract

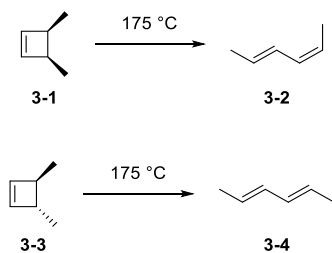
Syntheses of strained cyclic dienes were accomplished via palladium(II)-catalyzed oxidative cyclizations of terminal bis(vinylboronate esters). The reactions generated strained (*E,E*)-1,3-dienes that underwent spontaneous  $4\pi$ -electrocyclizations to form bicyclic cyclobutenes. Formation of the cyclobutenes is driven by strain in the medium-ring (*E,E*)-1,3-diene intermediates. Thermal ring openings of the cyclobutenes give (*Z,Z*)-1,3-diene products, again for thermodynamic reasons. These results are in contrast with typical acyclic *trans*-3,4-dialkyl cyclobutenes, which favor outward torquoselective ring-openings to give (*E,E*)-1,3-dienes. DFT calculations verified the thermodynamic versus kinetic control of the reactions and kinetic studies are in excellent agreement with the calculated energy changes.

#### 3.2. Introduction

Strained ring systems have captivated organic chemists due to their intriguing chemical structures as well as the synthetic challenges their preparation requires.<sup>1</sup> A particularly challenging aspect of their synthesis is reflected in their inherent reactivity due to their ring strain. For example, *trans*-cycloheptene, first generated by the elimination of cyclic dithiocarbamates and trapped by diphenylisobenzofuran,<sup>2</sup> is highly unstable, which has precluded its use in synthesis other than as a reactive intermediate. Consequently, *trans*-cyclooctene is the smallest cyclic *trans*-alkene isolable at room temperature.<sup>3</sup> Similarly, bridgehead alkenes in bicyclic ring structures are unstable in small ring sizes. Typically, the ring containing the bridgehead *trans*-alkene must be 8-membered

or larger, whereas 7-membered rings and smaller are useful primarily as reactive intermediates. This generalization was established from a series of empirical observations which would later become known as Bredt's rule.<sup>4,5</sup> An extension of this research interest is the study of strained monocyclic dienes, the subject of this study.

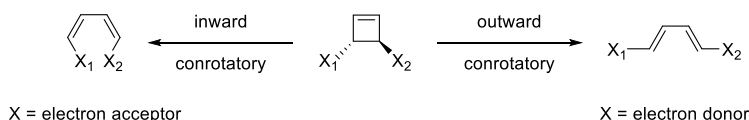
Research interest in strained cyclic dienes stems from work on electrocyclic ring opening of monocyclic cyclobutenes. Early work by Vogel provided the first examples of cyclobutene ring opening to linear dienes.<sup>6,7</sup> Winter and Criegee later extended this method to *cis*- and *trans*-cyclobutenes which underwent clean electrocyclic ring opening to form linear dienes.<sup>8,9</sup> In these examples, *cis*-3,4-disubstituted cyclobutenes ring open to (*E,Z*)-dienes, whereas their *trans*-isomers open to (*E,E*)-dienes (Scheme 3.1).<sup>10</sup> Two key observations could be made on the basis of these cyclobutene ring openings: 1) diene products were formed stereospecifically and 2) substituents at the 3-, and 4-positions appear to rotate in a conrotatory manner. These observations were later formalized in what later became known as the Woodward-Hoffman rules.<sup>11,12</sup>



**Scheme 3.1. Electrocyclic ring opening of *cis*- and *trans*-3,4-dimethyl substituted cyclobutenes.**

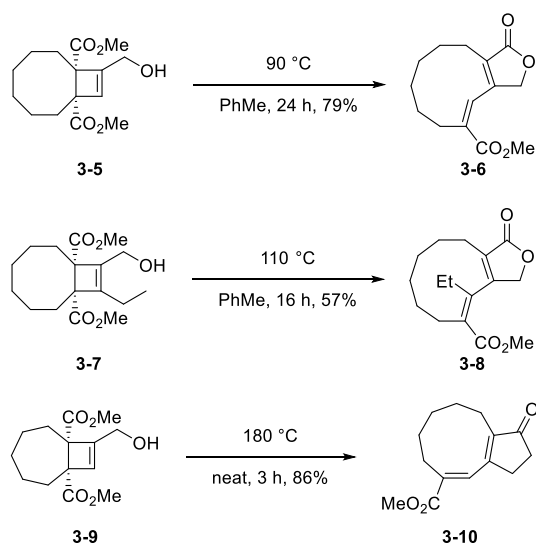
Computational investigations by the Houk group established the theory of torquoselectivity in electrocyclic ring opening of cyclobutenes, where electron withdrawing substituents (X = CHO, CO<sub>2</sub>R, CN, NO<sub>2</sub>, etc.) preferentially undergo outward rotation, whereas electron donating

substituents (OR, NR<sub>2</sub>, halogen, alkyl, etc.) preferentially undergo inward rotation (Scheme 3.2).<sup>13,14</sup> In each case, substituents rotate in a conrotatory manner. In the case of 3,4-disubstituted cyclobutenes, outward rotation of electron donating group gives the (*E,E*)-diene products. On the other hand, electron accepting substituents preferentially rotate inward to give (*Z,Z*)-diene products.



### Scheme 3.2. Preferential modes of cyclobutene ring openings.

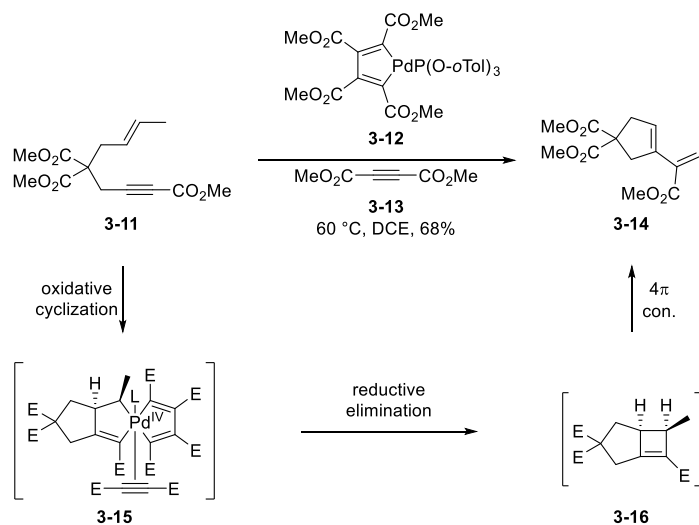
*cis*-Bicyclic 3,4-disubstituted cyclobutenes would be expected to undergo conrotatory electrocyclic ring opening to give *cis,trans*-diene configurations. The Booker-Milburn group demonstrated that *cis*-3,4-disubstituted bicyclic cyclobutenes undergo conrotatory electrocyclic ring openings to give cyclic *cis,trans*-dienes (**3-6** and **3-8**, Scheme 3.3).<sup>15</sup> Similar bicyclic cyclobutenes with fused rings smaller than 8-members open in a conrotatory manner to give *cis,trans*-dienes, but quickly undergo 1,5-hydride shifts to form the corresponding *cis,cis*-diene products. The conversion of cyclobutene **3-9** to **3-10** is a representative example. In each case, the appended alcohol and its proximal ester lactonize after the electrocyclic ring opening reaction.



**Scheme 3.3. Electrocyclic ring opening of highly substituted bicyclic cyclobutenes.**

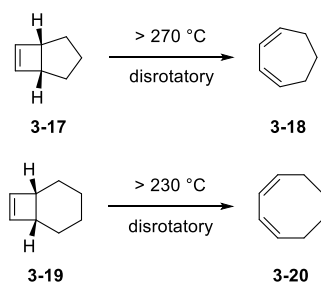
A palladium-catalyzed oxidative cyclization of 1,6-enynes lead to unstable cyclobutenes that undergo electrocyclic ring openings *in situ*. Treatment of *trans*-1,6-enyne **3-11** with palladacyclobutadiene complex **3-12** in the presence of dimethyl acetylene dicarboxylate **3-13**, DMAD) gave diene **3-14** (Scheme 3.4).<sup>16</sup> Mechanistic studies suggest the unusual rearrangement starts by a Pd(II)-catalyzed oxidative cyclization of **3-11** to form spirocyclic palladacycle intermediate **3-15**, which undergoes reductive elimination from Pd(IV) to give bicyclic cyclobutene **3-16**. The strained anti-Bredt olefin<sup>4,5</sup> in cyclobutene **3-16** renders it unstable, giving rise to a  $4\pi$ -conrotatory electrocyclic ring opening resulting in the formation of diene **3-14**.





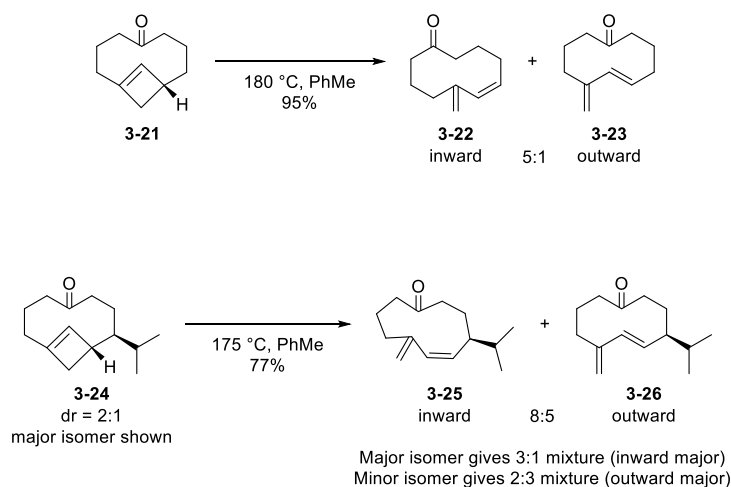
**Scheme 3.4. Palladium-catalyzed synthesis of unstable cyclobutenes from 1,6-enynes and their electrocyclic ring opening.**

Electrocyclic ring opening of small *cis*-bicyclic cyclobutenes occurs via an unusual disrotatory ring opening. Rather than undergo conrotatory electrocyclic ring opening to give highly strained (*E,Z*)-cycloheptadiene, bicyclic cyclobutene **3-17** opens to (*Z,Z*)-cycloheptadiene **3-18** via a high energy disrotatory pathway (Scheme 3.5).<sup>17</sup> Bicyclic cyclobutene **3-19** ring opens in a similar manner to give (*Z,Z*)-cyclooctadiene **3-20**.<sup>18</sup> These examples highlight that given sufficient ring strain in the diene product, the disrotatory pathway may become favored over the conrotatory pathway.



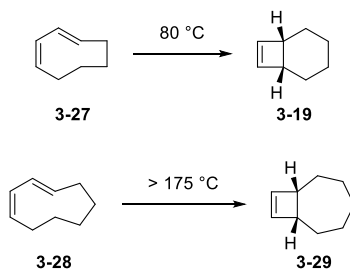
**Scheme 3.5. Disrotatory electrocyclic ring opening of bicyclic cyclobutenes.**

Though technically not a violation of torquoselectivity, high energy ring opening pathways with inward rotation of electron donating alkyl groups may occur to form products with less ring strain. Schreiber demonstrated that 1,3-disubstituted cyclobutene **3-21**, a model substrate for the total synthesis of periplanone B, underwent electrocyclic ring opening to give a 5:1 mixture of products in favor of inward alkyl group rotation (Scheme 3.6).<sup>19</sup> Electrocyclic ring opening via the outward rotation pathway was likely favored kinetically to give **3-23**, but due to high temperature reaction conditions, equilibration to the thermodynamic product **3-22** was favored. Electrocyclic ring opening of a diastereomeric mixture of bicyclic cyclobutenes (**3-24**) displayed a similar thermodynamically favored inward alkyl group rotation to give **3-25** as the major product in Schreiber's total synthesis of periplanone B.<sup>20</sup>



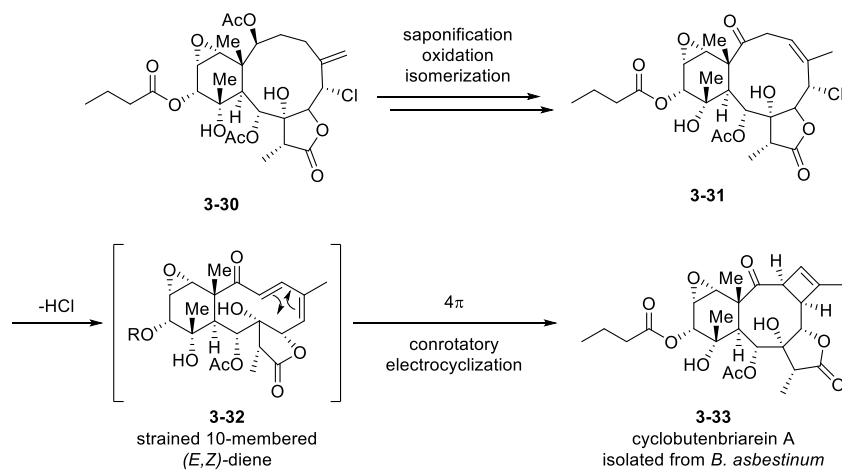
**Scheme 3.6. Electrocyclic ring opening of bicyclic cyclobutenes with inward rotation of alkyl groups.**

On the other hand, cyclic dienes with significant ring strain undergo electrocyclic ring closure to bicyclic cyclobutenes upon heating. For example, (*E,Z*)-1,3-cyclooctadiene **3-27** and (*E,Z*)-1,3-cyclononadiene **3-28** undergo electrocyclic ring-closure to *cis*-bicyclic cyclobutenes, yet only at temperatures above 80 °C and 175 °C, respectively (Scheme 3.7).<sup>21</sup> Evidently the starting cyclic dienes are higher in energy than bicyclic cyclobutenes. This is opposite what would be expected as electrocyclic ring openings of simple monocyclic cyclobutene ring openings give linear dienes upon heating (Scheme 3.1).



**Scheme 3.7. Electrocyclic ring closure of strained cyclic dienes to bicyclic cyclobutenes.**

The biosynthesis of cyclobutenbriarein A,<sup>22</sup> a natural product with a fused bicyclic cyclobutene core isolated from *B. asbestinum*, is proposed to proceed via a  $4\pi$ -electrocyclization of a macrocyclic (*E,Z*)-1,3-diene intermediate (Scheme 3.8).<sup>23</sup> Intermediate **3-30**, also isolable from *B. asbestinum*, is proposed to undergo saponification, followed by oxidation to the ketone, and double bond isomerization. Loss of hydrogen chloride gives the strained cyclic diene **3-32** which is proposed to undergo a  $4\pi$ -conrotatory electrocyclization to cyclobutenbriarein A (**3-33**). Note that the electrocyclization is also torquoselective. This is reminiscent of the electrocyclic ring closure of strained cyclic dienes **3-27** and **3-28** which undergo electrocyclization to bicyclic cyclobutenes (Scheme 3.7). Clearly, the barrier to electrocyclization must be substantially reduced for this natural product to be biosynthesized under ambient conditions.



### Scheme 3.8. Electrocyclic ring closure in the biosynthesis of cyclobutenbriarein A.

From these examples and further investigation into the literature, it became clear there are four types of 1,3-diene free-energy profiles for thermal interconversion of isomeric dienes via cyclobutene intermediates by conrotatory electrocyclizations (Figure 3.1). Figure 3.1a is typical of acyclic dienes, where the (*E,E*)-diene is lowest in energy, followed by the (*Z,Z*)-diene, and the cyclobutene is highest.<sup>6–10,14,18,24–27</sup> Macrocyclic (*E,Z*)-dienes typically have similar free-energy profiles (Figure 3.1b) where the cyclobutene is higher in energy than each diene isomer.<sup>15,17,28</sup> Computational studies have verified this type of free-energy profile.<sup>28,29</sup> An energy profile as shown in Figure 3.1c is known for select symmetric cyclic (*E,Z*)-dienes where cyclobutenes are lower in energy than the diene.<sup>21</sup> A fourth energy profile, where cyclic (*E,E*)-dienes are highest in energy (Figure 3.1d), followed by the cyclobutene, and finally the (*Z,Z*)-diene was unknown at the beginning of this work and is the subject of this study.

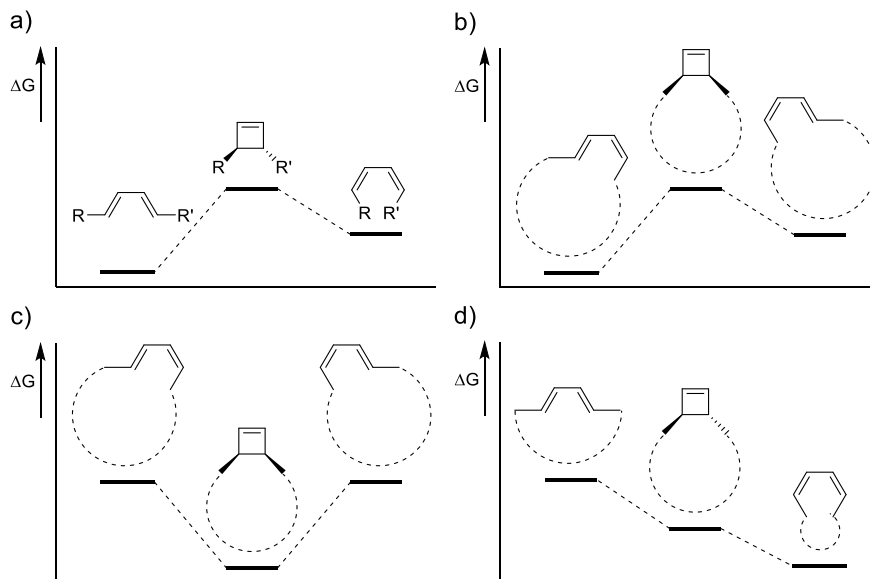
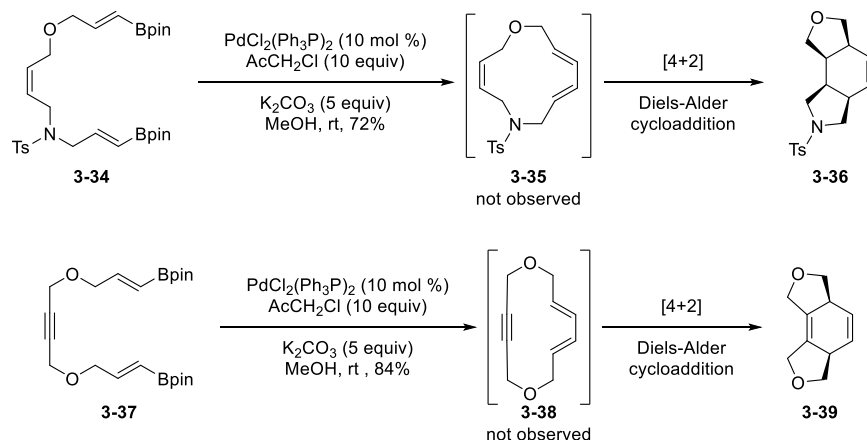


**Figure 3.1. Free-energy profiles of (a) acyclic dienes, (b) asymmetric macrocyclic (*E,Z*)-dienes, (c) symmetric strained cyclic (*E,Z*)-dienes, and (d) strained cyclic (*E,E*)-dienes.**

Members of the Merlic research group recently reported the synthesis of strained macrocyclic dienes that underwent room temperature transannular Diels-Alder (TADA) cycloaddition reactions (Scheme 3.9).<sup>30</sup> These TADA reactions were successful without activating substituents on the diene or dienophile allowing intermediates **3-35** and **3-38** to proceed directly to TADA products. Due to the large amount of ring strain, the intermediate trienes or dienynes were not able to be observed under the reactions conditions. Given the success of the palladium-catalyzed reaction conditions to generate strained cyclic trienes and dienynes which undergo the TADA reaction, we suspected these reaction conditions could be applied to the synthesis of strained cyclic dienes that could undergo electrocyclizations to bicyclic cyclobutenes. Furthermore, palladium catalysis has been applied to the synthesis of a variety of strained rings and natural products, as highlighted in Chapter 1. The electrocyclic ring closure of cyclic (*E,E*)-

1,3-dienes to bicyclic *trans*-cyclobutenes was unknown at the outset of this project (Figure 3.1d), and we began to explore this avenue of research.



**Scheme 3.9. Transannular Diels-Alder reactions of a strained triene and dienyne intermediates.**

### 3.3. Results and Discussion

We turned to calculations to quantify the relative strain in medium ring 1,3-dienes. Ring strain energies were calculated by my colleague Dr. Aaron Green<sup>31</sup> using homodesmotic reactions,<sup>32</sup> as strain energies of many cyclic compounds have previously been determined in this manner.<sup>33–35</sup> As shown in Figure 3.2, ring strain energies were calculated from the heat of dehydrogenation of the parent cycloalkane to form the 1,3-diene ring plus two equivalents of hydrogen, minus the heat of dehydrogenation of hexane to (*E,E*)-2,4-hexadiene and two equivalents of hydrogen. Ring strain energies were calculated for cyclic 1,3-dienes with (*E,E*)-, (*E,Z*)-, and (*Z,Z*)-double bond configurations in 9-, 10-, and 11-membered rings.

Several conclusions can be drawn from these calculated ring strain energies (Figure 3.2). Diene **3-40** is the most strained cyclic diene with a +46 kcal/mol ring strain energy, due to a (*E,E*)-

diene confined in a 9-membered ring. The least strained diene **3-47** has -5 kcal/mol strain energy, corresponding to (*Z,Z*)-double configuration in a 10-membered ring. For cyclic dienes with identical double bond configurations, strain energies decrease with increasing ring size, where 11-membered rings are less strained than 10-membered rings, and 9-membered rings are the most strained. For identical ring sizes, ring strain increases as the quantity of *trans*-double bonds increases, where (*Z,Z*)-dienes are the least strained, (*E,Z*)-dienes are higher in energy, and (*E,E*)-dienes are the most strained. These results suggested a broad range of ring strains would be accessible by modification of ring size and double bond configuration.

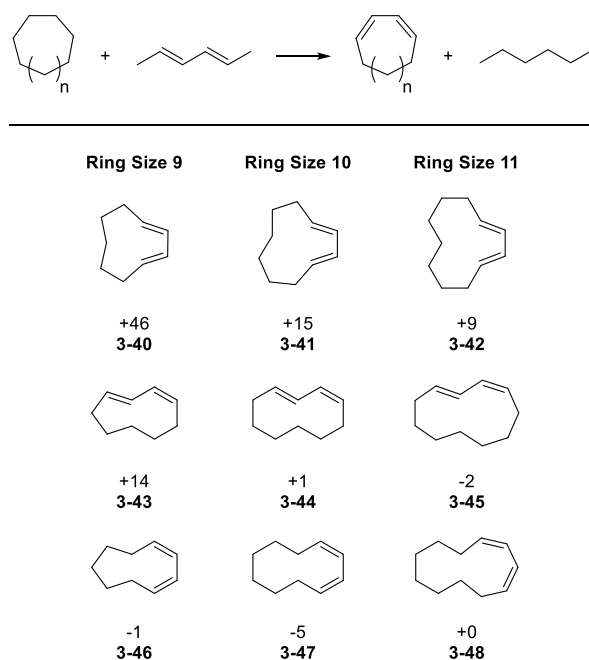
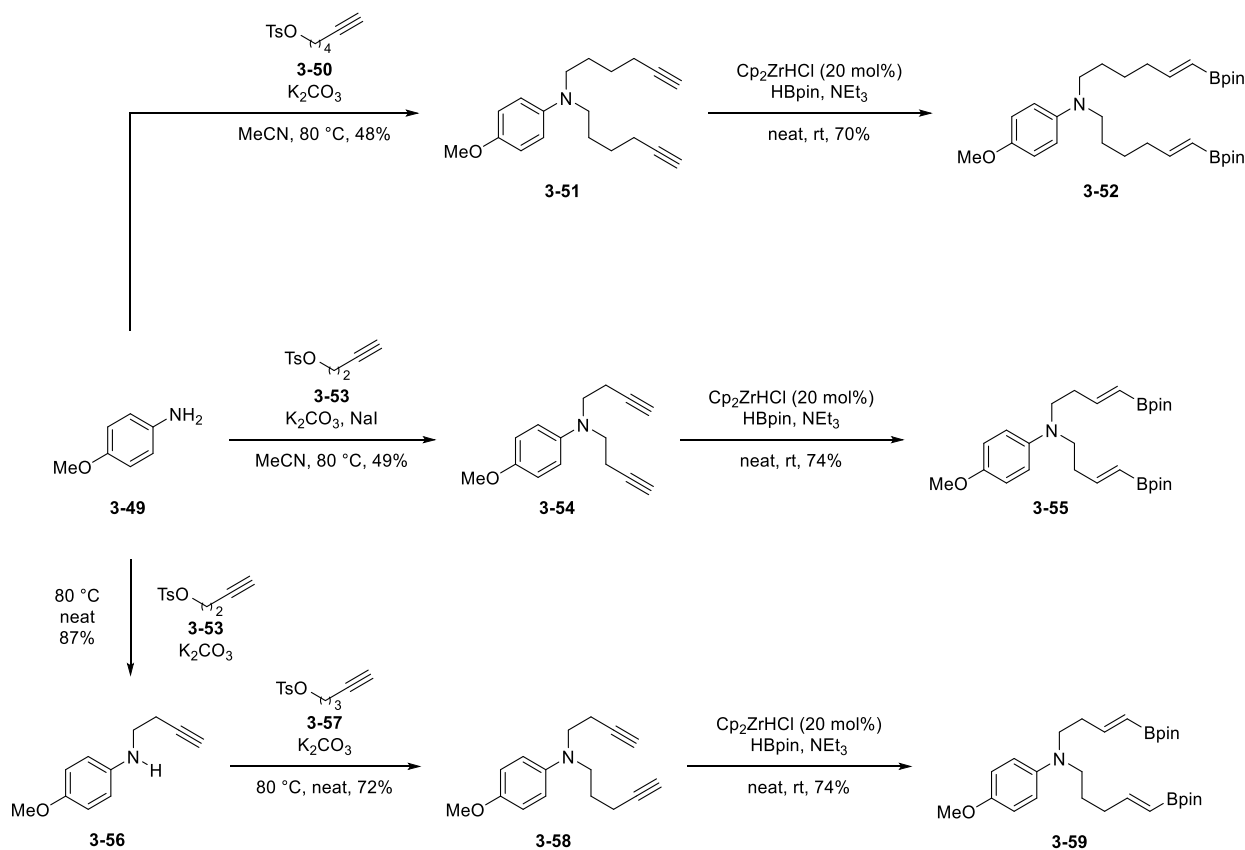


**Figure 3.2. Predicted strain energies (kcal/mol) of cyclic dienes. (Calculated at the M06/6-311++G(d,p)//B3LYP/6-31G(d) level of theory).**

Our experimental studies commenced with the synthesis of a series of bis(vinylboronate esters) with (*E,E*)- and (*E,Z*)-double bond configurations. The preparation of (*E,E*)-bis(vinylboronate esters) is shown in Scheme 3.10. Double alkylation of *p*-anisidine with tosylates

**3-50** or **3-53** gave bis(alkynes) **3-51** and **3-54**, which upon hydroboration catalyzed by Schwartz's reagent<sup>36</sup> gave symmetric (*E,E*)-bis(vinylboronate esters) **3-52** and **3-55**. Nonsymmetric (*E,E*)-bis(vinylboronate ester) **3-59** was prepared by sequential alkylation of *p*-anisidine by tosylates **3-53** and **3-57**, followed by double hydroboration.

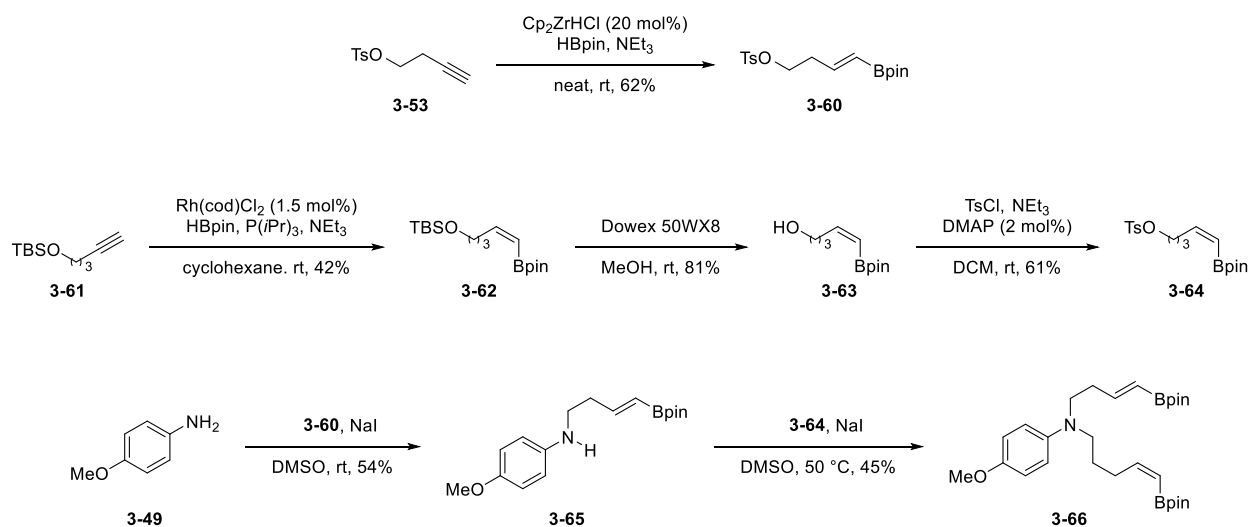


**Scheme 3.10.** Synthesis of (*E,E*)-bis(vinylboronate esters) **3-52**, **3-55**, and **3-59**.

A nonsymmetric (*E,Z*)-bis(vinylboronate ester) **3-66** was prepared by sequential alkylation of *p*-anisidine with different vinylboronate ester fragments (Scheme 3.11). The (*E*)-vinylboronate ester fragment **3-60** was easily prepared by the Schwartz-catalyzed hydroboration of tosylate **3-53**.<sup>36</sup> The (*Z*)-vinylboronate ester fragment **3-64** was prepared by the rhodium catalyzed *trans*-hydroboration of silyl ether **3-61**.<sup>37</sup> Mixtures of (*E*)- and (*Z*)-isomers were observed, requiring a challenging chromatographic separation to isolate **3-62** as a single isomer. Silyl group deprotection



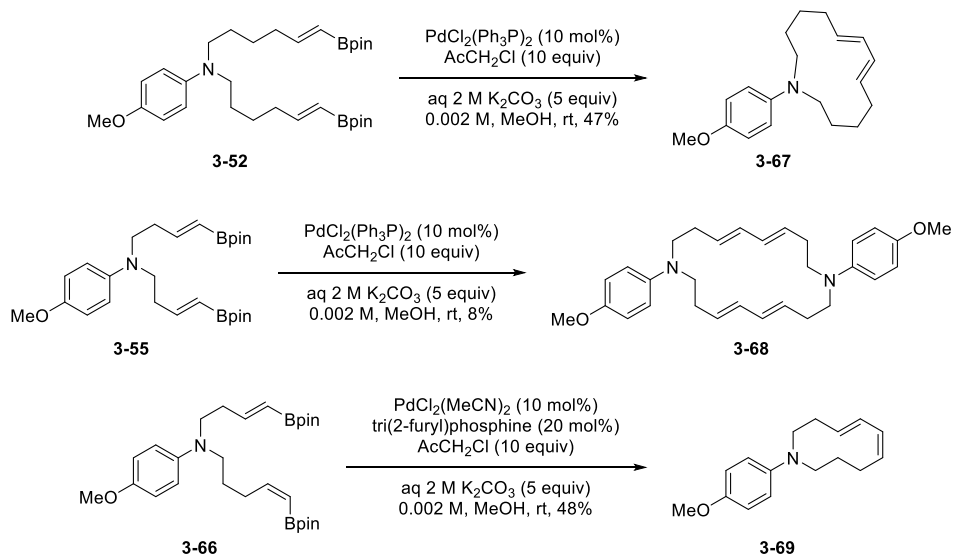
gave the free alcohol **3-63**, which was converted to tosylate **3-64**. Sequential alkylation of *p*-anisidine with vinylboronate fragments was successful in DMSO in the absence of base to prevent protodeboronation.<sup>38</sup> Alkylation of *p*-anisidine with the vinylboronate fragments starting with **3-60** gave the secondary amine **3-65**, which upon a second alkylation with **3-64** gave the nonsymmetric **3-66**.



**Scheme 3.11. Synthesis of (*E,Z*)-bis(vinylboronate ester) **3-66**.**

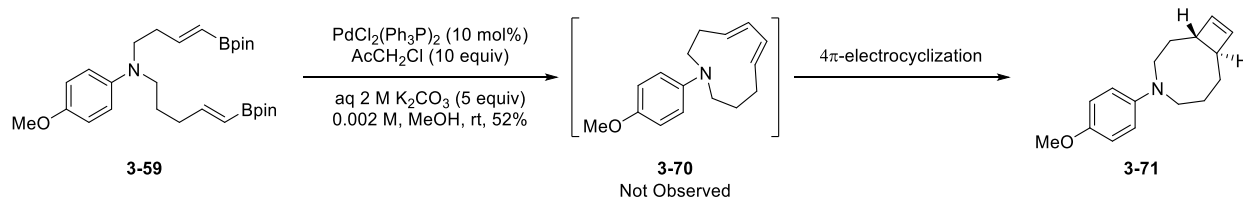
Oxidative cyclization experiments started with bis(vinylboronate esters) **3-52**, **3-55** and **3-66**. The unstrained macrocyclic 13-membered (*E,E*)-diene **3-67** was formed readily with our palladium(II)-catalyzed oxidative macrocyclization conditions, as previously discussed in Chapter 2.<sup>39</sup> In contrast, cyclization of **3-55** resulted in dimerization, giving cyclic tetraene dimer **3-68** in low yield. According to the strain energy calculations, the carbocyclic analogue for direct cyclization would give the medium-ring with +46 kcal/mol ring strain (**3-40**, Figure 3.2). Therefore, cyclization products with strain energies as high as +46 kcal/mol are likely too strained to form via palladium-catalyzed conditions. On the other hand, stable cyclic medium-ring diene **3-69** from the cyclization of bis(vinylboronate) ester **3-66** gave a lower limit for reactive rings, where

products with a strain energy of +1 kcal/mol or lower are expected to be quite stable (**3-44**, Figure 3.2).



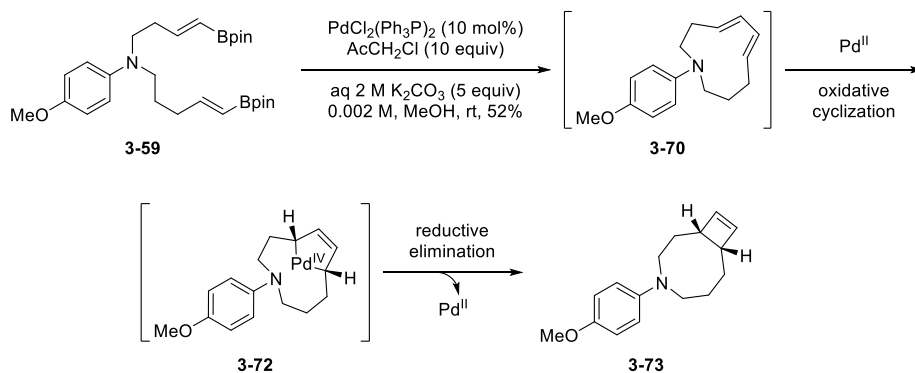
**Scheme 3.12. Macrocyclic and medium sized rings from cyclization of bis(vinylboronate esters) featuring *p*-anisidine linkers.**

Bis(vinylboronate) ester **3-59** was expected to generate a cyclic diene with strain in-between products derived from **3-55** and **3-66**. Its carbocyclic analog has ring strain of +15 kcal/mol (**3-41**, Figure 3.2) between that of rings derived from **3-55** and **3-66**, whose carbocyclic forms have ring strains corresponding to +46 and +1 kcal/mol, respectively (**3-40** and **3-44**, Figure 3.2). Surprisingly, cyclization gave bicyclic cyclobutene **3-71** rather than the cyclic (*E,E*)-1,3-diene **3-70** (Scheme 3.13). This was readily observed by  $^1\text{H}$  NMR where only two alkene proton signals at 5.98 and 6.08 ppm were observed. The structure was tentatively assigned as the *trans*-cyclobutene isomer, which would likely arise from a  $4\pi$ -electrocyclization of the strained intermediate diene **3-70**.



**Scheme 3.13. A *trans*-bicyclic cyclobutene from an oxidative cyclization/ $4\pi$ -electrocyclization pathway.**

The proposed mechanism of formation assumed that the *trans*-cyclobutene **3-71** arises from an ambient temperature electrocyclization, although due to the uncertain assignment of stereochemistry we could not exclude the possibility of a palladium-catalyzed reaction of **3-59** to give a *cis*-cyclobutene product. Trost and co-workers demonstrated that 1,6- and 1,7-enynes underwent Pd(II)-catalyzed oxidative cyclizations to form 5-membered palladacycle intermediates, which upon reductive elimination gave bicyclic cyclobutenes (Scheme 3.4).<sup>16,40</sup> Scheme 3.14 highlights the mechanistic steps of the possible Pd(II)-catalyzed formation of the hypothetical *cis*-cyclobutene **3-73**. Upon formation of the strained cyclic diene **3-70**, an oxidative cyclization by reaction with Pd(II) could give a palladacycle intermediate **3-72**, which upon reductive elimination would give the *cis*-cyclobutene **3-73**. Clearly determining the stereochemistry of the product would help eliminate one of these mechanistic pathways.



**Scheme 3.14. Mechanism of *cis*-cyclobutene formation by oxidative palladacycle formation and reductive elimination.**

Assignment of the cyclobutene stereochemistry was initially inconclusive due to conflicting literature data on the coupling constants of bridgehead hydrogens of 3,4-dialkyl substituted cyclobutenes. Experimental work by the Roberts group established that vicinal coupling within bridgehead cyclobutenes is larger for *trans*-cyclobutenes, measured at 4.35 Hz, compared to of 1.65 Hz for *cis*-cyclobutenes.<sup>41</sup> In contrast, computations at the B3LYP/cc-pVXZ level of theory by the Helgaker group showed that *cis*-cyclobutenes have larger coupling constants of 5.3 Hz, compared to 2.1 Hz the *trans*-cyclobutenes.<sup>42</sup> Further complicating the matter was difficulty in measuring the exact coupling constants of the cyclobutene bridgehead protons due to broad signals, although a coupling constant of 1-3 Hz was estimated based on each peak width. In search of a method to settle the disagreement in literature data, we turned to chemical shift<sup>43</sup> and coupling constant<sup>44</sup> calculations established by the Tantillo group, which have proven to be effective in the structural elucidation of natural products.<sup>44</sup>

The optimized structures of *cis*-**3-74** and *trans*-**3-74** as well as their relevant bridgehead proton coupling constants are shown in Figure 3.3, from calculations by Dr. Aaron Green.<sup>31</sup> Computations were carried out on the demethoxy structures of **3-71** to simplify calculations,

namely *cis*- and *trans*-**3-74**. The results of the calculations show that the *cis*-**3-74** has a larger geminal coupling constant of 4.1 Hz compared to the geminal coupling of *trans*-**3-74** of 2.1 Hz. The larger coupling constant in the *cis*-isomer is consistent with the nearly eclipsed bridgehead hydrogens which have a dihedral angle of 2°, in contrast to the larger 140° dihedral angle for the *trans*-isomer. In comparison to the estimated experimental coupling constant of 1-3 Hz, we propose that the cyclobutene isolated from cyclization of **3-59** was in fact the *trans*-isomer **3-71**. With this information in hand, we eliminated the possibility of cyclobutene formation directly catalyzed by Pd(II) to give *cis*-cyclobutene **3-73** (Scheme 3.14). Instead, these computational results suggest that the observed cyclobutene is the result of a 4 $\pi$ -electrocyclization from the strained cyclic diene **3-70** to give the *trans*-cyclobutene **3-71** (Scheme 3.13).

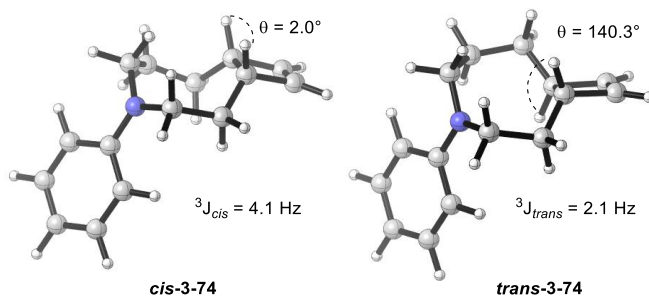
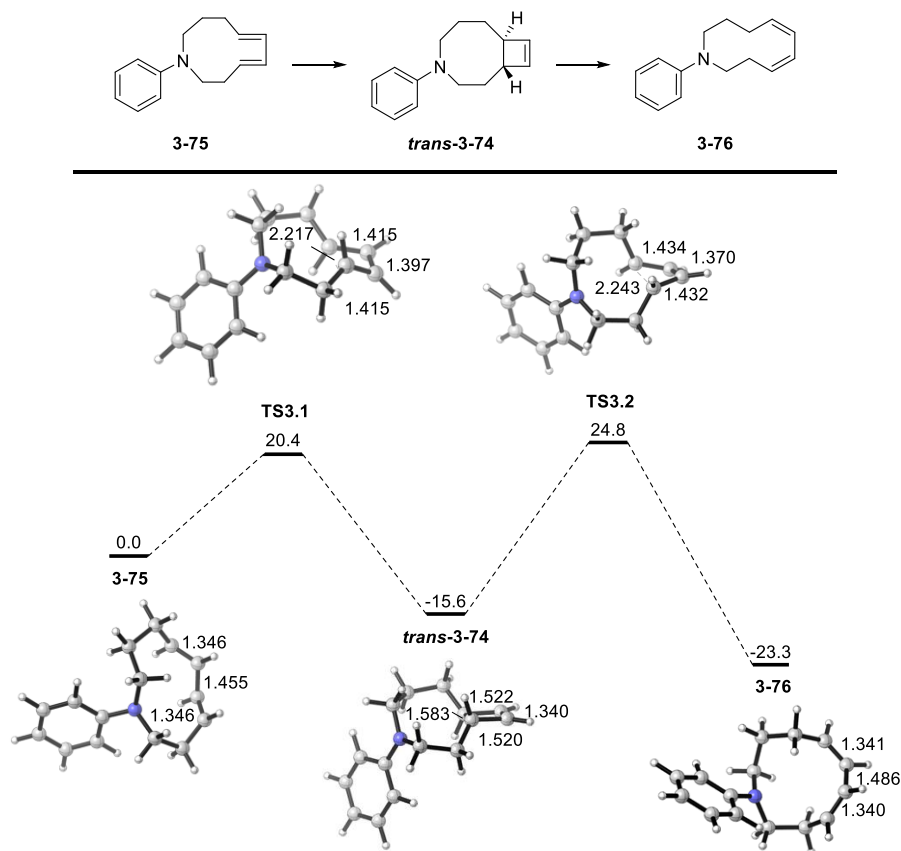


**Figure 3.3. Predicted lowest energy structures, dihedral angles and relevant coupling constants for *cis*-**3-74** and *trans*-**3-74** (calculated at the GIAO/B3LYP/6-31G(d) level of theory).**

The possibility that cyclobutene **3-71** arose from a 4 $\pi$ -electrocyclization of diene **3-59** intrigued us since the formation of cyclobutenes from strained cyclic dienes is an extremely rare process, known only for (*E,Z*)-1,3-cyclooctadiene and (*E,Z*)-1,3-cyclononadiene, **3-27** and **3-28**, which undergo electrocyclic ring-closure to *cis*-bicyclic cyclobutenes (Scheme 3.7). Computations from Dr. Aaron Green helped model the relative energy levels of dienes **3-75** and **3-76** and their

transitions states from electrocyclic ring opening/closing pathways.<sup>31</sup> The free-energy profile for electrocyclic ring closure of (*E,E*)-diene **3-75** to cyclobutene *trans*-**3-74** and electrocyclic ring opening to give (*Z,Z*)-diene **3-76** is shown in Scheme 3.15. Of the three isomers, the (*E,E*)-diene **3-75** is highest in energy, 15.6 kcal/mol higher in energy than the cyclobutene *trans*-**3-74**, and 23.3 kcal/mol higher in energy than (*Z,Z*)-diene **3-76**. Electrocyclic ring closure from (*E,E*)-diene **3-75** proceeds via transition state **TS3.1** with an activation barrier of only +20.4 kcal/mol. This low activation energy barrier explains why (*E,E*)-diene **3-70** was not observed as an isolable intermediate in the formation of **3-71**.

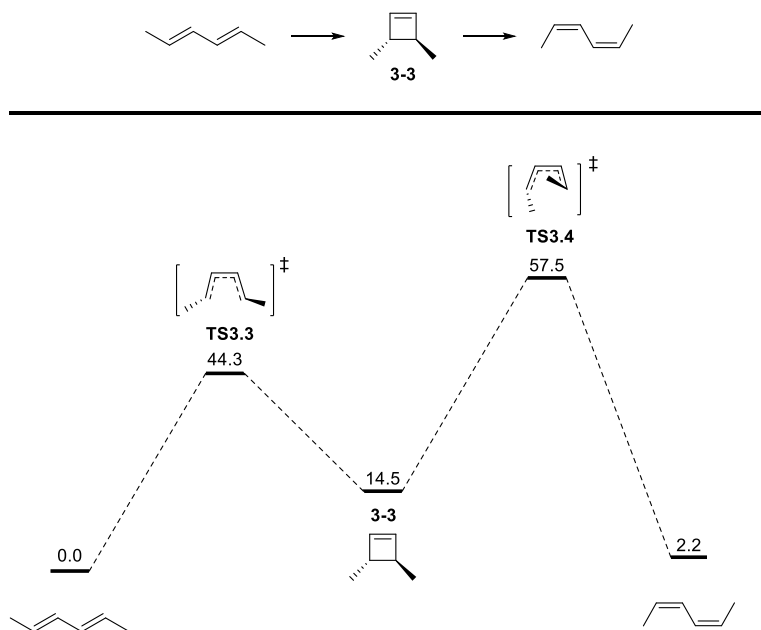


**Scheme 3.15.** Computed free-energy surface (gas phase; 298K) for electrocyclic ring-closure of (*E,E*)-diene **3-75** to give *trans*-**3-74** and ring-opening to yield (*Z,Z*)-diene **3-76** (calculated at the M06/6-311++G(d,p)//B3LYP/6-31G(d) level of theory).

The free-energy profile revealed that electrocyclic ring opening from cyclobutene *trans*-**3-74** may occur via high energy transition states **TS3.1** or **TS3.2**. Activation energy barriers of 36.0 and 40.4 kcal/mol for **TS3.1** and **TS3.2** explain why cyclobutene **3-71** was isolable at room temperature. However, given sufficient energy, ring opening by the lower energy **TS3.1** is expected to be kinetically favored, leading to the reversible formation of the (*E,E*)-diene **3-74**. On the other hand, ring opening via the higher energy **TS3.2** leads to the thermodynamic (*Z,Z*)-diene product **3-76**. The high activation energy barrier of 48.1 kcal/mol required to return to *trans*-**3-74** makes formation of (*Z,Z*)-diene **3-76** irreversible. The relative energies of **TS3.1** and **TS3.2** reflect the standard kinetics of torquoselective electrocyclic ring openings.<sup>13,14</sup> Outward rotation of cyclobutene alkyl substituents is favored kinetically, minimizing steric interactions in **TS3.1**, whereas inward alkyl group rotation in **TS3.2** has larger steric interactions and a higher energy of activation.

This unique free-energy profile of the bicyclic cyclobutene/diene interconversion is highlighted when compared to the free-energy profile of monocyclic cyclobutenes. The free-energy profile for inward and outward ring opening of *trans*-3,4-dimethylcyclobutene **3-3** to give (*E,E*)-2,4-hexadiene or (*Z,Z*)-2,4-hexadiene was calculated at the M06/6-311++G(d,p)//B3LYP/6-31G(d) level of theory by Dr. Aaron Green (Scheme 3.16).<sup>31</sup> In contrast to the free-energy profile for bicyclic cyclobutenes (Scheme 3.15) the cyclobutene is highest in energy, followed by the (*Z,Z*)-diene, and the (*E,E*)-diene is lowest in energy. Thermal ring opening of the cyclobutene by either **TS3.3** or **TS3.4** are both high energy pathways, but the (*E,E*)-diene is the thermodynamic product via the kinetically favored **TS3.3**. In the case of bicyclic cyclobutene *trans*-**3-74**, selectivity for the cyclic (*Z,Z*)-diene was observed by the higher energy **TS3.2**. Still, one key

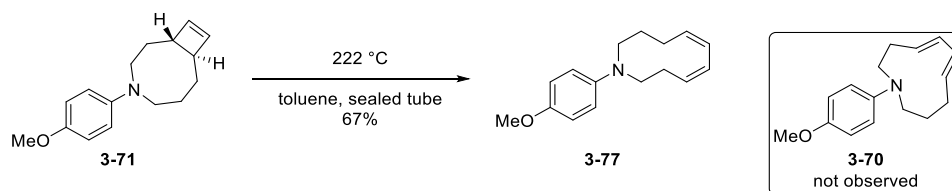
similarity remains. Outward alkyl group rotation via **TS3.1** or **TS3.3** is the kinetically favored ring opening pathway due to minimized steric interactions for both *trans*-**3-74** and **3-3**.



**Scheme 3.16. Computed free-energy surface (gas phase; 298K) for electrocyclic ring opening of 3-3 to give either (*E,E*) or (*Z,Z*)-1,3-dienes (calculated at the M06/6-311++G(d,p)//B3LYP/6-31G(d) level of theory).**

These computational results suggested that (*Z,Z*)-diene **3-77** could be obtained experimentally from the inward ring-opening of cyclobutene **3-71**. Indeed, heating a solution of **3-71** in toluene at 222 °C in a sealed tube gave (*Z,Z*)-diene **3-77** in 67% yield, the product of a torquoselective ring opening (Scheme 3.17). Clearly the higher energy transition state pathway **TS3.2** was operative to allow inward alkyl group rotation, leading to the thermodynamic (*Z,Z*)-diene **3-77**. The (*E,E*)-diene **3-70** was not detected by <sup>1</sup>H NMR analysis of the reaction mixture.





**Scheme 3.17. Electrocyclic ring opening of cyclobutene 3-71 to give *(Z,Z)*-diene 3-77.**

Examples of *trans*-bicyclic cyclobutenes that undergo electrocyclic ring opening via conrotatory inward alkyl group rotation are rare. More commonly, *cis*-bicyclic 3,4-dialkyl substituted cyclobutenes undergo conrotatory electrocyclic ring openings via inward rotation of one alkyl group.<sup>15,28</sup> On the other hand, bicyclic 1,3-disubstituted cyclobutenes were shown to undergo electrocyclic ring openings via inward rotation of the 3-alkyl group, although only two examples of this type are known (Scheme 3.6).<sup>19,20</sup> In contrast, conrotatory electrocyclic ring openings of *trans*-3,4-dialkyl cyclobutenes via outward rotation of alkyl groups is common,<sup>8-10,13,14</sup> highlighting the unique reactivity in our process.

We executed kinetic studies to verify the calculated free-energy of activation for the ring opening of cyclobutene **3-71** to give *(Z,Z)*-diene **3-77**. The rate of ring opening was measured at temperatures 185, 190, 197, and 218 °C and plotted in the form of an Eyring plot (Figure 3.4). Silicone oil was selected as the solvent for reaction due to its thermal stability in the high temperature reaction conditions. The Eyring plot was constructed by plotting  $\ln[k/T]$  vs  $1/T$  from data gathered by <sup>1</sup>H NMR analysis of the reaction mixture.<sup>45</sup>

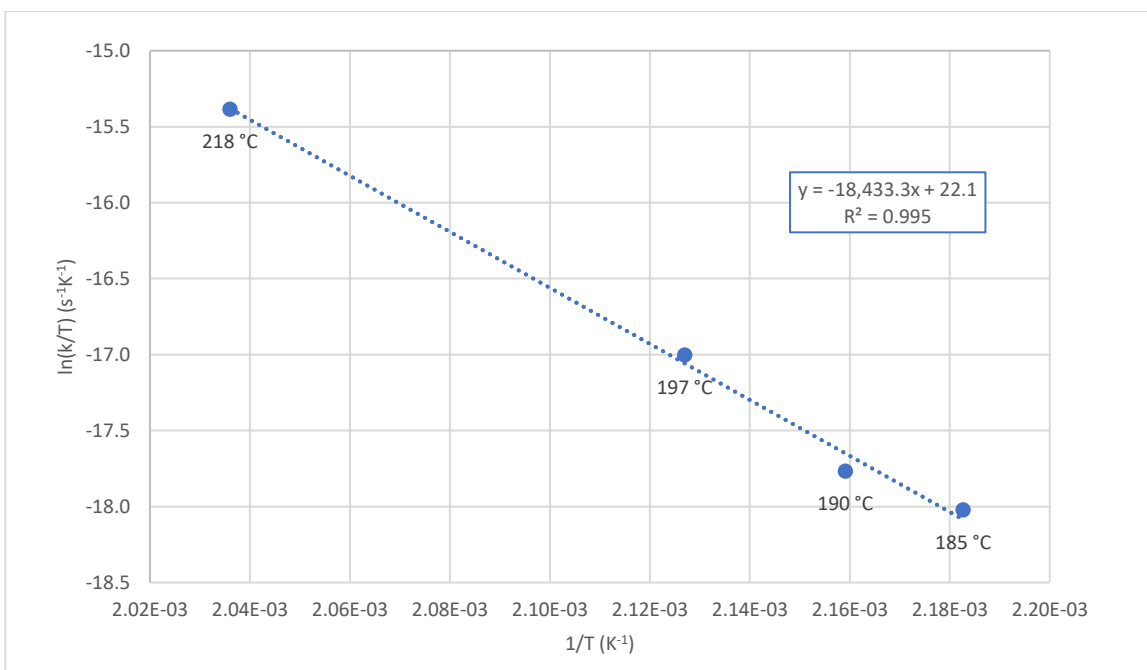
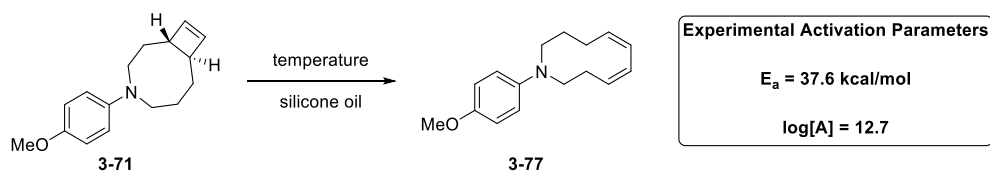


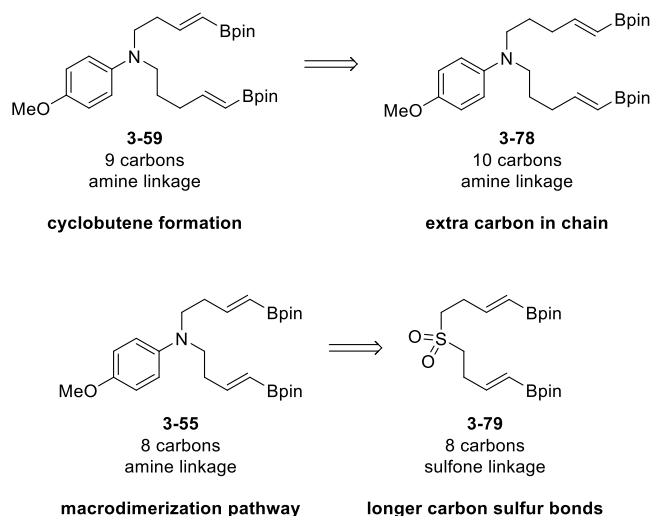
**Figure 3.4. Eyring plot for ring opening of cyclobutene 3-71 to (Z,Z)-diene 3-77.**

Experimental activation parameters were calculated from the lines of best fit from Eyring and Arrhenius plots for the electrocyclic ring opening of cyclobutene **3-71**. The results are summarized in Scheme 3.18. The experimental free-energy of activation of 37.6 kcal/mol differs only slightly from the calculated free-energy of activation of 40.4 kcal/mol at 298 K. The experimental free-energy of activation lies between that of monocyclic *trans*-3,4-dimethyl cyclobutene **3-3** (30.6 kcal/mol)<sup>13</sup> and bicyclic cyclobutenes *cis*-bicyclo [4.2.0]oct-7-ene **3-19** (43.2 kcal/mol)<sup>18</sup> and *cis*-bicyclo[3.2.0]hept-6-ene (45.5 kcal/mol)<sup>17</sup> which open to (Z,Z)-cyclooctadiene **3-20** and (Z,Z)-cycloheptadiene **3-18** (Scheme 3.5) via disrotatory pathways, respectively. The experimental log[A] parameter of 12.7 is comparable to other monocyclic<sup>13,26,46,47</sup> and bicyclic<sup>17,18</sup> cyclobutene ring opening reactions.



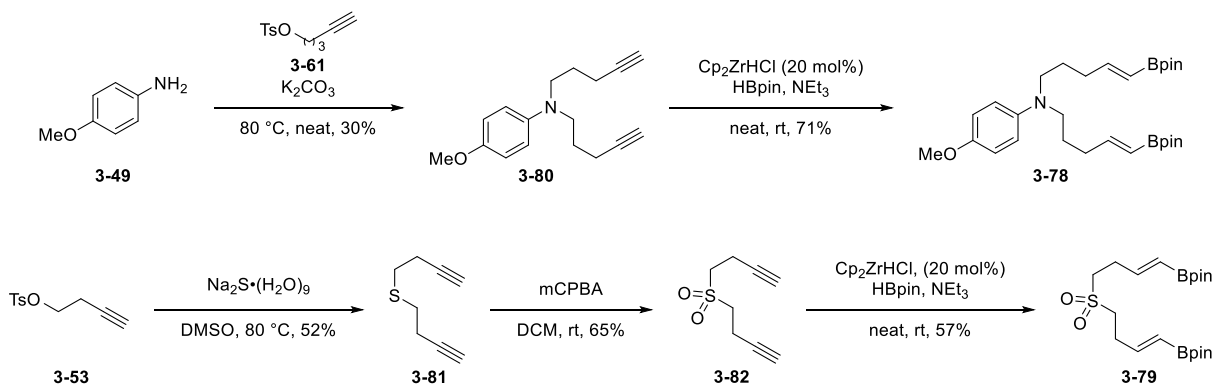
**Scheme 3.18. Experimental activation parameters and conditions for ring opening of cyclobutene 3-71.**

Structural modification of earlier substrates provided the basis for discovery of other cyclic dienes which undergo electrocyclization to bicyclic cyclobutenes (Scheme 3.19). Bis(vinylboronate ester) **3-59**, previously shown to cyclize to the cyclobutene **3-71** (Scheme 3.13) was redesigned as the one carbon elongated anisidine **3-78**. We expected cyclization products from **3-59** and **3-78** to have approximately equivalent ring strains, where the carbocyclic forms have ring strain energies of +15 and +9 kcal/mol, respectively, according to our calculations (**3-41** and **3-42**, Figure 3.2). Bis(vinylboronate ester) **3-55**, unable to undergo direct cyclization due to the favored dimerization pathway (Scheme 3.12), was redesigned by replacing the nitrogen linkage with a sulfone linkage. By replacing short carbon-nitrogen bonds with the longer carbon-sulfur analog (C-N 1.47 Å vs C-SO<sub>2</sub> 1.78 Å),<sup>48</sup> cyclization of sulfone **3-79** would be expected to yield a cyclobutene product after macrocyclization and electrocyclization



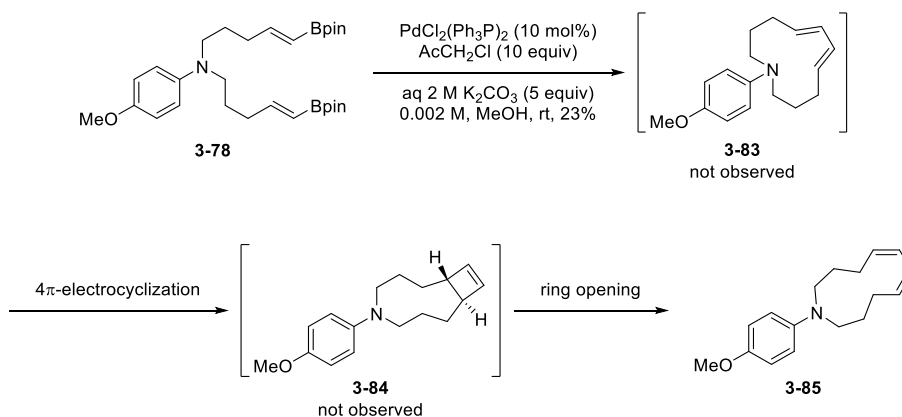
### Scheme 3.19. Structural modifications of known substrates.

We embarked upon the syntheses of these new bis(vinylboronate) structures to determine whether cyclobutene formation would be possible under the palladium-catalyzed cyclization conditions. Double alkylation of *p*-anisidine with tosylate **3-61** followed by double hydroboration gave **3-78** in a short two step sequence (Scheme 3.20). The bis(vinylboronate ester) **3-79** was easily prepared in a three-step sequence involving alkylation of sodium sulfide with tosylate **3-53**, oxidation to sulfone **3-82** with mCPBA, and finally double hydroboration catalyzed by Schwartz's reagent.



### Scheme 3.20. Synthesis of bis(vinylboronate esters) **3-75** and **3-79**.

With the new bis(vinylboronate esters) in hand, we tested the cyclization reaction of **3-78**. Upon treatment of **3-78** with the palladium-catalyzed oxidative cyclization conditions we observed the formation of a symmetric diene product. This was surprising as we had expected formation of a cyclobutene product, similar to the reaction of **3-59** to give cyclobutene **3-71** (Scheme 3.13). Upon careful examination of the  $^1\text{H}$  NMR spectrum of the isolated product we were surprised to find a small  $^3\text{J}$  alkene coupling constant of 9.8 Hz. Typically, macrocyclic (*E,E*)-dienes have coupling constants on the order of about 15-18 Hz. Clearly the observed coupling constant suggested the existence of (*Z*)-double bonds in the product. With this information, it became clear that the unexpected (*Z,Z*)-diene product **3-85** was isolated from the reaction (Scheme 3.21).

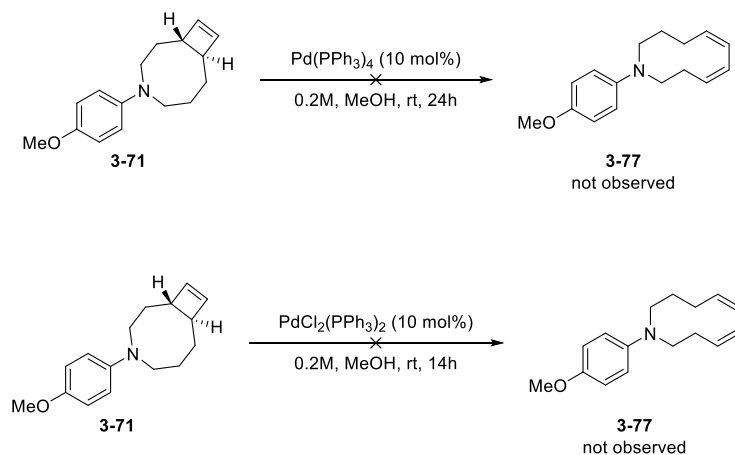


**Scheme 3.21. Possible mechanism for the formation of (*Z,Z*)-diene **3-85**.**

Considering our observation that bicyclic cyclobutene **3-71** required temperatures greater than 200 °C to undergo electrocyclic ring opening to cyclic (*Z,Z*)-diene **3-77** (Scheme 3.17), the isolation of (*Z,Z*)-diene **3-86** was puzzling. One possible mechanism of formation involves oxidative cyclization to cyclic (*E,E*)-diene **3-83**, which would be expected to undergo a  $4\pi$ -conrotatory electrocyclic ring closure to give the *trans*-cyclobutene **3-84**. The (*Z,Z*)-diene **3-85** would result from the  $4\pi$ -conrotatory electrocyclic ring opening of the bicyclic cyclobutene

intermediate **3-84**. On the other hand, examples of thermal ring opening of bicyclic cyclobutenes via disrotatory alkyl group rotation require high temperature reaction conditions,<sup>17,18</sup> so a thermal ring opening would be unexpected by a disrotatory mechanism.

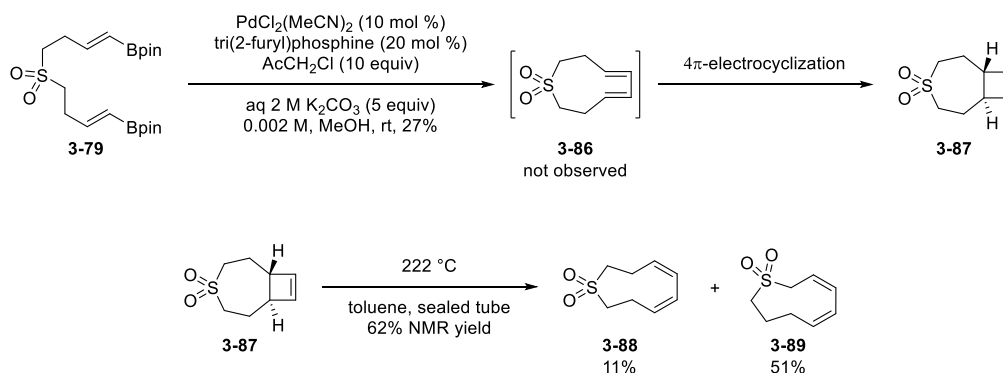
We considered the possibility that palladium could promote a  $4\pi$ -conrotatory electrocyclic ring opening of the proposed intermediate *trans*-cyclobutene **3-84** to give (*Z,Z*)-diene **3-85**. To test this possibility, a stable cyclobutene **3-71** was stirred in concentrated solutions of Pd(0) or Pd(II) in methanol and monitored for the formation of (*Z,Z*)-diene **3-77**. Cyclobutene ring opening was not observed in either case. Analysis of crude reaction mixtures by <sup>1</sup>H NMR showed that cyclobutene **3-71** was stable to the reaction conditions upon stirring with Pd(PPh<sub>3</sub>)<sub>4</sub> or PdCl<sub>2</sub>(PPh<sub>3</sub>)<sub>2</sub> without the formation of side products. At this point the formation of **3-85** is not understood and will require further studies.



**Scheme 3.22. Attempted palladium-catalyzed ring opening of cyclobutene 3-71.**

With continued interest in finding a third example of electrocyclic ring closure to bicyclic cyclobutenes from strained cyclic dienes, we turned to the reaction of bis(vinylboronate ester) **3-79**. After submitting sulfone **3-79** to the palladium-catalyzed oxidative cyclization conditions, we were pleased to find that cyclization had occurred, giving *trans*-bicyclic cyclobutene **3-87** (Scheme

3.23). Intermediate (*E,E*)-1,3-diene **3-86** was not observed under the reaction conditions, analogous to the cyclization of **3-59**, where (*E,E*)-1,3-diene intermediate **3-70** was not observed (Scheme 3.13). Cyclobutene **3-87** was evident by one alkene proton signal in the  $^1\text{H}$  NMR spectrum at 6.12 ppm and one alkene carbon signal in the  $^{13}\text{C}$  NMR spectrum. Thermolysis of *trans*-cyclobutene **37** in toluene in a sealed tube at 222 °C gave the ring-opened product (*Z,Z*)-diene **3-88** analogous to the ring-opening of cyclobutene **3-71** to give **3-77** (Scheme 3.17), although it was the minor product of electrocyclic ring opening. The unexpected diene isomer **3-89** was isolated as the major product. We propose that upon formation of **3-88** a subsequent thermal 1,5-hydride shift occurs giving diene **3-89**.<sup>15</sup> This was confirmed by heating an isolated mixture of **3-88** and **3-89** and observing the slow conversion of **3-88** to **3-89** by  $^1\text{H}$  NMR.

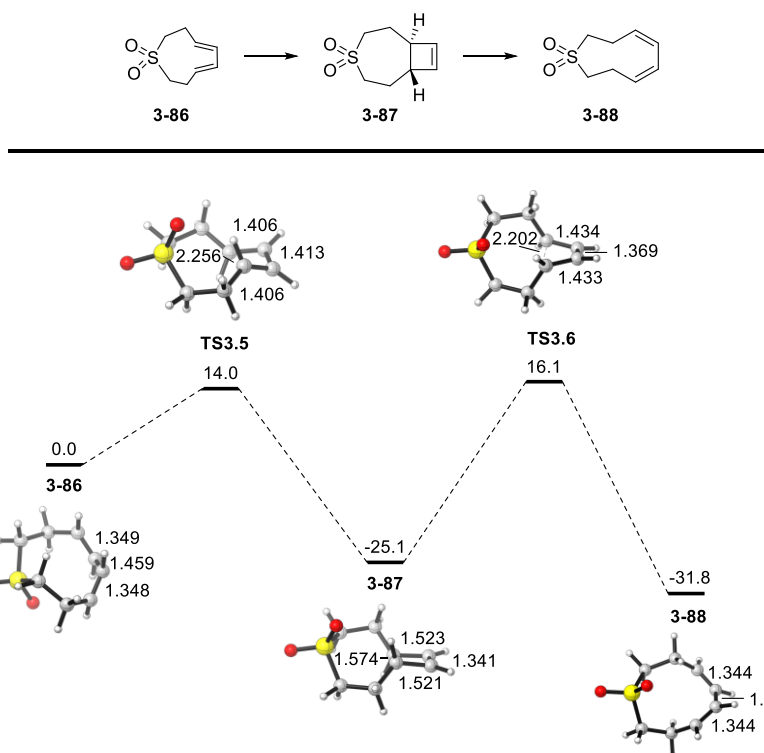


**Scheme 3.23. Formation of sulfone cyclobutene 3-87 and thermal ring opening reactions.**

Computations from Dr. Aaron Green helped model the relative energy levels of (*E,E*)-diene **3-86**, *trans*-cyclobutene **3-87**, and (*Z,Z*)-diene **3-88** and their transition states from the electrocyclic ring opening/closing pathways (Scheme 3.24).<sup>31</sup> The free-energy profile is reminiscent of the anisidine cyclobutene case (Scheme 3.15). We observe the same relative ordering of energy levels, where (*E,E*)-diene **3-86** is highest in energy, followed by the *trans*-cyclobutene **3-87**, with the (*Z,Z*)-diene **3-88** lowest in energy. The +14 kcal/mol activation energy

barrier for electrocyclic ring closure from (*E,E*)-diene **3-86** is substantially smaller than the 20.4 kcal observed in the anisidine case for conversion of (*E,E*)-diene **3-75** to *trans*-**3-74**. The low energy of activation explains why (*E,E*)-diene **3-86** was not observed from the oxidative cyclization of bis(vinylboronate ester) **3-79**. Electrocyclic ring opening from cyclobutene **3-87** via high energy transition states **TS3.5** or **TS3.6** are higher in energy relative to cyclobutene *trans*-**3-74**, corresponding to 39.1 and 41.2 kcal/mol, respectively. Once again, electrocyclic ring opening via **TS3.5** is kinetically favored leading to reversible formation of (*E,E*)-diene **3-86** via outward alkyl group rotation. On the other hand, ring opening via the higher energy **TS3.6** leads to irreversible formation of the thermodynamic (*Z,Z*)-diene **3-88**. The higher activation energy barrier of **TS3.6** can be attributed to the steric interaction between alkyl groups from inward rotation, as would be expected on the basis of studies on torquoselective electrocyclic ring openings.<sup>13,14</sup>





**Scheme 3.24.** Computed free-energy surface (gas phase; 298K) for electrocyclic ring-closure of (*E,E*)-diene 3-86 to give the trans-cyclobutene 3-87 and ring-opening to yield (*Z,Z*)-diene 3-88 (calculated at the M06/6-311++G(d,p)//B3LYP/6-31G(d) level of theory).

To quantify these experimental results, ring strain energies of the (*E,E*)-dienes **3-75** and **3-86** and their (*Z,Z*)-diene isomers **3-76** and **3-88** were calculated by Dr. Aaron Green (Figure 3.5).<sup>31</sup> We may that expect thermal  $4\pi$ -electrocyclizations may occur spontaneously for cyclic dienes with strain energies near or above +18 kcal/mol, although less strained rings may exhibit this reactivity. We should not expect cyclic dienes with ring strains of -3 kcal/mol or lower to undergo electrocyclic ring openings, highlighted by the stability of **3-76** and **3-88**. Synthesis of cyclic (1,3)-dienes with ring strain between -3 and +18 kcal/mol may provide more substrates capable of undergoing these unusual ambient temperature electrocyclic ring closures to bicyclic cyclobutenes.

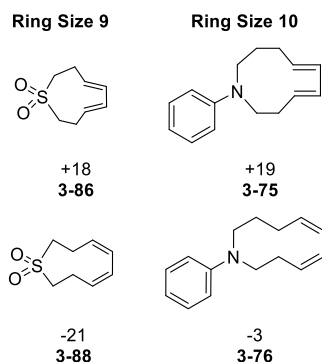


**Figure 3.5. Predicted strain energy (kcal/mol) of heterocyclic dienes (Calculated at the M06/6-311++G(d,p)//B3LYP/6-31G(d) level of theory).**

### 3.4 Conclusions

We demonstrated a novel cascade process where palladium(II)-catalyzed oxidative cyclization reactions of bis(vinylboronate esters) allowed the synthesis of highly strained medium ring (*E,E*)-1,3-dienes that undergo spontaneous thermal  $4\pi$ -electrocyclic ring closure to form *trans*-bicyclic cyclobutenes. DFT calculations by my colleague Dr. Aaron Green revealed that ring strain substantially raises the energies of the cyclic (*E,E*)-1,3-dienes relative to the corresponding *trans*-cyclobutenes. These same calculations showed that the cyclic (*Z,Z*)-1,3-

dienes were lowest in energy of the three isomers. Experimental thermal ring opening of the *trans*-cyclobutenes gave the thermodynamically favored medium ring (*Z,Z*)-1,3-dienes confirming the calculations. These unusual examples are in contrast with typical acyclic *trans*-3,4-dialkyl cyclobutenes, which favor outward torquoselective ring-openings to give (*E,E*)-1,3-dienes. As predicted by the DFT calculations, ring opening via outward alkyl group rotation to the (*E,E*)-1,3-dienes is favored kinetically, but due to the high temperature ring opening conditions, inward rotation of alkyl groups via a higher energy transition state gave the observed (*Z,Z*)-1,3-dienes. Kinetic studies were conducted to measure the free-energy of activation for the thermal ring opening of a *trans*-cyclobutene to (*Z,Z*)-dienes and were in excellent agreement with calculated values. These results highlight a novel important free-energy profile for diene/cyclobutene interconversions which may be applicable to future syntheses of stable *trans*-cyclobutenes from cyclic (*E,E*)-1,3-dienes as well as their ring opened (*Z,Z*)-1,3-diene products.

### 3.5 Experimental

#### General Information

All commercial compounds were used as received. Dichloromethane, triethylamine, and acetonitrile were purified by distillation over CaH<sub>2</sub>. Methanol was distilled over Mg. Tetrahydrofuran and ether were distilled prior to use from sodium-benzophenone ketyl. All reactions were carried out in flame-dried glassware under a nitrogen atmosphere. Bis(triphenylphosphine)palladium(II) dichloride (PdCl<sub>2</sub>(Ph<sub>3</sub>P)<sub>2</sub>, Aldrich, ≥ 99%) and bis(acetonitrile)dichloropalladium(II) (PdCl<sub>2</sub>(MeCN)<sub>2</sub>, Alpha Aesar) were used as received. Chloro(1,5-cyclooctadiene)rhodium(I) dimer ([Rh(cod)Cl]<sub>2</sub> Strem, 98%) was stored under nitrogen and used as received. Schwartz's catalyst (Strem) was stored in a glovebox and used as received. Reactions were monitored using TLC, and the plates were developed using vanillin,

cerium ammonium molybdate, or potassium permanganate stains. Column chromatography was performed using silica gel (40–63  $\mu\text{m}$ ) and reagent grade solvents without deactivation, unless noted. NMR spectra were recorded at 300, 400, 500, or 600 MHz as noted and calibrated to the solvent signal ( $\text{CDCl}_3$   $\delta = 7.26$  ppm,  $\text{DMSO-}d_6$   $\delta = 2.50$  ppm,  $\text{C}_6\text{D}_6$   $\delta = 7.16$  ppm for  $^1\text{H}$  NMR, and  $\text{CDCl}_3$   $\delta = 77.0$  ppm,  $\text{DMSO-}d_6$   $\delta = 39.5$  ppm,  $\text{C}_6\text{D}_6$   $\delta = 128.1$  for  $^{13}\text{C}$  NMR). Multiplicities are indicated by s (singlet), d (doublet), t (triplet), q (quartet), p (pentet), m (multiplet), or b (broadened). IR spectra were recorded with an ATR attachment, and selected peaks are reported in  $\text{cm}^{-1}$ . High resolution mass spectral data were recorded with an IonSense ID-CUBE DART source or ESI LC-TOF Micromass LCT.

### Kinetic Studies

Cyclobutene **3-71** (9 mg, 0.0370 mmol) and silicone oil (0.4 mL) were added to a 1 mL test tube and capped with a rubber septa. The cap was sealed with Teflon tape and a layer of electrical tape. The vial was backfilled with nitrogen after three freeze–pump–thaw cycles, and the reaction was stirred in a molten potassium nitrate/sodium nitrite (1:1 by wt.) bath under nitrogen. Kinetic runs were conducted at four temperatures (185, 190, 197, and 218  $^\circ\text{C}$ ), monitored with a mercury thermometer. A 20  $\mu\text{L}$  sample was removed from the reaction mixture and diluted in 0.45 mL  $\text{CDCl}_3$  in an NMR tube every 2 h (except the reaction at 218  $^\circ\text{C}$ , sampled every 40 min) and was analyzed by  $^1\text{H}$  NMR where the ratio of remaining starting material to ring-opened product was determined from signals at 5.92 ppm for cyclobutene **3-71** and the average of 5.71 and 5.49 ppm signals for (*Z,Z*)-diene product **3-77**. Presaturation of the silicone oil resonance (0.68 ppm) provided an adequate signal-to-noise ratio for analysis. Each trial included at least 5 data points. The rate of reaction at each temperature was determined from the slope of the best fit line from the plot of  $\ln[A/A_0]$  vs time, where  $A$  is the concentration of the starting material and  $A_0$  is the initial

concentration of the starting material.<sup>49</sup> An Arrhenius plot was constructed by plotting  $\ln[k]$  vs  $1/T$ , and  $\log[A]$  was calculated from the best fit line. An Eyring plot was constructed by plotting  $\ln[k/T]$  vs  $1/T$ , and the Gibbs free-energy of activation was calculated from the best fit line.

### **General Procedure A: Hydroboration Catalyzed by Schwartz's Reagent**

This is a modification of a known procedure.<sup>36</sup> A flame-dried flask containing the bis(alkyne) (1 equiv) was evacuated and replenished with nitrogen three times followed by addition of pinacolborane (4 equiv) and  $\text{NEt}_3$  (0.2 equiv). The mixture was transferred to a flask containing  $\text{Cp}_2\text{ZrHCl}$  (Schwartz's reagent, 0.2 equiv) via cannula. The mixture was stirred at rt overnight. The reaction was passed through a silica gel plug with EtOAc and then concentrated *in vacuo*. The crude product was purified by column chromatography.

### **General Procedure B: Tosylation of Primary Alcohols**

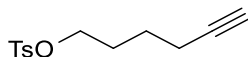
A flame-dried flask equipped with DMAP (0.01 equiv) was evacuated and replenished with nitrogen three times, and then DCM was added. After the addition of the alcohol (1 equiv) and  $\text{NEt}_3$  (1.1 equiv), the flask was cooled to 0 °C, and *p*-TsCl (1.1 equiv) was added slowly. The flask was warmed to rt and stir overnight. The mixture was diluted with water, extracted with DCM, and dried with  $\text{MgSO}_4$ . Solvent was removed *in vacuo*, and the crude product was purified by column chromatography.

### **General Procedure C: Alkylation with Alkynyl Tosylates**

A flame-dried flask containing alkylation substrate, alkynyl tosylate, and  $\text{K}_2\text{CO}_3$  was evacuated and replenished with nitrogen three times (see specific procedure for equivalents of reagents). The mixture was stirred at 80 °C overnight. The reaction was passed through a silica gel plug with EtOAc then concentrated *in vacuo*. The crude product was purified by column chromatography.

## General Procedure D: Oxidative Macrocyclization

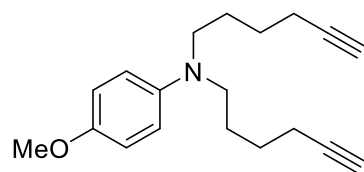
A flame-dried flask containing PdCl<sub>2</sub>(Ph<sub>3</sub>P)<sub>2</sub> (0.1 equiv) was evacuated and replenished three times with nitrogen, then charged with MeOH and chloroacetone (10 equiv). A separate flask containing bis(vinylboronate ester) (1 equiv) was evacuated and replenished with nitrogen three times, charged with MeOH, and transferred via cannula to the first flask. After addition of aq K<sub>2</sub>CO<sub>3</sub> (2 M, 5 equiv), the mixture was stirred at rt overnight. The reaction was passed through a Celite plug with EtOAc and then concentrated *in vacuo*. The mixture was diluted with water, extracted with DCM, and dried with MgSO<sub>4</sub>. Solvent was removed *in vacuo*, and the crude product was purified by column chromatography.



### hex-5-yn-1-yl 4-methylbenzenesulfonate (3-50)

To a flame-dried flask was added DMAP (200 mg, 1.64 mmol). The flask was evacuated and replenished with nitrogen three times, and then DCM (23 mL) was added. After the addition of hex-5-yn-1-ol (2.1 mL, 19.0 mmol) and NEt<sub>3</sub> (2.9 mL, 20.9 mmol), the flask was cooled to 0 °C, and *p*-TsCl (6.570 g, 34.5 mmol) was added slowly. The flask was warmed to rt and stir for 40 min. The mixture was diluted with saturated aqueous ammonium chloride (60 mL), extracted with DCM (2 × 60 mL), and dried with MgSO<sub>4</sub>. Solvent was removed *in vacuo*, and column chromatography with a 0% to 20% Hex:EtOAc gradient solvent system gave 3.860 g (80% yield) of the known<sup>50</sup> clear colorless oil.

<sup>1</sup>H NMR (400 MHz, CDCl<sub>3</sub>, ppm) δ 7.79 (d, *J* = 8.4 Hz, 2H), 7.35 (d, *J* = 8.0 Hz, 2H), 4.06 (t, *J* = 6.2 Hz, 2H), 2.45 (s, 3H), 2.17 (td, *J* = 6.9, 2.7 Hz, 2H), 1.92 (t, *J* = 2.6 Hz, 1H), 1.82–1.75 (m, 2H), 1.56 (p, *J* = 7.2 Hz, 2H).



***N,N*-di(hex-5-yn-1-yl)-4-methoxyaniline (3-51)**

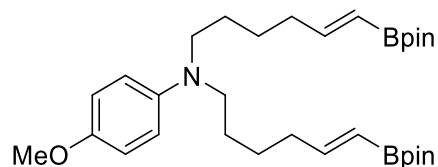
Following general procedure C, 4-methoxyaniline (803 mg, 6.52 mmol) was reacted with **3-50** (3.292 g, 13.0 mmol) in the presence of  $K_2CO_3$  (2.704 g, 19.6 mmol) and MeCN (21 mL). Chromatography with 7:1 Hex/Et<sub>2</sub>O gave 883 mg (48% yield) of a clear yellow oil.

$R_f = 0.37$  (6:1 Hex/EtOAc);

<sup>1</sup>H NMR (400 MHz, CDCl<sub>3</sub>, ppm)  $\delta$  6.84–6.79 (m, 2H), 6.70–6.66 (m, 2H), 3.75, (s, 3H), 3.20 (t,  $J = 7.4$  Hz, 4H), 2.21 (dt,  $J = 7.0, 2.7$  Hz, 4H), 1.95 (t,  $J = 2.6$  Hz, 2H), 1.69–1.61 (m, 4H), 1.59–1.51 (m, 4H);

<sup>13</sup>C NMR (100 MHz, CDCl<sub>3</sub>, ppm)  $\delta$  151.5, 143.0, 115.1, 114.7, 84.1, 68.4, 55.7, 51.5, 26.4, 26.0, 18.2; IR (neat, ATR, cm<sup>-1</sup>): 3293, 3045, 2991, 2937, 2862, 2833, 2116, 1508, 1462, 1441, 1372, 1239, 1181, 1038, 812, 624;

HRMS (DART): calcd [M + H]<sup>+</sup> (C<sub>19</sub>H<sub>26</sub>NO) 284.20089, found 284.20035.



**4-methoxy-*N,N*-bis((*E*)-6-(4,4,5,5-tetramethyl-1,3,2-dioxaborolan-2-yl)hex-5-en-1-yl)aniline (3-52)**

Following general procedure A, **3-51** (495 mg, 1.75 mmol) was reacted with pinacolborane (1.0 mL, 6.99 mmol) in the presence of NEt<sub>3</sub> (50 μL, 0.349 mmol) and Cp<sub>2</sub>ZrHCl (90 mg, 0.623 mmol). Chromatography with 7:1 Hex:EtOAc gave 661 mg (70% yield) of a light yellow oil.

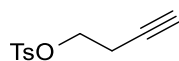
$R_f = 0.27$  (7:1 Hex:EtOAc);

**<sup>1</sup>H NMR** (400 MHz, CDCl<sub>3</sub>, ppm) δ 6.82–6.78 (m, 2H), 6.65–6.59 (m, 4H), 5.43 (dt,  $J = 18.0, 1.8$  Hz, 2H), 3.75 (s, 3H), 3.15 (t,  $J = 7.4$  Hz, 4H), 2.17 (q,  $J = 7.1$  Hz, 4H), 1.57–1.50 (m, 4H), 1.46–1.39 (m, 4H), 1.26 (s, 24H);

**<sup>13</sup>C NMR** (100 MHz, CDCl<sub>3</sub>, ppm) δ 154.1, 151.1, 143.1, 114.7, 114.5, 82.9, 55.7, 51.7, 35.6, 26.8, 25.7, 24.7 (boron substituted carbons, absent);

**IR** (neat, ATR, cm<sup>-1</sup>): 2977, 2934, 2858, 1637, 1512, 1466, 1358, 1318, 1243, 1143, 1038, 999, 970, 848, 751;

**HRMS** (DART): calcd [M + H]<sup>+</sup> (C<sub>31</sub>H<sub>52</sub>B<sub>2</sub>NO<sub>5</sub>) 540.40261, found 540.40196.

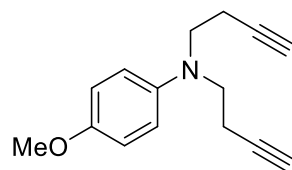


### but-3-yn-1-yl 4-methylbenzenesulfonate (**3-53**)

Following general procedure B, but-3-yn-1-ol (3.4 mL, 44.6 mmol) was reacted with *p*-TsCl (9.351 g, 49.0 mmol) in the presence of NEt<sub>3</sub> (6.8 mL, 49.0 mmol) and DMAP (54 mg, 0.446 mmol). Chromatography with 5:1 Hex:EtOAc gave 9.255 g (93% yield) of the known<sup>51</sup> clear yellow oil.

**<sup>1</sup>H NMR** (400 MHz, CDCl<sub>3</sub>, ppm) δ 7.80 (d,  $J = 8.4$  Hz, 2H), 7.35 (d,  $J = 8.4$  Hz, 2H), 4.10 (t,  $J = 7.2$  Hz, 2H), 2.55 (td,  $J = 7.0, 2.7$  Hz, 2H), 2.45 (s, 3H), 1.96 (t,  $J = 2.6$  Hz, 1H).





***N,N*-di(but-3-yn-1-yl)-4-methoxyaniline (3-54)**

Following general procedure C, 4-methoxyaniline (0.751 g, 6.1 mmol) was reacted with **3-53** (5.470 g, 24.4 mmol) in the presence of K<sub>2</sub>CO<sub>3</sub> (3.371 g, 24.3 mmol) and NaI (0.182 g, 1.19 mmol). Chromatography with 8:1 Hex:EtOAc gave 682 mg (49% yield) of a light brown oil.

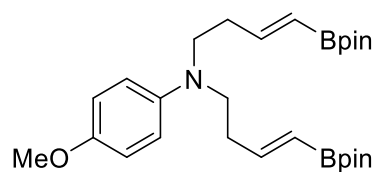
*R<sub>f</sub>* = 0.32 (7:1 Hex:EtOAc);

<sup>1</sup>H NMR (400 MHz, CDCl<sub>3</sub>, ppm) δ 6.86–6.82 (m, 2H), 6.70–6.66 (m, 2H), 3.76 (s, 3H), 3.50 (t, *J* = 7.6 Hz, 4H), 2.42 (td, *J* = 7.4, 2.5 Hz, 4H), 2.00 (t, *J* = 2.6 Hz, 2H);

<sup>13</sup>C NMR (100 MHz, CDCl<sub>3</sub>, ppm) δ 152.1, 141.1, 115.1, 114.6, 82.2, 69.6, 55.8, 51.1, 17.4;

IR (neat, ATR, cm<sup>-1</sup>): 3300, 2938, 2834, 2249, 1512, 1362, 1242, 1039, 910, 744, 654;

HRMS (ES): calcd [M + H]<sup>+</sup> (C<sub>15</sub>H<sub>18</sub>NO) 228.1383, found 228.1385.



**4-methoxy-*N,N*-bis(*E*)-4-(4,4,5,5-tetramethyl-1,3,2-dioxaborolan-2-yl)but-3-en-1-yl)aniline (3-55)**

Following general procedure A, **3-54** (682 mg, 3.00 mmol) was reacted with pinacolborane (1.7 mL, 12.0 mmol) in the presence of NEt<sub>3</sub> (80 μL, 0.60 mmol) and Cp<sub>2</sub>ZrHCl (155 mg, 0.60 mmol). Chromatography with 4:1 Hex:EtOAc gave 1.072 g (74% yield) of a clear light brown oil.

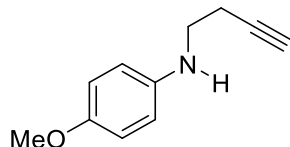
$R_f = 0.25$  (4:1 Hex/EtOAc);

$^1\text{H NMR}$  (400 MHz,  $\text{CDCl}_3$ , ppm)  $\delta$  6.83–6.78 (m, 2H), 6.66–6.57 (m, 4H), 5.50, (dt,  $J = 18.0$ , 1.4 Hz, 2H), 3.74 (s, 3H), 3.29 (t,  $J = 7.6$  Hz, 4H), 2.38 (q,  $J = 6.9$  Hz, 4H), 1.26 (s, 24H);

$^{13}\text{C NMR}$  (125 MHz,  $\text{C}_6\text{D}_6$ , ppm)  $\delta$  152.2, 151.6, 142.3, 115.5, 114.7, 82.5, 54.9, 50.9, 33.6, 24.5 (boron substituted carbons, absent);

**IR** (neat, ATR,  $\text{cm}^{-1}$ ): 2976, 2934, 2831, 1636, 1512, 1355, 1321, 1242, 1143, 969, 849, 811;

**HRMS** (ES): calcd  $[\text{M} + \text{Na}]^+(\text{C}_{27}\text{H}_{43}\text{O}_5\text{B}_2\text{NNa})$  506.3220, found 506.3223.



### ***N*-(but-3-yn-1-yl)-4-methoxyaniline (3-56)**

Following general procedure C, 4-Methoxyaniline (3.036 g, 24.7 mmol) was reacted with **3-53** (1.843 g, 8.22 mmol) in the presence of  $\text{K}_2\text{CO}_3$  (2.271 g, 16.4 mmol). Chromatography with 8:1 Hex:EtOAc gave 1.253 g (87% yield) of a clear orange oil.

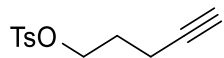
$R_f = 0.24$  (6:1 Hex:EtOAc);

$^1\text{H NMR}$  (400 MHz,  $\text{CDCl}_3$ , ppm)  $\delta$  6.81–6.77 (m, 2H), 6.64–6.60 (m, 2H), 3.75 (s, 3H), 3.27 (t,  $J = 6.6$  Hz, 2H), 2.48 (td,  $J = 6.5$  Hz, 2.7 Hz, 2H), 2.04 (t,  $J = 2.8$  Hz, 1H) (NH proton absent);

$^{13}\text{C NMR}$  (100 MHz,  $\text{CDCl}_3$ , ppm)  $\delta$  152.5, 141.7, 115.0, 114.7, 81.9, 70.0, 55.8, 43.6, 19.2;

**IR** (neat, ATR,  $\text{cm}^{-1}$ ): 3384, 3287, 2997, 2936, 2115, 1619, 1510, 1467, 1236, 1180, 1033, 821, 633;

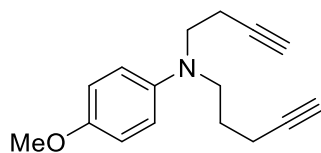
**HRMS** (DART): calcd  $[M + H]^+$  ( $C_{11}H_{14}NO$ ) 176.10699, found 176.10677.



**pent-4-yn-1-yl 4-methylbenzenesulfonate (3-57)**

Following general procedure B, pent-4-yn-1-ol (1.6 mL, 16.8 mmol) was reacted with *p*-TsCl (3.840 g, 20.1 mmol) in the presence of  $NEt_3$  (2.8 mL, 20.1 mmol) and DMAP (205 mg, 1.68 mmol). Chromatography with 5:1 Hex:EtOAc gave 3.364 g (84% yield) of the known<sup>52</sup> clear yellow oil.

**$^1H$  NMR** (400 MHz,  $CDCl_3$ , ppm)  $\delta$  7.80 (d,  $J = 8.0$  Hz, 2H), 7.35 (d,  $J = 8.0$  Hz, 2H), 4.15 (t,  $J = 6.2$  Hz, 2H), 2.45 (s, 3H), 2.26 (td,  $J = 7.0, 2.7$  Hz, 2H), 1.88 (t,  $J = 2.8$  Hz, 1H), 1.86 (p,  $J = 6.5$  Hz, 2H).



***N*-(but-3-yn-1-yl)-4-methoxy-*N*-(pent-4-yn-1-yl)aniline (3-58)**

Following general procedure C, **3-56** (1.000 g, 5.71 mmol) was reacted with **3-57** (2.720 g, 11.4 mmol) in the presence of  $K_2CO_3$  (1.577 g, 11.4 mmol). Chromatography with 8:1 Hex:EtOAc gave 990 mg (72% yield) of a clear light yellow oil.

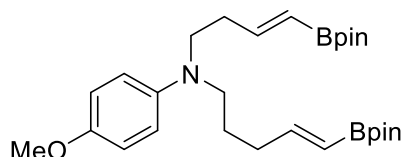
$R_f = 0.45$  (5:1 Hex/EtOAc);

**$^1H$  NMR** (400 MHz,  $CDCl_3$ , ppm)  $\delta$  6.85–6.81 (m, 2H), 6.74–6.70 (m, 2H), 3.76 (s, 3H), 3.46 (t,  $J = 7.4$  Hz, 2H), 3.35 (t,  $J = 7.2$  Hz, 2H), 2.40 (td,  $J = 7.5, 2.5$  Hz, 2H), 2.25 (td,  $J = 6.8, 2.4$  Hz, 2H), 2.002 (t,  $J = 2.6$  Hz, 1H), 1.995 (t,  $J = 2.6$  Hz, 1H), 1.77 (p,  $J = 7.0$  Hz, 2H);

$^{13}\text{C}$  NMR (100 MHz,  $\text{CDCl}_3$ , ppm)  $\delta$ : 152.0, 142.0, 115.3, 114.9, 83.9, 82.4, 69.5, 68.9, 55.8, 51.5, 50.5, 26.2, 17.1, 15.9;

IR (neat, ATR,  $\text{cm}^{-1}$ ): 3307, 2949, 2832, 2248, 2115, 1514, 1249, 1039, 914, 745;

HRMS (DART): calcd  $[\text{M} + \text{H}]^+$  ( $\text{C}_{16}\text{H}_{20}\text{NO}$ ) 242.15394, found 242.15282.



**4-methoxy-N-((E)-4-(4,4,5,5-tetramethyl-1,3,2-dioxaborolan-2-yl)but-3-en-1-yl)-N-((E)-5-(4,4,5,5-tetramethyl-1,3,2-dioxaborolan-2-yl)pent-4-en-1-yl)aniline (3-59)**

Following general procedure A, **3-58** (990 mg, 4.10 mmol) was reacted with pinacolborane (2.4 mL, 16.4 mmol) in the presence of  $\text{NEt}_3$  (0.11 mL, 0.820 mmol) and  $\text{Cp}_2\text{ZrHCl}$  (211 mg, 0.820 mmol). Chromatography with 6:1 Hex:EtOAc afforded 1.516 g (74% yield) of a clear light yellow oil.

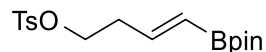
$R_f$  = 0.38 (3:1 Hex:EtOAc);

$^1\text{H}$  NMR (400 MHz,  $\text{CDCl}_3$ , ppm)  $\delta$  6.82–6.78 (m, 2H), 6.66–6.60 (m, 4H), 5.49 (bd,  $J$  = 18.0 Hz, 1H), 5.45 (bd,  $J$  = 18.4, 1H), 3.75 (s, 3H), 3.30–3.26 (m, 2H), 3.19–3.15 (m, 2H), 2.37 (q,  $J$  = 6.9, 2H) 2.17 (q,  $J$  = 6.7 Hz, 2H), 1.66 (p,  $J$  = 7.6 Hz, 2H), 1.262 (s, 12H), 1.259 (s, 12H);

$^{13}\text{C}$  NMR (100 MHz,  $\text{CDCl}_3$ , ppm)  $\delta$  153.7, 151.5, 151.4, 142.7, 115.0, 114.8, 83.1, 83.0, 55.8, 51.5, 51.0, 33.4, 33.3, 26.0, 24.8 (boron substituted carbons, absent);

IR (neat, ATR,  $\text{cm}^{-1}$ ): 3030, 2977, 2941, 1639, 1510, 1362, 1221, 1144, 914, 769;

**HRMS** (ES): calcd  $[M + Na]^+$  ( $C_{28}H_{45}B_2NO_5Na$ ) 520.3376, found 520.3395.

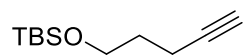


**(E)-4-(4,4,5,5-tetramethyl-1,3,2-dioxaborolan-2-yl)but-3-en-1-yl 4-methylbenzenesulfonate (3-60)**

Following general procedure A, **3-53** (2.349 g, 10.5 mmol) was reacted with pinacolborane (3.0 mL, 21.0 mmol) in the presence of  $NEt_3$  (0.15 mL, 1.05 mmol) and  $Cp_2ZrHCl$  (270 mg, 1.05 mmol). Chromatography with 7:2 Hex:EtOAc gave 2.275 g (62% yield) of the known<sup>36</sup> white solid.

$R_f = 0.21$  (3:1 Hex:EtOAc);

$^1H$  NMR (300 MHz,  $CDCl_3$ , ppm)  $\delta$  7.78 (d,  $J = 8.4$  Hz, 2H), 7.34 (d,  $J = 8.1$  Hz, 2H), 6.44, (dt,  $J = 18.1, 6.4$  Hz, 1H), 5.46 (dt,  $J = 18.0, 1.6$  Hz, 1H), 4.08, (t,  $J = 6.9$  Hz, 2H), 2.49 (td,  $J = 6.6, 1.5$  Hz, 2H), 2.45 (s, 3H), 1.25 (s, 12H).

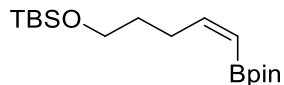


**tert-butyldimethyl(pent-4-yn-1-yloxy)silane (3-61)**

To a flame-dried flask was added TBSCl (2.687 g, 17.83 mmol, 50% w/w in toluene) and imidazole (2.0202 g, 29.7 mmol). The flask was evacuated and replenished with nitrogen three times, and then DMF (19 mL) was added and the mixture was cooled to 0 °C. Pent-4-yn-1-ol (1.10 mL, 11.9 mmol) was added dropwise, then the reaction was stirred at 0 °C for 30 min, and overnight at rt. Toluene was removed *in vacuo*. The reaction was diluted with water, extracted with  $Et_2O$ . The organic extracts were combined and rinsed with brine and dried with  $MgSO_4$ .

Solvent was removed *in vacuo*. Chromatography with 100:1 Hex:EtOAc gave 1.906 g (72% yield) of the known<sup>53</sup> product.

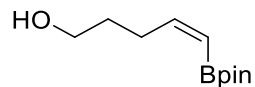
<sup>1</sup>H NMR (400 MHz, CDCl<sub>3</sub>, ppm) δ 3.70 (t, *J* = 6.0 Hz, 2H), 2.27 (td, *J* = 7.1, 2.7 Hz, 2H), 1.93 (t, *J* = 2.7 Hz, 1H), 1.76-1.69 (m, 2H).



**(Z)-tert-butyl dimethyl((5-(4,4,5,5-tetramethyl-1,3,2-dioxaborolan-2-yl)pent-4-en-1-yl)oxy)silane (3-62)**

This compound was prepared by a modification of a known procedure.<sup>37</sup> A flame-dried flask containing [Rh(cod)Cl]<sub>2</sub> (12 mg, 0.0252 mmol) was evacuated and replenished with nitrogen three times, followed by addition of cyclohexane (5 mL), PiPr<sub>3</sub> (16 mg, 0.101 mmol), NEt<sub>3</sub> (1.17 mL, 8.40 mmol), and pinacolborane (0.25 mL, 1.68 mmol). The solution was stirred at rt for 30 min. Next, **3-61** (400 mg, 2.02 mmol)<sup>54</sup> was added in one portion. The reaction was stirred for 21 h. The reaction mixture was passed through a silica gel plug with EtOAc and concentrated *in vacuo* and further concentrated in MeOH twice more. Chromatography with 20:1 Hex:EtOAc gave 228 mg (42% yield) of the known<sup>37</sup> light brown oil.

<sup>1</sup>H NMR (400 MHz, CDCl<sub>3</sub>, ppm) δ 6.44 (dt, *J* = 13.6, 7.1 Hz, 1H), 5.33 (dt, *J* = 13.6, 1.2 Hz, 1H), 3.63 (t, *J* = 6.6 Hz, 2H), 2.43 (qd, *J* = 7.6, 1.2 Hz, 2H), 1.61 (p, *J* = 7.2, 2H), 1.26 (s, 12H), 0.90 (s, 9H), 0.05 (s, 6H).



**(Z)-5-(4,4,5,5-tetramethyl-1,3,2-dioxaborolan-2-yl)pent-4-en-1-ol (3-63)**

A flame-dried flask containing 50WX8 Dowex cation exchange resin (20–50 mesh, hydrogen form, 185 mg) was evacuated and replenished three times with nitrogen. The flask was charged with MeOH (2.2 mL) followed by **3-62** (642 mg, 1.97 mmol). The reaction was stirred for 18 h. The exchange resin was filtered and rinsed with MeOH. Solvent was removed *in vacuo*, and chromatography with 3:1 Hex:EtOAc gave 338 mg (81% yield) of a clear colorless oil.

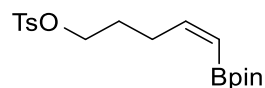
$R_f = 0.33$  (3:1 Hex:EtOAc);

$^1\text{H NMR}$  (400 MHz,  $\text{CDCl}_3$ , ppm)  $\delta$  6.39 (dt,  $J = 13.2, 6.9$  Hz, 1H), 5.44 (dd,  $J = 13.2, 0.8$  Hz, 1H), 3.57 (bs, 2H), 3.04 (bs, 1H), 2.47 (q,  $J = 7.1$  Hz, 2H), 1.64 (p,  $J = 6.1$  Hz, 2H), 1.29 (s, 12H);

$^{13}\text{C NMR}$  (100 MHz,  $\text{CDCl}_3$ , ppm)  $\delta$  153.4, 83.4, 60.0, 30.9, 27.9, 24.7 (boron substituted carbon, absent);

**IR** (neat, ATR,  $\text{cm}^{-1}$ ): 3437, 2980, 2934, 2869, 1627, 1422, 1311, 1260, 1143, 1064, 966;

**HRMS** (ES): calcd  $[\text{M} - \text{H}]^-$  ( $\text{C}_{11}\text{H}_{20}\text{BO}_3$ ) 211.1511, found 211.1515.



**(Z)-5-(4,4,5,5-tetramethyl-1,3,2-dioxaborolan-2-yl)pent-4-en-1-yl 4-methylbenzenesulfonate (3-64)**

To a flame-dried flask was added DMAP (2 mg, 0.002 mmol). The flask was evacuated and replenished with nitrogen three times, and then DCM (2 mL) was added. After the addition of

**3-63** (266 mg, 1.25 mmol) and NEt<sub>3</sub> (0.23 mL, 1.63 mmol), the flask was cooled to 0 °C, and *p*-TsCl (311 mg, 1.63 mmol) was added slowly. The flask was warmed to rt and stir overnight. The mixture was passed through a silica gel plug and concentrated *in vacuo*, and chromatography with 5:1 Hex:EtOAc gave 282 mg (61% yield) of the product.

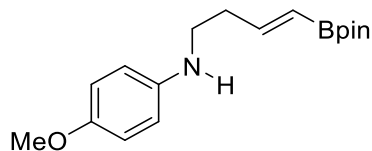
*R<sub>f</sub>* = 0.32 (5:1 Hex:EtOAc);

**<sup>1</sup>H NMR** (400 MHz, CDCl<sub>3</sub>, ppm) δ 7.79, (d, *J* = 8.4 Hz, 2H), 7.34 (d, *J* = 8.6, 2H), 6.31 (dt, *J* = 13.2, 7.1 Hz, 1H), 5.36 (dt, *J* = 13.6, 1.2 Hz, 1H), 4.03, (t, *J* = 6.8 Hz), 2.45 (s, 3H), 2.42 (tdd, *J* = 7.3, 7.3, 1.0 Hz, 2H), 1.74 (p, *J* = 7.1 Hz, 2H), 1.25 (s, 12H);

**<sup>13</sup>C NMR** (100 MHz, CDCl<sub>3</sub>, ppm) δ 152.3, 144.6, 133.3, 129.8, 127.9, 83.0, 70.1, 28.7, 28.0, 24.8, 21.6 (boron substituted carbon, absent);

**IR** (neat, ATR, cm<sup>-1</sup>): 2980, 2930, 2872, 1627, 1598, 1422, 1358, 1322, 1257, 1174, 1143, 966, 923;

**HRMS** (ES): calcd [M + Na]<sup>+</sup> (C<sub>18</sub>H<sub>27</sub>BO<sub>5</sub>SNa) 389.1565, found 389.1569.



**(*E*)-4-methoxy-*N*-(4-(4,4,5,5-tetramethyl-1,3,2-dioxaborolan-2-yl)but-3-en-1-yl)aniline (3-65)**

To a flame-dried flask were added 4-methoxyaniline (1.665 g, 13.5 mmol) and NaI (101 mg, 0.676 mmol). The flask was then evacuated and replenished with nitrogen three times. In a separate flask was added **3-60** (2.275 g, 6.45 mmol), which was then evacuated and replenished with nitrogen three times, followed by addition of DMSO (13.8 mL). The solution was transferred



via cannula to the first flask and was stirred overnight. The mixture was diluted with 1% aq NaOH, and extracted with Et<sub>2</sub>O. Organic extracts were washed with brine and then dried with MgSO<sub>4</sub>. Solvent was removed *in vacuo*, and chromatography with 4:1 Hex:EtOAc gave 1.059 g (54% yield) of a clear yellow oil.

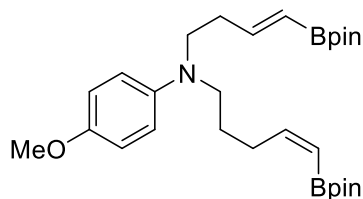
*R<sub>f</sub>* = 0.27 (4:1 Hex:EtOAc);

**<sup>1</sup>H NMR** (400 MHz, CDCl<sub>3</sub>, ppm) δ 6.72–6.68 (m, 2H), 6.55 (dt, *J* = 17.8, 6.7 Hz, 1H), 6.52–6.48 (m, 2H), 5.48 (dt, *J* = 18.0, 1.4 Hz, 1H), 3.67 (s, 3H), 3.11 (t, *J* = 6.8 Hz, 2H), 2.39 (tdd, *J* = 6.7, 6.7, 1.6 Hz, 2H), 1.20 (s, 12H) (NH proton absent);

**<sup>13</sup>C NMR** (100 MHz, CDCl<sub>3</sub>, ppm) δ 152.2, 151.0, 142.4, 114.9, 114.3, 83.2, 55.8, 43.4, 35.7, 24.8 (boron substituted carbon, absent);

**IR** (neat, ATR, cm<sup>-1</sup>): 3386, 2977, 2930, 2830, 1637, 1512, 1358, 1318, 1232, 1143, 1038, 966, 848, 816;

**HRMS** (ES): calcd [M + Na]<sup>+</sup> (C<sub>17</sub>H<sub>26</sub>NO<sub>3</sub>BNa) 326.1898, found 326.1909.



**4-methoxy-*N*-((*E*)-4-(4,4,5,5-tetramethyl-1,3,2-dioxaborolan-2-yl)but-3-en-1-yl)-*N*-((*Z*)-5-(4,4,5,5-tetramethyl-1,3,2-dioxaborolan-2-yl)pent-4-en-1-yl)aniline (3-66)**

To a flame-dried flask was added **3-65** (482 mg, 1.59 mmol), NaI (8 mg, 0.0530 mmol), and **3-64** (194 mg, 0.530 mmol). The flask was then evacuated and replenished with nitrogen three times, followed by addition of DMSO (1.0 mL). The mixture was stirred overnight at 50 °C. Upon

completion the reaction was neutralized with saturated aq NaHCO<sub>3</sub> and extracted with Et<sub>2</sub>O. Organic extracts were washed with brine and then dried with MgSO<sub>4</sub>. Solvent was removed *in vacuo*, and chromatography with 7:1 Hex:EtOAc gave 119 mg (45% yield) of a clear reddish-orange oil.

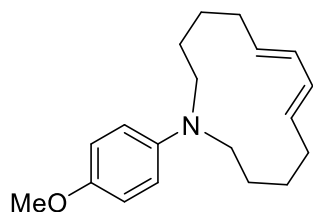
*R<sub>f</sub>* = 0.33 (7:1 Hex:EtOAc);

**<sup>1</sup>H NMR** (400 MHz, CDCl<sub>3</sub>, ppm) δ 6.83–6.78 (m, 2H), 6.67–6.58 (m, 3H), 6.44, (dt, *J* = 13.2, 7.1 Hz, 1H) 5.50 (dt, *J* = 18.0, 1.4 Hz, 1H), 5.37 (dt, *J* = 13.6, 1.2 Hz, 1H), 3.75 (s, 3H) 3.33–3.29 (m, 2H), 3.21–3.18 (m, 2H), 2.46–2.35 (m, 4H), 1.63 (p, *J* = 7.5, 2H), 1.266 (s, 12H), 1.265 (s, 12H);

**<sup>13</sup>C NMR** (100 MHz, CDCl<sub>3</sub>, ppm) δ 154.1, 151.4, 151.3, 142.7, 114.9, 114.5, 83.1, 82.9, 55.8, 51.2, 50.8, 33.5, 29.9, 27.1, 24.9, 24.8 (boron substituted carbons, absent);

**IR** (neat, ATR, cm<sup>-1</sup>): 2977, 2930, 1634, 1512, 1358, 1243, 1143, 1038, 970, 848, 812;

**HRMS** (ES): calcd [M + Na]<sup>+</sup> (C<sub>28</sub>H<sub>45</sub>NO<sub>5</sub>B<sub>2</sub>Na) 520.3376, found 520.3391.



**(6*E*,8*E*)-1-(4-methoxyphenyl)azacyclotrideca-6,8-diene (3-67)**

Following general procedure D, **3-52** (200 mg, 0.371 mmol) was reacted in the presence of chloroacetone (0.30 mL, 3.71 mmol), aq K<sub>2</sub>CO<sub>3</sub> (2 M, 0.9 mL, 1.85 mmol), and PdCl<sub>2</sub>(Ph<sub>3</sub>P)<sub>2</sub> (26 mg, 0.0371 mmol). Compound **3-52** was dissolved in 15 mL of MeOH prior to

transfer via cannula, and the total volume of MeOH was adjusted to 175 mL after the transfer. Chromatography with 20:1 petroleum ether/Et<sub>2</sub>O gave 50 mg (47% yield) of a white solid.

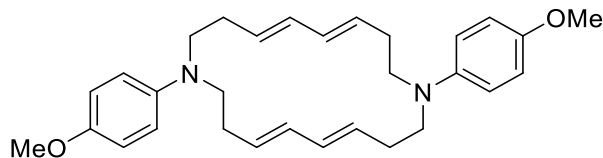
$R_f$  = 0.30 (20:1 petroleum ether/Et<sub>2</sub>O);

<sup>1</sup>H NMR (400 MHz, C<sub>6</sub>D<sub>6</sub>, ppm) δ 6.90–6.86 (m, 2H), 6.52–6.48 (m, 2H), 5.92–5.85 (m, 2H), 5.15–5.07 (m, 2H), 3.44 (s, 3H), 2.82–2.77 (m, 4H), 1.90 (q,  $J$  = 6.5 Hz, 4H), 1.36 (bs, 4H), 1.07 (bs, 4H);

<sup>13</sup>C NMR (100 MHz, CDCl<sub>3</sub>, ppm) δ 149.6, 143.1, 131.6, 131.3, 115.2, 110.5, 56.0, 48.9, 34.0, 23.3, 22.6;

IR (neat, ATR, cm<sup>-1</sup>): 3009, 2920, 2847, 1516, 1243, 1227, 1040, 1001, 803, 694;

HRMS (DART): calcd [M + H]<sup>+</sup> (C<sub>19</sub>H<sub>28</sub>NO) 286.21654, found 286.21564.



**(4E,6E,13E,15E)-1,10-bis(4-Methoxyphenyl)-1,10-diazacyclooctadeca-4,6,13,15-tetraene (3-68)**

Following general procedure D, **3-55** (271 mg, 0.561 mmol) was reacted in the presence of chloroacetone (0.45 mL, 5.61 mmol), aq K<sub>2</sub>CO<sub>3</sub> (2 M, 1.4 mL, 2.8 mmol), and PdCl<sub>2</sub>(Ph<sub>3</sub>P)<sub>2</sub> (39 mg, 0.0561 mmol). Compound **3-55** was dissolved in 50 mL of MeOH prior to transfer via cannula, and the total volume of MeOH was adjusted to 280 mL after the transfer. Chromatography with 6:1 Hex:EtOAc gave 10 mg (8% yield) of an off-white solid.

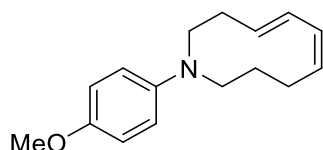
$R_f$  = 0.51 (6:1 Hex/EtOAc);

**<sup>1</sup>H NMR** (400 MHz, CDCl<sub>3</sub>, ppm) δ 6.83 (m, 8H) 6.10–6.03 (m, 4H), 5.67–5.60 (m, 4H), 3.77 (s, 6H), 3.17 (m, 8H), 2.25 (q, *J* = 6.1 Hz, 8H);

**<sup>13</sup>C NMR** (100 MHz, CDCl<sub>3</sub>, ppm) δ 153.5, 144.6, 131.0, 130.7, 120.0, 114.6, 55.7, 53.7, 31.5;

**IR** (neat, ATR, cm<sup>-1</sup>): 3012, 2948, 2926, 2833, 2812, 1512, 1458, 1441, 1239, 1181, 1035, 974, 822, 758, 693, 672;

**HRMS** (ES): calcd [M + H]<sup>+</sup> (C<sub>30</sub>H<sub>39</sub>N<sub>2</sub>O<sub>2</sub>) 459.30060, found 459.29927.



**(5Z,7E)-1-(4-methoxyphenyl)-1,2,3,4,9,10-hexahydroazecine (3-69)**

A flame-dried flask containing **3-66** (115 mg, 0.231 mmol) was evacuated and replenished three times with nitrogen. The flask was charged with MeOH (92 mL). A separate flask containing PdCl<sub>2</sub>(MeCN)<sub>2</sub> (6 mg, 0.0231 mmol) and tri(2-furyl)phosphine (11 mg, 0.0463 mmol) was evacuated and replenished three times with nitrogen, charged with MeOH (3 mL), and then stirred for 4 h. The solution was transferred via cannula, and the total volume of the reaction mixture was diluted to 116 mL with MeOH. Chloroacetone (0.18 mL, 1.16 mmol) was added, followed by aq K<sub>2</sub>CO<sub>3</sub> (2M, 0.58 mL, 2.31 mmol). The mixture was stirred at rt overnight. The reaction was passed through a Celite plug with EtOAc and then concentrated *in vacuo*. Chromatography with 10:1 Hex:EtOAc gave 27 mg (48% yield) of a clear light brown oil.

*R<sub>f</sub>* = 0.33 (10:1 Hex:EtOAc);

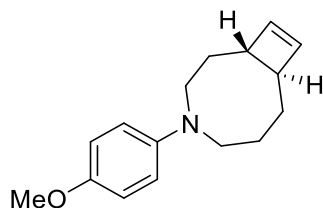
**<sup>1</sup>H NMR** (400 MHz, CDCl<sub>3</sub>, ppm) δ 6.85–6.81 (m, 2H), 6.73–6.69 (m, 2H), 6.06 (ddq, *J* = 10.5, 3.9, 1.2 Hz, 1H), 5.95 (ddq, *J* = 16.1, 4.0, 1.0 Hz, 1H), 5.73 (dtd, *J* = 10.4, 7.2, 1.2 Hz, 1H),

5.62 (dtd,  $J = 16.1, 7.5, 1.5$  Hz, 1H), 3.77 (s, 3H), 3.37–3.34 (m, 2H), 3.21–3.18 (m, 2H), 2.36 (q,  $J = 6.3$  Hz, 2H), 2.22 (q,  $J = 6.8$  Hz, 2H) 1.80 (p,  $J = 6.1$  Hz, 2H);

$^{13}\text{C}$  NMR (100 MHz,  $\text{CDCl}_3$ , ppm)  $\delta$  151.2, 144.0, 132.8, 132.5, 129.5, 129.4, 114.6, 114.4, 55.7, 55.32, 53.25, 32.0, 28.8, 24.0;

IR (neat, ATR,  $\text{cm}^{-1}$ ): 3011, 2928, 2830, 1508, 1463, 1356, 1291, 1238, 1181, 1037, 972, 1037, 972, 810, 745, 705, 665;

HRMS (ES): calcd  $[\text{M} + \text{H}]^+$  ( $\text{C}_{16}\text{H}_{22}\text{NO}$ ) 244.1701, found 244.1708.



#### 4-(4-methoxyphenyl)-4-azabicyclo[6.2.0]dec-9-ene (3-71)

Following general procedure D, **3-59** (200 mg, 0.402 mmol) was reacted in the presence of chloroacetone (0.32 mL, 4.02 mmol), aq  $\text{K}_2\text{CO}_3$  (2 M, 1.0 mL, 2.0 mmol), and  $\text{PdCl}_2(\text{Ph}_3\text{P})_2$  (28 mg, 0.0402 mmol). Compound **3-59** was dissolved in 40 mL of MeOH prior to transfer via cannula, and the total volume of MeOH was adjusted to 201 mL after the transfer. Chromatography with 20:1 Hex:EtOAc gave 51 mg (52% yield) of a clear light yellow oil.

$R_f = 0.71$  (8:1 Hex:EtOAc);

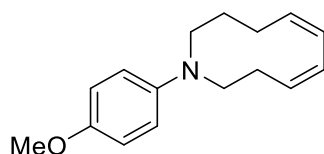
$^1\text{H}$  NMR (400 MHz,  $\text{CDCl}_3$ , ppm)  $\delta$  6.85–6.82 (m, 2H), 6.59–6.55 (m, 2H), 6.08 (ddd,  $J = 2.6, 1.2, 1.2$  Hz, 1H), 5.98 (ddd,  $J = 2.5, 1.1, 1.1$  Hz, 1H), 4.00 (dd,  $J = 15.2, 4.0$  Hz, 1H), 3.83 (ddd,  $J = 15.2, 2.9, 2.9$  Hz, 1H), 3.75 (s, 3H), 3.15 (ddd,  $J = 15.2, 12.6, 2.8$  Hz, 1H), 3.02 (dd,  $J = 14.8, 11.6$  Hz, 1H), 2.55 (dd,  $J = 12.2, 1.0$  Hz, 1H), 2.43 (d,  $J = 11.6$  Hz, 1H),

2.00–1.89 (m, 1H), 1.86–1.75 (m, 2H), 1.67 (dddd,  $J = 13.2, 2.6, 2.6, 2.5$  Hz, 1H), 1.57–1.46 (m, 2H);

$^{13}\text{C}$  NMR (100 MHz,  $\text{CDCl}_3$ , ppm)  $\delta$  150.2, 142.0, 139.7, 137.7, 115.0, 111.8, 56.0, 55.5, 52.7, 52.3, 50.7, 32.4, 32.0, 25.1;

IR (neat, ATR,  $\text{cm}^{-1}$ ): 3039, 2951, 2917, 2844, 1513, 1358, 1243, 1206, 1043, 910, 811, 744;

HRMS (ES): calcd  $[\text{M} + \text{H}]^+$  ( $\text{C}_{16}\text{H}_{22}\text{NO}$ ) 244.1696, found 244.1705.



**(5Z,7Z)-1-(4-methoxyphenyl)-1,2,3,4,9,10-hexahydroazecine (3-77)**

A flame-dried pressure tube containing **3-71** (200 mg, 0.0.822 mmol) and toluene (4 mL) was capped with a rubber stopper. The cap was sealed with Teflon tape and then electrical tape. The flask was backfilled with nitrogen after three freeze–pump–thaw cycles, and then the rubber stopper was replaced with a pressure tube cap. The flask was heated at 222 °C for 96 h with stirring behind a blast shield. Toluene was removed *in vacuo*, and chromatography with 20:1 Hex:EtOAc gave 134 mg (67% yield) of a yellow solid.

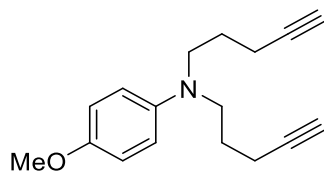
$R_f = 0.38$  (20:1 Hex:EtOAc);

$^1\text{H}$  NMR (400 MHz,  $\text{CDCl}_3$ , ppm)  $\delta$  6.87–6.79 (m, 4H), 5.99 (bd,  $J = 10.8$  Hz, 1H), 5.92 (bd,  $J = 11.2$  Hz, 1H), 5.74–5.67 (m, 1H), 5.51–5.46 (m, 1H), 3.76 (s, 3H), 3.19–3.16 (m, 2H), 3.05–3.02 (m, 2H), 2.37 (q,  $J = 6.1$  Hz, 2H), 2.11 (q,  $J = 6.1$  Hz, 2H), 1.57 (p,  $J = 6.0$  Hz, 2H);

$^{13}\text{C}$  NMR (125 MHz,  $\text{CDCl}_3$ , ppm)  $\delta$  152.8, 145.0, 133.2, 130.9, 128.9, 127.8, 119.8, 114.2, 55.7, 55.6, 43.4, 28.4, 24.7, 24.1;

IR (neat, ATR,  $\text{cm}^{-1}$ ): 3039, 2993, 2934, 2904, 2828, 1508, 1464, 1438, 1240, 1184, 1149, 1038, 824, 790, 770, 711, 664, 623;

HRMS (DART): calcd  $[\text{M} + \text{H}]^+$  ( $\text{C}_{16}\text{H}_{22}\text{NO}$ ) 244.16959, found 244.16852.



#### 4-methoxy-N,N-di(pent-4-yn-1-yl)aniline (3-80)

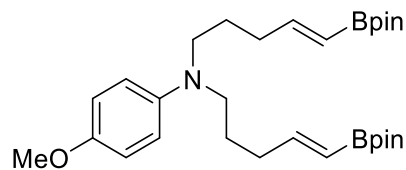
To a round bottom flask containing **3-61** (1.554 g, 6.52 mmol) equipped with a stir bar was added 4-methoxyaniline (402 mg, 3.26 mmol) and  $\text{K}_2\text{CO}_3$  (991 mg, 7.17 mmol). The flask was evacuated and replenished with nitrogen three times. The mixture was heated to 80 °C and stirred overnight. The mixture was passed through a short plug of silica with EtOAc and concentrated *in vacuo*. Chromatography with 6:1 Hex:EtOAc afforded 242 mg (30 % yield) of a clear yellow oil.

$^1\text{H}$  NMR (400 MHz,  $\text{CDCl}_3$ , ppm)  $\delta$  8.84-6.80 (m, 2H), 6.75-6.71 (m, 2H), 3.76 (s, 3H), 3.32 (t,  $J = 7.2$  Hz, 4H), 2.23 (td,  $J = 8.2, 2.8$  Hz, 4H), 1.99 (t,  $J = 2.8$  Hz, 2H), 1.76 (quin,  $J = 7.0$  Hz, 4H);

$^{13}\text{C}$  NMR (100 MHz,  $\text{CDCl}_3$ , ppm)  $\delta$  151.7, 142.7, 115.3, 114.7, 83.8, 68.6, 55.7, 50.9, 25.9, 15.9;

IR (neat, ATR): 3291, 3041, 2989, 2941, 2832, 2115, 1510, 1462, 1442, 1369, 1277, 1245, 1184, 1035, 814;

HRMS (DART): calcd  $[\text{M}]^+$  ( $\text{C}_{17}\text{H}_{21}\text{NO}$ ) 255.16231, found 255.16177.



**4-methoxy-*N,N*-bis((*E*)-5-(4,4,5,5-tetramethyl-1,3,2-dioxaborolan-2-yl)pent-4-en-1-yl)aniline (3-78)**

A flame dried round bottom flask containing **3-80** (242 mg, 0.948 mmol) and a stir bar was evacuated and replenished with nitrogen three times followed by addition of pinacolborane (0.55 mL, 3.79 mmol), NEt<sub>3</sub> (26 μL, 0.190 mmol). The mixture was transferred to a flask containing Cp<sub>2</sub>ZrHCl (49 mg, 0.190 mmol) via cannula and stirred overnight. The reaction was passed through a silica plug with EtOAc then concentrated *in vacuo*. Chromatography with 4:1 Hex:EtOAc gave 0.344 g (71 % yield) of a white solid.

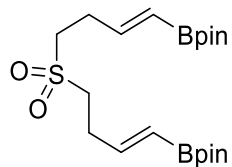
**<sup>1</sup>H-NMR** (400 MHz, C<sub>6</sub>D<sub>6</sub>, ppm) δ: 6.86 (dt, *J* = 18.0, 7.7 Hz, 2H), 6.79-6.76 (m, 2H), 6.57-6.54 (m, 2H), 5.71 (dt, *J* = 18.0, 1.5 Hz, 2H), 3.39 (s, 3H), 2.84 (t, *J* = 7.4 Hz, 4H), 1.92 (t, *J* = 7.1 Hz, 4H), 1.42 (p, *J* = 7.5 Hz, 4H), 1.05 (s, 24H);

**<sup>13</sup>C-NMR** (100 MHz, CDCl<sub>3</sub>, ppm) δ: 153.6, 151.4, 143.0, 115.1, 114.7, 82.9, 55.7, 51.6, 33.3, 25.8, 24.7;

**IR** (neat, ATR): 2977, 2932, 2876, 2836, 1639, 1510, 1362, 1349, 1321, 1241, 1140, 1039, 999, 966, 846, 818, 668, 644, 620;

**HRMS** (DART): calcd [M]<sup>+</sup> (C<sub>29</sub>H<sub>47</sub>B<sub>2</sub>NO<sub>5</sub>) 511.36403, found 511.36348.





**2,2'-((1E,1'E)-sulfonylbis(but-1-ene-4,1-diyl))bis(4,4,5,5-tetramethyl-1,3,2-dioxaborolane)**

**(3-79)**

Following general procedure A, **3-82** (1.276 g, 7.50 mmol) in DCM (5 mL) was reacted with pinacolborane (4.3 mL, 30.0 mmol) in the presence of NEt<sub>3</sub> (0.21 mL, 1.50 mmol) and Cp<sub>2</sub>ZrHCl (386 mg, 1.50 mmol). Chromatography with 3:2 Hex:EtOAc gave 1.808 g (57% yield) of a white solid.

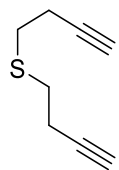
*R<sub>f</sub>* = 0.38 (2:1 Hex/EtOAc);

<sup>1</sup>H NMR (400 MHz, CDCl<sub>3</sub>, ppm) δ 6.55 (dt, *J* = 18.0, 6.2 Hz, 2H), 5.54 (dt, *J* = 17.9, 1.4 Hz, 2H), 3.07–3.03 (m, 4H), 2.70–2.64 (m, 4H), 1.25, (s, 24H);

<sup>13</sup>C NMR (100 MHz, CDCl<sub>3</sub>, ppm) δ 147.8, 83.3, 51.4, 27.6, 24.7 (boron substituted carbons, absent);

IR (neat, ATR, cm<sup>-1</sup>): 2979, 2927, 1637, 1364, 1320, 1265, 1143, 972, 846, 746, 639;

HRMS (DART): calcd [M + H]<sup>+</sup> (C<sub>20</sub>H<sub>37</sub>B<sub>2</sub>O<sub>6</sub>S) 427.24915, found 427.24824.



**di(but-3-yn-1-yl)sulfane (3-81)**

To a flask containing **3-53** (9.580 g, 42.7 mmol) was added sodium sulfide nonahydrate (4.663 g, 19.4 mmol). The flask was evacuated and replenished with nitrogen three times, followed by addition of DMSO (19 mL). The mixture was stirred at 80 °C overnight. The reaction was diluted with water and extracted with Et<sub>2</sub>O. The organic layer was washed with water and brine and then dried with MgSO<sub>4</sub>. The solvent was removed *in vacuo*. The crude mixture was purified by short path distillation at reduced pressure giving 1.391 g (52% yield) of the known<sup>55</sup> clear colorless oil.

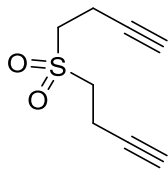
**Bp** = 97 °C (13 mmHg); *R<sub>f</sub>* = 0.37 (15:1 Hex/EtOAc);

**<sup>1</sup>H NMR** (400 MHz, CDCl<sub>3</sub>, ppm) δ 2.75 (t, *J* = 7.4 Hz, 4H), 2.50 (td, *J* = 7.3, 2.5 Hz, 4H), 2.04 (t, *J* = 2.6 Hz, 2H);

**<sup>13</sup>C NMR** (100 MHz, CDCl<sub>3</sub>, ppm) δ 82.3, 69.4, 30.8, 19.9;

**IR** (neat, ATR, cm<sup>-1</sup>): 3292, 2959, 2923, 2837, 2116, 1431, 1324, 1284, 1225, 643;

**HRMS** (DART): calcd [M + H]<sup>+</sup> (C<sub>8</sub>H<sub>11</sub>S) 139.05760, found 139.05713.



#### **4-(but-3-yn-1-ylsulfonyl)but-1-yne (3-82)**

A flask containing **3-81** (1.391 g, 10.1 mmol) was evacuated and replenished with nitrogen three times. After addition of DCM (67 mL), the mixture was cooled to 0 °C, followed by careful addition of mCPBA (3.647 g, 21.1 mmol). The mixture was stirred at 0 °C for 1 h, then warmed to rt, and stirred overnight. The mixture was diluted with water, extracted with DCM, and washed

with a saturated aq. NaHCO<sub>3</sub>. The organic layer was dried with MgSO<sub>4</sub> and concentrated *in vacuo*. Chromatography with 2:1 Hex:EtOAc gave 1.122 g (65% yield) of a white solid.

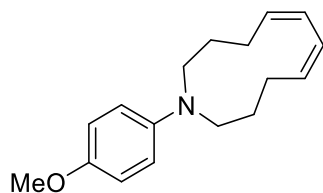
*R<sub>f</sub>* = 0.35 (2:1 Hex/EtOAc);

<sup>1</sup>H NMR (400 MHz, CDCl<sub>3</sub>, ppm) δ 3.28 (t, *J* = 7.2 Hz, 4H), 2.78 (td, *J* = 7.2, 2.8 Hz, 4H), 2.13 (t, *J* = 2.6 Hz, 2H);

<sup>13</sup>C NMR (100 MHz, CDCl<sub>3</sub>, ppm) δ 79.5, 71.1, 51.8, 12.7;

IR (neat, ATR, cm<sup>-1</sup>): 3276, 2935, 2361, 2337, 1305, 1257, 1115, 798, 648;

HRMS (DART): calcd [M + H]<sup>+</sup> (C<sub>8</sub>H<sub>11</sub>O<sub>2</sub>S) 170.04743, found 170.04679.



**(5Z,7Z)-1-(4-methoxyphenyl)azacycloundeca-5,7-diene (3-85)**

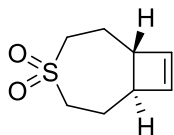
Following general procedure D, **3-78** (150 mg, 0.293 mmol) was reacted in the presence of chloroacetone (0.23 mL, 2.93 mmol), aq K<sub>2</sub>CO<sub>3</sub> (2 M, 0.73 mL, 1.47 mmol), and PdCl<sub>2</sub>(Ph<sub>3</sub>P)<sub>2</sub> (21 mg, 0.0293 mmol). Compound **3-78** was dissolved in 15 mL of MeOH prior to transfer via cannula, and the total volume of MeOH was adjusted to 147 mL after the transfer. Chromatography with 20:1 Hex:EtOAc gave 17 mg (23% yield) of the product.

<sup>1</sup>H NMR (400 MHz, CDCl<sub>3</sub>, ppm) δ 6.84-6.78 (m, 4H), 5.80 (d, *J* = 9.8 Hz, 2H), 5.50 (dt, *J* = 10.0, 7.4 Hz, 2H), 3.76 (s, 3H), 3.18-3.15 (m, 4H), 2.25 (q, *J* = 6.9 Hz, 4H), 1.76-1.72 (m, 4H);

$^{13}\text{C}$  NMR (100 MHz,  $\text{CDCl}_3$ , ppm)  $\delta$  152.3, 144.4, 132.2, 125.8, 117.6, 114.3, 55.6, 52.9, 26.8, 26.4;

IR (neat, ATR,  $\text{cm}^{-1}$ ): 3037, 2994, 2919, 2830, 1508, 1242, 1038, 816;

HRMS (DART): calcd  $[\text{M} + \text{H}]^+$  ( $\text{C}_{17}\text{H}_{24}\text{NO}$ ) 258.18579, found 288.18435.



#### 4-thiabicyclo[5.2.0]non-8-ene 4,4-dioxide (3-87)

A 1 dram vial was charged with  $\text{PdCl}_2(\text{MeCN})_2$  (5 mg, 0.0176 mmol) and tri(2-furyl)phosphine (8 mg, 0.0352 mmol), then capped with a rubber septa, and evacuated and backfilled with nitrogen three times. MeOH was added (3 mL), and the mixture was stirred for 90 min. This mixture was added via cannula to a separate flask sealed with a rubber septum, previously evacuated, and backfilled with nitrogen three times. MeOH (67 mL) was added to the mixture, followed by addition of chloroacetone (0.14 mL, 1.76 mL). A separate flask containing **3-79** (75 mg, 0.176 mmol) was capped with a rubber septum, then evacuated, and replenished with nitrogen three times. MeOH (18 mL) was added, and then the mixture was transferred via cannula to the palladium solution. After addition of aq  $\text{K}_2\text{CO}_3$  (2M, 0.44 mL, 0.880 mmol), the mixture was stirred for 24 h at rt. The reaction was passed through a Celite plug with EtOAc and then concentrated *in vacuo*. The mixture was diluted with water, extracted with DCM, and dried with  $\text{MgSO}_4$ . Solvent was removed *in vacuo*, and chromatography with 1.25:1 Hex:EtOAc gave 10 mg of an impure white solid product. Recrystallization with hexanes gave 8 mg (27%) of the white solid product.

$R_f$  = 0.20 (3:1  $\text{Et}_2\text{O}$ /petroleum ether);

**<sup>1</sup>H NMR** (400 MHz, CDCl<sub>3</sub>, ppm) δ 6.12 (d, *J* = 0.8 Hz, 2H) 3.36 (dddd, *J* = 15.1, 6.4, 6.4, 1.8 Hz, 2H), 3.25 (dddd, *J* = 15.1, 6.7, 6.7, 1.7 Hz, 2H), 2.99 (bdd, *J* = 12.0, 3.6 Hz, 2H), 2.11–2.04 (m, 2H), 1.80–1.70 (m, 2H);

**<sup>13</sup>C NMR** (100 MHz, CDCl<sub>3</sub>, ppm) δ 137.5, 58.0, 48.6, 24.2;

**IR** (neat, ATR, cm<sup>-1</sup>): 3038, 2927, 2876, 1415, 1268, 1134, 1107, 853, 767, 691;

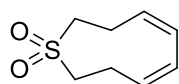
**HRMS** (DART): calcd [M + H]<sup>+</sup> (C<sub>8</sub>H<sub>13</sub>O<sub>2</sub>S), 173.06308 found 173.06250.

### **Thermal Ring Opening of 3-87 and Purification of (4Z,6Z)-2,3,8,9-tetrahydrothionine 1,1-dioxide (3-88) and (5Z,7Z)-2,3,4,9-tetrahydrothionine 1,1-Dioxide (3-89)**

A flame-dried pressure tube containing **3-87** (22 mg, 0.128 mmol) and toluene (6.1 mL) was capped with a rubber stopper, which was held on by one layer of Teflon tape and electrical tape each. The pressure tube was backfilled with nitrogen after three freeze–pump cycles, and then the rubber stopper was replaced with a pressure tube cap. The pressure tube was heated at 222 °C over the course of 7 days with stirring behind a blast shield. Toluene was removed *in vacuo*. Chromatography with 1.5:1 Hex:EtOAc gave 5 mg of **3-89** as a white solid, plus 9 mg of a 1.0:2.5:0.07 mixture of **3-88:3-89:3-79**, corresponding to a total of 2.5 mg of **3-88** (11% yield, calculated by <sup>1</sup>H NMR analysis) and 11.3 mg (51% yield, calculated by <sup>1</sup>H NMR analysis) of **3-89**, for a combined yield of 62%.

An analytically pure sample of **3-88** was obtained by further chromatographic separation with silver nitrate impregnated silica gel. First, silver nitrate (78 mg) was dissolved in water (5 mL) and then added to silica gel (780 mg) in a beaker, stirred, covered in foil, and let dry in the oven overnight to make a 10% by weight silver nitrate impregnated silica gel. Chromatography with 1:1 Hex:EtOAc gave two mixtures, and all fractions containing **3-87** were discarded and the

rest were subject to further chromatography. Silver nitrate (117 mg) was dissolved in water (5 mL), then added to silica gel (780 mg) in a beaker, stirred, covered in foil, and let dry in the oven overnight to make a 15% by weight silver nitrate impregnated silica gel. Chromatography with 3:1 Hex:EtOAc gave 1 mg of the white solid **3-88**.



**(4Z,6Z)-2,3,8,9-tetrahydrothionine 1,1-dioxide (3-88)**

Yield: 11%, calculated by  $^1\text{H}$  NMR analysis.

$R_f$  = 0.38 (1:1 Hex:EtOAc);

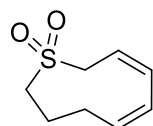
$^1\text{H}$  NMR (400 MHz,  $\text{CDCl}_3$ , ppm)  $\delta$  6.01–5.97(m, 2H), 5.73–5.66 (m, 2H), 3.33–3.30 (m, 2H), 2.65–2.60 (m, 2H);

$^{13}\text{C}$  NMR (125 MHz,  $\text{CDCl}_3$ , ppm)  $\delta$  128.4 (b), 54.5, 23.0;

$^{13}\text{C}$  NMR (125 MHz, DEPT-45, 45 °C,  $\text{CDCl}_3$ , ppm)  $\delta$  128.4, 128.3, 54.5, 23.0;

IR (neat, ATR,  $\text{cm}^{-1}$ ): 3004, 2926, 2853, 1460, 1442, 1371, 1335, 1280, 1204, 1119, 805, 779, 671, 655;

HRMS (DART): calcd  $[\text{M} + \text{H}]^+$  ( $\text{C}_8\text{H}_{13}\text{O}_2\text{S}$ ) 173.06308, found 173.06273.



**(5Z,7Z)-2,3,4,9-tetrahydrothionine 1,1-dioxide (3-89)**

Yield: 51%, calculated by  $^1\text{H}$  NMR analysis.

$R_f = 0.47$  (1:1 Hex:EtOAc);

$^1\text{H NMR}$  (400 MHz,  $\text{C}_6\text{D}_6$ , ppm)  $\delta$  5.67 (dm,  $J = 10.8$  Hz, 1H), 5.36 (dm,  $J = 10.8$  Hz, 1H), 5.29 (dddd,  $J = 10.2, 8.5, 8.5, 1.7$  Hz, 1H), 5.00 (dddd,  $J = 10.2, 8.6, 8.6, 1.5$  Hz, 1H), 3.21 (dm,  $J = 8.4$ , Hz, 2H), 2.61–2.57 (m, 2H), 1.90 (q,  $J = 6.9$  Hz, 2H), 1.29 (bp,  $J = 6.2$  Hz, 2H);

$^{13}\text{C NMR}$  (125 MHz,  $\text{CDCl}_3$ , ppm)  $\delta$  135.2, 133.7, 128.3, 119.9, 57.3, 56.2, 27.2, 22.6;

**IR** (neat, ATR,  $\text{cm}^{-1}$ ): 3007, 2967, 2920, 2851, 1739, 1368, 1308, 1284, 1228, 1201, 1116, 1037, 815, 769, 741, 716, 665, 620;

**HRMS** (DART): calcd  $[\text{M} + \text{H}]^+$  ( $\text{C}_8\text{H}_{13}\text{O}_2\text{S}$ ) 173.06308, found 173.0626.

### 3.6 Supporting Information

Detailed experimental kinetic data is provided in Appendix B.

### 3.7 Copyright Information

Portions of chapter are duplicated with permission from the following publication:

Boon, B. A.; Green, A. G.; Liu, P.; Houk, K. N.; Merlic, C. A. *J. Org. Chem.* **2017**, 82, 4613. DOI: 10.1021/acs.joc.7b00203

ACS Articles on Request Direct Link:

<http://pubs.acs.org/articlesonrequest/AOR-Qfhb48aDT6iNzfyX4jv>

### 3.8 References and Notes

- (1) Wiberg, K. B. *Angew. Chem. Int. Ed. Engl.* **1986**, 25, 312.
- (2) Corey, E. J.; Carey, F. A.; Winter, R. A. E. *J. Am. Chem. Soc.* **1965**, 87, 934.
- (3) Cope, A. C.; Bach, R. D. *Org. Synth.* **1969**, 49, 39.

- (4) Brecht, J. *Justus Liebigs Ann. Chem.* **1924**, 437, 1.
- (5) Shea, K. J. *Tetrahedron* **1980**, 36, 1683.
- (6) Vogel, E. *Angew. Chem.* **1954**, 66, 640.
- (7) Vogel, E. *Justus Liebigs Ann. Chem.* **1958**, 615, 14.
- (8) Criegee, R.; Noll, K. *Justus Liebigs Ann. Chem.* **1959**, 627, 1.
- (9) Criegee, R.; Seebach, D.; Winter, R. E.; Börretzen, B.; Brune, H.-A. *Chem. Ber.* **1965**, 98, 2339.
- (10) Winter, R. E. K. *Tetrahedron Lett.* **1965**, 6, 1207.
- (11) Woodward, R. B.; Hoffmann, R. *J. Am. Chem. Soc.* **1965**, 87, 395.
- (12) Woodward, R. B.; Hoffmann, R. *Angew. Chem. Int. Ed. Engl.* **1969**, 8, 781.
- (13) Kirmse, W.; Rondan, N. G.; Houk, K. N. *J. Am. Chem. Soc.* **1984**, 106, 7989.
- (14) Dolbier, W. R.; Koroniak, H.; Houk, K. N.; Sheu, C. *Acc. Chem. Res.* **1996**, 29, 471.
- (15) Ralph, M. J.; Harrowven, D. C.; Gaulier, S.; Ng, S.; Booker-Milburn, K. I. *Angew. Chem. Int. Ed.* **2015**, 54, 1527.
- (16) Trost, B. M.; Tanoury, G. J. *J. Am. Chem. Soc.* **1988**, 110, 1636.
- (17) Branton, G. R.; Frey, H. M.; Montague, D. C.; Stevens, I. D. R. *Trans. Faraday Soc.* **1966**, 62, 659.
- (18) Branton, G. R.; Frey, H. M.; Skinner, R. F. *Trans. Faraday Soc.* **1966**, 62, 1546.
- (19) Schreiber, S. L.; Santini, C. *Tetrahedron Lett.* **1981**, 22, 4651.



- (20) Schreiber, S. L.; Santini, C. *J. Am. Chem. Soc.* **1984**, *106*, 4038.
- (21) Shumate, K. M.; Neuman, P. N.; Fonken, G. J. *J. Am. Chem. Soc.* **1965**, *87*, 3996.
- (22) González, N.; Rodríguez, J.; Kerr, R. G.; Jiménez, C. *J. Org. Chem.* **2002**, *67*, 5117.
- (23) Beaudry, C. M.; Malerich, J. P.; Trauner, D. *Chem. Rev.* **2005**, *105*, 4757.
- (24) Gil-Av, E.; Shabtai, J. *J. Org. Chem.* **1964**, *29*, 257.
- (25) Brauman, J. I.; Archie, W. C. *J. Am. Chem. Soc.* **1972**, *94*, 4262.
- (26) Srinivasan, R. *J. Am. Chem. Soc.* **1969**, *91*, 7557.
- (27) Souris, C.; Misale, A.; Chen, Y.; Luparia, M.; Maulide, N. *Org. Lett.* **2015**, *17*, 4486.
- (28) Wang, X.-N.; Krenske, E. H.; Johnston, R. C.; Houk, K. N.; Hsung, R. P. *J. Am. Chem. Soc.* **2014**, *136*, 9802.
- (29) Sader, C. A.; Houk, K. N. *J. Org. Chem.* **2012**, *77*, 4939.
- (30) Iafe, R. G.; Kuo, J. L.; Hochstatter, D. G.; Saga, T.; Turner, J. W.; Merlic, C. A. *Org. Lett.* **2013**, *15*, 582.
- (31) Boon, B. A.; Green, A. G.; Liu, P.; Houk, K. N.; Merlic, C. A. *J. Org. Chem.* **2017**, *82*, 4613.
- (32) Wheeler, S. E.; Houk, K. N.; Schleyer, P. v. R.; Allen, W. D. *J. Am. Chem. Soc.* **2009**, *131*, 2547.
- (33) Zhao, M.; Gimarc, B. M. *J. Phys. Chem.* **1993**, *97*, 4023.
- (34) Qin, C.; Davis, S. R.; Zhao, Z.; Magers, D. H. *J. Phys. Chem. A* **2006**, *110*, 2034.

- (35) Tan, B.; Long, X.; Li, J. *Comput. Theor. Chem.* **2012**, *993*, 66.
- (36) Wang, Y. D.; Kimball, G.; Prashad, A. S.; Wang, Y. *Tetrahedron Lett.* **2005**, *46*, 8777.
- (37) Ohmura, T.; Yamamoto, Y.; Miyaura, N. *J. Am. Chem. Soc.* **2000**, *122*, 4990.
- (38) Tumey, L. N.; Bhagirath, N.; Brennan, A.; Brooijmans, N.; Lee, J.; Yang, X.; Boschelli, D. H. *Bioorg. Med. Chem.* **2009**, *17*, 7933.
- (39) Iafe, R. G.; Chan, D. G.; Kuo, J. L.; Boon, B. A.; Faizi, D. J.; Saga, T.; Turner, J. W.; Merlic, C. A. *Org. Lett.* **2012**, *14*, 4282.
- (40) Trost, B. M.; Yanai, M.; Hoogsteen, K. *J. Am. Chem. Soc.* **1993**, *115*, 5294.
- (41) Borčić, S.; Roberts, J. D. *J. Am. Chem. Soc.* **1965**, *87*, 1056.
- (42) Lutnæs, O. B.; Ruden, T. A.; Helgaker, T. *Magn. Reson. Chem.* **2004**, *42*, S117.
- (43) Lodewyk, M. W.; Siebert, M. R.; Tantillo, D. J. *Chem. Rev.* **2011**, *112*, 1839.
- (44) Lodewyk, M. W.; Soldi, C.; Jones, P. B.; Olmstead, M. M.; Rita, J.; Shaw, J. T.; Tantillo, D. J. *J. Am. Chem. Soc.* **2012**, *134*, 18550.
- (45) See Experimental section for further details.
- (46) Cooper, W.; Walters, W. D. *J. Am. Chem. Soc.* **1958**, *80*, 4220.
- (47) Frey, H. M.; Marshall, D. C. *Trans. Faraday Soc.* **1965**, *61*, 1715.
- (48) Allen, F. H.; Kennard, O.; Watson, D. G.; Brammer, L.; Orpen, A. G.; Taylor, R. *J. Chem. Soc. Perkin Trans. 2* **1987**, 1.
- (49) Detailed experimental kinetic data is provided in Appendix B.

- (50) Davison, E. C.; Fox, M. E.; Holmes, A. B.; Roughley, S. D.; Smith, C. J.; Williams, G. M.; Davies, J. E.; Raithby, P. R.; Adams, J. P.; Forbes, I. T.; Press, N. J.; Thompson, M. J. *J. Chem. Soc. Perkin Trans. 1* **2002**, 1494.
- (51) Erixon, K. M.; Dabalos, C. L.; Leeper, F. J. *Org. Biomol. Chem.* **2008**, *6*, 3561.
- (52) Berná, J.; Crowley, J. D. D.; Goldup, S. M. M.; Hänni, K. D. D.; Lee, A.-L.; Leigh, D. A. *Angew. Chem. Int. Ed.* **2007**, *46*, 5709.
- (53) Balas, L.; Bertrand-Michel, J.; Viars, F.; Faugere, J.; Lefort, C.; Caspar-Bauguil, S.; Langin, D.; Durand, T. *Org. Biomol. Chem.* **2016**, *14*, 9012.
- (54) Guo, H.; O'Doherty, G. A. *Org. Lett.* **2005**, *7*, 3921.
- (55) Miles, L. W. C.; Owen, L. N. *J. Chem. Soc.* **1952**, 817.

## Chapter 4

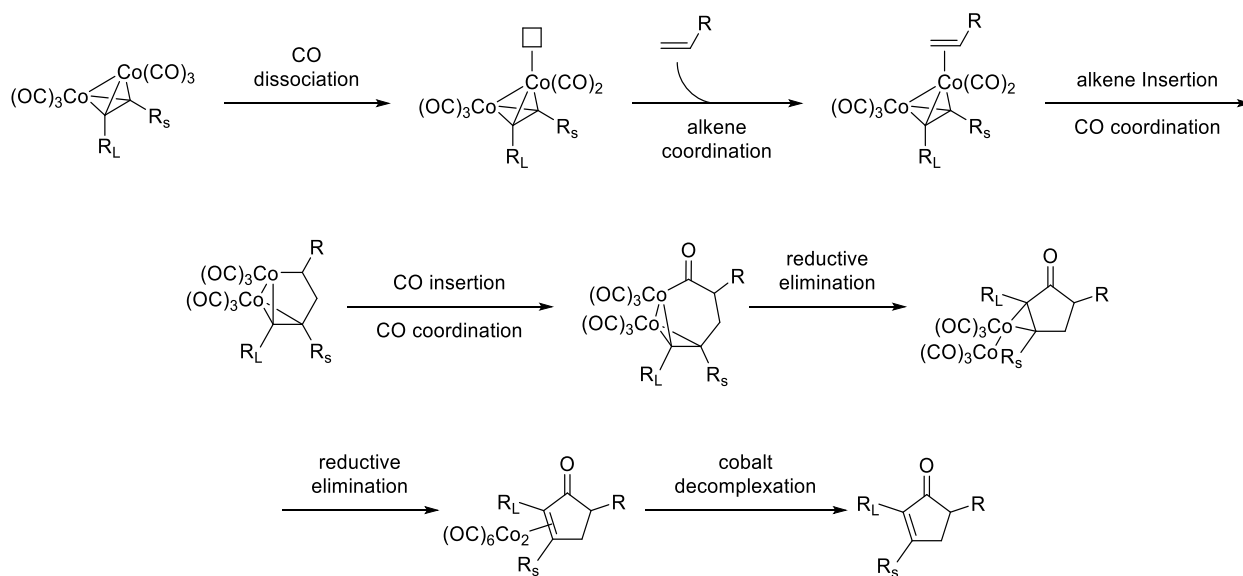
### The Transannular Pauson-Khand Reaction

#### 4.1 Abstract

The Pauson-Khand reaction is a powerful tool for the synthesis of cyclopentenones through the efficient [2+2+1] cycloaddition of dicobalt alkyne complexes with alkenes. While intermolecular and intramolecular variants are widely known, transannular versions of this reaction are unknown and the basis of this study. First, previous experimental studies by Dr. Sedef Karabiyikoglu are highlighted that established the key structural requirements leading to her discovery of the first transannular Pauson-Khand reaction. This successful reaction required a cyclic enyne substrate with one long chain and one short three-atom chain linking the alkene and alkyne moieties. Formation of the transannular Pauson-Khand product rather than products from transannular [4+2], intermolecular [2+2+2], or intermolecular [2+2+1] pathways was enabled by judicious choice of promoter. From the insights gleaned from these studies, further substrate modification lead to our second demonstration of the transannular Pauson-Khand reaction of a cyclic enyne incorporating a rigid aryl linker in the backbone of the long linker chain. This rigid aryl linker is proposed to facilitate the transannular [2+2+1] cyclization. Furthermore, computational studies revealed that transannular Pauson-Khand reactions are thermodynamically favored for cyclic enynes featuring a long linker of at least 5 carbons, but with smaller chains the reactions are thermodynamically disfavored. Experimental studies show that linking chains with more than 5 members are required to prevent to steric interactions between the dicobalt hexacarbonyl moiety and the linking chain to allow the reaction to be kinetically favored.

## 4.2 Introduction

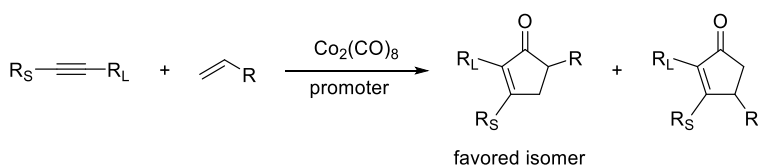
Of the many modes of reactivity exhibited by dicobalt hexacarbonyl alkyne complexes, one of the most useful and well-studied is the Pauson-Khand (PK) reaction. The reaction allows the efficient synthesis of cyclopentenones from simple alkene and alkyne starting materials in the presence of dicobalt octacarbonyl or from alkenes and dicobalt hexacarbonyl alkyne complexes (Scheme 4.1).<sup>1-7</sup> The method's utility and efficiency is demonstrated in many total syntheses.<sup>8-16</sup> Transannular reactions catalyzed or promoted by organometallic species, although known, are not well explored.<sup>17-19</sup> Since transannular reactions are exceptionally powerful at generating molecular complexity,<sup>20</sup> as exemplified by the transannular Diels-Alder reaction,<sup>21-26</sup> we seized this opportunity to expand the scope of these methodologies to demonstrate examples of the transannular Pauson-Khand reaction.



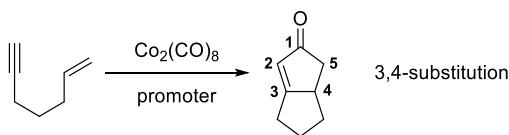
**Scheme 4.1. Mechanism of the Pauson-Khand reaction.**

Generally, intermolecular and intramolecular PK reactions give complementary regiochemistries.<sup>3,27,28</sup> Intermolecular PK reactions preferentially give cyclopentenones with large substituents at the alpha positions (Figure 4.1a). Intramolecular reactions of 1,6- and 1,7-enynes give bicyclic 3,4-disubstituted cyclopentenones (Figure 4.1b). On the other hand, a transannular Pauson-Khand (TAPK) reaction would be expected to yield bridged tricyclic cyclopentenone derivatives (Figure 4.1c), but the reaction is unprecedented in the PK literature.

a) Intermolecular PK Reactions



b) Intramolecular PK Reactions



c) This Work: Transannular PK Reactions

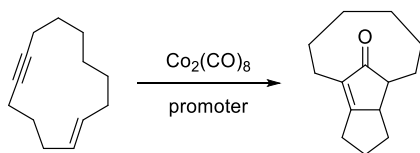
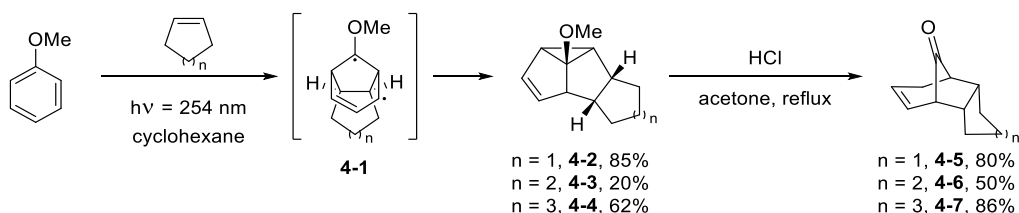


**Figure 4.1. Regioselectivity of inter- and intramolecular Pauson-Khand reactions and the transannular Pauson-Khand reaction.**

Although bridged tricyclic cyclopentenones with bridgehead alkenes expected from the proposed TAPK reaction are unknown (Figure 4.1c), isomeric tricyclic enones with a similar tricyclic framework are known. Photochemical 1,3-additions of anisole derivatives to cyclic olefins give tetracyclic adducts, which upon treatment with acid rearrange to tricyclic enones with fused bicyclo[3.2.1]octenone frameworks.<sup>29,30</sup> A selection of cyclic olefins are highlighted in

Scheme 4.2.<sup>31</sup> The substrate scope is limited to the fused bicyclo[3.2.1] core structure due to the requirement for aromatic starting materials, although different cyclic alkenes allow different sized fused rings. On the other hand, discovery of a general TAPK reaction process would provide access to a similar library of compounds with a variety of bridging ring lengths.

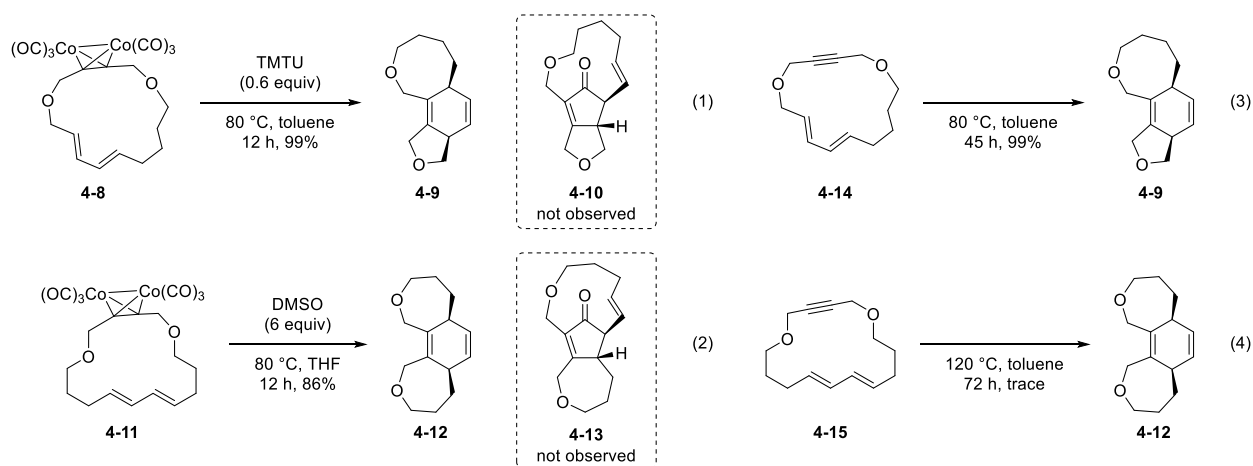


**Scheme 4.2. Synthesis of fused bicyclo[3.2.1]octenone rings.**

The remainder of this introduction highlights the extensive work to establish the structural requirements and reaction conditions leading to the first TAPK reaction by my colleague Dr. Sedef Karabiyikoglu during her graduate studies.<sup>32</sup> These studies provided the groundwork for our discovery of the second TAPK reaction. Further examination of the reactivity of these dicobalt-hexacarbonyl alkyne complexes will be discussed to highlight [4+2], [2+2+2], and [2+2+1+1] reactions observed of these macrocyclic enynes and dienyne, controlled by proper choice of reaction conditions.

Macrocyclic dicobalt hexacarbonyl dienyne complexes served as entry points for the proposed TAPK reaction as they were easily prepared employing our palladium-catalyzed oxidative macrocyclization of terminal bis(vinylboronate esters),<sup>33,34</sup> followed by dicobalt octacarbonyl complexation.<sup>35,36</sup> Previously, Dr. Karabiyikoglu reported the serendipitous discovery that dienyne complexes **4-8** and **4-11** undergo smooth transannular Diels-Alder (TADA) reactions (eq 1 and 2, Scheme 4.3) under mild reaction conditions, rather than the TAPK reaction.<sup>34</sup> This mode of reactivity is due to low transition state distortion energies imparted on the diene and

dienophile by their linking tethers and the strain release of the tethers in the transition state.<sup>37</sup> Choice of promoter to activate loss of a carbonyl group was critical for success of the reaction, as is known for many reactions with dicobalt hexacarbonyl alkyne complexes.<sup>38</sup> Tetramethylthiourea (TMTU)<sup>39</sup> and DMSO<sup>40</sup> were found to be the optimal promoters for **4-8** and **4-11**, respectively. On the other hand, cobalt-free Diels-Alder reactions were less efficient. Heating dienyne **4-14** at high temperatures to form TADA product **4-9** required 45 h for completion (eq 3), compared to 12 hours for the analogous cobalt complex **4-8** (eq 1). The TADA reaction of dienyne **4-15** only gave trace amounts of **4-12** at high temperature (eq 4), compared to the efficient TADA reaction of complex **4-11** to form **4-12** (eq 2).

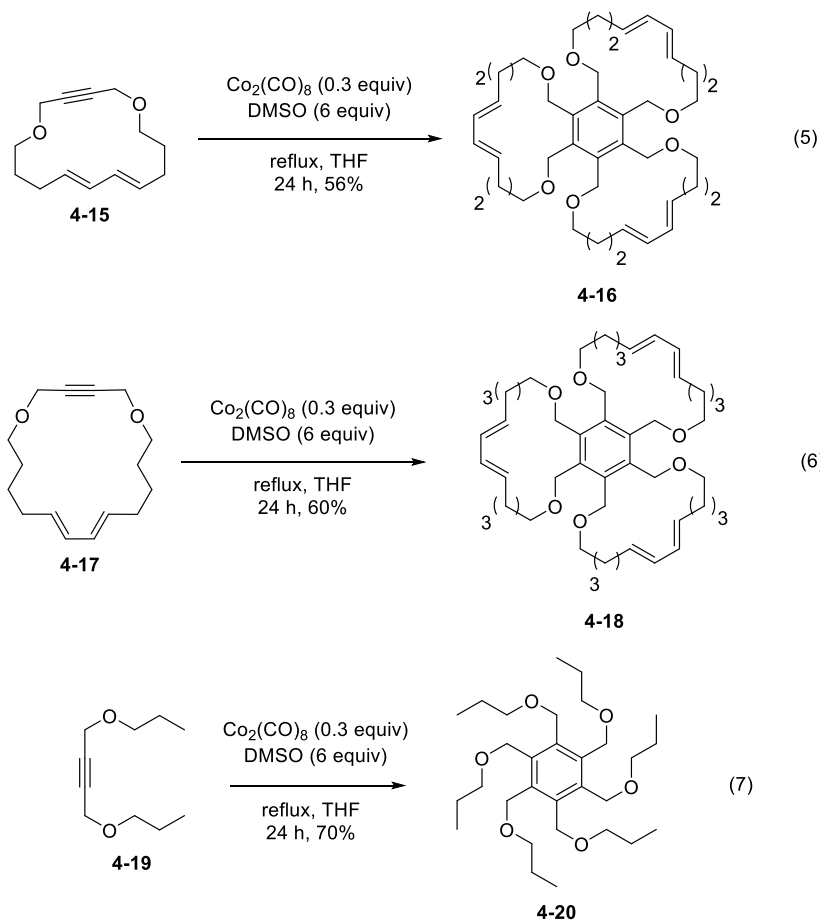


**Scheme 4.3. Transannular Diels-Alder reactions of macrocyclic dienynes and dienyne cobalt complexes.**

The reaction of free dienynes with catalytic dicobalt octacarbonyl were similarly unsuitable for the TAPK reactions, but underwent intermolecular [2+2+2] reactions instead.<sup>32</sup> Heating dienyne **4-15** in the presence of catalytic dicobalt octacarbonyl (0.3 equiv) gave trimer **4-16** from a [2+2+2] cycloaddition reaction in moderate yield (eq 5, Scheme 4.4). In contrast, the preformed dicobalt alkyne complex **4-11** underwent the TADA reaction under identical reaction conditions

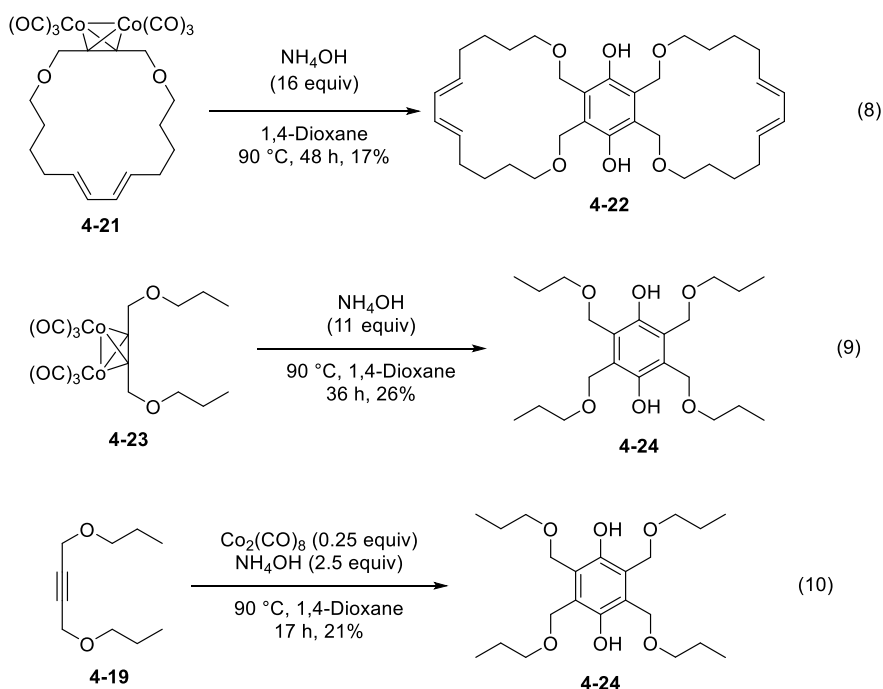


(eq 2, Scheme 4.3). The larger 18-membered dienyne **4-17** underwent a similar [2+2+2] cycloaddition reaction to give **4-18** (eq 6). Neither TADA or TAPK reaction products were observed in either case. The method was demonstrated to be equally effective for the [2+2+2] cycloaddition of non-macrocyclic alkyne **4-19** (eq 7).



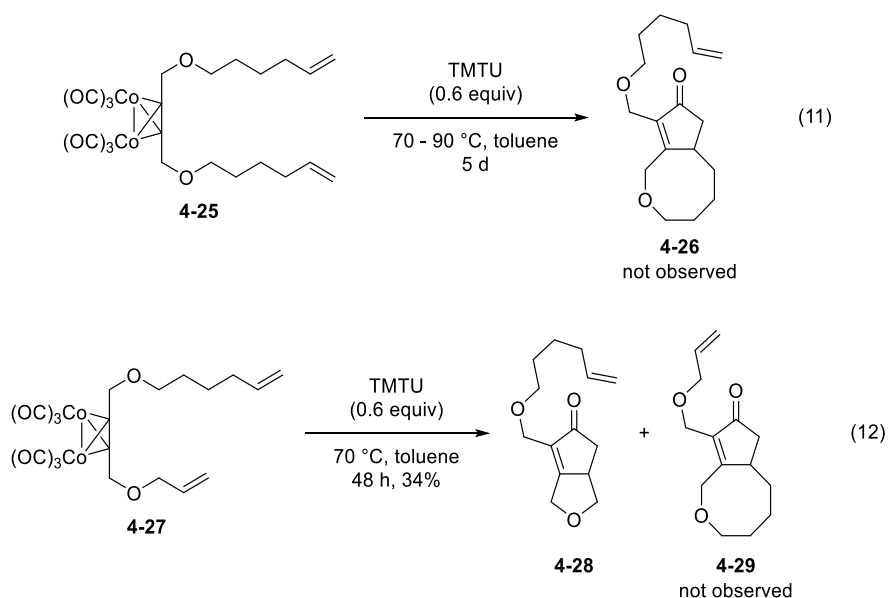
**Scheme 4.4. Dicobalt octacarbonyl catalyzed intermolecular [2+2+2] cycloaddition reactions.**

Different reaction promoters were demonstrated to affect the CO dissociation pathway, leading to alternative reaction pathways for dicobalt hexacarbonyl dienyne complexes.<sup>32</sup> The 18-membered diene **4-17**, shown to undergo a [2+2+2] cycloaddition in the presence of catalytic dicobalt octacarbonyl (eq 6, Scheme 4.4) was tested as the dicobalt hexacarbonyl complex **4-21** with ammonium hydroxide as a promoter.<sup>41</sup> Under these conditions the [2+2+1+1] cycloaddition product **4-22** was formed as the sole identifiable product (eq 8, Scheme 4.5). It is noteworthy that while complex **4-21** and its cobalt-free analog **4-17** participated in the [2+2+1+1] and [2+2+2] cycloaddition reactions, neither gave a successful TADA reaction. A non-macrocylic example of the [2+2+1+1] process was also discovered by converting alkyne complex **4-23** to hydroquinone **4-24** (eq 9). This reactivity mode promoted by ammonium hydroxide was even observed for the cobalt-free alkyne **4-19** in the presence of catalytic dicobalt octacarbonyl (eq 10).



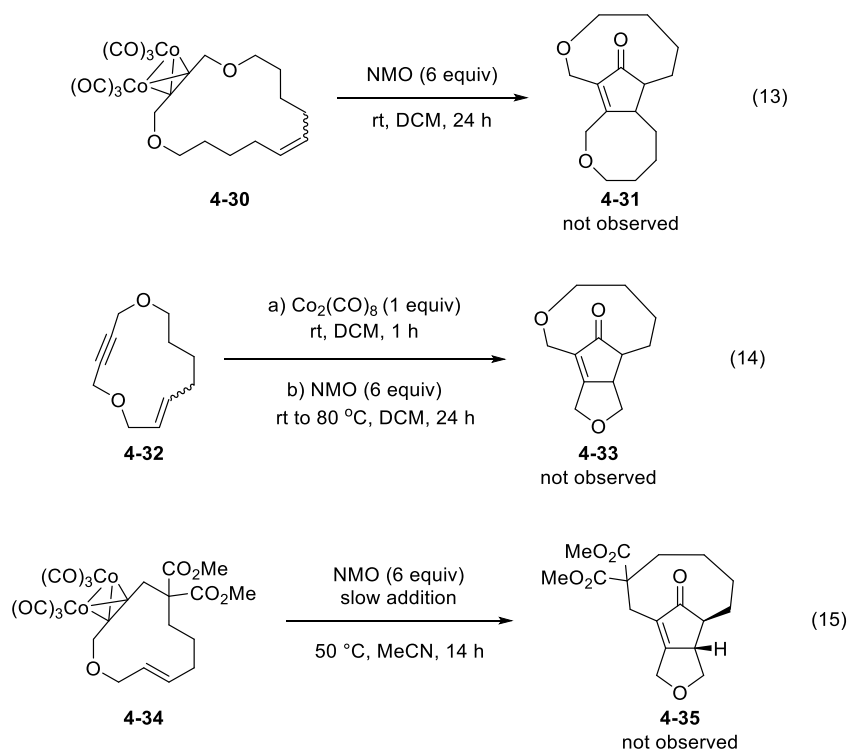
**Scheme 4.5. Intermolecular [2+2+1+1] cycloaddition reactions promoted by NH<sub>4</sub>OH.**

The effect of chain length between the alkene and dicobalt hexacarbonyl alkyne moieties in intramolecular reactions highlighted that chain length would be an important factor in the TAPK reaction.<sup>32</sup> Heating dienyne complex **4-25** in toluene over 5 days in the presence of TMTU gave a complex mixture of inseparable and unidentifiable compounds (eq 11, Scheme 4.6). The expected intramolecular PK reaction product **4-26** could not be isolated or detected. In contrast, unsymmetrical acyclic dienyne complex **4-27** gave cyclopentenone product **4-28** in 34% yield in the presence of TMTU (eq 12). Regioisomer **4-29** from the reaction with the alkene separated by the longer tether which would lead to an unfavored 8-membered ring was not observed. These results suggested that successful TAPK reactions might require formation of a 5-membered ring fused at the 3- and 4-positions of the cyclopentenone ring.



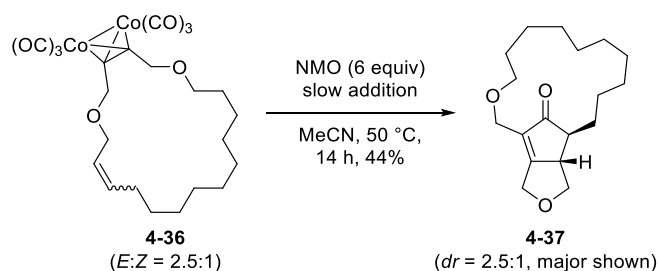
**Scheme 4.6. Effects of tether chain length on intramolecular PK reactions.**

Treatment of three substrates with PK reaction conditions established the basis for optimal chain lengths between the alkene and dicobalt hexacarbonyl moieties.<sup>32</sup> Similar to the failed intramolecular PK reaction of linear cobalt complex **4-25** (eq 11, Scheme 4.6), complex **4-30** was unable to form the fused eight-membered cyclopentenone TAPK product **4-31** (eq 13, Scheme 4.7). Enyne **4-32** was expected to form the fused five-membered cyclopentenone TAPK product **4-33** based on the successful intramolecular PK reaction of **4-27** to give **4-28** (eq 12, Scheme 4.6), but did not. These data suggested the length of the second bridging chain should be modified to find an optimal TAPK substrate. The inability of complex **4-34** to undergo the TAPK reaction to give cyclopentenone **4-35** (eq 15) confirmed that the length of the second chain was an opportunity for further substrate modification.



**Scheme 4.7. Attempted TAPK reactions to investigate the effect of linking tether lengths.**

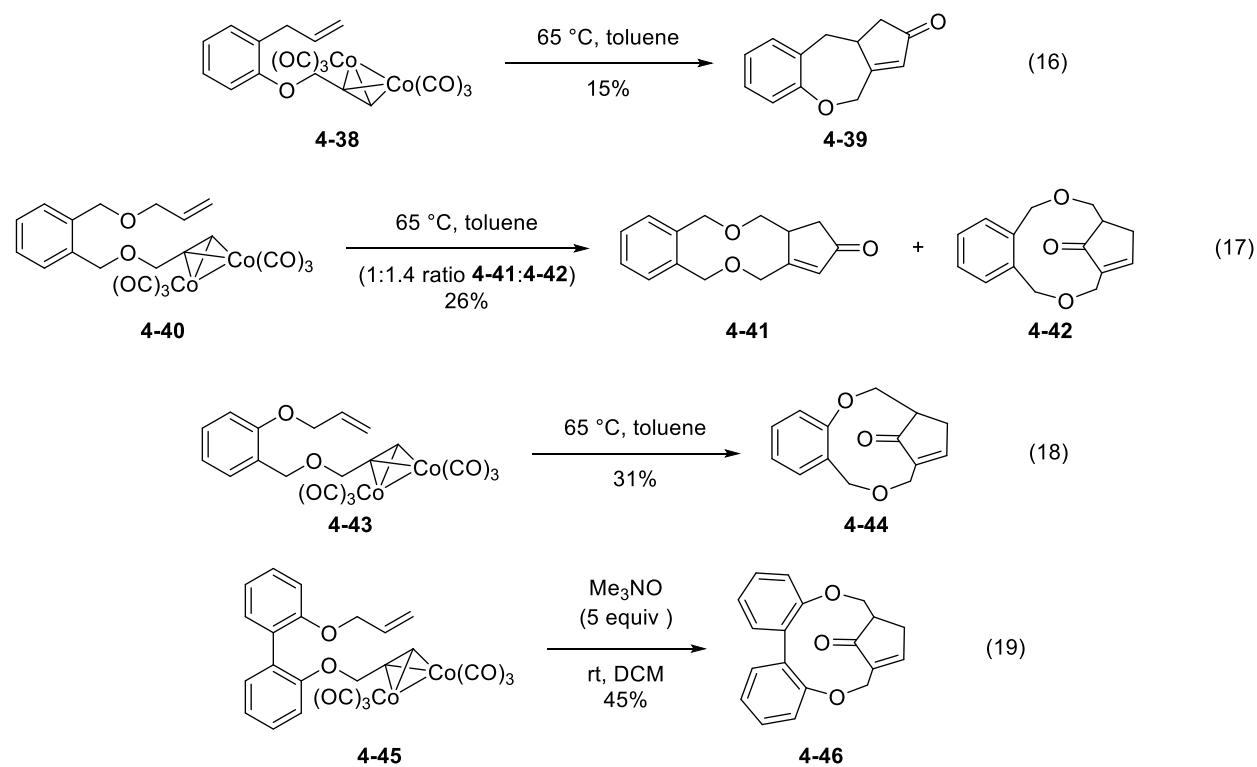
These results led to the prediction that even when forming 5-membered rings fused at the 3- and 4-positions of the cyclopentenone, TAPK reactions may require significantly longer bridging chains between the 2- and 5-positions, a challenging reaction requiring formation of a medium or large-sized rings in the TAPK product. Dr. Karabiyikoglu designed complex **4-36**, featuring a 3-membered short linking chain to favor 5-membered ring formation and a long 12-membered linking chain that would link the 2- and 5-positions of the hypothetical TAPK product **4-37** (Scheme 4.8).<sup>32</sup> Upon treatment of complex **4-36** with NMO in acetonitrile at 50 °C she was able to observe the first example of the TAPK reaction. Slow addition of NMO was required to decrease the rate of dicobalt hexacarbonyl decomplexation relative to the TAPK reaction.



#### Scheme 4.8. First transannular Pauson-Khand reaction.

Excited by these results, we began a search for a second example of the TAPK reaction. Previously, the Krafft group had demonstrated preparation of medium-sized rings in intramolecular PK reactions of 1,8-, 1,10-, and 1,11-enynes (Scheme 4.9). Their success stemmed from rigid aromatic linkers which placed the alkene and alkyne termini in close proximity to allow cyclization to occur.<sup>42</sup> 1,8-Enyne complex **4-38** proceeded with the standard intramolecular regiochemistry giving 3,4-disubstituted cyclopentenone **4-39** (eq 16). On the other hand, 1,11-enyne complex **4-40** gave a mixture of standard regioisomeric product **4-41** plus the unusual 2,5-disubstituted isomer **4-42** (eq 17). On the other hand, 1,10-enyne complex **4-43** gave a single 2,5-

disubstituted cyclopentenone **4-44** (eq 18). 1,11-Enyne complex **4-45** gave similar regioselectivity forming 2,5-disubstituted cyclopentenone **4-46** (eq 19). This demonstrated that as the length of linking chains increased, regioselectivity in favor of 3,4-disubstituted cyclopentenones diminishes as 2,5-disubstituted cyclopentenone formation occurs competitively. Also notable are the low yields of **4-39** and **4-41** where the ring fused to the cyclopentenone was a medium-sized ring. This again highlights the importance of forming a 5,5-fused ring product.



**Scheme 4.9. Successful intermolecular PK reactions to form medium ring fused and bridged bicyclic cyclopentenones.**

With this information in mind, we designed complex **4-47**, expecting that a small linking chain would favor formation of a 5-membered ring fused at the 3- and 4-positions of the cyclopentenone **4-48**, while a significantly longer linking chain would bridge the 2- and 5-positions (Figure 4.2), analogous to **4-36** which successfully underwent the TAPK reaction (Scheme 4.8). Substrate **4-47** benefits from incorporation of the rigid aryl group to restrict the conformational freedom for cyclization, similar to the work of the Krafft group (Scheme 4.9).<sup>42</sup>

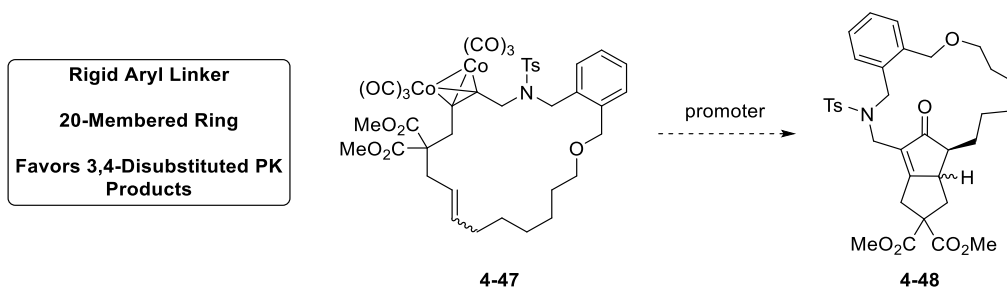
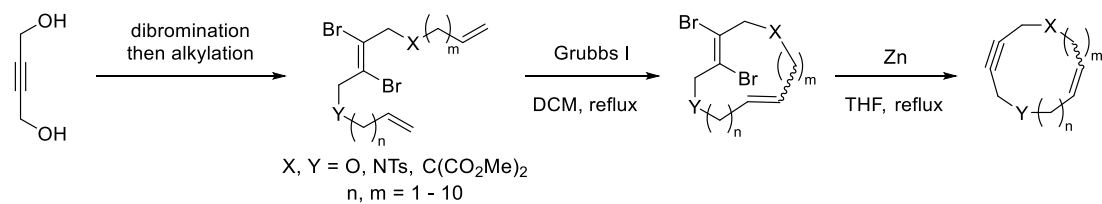
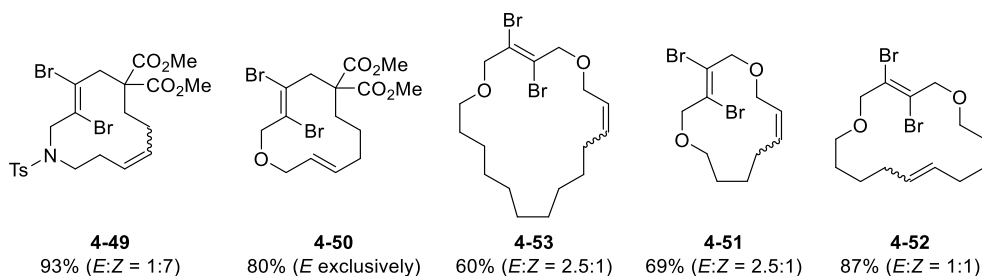


**Figure 4.2. Proposed TAPK reaction.**

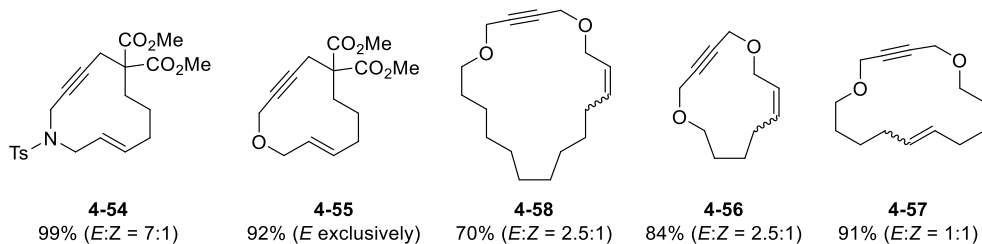
We anticipated that **4-47** would be accessible by cobalt complexation of the cyclic enyne. Synthesis of macrocyclic enynes has recently been reported by our group using a ring closing metathesis strategy of *vic*-dibromo trienes followed by zinc deprotection.<sup>43</sup> Alkyne protection as the *vic*-dibromoalkene prevented enyne metathesis, which is thermodynamically favored over the ring closing metathesis pathway.<sup>44-46</sup> Select examples of the method are highlighted in Scheme 4.10. Ring closure with Grubbs' first generation catalyst gave cyclic to *vic*-dibromoalkenes **4-49**–**4-53** in good yields. Alkyne deprotection with zinc in refluxing THF gave enynes products **4-54**–**4-58**. These high yielding and operationally simple reactions provided the groundwork to synthesize complex **4-47**.



#### cyclic *vic*-dibromodienes



#### cyclic enynes



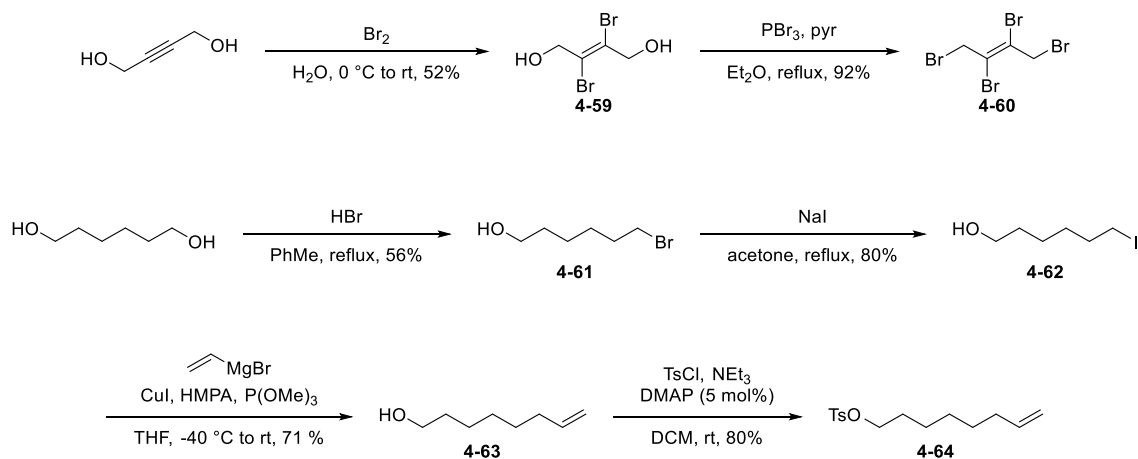
### Scheme 4.10. Ring closing metathesis and deprotection sequence of *vic*-dibromotrienes to give cyclic enynes.

## 4.3 Results and Discussion

With these methods in hand we embarked upon the synthesis of TAPK substrate **4-47**. Alkyne protection of butyne-1,4-diol with bromine gave the *vic*-dibromoalkene **4-59**, which was then converted to the tetrabromoalkene **4-60** with  $PBr_3$  (Scheme 4.11). Alkene **4-60** would serve as the linchpin for the terminal alkene carbon fragments prior to ring closing metathesis. The synthesis of the terminal alkene **4-64** began from hexane-1,6-diol. Monohalogenation by a known procedure gave the bromo alcohol **4-61**,<sup>47</sup> which was converted to iodo alcohol **4-62** in the

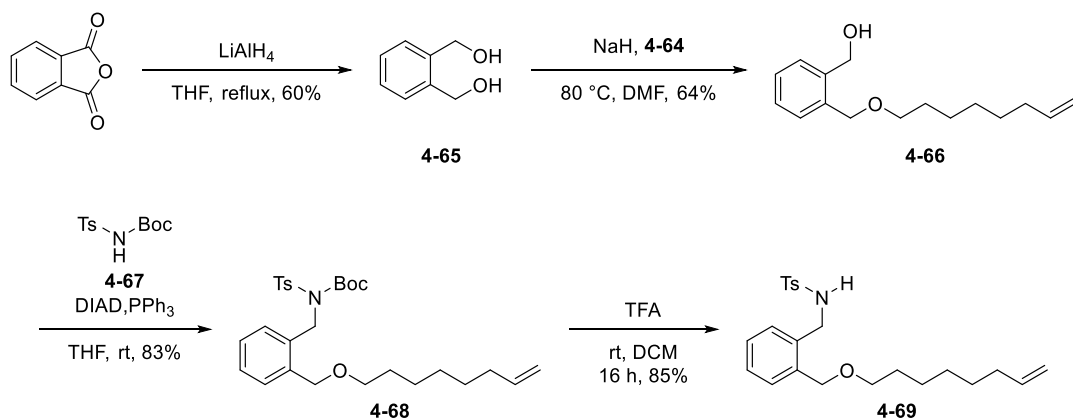


presence of sodium iodide. Gilman coupling with vinyl magnesium bromide<sup>48</sup> followed by tosylation the gave the requisite terminal alkene linker **4-64**.



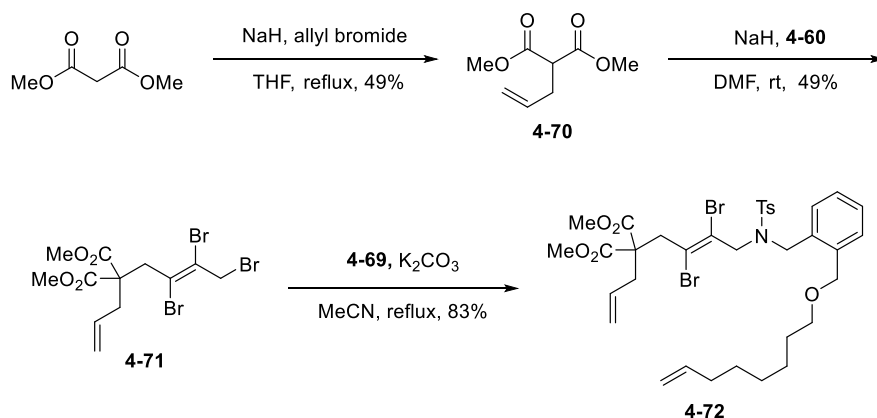
**Scheme 4.11. Syntheses of linchpin 4-60 and alkene 4-64.**

The rigid aryl backbone of **4-47** originated from phthalic anhydride. Reduction with lithium aluminum hydride gave diol **4-65**, which was monoalkylated by deprotonation with sodium hydride and by treatment with tosylate **4-64** (Scheme 4.12). A Mitsunobu reaction converted the alcohol to the Boc-protected sulfonamide **4-68**, which was deprotected with trifluoroacetic acid to give sulfonamide **4-69**.



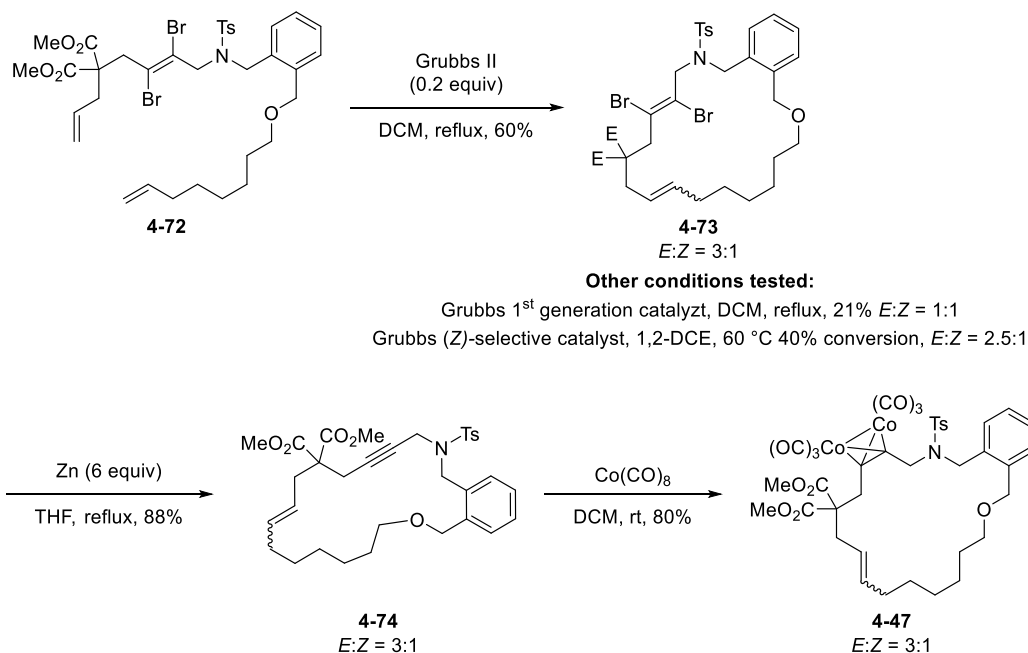
**Scheme 4.12. Synthesis of sulfonamide 4-69.**

The second terminal alkene unit was prepared by alkylation of dimethyl malonate with allyl bromide to give **4-70** (Scheme 4.13) The *vic*-dibromoalkene linchpin was alkylated in a two-step sequence to provide the macrocyclization precursor. Alkylation of malonate **4-70** with tetrabromo alkene **4-60**, facilitated by sodium hydride, gave the tribromoalkene **4-71**. A second alkylation with sulfonamide **4-69** in the presence of potassium carbonate gave the linear *vic*-dibromotriene **4-72** for the key macrocyclization step.



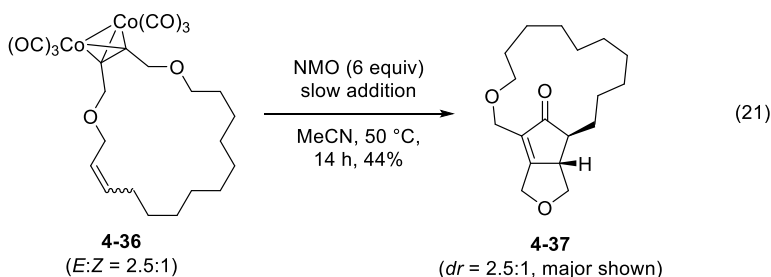
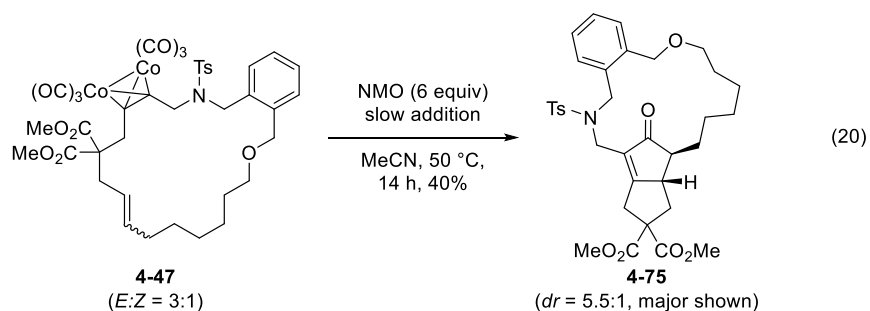
**Scheme 4.13. Synthesis of macrocyclization precursor 4-72.**

With the macrocyclization precursor in hand, we submitted **4-72** to the macrocyclization and deprotection sequence.<sup>43</sup> These conditions featured Grubbs' 1<sup>st</sup> generation catalyst,<sup>49</sup> but in this case it was found to give low conversion leading to equal amounts of (*E*)- and (*Z*)-isomers (Scheme 4.14). We attempted the cyclization with Grubbs' (*Z*)-selective metathesis catalyst,<sup>50</sup> but this also exhibited low conversion to product in a 2.5:1 *E*:*Z* ratio. Success was realized when ring closing metathesis with Grubbs' 2<sup>nd</sup> generation catalyst<sup>51</sup> gave macrocyclic product **4-73** in a 3:1 *E*:*Z* ratio in a good 60% yield. Facile deprotection employing the standard deprotection conditions with zinc in refluxing THF gave the cyclic enyne **4-74** in 88% yield. The synthesis of complex **4-47** was completed upon cobalt complexation with dicobalt octacarbonyl.



**Scheme 4.14. Key macrocyclization and deprotection steps in the synthesis of dicobalt enyne complex 4-47.**

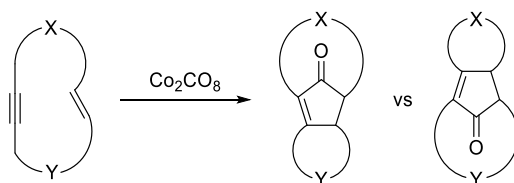
When complex **4-47** was submitted to the NMO-promoted PK reaction conditions we were delighted to find that the TAPK reaction had occurred to give the tricyclic cyclopentenone **4-75** in a 40% yield (eq 20, Scheme 4.15). In this case, the starting 3:1 *E:Z* ratio, derived from the limited selectivity in the metathesis macrocyclization reaction, led to a 5.5:1 diastereomeric ratio of products. Thus, the *E*-isomer undergoes a more productive TAPK reaction than the reaction than the *Z*-isomer, as shown by the increase in the diastereomeric ratio compared to the starting material. The identical reaction conditions were demonstrated previously to convert complex **4-36** to tricyclic cyclopentenone **4-37** in a similar 44% yield (eq 21) by Dr. Karabiyikoglu.<sup>32</sup> In this case the starting 2.5:1 *E:Z* ratio is conserved in the 2.5:1 diastereomeric ratio in the product. From these results, we can suggest that TAPK product formation is favored upon formation of a 5-membered fused ring at the 3- and 4-positions of the cyclopentenone with long bridging chains between the 2- and 5-positions.



**Scheme 4.15. Successful examples of the transannular Pauson-Khand reaction.**

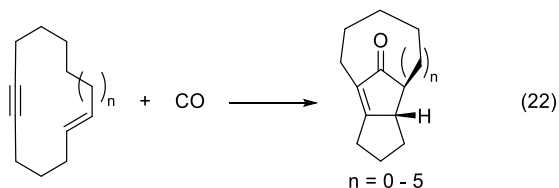
Critical to the success of the TAPK reaction of complex **4-47** to form **4-75** was the method used to clean glassware prior to the reaction. Glassware soaked in nitric acid, followed by soaking in a KOH/isopropanol bath, followed by rinsing with deionized water, and oven drying gave successful reactions. On the other hand, reactions in glassware cleaned only by acetone lead to poor conversions and complex mixtures of products. This is similar to results reported by the Krafft group in the case intermolecular PK reactions catalytic in dicobalt octacarbonyl.<sup>52</sup>

A distinct advantage of our substrate design is that we were also able to achieve a completely regioselective reaction. If both chains linking the alkene and alkyne groups are sufficiently long, it should be possible to obtain mixture of regioisomers as illustrated in Scheme 4.16. However, by having a short linker in **4-36** and **4-47** we were able to selectively favor a single regioisomer.



**Scheme 4.16. Possible regioisomers of the transannular Pauson-Khand reaction.**

To improve our understanding of the TAPK reaction, we sought to determine whether the unsuccessful TAPK reactions were favored thermodynamically, yet the steric interactions between the dicobalt carbonyl moiety and the linking chain disfavored the transformation kinetically. Calculations were performed to determine the change in Gibbs free-energy for the formation of TAPK products from cyclic enynes and carbon monoxide using substrates with a variety of long linking chains bridging the 2- and 5-positions of the cyclopentenone (Scheme 4.17). Energies of products and reactants were calculated for linking chains ranging from 4 ( $n=0$ ) to 9 ( $n=5$ ) atoms at the M06-2x/6-311+G(d,p)//B3LYP/6-31G(d) level of theory,<sup>53,54</sup> and Gibbs free-energies of reactions were calculated from the differences in energies between the products and the reactants.<sup>55</sup>



**Scheme 4.17. Formation of TAPK products for Gibbs free-energy calculations.**

The Gibbs free-energy of reaction is shown as a function of the number of carbon atoms in the linking chain (Figure 4.3). As the chain length increases, the Gibbs free-energy of the TAPK reaction decreases. This is attributed to decreasing ring strain, although none of these products are technically Bredt's Rule violations.<sup>56</sup> The computational results show that linking chains  $n = 0$  (or smaller), corresponding to 4-membered linking chains, are disfavored thermodynamically with a positive Gibbs free-energy, whereas ring sizes with  $n = 1$ , corresponding to 5-membered linking chains, and larger are thermodynamically favorable with negative Gibbs free-energies.

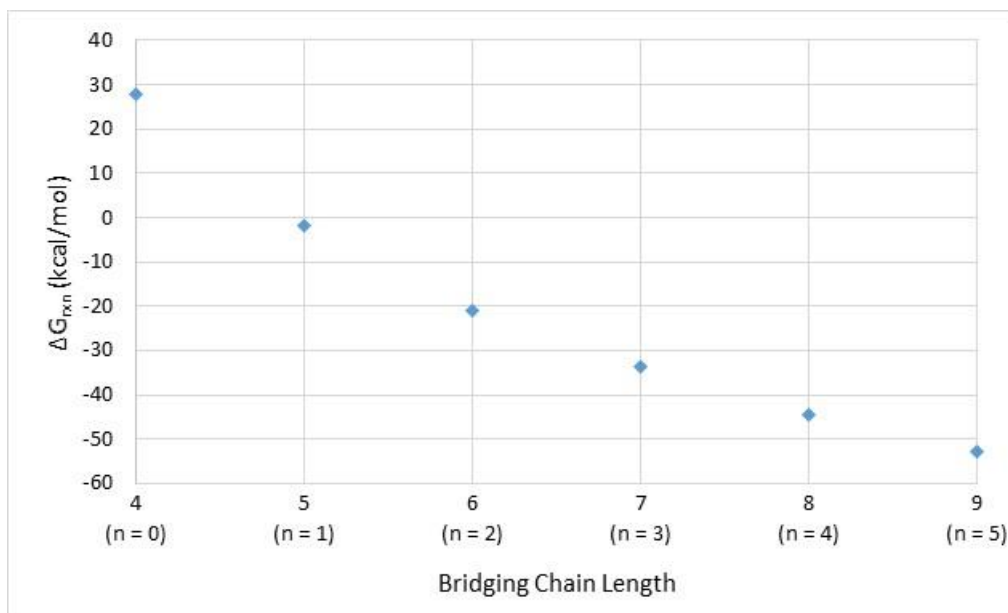
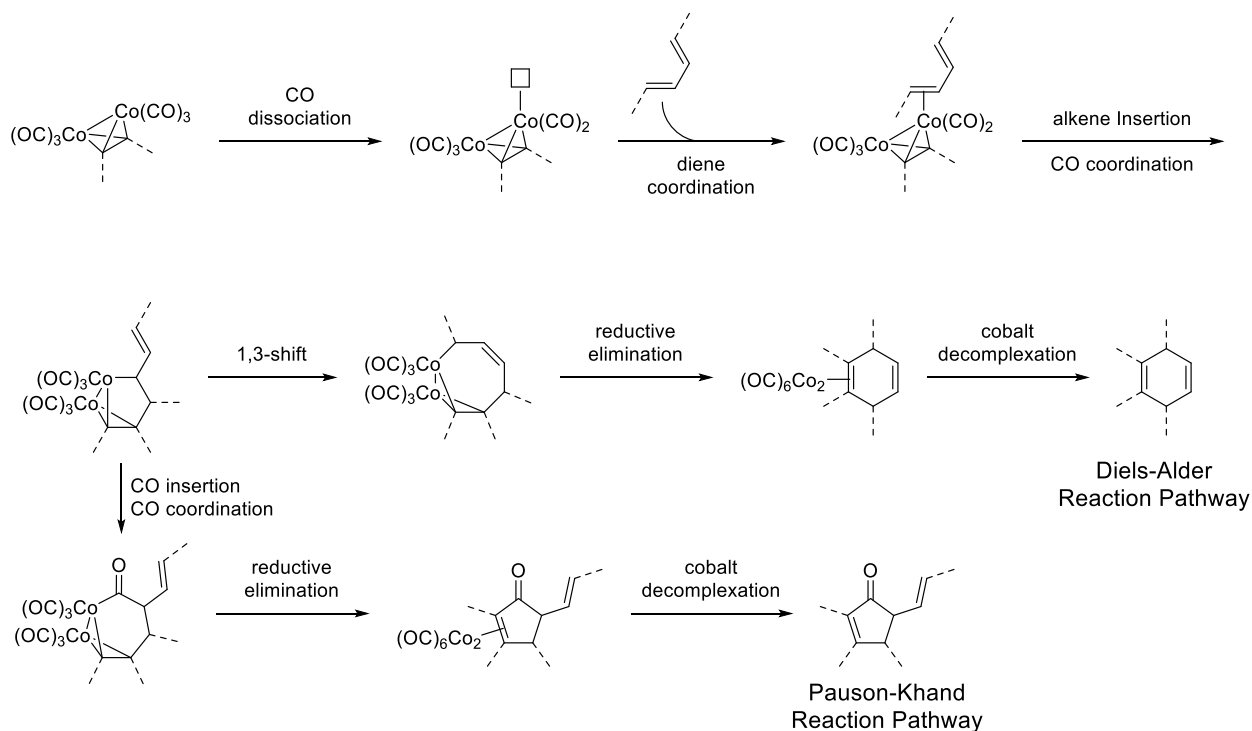


**Figure 4.3. Gibbs free-energy of the TAPK reaction (energies calculated at the M06-2x/6-311+G(d,p)//B3LYP/6-31G(d) level of theory).**

Examination of the computational results revealed that complexes **4-33** and **4-35** (Scheme 4.7) should be expected to undergo thermodynamically favored TAPK reactions, but the experimental results were ultimately unsuccessful. We propose that while TAPK reactions for these substrates may be favored thermodynamically, they are kinetically disfavored due to steric interactions of the bulky dicobalt hexacarbonyl moiety with the linking chains. Steric interactions

likely disfavor the alkene coordination, insertion, and reductive elimination steps required for the TAPK reaction pathway (Scheme 4.18). Complexes **4-36** and **4-47** have larger linking chains that may allow sufficient conformational freedom to prevent these unfavorable steric interactions leading to a thermodynamically and kinetically favored TAPK. On the other hand, complexes **4-8** and **4-11** undergo the TADA reaction due to a kinetically favored 1,3-shift in preference to CO insertion. Further studies are required to refine the structural requirements to favor either of these processes.



**Scheme 4.18. Mechanism of cobalt-promoted Pauson-Khand and [4 + 2] reactions.**

## 4.4 Conclusions

The scope of the transannular Pauson-Khand reaction has been expanded. Driven by previously established structural and reaction requirements established by Dr. Karabiyikoglu and the Krafft group, this example of the transannular Pauson-Khand reaction features a short 3-membered linking chain between the alkene and alkyne groups, as well as long linking chain with a rigid aryl segment. Computational studies predicted that transannular-Pauson Khand reactions are thermodynamically favored for cyclic enynes with a three-membered linking chain between the alkene and alkyne, provided that the second linking chain is 5-membered or larger. Substrates within this category, while expected to be thermodynamically favored based on these calculations, do not lead to transannular Pauson-Khand reactions in experimental studies unless the 2,5-bridging chain is 12 or more atoms in length. Although the experimental substrates with bridging chains less than 12 atoms are not directly comparable to the carbocyclic rings used in calculations, we propose that these reactions, while possibly favored thermodynamically, are likely disfavored kinetically due to the steric interaction between the bulky dicobalt hexacarbonyl group and the linking chain. Further experimental studies will be required to test the transannular Pauson-Khand reactivity of these carbocyclic enynes to confirm this hypothesis.

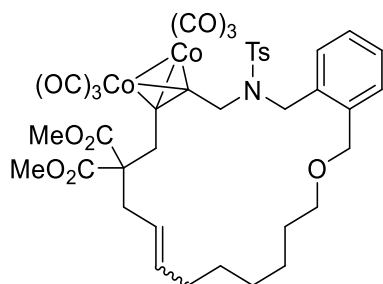
## 4.5 Experimental

### General Procedures

All commercial compounds were used as received. Dicobalt octacarbonyl was purchased from Strem Chemicals, Inc. as a solid, stabilized with 1–5 % hexane, and was stored at 0 °C. Dichloromethane, triethylamine, and acetonitrile were purified by distillation over CaH<sub>2</sub>. Methanol was distilled over Mg. Tetrahydrofuran and ether were distilled prior to use from



sodium-benzophenone ketyl. All reactions were carried out in flame-dried glassware under a nitrogen atmosphere. Metathesis catalysts (Materia) were stored in a glovebox and used as received. Reactions were monitored using TLC and the plates were developed using vanillin, cerium ammonium molybdate, or potassium permanganate stains. Column chromatography was performed using silica gel (40-63 micron) and reagent grade solvents without deactivation, unless noted. NMR spectra were recorded at 400 or 500 MHz as noted and calibrated to the solvent signal ( $\text{CDCl}_3$   $\delta = 7.26$  ppm or  $\text{C}_6\text{D}_6$   $\delta = 7.16$  ppm for  $^1\text{H}$  NMR, and  $\text{CDCl}_3$   $\delta = 77.0$  ppm or  $\text{C}_6\text{D}_6$   $\delta = 128.1$  for  $^{13}\text{C}$  NMR). Multiplicities are indicated by s (singlet), d (doublet), t (triplet), q (quartet), p (pentet), m (multiplet), or b (broadened). IR spectra were recorded with an ATR attachment and selected peaks are reported in  $\text{cm}^{-1}$ . High resolution mass spectral data was recorded with an IonSense ID-CUBE DART source or an Agilent 6530 Q-TOF ESI.



### Complex 4-47

A flame dried flask with dicobalt octacarbonyl (236 mg, 0.690 mmol), **4-74** (316 mg, 0.530 mmol), and a stir bar was flushed with nitrogen, then DCM (22 mL) was added. The mixture was stirred at rt 16 h. Solvent was removed *in vacuo*. Chromatography with 3:1 Hex:EtOAc gave 327 mg (80% yield, *E:Z* ratio 3:1) of a red viscous oil.

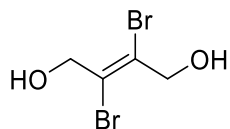
$^1\text{H}$  NMR (500 MHz,  $\text{CDCl}_3$ , ppm)  $\delta$  (***E* isomer**) 7.45 (d,  $J = 8.5$  Hz, 2H), 7.19-7.04 (m, 4H), 7.12 (d,  $J = 8.0$  Hz, 2H), 5.48 (dt,  $J = 14.5, 7.1$  Hz, 1H), 5.24 (dt,  $J = 15.3, 7.6$  Hz, 1H), 4.74

(s, 2H), 4.64 (s, 2H), 4.39 (s, 2H), 3.73 (s, 6H), 4.47 (t,  $J = 6.5$  Hz, 2H), 3.40 (s, 2H), 2.82 (d,  $J = 7.5$  Hz 2H), 2.36 (s, 3H), 2.01 (td,  $J = 5.8, 5.8$  Hz, 2H), 1.56 (p,  $J = 6.6$  Hz, 2H), 1.43-1.29 (m, 6H); (**Z isomer**) 7.27-7.26 (m, 2H), 7.19-7.04 (m, 6H), 5.51-5.45 (m, 1H), 5.33 (dt,  $J = 11.0, 6.8$  Hz, 1H), 4.73 (s, 2H), 4.60 (s, 2H), 4.22 (s, 2H), 3.75 (s, 6H), 3.68 (s, 2H), 3.33 (t,  $J = 6.0$  Hz, 2H), 2.70 (d,  $J = 7.0$  Hz, 2H), 2.33 (s, 3H), 2.04 (td,  $J = 7.0$  Hz, 2H), 1.58-1.29 (m, 8H);

$^{13}\text{C}$  NMR (125 MHz,  $\text{CDCl}_3$ , ppm)  $\delta$  (**E isomer**) 199.2, 170.7, 143.0, 137.1, 136.8, 135.7, 133.9, 129.6, 129.4, 129.3, 127.8, 127.6, 127.2, 123.5, 90.5, 90.3, 71.0, 70.2, 58.7, 53.0, 52.5, 50.5, 35.7, 34.7, 31.1, 29.0, 27.0, 26.5, 24.7, 21.4; (**Z isomer**) 199.2, 170.7, 142.7, 137.3, 136.7, 134.0, 131.6, 129.7, 129.1, 128.0, 126.9, 122.8, 94.7, 90.4, 71.4, 70.4, 58.2, 54.2, 52.7, 51.7, 39.0, 32.0, 30.9, 27.7, 27.1, 25.7, 24.8 (3 C's, absent);

IR (neat, ATR,  $\text{cm}^{-1}$ ): 3031, 2934, 2093, 2051, 2018, 1735, 1437, 1207, 1160, 1092;

HRMS (ESI): calcd  $[\text{M}+\text{Na}]^+$  ( $\text{C}_{39}\text{H}_{41}\text{Co}_2\text{NO}_{13}\text{SNa}$ ) 904.0860, found 904.0974.

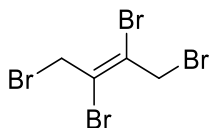


#### (**E**)-2,3-dibromobut-2-ene-1,4-diol (**4-59**)

A flame dried flask containing butyne-1,4-diol (5.252 g, 61.0 mmol) and a stir bar was flushed and with nitrogen, then water (145 mL) was added. The mixture was cooled to 0 °C, then bromine (4.2 mL, 80.5 mmol) was added dropwise with stirring. The mixture was stirred 30 min at 0 °C, then 90 min at rt. The reaction was quenched with saturated aq  $\text{Na}_2\text{S}_2\text{O}_3$  and neutralized with aq 1M NaOH. The mixture was extracted with EtOAc and dried with  $\text{MgSO}_4$ , then filtered

through silica gel. Solvent was removed *in vacuo* to give 7.874 g (52% yield) of the known<sup>57</sup> off white solid.

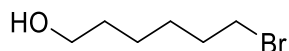
<sup>1</sup>H NMR (400 MHz, CDCl<sub>3</sub>, ppm) δ 4.54 (d, *J* = 7.1 Hz, 4H), 2.04 (t, *J* = 2.1 Hz, 2H).



**(E)-1,2,3,4-tetrabromobut-2-ene (4-60)**

A flame dried flask containing **4-59** (7.874 g, 32.0 mmol), fitted with a reflux condenser, and equipped with a stir bar was flushed and with nitrogen, then ether (39 mL) was added, followed by pyridine (0.47 mL, 5.75 mmol). The mixture was cooled to 0 °C, then phosphorus tribromide (2.4 mL, 25.6 mmol) was added dropwise with stirring. The mixture was stirred 30 min at 0 °C, then 4 h at reflux. The mixture was diluted with water and extracted with ether. The organic extracts were washed with saturated aq. NaHCO<sub>3</sub>, then brine, and dried with MgSO<sub>4</sub>. The mixture was filtered through silica gel and solvent was removed *in vacuo* to give 10.903 g (92% yield) of the known<sup>58</sup> white solid.

<sup>1</sup>H NMR (400 MHz, CDCl<sub>3</sub>, ppm) δ 4.43 (s, 4H).

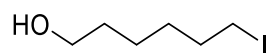


**6-bromohexan-1-ol (4-61)**

This compound was obtained by a modification of a known procedure.<sup>47</sup> A flame dried flask with 1,6-hexanediol (9.789 g, 82.8 mmol) and a stir bar was evacuated and replenished with nitrogen three times, then toluene (196 mL) was added. Hydrobromic acid (11.0 mL, 98.7 mmol, 48% aq solution, 9M) was added dropwise at rt. The mixture was heated to reflux and stirred

overnight. The mixture was diluted with water, and extracted with ether. The organic layer was separated and washed with 1M aq KOH, brine, then water, and dried with MgSO<sub>4</sub>. Solvent was removed *in vacuo*. Chromatography with 8:1 Hex:EtOAc gave 8.363 g (56% yield) of the known<sup>59</sup> clear light yellow oil.

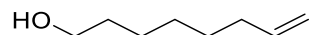
<sup>1</sup>H-NMR (400 MHz, CDCl<sub>3</sub>, ppm) δ 3.63 (t, *J* = 7.3 Hz, 2H), 3.40 (t, *J* = 6.6 Hz, 2H), 1.86 (p, *J* = 7.1 Hz, 2H), 1.57 (t, *J* = 7.0 Hz, 2H), 1.50-1.34 (m, 4H).



#### 6-iodohexan-1-ol (4-62)

A flame dried flask containing **4-61** (8.363 g, 46.2 mmol) and a stir bar was flushed and with nitrogen, then acetone (123 mL) was added. After the addition of NaI (24.260 g, 161 mmol) the mixture was heated to reflux and stirred 16 h. The mixture was diluted with water and extracted with EtOAc. The organic layers were washed with 1% aq Na<sub>2</sub>S<sub>2</sub>O<sub>3</sub> and brine, then dried with MgSO<sub>4</sub>. Solvent was removed *in vacuo*. Chromatography with 2:1 Hex:EtOAc gave 9.542 g (80% yield) of the known<sup>60</sup> clear light yellow oil.

<sup>1</sup>H NMR (400 MHz, CDCl<sub>3</sub>, ppm) δ 3.63 (t, *J* = 6.6 Hz, 2H), 3.18 (t, *J* = 7.0 Hz, 2H), 1.83 (p, *J* = 7.0 Hz, 2H), 1.57 (p, *J* = 6.9 Hz, 2H), 1.47-1.34 (m, 4H).

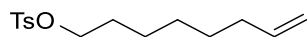


#### oct-7-en-1-ol (4-63)

A flame dried flask with copper(I) iodide (7.634 g, 40.1 mmol) and a stir bar was flushed with nitrogen, then THF (55 mL) was added. The flask was cooled to -40 °C, then vinylmagnesium bromide (120 mL, 120 mmol, 1M in hexanes), was added, and the mixture was stirred for 15 min

at that temperature. Next, HMPA (13.9 mL, 80.2 mmol), triethyl phosphite (13.7 mL, 80.2 mmol), and a solution of **4-62** (9.142 g, 40.1 mmol) in THF (55 mL) were added sequentially at -40 °C, then stirred 1 h. The mixture was warmed to rt and stirred for 2 h, then the reaction was quenched with saturated aq NH<sub>4</sub>Cl, extracted with EtOAc, washed with brine, and dried with MgSO<sub>4</sub>. Solvent was removed *in vacuo*. Chromatography with 3:1 Hex:Et<sub>2</sub>O gave 3.638 g (71% yield) of the known<sup>48</sup> clear light yellow oil.

<sup>1</sup>H NMR (400 MHz, CDCl<sub>3</sub>, ppm) δ 5.80 (dtd, *J* = 17.1, 10.3, 6.7 Hz, 1H), 4.99 (bd, *J* = 17.2 Hz, 1H), 4.93 (bd, *J* = 10.0 Hz, 1H), 3.63, (t, *J* = 6.6 Hz, 2H) 2.04 (td, *J* = 6.8 Hz, 2H), 1.56 (p, *J* = 6.9 Hz, 2H), 1.43-1.27 (m, 6H).



#### oct-7-en-1-yl 4-methylbenzenesulfonate (**4-64**)

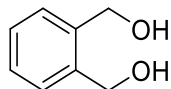
A flame dried flask with DMAP (69 mg, 0.567 mmol) and a stir bar was flushed with nitrogen, then DCM (57 mL) was added. After the addition of **4-63** (3.638 g, 28.4 mmol) and NEt<sub>3</sub> (5.14 mL, 36.9 mmol), the flask was cooled to 0 °C, and *p*-TsCl (5.950 g, 31.2 mmol) was added slowly. The mixture was warmed to rt and stirred 16 h. The mixture was diluted with water, washed with brine, and dried with MgSO<sub>4</sub>. Solvent was removed *in vacuo*. Chromatography with 5:1 Hex:Et<sub>2</sub>O gave 6.437 g (80% yield) of a clear colorless oil.

<sup>1</sup>H NMR (400 MHz, CDCl<sub>3</sub>, ppm) δ 7.79 (d, *J* = 8.0 Hz, 2H), 7.34 (d, *J* = 8.0 Hz, 2H), 5.76 (ddt, *J* = 17.0, 10.2, 6.7 Hz, 1H), 4.97 (dtd, *J* = 17.2, 1.8, 1.6 Hz, 1H), 4.92 (ddt, *J* = 10.3, 2.1, 1.1 Hz, 1H) 4.01 (t, *J* = 6.6 Hz, 2H), 2.44 (s, 3H) 1.99 (q, *J* = 7.1 Hz, 2H), 1.63 (p, *J* = 6.9 Hz, 2H), 1.36-1.19 (m, 6H);

$^{13}\text{C}$  NMR (100 MHz,  $\text{CDCl}_3$ , ppm)  $\delta$  144.6, 138.8, 133.3, 129.8, 127.9, 114.4, 70.6, 33.6, 28.8, 28.6, 28.4, 25.2, 21.6;

IR (neat, ATR,  $\text{cm}^{-1}$ ): 3077, 2973, 2930, 2855, 1358, 1174, 956, 912, 812;

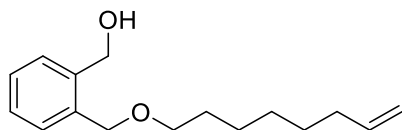
HRMS (DART): calcd  $[\text{M}+\text{H}]^+$  ( $\text{C}_{15}\text{H}_{23}\text{O}_3\text{S}$ ) 283.13624, found 283.13682.



### 1,2-phenylenedimethanol (4-65)

A flame dried flask with LAH (5.210 g, 137.3 mmol) and a stir bar was flushed with nitrogen, then THF (145 mL) was added. The flask was cooled to 0 °C, then a solution of phthalic anhydride (10.719g, 72.4 mmol) in THF (106 mL) was added dropwise. The mixture was stirred at rt for 30 min, then at reflux for 3 h. The mixture was cooled to 0 °C, diluted with  $\text{Et}_2\text{O}$ , and water (5.5 mL) was added dropwise, followed by 15% aq NaOH (5.5 mL), then water (13.7 mL). The solution was warmed to rt, then stirred 15 minutes, then another 15 minutes after addition of magnesium sulfate. The mixture was filtered through Celite and solvent was removed in vacuo. Crystallization with hexanes gave 6.002 g (60% yield) of the known compound<sup>61</sup> as off white crystals.

$^1\text{H}$  NMR (400 MHz,  $\text{CDCl}_3$ , ppm)  $\delta$  7.30 (s, 4H), 4.62 (s, 4H), 3.77 (s, 2H).



### 2-((oct-7-en-1-yloxy)methyl)phenylmethanol (4-66)

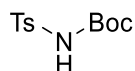
A flame dried flask with NaH (603 mg, 15.1 mmol) and a stir bar was flushed with nitrogen, then DMF (16 mL) was added. A solution of **4-65** (2.092 g, 15.1 mmol) in DMF (16 mL) was added dropwise at 0 °C, then stirred 15 minutes. Next, a solution of **4-64** (4.257 g, 15.1 mmol) in DMF (16 mL) was added at 0 °C, then stirred 15 minutes. The mixture was warmed to 80 °C and stirred 16 h. The mixture was diluted with water, extracted with Et<sub>2</sub>O, and dried with MgSO<sub>4</sub>. Solvent was removed *in vacuo*. Chromatography with 3:2 Hex:Et<sub>2</sub>O gave 2.379 g (64% yield) of a clear light yellow oil.

**<sup>1</sup>H NMR** (400 MHz, CDCl<sub>3</sub>, ppm) δ 7.40 (d, *J* = 6.8 Hz, 1H), 7.36-7.27 (m, 3H), 5.79 (ddt, *J* = 16.8, 10.4, 6.7, 1H), 4.98 (dtd, *J* = 17.1, 1.8, 1.8, 1H), 4.92 (ddt, *J* = 10.2, 2.2, 1.1 Hz, 1H), 4.66 (d, *J* = 6.4 Hz, 2H), 4.60 (s, 2H), 3.52 (t, *J* = 6.6 Hz, 3H), 3.31 (t, *J* = 6.4 Hz, 1H), 2.03 (td, *J* = 7.1, 7.1 Hz, 2H), 1.61 (p, *J* = 7.1 Hz, 2H), 1.41-1.27 (m, 6H);

**<sup>13</sup>C NMR** (100 MHz, CDCl<sub>3</sub>, ppm) δ 140.9, 139.0, 136.3, 130.1, 129.8, 128.9, 128.0, 114.3, 72.4, 70.9, 64.0, 33.7, 29.6, 28.9, 28.8, 26.0;

**IR** (neat, ATR, cm<sup>-1</sup>): 3401, 3074, 2926, 2855, 1641, 1362, 1089, 1006, 908, 747;

**HRMS** (DART): calcd [M+H]<sup>+</sup> (C<sub>16</sub>H<sub>25</sub>O<sub>2</sub>) 249.18491, found 249.18455.

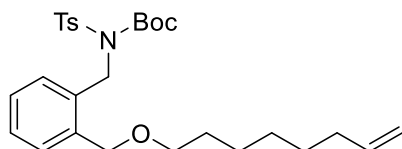


#### ***tert*-butyl tosylcarbamate (**4-67**)**

A flame dried flask with *p*-toluenesulfonamide (3.470 g, 20.3 mmol), DMAP (248 mg, 2.03 mmol), NEt<sub>3</sub> (3.1 mL), and a stir bar was flushed with nitrogen, then DCM (40 mL) was added. Di-*tert*-butyldicarbonate (4.866 g, 22.3 mmol) was added in one portion. The mixture was stirred at rt 16 h. The reaction mixture was washed with aq. 1M HCl (13 mL), followed by water

(13mL), then brine (13mL). The organic layer was dried with MgSO<sub>4</sub>. Solvent was removed *in vacuo*. Crystallization from petroleum ether/Et<sub>2</sub>O, followed by chromatography with 4:1 Hex:EtOAc gave 2.714 g (49% yield) of a the known<sup>62</sup> white solid.

<sup>1</sup>H NMR (400 MHz, CDCl<sub>3</sub>, ppm) δ 7.89 (d, *J* = 8.4 Hz, 2H), 7.33 (d, *J* = 8.1 Hz, 2H), 7.20 (s, 1H), 2.45 (s, 3H), 1.38 (s, 9H).



***tert*-butyl (2-((oct-7-en-1-yloxy)methyl)benzyl)(tosyl)carbamate (4-68)**

A flame dried flask with **4-66** (614 mg, 2.47 mmol), PPh<sub>3</sub> (778 mg, 2.97 mmol), **4-67** (805 mg, 2.97 mmol), and a stir bar was flushed with nitrogen, then THF (5 mL) was added. The mixture was cooled to 0 °C, then DIAD (0.49 mL, 2.47 mmol) was added dropwise. The mixture warmed to rt and stirred 16 h. Solvent was removed *in vacuo*. Chromatography with 6:1 Hex:EtOAc gave 1.031 g (83% yield) of a clear colorless oil.

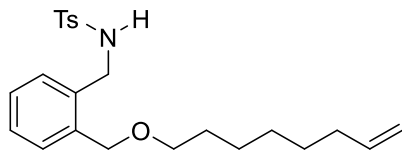
<sup>1</sup>H NMR (400 MHz, CDCl<sub>3</sub>, ppm) δ 7.68 (d, *J* = 8.4 Hz, 2H), 7.32-7.21 (m, 6H), 5.80 (ddt, *J* = 17.2, 10.4, 6.7 Hz), 5.14 (s, 2H), 4.98 (dtd, *J* = 17.2, 1.9, 1.9 Hz, 1H), 4.92 (ddt, *J* = 10.1, 2.3, 1.1 Hz, 1H), 4.60 (s, 2H) 3.44 (t, *J* = 6.6 Hz, 2H), 2.43 (s, 3H), 2.04 (td, *J* = 6.9, 6.9 Hz, 2H), 1.60 (p, *J* = 6.9 Hz, 2H), 1.42-1.33 (m, 6H), 1.31 (s, 9H);

<sup>13</sup>C NMR (125 MHz, CDCl<sub>3</sub>, ppm) δ 151.2, 144.2, 139.1, 137.0, 136.5, 135.3, 129.12, 129.08, 128.3, 128.2, 126.9, 126.5, 114.2, 84.3, 71.3, 70.3, 47.0, 33.7, 29.7, 29.0, 28.9, 27.8, 26.1, 21.6;

IR (neat, ATR, cm<sup>-1</sup>): 3070, 2977, 2930, 2858, 1727, 1358, 1153, 1089;



**HRMS** (DART): calcd  $[M-C_5H_9O_2]^+$  ( $C_{23}H_{30}NO_3S$ ) 400.19464, found 400.19368.



**4-methyl-N-(2-((oct-7-en-1-yloxy)methyl)benzyl)benzenesulfonamide (4-69)**

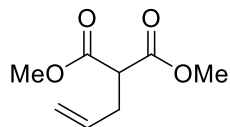
A flame dried flask with **4-68** (1.031 g, 2.05 mmol) and a stir bar was flushed with nitrogen, then DCM (35 mL) was added. TFA (3.3 mL, 42.5 mmol) was added dropwise, and the mixture was warmed to rt and stirred 16 h. The mixture was quenched with saturated aq  $NaHCO_3$ , extracted with DCM, and dried with  $MgSO_4$ . Solvent was removed *in vacuo*. Chromatography with 4:1 Hex:EtOAc gave 702 mg (85% yield) of a clear colorless oil.

**$^1H$  NMR** (400 MHz,  $CDCl_3$ , ppm)  $\delta$  7.72 (d,  $J = 8.4$  Hz, 2H), 7.27-7.14 (m, 6H), 5.80 (ddt,  $J = 17.2, 10.4, 6.7$  Hz, 1H), 5.65 (t,  $J = 5.8$  Hz, 1H), 4.99 (dtd,  $J = 17.2, 1.8, 1.8$  Hz, 1H), 4.93 (ddt,  $J = 10.3, 2.3, 1.3$  Hz, 1H), 4.39 (s, 3H), 4.14 (d,  $J = 8.0$  Hz, 2H), 3.42 (t,  $J = 6.8$  Hz, 2H), 2.07 (s, 3H), 2.05 (td,  $J = 7.0$  Hz, 2H), 1.60 (p,  $J = 6.0$  Hz, 2H), 1.43-1.30 (m, 6H);

**$^{13}C$  NMR** (100 MHz,  $CDCl_3$ , ppm)  $\delta$  143.2, 139.1, 137.2, 136.2, 135.8, 130.4 (2C), 129.6, 128.7, 128.2, 127.2, 114.3, 70.7, 70.8, 45.7, 33.7, 29.6, 28.9, 28.8, 26.0, 21.5;

**IR** (neat, ATR,  $cm^{-1}$ ): 3282, 3066, 2926, 2858, 1738, 1329, 1156, 1092;

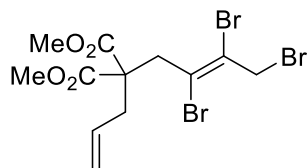
**HRMS** (DART): calcd  $[M+H]^+$  ( $C_{23}H_{32}NO_3S$ ) 402.20974, found 402.20858.



### dimethyl 2-allylmalonate (4-70)

A flame dried flask with a reflux condenser containing NaH (3.903 g, 97.6 mmol, 60% w/w dispersion mineral oil) and a stir bar was flushed with nitrogen, then THF (70 mL) was added. Dimethyl malonate (10.0 mL, 87.1 mmol) was added dropwise at rt with stirring. After 30 minutes, allyl bromide (7.5 mL, 87.1 mmol) was added dropwise at rt. The mixture was heated at reflux 16 h with stirring. The reaction was quenched with water, extracted with Et<sub>2</sub>O, washed with brine, and dried with MgSO<sub>4</sub>. Solvent was removed *in vacuo*. Chromatography with 4:1 petroleum ether:Et<sub>2</sub>O two times gave 7.399 g (49% yield) of the known<sup>63</sup> clear light yellow oil.

<sup>1</sup>H NMR (400 MHz, CDCl<sub>3</sub>, ppm) δ 5.76 (ddt, *J* = 17.1, 10.2, 6.8 Hz, 1H), 5.11 (ddt, *J* = 17.1, 1.5, 1.5 Hz, 1H), 5.06 (ddt, *J* = 10.2, 1.2, 1.2 Hz, 1H), 3.73 (s, 6H), 3.46 (t, *J* = 7.6 Hz, 1H), 2.66-2.62 (m, 2H).

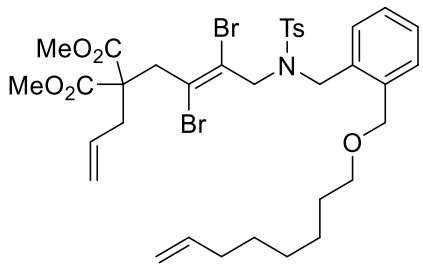


### dimethyl (*E*)-2-allyl-2-(2,3,4-tribromobut-2-en-1-yl)malonate (4-71)

A flame dried flask with NaH (3.903 g, 97.6 mmol, 60% w/w dispersion mineral oil) and a stir bar was flushed with nitrogen, then DMF (37 mL) was added and the mixture was cooled to 0 °C. **4-70** (3.868 g, 22.5 mmol) was added dropwise at 0 °C with stirring. After 30 minutes, **4-60** (10.903 g, 29.3 mmol) was added dropwise at 0 °C. The mixture was warmed to rt and stirred 24 h. The reaction was quenched with water and extracted with Et<sub>2</sub>O. The organic layer was washed

with water, then brine, and dried with MgSO<sub>4</sub>. Solvent was removed *in vacuo*. Chromatography with 7:1 Hex:Et<sub>2</sub>O gave 9.591 g (48% yield) of the known<sup>32</sup> clear light brown oil.

<sup>1</sup>H NMR (300 MHz, CDCl<sub>3</sub>, ppm) δ 5.84 (ddt, *J* = 16.9, 10.3, 7.3 Hz, 1H), 5.20-5.13 (m, 2H), 4.50 (s, 2H), 3.78 (s, 6H), 3.56 (s, 2H), 2.76 (dt, *J* = 7.3, 1.1 Hz, 2H).



**dimethyl (*E*)-2-allyl-2-(2,3-dibromo-4-((4-methyl-*N*-(2-((oct-7-en-1-yloxy)methyl)benzyl)phenyl)sulfonamido)but-2-en-1-yl)malonate (4-72)**

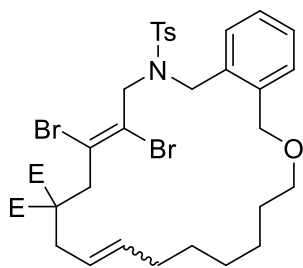
A flame dried flask with **4-71** (702 mg, 1.75 mmol), **4-69** (890 mg, 1.92 mmol), K<sub>2</sub>CO<sub>3</sub> (483 mg, 3.50 mmol), and a stir bar was flushed with nitrogen, then MeCN (8.7 mL) was added. The mixture was heated at reflux 16 h with stirring. The mixture was passed through a silica plug with DCM, then solvent was removed *in vacuo*. Chromatography with 4:1 Hex:EtOAc gave 1.138 g (83% yield) of a clear light yellow oil.

<sup>1</sup>H NMR (500 MHz, CDCl<sub>3</sub>, ppm) δ 7.73 (d, *J* = 8.0 Hz, 2H), 7.33-7.27 (m, 2H), 7.30 (d, *J* = 8.0 Hz, 2H), 7.23-7.20 (m, 2H), 5.80 (ddt, *J* = 17.1, 10.1, 6.8 Hz, 1H), 5.78-5.71 (m, 1H), 5.03 (bd, *J* = 10.0 Hz, 1H), 5.02 (bd, *J* = 17.0 Hz, 1H), 4.99 (dtd, *J* = 17.0, 1.8, 1.8 Hz, 1H), 4.93, (ddt, *J* = 10.1, 2.1, 1.1 Hz, 1H), 4.52 (s, 2H), 4.48 (s, 2H), 4.33 (s, 2H), 3.67 (s, 6H), 3.43 (t, *J* = 6.8 Hz, 2H), 2.49, (d, *J* = 7.5 Hz, 2H), 2.44 (s, 3H), 2.04 (td, *J* = 7.0, 7.0 Hz, 2H), 1.58 (p, *J* = 6.7 Hz, 2H), 1.41-1.27 (m, 6H);

$^{13}\text{C}$  NMR (125 MHz,  $\text{CDCl}_3$ , ppm)  $\delta$  170.5, 143.6, 139.1, 136.9, 136.4, 133.7, 132.7, 129.7, 129.2, 129.1, 127.9, 127.8, 127.6, 122.5, 119.2, 118.9, 114.3, 70.9, 70.6, 57.6, 54.8, 52.6, 49.8, 43.1, 36.7, 33.8, 29.7, 29.0, 28.9, 26.1, 21.6;

IR (neat, ATR,  $\text{cm}^{-1}$ ): 3073, 2930, 2855, 1735, 1437, 1343, 1218, 1160, 1092, 908;

HRMS (ESI): calcd  $[\text{M}+\text{Na}]^+$  ( $\text{C}_{35}\text{H}_{45}\text{Br}_2\text{NO}_7\text{SNa}$ ) 804.1181, found 804.1184.



**dimethyl (14E)-14,15-dibromo-17-tosyl-4,5,6,7,8,11,13,16,17,18-decahydro-1H-benzo[c][1]oxa[6]azacycloicosine-12,12(3H)-dicarboxylate (4-73)**

A flame dried round bottom flask containing Grubbs' 2<sup>nd</sup> generation catalyst (123 mg, 0.145 mmol) and a stir bar was dissolved in DCM (600 mL). After addition of a solution of **4-72** (1.138 g, 1.45 mmol) in DCM (100 mL) the reaction was warmed to reflux for 16 h. Another portion of Grubbs' 2<sup>nd</sup> generation catalyst was added (123 mg, 0.145 mmol), and the reaction was stirred under reflux for another 24 h. Solvent was removed *in vacuo*. Chromatography with 1:1 Hex:Et<sub>2</sub>O gave 654 mg (60% yield, *E:Z* ratio 3:1) of a white foam.

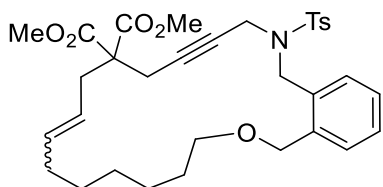
$^1\text{H}$  NMR (500 MHz,  $\text{CDCl}_3$ , ppm)  $\delta$  (**E isomer**) 7.73 (d,  $J = 8.5$  Hz, 2H), 7.37 (d,  $J = 7.0$  Hz, 1H), 7.29 (d, 2H), 7.27-7.19 (m, 3H), 5.48 (td,  $J = 14.3, 7.0$  Hz, 1H), 5.19 (td,  $J = 15.0, 7.4$  Hz, 1H), 4.57 (s, 2H), 4.47 (s, 2H), 4.34 (s, 2H), 3.71 (s, 6H), 3.53 (t,  $J = 6.5$  Hz, 2H), 3.41 (s, 2H), 2.65 (d,  $J = 7.0$  Hz, 2H), 2.43 (s, 3H), 1.96 (p,  $J = 6.4$  Hz, 2H), 1.62 (p,  $J = 6.7$  Hz, 2H), 1.40-1.25 (m, 6H); (**Z isomer**) 7.66 (d,  $J = 8.5$  Hz, 2H), 7.41 (d,  $J = 7.5$  Hz, 1H), 7.30-

7.19 (m, 5H), 5.47-5.42 (m, 1H), 5.33 (td,  $J = 10.8, 6.8$  Hz, 1H), 4.70 (s, 2H), 4.92 (s, 2H), 4.45 (s, 2H), 3.71 (s, 6H), 3.454 (t,  $J = 6.5$  Hz, 2H), 3.450 (s, 2H), 2.55 (d,  $J = 8.0$  Hz, 2H), 2.42 (s, 3H), 1.98-1.92 (m, 2H), 1.56-1.51 (m, 2H), 1.40-1.25 (m, 6H);

$^{13}\text{C}$  NMR (125 MHz,  $\text{CDCl}_3$ , ppm)  $\delta$  (**E isomer**) 170.6, 143.6, 137.5, 136.4, 135.5, 132.8, 129.6, 128.6, 128.0, 127.8, 127.63, 127.61, 123.5, 122.0, 119.6, 70.2, 69.8, 57.4, 53.9, 52.8, 49.5, 41.5, 35.3, 31.4, 28.8, 27.5, 27.0, 25.1, 21.6; (**Z isomer**) 170.8, 143.4, 137.4, 136.3, 134.7, 133.2, 129.4, 128.4, 127.5, 127.4, 122.7, 123.9, 119.1, 71.1, 70.4, 57.0, 54.2, 52.7, 49.6, 44.1, 30.2, 29.3, 28.1, 27.7, 26.3, 24.9 (3 C's, absent);

IR (neat, ATR,  $\text{cm}^{-1}$ ): 3027, 2926, 2855, 1735, 1437, 1156, 1089;

HRMS (ESI): calcd  $[\text{M}+\text{Na}]^+$  ( $\text{C}_{33}\text{H}_{41}\text{Br}_2\text{O}_7\text{S}$ ) 776.0868, found 776.0822.



**dimethyl 14,15-dehydro-17-tosyl-4,5,6,7,8,11,13,16,17,18-decahydro-1H-benzo[c][1]oxa[6]azacycloicosine-12,12(3H)-dicarboxylate (4-74)**

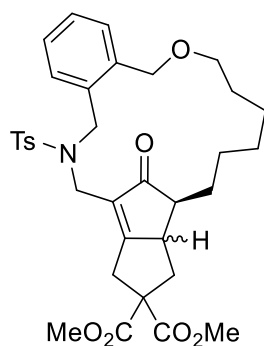
A flame dried flask equipped with a reflux condenser and a stir bar was charged with zinc dust (339 mg, 5.19 mmol). The zinc dust was stirred with 1M HCl, rinsed with water, and flame dried in a flask prior to use. A solution of **4-73** (654 mg, 0.866 mmol) in THF (43 mL) was added. The mixture was heated at reflux and stirred 16 h. The mixture was diluted with EtOAc and filtered over Celite. Solvent was removed *in vacuo*. Chromatography with 3:1 Hex:EtOAc gave 452 mg (88% yield, *E:Z* ratio 3:1) of a white solid.

**<sup>1</sup>H NMR** (500 MHz, CDCl<sub>3</sub>, ppm) δ (***E* isomer**) 7.81 (d, *J* = 8.5 Hz, 2H), 7.59 (d, *J* = 8.0 Hz, 1H), 7.37 (d, *J* = 8.5 Hz, 2H), 7.34-7.24 (m, 3H), 5.07 (dt, *J* = 14.7, 7.1 Hz), 4.92 (dt, *J* = 14.8, 7.4 Hz, 1H), 4.49 (s, 2H), 4.48 (s, 2H), 3.98 (s, 2H), 3.72 (s, 6H), 3.45 (t, *J* = 6.0 Hz, 2H), 2.63 (s, 2H), 2.52 (d, *J* = 7.5 Hz, 2H), 2.42 (s, 3H), 1.96 (td, *J* = 6.0, 6.0 Hz, 2H), 1.58 (p, *J* = 6.3 Hz, 2H), 1.39-1.27 (m, 4H), 1.22-1.16 (m, 2H); (***Z* isomer**) 7.75 (d, *J* = 8.0 Hz, 2H), 7.54 (d, *J* = 7.5 Hz, 1H), 7.34-7.24 (m, 5H), 5.46 (dt, *J* = 11.0, 7.5 Hz, 1H), 4.95-4.89 (m, 1H), 4.55 (s, 2H), 4.48 (s, 2H), 4.07 (s, 2H), 3.72 (s, 6H), 3.40 (t, *J* = 5.7 Hz, 2H), 2.60 (d, *J* = 8.0 Hz, 2H), 2.59 (s, 2H), 2.43 (s, 3H), 1.88 (td, *J* = 7.2 Hz, 2H), 1.52 (p, *J* = 6.4 Hz, 2H), 1.39-1.27 (m, 4H), 1.22-1.16 (m, 2H);

**<sup>13</sup>C NMR** (125 MHz, CDCl<sub>3</sub>, ppm) δ (***E* isomer**) 170.23, 143.45, 137.1, 136.50, 135.2, 129.8, 129.6, 129.1, 128.8, 127.6, 127.5, 122.7, 80.7, 76.7, 71.67, 69.4, 56.4, 52.82, 45.0, 36.2, 35.3, 31.9, 28.4, 27.9, 26.6, 24.9, 22.5, 21.5 (one C, absent); (***Z* isomer**) 170.19, 143.36, 136.48, 135.3, 134.8, 130.2, 129.5, 129.3, 128.6, 127.8, 127.5, 122.2, 80.8, 76.6, 71.7, 69.2, 56.8, 52.8, 46.5, 37.4, 30.2, 29.0, 28.6, 27.6, 26.5, 25.1, 23.1, 21.6 (one C, absent);

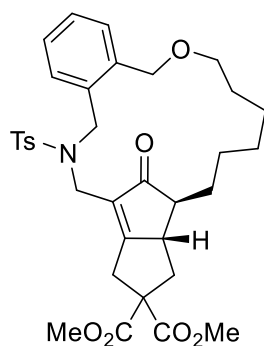
**IR** (neat, ATR, cm<sup>-1</sup>): 3027, 2926, 2858, 2359, 1735, 1437, 1347, 1210, 1160, 1089, 1066;

**HRMS** (DART): calcd [M+H]<sup>+</sup> (C<sub>33</sub>H<sub>42</sub>NO<sub>7</sub>S) 596.26765, found 596.26750.



**dimethyl 15-oxo-3-tosyl-11,12,13,13a,14,15-hexahydro-7-oxa-3-aza-1(6,4)-pentalena-5(1,2)-benzenacyclotridecaphane-1<sup>2</sup>,1<sup>2</sup>-dicarboxylate (4-75)**

Prior to reaction, glassware was soaked in concentrated nitric acid for 24 h, then KOH/*i*PrOH/H<sub>2</sub>O for 24 h.<sup>52</sup> MeCN was submitted to 3 freeze/pump/thaw cycles prior to use. A flame dried flask with complex **4-47** (100 mg, 0.113 mmol) and a stir bar was flushed with nitrogen, then MeCN (11 mL) was added. An MeCN (5.0 mL) solution of NMO (80 mg, 0.681 mmol) was added dropwise with stirring at 50 °C over 14 h. The mixture was stirred at 50 °C for another 4 h. Solvent was removed *in vacuo*. Chromatography with 3:1 Hex:EtOAc gave 28 mg (40% yield, 5.5:1 diastereomeric ratio, *trans* major) of a clear colorless oil. Further chromatography was repeated with preparative TLC with 2:1 Hex:EtOAc to yield pure diastereomers for characterization (see *trans*-**4-75** and *cis*-**4-75**, below).



**dimethyl *trans*-15-oxo-3-tosyl-11,12,13,13a,14,15-hexahydro-7-oxa-3-aza-1(6,4)-pentalena-5(1,2)-benzenacyclotridecaphane-1<sup>2</sup>,1<sup>2</sup>-dicarboxylate (*trans*-4-75)**

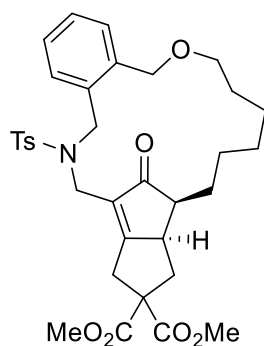
**<sup>1</sup>H NMR** (400 MHz, CDCl<sub>3</sub>, ppm) δ 7.69 (d, *J* = 8.4 Hz, 2H), 7.53-7.49 (m, 1H), 7.37-7.35 (m, 1H), 7.31 (d, *J* = 8.0 Hz, 2H), 7.19-7.16 (m, 2H), 4.37 (d, *J* = 16.4 Hz, 1H), 4.35 (d, *J* = 12.4 Hz, 1H), 4.30 (d, *J* = 12.8 Hz, 1H), 4.15 (d, *J* = 16.4 Hz, 1H), 4.13 (d, *J* = 14.0 Hz, 1H), 3.85 (d, *J* = 14.0 Hz, 1H), 3.80 (s, 3H), 3.76 (s, 3H), 3.58-3.47 (m, 2H), 3.32 (d, *J* = 19.6 Hz, 1H), 3.23 (d, *J* = 19.6 Hz, 1H), 2.63 (dd, *J* = 12.6, 7.8 Hz, 1H), 2.44 (s, 3H), 2.31 (bdd, *J* = 12.4, 7.8 Hz, 1H), 1.84 (m, 1H), 1.63-1.37 (m, 8H), 1.41 (dd, *J* = 12.4, 12.4 Hz, 1H), 1.27 (p, *J* = 6.5 Hz, 2H);

**<sup>13</sup>C NMR** (125 MHz, CDCl<sub>3</sub>, ppm) δ 210.1, 183.4, 171.7, 171.1, 143.6, 136.0, 135.8, 134.7, 130.7, 129.8, 127.5, 127.32, 127.30, 127.2, 127.0, 70.0, 68.7, 60.9, 53.2, 53.1, 51.9, 48.9, 48.4, 42.1, 38.1, 34.7, 26.9, 26.8, 26.4, 24.1, 23.7, 21.5;

**IR** (neat, ATR, cm<sup>-1</sup>): 3006, 2951, 2864, 1737, 1715, 1365, 1218, 1159, 665;

**HRMS** (DART): calcd [M+H]<sup>+</sup> (C<sub>34</sub>H<sub>42</sub>NO<sub>8</sub>S) 624.26526, found 624.26290.





**dimethyl *cis*-15-oxo-3-tosyl-11,12,13,13a,14,15-hexahydro-7-oxa-3-aza-1(6,4)-pentalena-5(1,2)-benzenacyclotridecaphane-1<sup>2</sup>,1<sup>2</sup>-dicarboxylate (*cis*-4-75)**

**<sup>1</sup>H NMR** (500 MHz, C<sub>6</sub>D<sub>6</sub>, ppm) δ 7.69 (d, *J* = 7.0 Hz, 1H), 7.67 (d, *J* = 8.5 Hz, 2H), 7.29 (d, *J* = 8.0 Hz, 1H), 7.12-7.09 (m, 1H), 7.03, (t, *J* = 7.5 Hz, 1H), 6.75 (d, *J* = 8.0 Hz, 2H), 4.65 (d, *J* = 17.0 Hz, 1H), 4.43 (d, *J* = 12.0 Hz, 1H), 4.41 (d, *J* = 16.5 Hz, 1H), 4.24 (d, *J* = 15.0 Hz, 1H), 4.04 (d, *J* = 12.0 Hz, 1H), 3.91 (d, *J* = 14.5 Hz, 1H), 3.60 (d, *J* = 20.5 Hz, 1H), 3.50 (d, *J* = 20.0 Hz, 1H), 3.40-3.28 (m, 2H), 3.283 (s, 6H), 2.66 (ddd, *J* = 13.5, 6.8, 6.8 Hz, 1H), 2.28 (dd, *J* = 12.5, 7.5 Hz, 1H), 2.66 (ddd, *J* = 13.5, 6.8, 6.8 Hz, 1H), 1.97 (ddd, *J* = 11.0, 6.8, 4.0 Hz, 1H) 1.85 (s, 3H), 1.67 (dd, *J* = 13.0 Hz, 1H), 1.37-1.08 (m, 10H);

**<sup>13</sup>C NMR** (125 MHz, CDCl<sub>3</sub>, ppm) δ 211.1, 181.8, 171.9, 170.8, 143.3, 136.6, 135.8, 135.2, 129.6, 128.8, 128.6, 127.7, 127.5, 127.3, 126.9, 70.2, 69.6, 60.6, 53.3, 53.1, 48.6, 48.5, 47.9, 41.7, 34.4, 33.8, 27.19, 27.17, 27.1, 24.3, 24.2, 21.5;

**IR** (neat, ATR, cm<sup>-1</sup>): 3022, 3003, 2970, 1738, 1435, 1366, 1355, 1228, 1217, 1206;

**HRMS** (DART): calcd [M+H]<sup>+</sup> (C<sub>34</sub>H<sub>42</sub>NO<sub>8</sub>S) 624.26526, found 624.26382.

## 4.6 Computational Methods

For all structures, a conformational search was first performed using MMFF (gas phase) with Spartan'16 by Wavefunction, Inc.<sup>64</sup> The lowest energy conformer from the search was optimized for geometry in the gas phase using the B3LYP/6-31G(d) level of theory.<sup>53</sup> Single point energy calculations for were performed using the M06-2x/6-311+G(d,p) level of theory in the gas phase at 298.15 K.<sup>54</sup> All geometry optimizations and single point calculations were done using Spartan'16. The Gibbs free-energies were calculated by adding the thermal corrections and zero point energies based on the B3LYP/6-31G(d) level of theory to the single point energies calculated at the M06-2x/6-311+G(d,p) calculations. Free energies of reactions were calculated from the difference between free energies of products and reactants.

## 4.7 Supporting Information

Cartesian coordinates and energies of all reported structures for computational studies are provided in Appendix C.

## 4.8 References and Notes

- (1) Khand, I. U.; Knox, G. R.; Pauson, P. L.; Watts, W. E.; Foreman, M. I. *J. Chem. Soc. Perkin Trans. 1* **1973**, 977.
- (2) Khand, I. U.; Knox, G. R.; Pauson, P. L.; Watts, W. E. *J. Chem. Soc. Perkin Trans. 1* **1973**, 975.
- (3) Magnus, P.; Principe, L. M. *Tetrahedron Lett.* **1985**, 26, 4851.
- (4) Blanco-Urgoiti, J.; Anorbe, L.; Perez-Serrano, L.; Dominguez, G.; Perez-Castells, J. *Chem. Soc. Rev.* **2004**, 33, 32.

- (5) Geis, O.; Schmalz, H.-G. *Angew. Chem. Int. Ed.* **1998**, *37*, 911.
- (6) Gibson, S. E.; Stevenazzi, A. *Angew. Chem. Int. Ed.* **2003**, *42*, 1800.
- (7) Lee, H.-W.; Kwong, F.-Y. *Eur. J. Org. Chem.* **2010**, *2010*, 789.
- (8) Hayashi, Y.; Inagaki, F.; Mukai, C. *Org. Lett.* **2011**, *13*, 1778.
- (9) Huang, J.; Fang, L.; Long, R.; Shi, L.-L.; Shen, H.-J.; Li, C.; Yang, Z. *Org. Lett.* **2013**, *15*, 4018.
- (10) Ishikawa, T.; Ishii, H.; Shimizu, K.; Nakao, H.; Urano, J.; Kudo, T.; Saito, S. *J. Org. Chem.* **2004**, *69*, 8133.
- (11) Liu, Q.; Yue, G.; Wu, N.; Lin, G.; Li, Y.; Quan, J.; Li, C.; Wang, G.; Yang, Z. *Angew. Chem. Int. Ed.* **2012**, *51*, 12072.
- (12) You, L.; Liang, X.-T.; Xu, L.-M.; Wang, Y.-F.; Zhang, J.-J.; Su, Q.; Li, Y.-H.; Zhang, B.; Yang, S.-L.; Chen, J.-H.; Yang, Z. *J. Am. Chem. Soc.* **2015**, *137*, 10120.
- (13) Shi, L.; Yang, Z. *Eur. J. Org. Chem.* **2016**, *2016*, 2356.
- (14) Lv, C.; Yan, X.; Tu, Q.; Di, Y.; Yuan, C.; Fang, X.; Ben-David, Y.; Xia, L.; Gong, J.; Shen, Y.; Yang, Z.; Hao, X. *Angew. Chem. Int. Ed.* **2016**, *55*, 7539.
- (15) Clark, J. S.; Xu, C. *Angew. Chem. Int. Ed.* **2016**, *55*, 4332.
- (16) Yamakoshi, H.; Sawayama, Y.; Akahori, Y.; Kato, M.; Nakamura, S. *Org. Lett.* **2016**, *18*, 3430.
- (17) Blaszykowski, C.; Harrak, Y.; Gonçalves, M.-H.; Cloarec, J.-M.; Dhimane, A.-L.; Fensterbank, L.; Malacria, M. *Org. Lett.* **2004**, *6*, 3771.

- (18) Gu, Z.; Zakarian, A. *Org. Lett.* **2010**, *12*, 4224.
- (19) Carrillo, R.; Martín, T.; López-Rodríguez, M.; Pinacho Crisóstomo, F. *Org. Lett.* **2014**, *16*, 552.
- (20) Reyes, E.; Uria, U.; Carrillo, L.; Vicario, J. L. *Tetrahedron* **2014**, *70*, 9461.
- (21) Deslongchamps, P. *Pure Appl. Chem.* **1992**, *64*, 1831.
- (22) Takao, K.; Munakata, R.; Tadano, K. *Chem. Rev.* **2005**, *105*, 4779.
- (23) Marsault, E.; Toró, A.; Nowak, P.; Deslongchamps, P. *Tetrahedron* **2001**, *57*, 4243.
- (24) Marsault, E.; Deslongchamps, P. *Org. Lett.* **2000**, *2*, 3317.
- (25) Tortosa, M.; Yakelis, N. A.; Roush, W. R. *J. Am. Chem. Soc.* **2008**, *130*, 2722.
- (26) Iafe, R. G.; Kuo, J. L.; Hochstatter, D. G.; Saga, T.; Turner, J. W.; Merlic, C. A. *Org. Lett.* **2013**, *15*, 582.
- (27) Boñaga, L. V. R.; Krafft, M. E. *Tetrahedron* **2004**, *60*, 9795.
- (28) Cambeiro, X. C.; Pericàs, M. A. In *The Pauson-Khand Reaction*; John Wiley & Sons, Ltd, 2012; pp 23–48.
- (29) Srinivasan, R.; Merritt, V. Y.; Subrahmanyam, G. *Tetrahedron Lett.* **1974**, *15*, 2715.
- (30) Sheridan, R. S. *Tetrahedron Lett.* **1982**, *23*, 267.
- (31) Ors, J. A.; Srinivasan, R. *J. Org. Chem.* **1977**, *42*, 1321.
- (32) Karabiyikoglu, S. Transition Metal-Mediated Synthesis and Functionalization of Macrocycles. Ph.D. Dissertation, University of California, Los Angeles, CA, 2015.

- (33) Iafe, R. G.; Chan, D. G.; Kuo, J. L.; Boon, B. A.; Faizi, D. J.; Saga, T.; Turner, J. W.; Merlic, C. A. *Org. Lett.* **2012**, *14*, 4282.
- (34) Karabiyikoglu, S.; Merlic, C. A. *Org. Lett.* **2015**, *17*, 4086.
- (35) Greenfield, H.; Sternberg, H. W.; Friedel, R. A.; Wotiz, J. H.; Markby, R.; Wender, I. J. *Am. Chem. Soc.* **1956**, *78*, 120.
- (36) Pauson, P. L.; Stambuli, J. P.; Chou, T.-C.; Hong, B.-C. In *Encyclopedia of Reagents for Organic Synthesis*; John Wiley & Sons, Ltd, 2001.
- (37) He, C. Q.; Chen, T. Q.; Patel, A.; Karabiyikoglu, S.; Merlic, C. A.; Houk, K. N. *J. Org. Chem.* **2015**, *80*, 11039.
- (38) Sugihara, T.; Yamaguchi, M.; Nishizawa, M. *Chem. – A Eur. J.* **2001**, *7*, 1589.
- (39) Tang, Y.; Deng, L.; Zhang, Y.; Dong, G.; Chen, J.; Yang, Z. *Org. Lett.* **2005**, *7*, 593.
- (40) Chung, Y. K.; Lee, B. Y.; Jeong, N.; Hudecek, M.; Pauson, P. L. *Organometallics* **1993**, *12*, 220.
- (41) Sugihara, T.; Yamada, M.; Ban, H.; Yamaguchi, M.; Kaneko, C. *Angew. Chem. Int. Ed. Engl.* **1997**, *36*, 2801.
- (42) Krafft, M. E.; Fu, Z.; Boñaga, L. V. R. *Tetrahedron Lett.* **2001**, *42*, 1427.
- (43) Karabiyikoglu, S.; Iafe, R. G.; Merlic, C. A. *Org. Lett.* **2015**, *17*, 5248.
- (44) Maifeld, S. V.; Lee, D. *Chem. – A Eur. J.* **2005**, *11*, 6118.
- (45) Hansen, E. C.; Lee, D. *Acc. Chem. Res.* **2006**, *39*, 509.
- (46) Clavier, H.; Correa, A.; Escudero-Adán, E. C.; Benet-Buchholz, J.; Cavallo, L.; Nolan, S.

- P. Chem. - A Eur. J.* **2009**, *15*, 10244.
- (47) Chong, J. M.; Heuft, M. A.; Rabbat, P. J. *Org. Chem.* **2000**, *65*, 5837.
- (48) Berube, M.; Poirier, D. *J. Enzyme Inhib. Med. Chem.* **2009**, *24*, 832.
- (49) Schwab, P.; France, M. B.; Ziller, J. W.; Grubbs, R. H. *Angew. Chem. Int. Ed. Engl.* **1995**, *34*, 2039.
- (50) Keitz, B. K.; Endo, K.; Patel, P. R.; Herbert, M. B.; Grubbs, R. H. *J. Am. Chem. Soc.* **2012**, *134*, 693.
- (51) Scholl, M.; Trnka, T. M.; Morgan, J. P.; Grubbs, R. H. *Tetrahedron Lett.* **1999**, *40*, 2247.
- (52) Krafft, M. E.; Bonaga, L. V. R.; Hirosawa, C. *Tetrahedron Lett.* **1999**, *40*, 9171.
- (53) Becke, A. D. *J. Chem. Phys.* **1993**, *98*, 1372.
- (54) Zhao, Y.; Truhlar, D. G. *Theor. Chem. Acc.* **2008**, *120*, 215.
- (55) See Computational Methods and Appendix C for complete details.
- (56) Brecht, J. *Justus Liebigs Ann. Chem.* **1924**, *437*, 1.
- (57) Kang, S. K.; Kim, W. S.; Moon, B. H. *Synthesis* **1985**, 1161.
- (58) Belmessieri, D.; Cordes, D. B.; Slawin, A. M. Z.; Smith, A. D. *Org. Lett.* **2013**, *15*, 3472.
- (59) Baldwin, J. E.; Adlington, R. M.; Ramcharitar, S. H. *Tetrahedron* **1992**, *48*, 3413.
- (60) Lee, C.-F.; Leigh, D. A.; Pritchard, R. G.; Schultz, D.; Teat, S. J.; Timco, G. A.; Winpenny, R. E. P. *Nature* **2009**, *458*, 314.
- (61) Wickel, H.; Agarwal, S. *Macromolecules* **2003**, *36*, 6152.

- (62) Barrett, S.; O'Brien, P.; Steffens, H. C.; Towers, T. D.; Voith, M. *Tetrahedron* **2000**, *56*, 9633.
- (63) Teller, H.; Corbet, M.; Mantilli, L.; Gopakumar, G.; Goddard, R.; Thiel, W.; Fürstner, A. *J. Am. Chem. Soc.* **2012**, *134*, 15331.
- (64) Spartan'16. **Wavefunction, Inc.** Irvine, CA.

## Chapter 5

### Progress Towards the Total Synthesis of (+)-Kingianin A

#### 5.1 Abstract

This chapter highlights progress towards the total synthesis of (+)-kingianin A. This natural product was isolated as a racemic mixture from the bark of *Endiandra kingiana* and is an inhibitor of antiapoptotic protein Bcl-Xl, highlighting its potential use in cancer treatments. Its structure is proposed to arise from an intermolecular Diels-Alder dimerization reaction of bicyclo[4.2.0]octadiene fragments derived from an  $8\pi/6\pi$ -electrocyclization cascade. Although two total syntheses of ( $\pm$ )-kingianin A have been reported, an enantioselective synthesis has not been achieved and is the purpose of this study. This synthetic route begins from L-(+)-dimethyl tartrate, a cheap and commercially available starting material, and aims to follow a biomimetic synthetic pathway featuring a substrate controlled diastereoselective palladium(II)-catalyzed oxidative cyclization and  $8\pi/6\pi$ -electrocyclization cascade. Although the feasibility of this cascade pathway has not yet been realized, key synthetic transformations to install the requisite carbocyclic framework of (+)-kingianin A have been discovered, paving the way for future investigations on the palladium(II)-catalyzed coupling/electrocyclization cascade and completion of the synthesis.

#### 5.2 Introduction

Programmed cell death, also known as apoptosis, is critical to the proper functioning of a cell population. Resistance to apoptosis leads to uncontrolled cell proliferation, a common feature in many forms of cancer.<sup>1</sup> In functioning cells, the Bcl-2 family of proteins regulate cytochrome C mediated apoptosis in a balance between proapoptotic (Bax, Bak, Bid, Bim) and antiapoptotic (Bcl-2, Bcl-XL, Bcl-W) proteins in the mitochondria.<sup>1-3</sup> Overexpression of Bcl-2 antiapoptotic



proteins gives rise to apoptosis resistance and increased cancer cell proliferation.<sup>3</sup> As a result, many cancer therapies are focused on inhibition of these Bcl-2 antiapoptotic proteins.<sup>4</sup> Of these antiapoptotic proteins, Bcl-XL has received considerable attention as a target for drug discovery,<sup>5</sup> leading to a search for selective small molecule inhibitors of this target.<sup>6</sup>

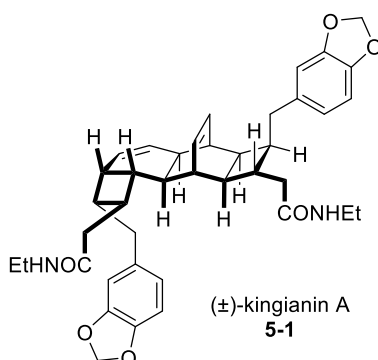


**Figure 5.1. Structure of (±)-kingianin A.**

The kingianin family of polyketide natural products, isolated from the bark of the tree *Endiandra kingiana*, was first reported in 2010 with the disclosure of (±)-kingianin A (**5-1**, Figure 5.1).<sup>7</sup> Kingianin A, along with its family of isomeric kingianins B-F (Figure 5.2), were later reported to bind to the Bcl-XL antiapoptotic protein in the micromolar range, highlighting their potential use for cancer therapy (Table 5.1).<sup>8</sup> Each member of the family was isolated as a racemic pair. Of the two enantiomers of kingianin A, (-)-kingianin A is the more bioactive component, and most active among all enantiomeric forms of the kingianins A-F.

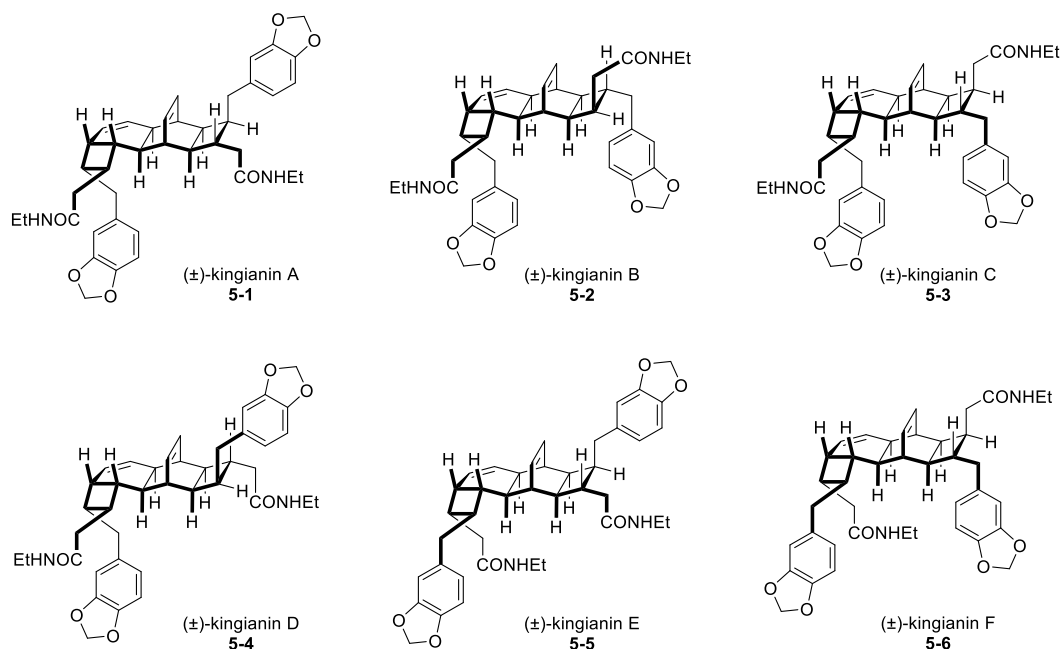


**Figure 5.2. Structure of kingianins A-F.**

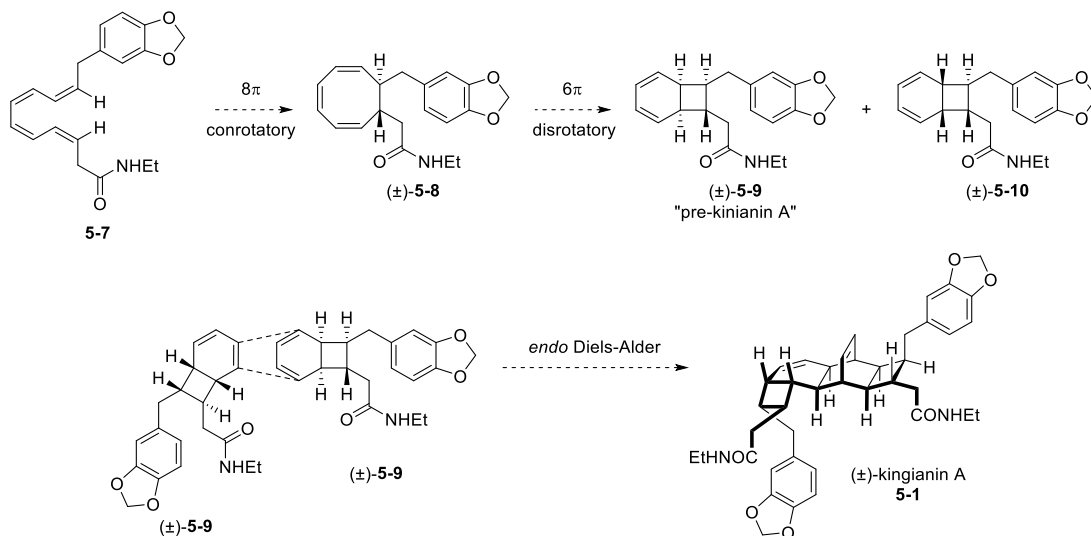
**Table 5.1. Bcl-XL binding affinity ( $K_i$ ) of kingianins A-F<sup>a</sup>**

Compound	Racemic Mixture $K_i$	Enantiomer (-) $K_i$	Enantiomer (+) $K_i$
<b>Kingianin A</b>	213 ± 53	60 ± 1.5	> 300
<b>Kingianin B</b>	> 300	N.D.	N.D.
<b>Kingianin C</b>	> 300	N.D.	N.D.
<b>Kingianin D</b>	> 300	N.D.	N.D.
<b>Kingianin E</b>	> 300	N.D.	N.D.
<b>Kingianin F</b>	231 ± 47	N.D.	N.D.

<sup>a</sup>  $K_i$  values are the mean value ± standard deviation, measured in  $\mu\text{M}$ . N.D. = not determined.

(±)-Kingianin A was proposed to arise from a pericyclic reaction cascade starting from (*Z,E,E,Z*)-tetraene **5-7** (Scheme 5.1).<sup>7</sup> Starting from **5-7**, an  $8\pi$ -electrocyclization gives the cyclic triene **5-8**. The  $8\pi$ -electrocyclic ring closure sets the *trans*-stereochemistry from a conrotatory

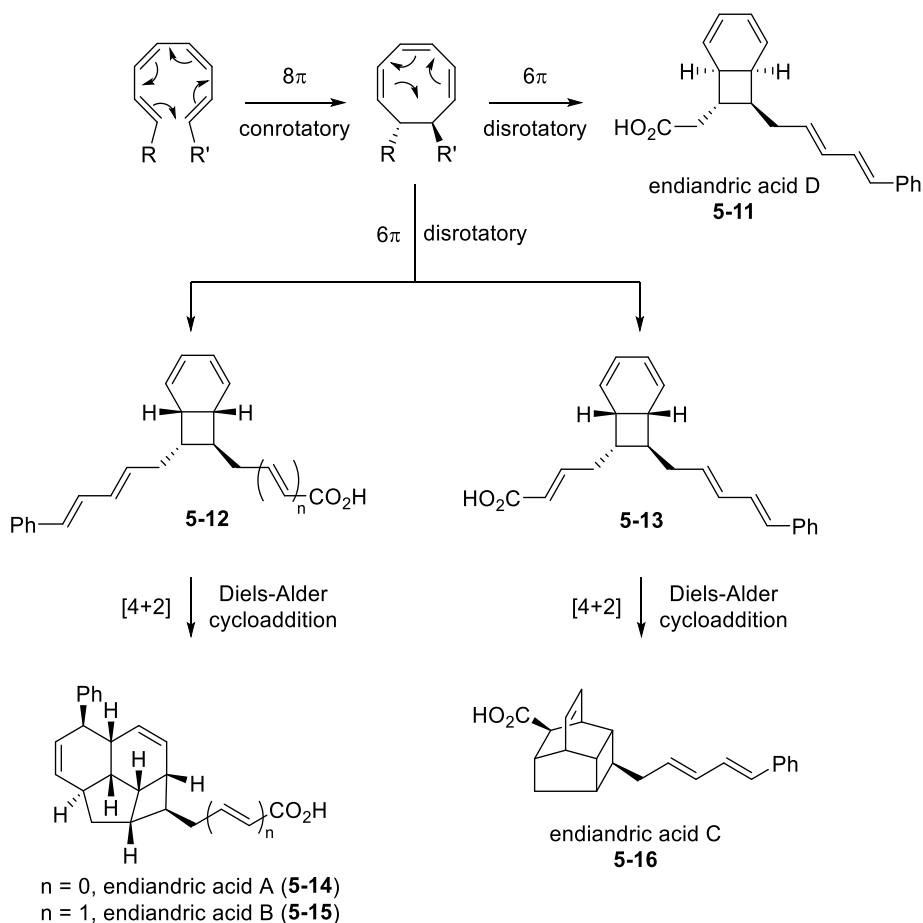
rotation of terminal substituents where enantiomeric rotations result in a racemic mixture. A  $6\pi$ -electrocyclic ring closure forms a diastereomeric pair of bicyclo[4.2.0] octadiene intermediates **5-9** and **5-10** where a thermal disrotatory mode sets the *cis*-ring juncture. The four isomers of **5-9** and **5-10** are the origin of the isomeric kingianin dimers. Diastereomer **5-9**, later named “pre-kingianin A,” is proposed to undergo an *endo*-Diels-Alder dimerization to give kingianin A, the homochiral dimer of **5-9**. On the other hand, the *endo* Diels-Alder dimerization of opposite enantiomers of **5-9** gives rise to the heterochiral dimer kingianin D (**5-4**, Figure 5.2). Crossed *endo* Diels-Alder cycloaddition reactions of racemic diastereomers **5-9** and **5-10** results in the formation of kingianins B, C, and E. Kingianin F is the homochiral dimer of **5-10**. These electrocyclic pathways helps explain why each kingianin natural product was isolated as a racemic mixture, where the  $8\pi/6\pi$ -electrocyclic ring closure cascade forms racemic products **5-9** and **5-10** that undergo dimerization.



### Scheme 5.1. Proposed biosynthesis of kingianin A.

The bicyclo[4.2.0]octadiene precursor structure of the kingianin natural products is similar to that of the endiandric acids, first discovered in the 1980's by Black and coworkers.<sup>9-14</sup> The

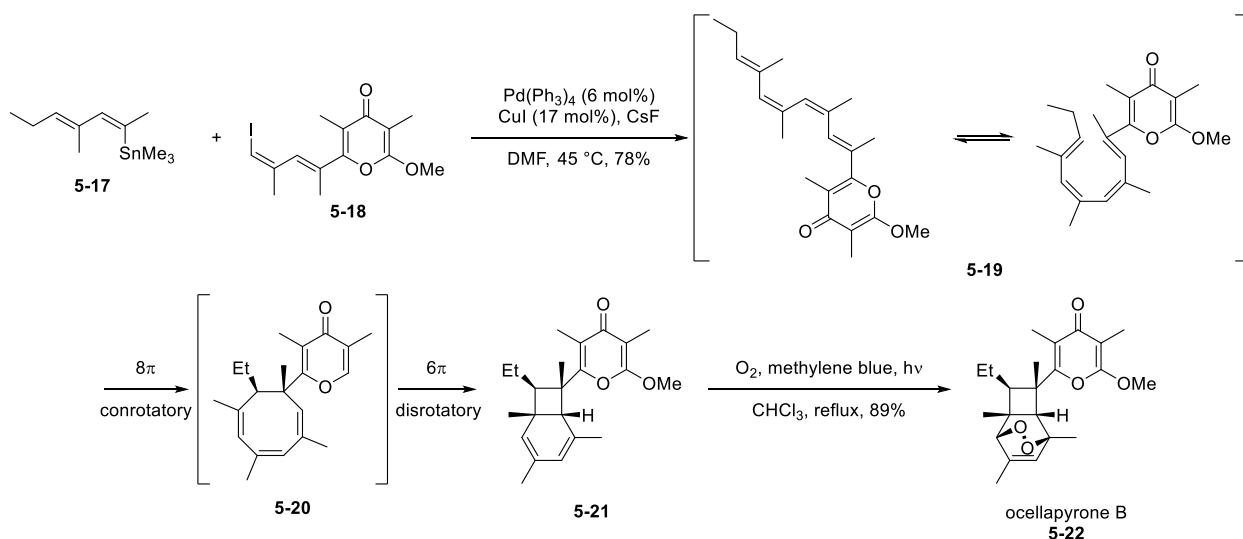
structures of the endiandric acids were proposed to arise from linear (*E,Z,Z,E*) or (*Z,Z,Z,Z*)-tetraenes that undergo  $8\pi/6\pi$ -cascade electrocyclizations to substituted bicyclo[4.2.0]octadiene structures (Scheme 5.2).<sup>10</sup> Endiandric acid D (**5-11**) is stable as a bicyclo[4.2.0]octadiene, but intramolecular Diels-Alder reactions occur for intermediates **5-12** and **5-13**, which accounts for the formation of endiandric acids A, B, and C. Similar to the kingianin natural products, the endiandric acids are isolated in their racemic forms, highlighting the possibility that the  $8\pi$ -conrotatory step of their biosynthesis proceeds by a non-enzymatic pathway.



**Scheme 5.2. Proposed biosynthesis of endiandric acids A-D.**

The  $8\pi/6\pi$ -electrocyclization cascade has been applied to the total synthesis of many natural products with bicyclo[4.2.0]octadiene cores. Nicolaou demonstrated an application of this

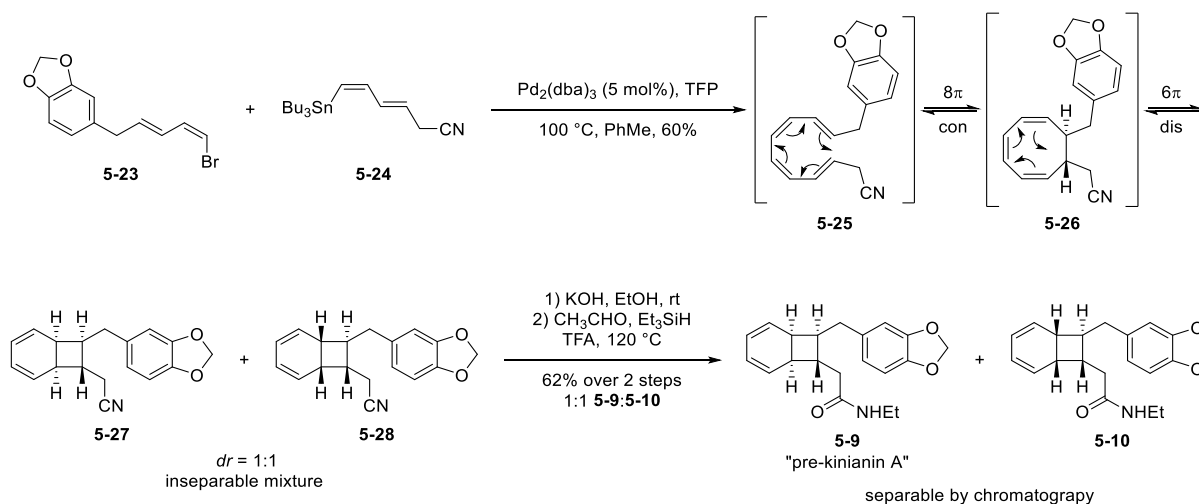
cascade reaction to the total synthesis of endiandric acids.<sup>15-17</sup> The immunosuppressants SNF4435C and SNF4435D have been synthesized by similar methods as well.<sup>18-21</sup> Ocellapyrone B (**5-22**, Scheme 5.3), isolated from *Placobranchus ocellatus*, also features a similar core with an endoperoxide bridge.<sup>22</sup> This natural product was first synthesized by the Trauner group in 2005.<sup>23</sup> The key step featured a Stille coupling/electrocyclization cascade. Palladium-catalyzed cross coupling of **5-17** and **5-18** gave the linear polyene **5-19** which underwent an  $8\pi/6\pi$ -electrocyclization cascade reaction to give the racemic bicyclo[4.2.0]octadiene **5-21** in 78% yield as the major diastereomer. To complete the synthesis, a [4+2] cycloaddition with singlet oxygen gave ocellapyrone B.



**Scheme 5.3. Total synthesis of ocellapyrone B by Trauner and co-workers.**

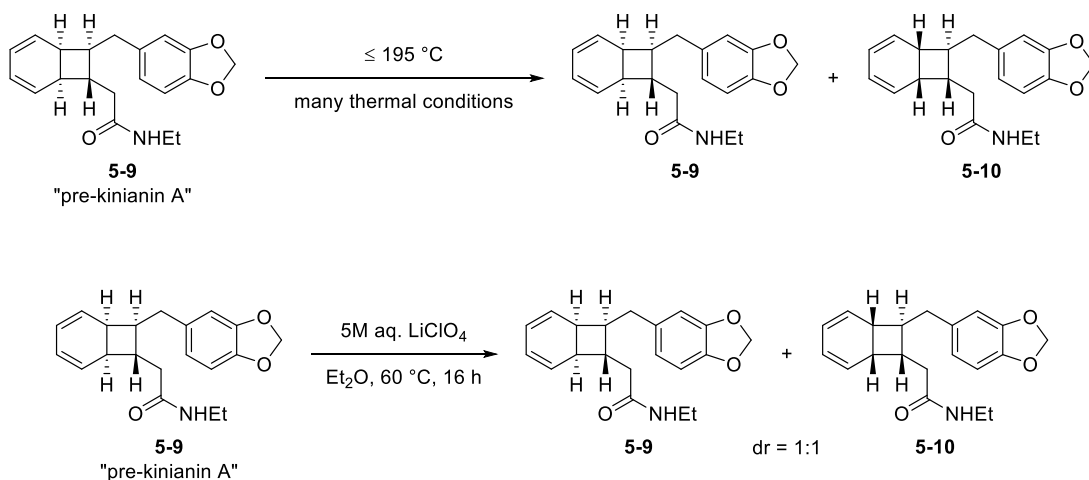
To test the proposed biosynthesis of kingianin A (Scheme 5.1), the Moses group synthesized the postulated bicyclo[4.2.0]octadiene precursor to kingianin A (**5-9**), which they termed “pre-kingianin A,” by an  $8\pi/6\pi$ -electrocyclization cascade (Scheme 5.4). Their key synthetic step involved a Stille coupling of dienyl bromide **5-23** and dienyl stannane **5-24** to give a linear tetraene **5-25**.<sup>24</sup> Due to the high temperature reaction conditions **5-25** was not isolable

under the reactions conditions and underwent the  $8\pi/6\pi$ -electrocyclization cascade to give a 1:1 mixture of inseparable diastereomeric bicyclo[4.2.0]octadienes **5-27** and **5-28**. Conversion of the nitrile groups to ethyl amides gave a separable mixture of pre-kingianin A (**5-9**), and its diastereomer **5-10**.



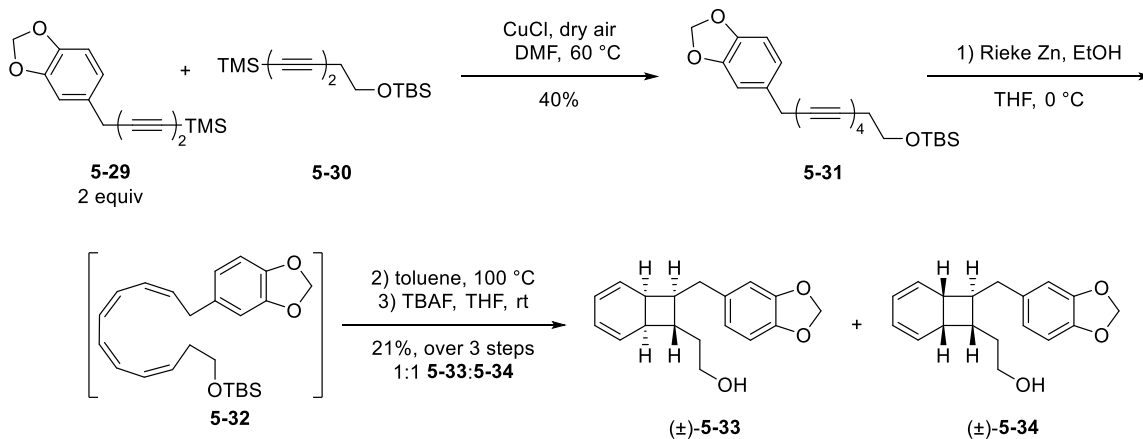
#### Scheme 5.4. Synthesis of pre-kingianin A by the Moses group.

The Moses group observed that pre-kingianin A (**5-9**) was isolable at room temperature and did not undergo a Diels-Alder dimerization reaction to give kingianin A under a variety of reaction conditions.<sup>24</sup> This is not surprising considering that Diels-Alder dimerization of 1,3-cyclohexadiene requires temperatures in excess of 150 °C.<sup>25–27</sup> Thermal dimerization conditions with temperatures up to 195 °C gave mixtures of pre-kingianin A and its diastereomer **5-10** due to a reversible  $6\pi$ -electrocyclization (Scheme 5.5). Room temperature Diels-Alder reactions have been observed in 5 M solutions of  $\text{LiClO}_4$  in ether,<sup>28</sup> but these conditions were unsuccessful for **5-9**. These experiments suggested that the proposed biosynthetic route to ( $\pm$ )-kingianin A (Scheme 5.1) involving a Diels-Alder dimerization required revision.



### Scheme 5.5. Attempted Diels-Alder dimerizations of pre-kingianin A.

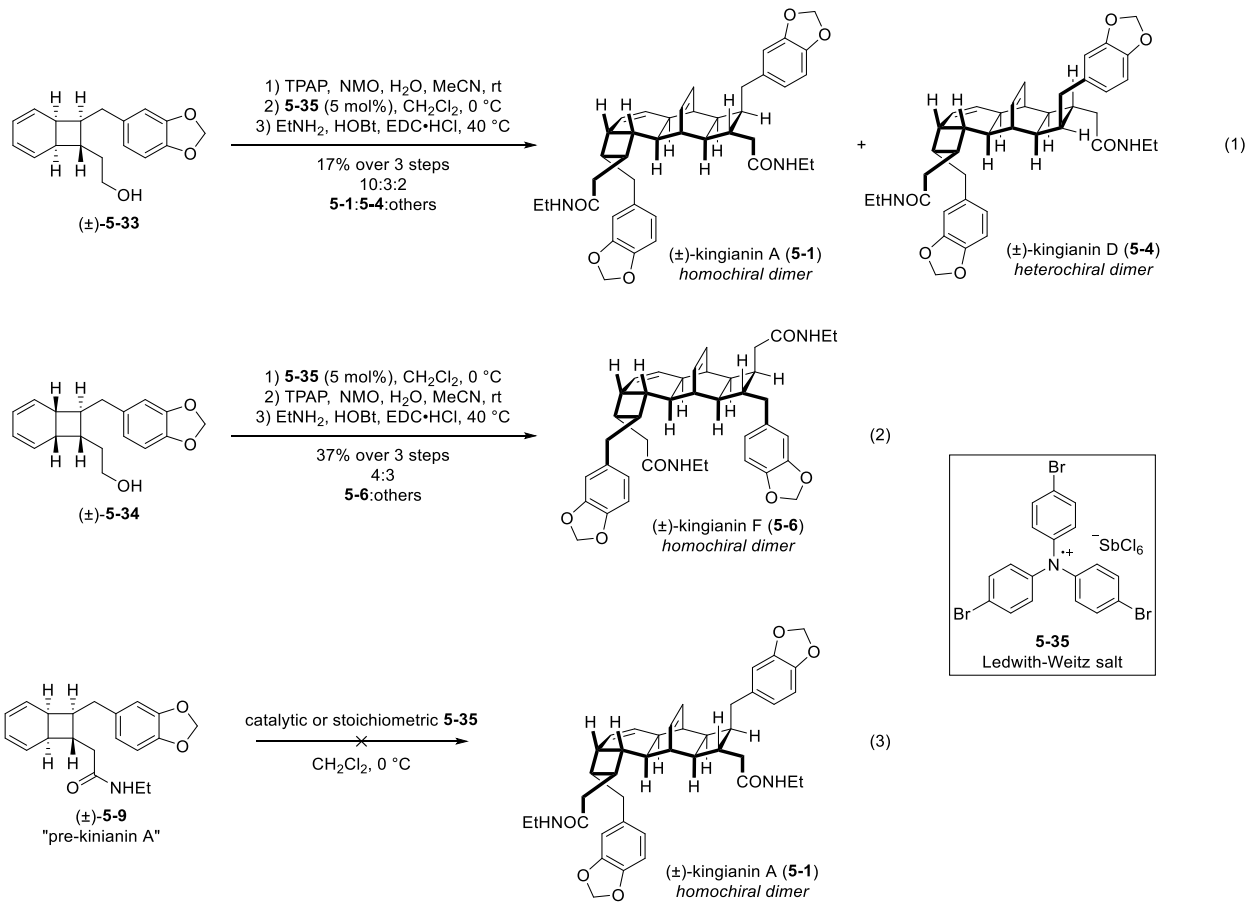
In light of the unsuccessful intermolecular Diels-Alder reaction of pre-kingianin A, the Sherburn group proposed a  $8\pi/6\pi$ -electrocyclization and a radical-cation catalyzed Diels-Alder biosynthetic pathway which they tested by total synthesis.<sup>29</sup> Their electrocyclization precursor was accessed from a linear tetrayne **5-31**, the product of an oxidative Mori-Hiyama coupling from diynes **5-29** and **5-30** (Scheme 5.6). Reduction with Rieke zinc gave the linear (*Z,Z,Z,Z*)-tetraene **5-32**, which was immediately dissolved in toluene and heated to 100 °C to cause the  $8\pi/6\pi$ -electrocyclization. After purification and deprotection, a 1:1 mixture of diastereomeric bicyclo[4.2.0]octadienes **5-33** and **5-34** were isolated in 21% yield over three steps. The successful electrocyclization cascade highlighted the possibility of a (*Z,Z,Z,Z*)-tetraene biosynthetic precursor to ( $\pm$ )-kingianin A, in contrast to the proposed (*E,Z,Z,E*)-tetraene intermediate (**5-7**, Scheme 5.1).



### Scheme 5.6. Sherburn's $8\pi/6\pi$ -electrocyclization cascade.

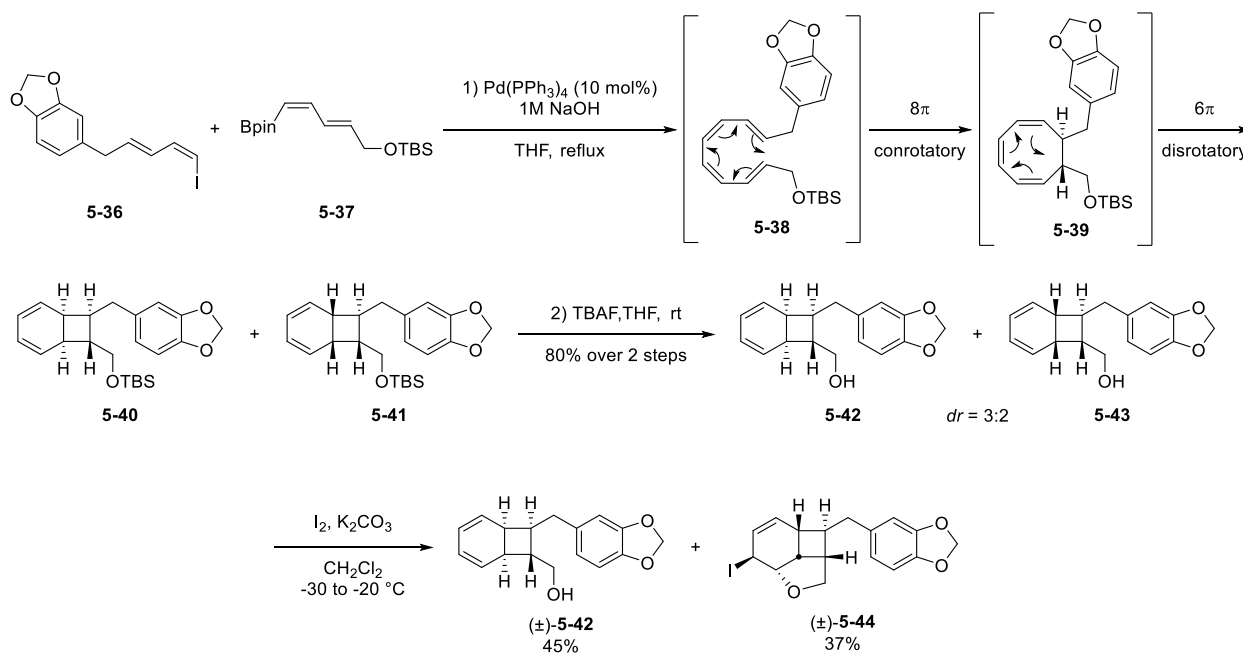
With the bicyclo[4.2.0]octadiene core prepared, the proposed radical-cation catalyzed Diels-Alder reaction was investigated. This step was catalyzed by the Ledwith-Weitz aminium salt **5-35**, which has been shown to catalyze Diels-Alder reactions of unactivated cyclohexadienes at  $0^\circ\text{C}$  in DCM by Bauld and co-workers.<sup>30</sup> A three-step sequence resulted in the successful completion of the total synthesis of ( $\pm$ )-kingianin A (Scheme 5.7). Oxidation of racemic alcohol **5-33** to the carboxylic acid, followed by treatment with the Ledwith-Weitz aminium salt, and subsequent amidation gave the homochiral dimer ( $\pm$ )-kingianin A as the major product, along with the minor heterochiral dimer ( $\pm$ )-kingianin D (eq 1). ( $\pm$ )-Kingianin F, the homochiral dimer of **5-34** was also successfully prepared by a similar reaction sequence (eq 2). Surprisingly, the proposed biosynthetic precursor “pre-kingianin A” (**5-9**) was unable to undergo the Diels-Alder dimerization to give kingianin A with either catalytic or stoichiometric Ledwith-Weitz salt (eq 3). These results suggest that while a single-electron transfer pathway may be involved in the biosynthesis of kingianin natural products, it is not operative starting from **5-9**, although an enzymatic pathway cannot be ruled out.





**Scheme 5.7. Sherburn's total synthesis of kingianin A, D, and F.**

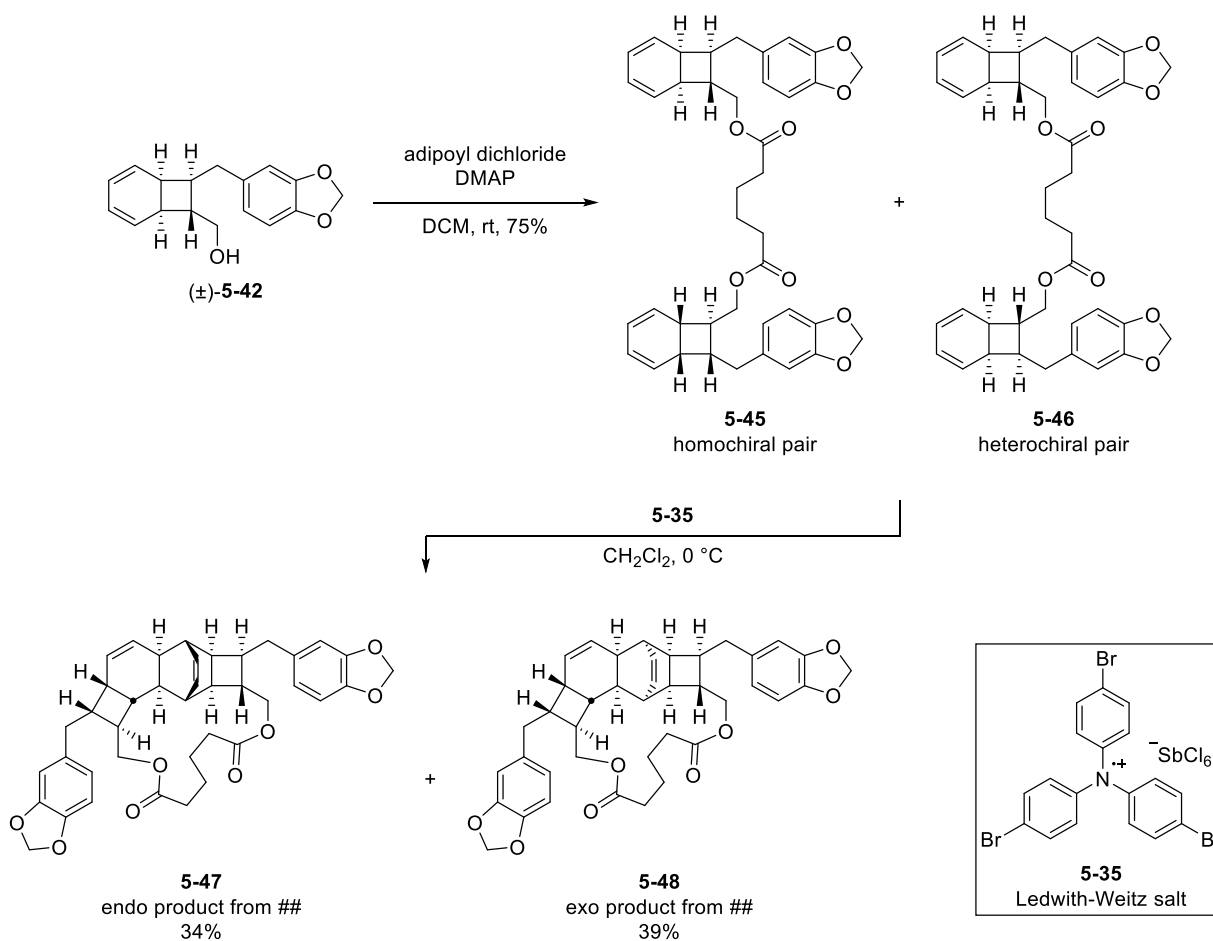
The Parker group synthesized ( $\pm$ )-kingianin A using a similar radical-cation Diels-Alder cyclization reaction of tethered bicyclo[4.2.0]octadiene precursors from an  $8\pi/6\pi$ -electrocyclization of a linear tetraene.<sup>31</sup> Suzuki coupling of dienyliodide **5-36** and boronate ester **5-37** gave an unstable linear tetraene **5-38** which underwent the  $8\pi/6\pi$ -electrocyclization to give a mixture of racemic bicyclo[4.2.0]octadienyl alcohols **5-40** and **5-41**. These were isolated after silyl group deprotection in a 3:2 diastereomeric ratio (Scheme 5.8). Upon treatment with iodine and potassium carbonate, the undesired diastereomer **5-43** underwent iodoetherification, allowing chromatographic separation to give pure racemic **5-42**, the requisite diastereomer to complete the synthesis.



**Scheme 5.8. Suzuki coupling/electrocyclization cascade.**

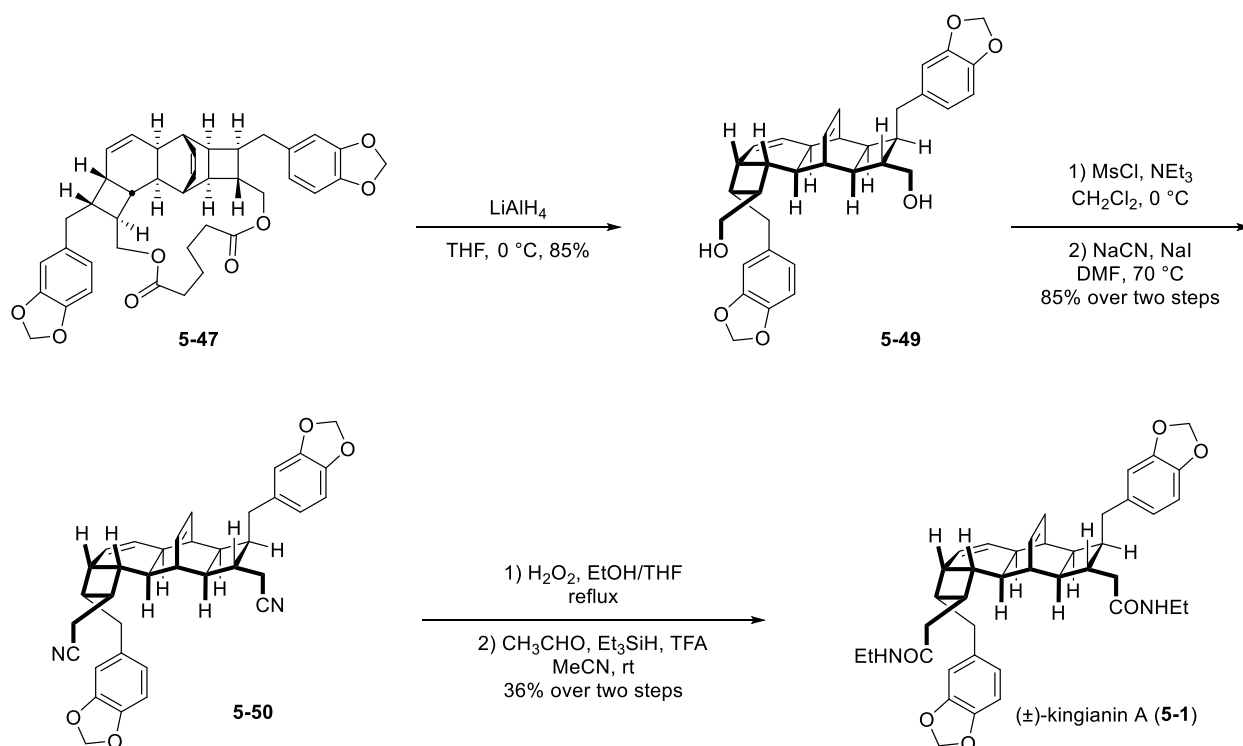
With the desired diastereomer in hand, tethering was successful by treatment with adipoyl chloride in the presence of DMAP to give a mixture of homochiral and heterochiral linked monomers from racemic **5-42** (Scheme 5.9). Kingianin A, the homochiral dimer of its proposed

biosynthetic precursor pre-kingianin A (**5-9**, Scheme 5.1) was expected to be accessible from the tethered homochiral pair **5-45**. The mixture of diastereomers **5-45** and **5-46** were treated with radical-cation Diels-Alder reaction conditions featuring the Ledwith-Weitz salt **5-35** in dichloromethane,<sup>30</sup> similar to those reported in the Sherburn group's total synthesis of kingianin A.<sup>29</sup> The desired radical-cation Diels-Alder dimerization of **5-45** was successful, giving the desired *endo* adduct **5-47**, with a nearly equal amount of the diastereomeric *exo* adduct **5-48**. It is notable there is no *endo/exo* selectivity compared with the intermolecular reaction. Surprisingly, the intramolecular cyclization of the heterochiral dimer **5-46** was not observed. Separation of the diastereomeric *endo* and *exo* products was possible prior to the final steps of the total synthesis.



**Scheme 5.9. Tethered radical-cation Diels-Alder reactions.**

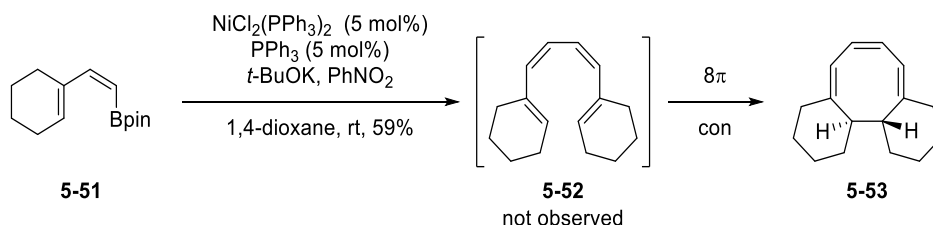
Completion of the total synthesis of ( $\pm$ )-kingianin A required removal of the tether and functionalization to the bis(ethyl amide). Lithium aluminum hydride removed the tether to give diol **5-49**, which was converted to the bis(nitrile) **5-50** by mesylation and treatment with sodium cyanide (Scheme 5.10). Hydrolysis promoted by hydrogen peroxide gave the bis(amide), which upon double reductive N-alkylation gave ( $\pm$ )-kingianin A.



**Scheme 5.10. Parker's completion of the total synthesis of ( $\pm$ )-kingianin A.**

Similar to the palladium-catalyzed access to  $8\pi/6\pi$ -electrocyclization cascades demonstrated earlier (Schemes 5.4, 5.6, and 5.8) we were interested to see whether bicyclo[4.2.0]octadiene structures would be accessible using our Pd(II)-catalyzed oxidative cyclization of bis(vinylboronate esters).<sup>32</sup> Inspiration arose from the serendipitous discovery by my co-worker Robert Tobolowsky, who discovered that treatment of *cis*-dienyl boronate ester **5-51** with catalytic nickel(II) in the presence of triphenyl phosphine, potassium carbonate, and

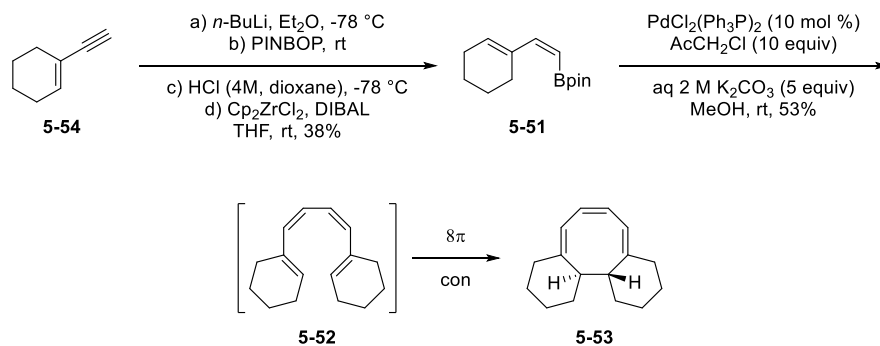
nitrobenzene gave the unexpected tricyclic polyene **5-53** (Scheme 5.11).<sup>33</sup> The linear tetraene **5-52** from the oxidative homocoupling reaction was unstable at room temperature and underwent an  $8\pi$ -electrocyclization at room temperature. Although the second  $6\pi$ -electrocyclization did not occur, as demonstrated for 1,8-disubstituted tetraenes, these 1,1,8,8-tetrasubstituted tetraenes have been shown to require considerably higher Gibbs free-energy of activation in computational studies.<sup>34</sup>



**Scheme 5.11. Ni(II)-catalyzed oxidative coupling/ $8\pi$ -electrocyclization cascade.**

### 5.3 Results and Discussion

We turned to our Pd(II)-catalyzed oxidative coupling conditions to explore the possibility of an oxidative coupling and  $8\pi/6\pi$ -coupling cascade. Similar to the Ni(II)-catalyzed oxidative coupling of bis(vinylboronate ester) **5-51** (Scheme 5.11), oxidative coupling catalyzed by palladium(II) in the presence of potassium carbonate and chloroacetone in methanol gave the unstable intermediate tetraene **5-52**, which underwent a conrotatory electrocyclic ring closure to the tricyclic polyene **5-53** (Scheme 5.12).



**Scheme 5.12. Pd(II)-catalyzed oxidative coupling/8 $\pi$ -electrocyclization cascade.**

Full characterization of **5-53** was not previously reported.<sup>35</sup> We found that **5-53** undergoes conformational change which complicated the spectral data. This was evidenced by broadened <sup>13</sup>C-NMR signals at room temperature that become 8 sharp signals at 45 °C, and 14 separate signals at -50 °C (two carbon signals are degenerate). Three alkene carbons were observed at 45 °C in the <sup>13</sup>C NMR spectrum, but six at -50 °C. This suggests that there is one preferred asymmetric conformer of **5-53** at low temperature which undergoes conformational change at higher temperatures. These data ruled out a second 6 $\pi$ -electrocyclization reaction that would create a strained four-membered ring, a reaction many related cyclooctatrienes undergo.<sup>34</sup>

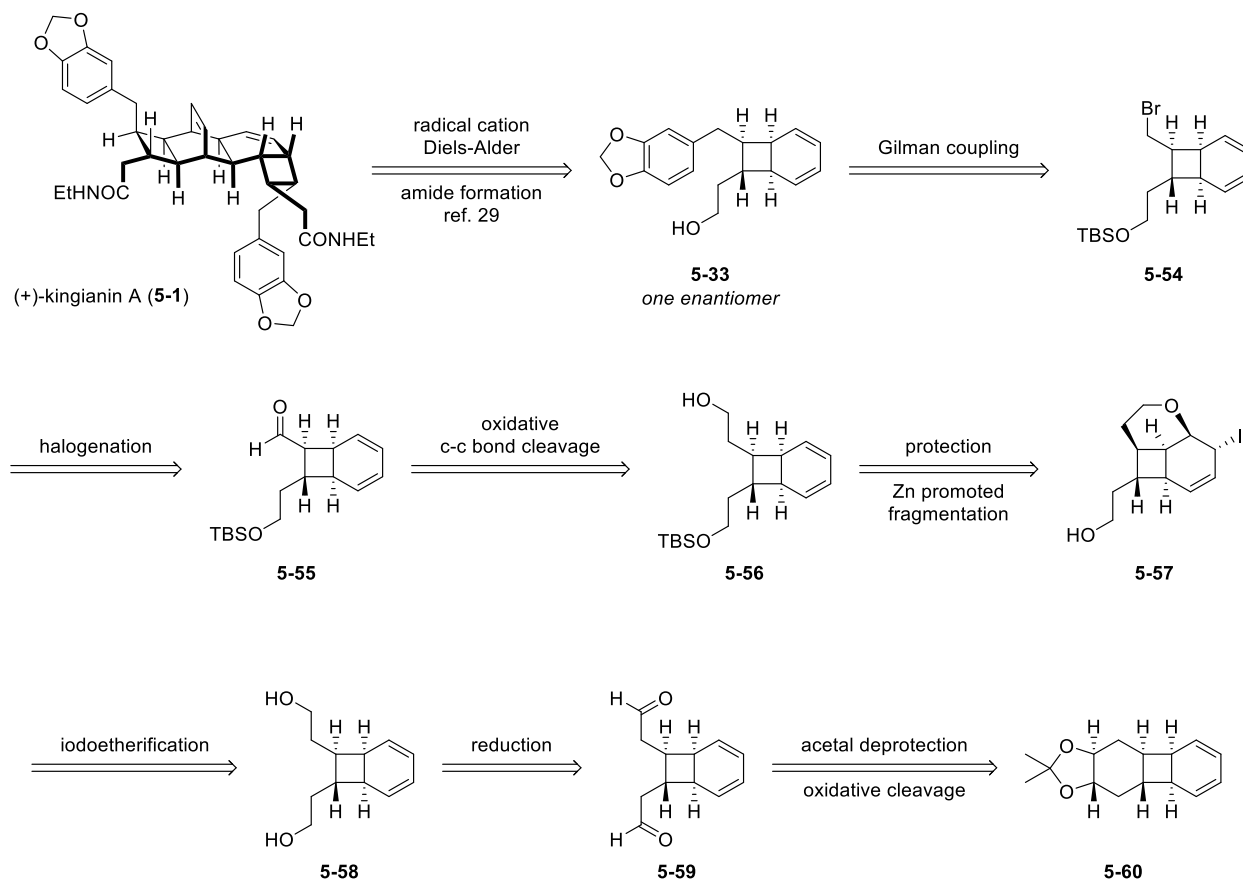
With the successful Pd(II)-catalyzed oxidative coupling/8 $\pi$ -electrocyclization cascade results, we suspected that an oxidative coupling and 8 $\pi$ /6 $\pi$ -electrocyclization coupling cascade reaction might be possible. Similar palladium-catalyzed cross coupling/8 $\pi$ /6 $\pi$ -electrocyclization cascades have been used to synthesize bicyclo[4.2.0]octadiene derivatives in key steps in total syntheses of kingianin A,<sup>29,31</sup> as well as the synthesis of its proposed biogenic precursor pre-kingianin A.<sup>24</sup>

With this inspiration, we set our sights on a synthetic route to kingianin A. Two synthetic pitfalls were observed in previous total syntheses of kingianin A. Previously, successful syntheses

relied upon radical-cation Diels-Alder dimerizations of racemic bicyclo[4.2.0]octadiene derivatives to give homochiral ( $\pm$ )-kingianin A.<sup>29,31</sup> These reactions suffered low yields due to competitive heterochiral dimer formation in the Diels-Alder cyclization step, or in the tethering step in tethered radical-cation Diels-Alder cyclization strategies (Scheme 5.7 and 5.9, respectively). In addition, each successful synthesis utilized a palladium-catalyzed cross coupling/electrocyclization cascade to give the racemic dimerization precursors in poor 1:1 diastereomeric ratios (Scheme 5.6 and 5.8). Thus, these syntheses necessitated tedious separation of the bicyclo[4.2.0]octadienes to isolate the desired diastereomer. Hence, an efficient synthesis of kingianin A would need to address these two key limitations.

To improve upon this synthetic groundwork, we propose an asymmetric synthesis of a kingianin precursor **5-33**, which upon dimerization will lead to enantiopure (+)-kingianin A (Scheme 5.13). Dimerization of a single enantiomer of the precursor prevents formation of heterochiral dimers, which will increase the overall yield of the dimerization reaction. Although (+)-kingianin A is less biologically active than its enantiomer, we chose to pursue its synthesis due to the cheaper cost of L-(+)-dimethyl tartrate relative to D-(-)-dimethyl tartrate while establishing an initial synthetic route. Alcohol **5-33** was previously demonstrated to undergo a radical-cation catalyzed Diels-Alder dimerization, followed by amide formation, to give ( $\pm$ )-kingianin A, as demonstrated by Sherburn and co-workers.<sup>29</sup> A Gilman coupling from **5-54** would provide the benzodioxole substituent. This would require a terminal halogen substituent, accessible from end group manipulations of aldehyde **5-55**. An oxidative C-C bond cleavage from alcohol **5-56** would provide **5-55**, likely via oxidation to the aldehyde, alpha hydroxylation, and oxidative cleavage with sodium periodate. Alcohol **5-56** would be prepared by a desymmetrization strategy from diol **5-58**, employing a selective iodoetherification of the alcohol proximal to the *cis*-cyclobutane ring

fusion, which would permit the free alcohol would be protected as the silyl ether. Diol **5-58** would be synthesized from aldehyde **5-59** formed in turn from acetal deprotection and oxidative cleavage of **5-60**.

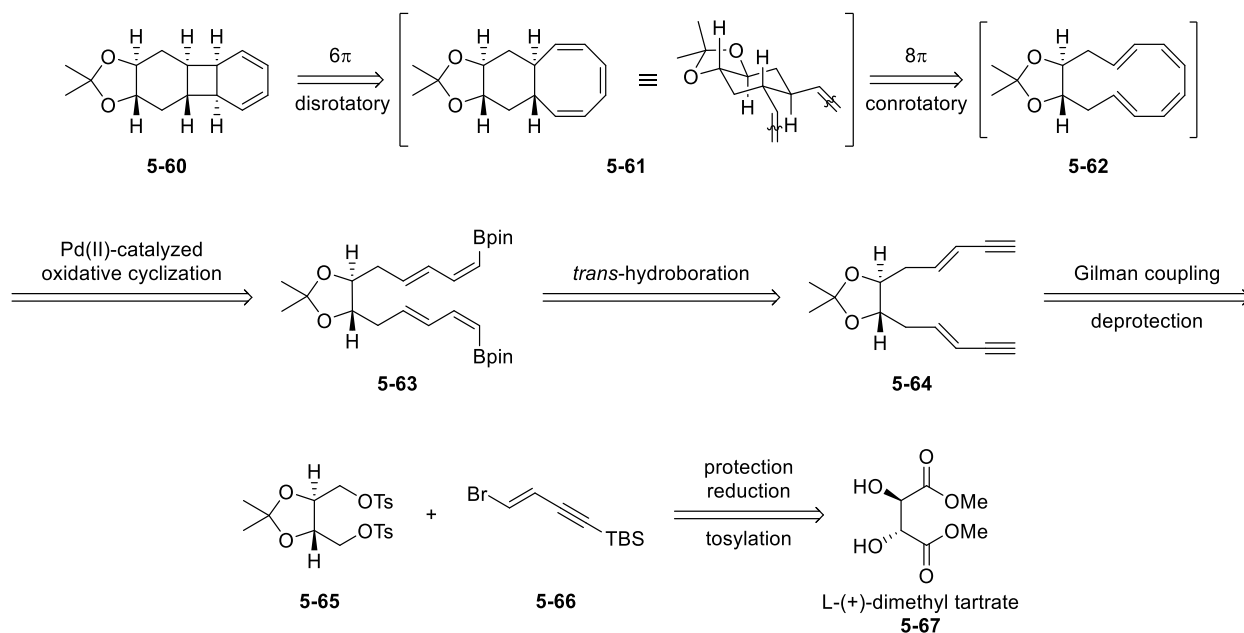


**Scheme 5.13. Retrosynthesis of (+)-kingianin A featuring a desymmetrization strategy.**

Tetracyclic diene **5-60** would be formed from the  $8\pi/6\pi$ -electrocyclization cascade reaction of cyclic tetraene **5-62** (Scheme 5.14). Oxidative cyclization of **5-63** with our Pd(II)-catalyzed oxidative cyclization conditions would be expected to yield the cyclic tetraene **5-62** under mild conditions.<sup>32</sup> Previous syntheses of kingianin A suffered from poor diastereoselectivity due to two diastereomeric directions of conrotatory electrocyclic ring closure in the  $8\pi$ -electrocyclization step. In the case of **5-62**, the  $8\pi$ -electrocyclization would be expected to yield triene **5-61**<sup>36</sup>



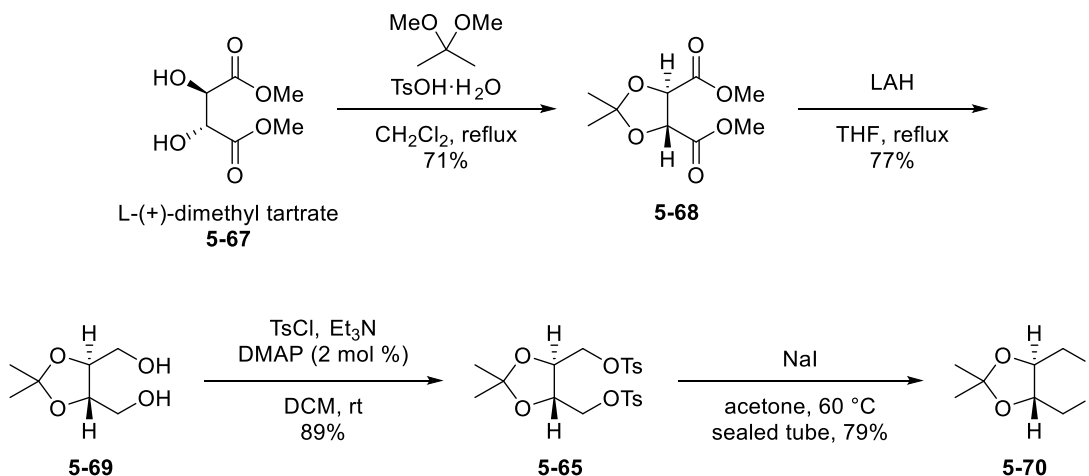
diastereoselectivity, where the triene ring extends from the equatorial positions of the newly formed cyclohexane ring. Ring closure via the opposite direction of rotation would be expected to yield a highly strained diaxial substituted cyclohexane linked by the triene moiety. The  $6\pi$ -electrocyclization may proceed by two disrotatory directions, but both give rise to the same enantiopure product **5-60**. Bis(dienylboronate ester) **5-63** would be prepared by a double *trans*-hydroboration of bis(enyne) **5-64**. A Gilman coupling of known bromoenyne **5-66**<sup>37</sup> and bis(tosylate) **5-65**<sup>38,39</sup> form the key carbon framework of kingianin A. The starting point of the synthesis is L-(+)-dimethyl tartrate (**5-67**), the source of chirality that is expected to give (+)-kingianin and impart diastereoselectivity on the  $8\pi/6\pi$ -electrocyclization cascade reaction.



**Scheme 5.14. Retrosynthesis of electrocyclization precursor **5-63** and the diastereoselective  $8\pi/6\pi$ -electrocyclization cascade.**

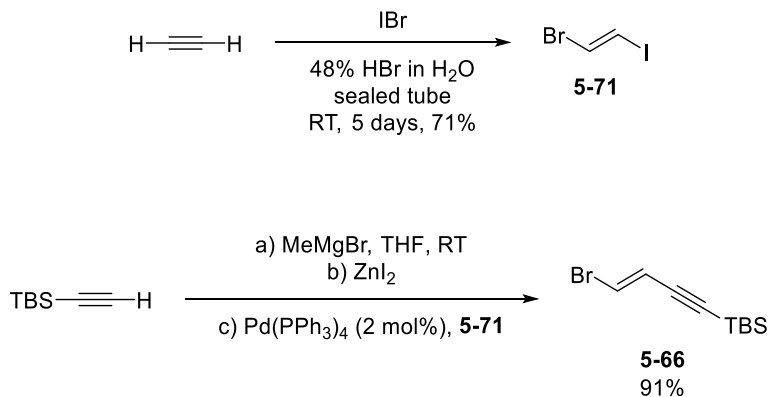
The forward synthesis commenced with preparation of bis(tosylate) **5-65** and diiodide **5-70** (Scheme 5.15). Acetonide protection of L-(+)-dimethyl tartrate with acetone dimethyl acetal

gave dimethyl acetonide **5-68** by a known procedure.<sup>40</sup> Lithium aluminum hydride gave diol **5-69**,<sup>41</sup> which was treated with tosyl chloride to give the bis(tosylate) **5-65**.<sup>42</sup> Diiodide **5-70** was prepared by a Finkelstein reaction of **5-65** in the presence of sodium iodide.<sup>43</sup>



**Scheme 5.15. Preparation of bis(tosylate) 5-65 and diiodide 5-70.**

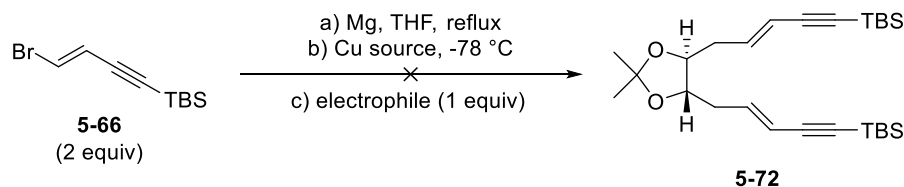
Bromoene **5-66** was prepared by a modification of a known procedure established by the Negishi group in their synthesis of the polyenyne natural product Xerulin.<sup>37</sup> Starting from acetylene, reaction with iodine monobromide in concentrated HBr gave the (*E*)-1-bromo-2-iodoethylene **5-71** stereoselectively. The literature procedure specified bubbling acetylene gas through a solution of IBr in HBr, but in our hands low yields of product was obtained. Success was eventually realized by condensing two equivalents of acetylene in a pressure tube with HBr and IBr, and allowing reaction to stir at room temperature over 5 days.<sup>44</sup> The subsequent Negishi coupling took place with TBS acetylene to provide enyne **5-66** in high yield.



**Scheme 5.16. Synthesis of bromoenyne 5-66.**

With the key coupling partners in hand, we tested the Gilman coupling with Grignard reagents formed from bromoenyne **5-66**. Two copper sources, CuCN and LiCuCl<sub>4</sub>, were tested for their ability to transfer one equivalent of Grignard without the requirement of a sacrificial equivalent of organometallic species, as would be expected for Gilman reactions using copper(I) halides.<sup>45</sup> Unfortunately, coupling reactions were unsuccessful using Grignard reagents derived from **5-66** using either copper source, regardless of whether bis(tosylate) **5-65** or diiodide **5-70** was used as the electrophilic coupling partner (Table 5.2, entries 1-4). Control experiments with allyl magnesium chloride or phenyl magnesium bromide were similarly unsuccessful (entries 5-7). This was surprising as Li<sub>2</sub>CuCl<sub>4</sub> has been demonstrated to effectively catalyze the coupling of Grignard reagents with **5-65**.<sup>46</sup> Complete consumption of vinyl or aryl starting material was observed in the formation of each Grignard reagent.

**Table 5.2. Attempted Gilman couplings with Grignard reagents.**



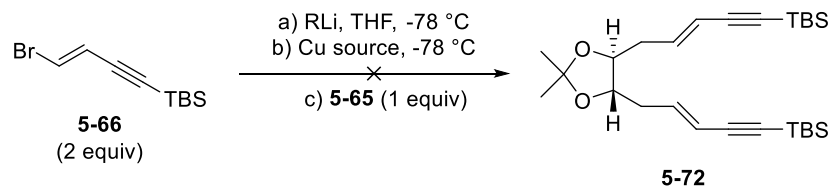
Entry	Equiv Mg	Cu source (equiv)	Electrophile
1	5	CuCN (2)	5.65
2	5	CuCN (2)	5.70
3	6	Li <sub>2</sub> CuCl <sub>4</sub> (0.1)	5.65
4	6	Li <sub>2</sub> CuCl <sub>4</sub> (0.1)	5.70
5 <sup>a</sup>	0	Li <sub>2</sub> CuCl <sub>4</sub> (0.05)	5.65
6 <sup>b</sup>	6	CuCN (0.05)	5.65
7 <sup>b</sup>	6	Li <sub>2</sub> CuCl <sub>4</sub> (0.1)	5.65

<sup>a</sup>Allyl magnesium chloride used in place of **5.66**. <sup>b</sup>Bromobenzene used in place of **5.66**.

We turned our attention to Gilman couplings of vinyl lithium reagents from the lithium halogen exchange of bromoenyne **5-66**. Two successful examples have previously been demonstrated where bis(tosylate) **5-65** underwent Gilman couplings with aryl and alkyl lithium compounds in the presence of Cu(I) sources.<sup>47,48</sup> Lithium halogen exchange of bromoenyne **5-66** with *n*-BuLi or *t*-BuLi was successful as evidenced by the disappearance of **5-66**, but Gilman coupling with **5-65** was unsuccessful in the presence of CuCN or Li<sub>2</sub>CuCl<sub>4</sub> copper sources (Table 5.3, entries 1,2). Attempts to carry out the carbon-carbon bond forming reaction with phenyl lithium, generated from lithium-halogen exchange on bromobenzene, were similarly unsuccessful

(entries 3,4). We also attempted the direct coupling of *n*-BuLi with **5.65**, but alkylation product was not detected (entry 5).

**Table 5.3. Attempted Gilman couplings with organolithium reagents.**

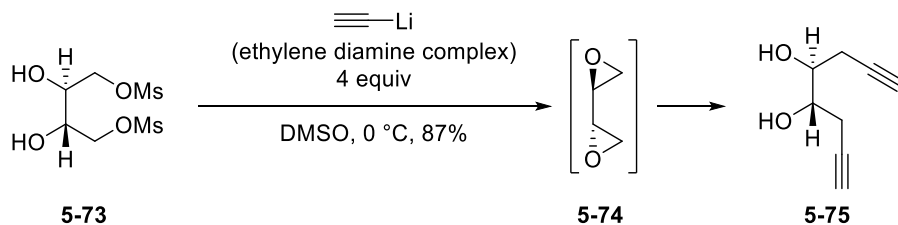


Entry	RLi (equiv)	Cu source (equiv)
<b>1</b>	<i>t</i> -BuLi (4)	CuCN (2)
<b>2</b>	<i>t</i> -BuLi (4)	Li <sub>2</sub> CuCl <sub>4</sub> (0.1)
<b>3<sup>a</sup></b>	<i>t</i> -BuLi (4)	CuCN (2)
<b>4<sup>a</sup></b>	<i>t</i> -BuLi (4)	Li <sub>2</sub> CuCl <sub>4</sub> (0.1)
<b>5<sup>b</sup></b>	<i>n</i> -BuLi (2)	CuCN (2)
<b>6<sup>b</sup></b>	<i>n</i> -BuLi (2)	Li <sub>2</sub> CuCl <sub>4</sub> (0.1)

<sup>a</sup>Bromobenzene used in place of **5.66**. <sup>b</sup>**5.66** was not used.

We focused our attention on the possibility of a nucleophilic ring opening of a bis(epoxide) reagent to carry out the double carbon-carbon bond forming reaction. Inspiration for this pathway arose from the total synthesis of (+)-muricatacin.<sup>49</sup> Enantiopure diol **5-73** was treated with 4 equivalents of lithium acetylide causing the formation of bis(epoxide) **5-74** by a double internal S<sub>N</sub>2 displacement. Excess lithium acetylide in the reaction mixture opened the epoxide by a double S<sub>N</sub>2 displacement, giving the alkylated diol **5-75** (Scheme 5.17). Although bis(epoxide) **5-74** had

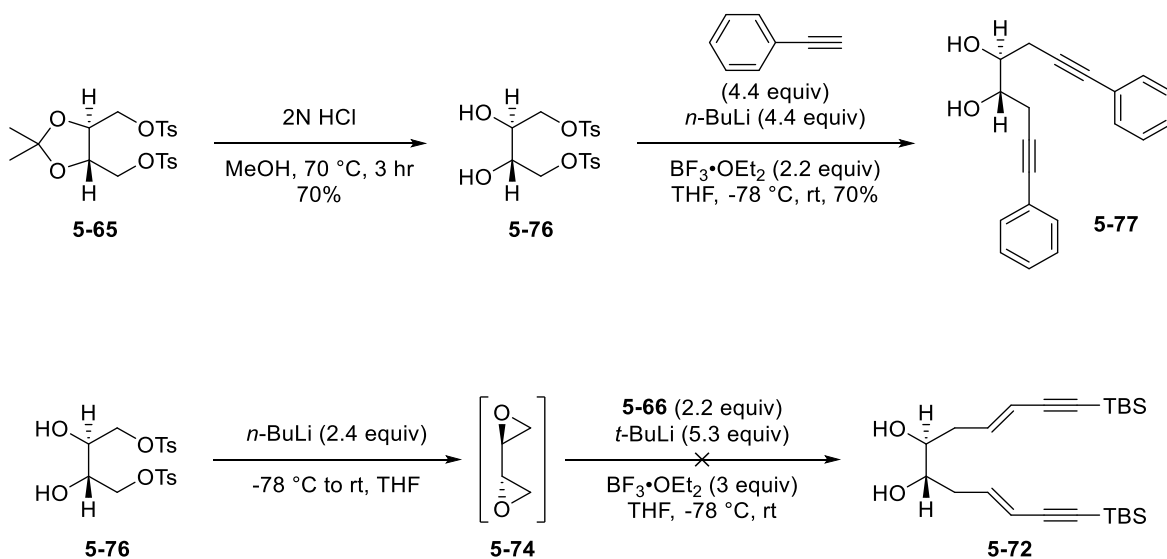
previously been isolated,<sup>50</sup> the preparation and isolation is challenging leading the authors to form **5-74** *in-situ*.



**Scheme 5.17. *In-situ* formation of a bis-epoxide 5-74 and double epoxide ring opening.**

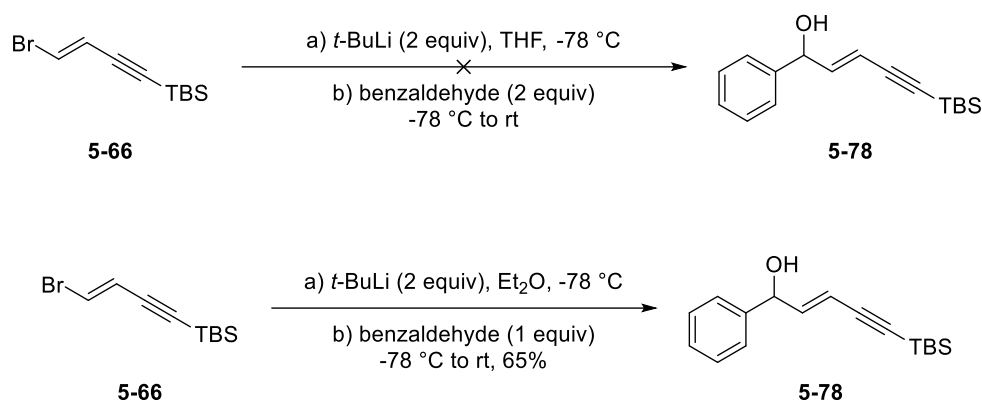
Deprotection of tosylate **5-65** by acetonide deprotection was facile leading to diol **5-76**.<sup>42</sup> Attempts to prepare the bis(epoxide) **5-74** by a double S<sub>N</sub>2 displacement by established procedures<sup>50</sup> were successful, although isolation of the product was difficult due to the low molecular weight leading to a challenging purification. Instead, we elected to form and react the bis(epoxide) *in-situ*.

We tested the feasibility of ring opening of the *in-situ* formed bis-epoxide from bis(tosylate) **5-76** with the lithium anion of phenyl acetylene (Scheme 5.18). Treatment of bis(tosylate) **5-76** with excess lithium phenyl acetylide promoted double deprotonation and internal S<sub>N</sub>2 displacement to generate the bis(epoxide) **5-74**, which underwent double ring opening to give diyne **5-77** in the presence of BF<sub>3</sub>·OEt<sub>2</sub> in good yield. On the other hand, attempted epoxide ring openings with the lithium anion derived from bromoenyne **5-66** were unsuccessful. In this example, the internal S<sub>N</sub>2 reaction to form bis(epoxide) **5-74** was promoted by *n*-BuLi rather than excess of the lithium anion from **5-66**.



**Scheme 5.18. Attempted bis(epoxide) formation and nucleophilic ring opening with lithium phenylacetylene and bromoenyne 5-66.**

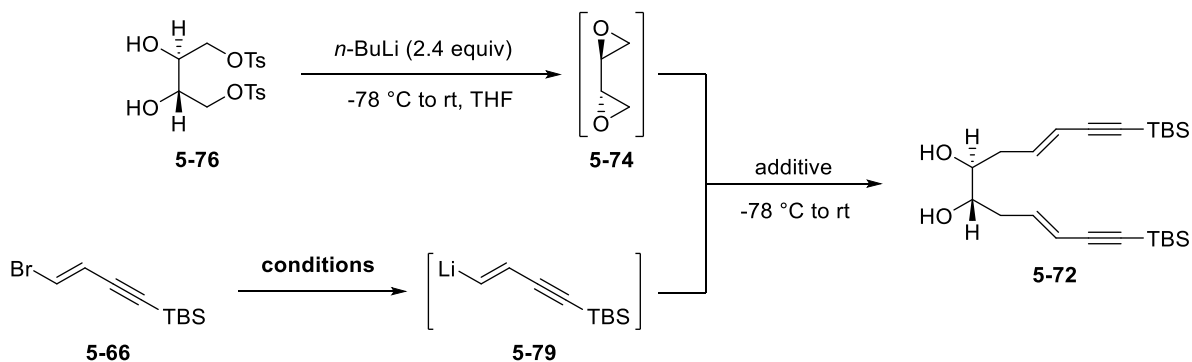
We suspected that organolithium compounds derived from bromoenyne **5-66** may be unstable in THF. Organolithium reagents are known to undergo decomposition in ethereal solvents at low temperatures, where *t*-BuLi has a half-life of 42 min at -20 °C in THF, and at half-life of greater than 8 hours in diethyl ether.<sup>51</sup> We compared the lithium halogen exchange of **5-66** and nucleophilic addition to benzaldehyde in THF and diethyl ether (Scheme 5.19). The reaction was unsuccessful in THF, but gave a modest 63% yield in diethyl ether. This was the first successful carbon-carbon bond forming reaction with **5-66** in our hands and suggested that its lithium anion is unstable in THF.



**Scheme 5.19. Addition of 5-66 to benzaldehyde.**

With this critical information in hand, we tested the addition of the organolithium derived from bromoenyne **5-66** to the *in-situ* formed epoxide **4-74**. Reaction conditions tested are shown in Table 5.4. Although we had discovered that the lithium anion of **5-66** was unstable in THF, bis(tosylate) **5-76** is sparingly soluble in organic solvents aside from THF. This required THF solvent to form epoxide **5-74**. The first successful coupling of bis(tosylate) **5-76** was carried out by forming the lithium anion **5-66** with excess *t*-BuLi in diethyl ether, followed by addition to the bis(epoxide) solution in THF. These reaction conditions gave the desired product **5-72** in 36% yield (entry 1). Replacement of THF with ether for the bis(epoxide) forming reaction was unsuccessful due to the insolubility of tosylate **5-76** in ether (entry 2). Employing excess organolithium reagent derived from **5-66** prevented the possibility to isolate any of the desired product (entry 3). Use of additives such as copper(I) cyanide or copper(I) iodide were unsuccessful in Gilman coupling reactions (entry 4 and 5). This successful reaction (entry 1) condition forms the carbocyclic framework for the future synthetic efforts towards (+)-kingianin A, which may later be applied to the total synthesis of the more biologically active enantiomer (-)-kingianin A. Further studies are currently underway to optimize this transformation and carry this synthetic effort forward.



**Table 5.4. Reaction conditions screen for double epoxide ring opening.**

Entry	Equiv 5-66	Base (equiv)	Solvent	Additive (equiv)	Isolated Yield (%)
1	2.2	$t\text{-BuLi}$ (4.4)	$\text{Et}_2\text{O}$	-	36%
2 <sup>a</sup>	2.2	$t\text{-BuLi}$ (4.4)	$\text{Et}_2\text{O}$	-	0%
3	4	$t\text{-BuLi}$ (8)	$\text{Et}_2\text{O}$	-	0%
4	2.2	$t\text{-BuLi}$ (4.4)	$\text{Et}_2\text{O}$	$\text{CuCN}$ (2.2)	0%
5	4.4	$t\text{-BuLi}$ (8.8)	$\text{Et}_2\text{O}$	$\text{CuI}$ (2.2)	0%

<sup>a</sup> $\text{Et}_2\text{O}$  used as solvent for epoxide formation and lithium halogen exchange, 1 equiv 5-76.

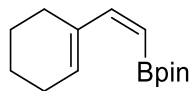
## 5.4 Conclusions

This work represents progress towards the total synthesis of (+)-kingianin A. This synthesis targets a bicyclo[4.2.0]octadiene intermediate, previously shown to undergo a radical-cation Diels-Alder dimerization to ( $\pm$ )-kingianin A. This synthetic method began from L-(+)-dimethyl tartrate, which served as the source of chirality for (+)-kingianin A. Progress towards this total synthesis has been highlighted, which features a key double carbon-carbon bond forming reaction from a highly reactive *in-situ* generated chiral bis(epoxide) intermediate and with enyne carbon fragments. Extensive screening of reactions conditions has identified successful reaction conditions for this transformation. This product features the complete carbon framework from

which (+)-kingianin A will be synthesized in future synthetic studies, where a Pd(II)-catalyzed oxidative cyclization is expected to yield the bicyclo[4.2.0] core diastereoselectively prior to the radical-cation Diels-Alder dimerization reaction.

## 5.5 Experimental

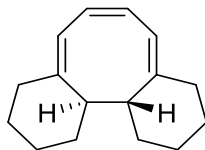
All commercial compounds were used as received. L-(+)-dimethyl tartrate (99%, 99% ee) and bis(triphenylphosphine)palladium(II) dichloride ( $\text{PdCl}_2(\text{Ph}_3\text{P})_2$ , Aldrich,  $\geq 99\%$ ) were used as received from Aldrich. Dichloromethane, triethylamine, and acetonitrile were purified by distillation over  $\text{CaH}_2$ . Methanol was distilled over Mg. Tetrahydrofuran and diethyl ether were distilled prior to use from sodium-benzophenone ketyl. All reactions were carried out in flame-dried glassware under a nitrogen atmosphere. Reactions were monitored using TLC and the plates were developed using vanillin, cerium ammonium molybdate, or potassium permanganate stains. Column chromatography was performed using silica gel (40-63 micron) and reagent grade solvents without deactivation, unless noted. NMR spectra were recorded at 300, 400, or 500 MHz as noted and calibrated to the solvent signal ( $\text{CDCl}_3$   $\delta = 7.26$  ppm or  $\text{C}_6\text{D}_6$   $\delta = 7.16$  ppm for  $^1\text{H}$  NMR, and  $\text{CDCl}_3$   $\delta = 77.0$  ppm or  $\text{C}_6\text{D}_6$   $\delta = 128.1$  for  $^{13}\text{C}$  NMR). Multiplicities are indicated by s (singlet), d (doublet), t (triplet), q (quartet), p (pentet), m (multiplet), or b (broadened). IR spectra were recorded with an ATR attachment and selected peaks are reported in  $\text{cm}^{-1}$ . High resolution mass spectral data was recorded with an IonSense ID-CUBE DART source. Specific rotations were measured on Rudolph Research Analytical Autopol III Automatic polarimeter in a Rudolph Research Analytical 32-5-50-1.0 sample cell (5 mm diameter, 50 mm path length, 1.0 mL volume) at 589 nm in  $\text{CHCl}_3$ .



**(Z)-2-(2-(cyclohex-1-en-1-yl)vinyl)-4,4,5,5-tetramethyl-1,3,2-dioxaborolane (5-51)**

A flame dried flask with 1-ethynylcyclohex-1-ene (1.51 mL, 12.8 mmol) and a stir bar was flushed with nitrogen. Et<sub>2</sub>O (21 mL) was added, then the mixture was cooled to -78 °C. Over the course of 15 min, *n*-BuLi (8 mL, 12.8 mmol, 1.6 M in hexanes) was added dropwise. The mixture was stirred 2 h. After warming to rt, 2-isopropoxy-4,4,5,5-tetramethyl-1,3,2-dioxaborolane (2.6 mL, 12.8 mmol) was added, and the reaction was stirred overnight. After cooling to -78 °C, HCl in dioxane (3.2 ml, 12.8 mmol, 4 M) was added. After the reaction was stirred for 1.5 h the reaction was warmed to rt, then filtered under nitrogen through Celite. All solvent was removed *in vacuo* for 5 h. Zirconocene dichloride (5.617 g, 19.2 mmol) was added to a separate flame dried flask. The flask was evacuated and backfilled with nitrogen three times, then THF was added (50 mL). To this mixture, DIBAL (17.9 mL, 17.9 mmol, 1 M in toluene) was added dropwise over 45 min at rt, whereupon it was transferred via cannula to the previously formed alkynyl boronate ester. After stirring at rt for 90 min, water was slowly added to quench the reaction. THF was removed *in vacuo*, and the water was extracted with DCM. The organic extracts were combined and dried with MgSO<sub>4</sub>. Solvent was removed *in vacuo* and chromatography with 25:1 Hex:EtOAc gave 1.153 g (38%) of the known<sup>52</sup> clear light yellow oil.

**<sup>1</sup>H-NMR** (400 MHz, CDCl<sub>3</sub>, ppm) δ 6.64 (d, *J* = 14.8 Hz, 1H), 5.83 (t, *J* = 3.4 Hz, 1H), 5.17 (d, *J* = 15.2 Hz, 1H), 2.27-2.24 (m, 2H), 2.15-2.11 (m, 2H), 1.67-1.55 (m, 4H), 1.28 (s, 12H).



**(4aZ,6Z,8Z)-1,2,3,4,9,10,11,12,12a,12b-decahydrodibenzo[a,c][8]annulene (5-53)**

A flame dried flask containing **5-51** (200 mg, 0.854 mmol) and a stir bar was flushed with nitrogen. The flask and was charged sequentially with MeOH (9.3 mL), chloroacetone (0.34 mL, 4.27 mmol), PdCl<sub>2</sub>(PPh<sub>3</sub>)<sub>2</sub> (30 mg, 0.0427 mmol), and aq K<sub>2</sub>CO<sub>3</sub> (2M, 1.1 mL, 2.14 mmol). The mixture was stirred at rt for two days. The reaction was passed through a Celite plug with EtOAc then concentrated *in vacuo*. Chromatography with hexanes gave 49 mg (53% yield) of the known<sup>35</sup> light yellow solid.

**<sup>1</sup>H-NMR** (400 MHz, CDCl<sub>3</sub>, ppm) δ 5.77 (dd, *J* = 3.0, 1.4 Hz, 2H), 5.70 (bs, 2H), 2.73 (bs, 2H), 2.27-2.15 (m, 4H), 1.66-1.41 (m, 12H);

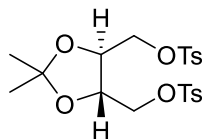
**<sup>13</sup>C-NMR** (125 MHz, -50 °C, CDCl<sub>3</sub>, ppm) δ 152.9, 149.7, 126.6, 125.5, 120.3, 118.4, 42.8, 38.4, 33.4, 33.1, 30.0, 27.5, 27.3, 20.3 (2 signals, degenerate);

**<sup>13</sup>C-NMR** (125 MHz, 20 °C, CDCl<sub>3</sub>, ppm) δ 150.9, 126.1, 119.6, 40.9 (b), 37.8 (b), 30.6 (b), 28.7, 23.9 (b);

**<sup>13</sup>C-NMR** (125 MHz, 45 °C, CDCl<sub>3</sub>, ppm) δ 150.3, 126.0, 120.0, 41.0, 37.8, 30.5, 28.6, 24.0;

**IR** (neat, ATR, cm<sup>-1</sup>): 3002, 2922, 2852, 1647, 1625, 1604, 1444, 989, 831, 795, 778;

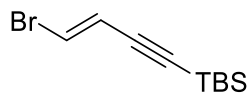
**HRMS** (DART): calcd [M+H]<sup>+</sup> (C<sub>16</sub>H<sub>23</sub>) 215.17943, found 215.17949.



**((4S,5S)-2,2-dimethyl-1,3-dioxolane-4,5-diyl)bis(methylene) bis(4-methylbenzenesulfonate)**  
**(5-65)**

A flame dried flask with DMAP (66 mg, 0.544 mmol), **5-69** (4.411 g, 27.2 mmol) and a stir bar was flushed with nitrogen, then DCM (56 mL) was added. The mixture was cooled to 0 °C, then NEt<sub>3</sub> (9.1 mL, 65.2 mmol) was added, followed by TsCl (12.444g, 65.2 mmol). The mixture was stirred 30 min at 0 °C, then warmed to rt and stirred overnight. The mixture was diluted with water, extracted with DCM, washed with brine, and dried with MgSO<sub>4</sub>. Solvent was removed *in vacuo*. Chromatography with 2:1 Hex:EtOAc gave 11.378 g (89% yield) of the known<sup>38,39</sup> white solid.

<sup>1</sup>H NMR (400 MHz, CDCl<sub>3</sub>, ppm) δ 7.78 (d, *J* = 8.3 Hz, 4H), 7.36 (d, *J* = 8.2 Hz, 4H), 4.12-4.05 (m, 4H), 4.02-3.99 (m, 2H), 2.45 (s, 6H), 1.29 (s, 6H).

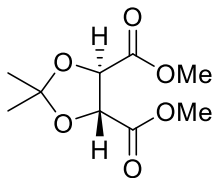


**(E)-(4-bromobut-3-en-1-yn-1-yl)(tert-butyl)dimethylsilane (5-66)**

This compound was prepared by a modification of a known procedure.<sup>37</sup> A flame dried flask containing *t*-butyldimethylsilyl acetylene (2.484 g, 17.7 mmol) and a stir bar was flushed with nitrogen, then THF (26.6 mL) was added. MeMgBr (7.1 mL, 3M in Et<sub>2</sub>O, 21.2 mmol) was added dropwise at rt and stirred 3 h. A separate flame dried round bottom flask containing ZnI<sub>2</sub> (7.348g, 23.0 mmol) and a stir bar was flushed with nitrogen and THF (8 mL) was added. The

mixture cooled to 0 °C, then the alkynyl Grignard solution was added via cannula. The mixture was warmed to rt and stirred 30 min. A THF (13.2 mL) solution of Pd(PPh<sub>3</sub>)<sub>4</sub> (409 mg, 0.354 mmol), **5-71** (4.535 g, 19.5 mmol) was added to the alkynyl zincate solution via cannula. The mixture was stirred at rt overnight. The reaction was quenched with saturated aq NH<sub>4</sub>Cl, extracted with Et<sub>2</sub>O, and dried with MgSO<sub>4</sub>. Solvent was removed *in vacuo*. Column chromatography with 100% hexanes gave 3.972 g (91% yield) of the known<sup>37</sup> clear light yellow oil.

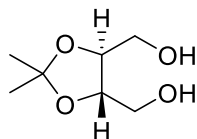
<sup>1</sup>H NMR (400 MHz, CDCl<sub>3</sub>, ppm) δ 6.75 (d, *J* = 14.0 Hz, 1H), 6.22 (d, *J* = 14.0 Hz, 1H), 0.93 (s, 9H), 0.12 (s, 6H).



**dimethyl (4*R*,5*R*)-2,2-dimethyl-1,3-dioxolane-4,5-dicarboxylate (5-68)**

This compound was prepared by modification of a known procedure.<sup>40</sup> A flame dried flask fitted with a reflux condenser and equipped with a stir bar was flushed and with nitrogen, then **5-67** (1.000 g, 5.61 mmol), *p*-toluenesulfonic acid monohydrate (534 mg, 2.81 mmol), and DCM (13.4 mL) were added. After addition of dimethoxypropane (4.5 mL, 36.8 mmol) the mixture was heated at reflux overnight with stirring. The mixture was cooled to rt, diluted with water, and extracted with DCM. The organic extracts were dried with MgSO<sub>4</sub>. Solvent was removed *in vacuo*. Column chromatography with 3:1 Hex:EtOAc gave 863 mg (71% yield) of the known<sup>53</sup> clear light yellow oil.

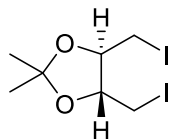
<sup>1</sup>H NMR (400 MHz, CDCl<sub>3</sub>, ppm) δ 4.80 (s, 2H), 3.82 (s, 6H), 1.49 (s, 6H).



**((4S,5S)-2,2-dimethyl-1,3-dioxolane-4,5-diyl)dimethanol (5-69)**

A flame dried flask equipped with a reflux condenser containing LAH (4.058 g, 106.9 mmol) and a stir bar was flushed with nitrogen, then THF (38 mL) was added (Note: a safer method would be to add LAH to a stirring solution of THF). The flask was cooled to 0 °C, then a solution of **5-68** (7.778 g, 35.6 mmol) in THF (19 mL) was added dropwise. The mixture was stirred at rt for 30 min, then at reflux for 3 h. The mixture was cooled to 0 °C, diluted with Et<sub>2</sub>O, and water (4.1 mL) was added dropwise, followed by 15% aq NaOH (4.1 mL), then another portion of water (12.2 mL). The solution was warmed to rt, stirred 15 min, then MgSO<sub>4</sub> was added until the reaction mixture became white. The mixture was stirred an additional 15 min then filtered through Celite. Solvent was removed *in vacuo*. Column chromatography with 100% EtOAc gave 4.461 g (77% yield) of the known<sup>41</sup> clear colorless oil.

<sup>1</sup>H NMR (400 MHz, CDCl<sub>3</sub>, ppm) δ 4.01-3.97 (m, 2H) 3.78 (bd, *J* = 11.7 Hz, 2H), 3.69 (bd, *J* = 11.8 Hz, 2H), 1.42 (s, 6H).

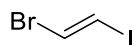


**((4R,5R)-4,5-bis(iodomethyl)-2,2-dimethyl-1,3-dioxolane (5-70)**

A flame dried pressure tube containing **5-65** (1.400 g, 2.98 mmol), NaI (1.783 g 11.9 mmol) and a stir bar was capped with a rubber septum. The pressure tube was flushed and with nitrogen, then acetone (17.5 mL) was added, and the rubber septum was replaced with a pressure cap. The

mixture was heated to 60 °C and stirred overnight. The mixture was diluted with water and extracted with EtOAc. The organic layers were washed with 5% aq NaS<sub>2</sub>O<sub>3</sub> and brine, then dried with MgSO<sub>4</sub>. Solvent was removed *in vacuo*. Column chromatography with a gradient elution from 15:1 to 10:1 Hex:EtOAc gave 900 mg (79% yield) of the known<sup>54,43</sup> clear colorless oil.

<sup>1</sup>H NMR (300 MHz, CDCl<sub>3</sub>, ppm) δ 3.92-3.85 (m, 2H), 3.46-3.36 (m, 4H), 1.50 (s, 6H).



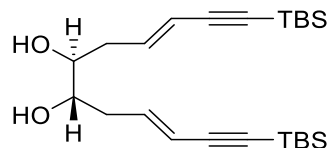
**(E)-1-bromo-2-iodoethene (5-71)**

This compound was prepared by modification of a known procedure.<sup>37</sup> A flame dried pressure tube containing IBr (4.000 g, 19.3 mmol) and a stir bar was capped with a rubber septum, sealed with electrical tape, and flushed with nitrogen. Concentrated HBr (48% aq, 25 mL) was added at rt. The reaction mixture was frozen by immersion in a liquid nitrogen bath. Acetylene gas (984 mg, 37.8 mmol) purified by passage through two cold fingers cooled to -78 ° was condensed into the pressure tube. While the mixture was frozen, the rubber septum was replaced with a pressure cap. The reaction was warmed to rt and stirred 5 days behind a blast shield. The reaction was opened carefully to vent excess acetylene gas, then extracted with pentanes. The organic layers were collected and rinsed with saturated aq NaS<sub>2</sub>O<sub>3</sub> and brine. Solvent was removed *in vacuo* carefully to prevent evaporation of the volatile product. The product was purified by short path distillation where the receiving flask was cooled at -78 °C to give 3.181 g (71% yield) of the known<sup>37</sup> clear colorless oil.

**Bp** 40 °C (90 mmHg);

<sup>1</sup>H NMR (400 MHz, CDCl<sub>3</sub>, ppm) δ 6.86 (d, *J* = 13.4 Hz, 1H), 6.76 (d, *J* = 13.4 Hz).





**(3E,6S,7S,9E)-1,12-bis(tert-butyldimethylsilyl)dodeca-3,9-dien-1,11-diyne-6,7-diol (5-72)**

A flame dried round bottom flask containing **5-76** (159 mg, 0.371 mmol) and a stir bar was flushed with nitrogen, then THF (1.1 mL) was added. The mixture was cooled to  $-78\text{ }^{\circ}\text{C}$ , then *n*-BuLi (0.33 mL, 2.5 M in hexanes, 0.813 mmol) was added dropwise. The mixture was stirred 15 min at  $-78\text{ }^{\circ}\text{C}$ , and 45 min at rt. A separate flame dried round bottom flask containing **5-66** (199 mg, 0.813 mmol) and a stir bar was flushed with nitrogen, then Et<sub>2</sub>O (1.1 mL) was added. The mixture was cooled to  $-78\text{ }^{\circ}\text{C}$ , then *t*-BuLi (0.86 mL, 1.9 M in pentane, 1.63 mmol) was added dropwise. This mixture was stirred at  $-78\text{ }^{\circ}\text{C}$  for 7 min. The solution originally containing **5-76** was added to the vinyl lithium solution dropwise at  $-78\text{ }^{\circ}\text{C}$ . The reaction was stirred 15 min at  $-78\text{ }^{\circ}\text{C}$ , then 30 min at rt. The reaction was quenched with saturated aq NH<sub>4</sub>Cl, extracted with DCM, and dried with MgSO<sub>4</sub>. Solvent was removed *in vacuo*. Chromatography with 4:1 pentanes:EtOAc gave 56 mg (36% yield) of the clear light yellow oil.

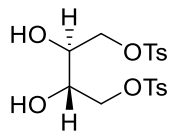
**<sup>1</sup>H-NMR** (400 MHz, CDCl<sub>3</sub>, ppm)  $\delta$  6.20 (dt, *J* = 15.4, 7.6 Hz, 2H), 5.62 (d, *J* = 15.9 Hz, 2H), 3.55 (s, 2H), 2.41-2.28 (m, 4H), 0.94 (s, 18H), 0.11 (s, 12H);

**<sup>13</sup>C-NMR** (100 MHz, CDCl<sub>3</sub>, ppm)  $\delta$  140.7, 113.2, 103.9, 92.2, 72.5, 37.6, 26.1, 16.6, -4.6;

**IR** (neat, ATR, cm<sup>-1</sup>): 3359, 2952, 2928, 2857, 2171, 2134, 1470, 1251, 1081, 823;

**HRMS** (DART): calcd [M+H]<sup>+</sup> (C<sub>24</sub>H<sub>43</sub>O<sub>2</sub>Si<sub>2</sub>) 419.27961, found 419.27732;

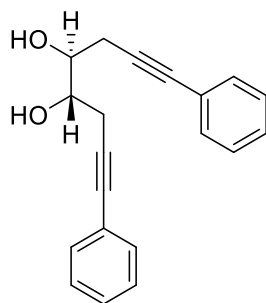
**[ $\alpha$ ]<sub>D</sub><sup>26</sup>** - 2.42 (c 1.57, CHCl<sub>3</sub>).



**(2*S*,3*S*)-2,3-dihydroxybutane-1,4-diyl bis(4-methylbenzenesulfonate) (5-76)**

A flame dried flask containing **5-65** (9.024 g, 19.2 mmol) and a stir bar was flushed and with nitrogen, then 2N aq HCl (19.2 mL, 38.4 mmol) was added. The mixture was heated to 75 °C and heated 3 h with stirring. The mixture was cooled to rt, quenched with 10% aq KOH (22 mL), extracted with CHCl<sub>3</sub>, and dried with MgSO<sub>4</sub>. Solvent was removed *in vacuo*. Column chromatography with 2:3 Hex:EtOAc gave 5.819 g (70% yield) of the known<sup>42</sup> white solid.

<sup>1</sup>H NMR (400 MHz, CDCl<sub>3</sub>, ppm) δ 7.77 (d, *J* = 8.3 Hz, 4H), 7.35 (d, *J* = 8.0 Hz, 4 H), 4.06 (d, *J* = 5.8 Hz, 4H), 3.71 (t, *J* = 5.1 Hz, 2H), 2.81 (s, 2H), 2.44 (s, 6H);



**(4*S*,5*S*)-1,8-diphenylocta-1,7-diyne-4,5-diol (5-77)**

This compound was prepared by a modification of a known procedure.<sup>55</sup> A flame dried flask containing phenyl acetylene (0.67 mL, 6.14 mmol) and a stir bar was flushed and with nitrogen, then THF (3.5 mL) was added. The mixture was cooled to -78 °C and *n*-BuLi (2.5 mL, 2.5 M in hexanes, 6.14 mmol) was added dropwise and stirred for 40 min at that temperature. A solution of **5-76** (600 mg, 1.39 mmol) in THF (3.5 mL) was added dropwise to the alkynyl lithium solution at -78 °C. The mixture was warmed to rt, and stirred 2 h, then BF<sub>3</sub>·Et<sub>2</sub>O (0.32 mL, 3.07

mmol) was added dropwise. The mixture was stirred 25 min at rt. The reaction was quenched with saturated aq NH<sub>4</sub>Cl, extracted with DCM, and dried with MgSO<sub>4</sub>. Solvent was removed *in vacuo*. Column chromatography with 2:3 Hex:EtOAc gave 285 mg (70% yield) of the light brown solid.

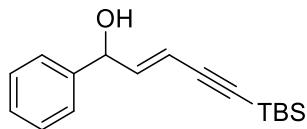
<sup>1</sup>H-NMR (400 MHz, CDCl<sub>3</sub>, ppm) δ 7.44-7.39 (m, 4H), 7.31-7.27 (m, 6H), 3.99 (t, *J* = 5.2 Hz, 2H), 2.79 (d, *J* = 6.1 Hz, 4 H), 2.57 (s, 2H);

<sup>13</sup>C-NMR (100 MHz, CDCl<sub>3</sub>, ppm) δ 131.7, 128.3, 128.1, 123.1, 85.5, 83.2, 71.3, 25.1;

IR (neat, ATR, cm<sup>-1</sup>): 3250, 3057, 2939, 2920, 2856, 2247, 2223, 1599, 1491, 1441, 1103, 1043, 954, 917;

HRMS (DART): calcd [M+H]<sup>+</sup> (C<sub>20</sub>H<sub>19</sub>O<sub>2</sub>) 291.13796, found 291.13692.

[α]<sub>D</sub><sup>24</sup> + 17.39 (c 0.89, CHCl<sub>3</sub>).



**(E)-5-(tert-butyldimethylsilyl)-1-phenylpent-2-en-4-yn-1-ol (5-78)**

A flame dried round bottom flask containing **5-66** (200 mg, 0.816 mmol) and a stir bar was flushed with nitrogen, then Et<sub>2</sub>O (1.1 mL) was added. The mixture was cooled to -78 °C, then *t*-BuLi (0.86 mL, 1.9 M in hexanes, 1.63 mmol) was added dropwise. The mixture was stirred 20 min at -78 °C, then benzaldehyde was added in dropwise at that temperature. The reaction was stirred 30 min at -78 °C, then 1 h at rt. The reaction was quenched with saturated aq NH<sub>4</sub>Cl, extracted with Et<sub>2</sub>O, and dried with MgSO<sub>4</sub>. Solvent was removed *in vacuo*. Chromatography with 8:1 Hex:EtOAc gave 144 mg (65% yield) of the clear light yellow oil.

**<sup>1</sup>H-NMR** (400 MHz, CDCl<sub>3</sub>, ppm) δ 7.37-7.29 (m, 5H), 6.32 (dd, *J* = 15.8, 5.8 Hz, 1H), 5.81 (dd, *J* = 16.0, 1.6 Hz, 1H), 5.17 (bd, *J* = 5.6 Hz, 1H), 2.61 (s, 1H), 0.98 (s, 9H), 0.15 (s, 6H);

**<sup>13</sup>C-NMR** (100 MHz, CDCl<sub>3</sub>, ppm) δ 145.4, 141.7, 128.7, 128.1, 126.5, 110.4, 103.7, 94.1, 74.4, 26.2, 16.7, -4.6;

**IR** (neat, ATR, cm<sup>-1</sup>): 3359, 3029, 2952, 2927, 2885, 2857, 2168, 2128, 1625, 1470, 1249, 1006, 954, 824;

**HRMS** (DART) calcd [M+H]<sup>+</sup> (C<sub>17</sub>H<sub>25</sub>OSi) 273.16692, found 273.16484.

## 5.6 References and Notes

- (1) Hanahan, D.; Weinberg, R. A. *Cell* **2000**, *100*, 57.
- (2) Green, D. R.; Reed, J. C. *Science* **1998**, *281*, 1309.
- (3) Kirkin, V.; Joos, S.; Zörnig, M. *Biochim. Biophys. Acta - Mol. Cell Res.* **2004**, *1644*, 229.
- (4) Fesik, S. W. *Nat. Rev. Cancer* **2005**, *5*, 876.
- (5) Lessene, G.; Czabotar, P. E.; Colman, P. M. *Nat Rev Drug Discov* **2008**, *7*, 989.
- (6) Lessene, G.; Czabotar, P. E.; Sleeb, B. E.; Zobel, K.; Lowes, K. N.; Adams, J. M.; Baell, J. B.; Colman, P. M.; Deshayes, K.; Fairbrother, W. J.; Flygare, J. A.; Gibbons, P.; Kersten, W. J. A.; Kulasegaram, S.; Moss, R. M.; Parisot, J. P.; Smith, B. J.; Street, I. P.; Yang, H.; Huang, D. C. S.; Watson, K. G. *Nat. Chem. Biol.* **2013**, *9*, 390.
- (7) Leverrier, A.; Dau, M. E. T. H.; Retailleau, P.; Awang, K.; Guéritte, F.; Litaudon, M. *Org. Lett.* **2010**, *12*, 3638.
- (8) Leverrier, A.; Awang, K.; Guéritte, F.; Litaudon, M. *Phytochemistry* **2011**, *72*, 1443.

- (9) Bandaranayake, W. M.; Banfield, J. E.; Black, D. S. C.; Fallon, G. D.; Gatehouse, B. M. *J. Chem. Soc., Chem. Commun.* **1980**, 162.
- (10) Bandaranayake, W. M.; Banfield, J. E.; Black, D. S. C. *J. Chem. Soc., Chem. Commun.* **1980**, 902.
- (11) Bandaranayake, W. M.; Banfield, J. E.; Black, D. S. C.; Fallon, G. D.; Gatehouse, B. M. *Aust. J. Chem.* **1981**, *34*, 1655.
- (12) Bandaranayake, W. M.; Banfield, J. E.; Black, D. S. C. *Aust. J. Chem.* **1982**, *35*, 557.
- (13) Bandaranayake, W. M.; Banfield, J. E.; Black, D. S. C.; Fallon, G. D.; Gatehouse, B. M. *Aust. J. Chem.* **1982**, *35*, 567.
- (14) Banfield, J. E.; Black, D. S. C.; Johns, S. R.; Willing, R. I. *Aust. J. Chem.* **1982**, *35*, 2247.
- (15) Nicolaou, K. C.; Petasis, N. A.; Zipkin, R. E.; Uenishi, J. *J. Am. Chem. Soc.* **1982**, *104*, 5555.
- (16) Nicolaou, K. C.; Zipkin, R. E.; Petasis, N. A. *J. Am. Chem. Soc.* **1982**, *104*, 5558.
- (17) Nicolaou, K. C.; Petasis, N. A.; Zipkin, R. E. *J. Am. Chem. Soc.* **1982**, *104*, 5560.
- (18) Beaudry, C. M.; Trauner, D. *Org. Lett.* **2002**, *4*, 2221.
- (19) Beaudry, C. M.; Trauner, D. *Org. Lett.* **2005**, *7*, 4475.
- (20) Moses, J. E.; Baldwin, J. E.; Marquez, R.; Adlington, R. M.; Cowley, A. R. *Org. Lett.* **2002**, *4*, 3731.
- (21) Jacobsen, M. F.; Moses, J. E.; Adlington, R. M.; Baldwin, J. E. *Org. Lett.* **2005**, *7*, 2473.
- (22) Manzo, E.; Ciavatta, M. L.; Gavagnin, M.; Mollo, E.; Wahidulla, S.; Cimino, G.

- Tetrahedron Lett.* **2005**, *46*, 465.
- (23) Miller, A. K.; Trauner, D. *Angew. Chem. Int. Ed.* **2005**, *44*, 4602.
- (24) Sharma, P.; Ritson, D. J.; Burnley, J.; Moses, J. E. *Chem. Commun.* **2011**, *47*, 10605.
- (25) Alder, K.; Stein, G. *Justus Liebigs Ann. Chem.* **1932**, *496*, 197.
- (26) Valentine, D.; Turro, N. J.; Hammond, G. S. *J. Am. Chem. Soc.* **1964**, *86*, 5202.
- (27) De Mare, G. R.; Huybrechts, G.; Toth, M.; Goldfinger, P. *Trans. Faraday Soc.* **1971**, *67*, 1397.
- (28) Grieco, P. A.; Nunes, J. J.; Gaul, M. D. *J. Am. Chem. Soc.* **1990**, *112*, 4595.
- (29) Drew, S. L.; Lawrence, A. L.; Sherburn, M. S. *Angew. Chem. Int. Ed.* **2013**, *52*, 4221.
- (30) Bellville, D. J.; Wirth, D. W.; Bauld, N. L. *J. Am. Chem. Soc.* **1981**, *103*, 718.
- (31) Lim, H. N.; Parker, K. A. *Org. Lett.* **2013**, *15*, 398.
- (32) Iafe, R. G.; Chan, D. G.; Kuo, J. L.; Boon, B. A.; Faizi, D. J.; Saga, T.; Turner, J. W.; Merlic, C. A. *Org. Lett.* **2012**, *14*, 4282.
- (33) Tobolowsky, R. Ph.D. Dissertation, University of California, Los Angeles, CA, 2017.
- (34) Patel, A.; Houk, K. N. *J. Org. Chem.* **2014**, *79*, 11370.
- (35) Marvell, E. N.; Seubert, J.; Vogt, G.; Zimmer, G.; Moy, G.; Siegmann, J. R. *Tetrahedron* **1978**, *34*, 1307.
- (36) Auchter-Krummel, P.; Krummel, G.; Müllen, K.; Lex, J. *Chem. Ber.* **1991**, *124*, 2819.
- (37) Negishi, E.; Alimardanov, A.; Xu, C. *Org. Lett.* **2000**, *2*, 65.

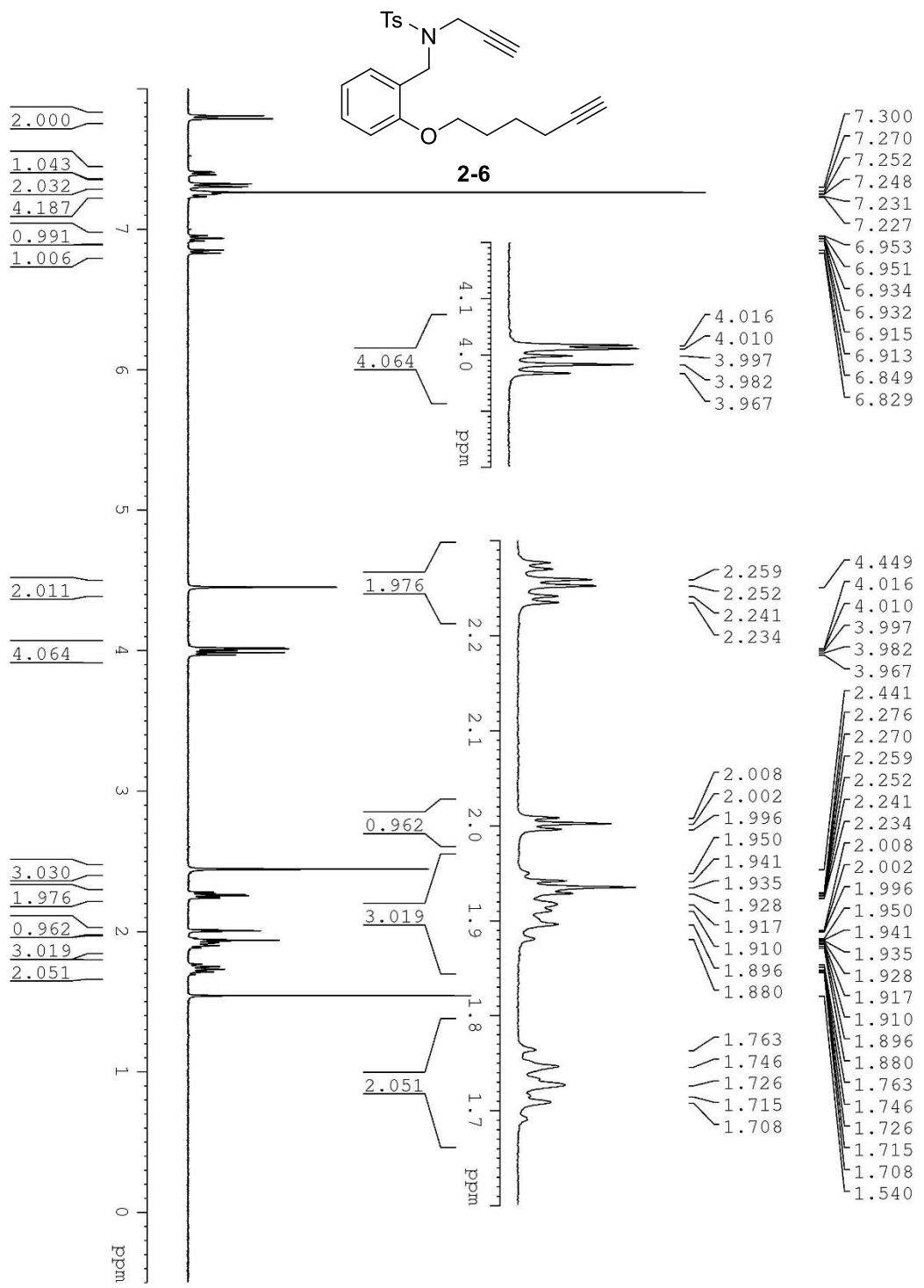
- (38) Kiełbasiński, P.; Albrycht, M.; Mikołajczyk, M.; Wieczorek, M. W.; Majzner, W. R.; Filipczak, A.; Ciołkiewicz, P. *Heteroat. Chem.* **2005**, *16*, 93.
- (39) Koschker, P.; Kähny, M.; Breit, B. *J. Am. Chem. Soc.* **2015**, *137*, 3131.
- (40) Gao, X.; Han, J.; Wang, L. *Org. Lett.* **2015**, *17*, 4596.
- (41) Mash, E. A.; Nelson, K. A.; Van Deusen, A.; Hemperly, S. B. *Org. Synth.* **1990**, *68*, 92.
- (42) Seebach, D.; Kalinowski, H.-O.; Bastani, B.; Crass, G.; Daum, H.; Dörr, H.; Dupreez, N. P.; Ehrig, V.; Langer, W.; Nüssler, C.; Oei, H.-A.; Schmidt, M. *Helv. Chim. Acta* **1977**, *60*, 301.
- (43) Khanapure, S. P.; Najafi, N.; Manna, S.; Yang, J.-J.; Rokach, J. *J. Org. Chem.* **1995**, *60*, 7548.
- (44) See Experimental section for further details.
- (45) *Organocopper Reagents, A Practical Approach*; Taylor, R. J., Ed.; Oxford University Press: Oxford, 1994.
- (46) Liu, G.; Wang, Z. *Chem. Commun.* **1999**, 1129.
- (47) Collins, D. J.; Crosby, I. T. *Aust. J. Chem.* **1998**, *51*, 1025.
- (48) Lee, W. H.; Bae, I. H.; Kim, B. M.; Seu, Y.-B. *Bull. Korean Chem. Soc.* **2016**, *37*, 1910.
- (49) Quayle, P.; Rahman, S.; Herbert, J. *Tetrahedron Lett.* **1995**, *36*, 8087.
- (50) Robbins, M. A.; Devine, P. N.; Oh, T. *Org. Synth.* **1999**, *76*, 101.
- (51) Stanetty, P.; Koller, H.; Mihovilovic, M. *J. Org. Chem.* **1992**, *57*, 6833.

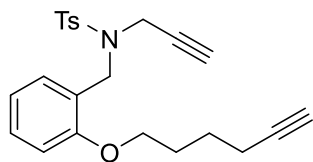
- (52) Mirzayans, P. M.; Pouwer, R. H.; Williams, C. M.; Bernhardt, P. V. *Tetrahedron* **2009**, *65*, 8297.
- (53) Beck, A. K.; Gysi, P.; La Vecchia, L.; Seebach, D. *Org. Synth.* **1999**, *76*, 12.
- (54) Townsend, J. M.; Blount, J. F.; Sun, R. C.; Zawoiski, S.; Valentine, D. *J. Org. Chem.* **1980**, *45*, 2995.
- (55) Yamakawa, M.; Kurachi, T.; Yoshikawa, Y.; Arisawa, M.; Okino, Y.; Suzuki, K.; Fujioka, H. *J. Org. Chem.* **2015**, *80*, 10261.



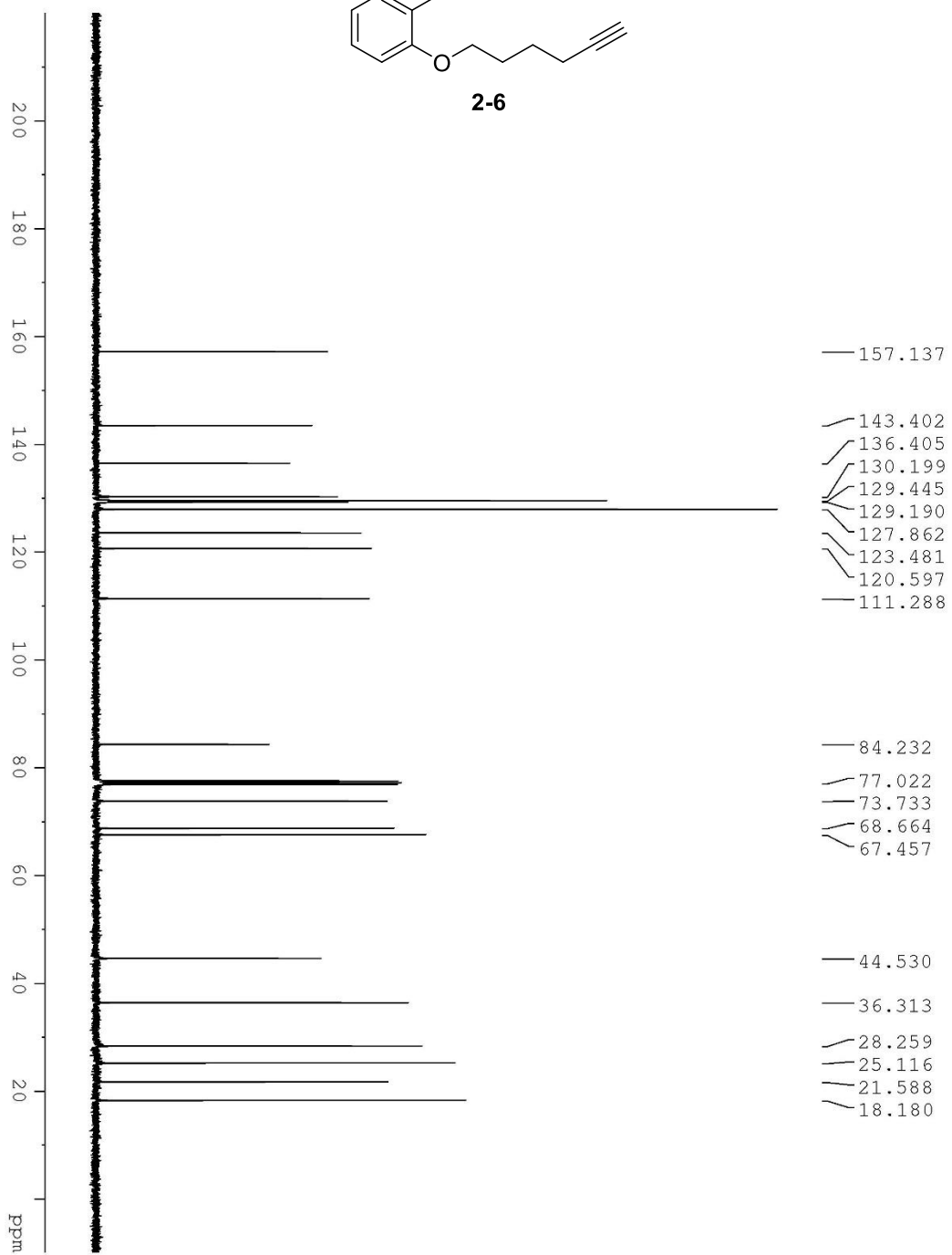
## **Appendix A**

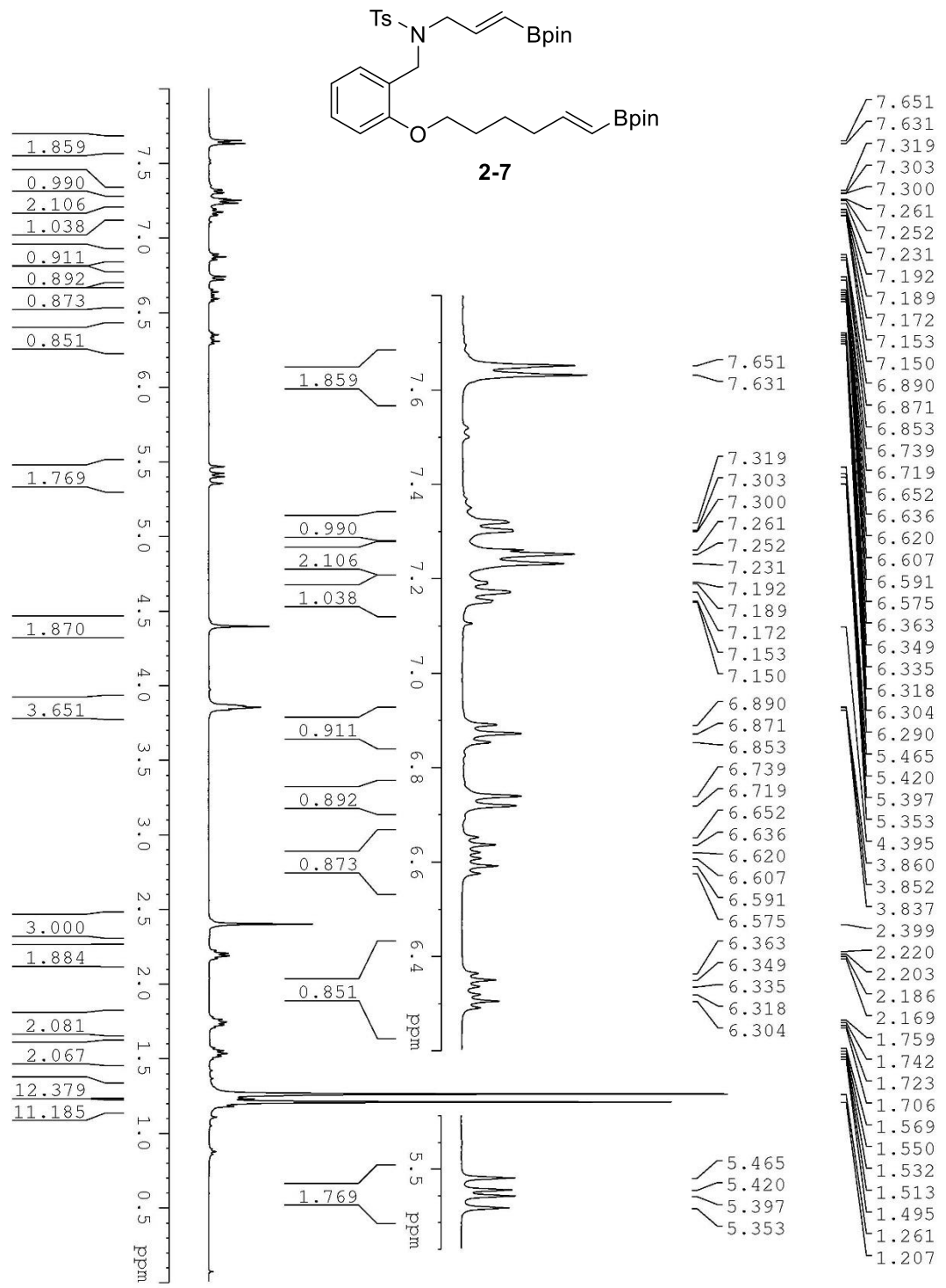
### **Spectral Data**

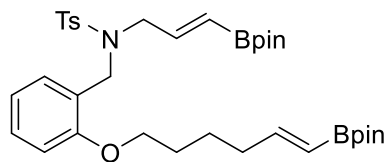




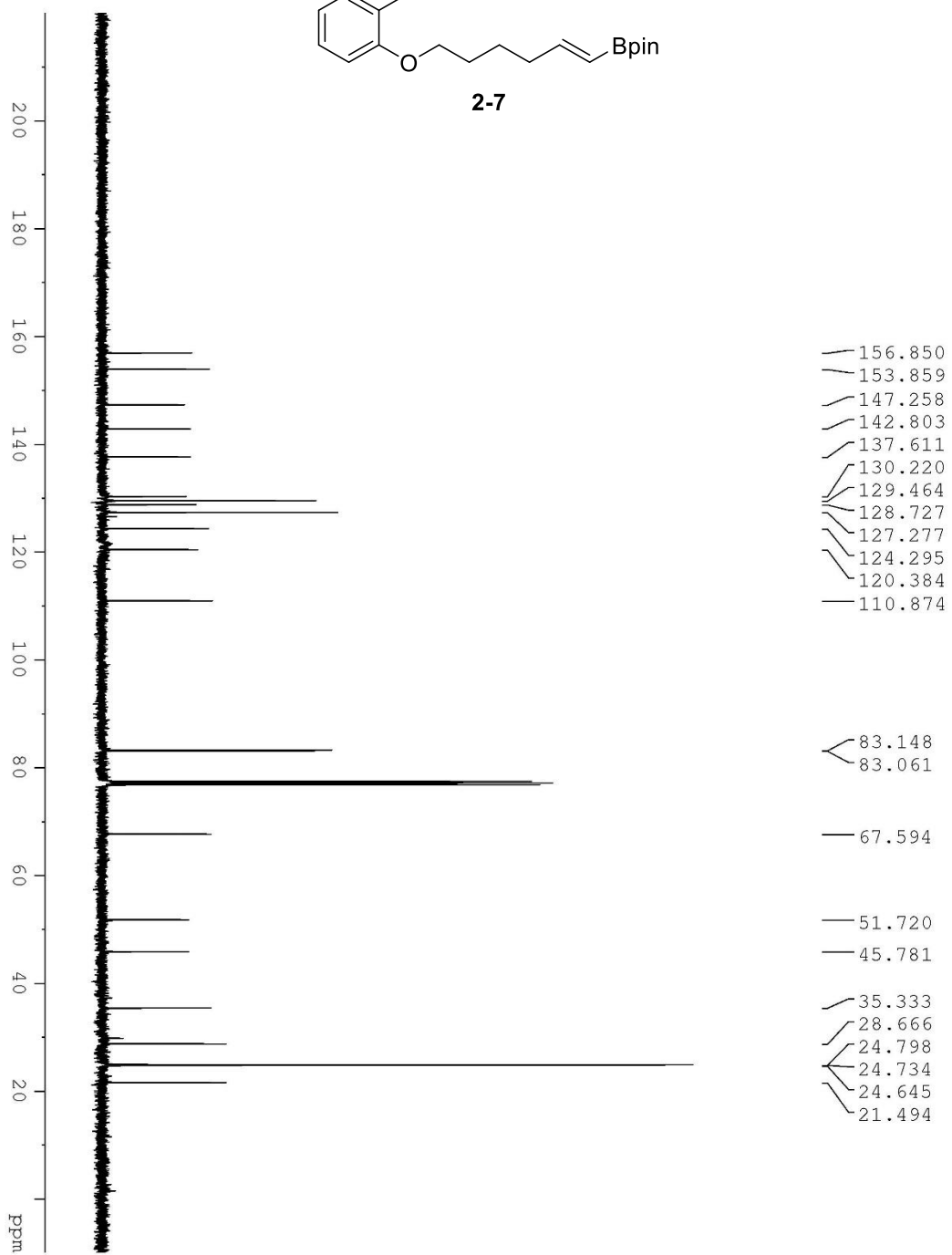
2-6

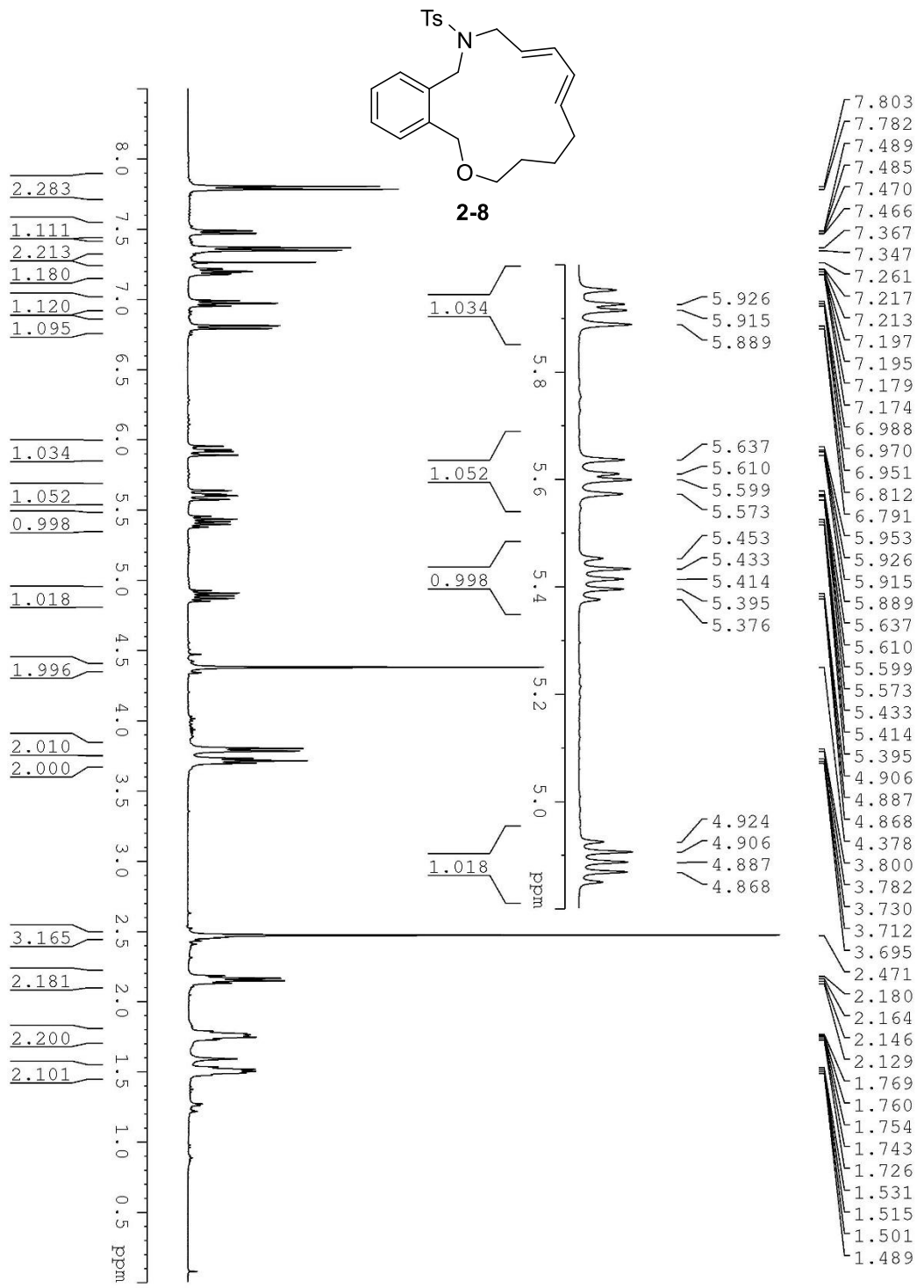


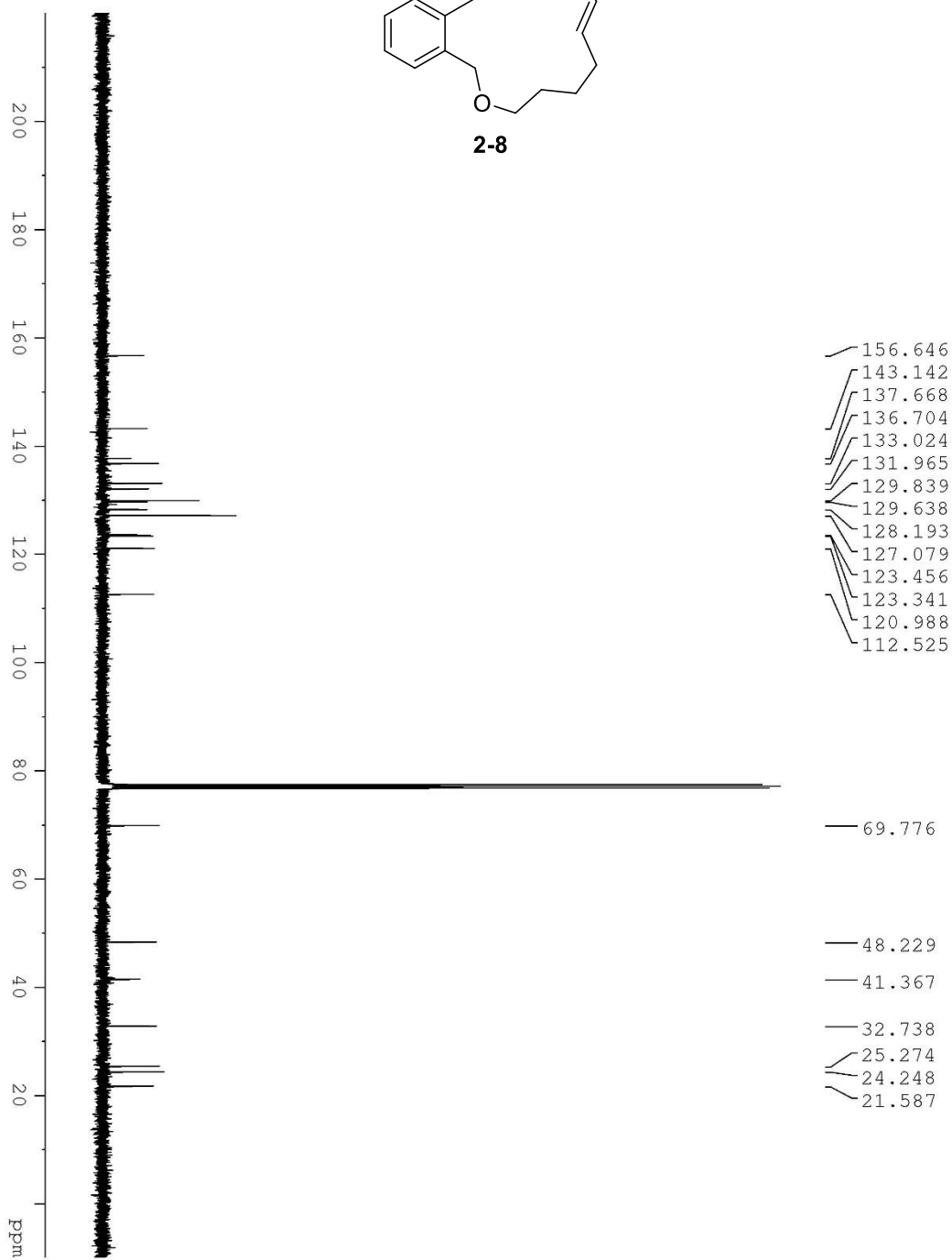
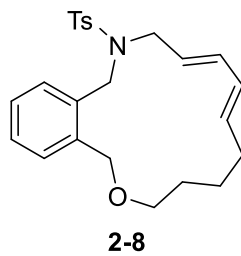


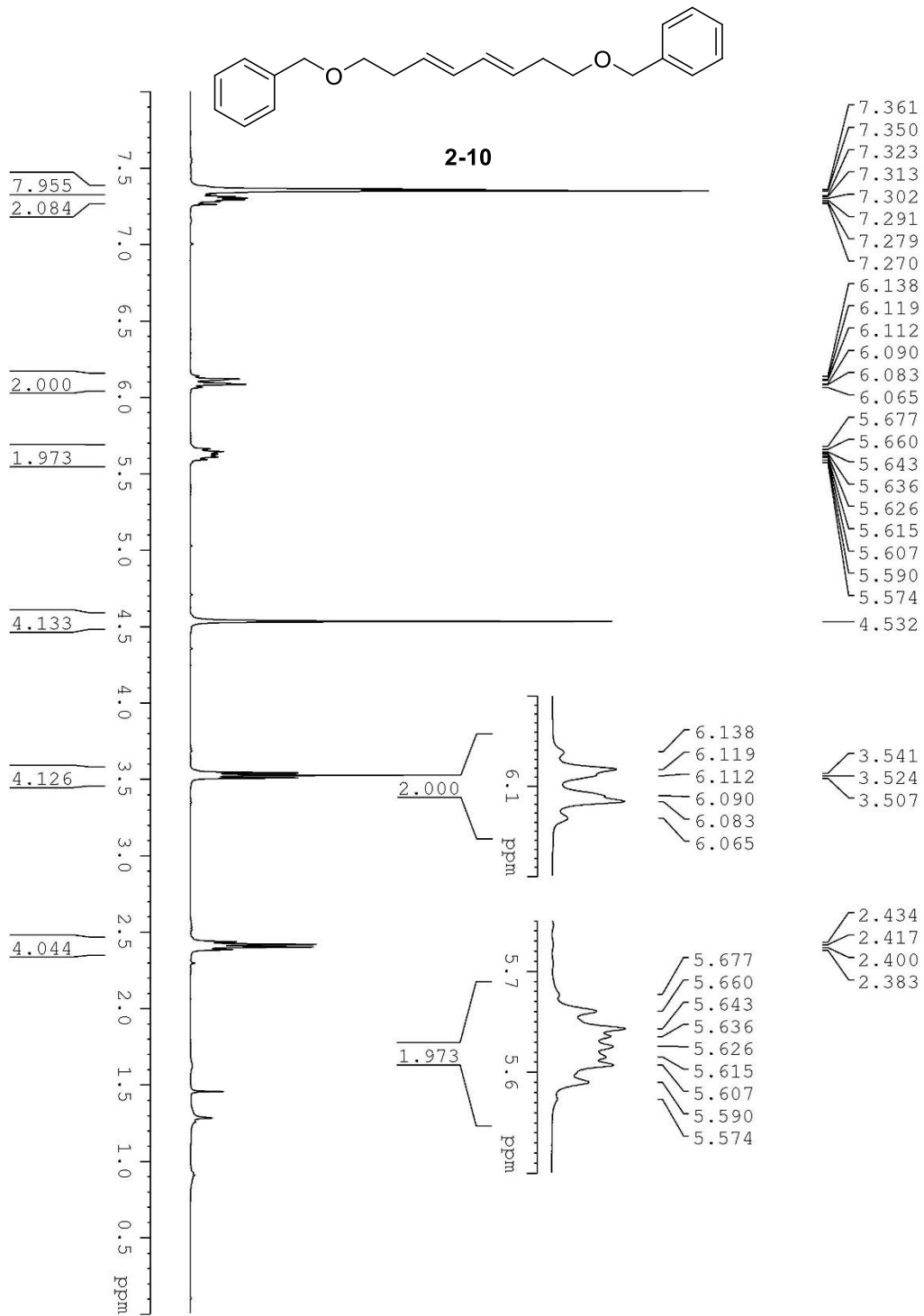


**2-7**

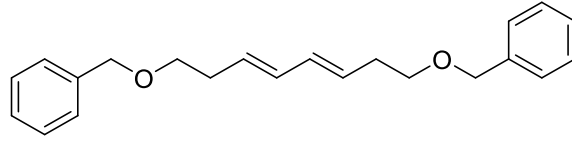




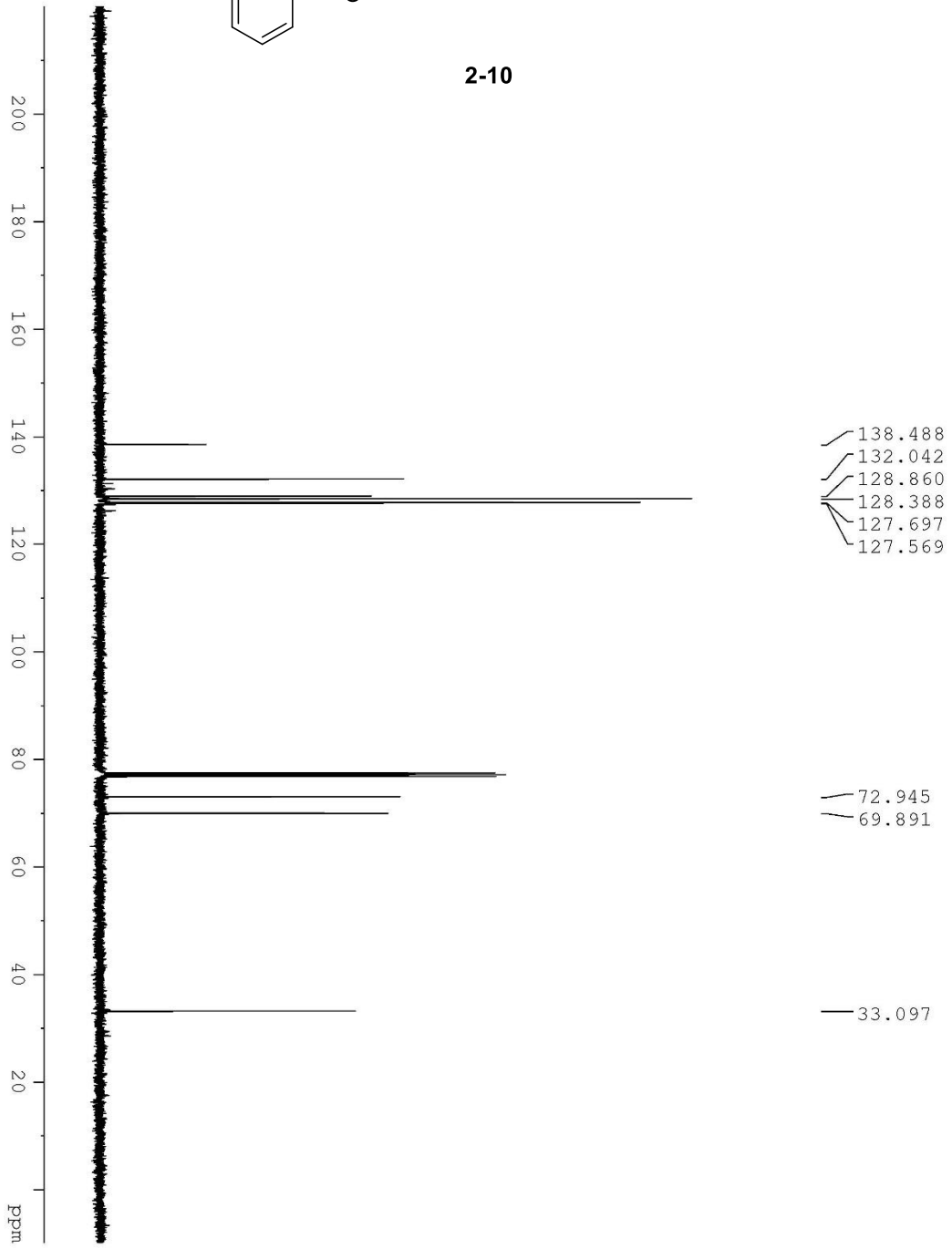


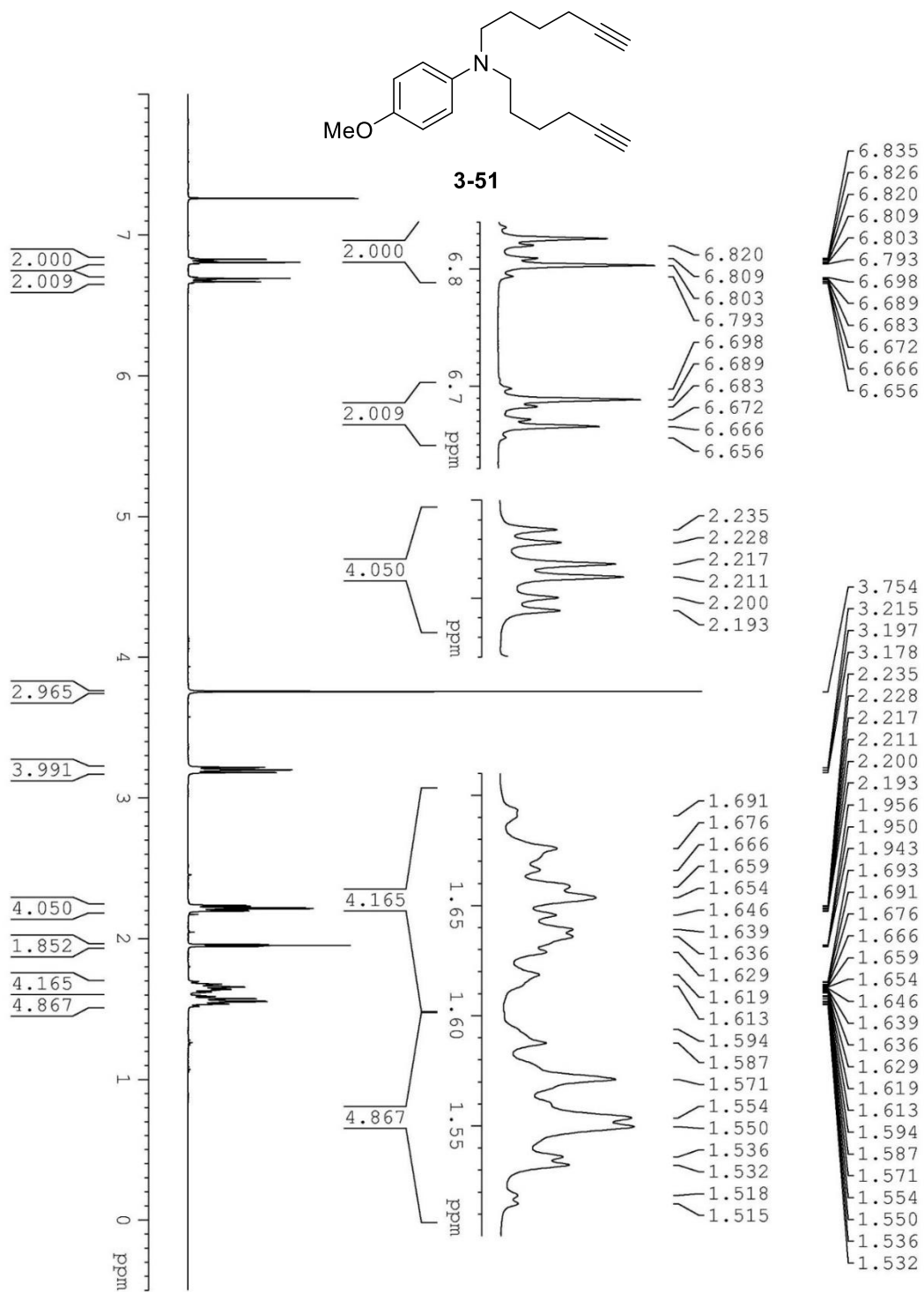


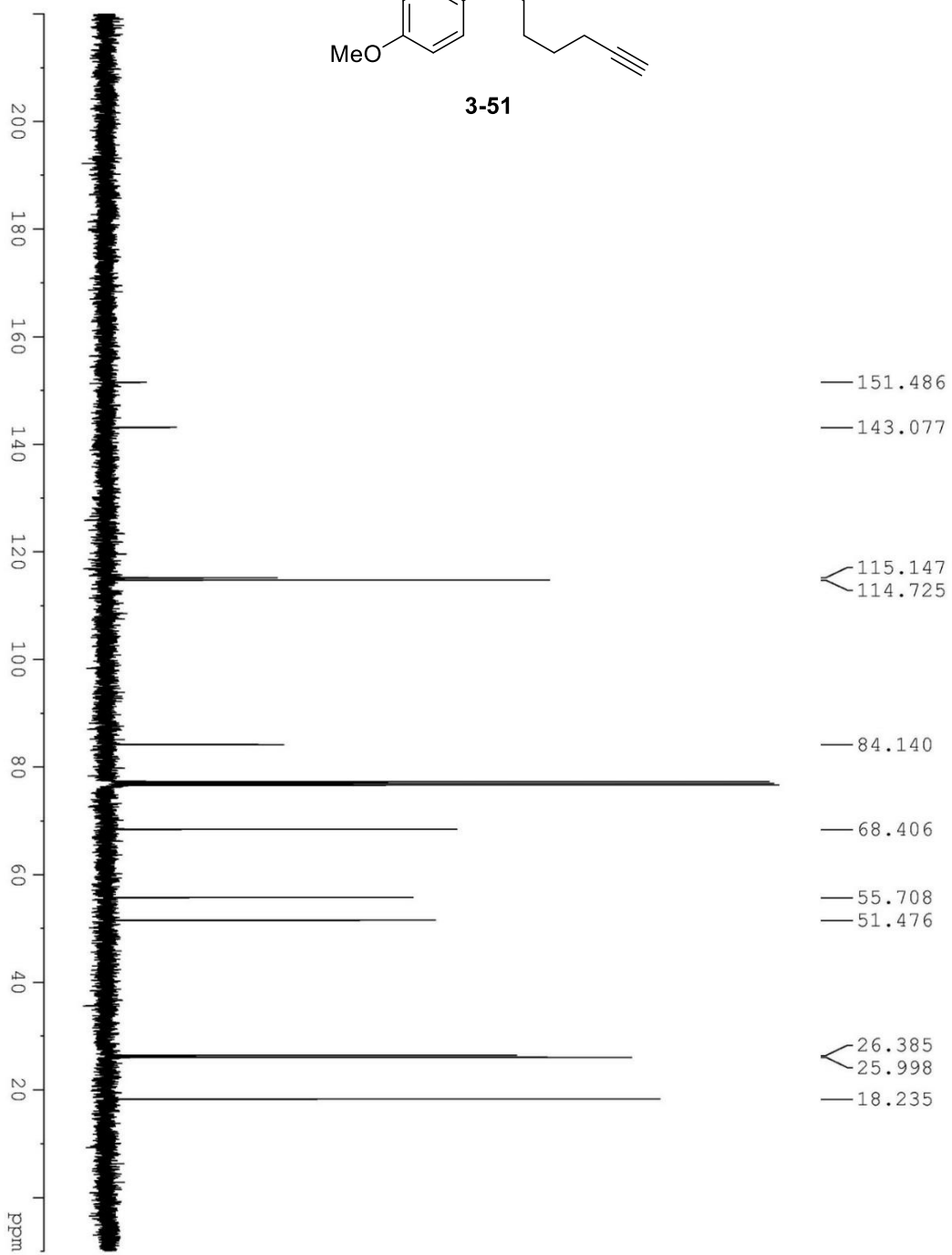
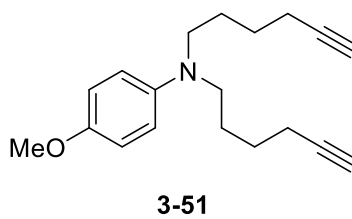


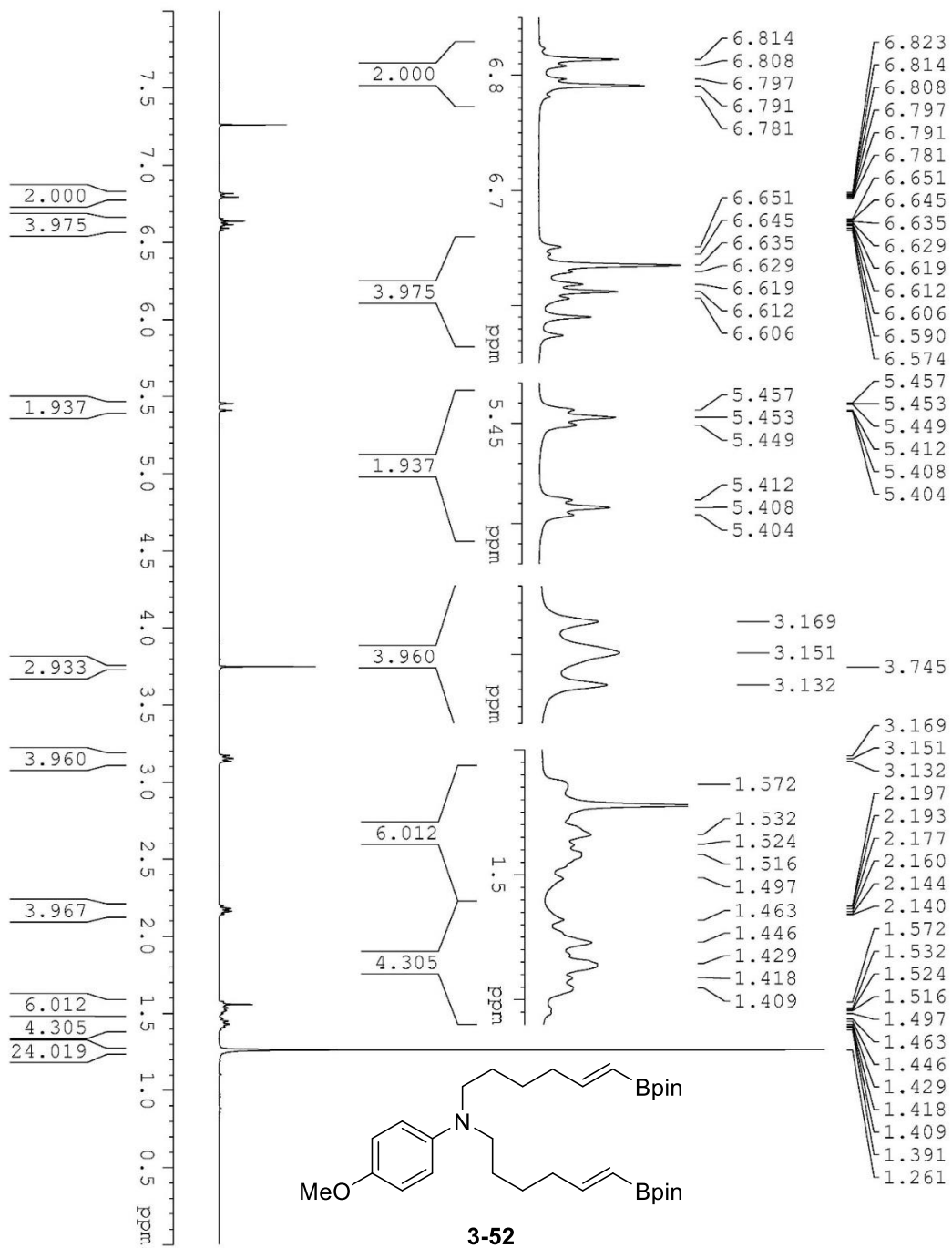


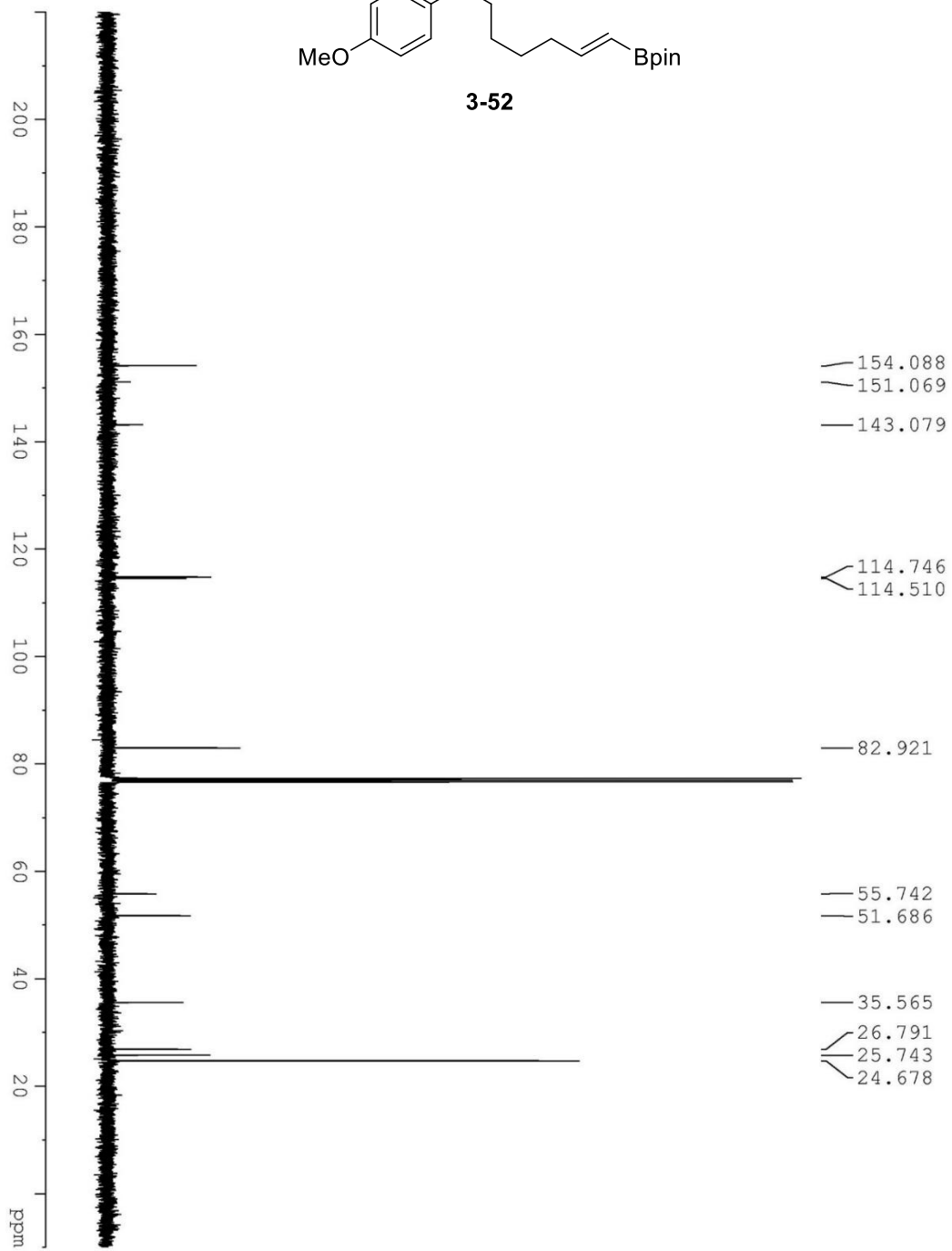
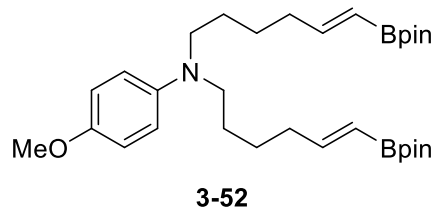
2-10

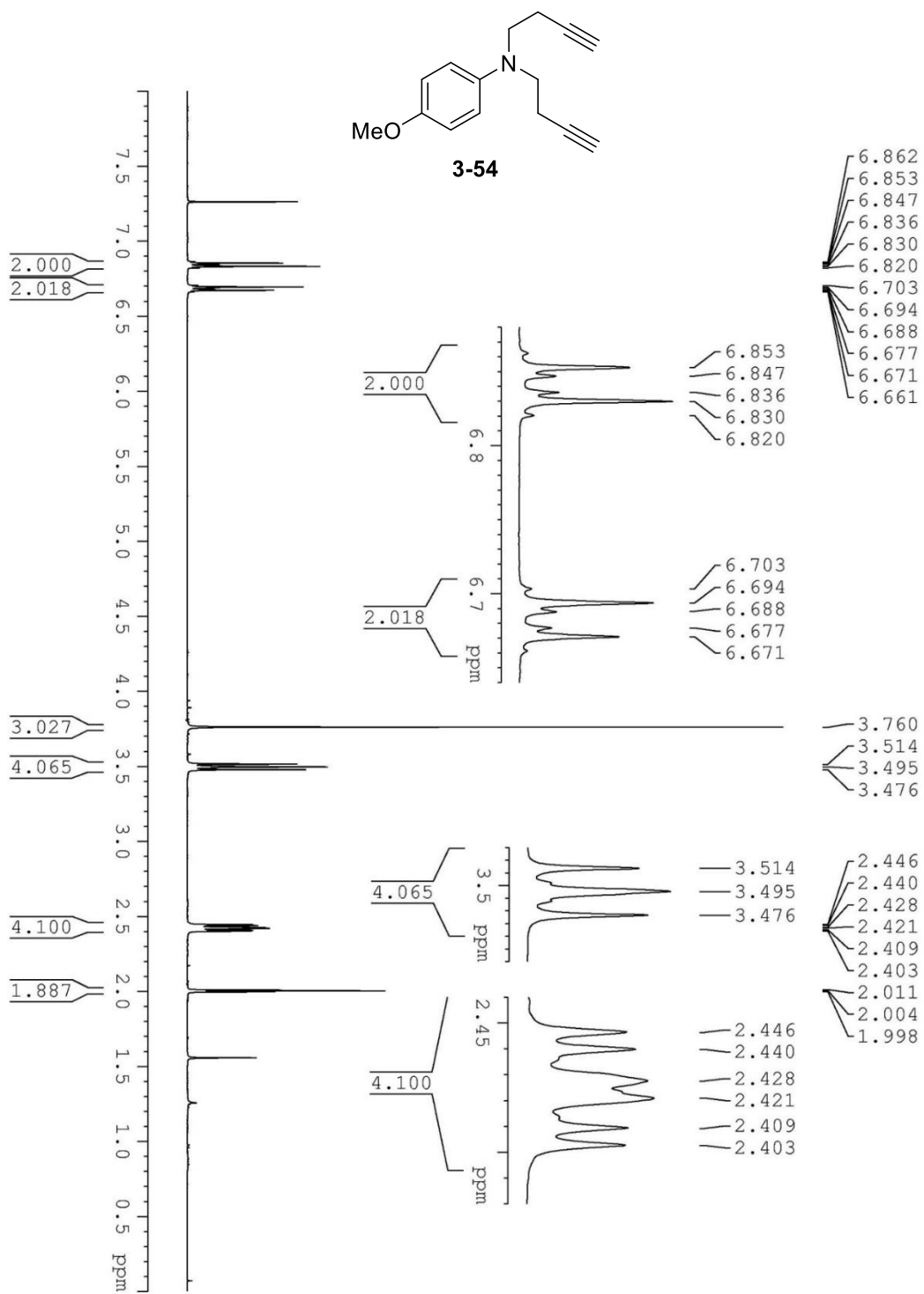


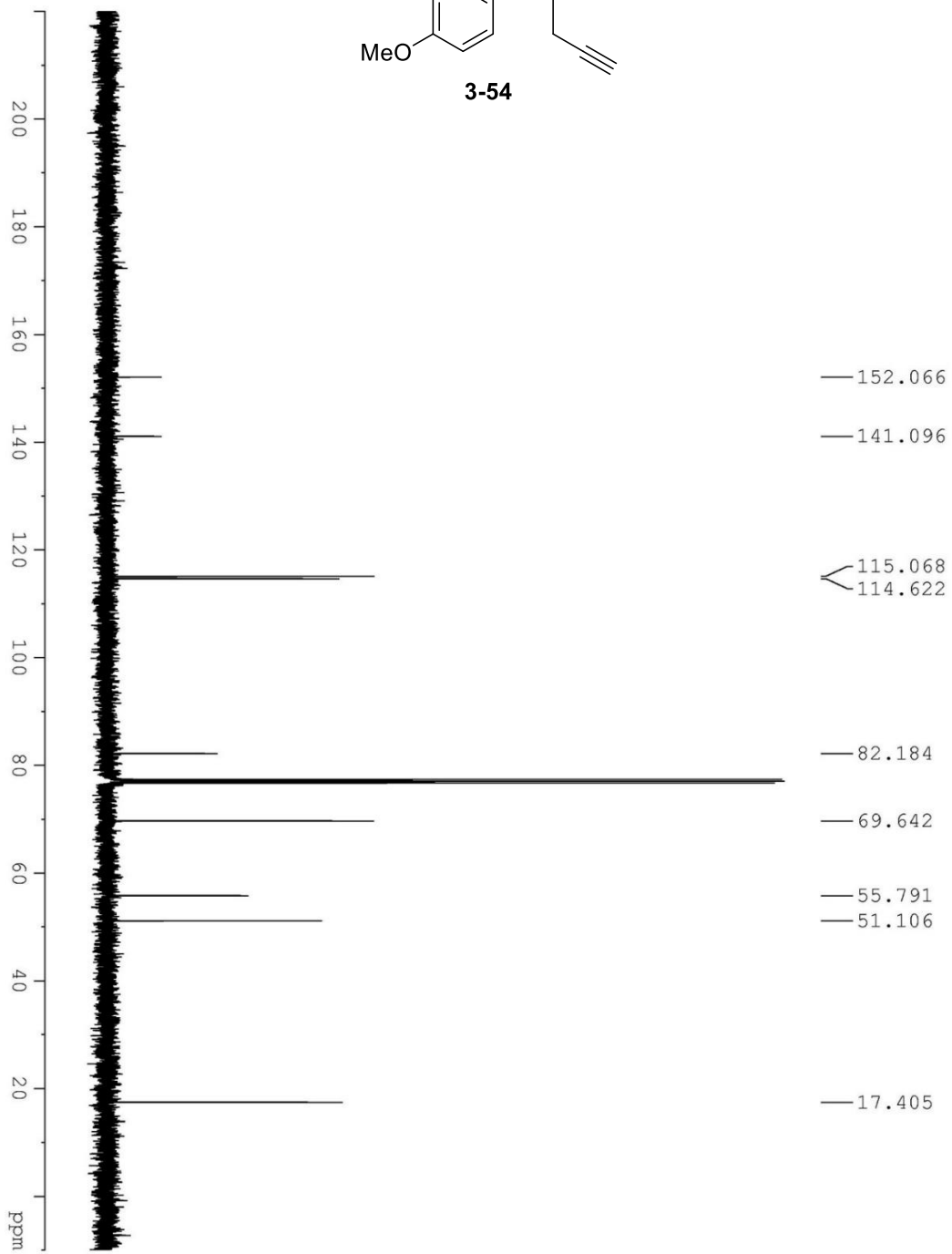
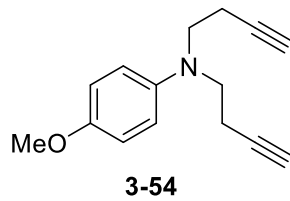


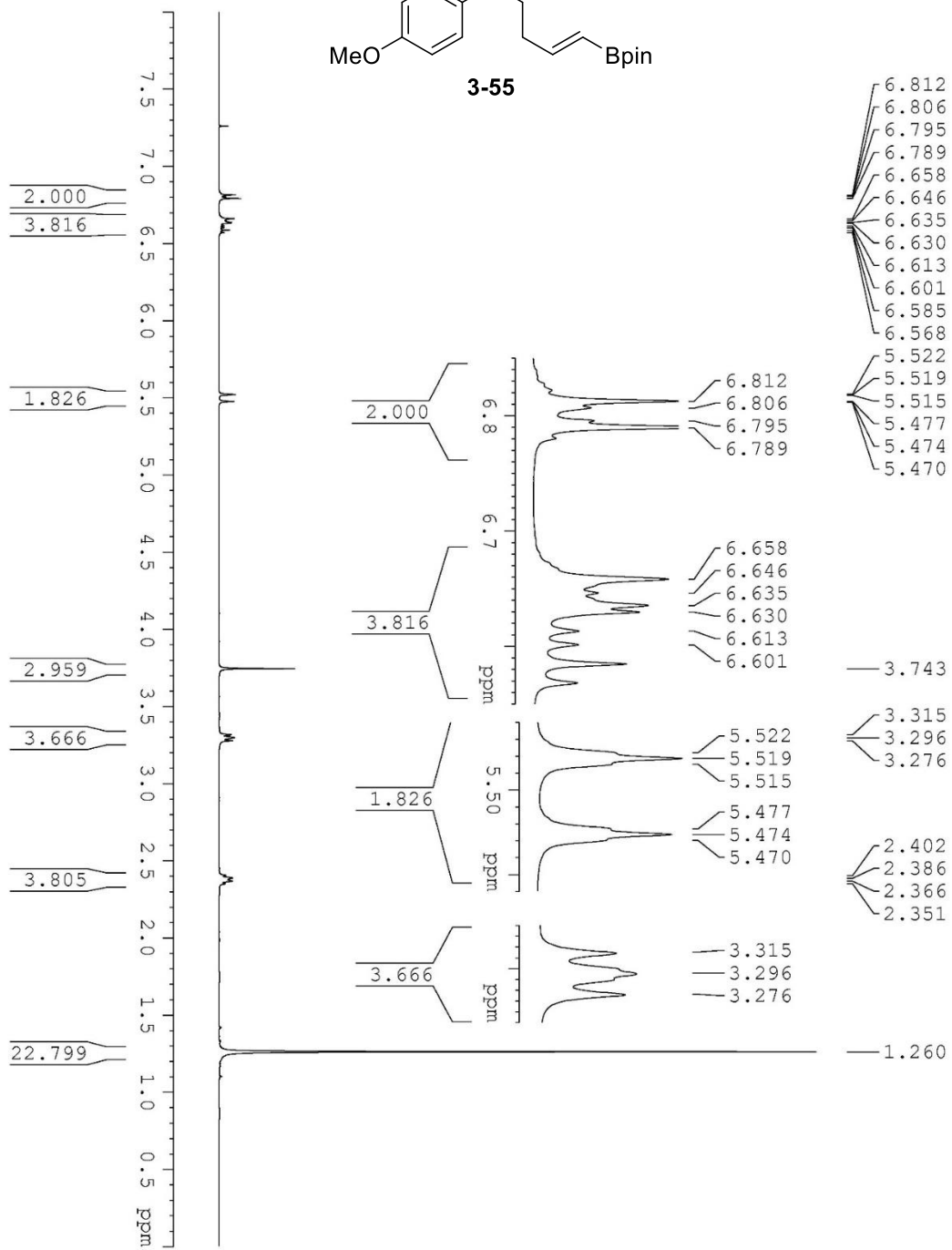
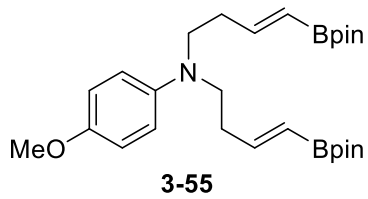




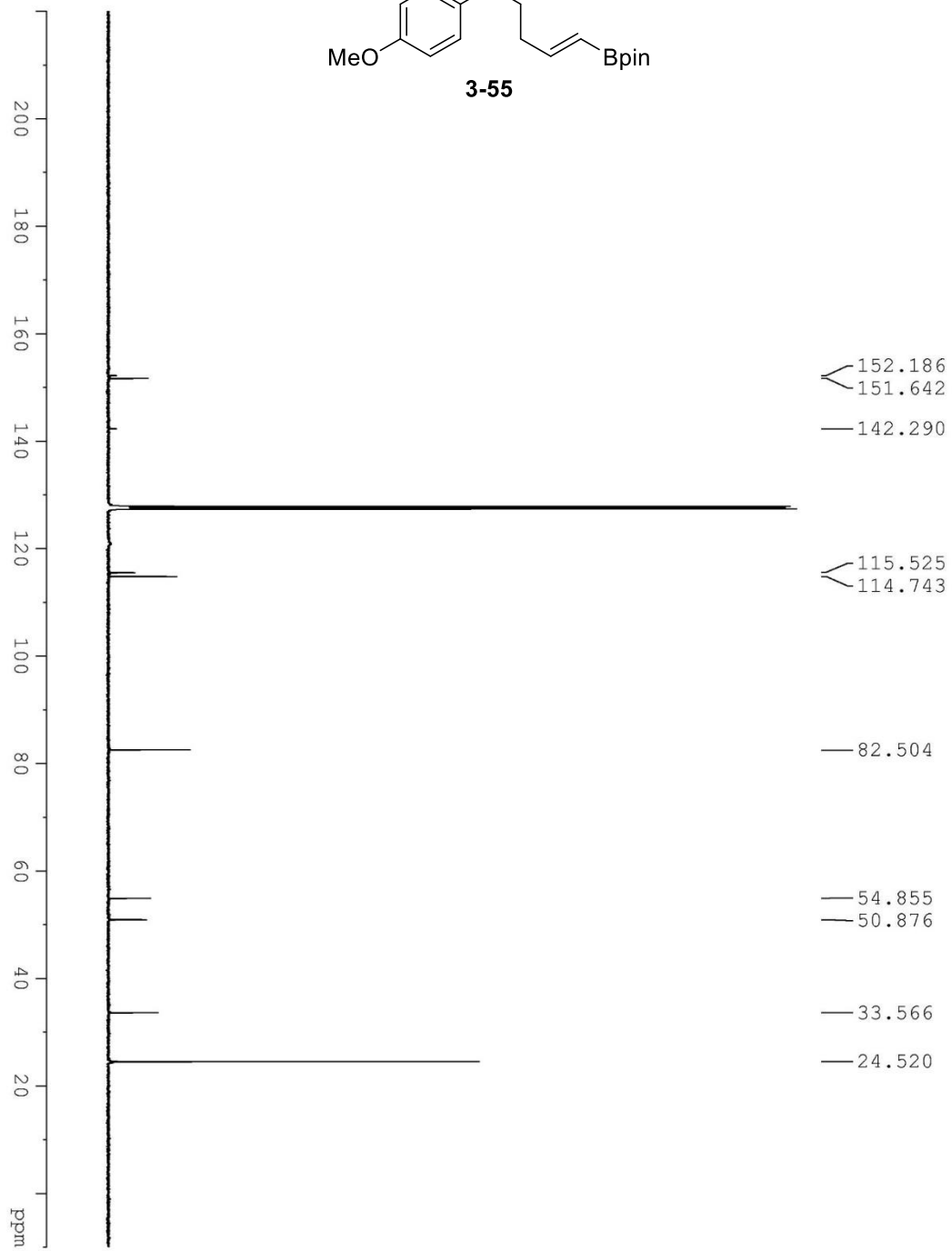
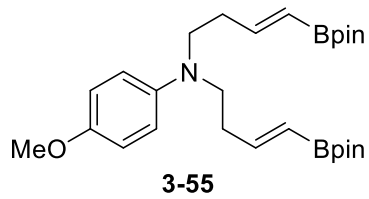


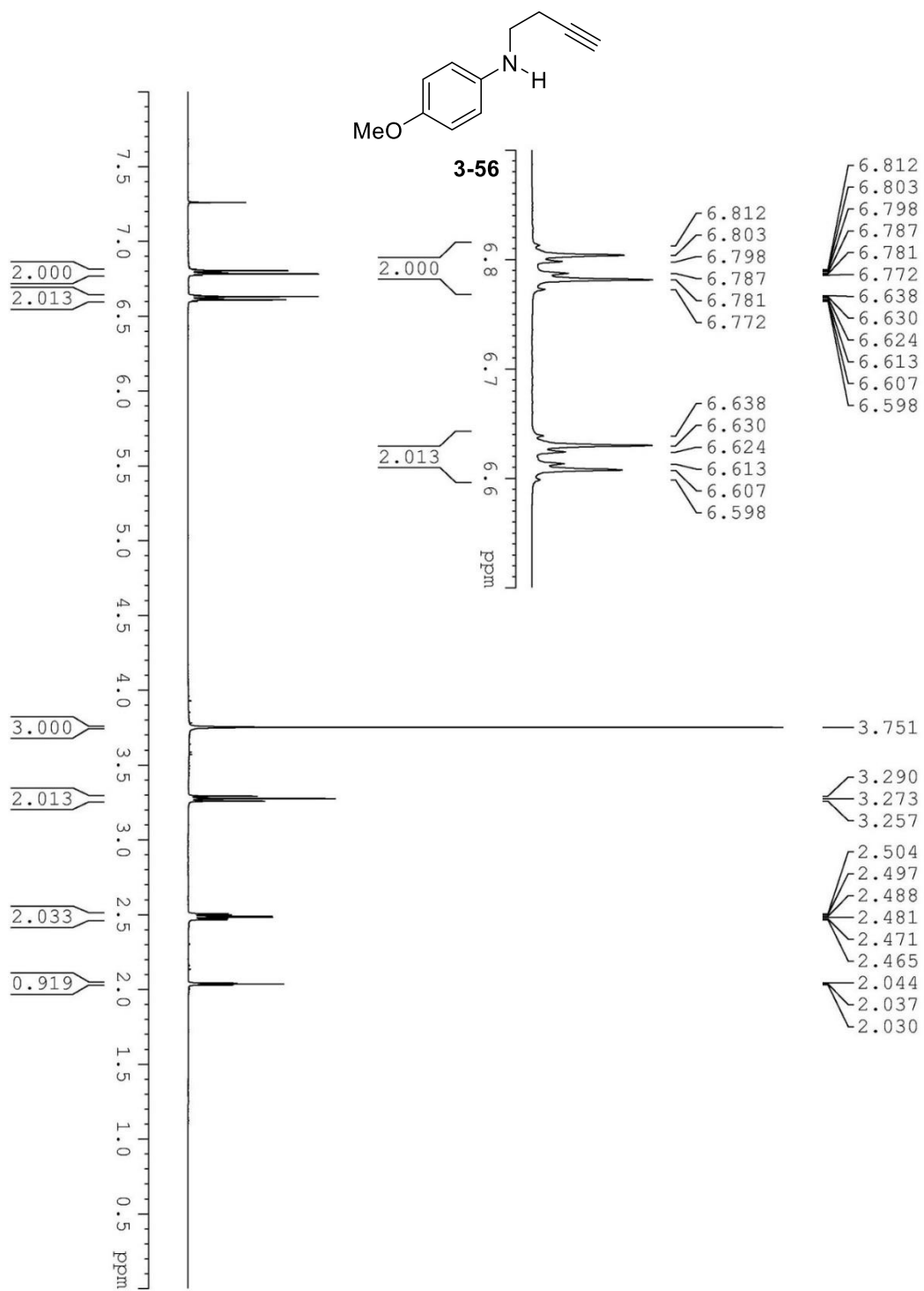


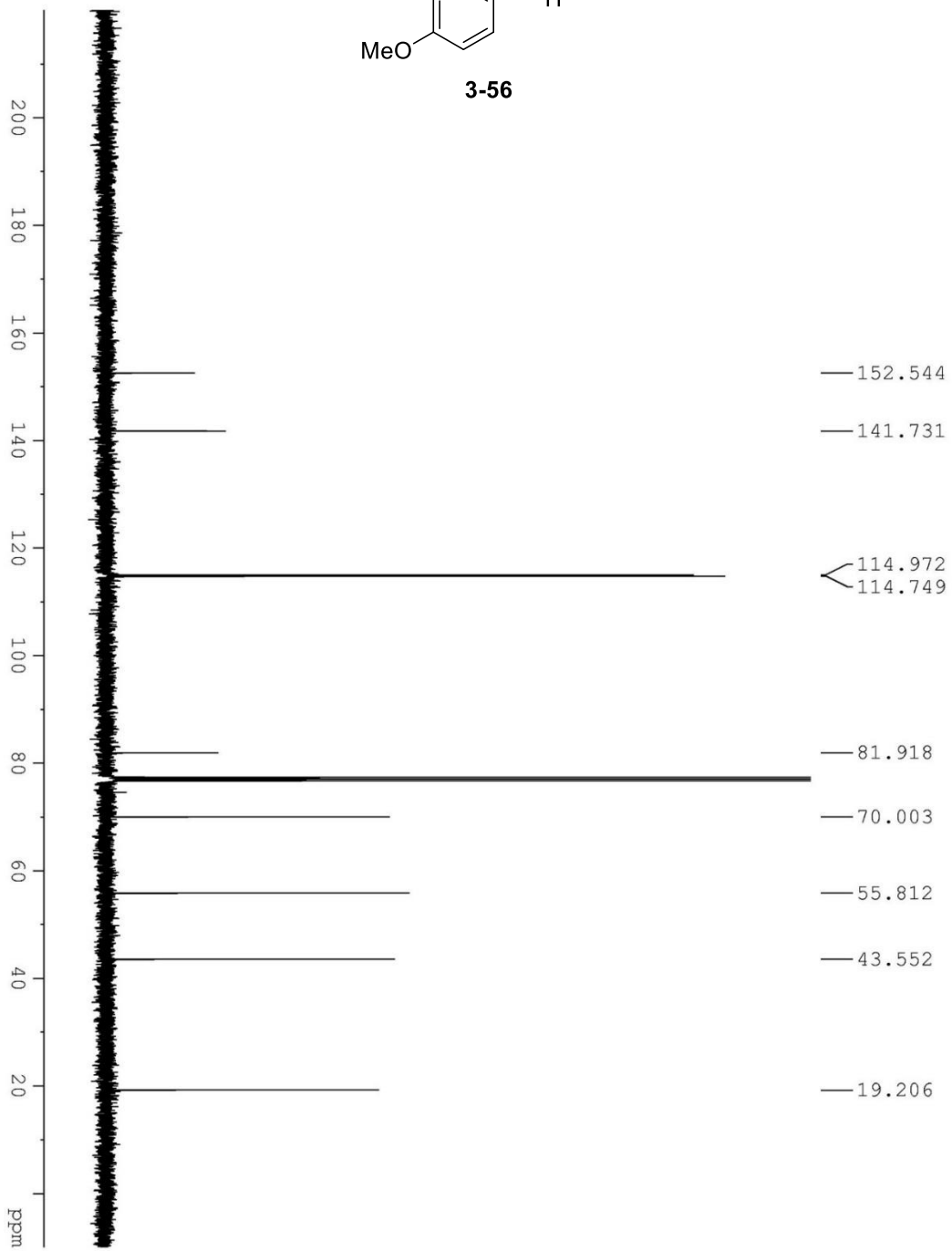
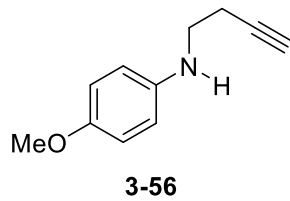




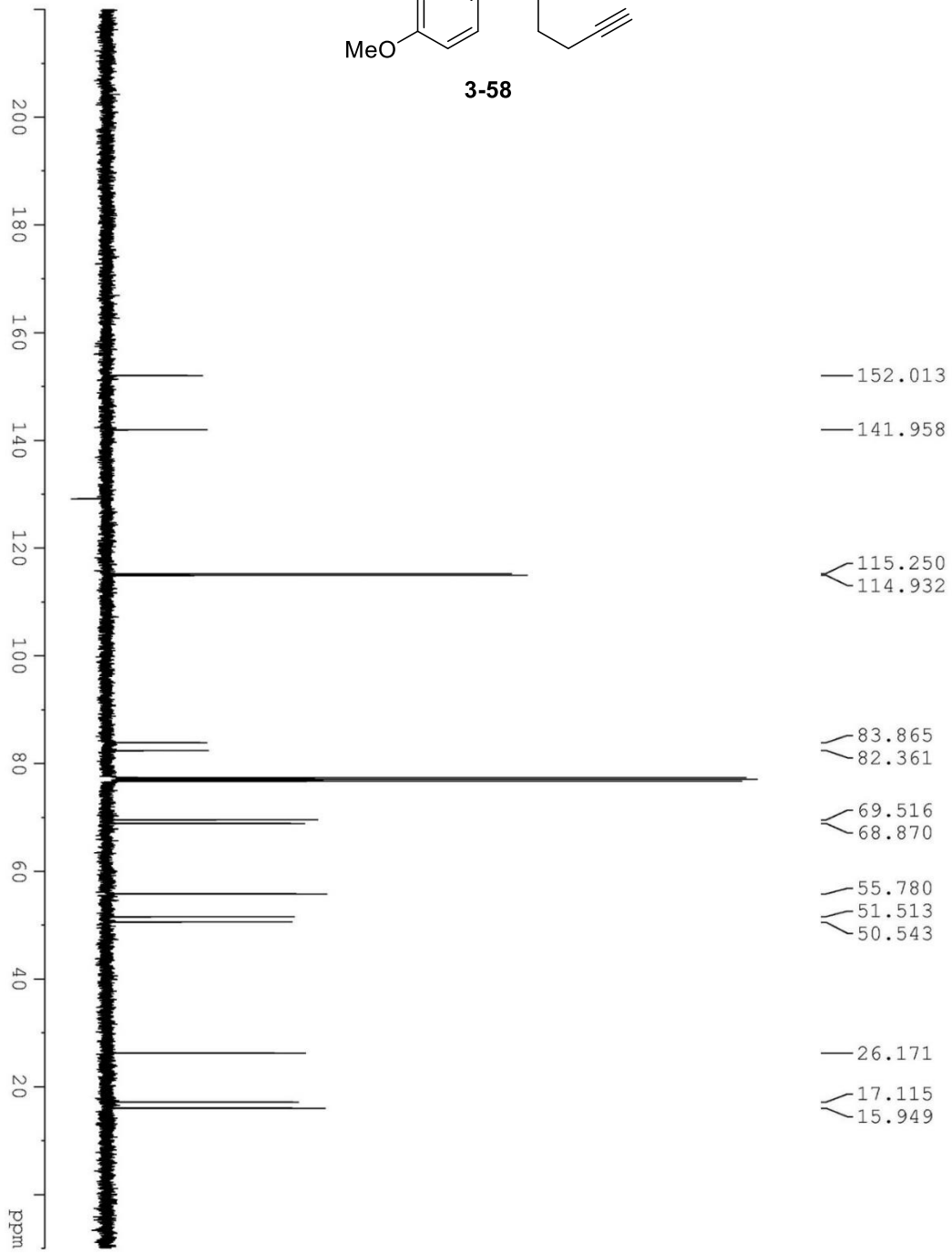
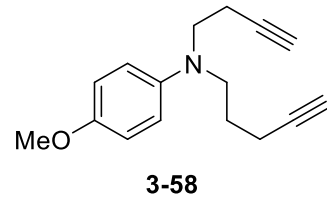


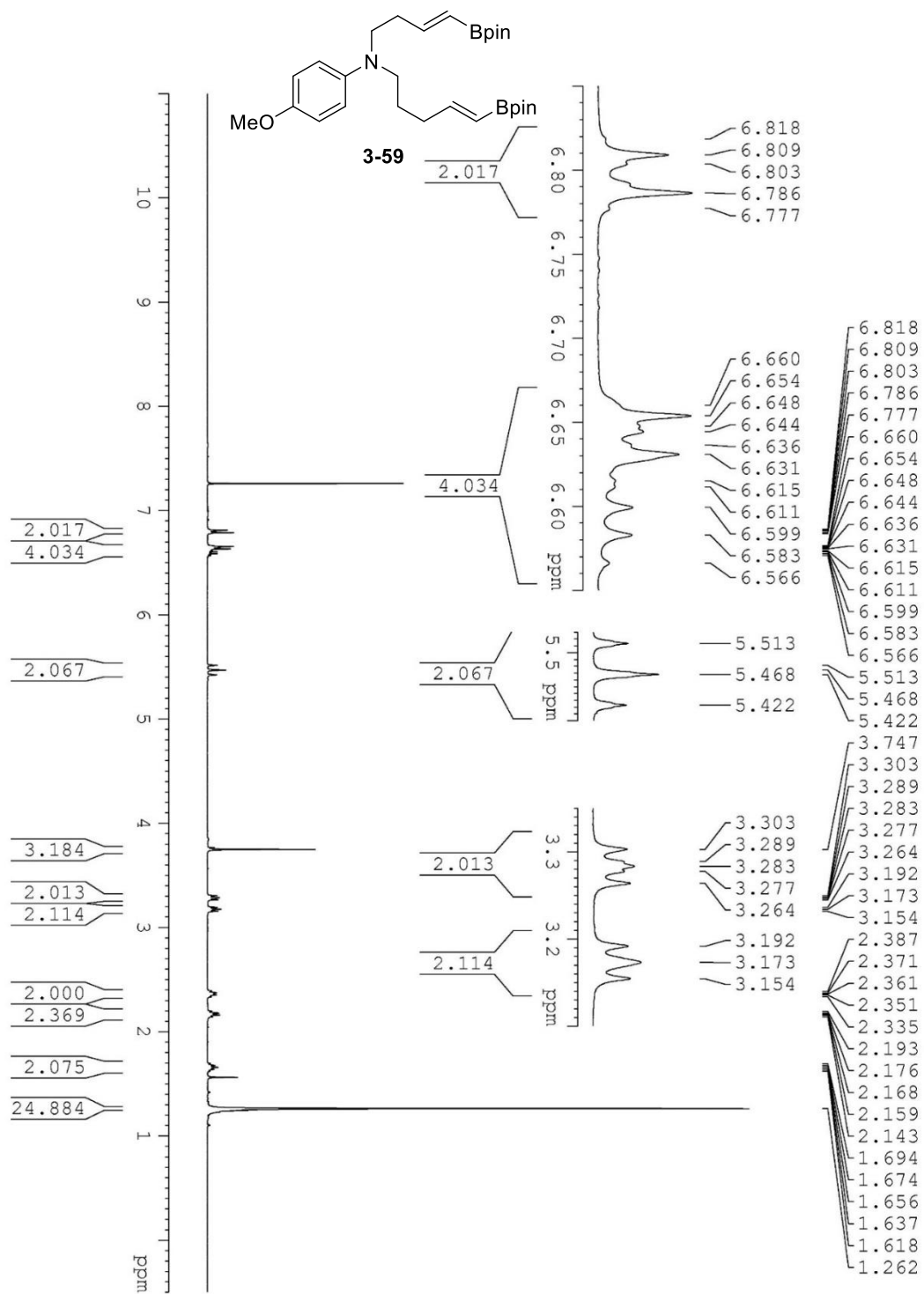


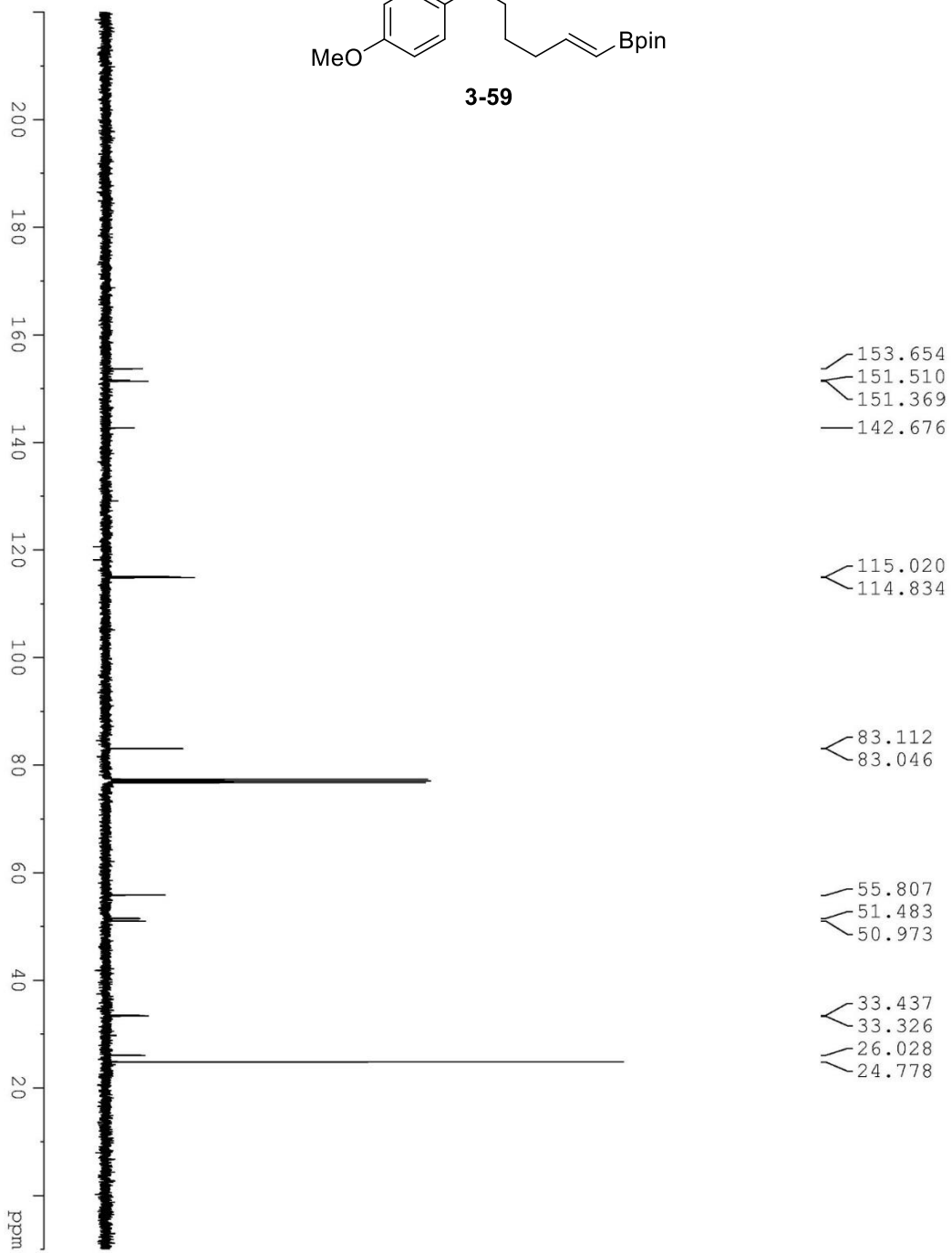
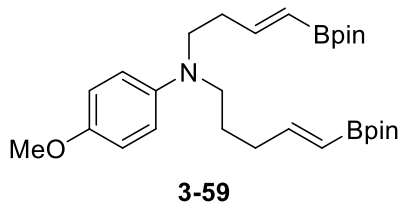


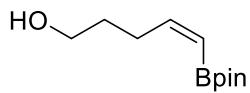




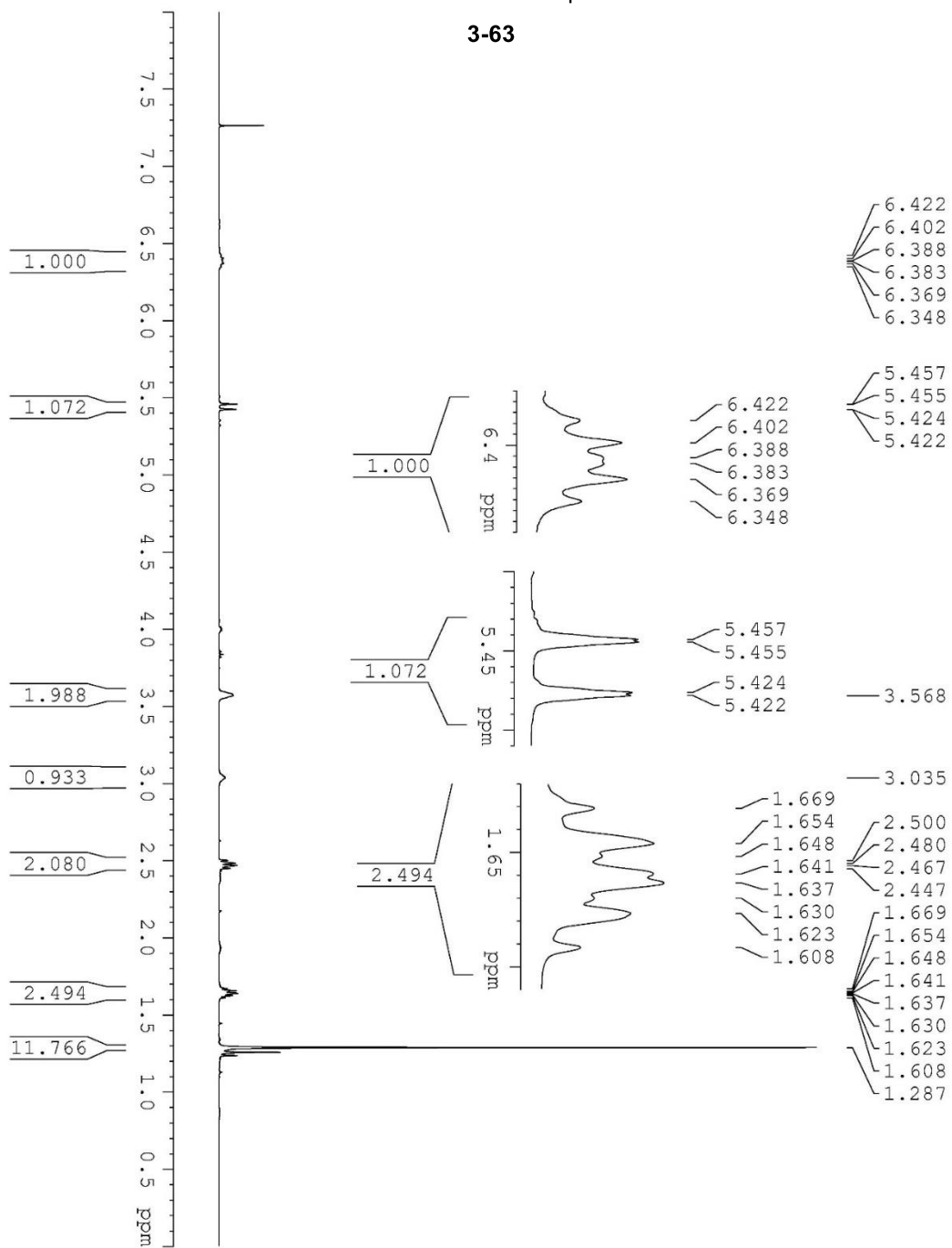




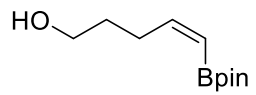




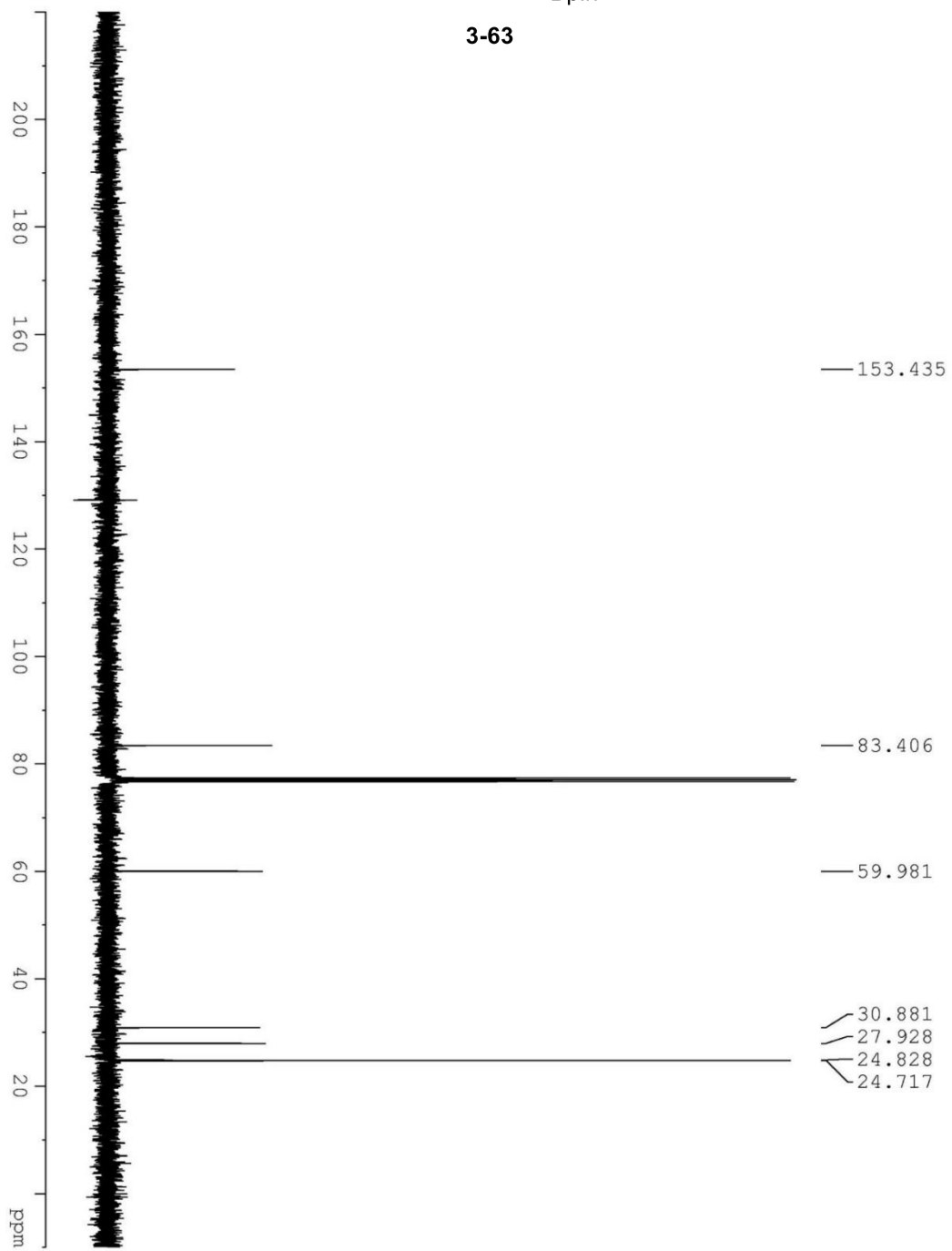
3-63

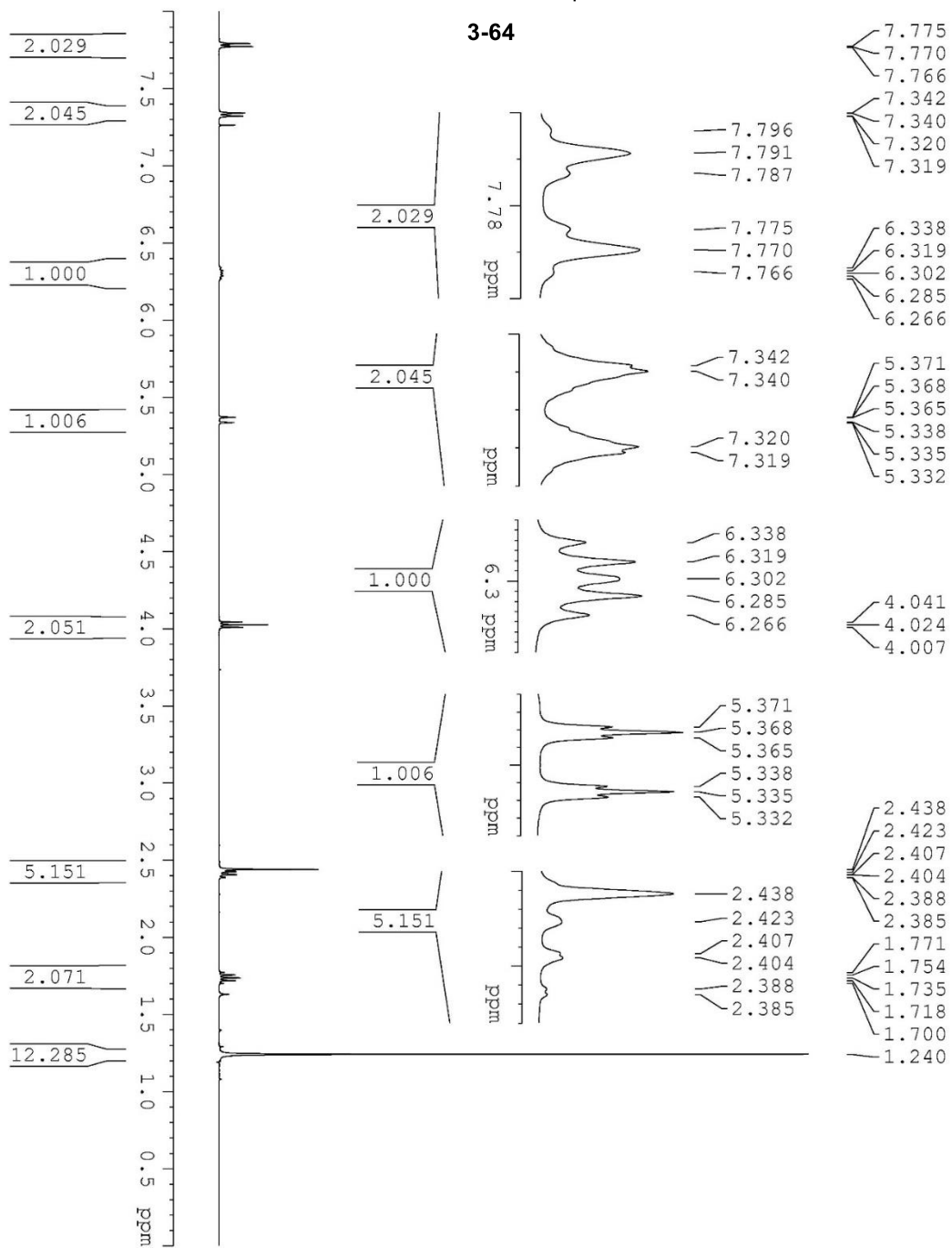
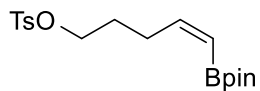


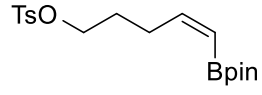




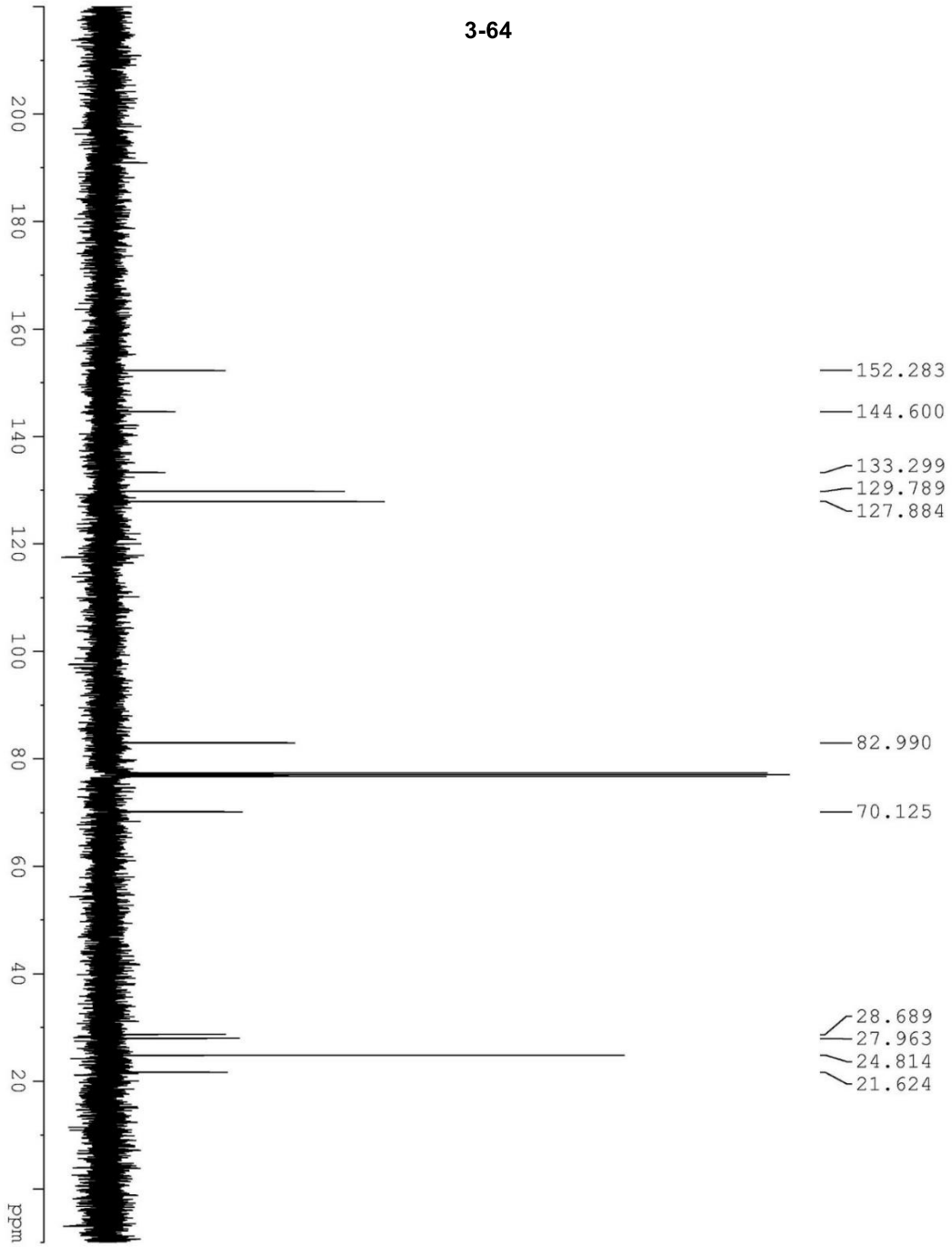
3-63

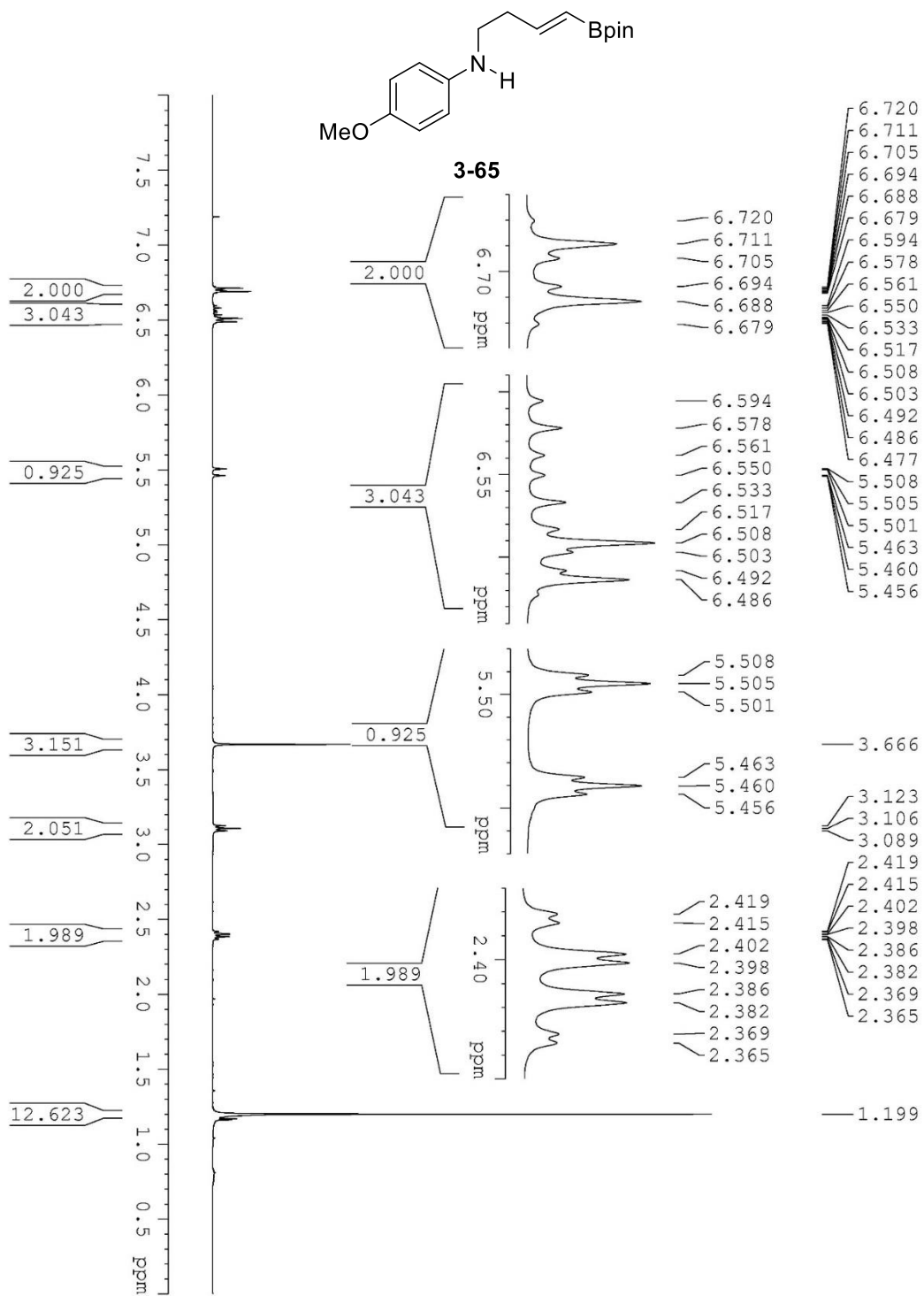


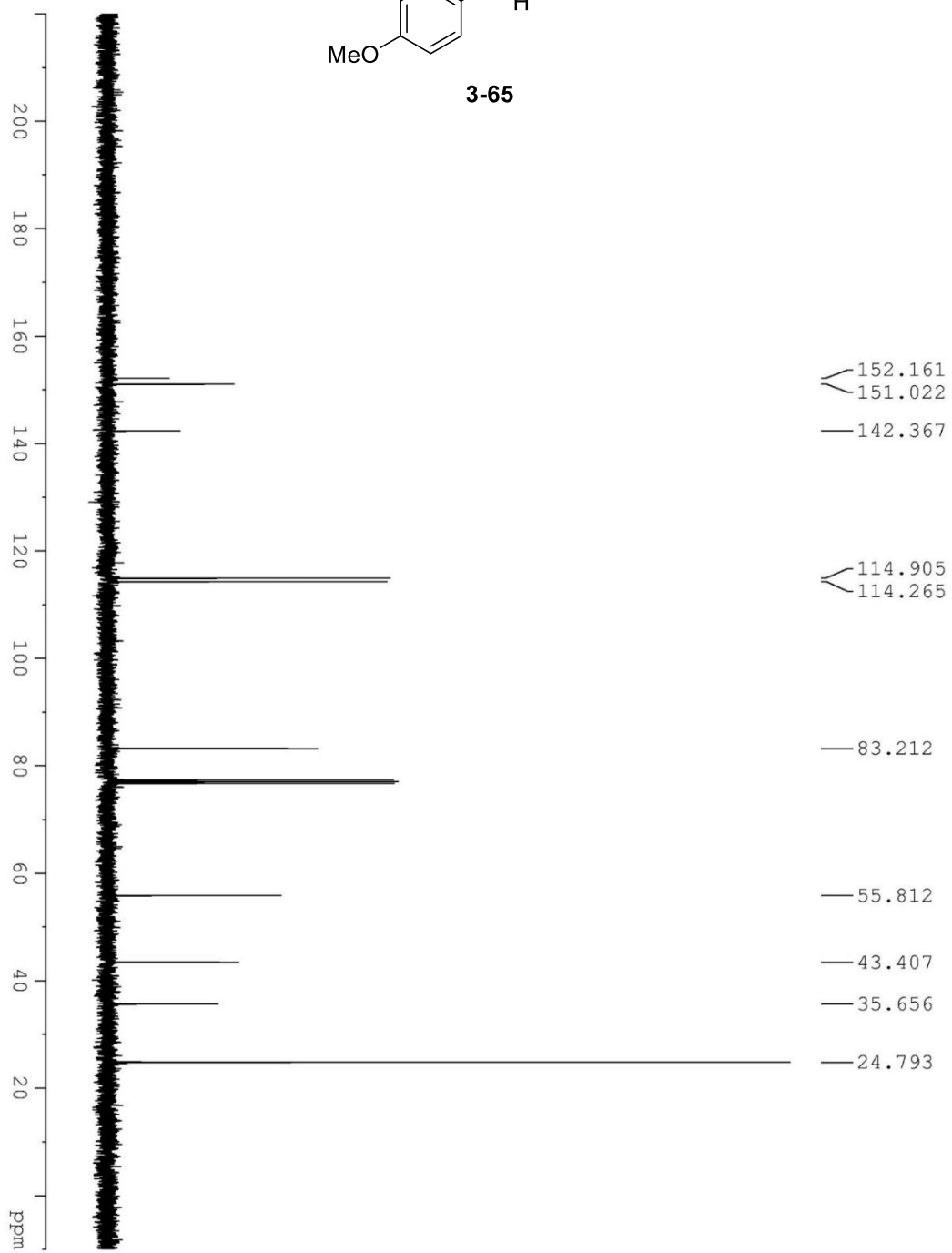
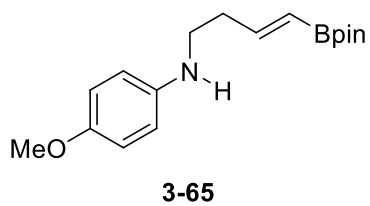


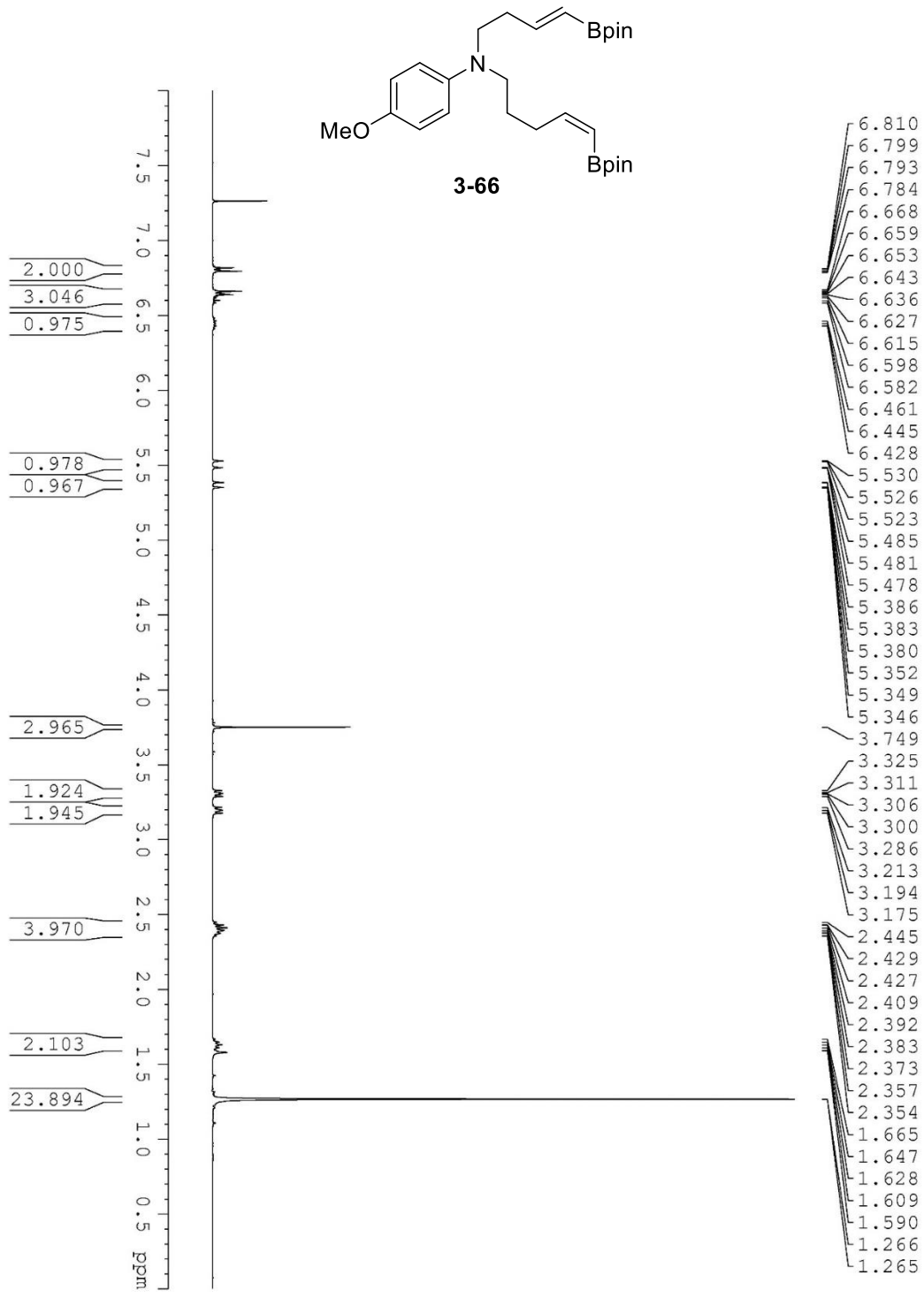


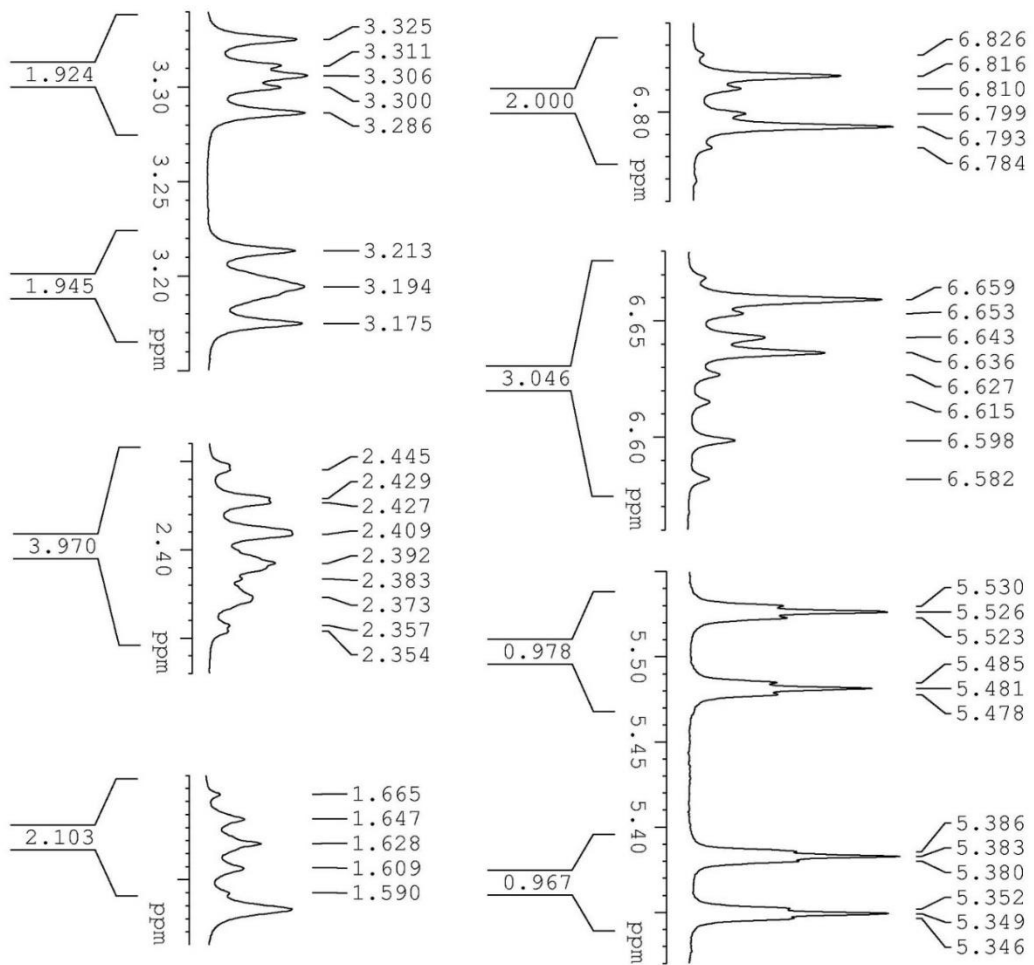
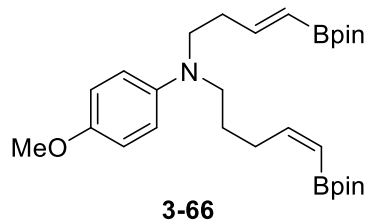
3-64

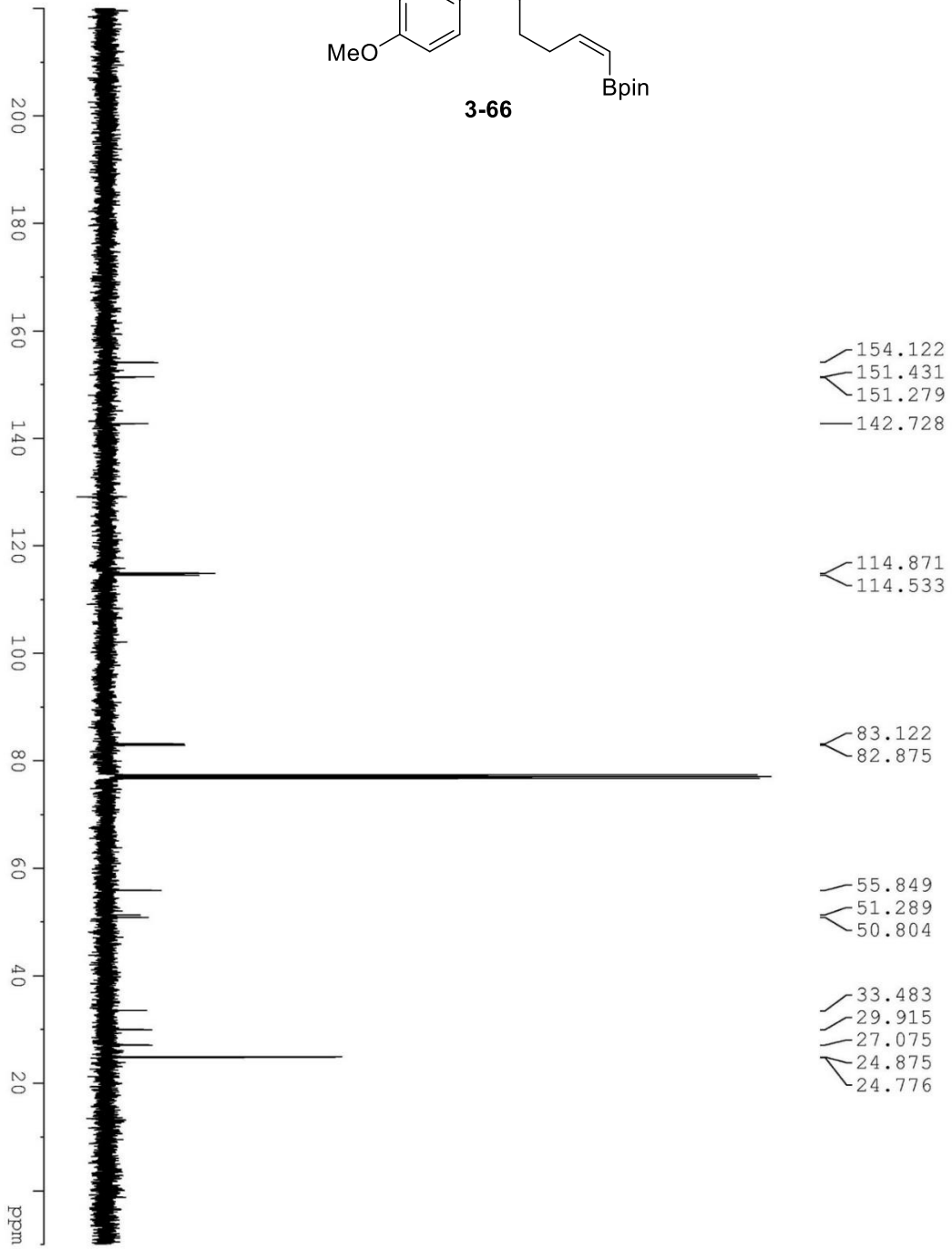
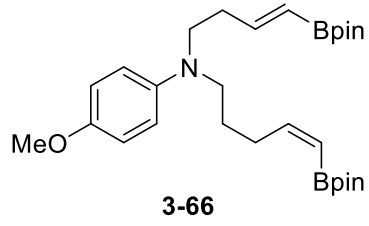




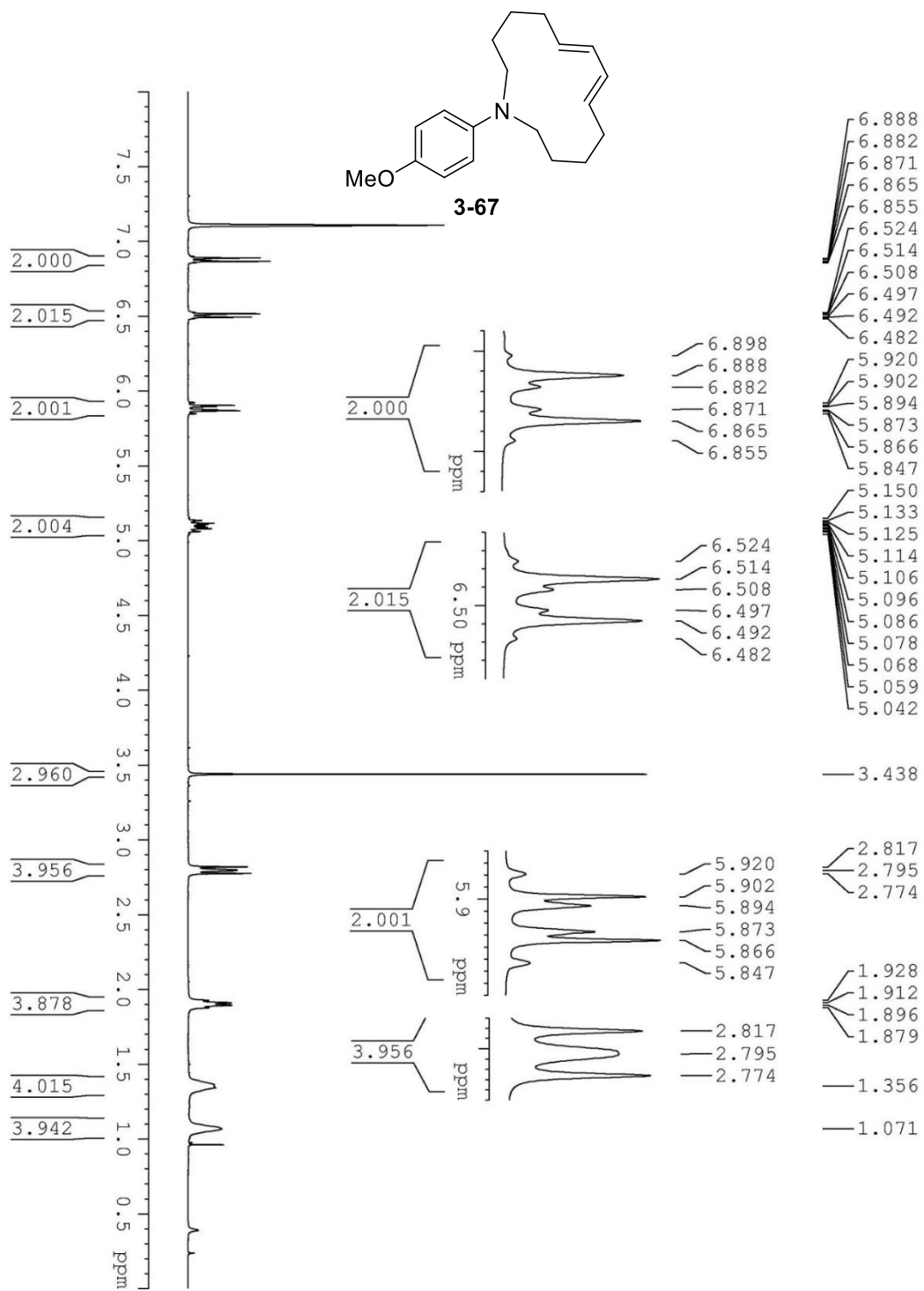


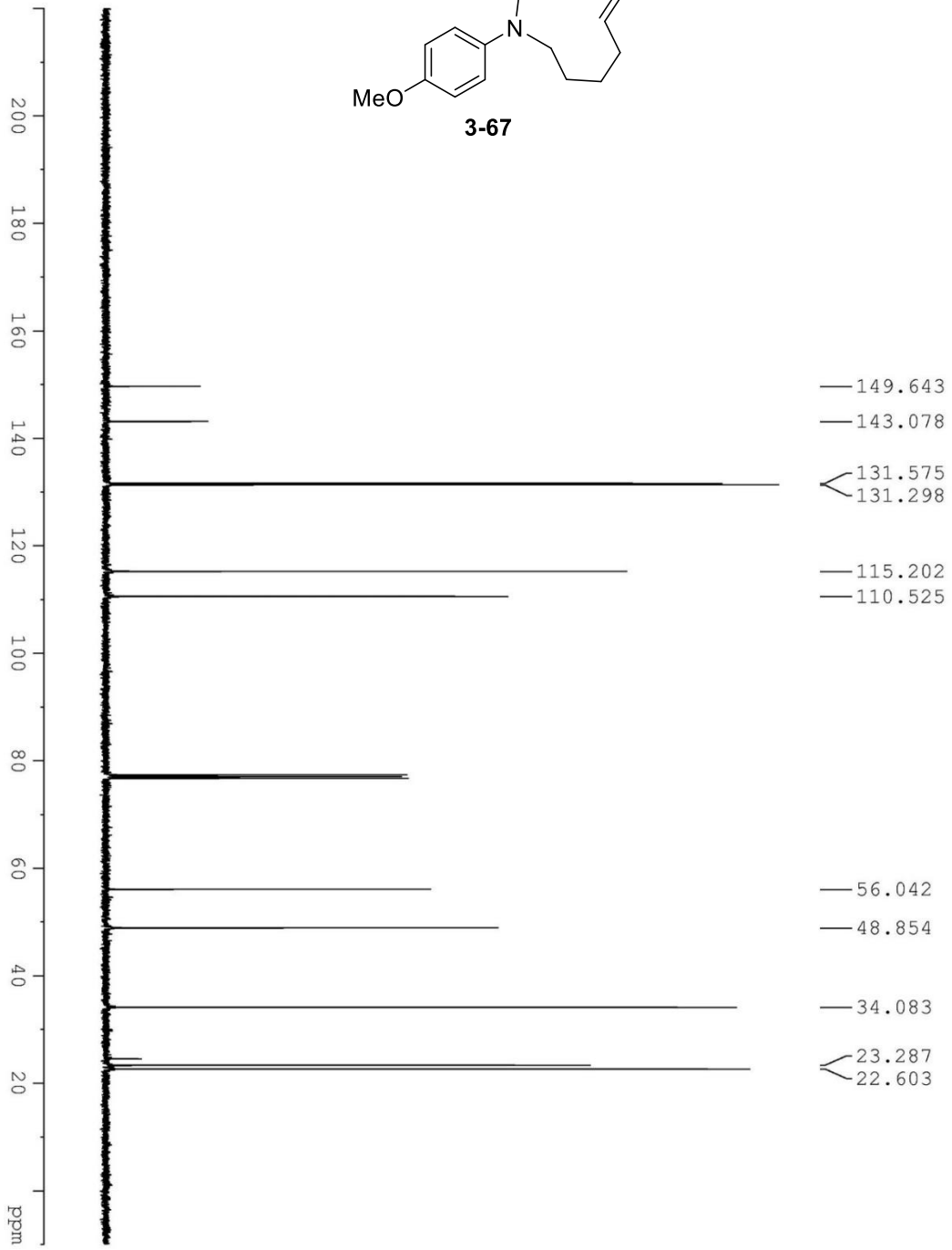
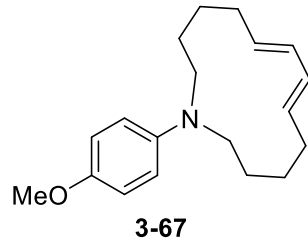


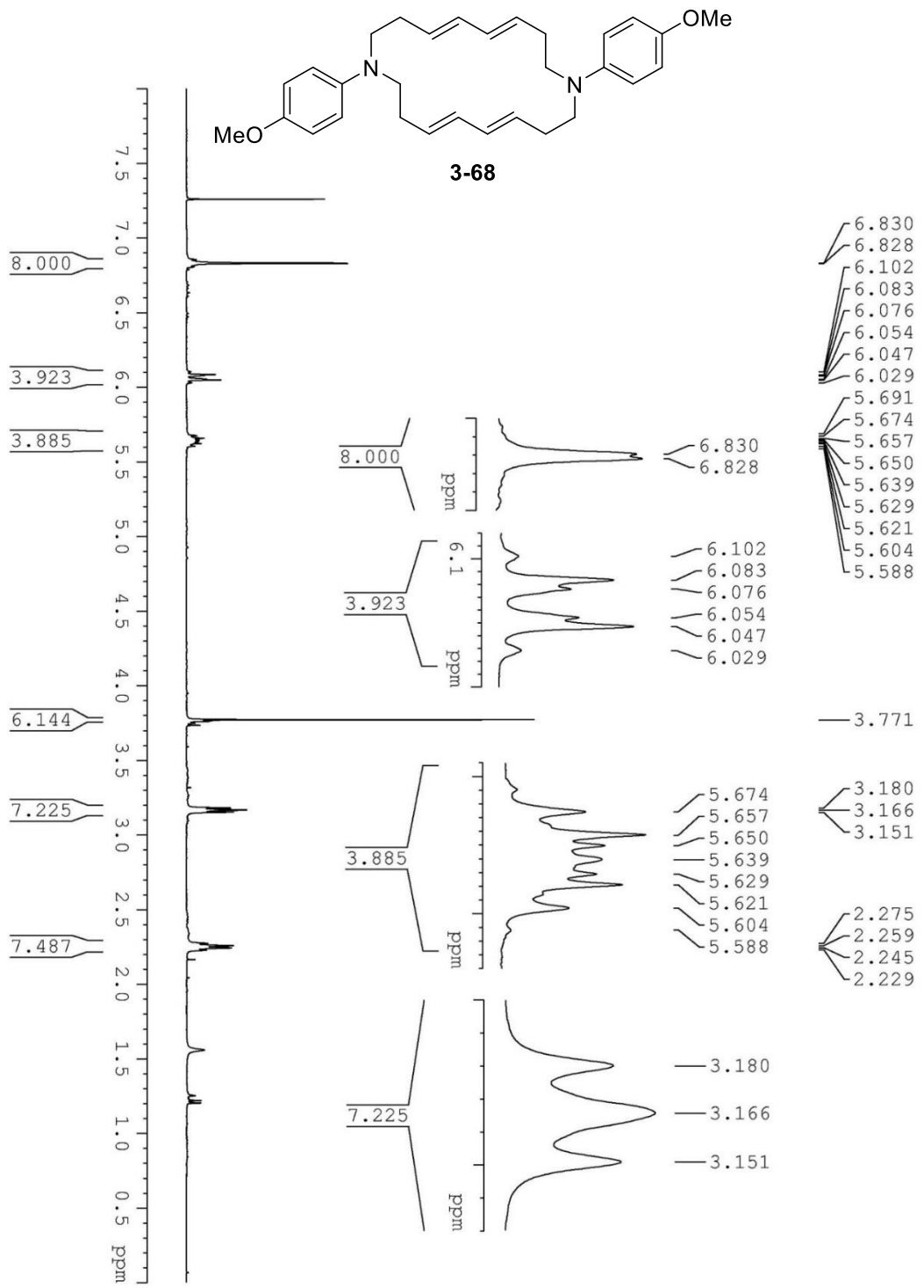


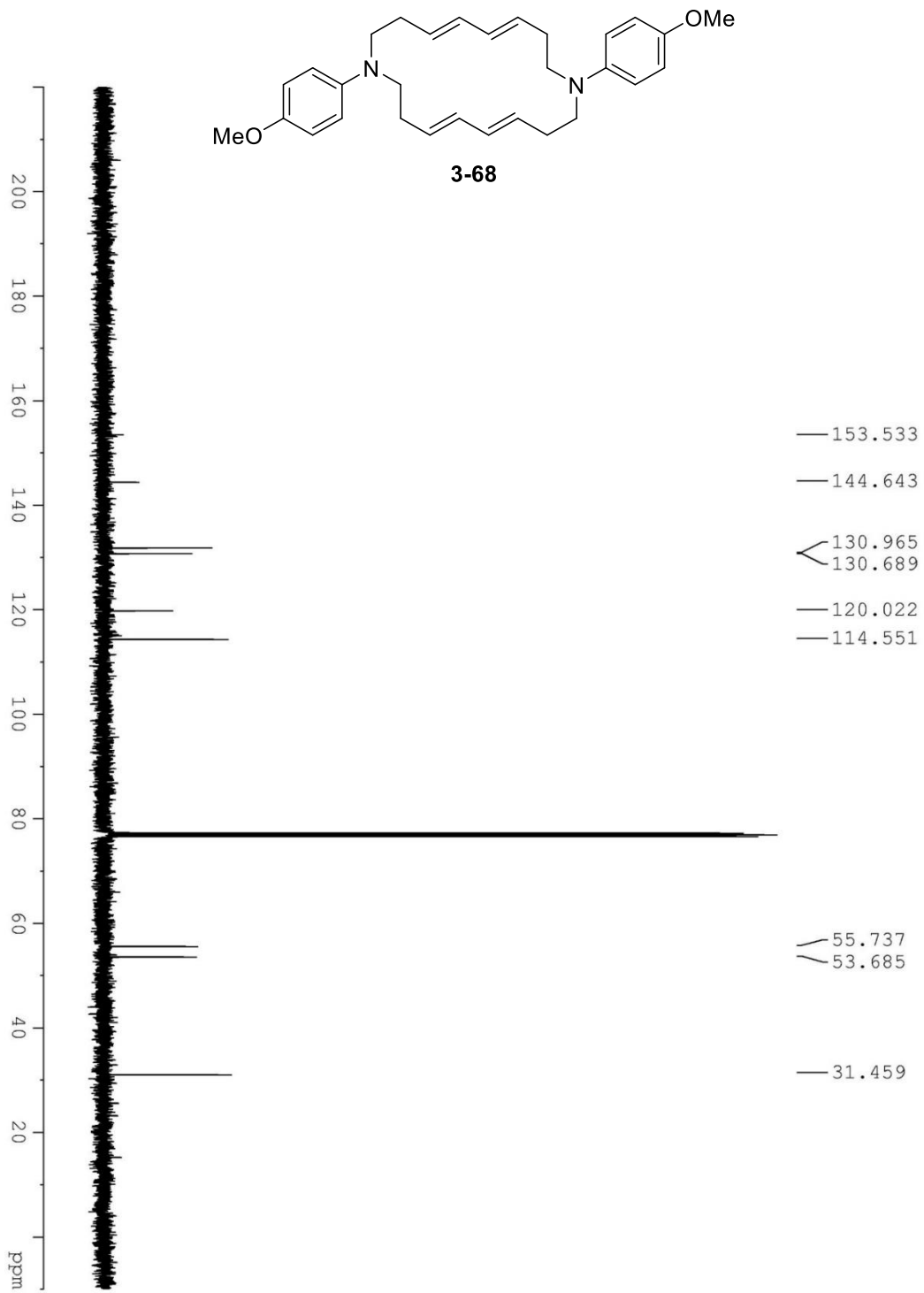


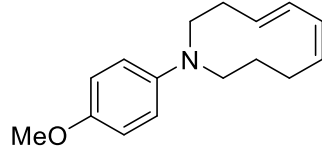




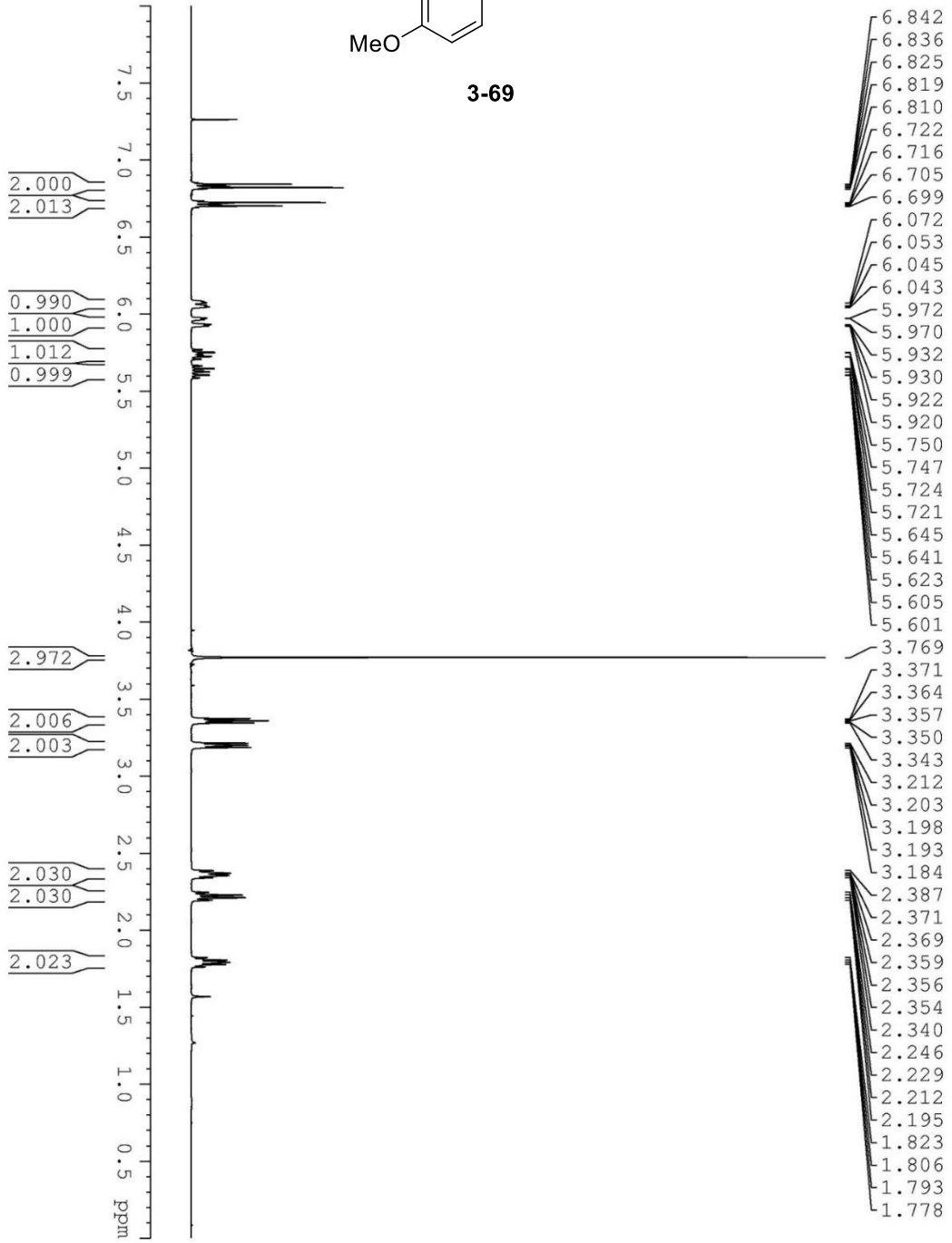


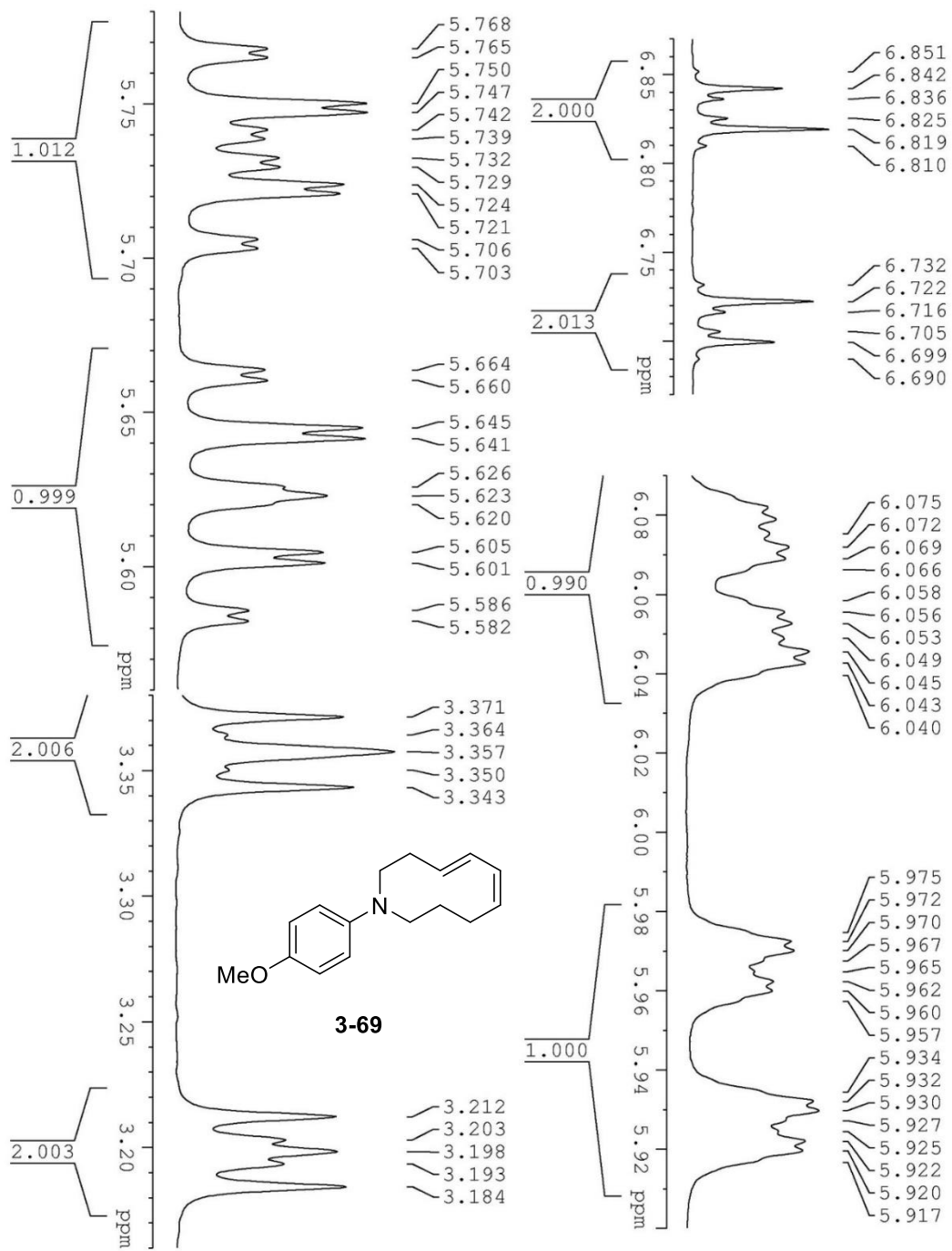


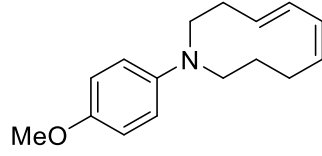




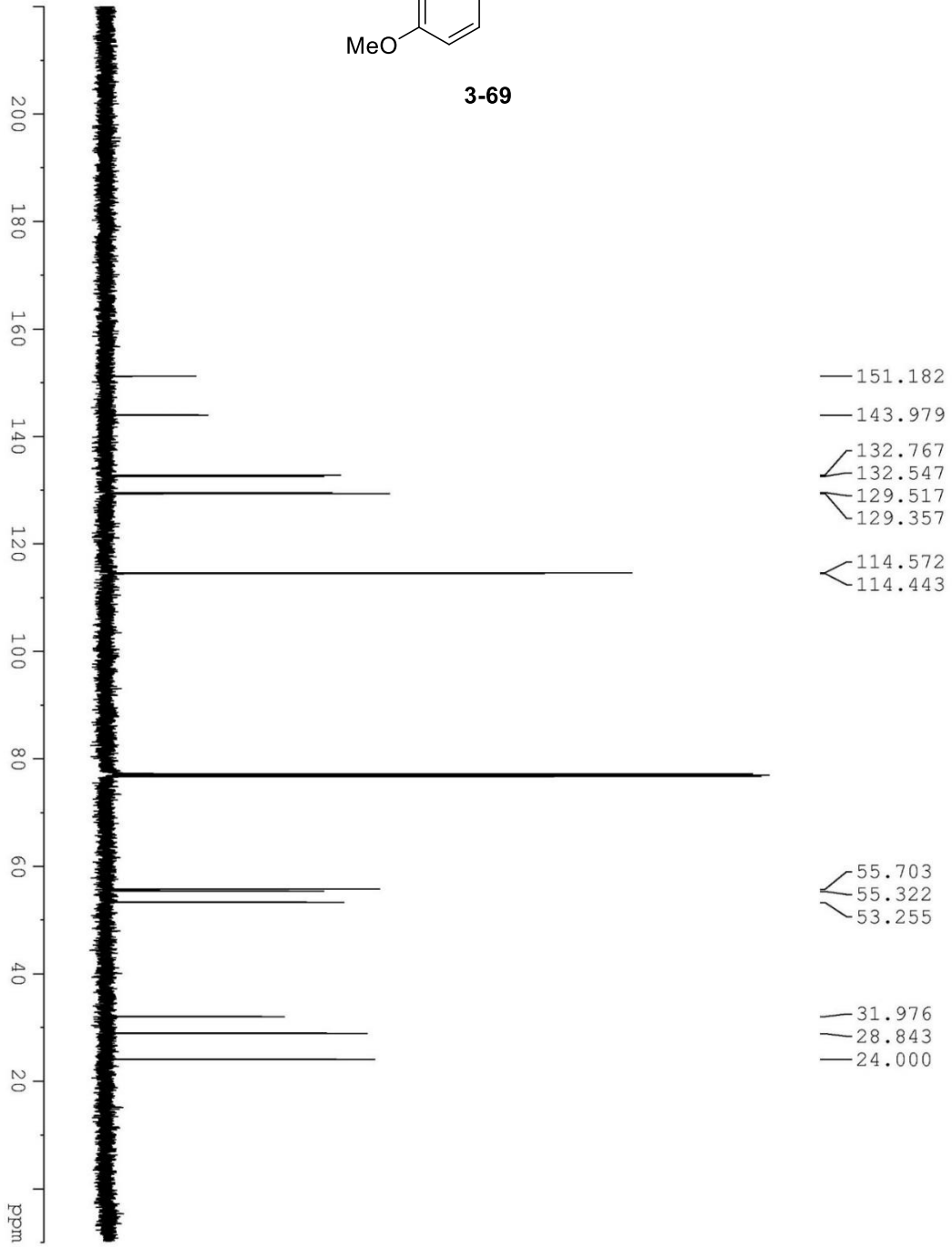
3-69

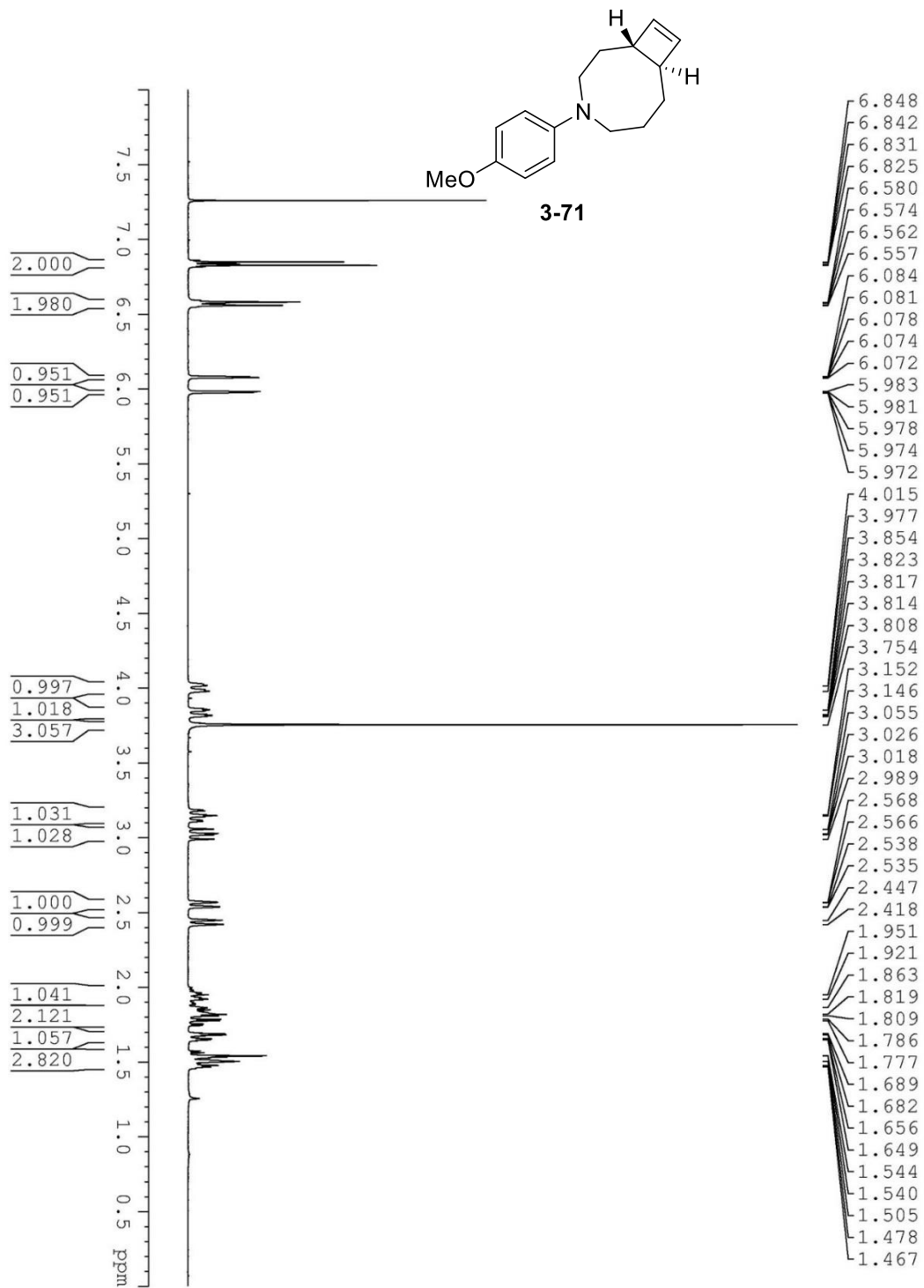




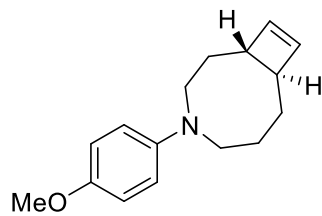
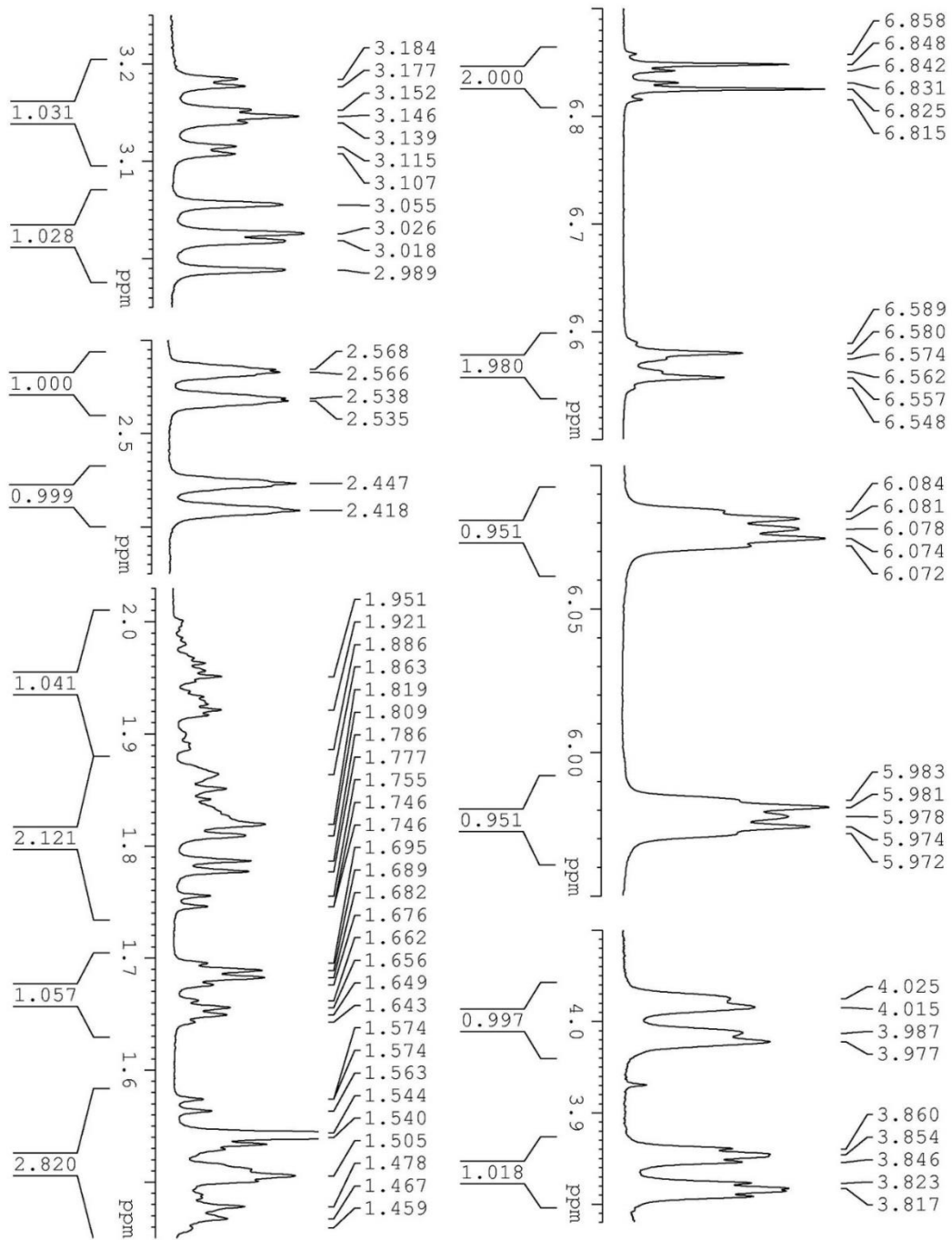


3-69

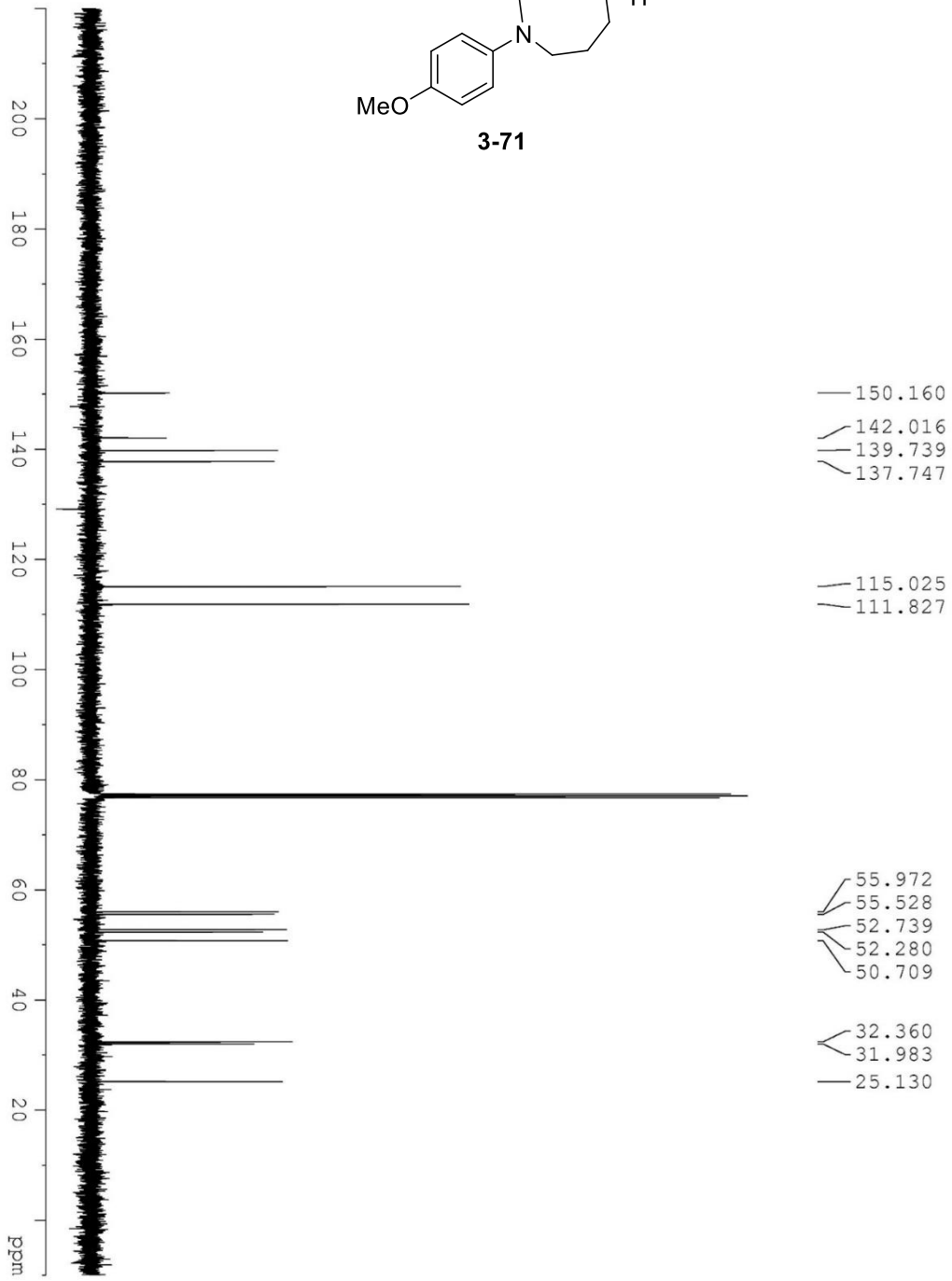
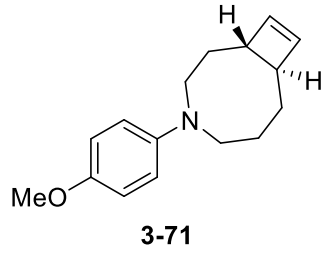


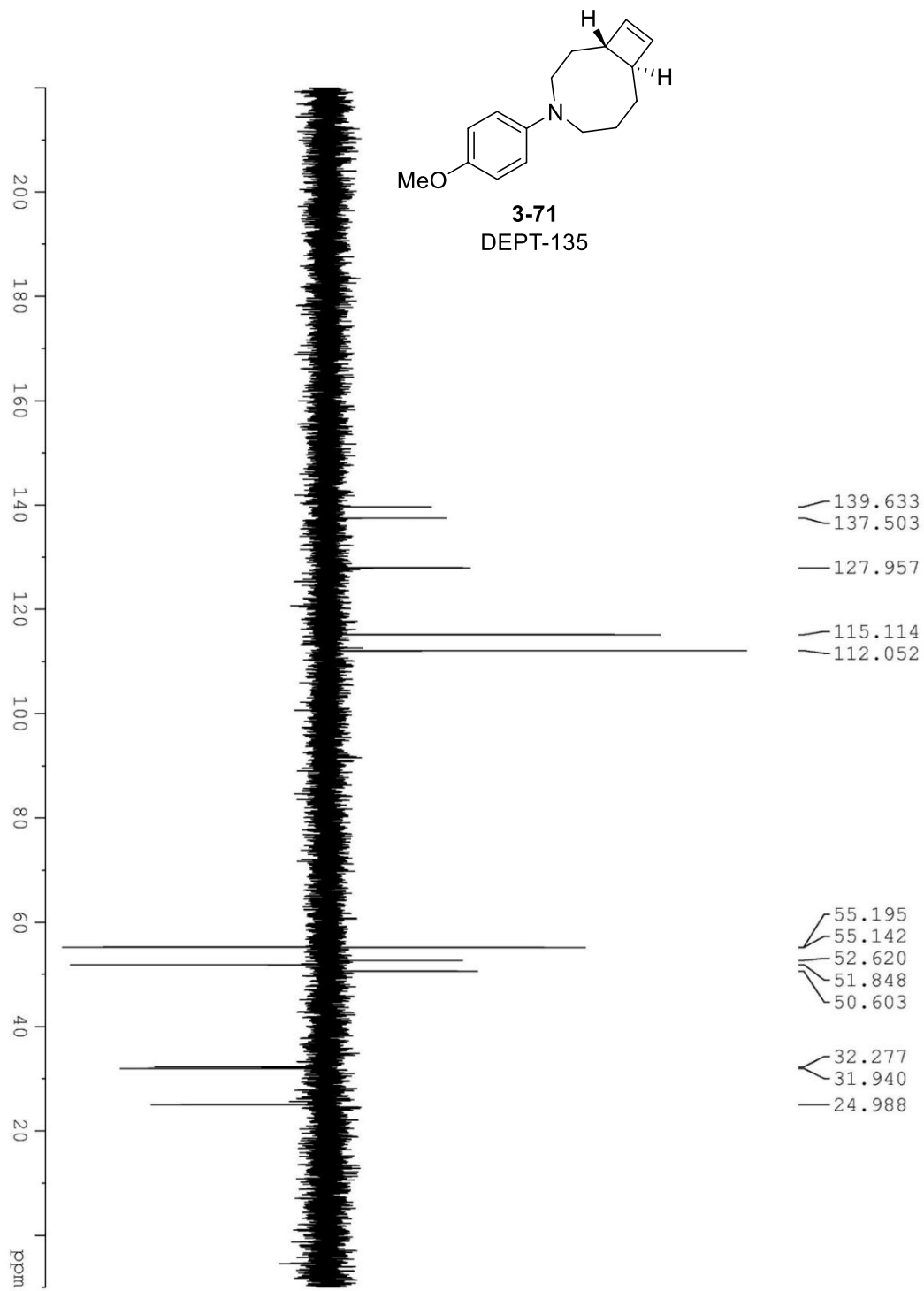


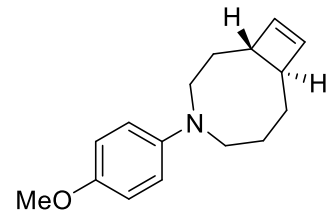




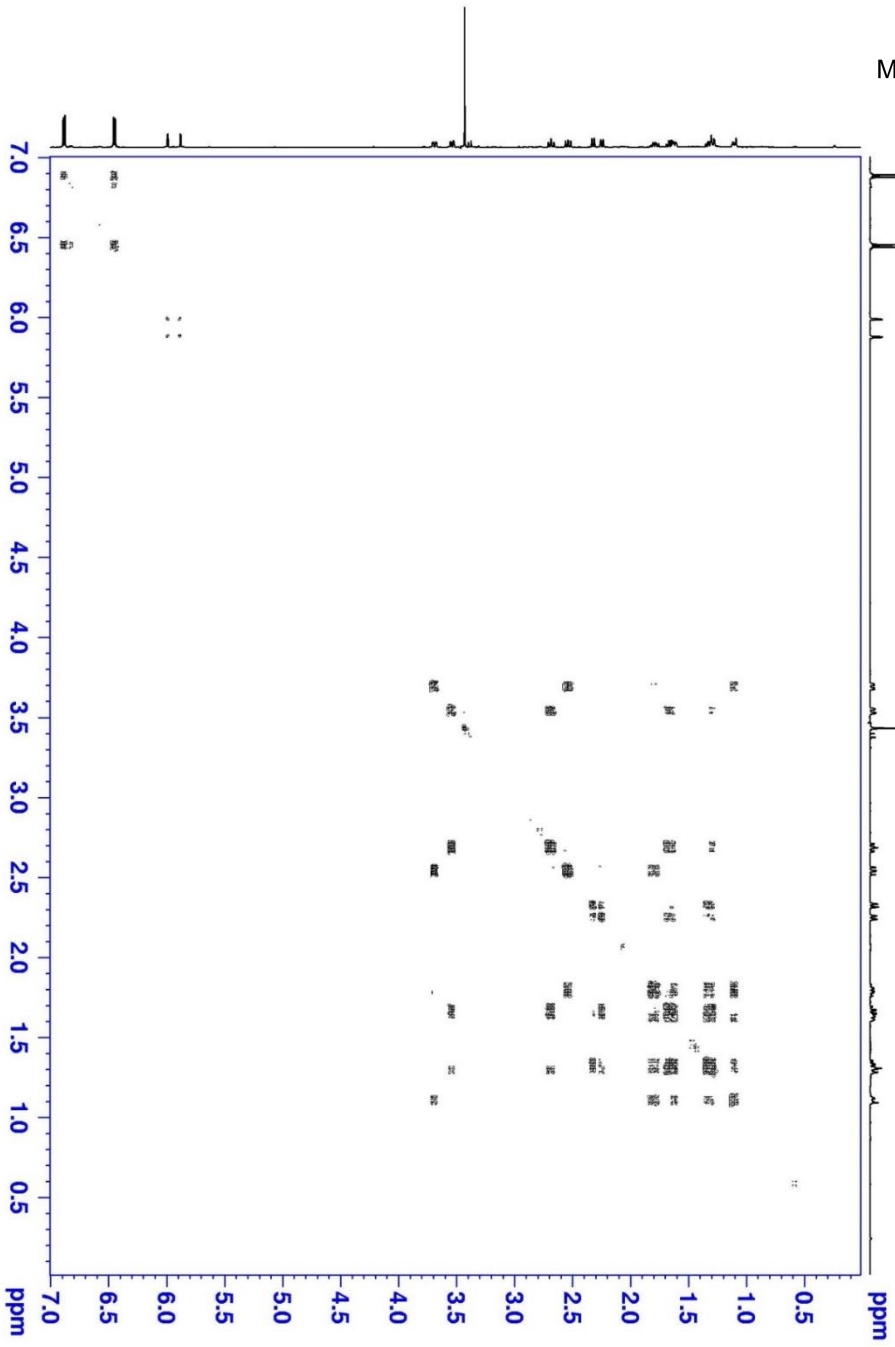
3-71

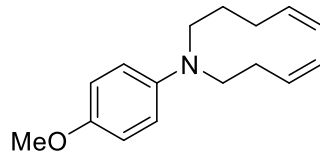




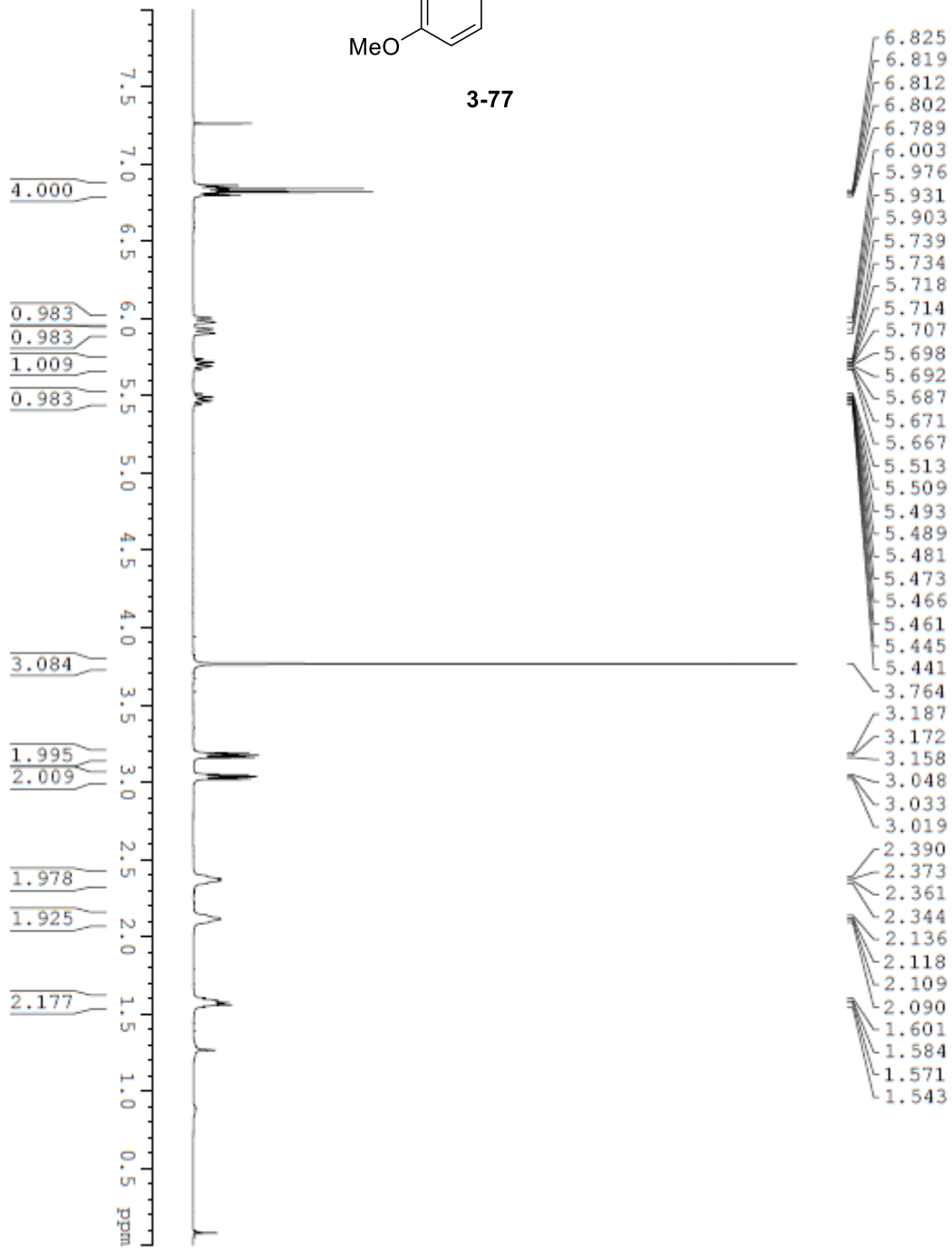


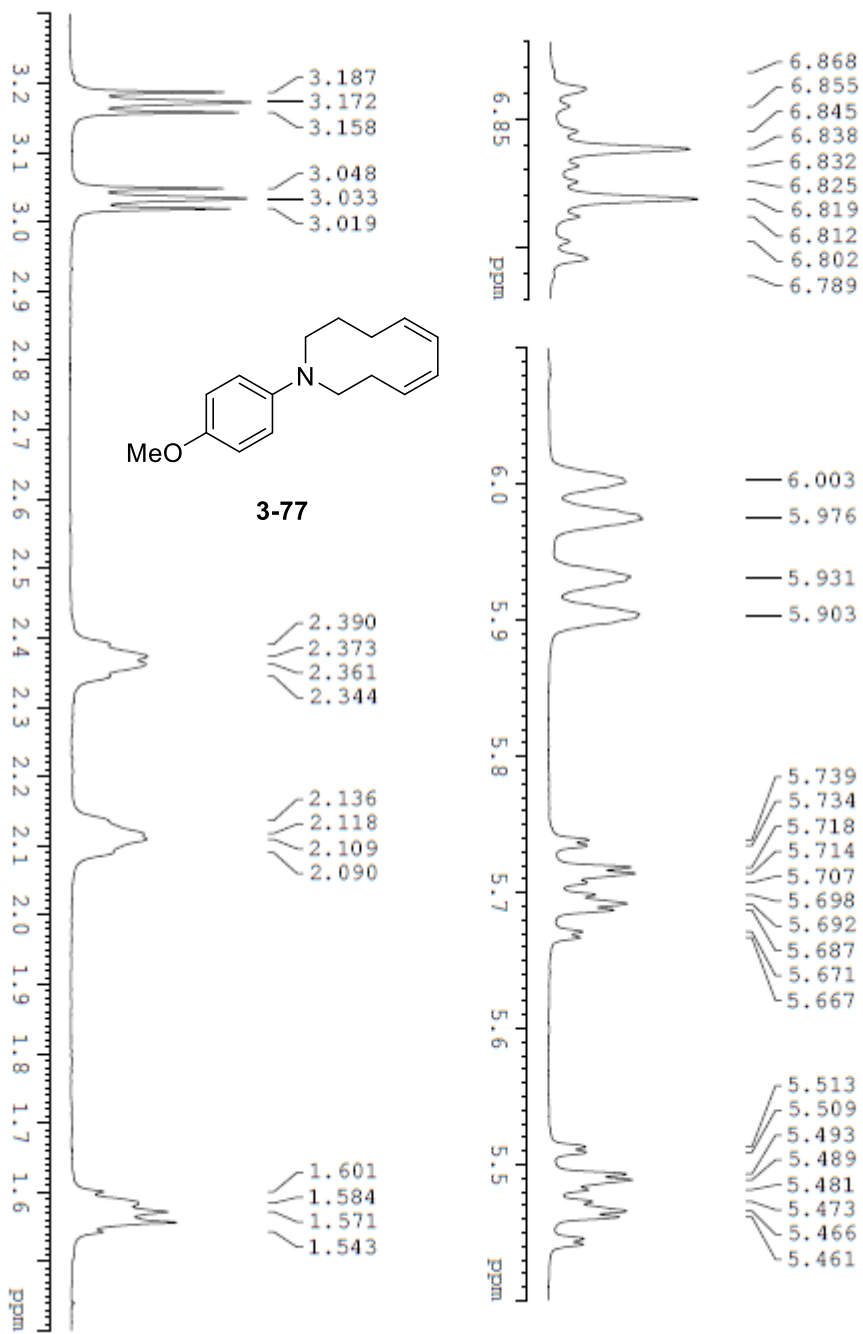
**3-71**  
<sup>1</sup>H COSY

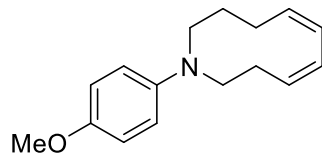




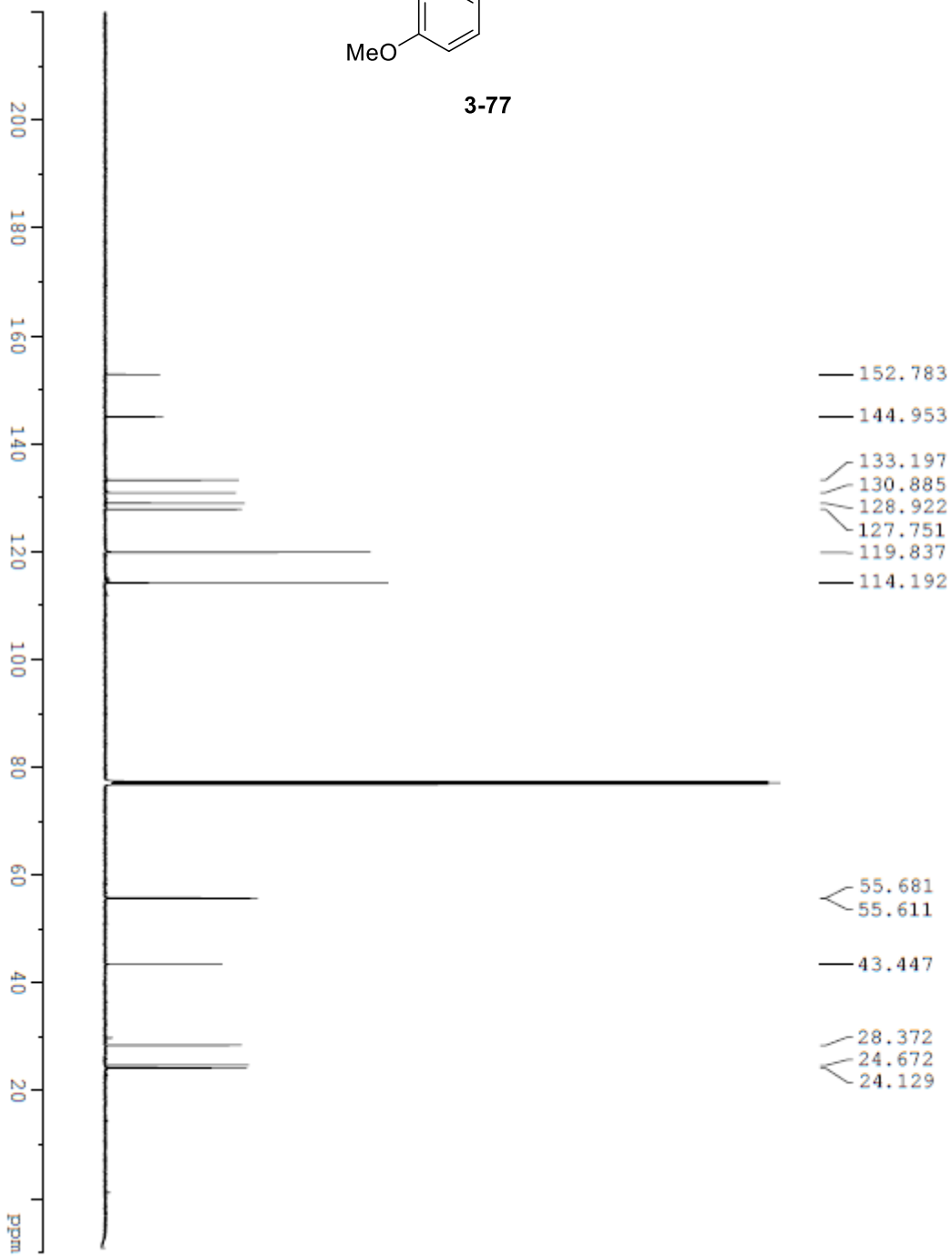
3-77

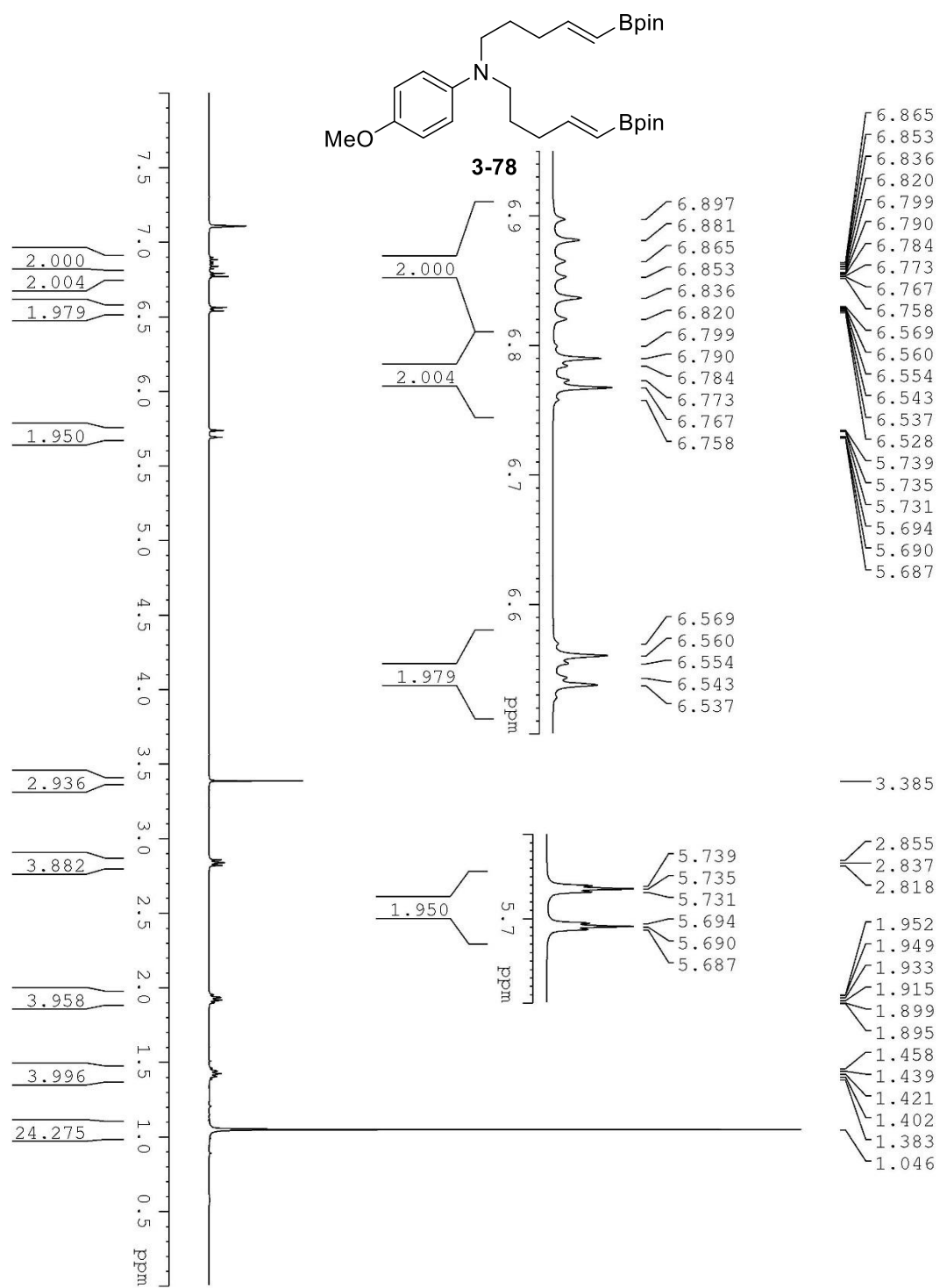




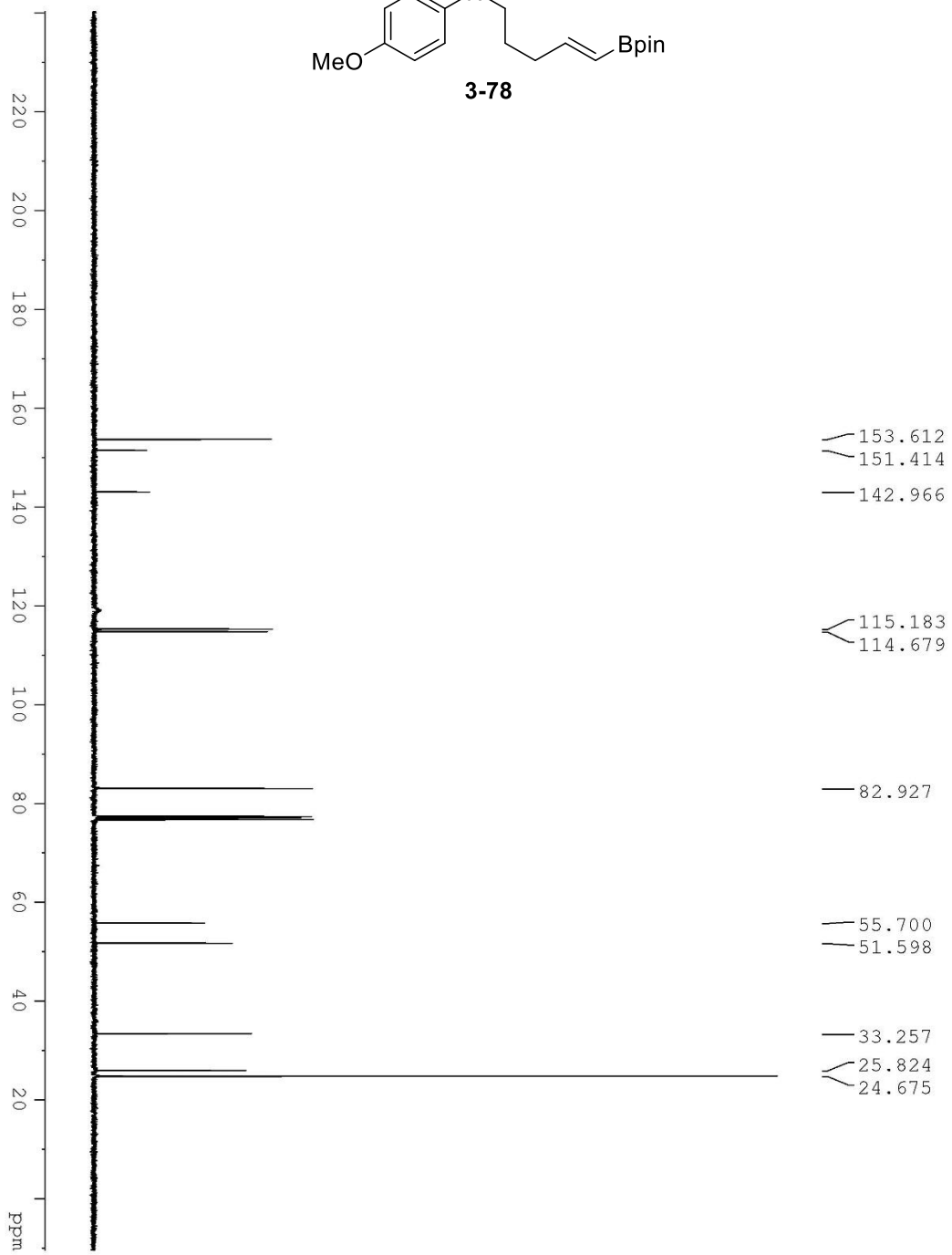
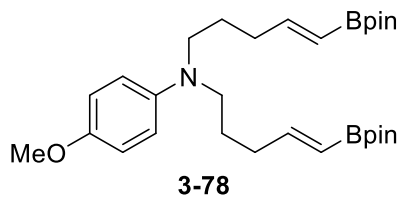


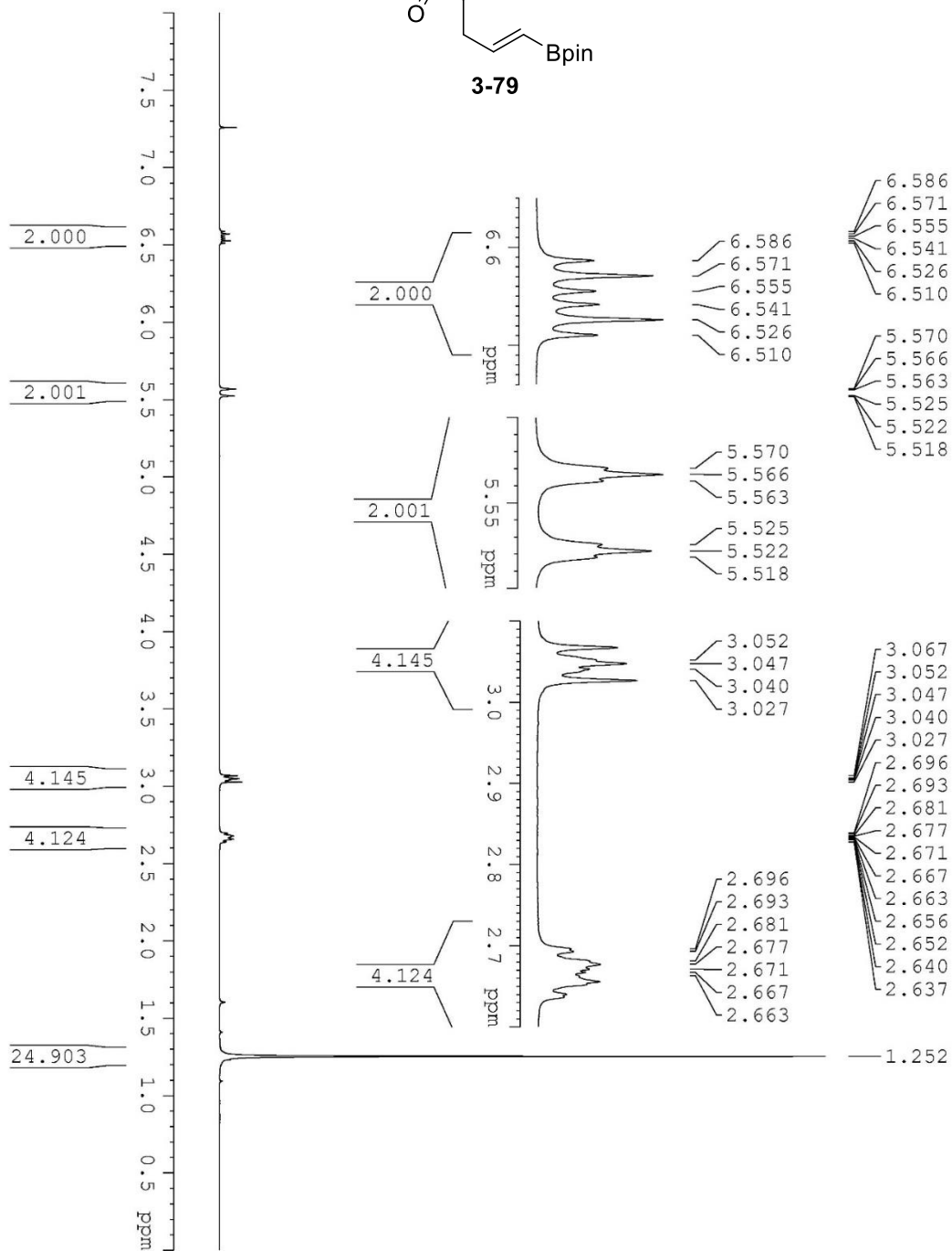
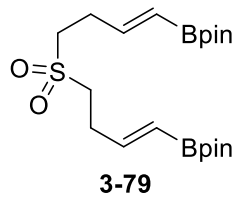
3-77

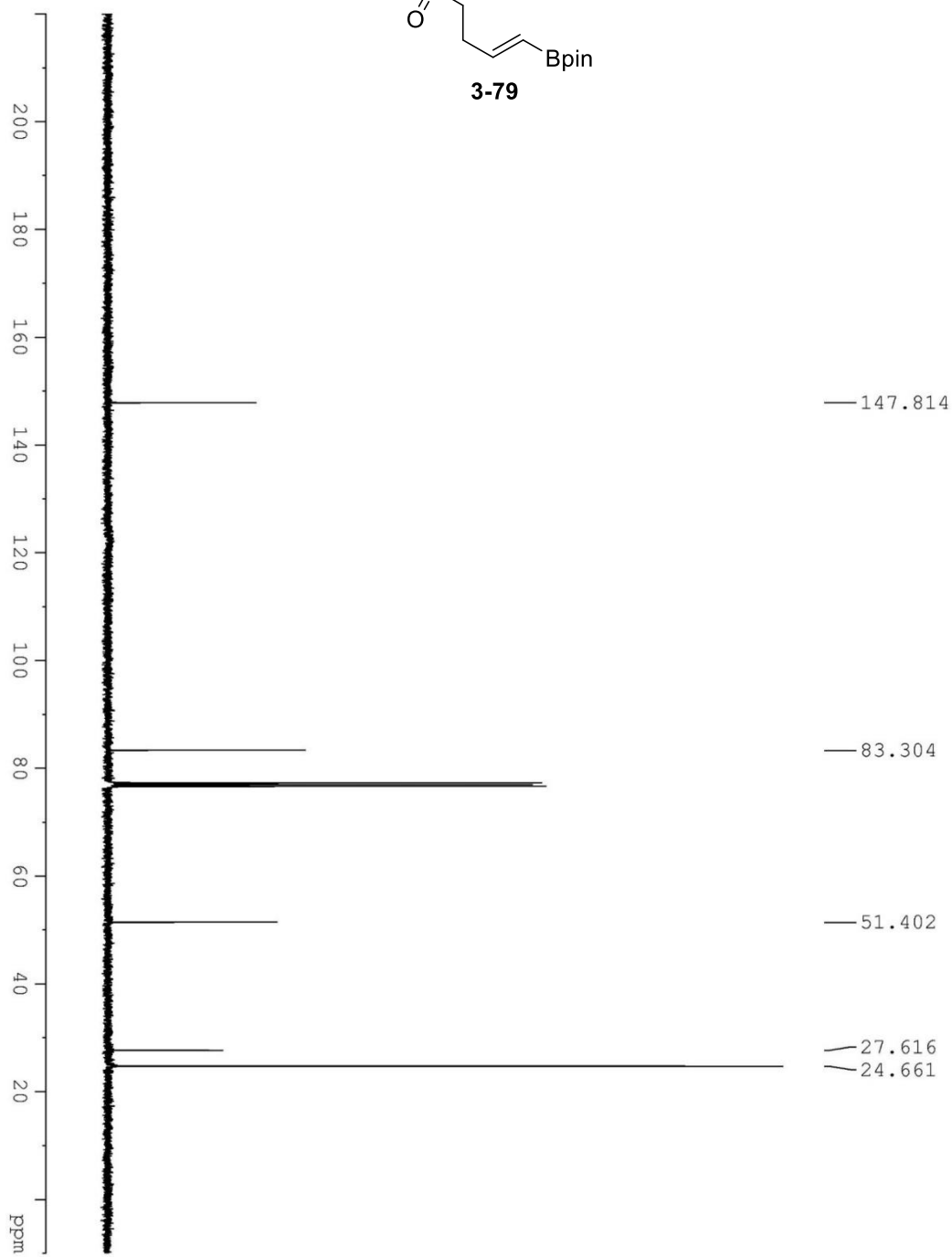
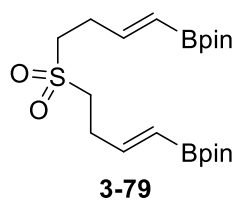


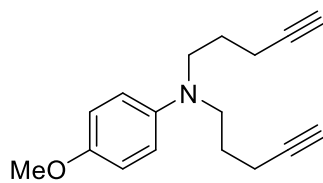
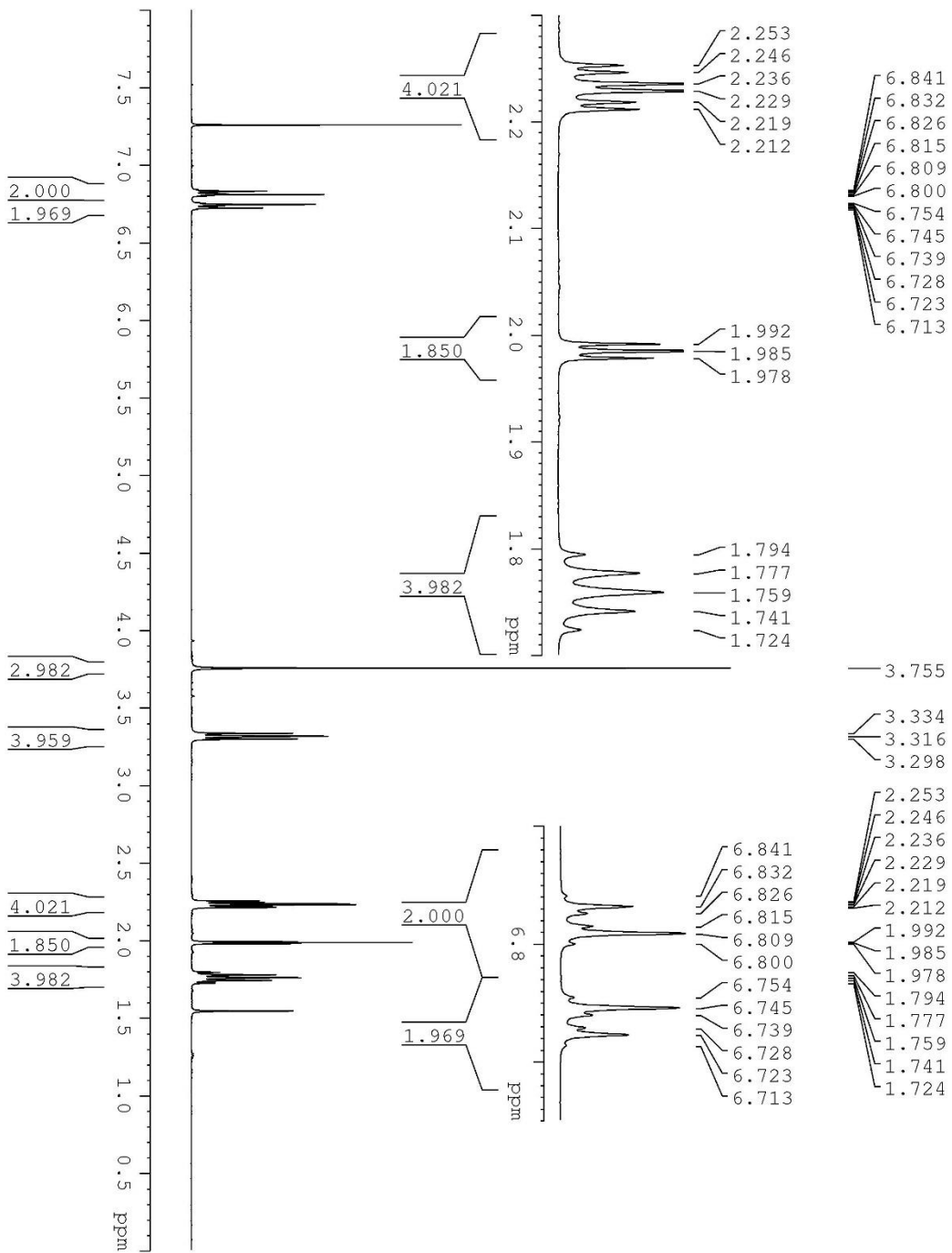




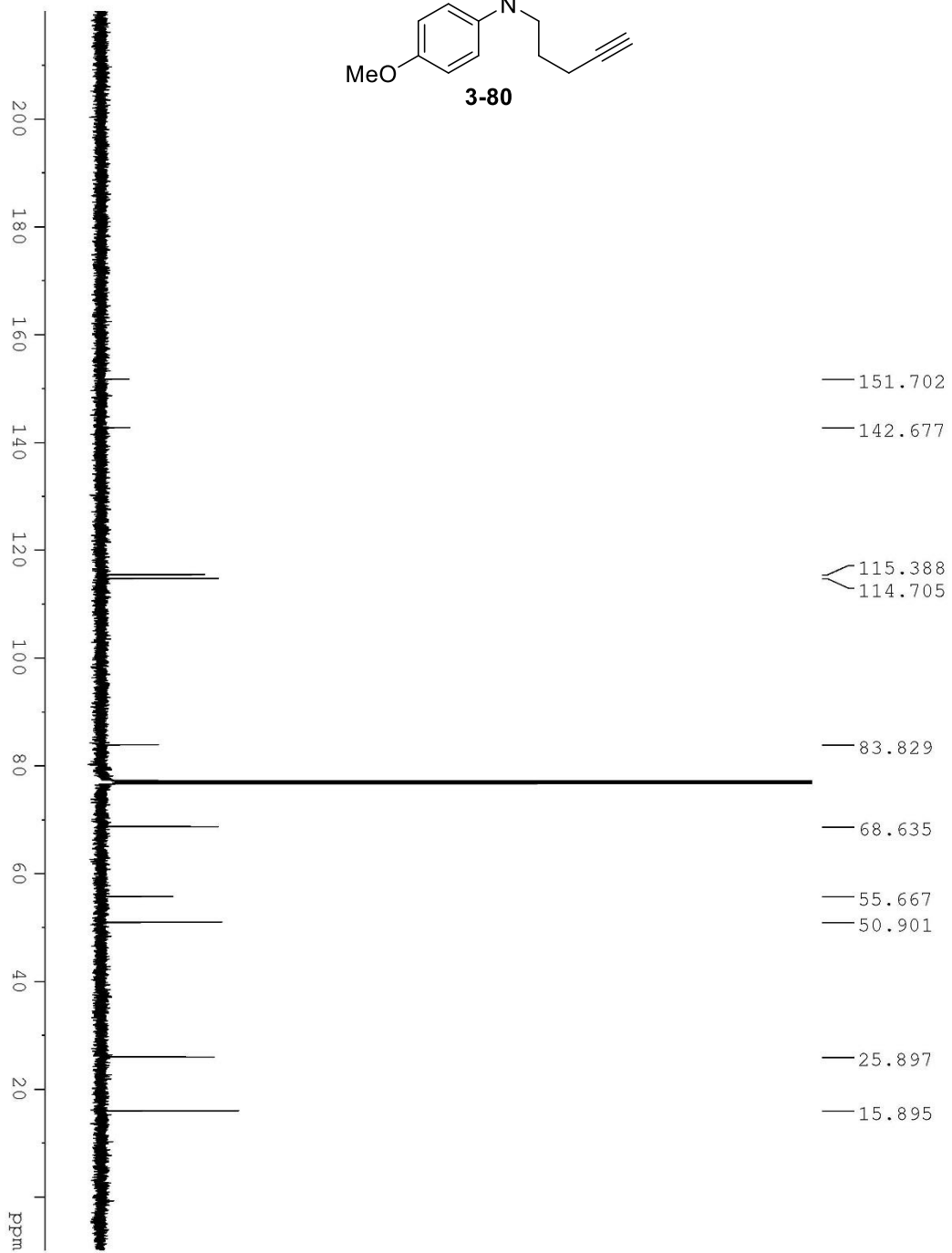
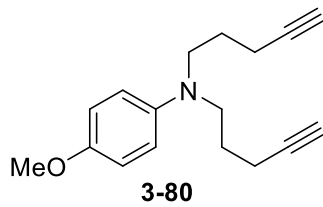


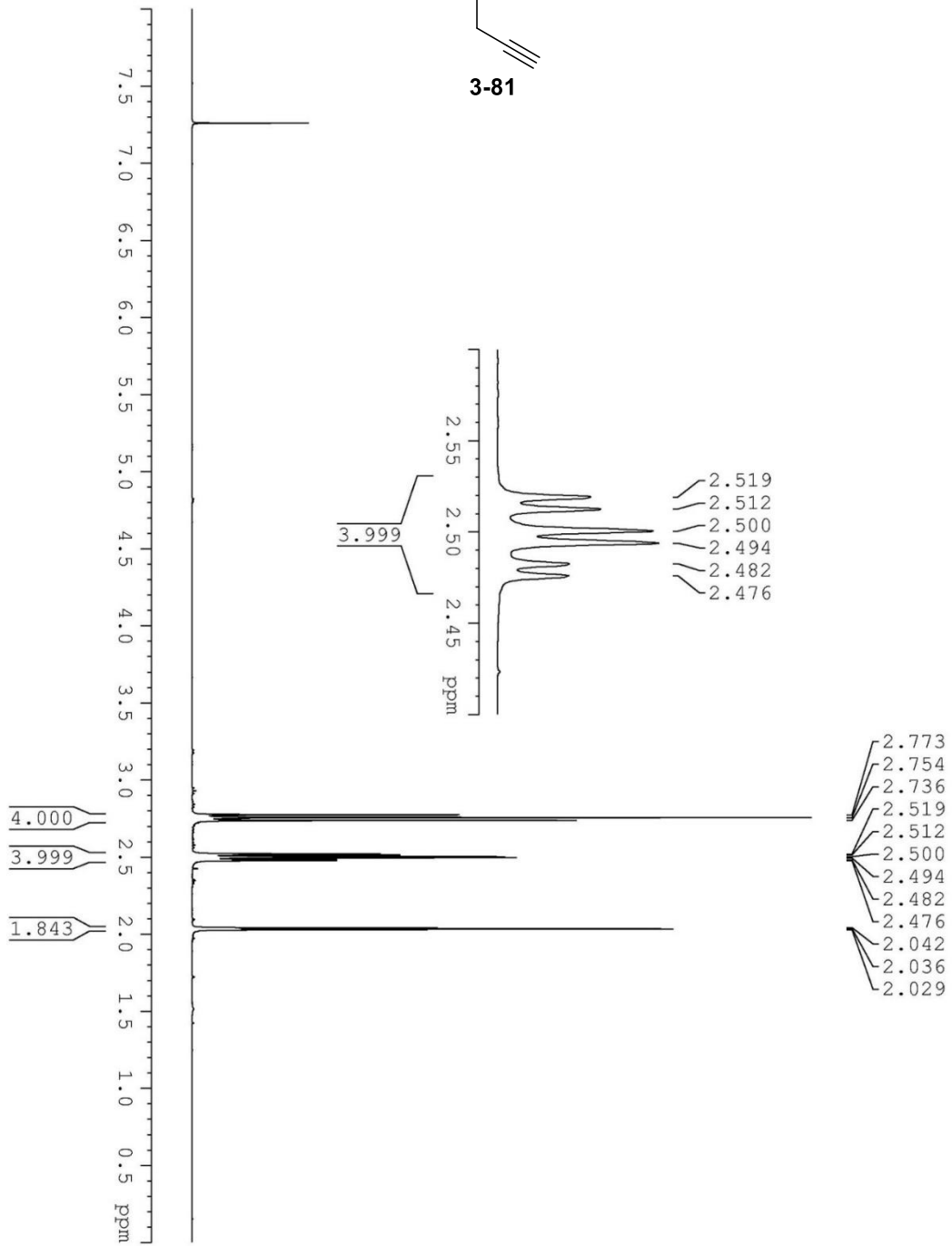
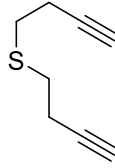


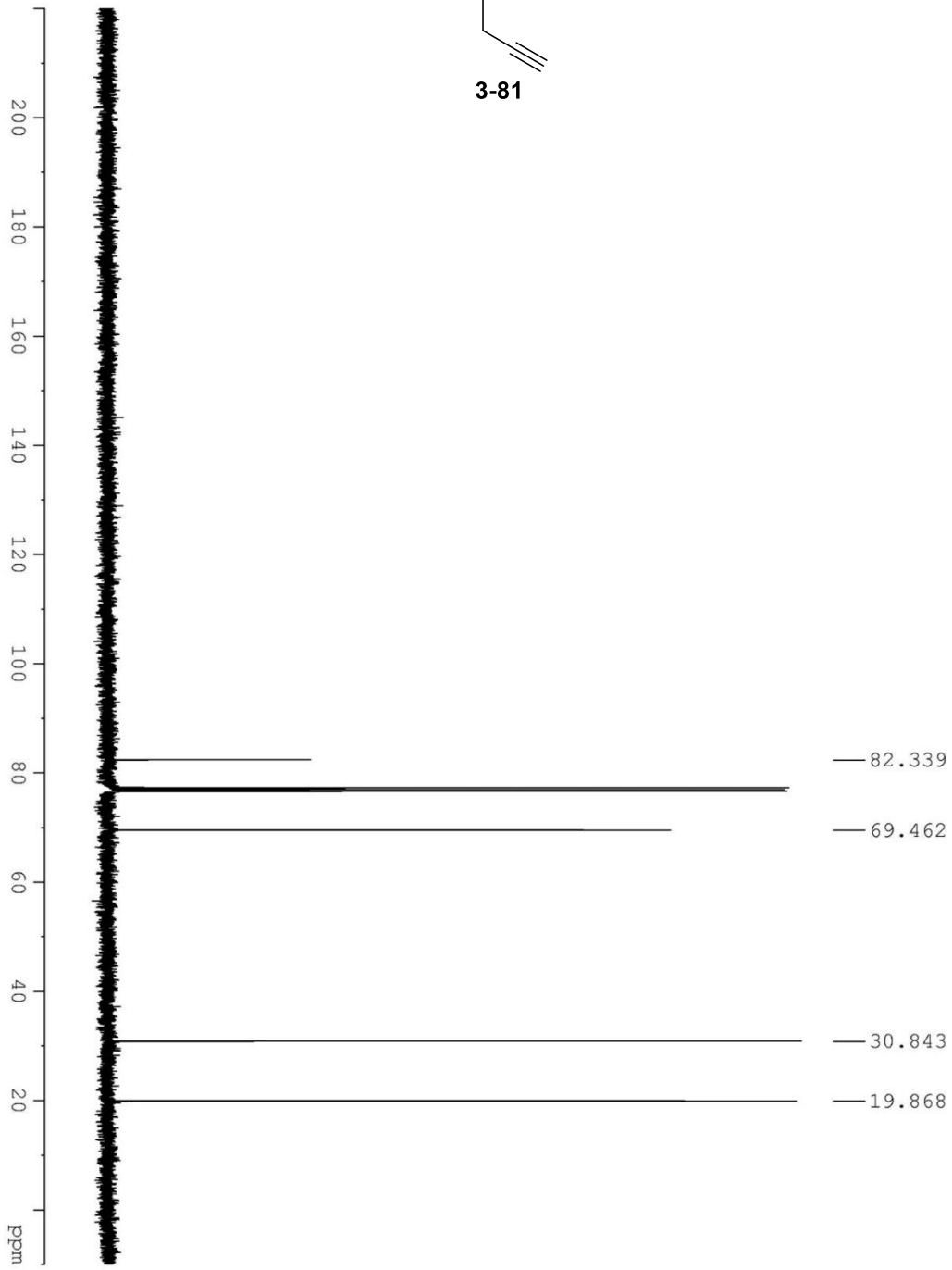
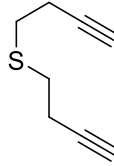


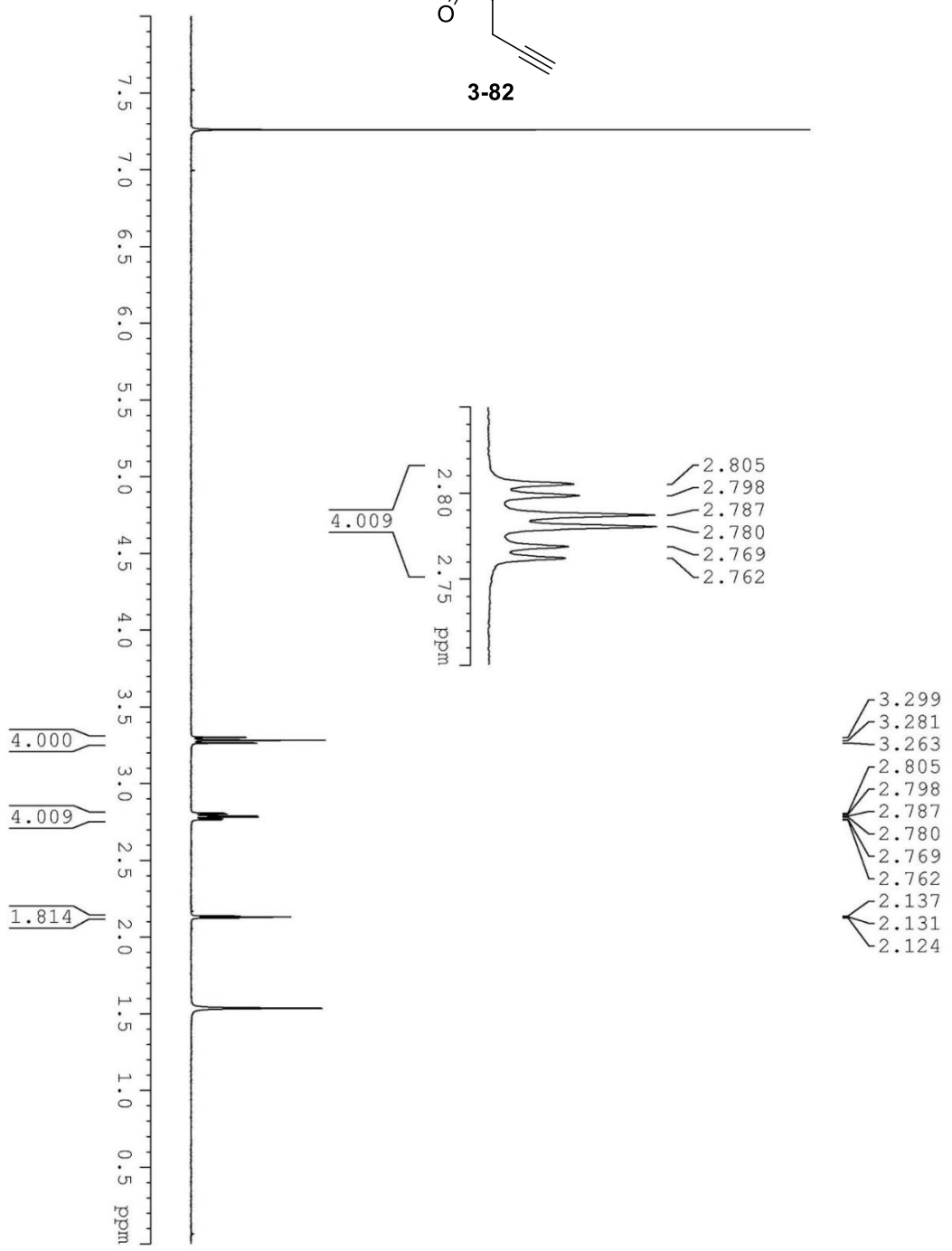
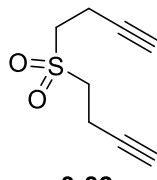


**3-80**

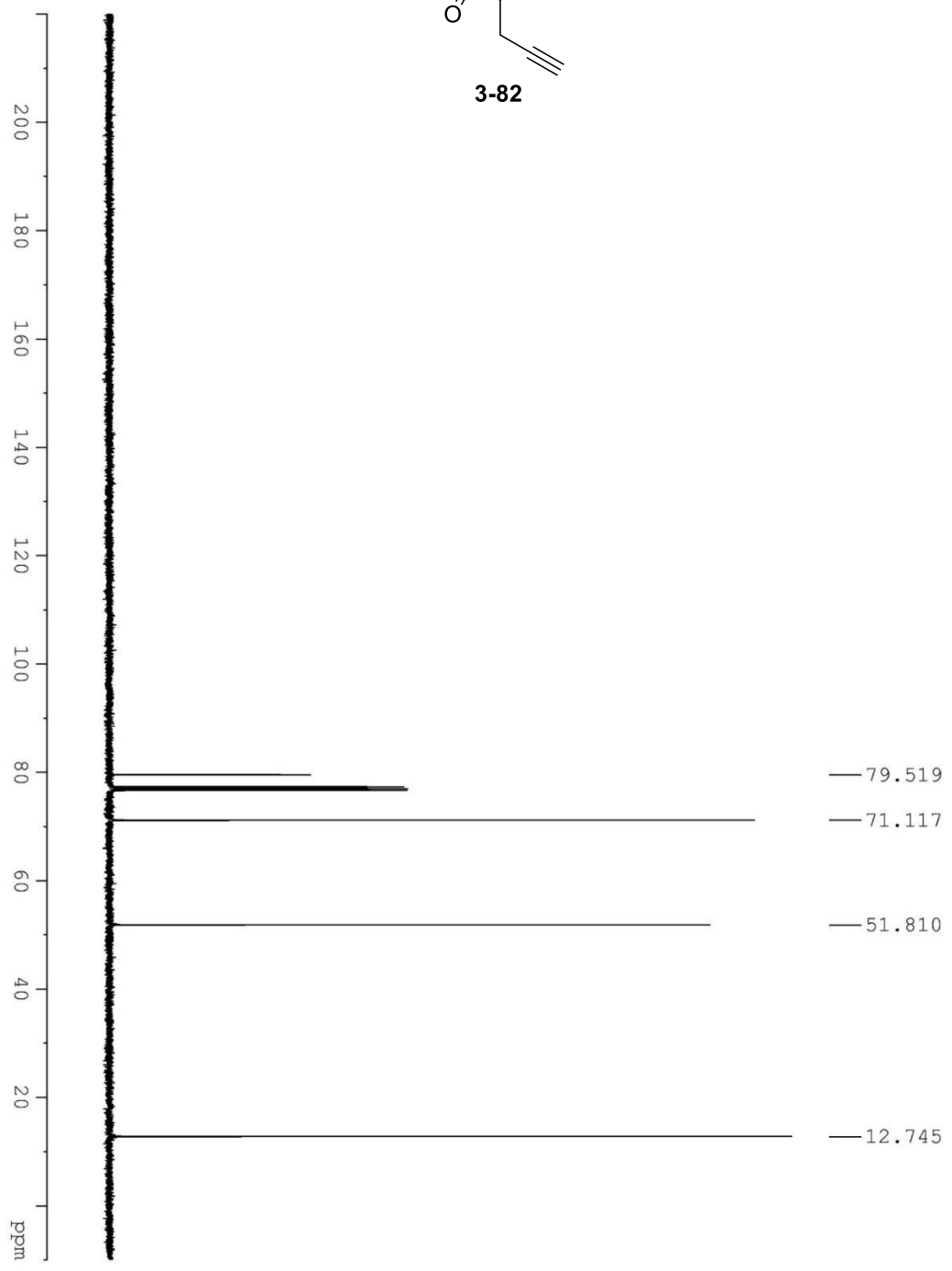
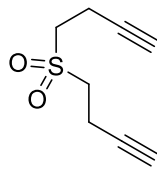


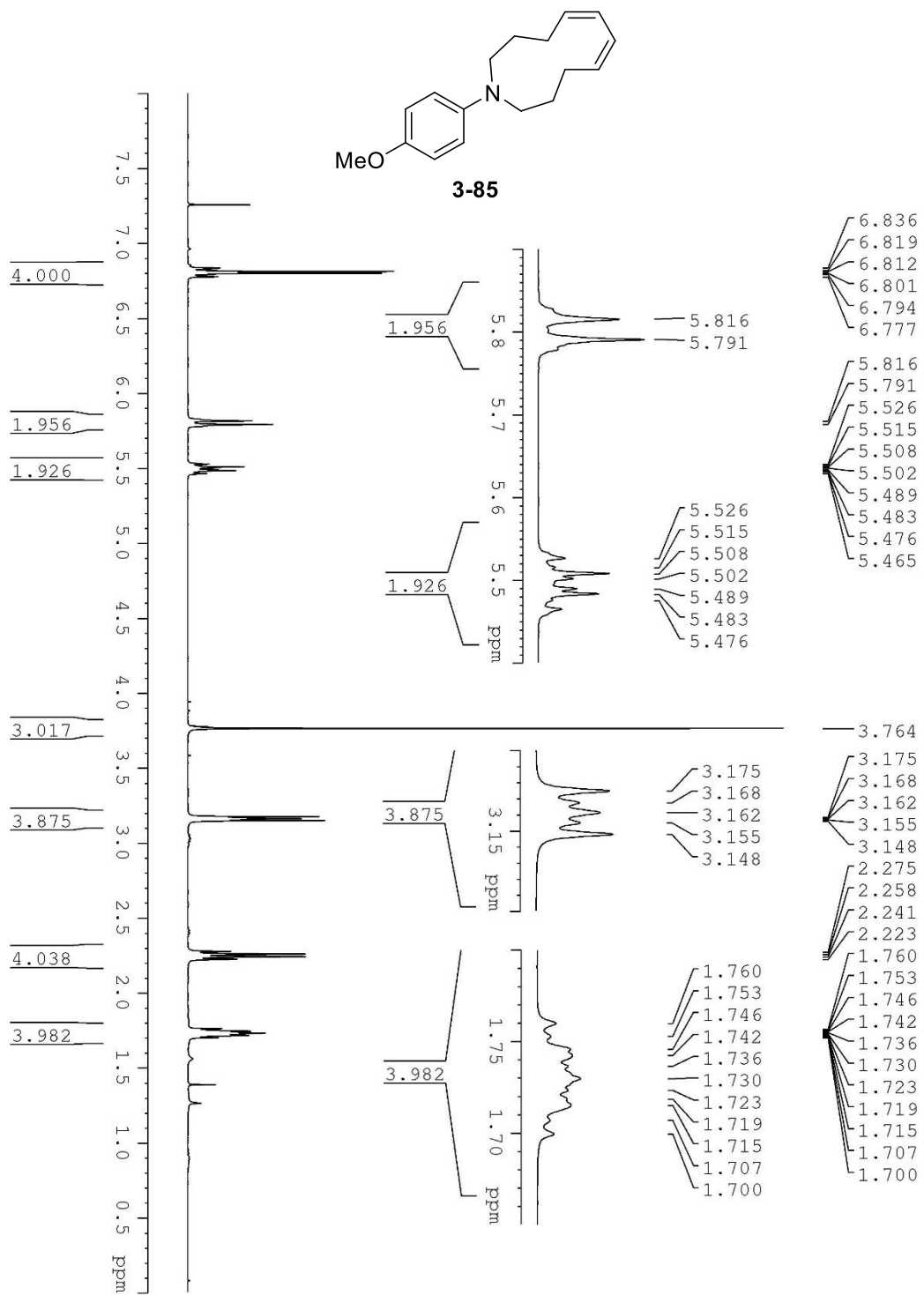


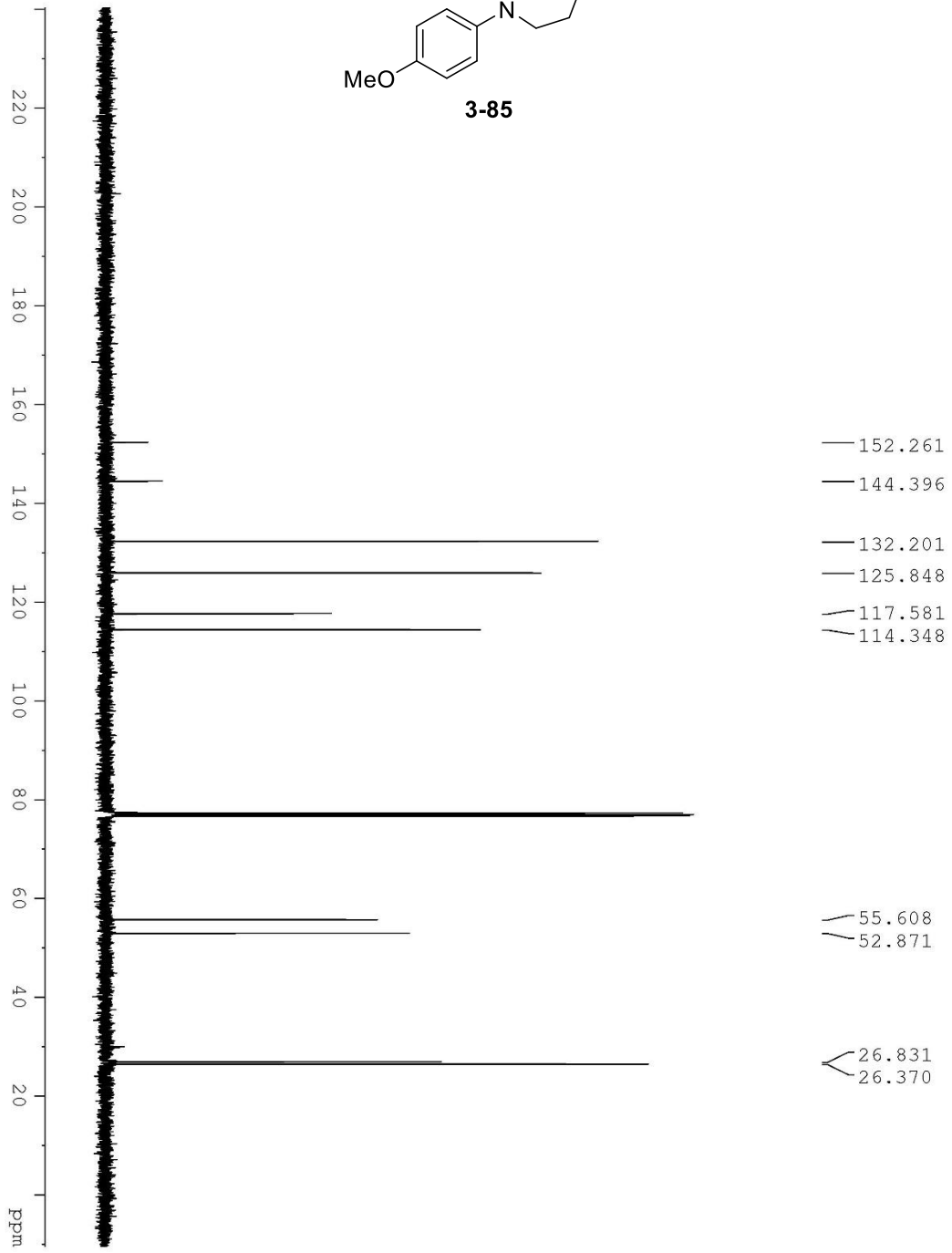
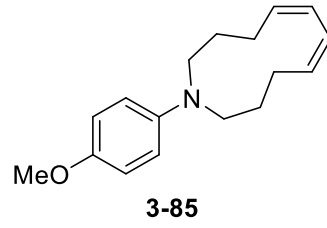


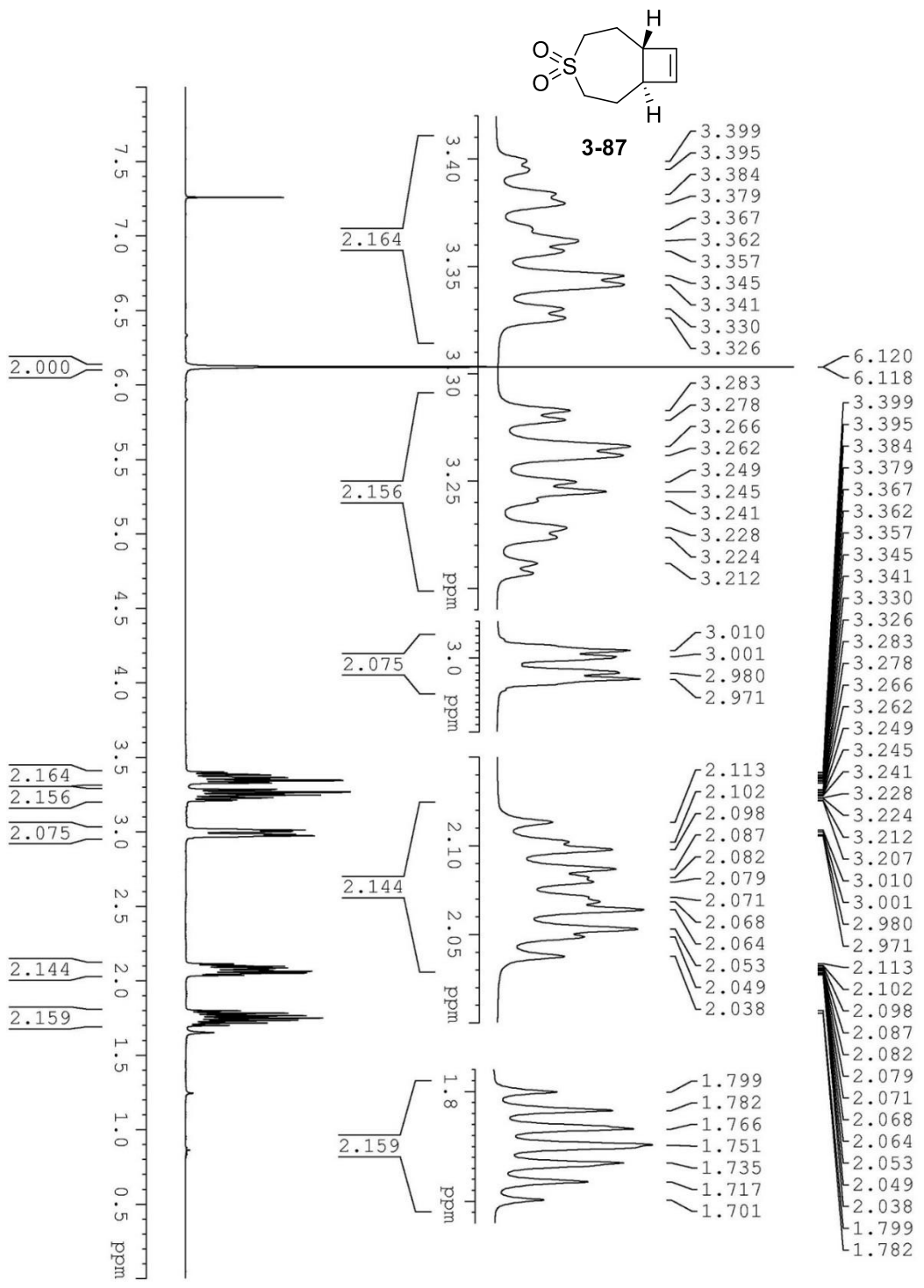


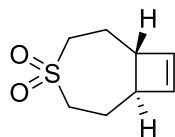




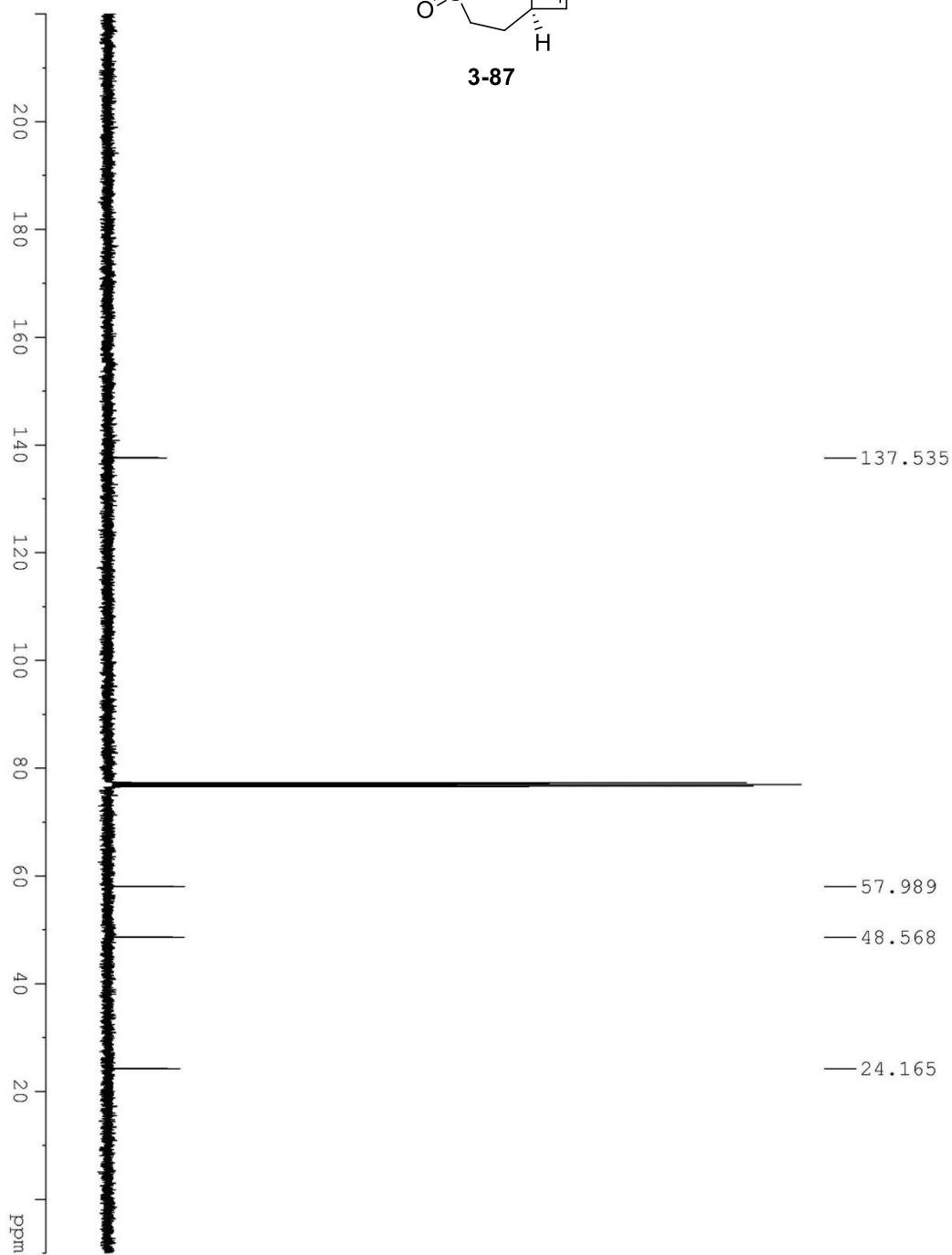


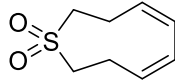




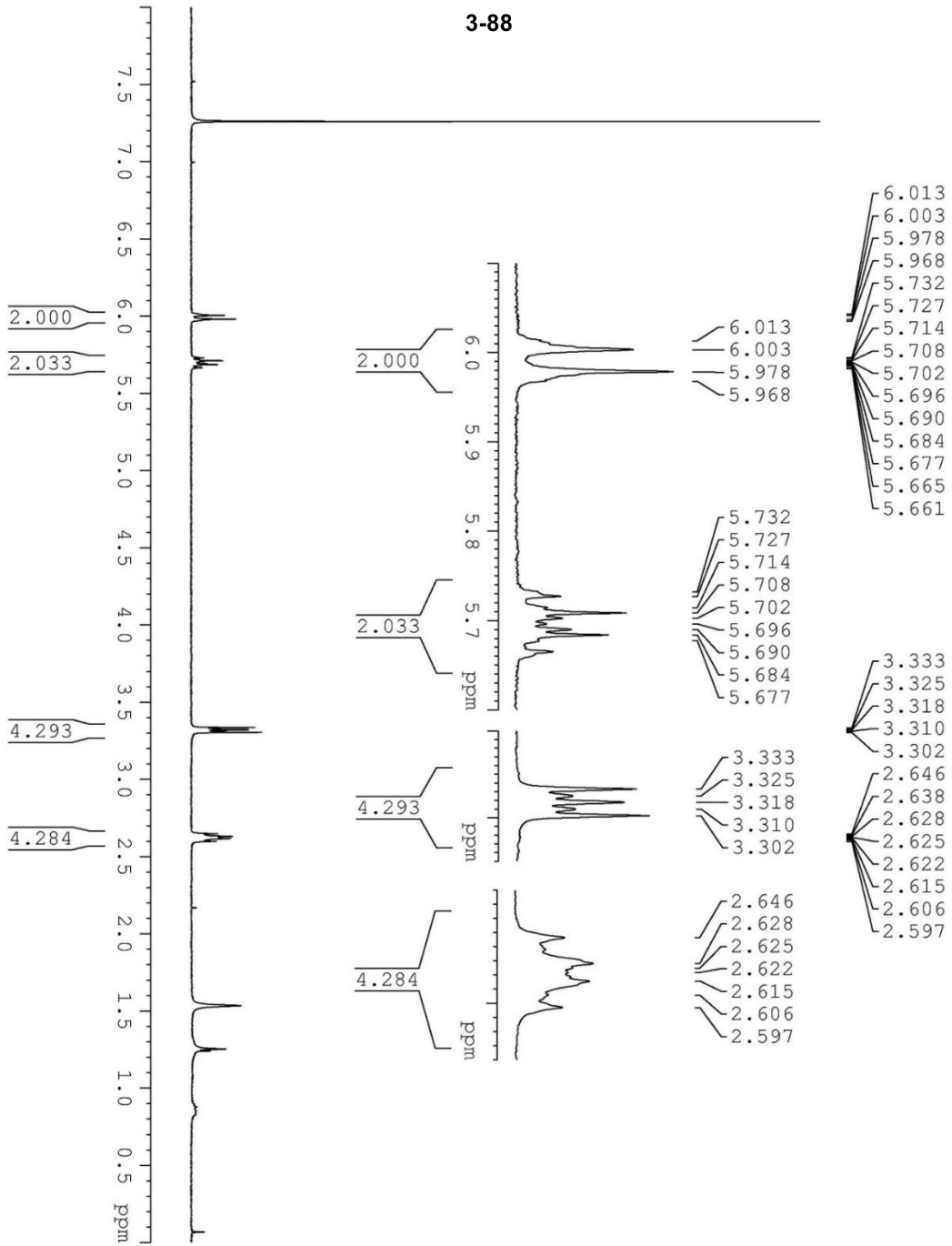


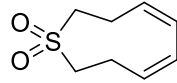
3-87



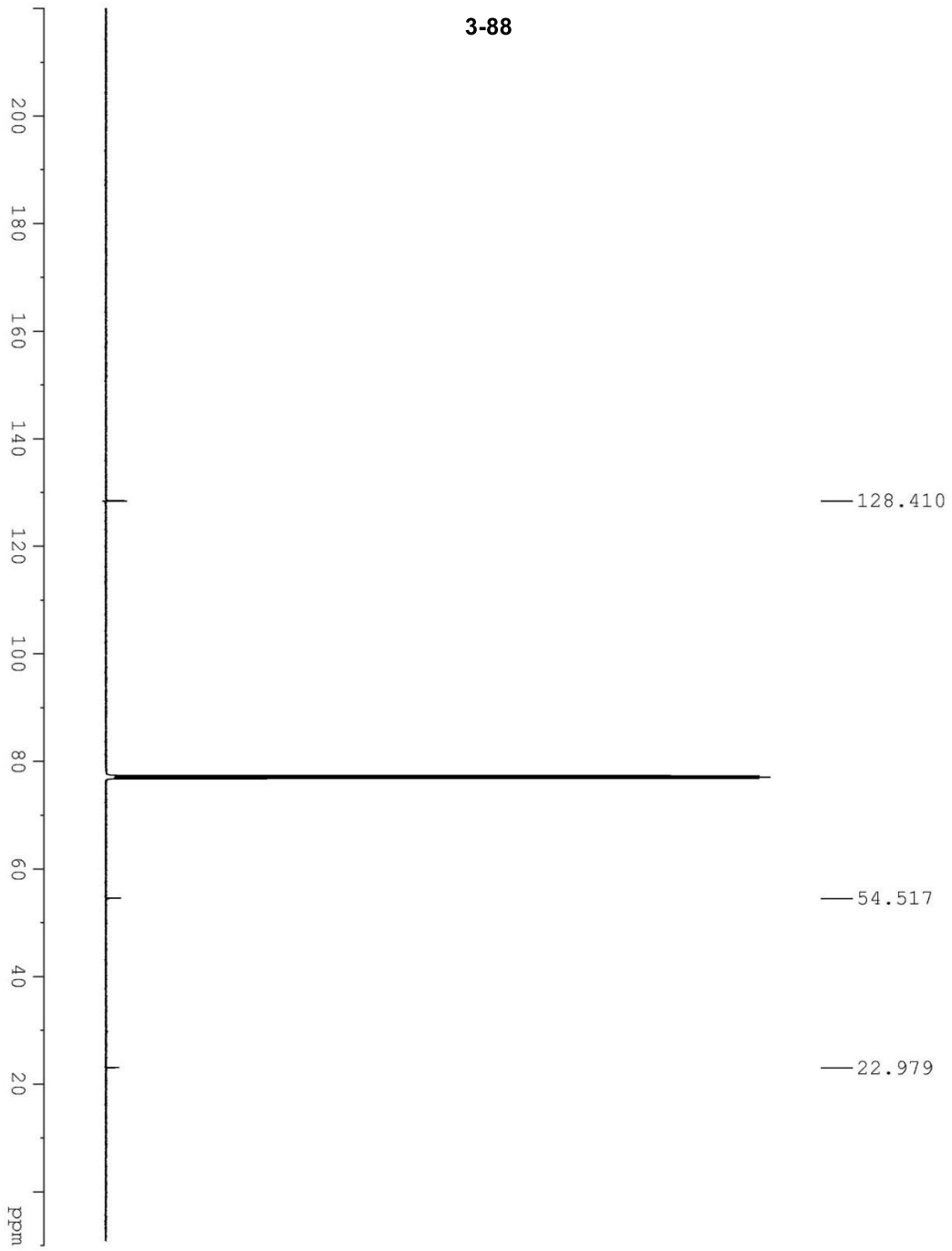


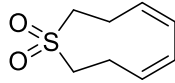
3-88



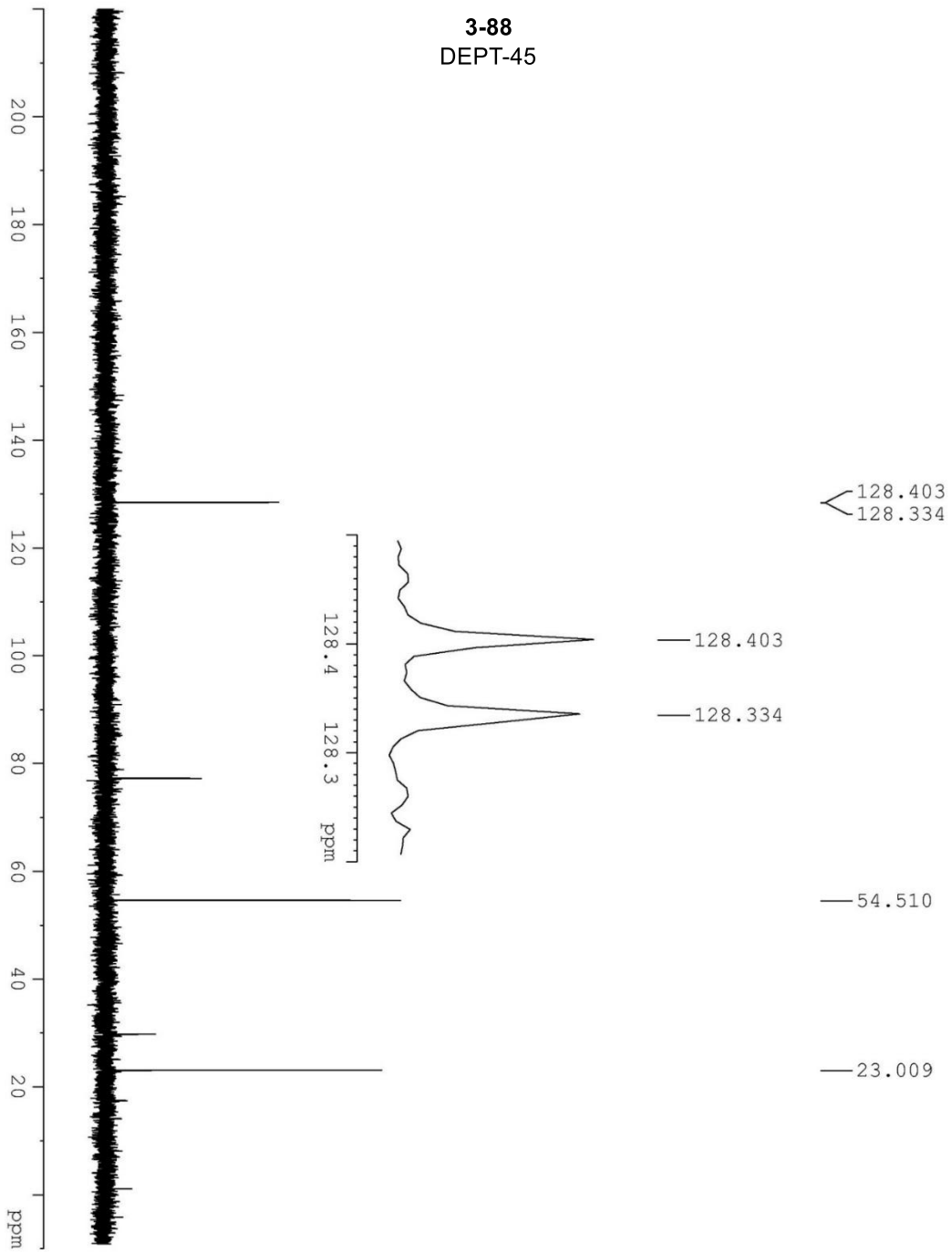


3-88

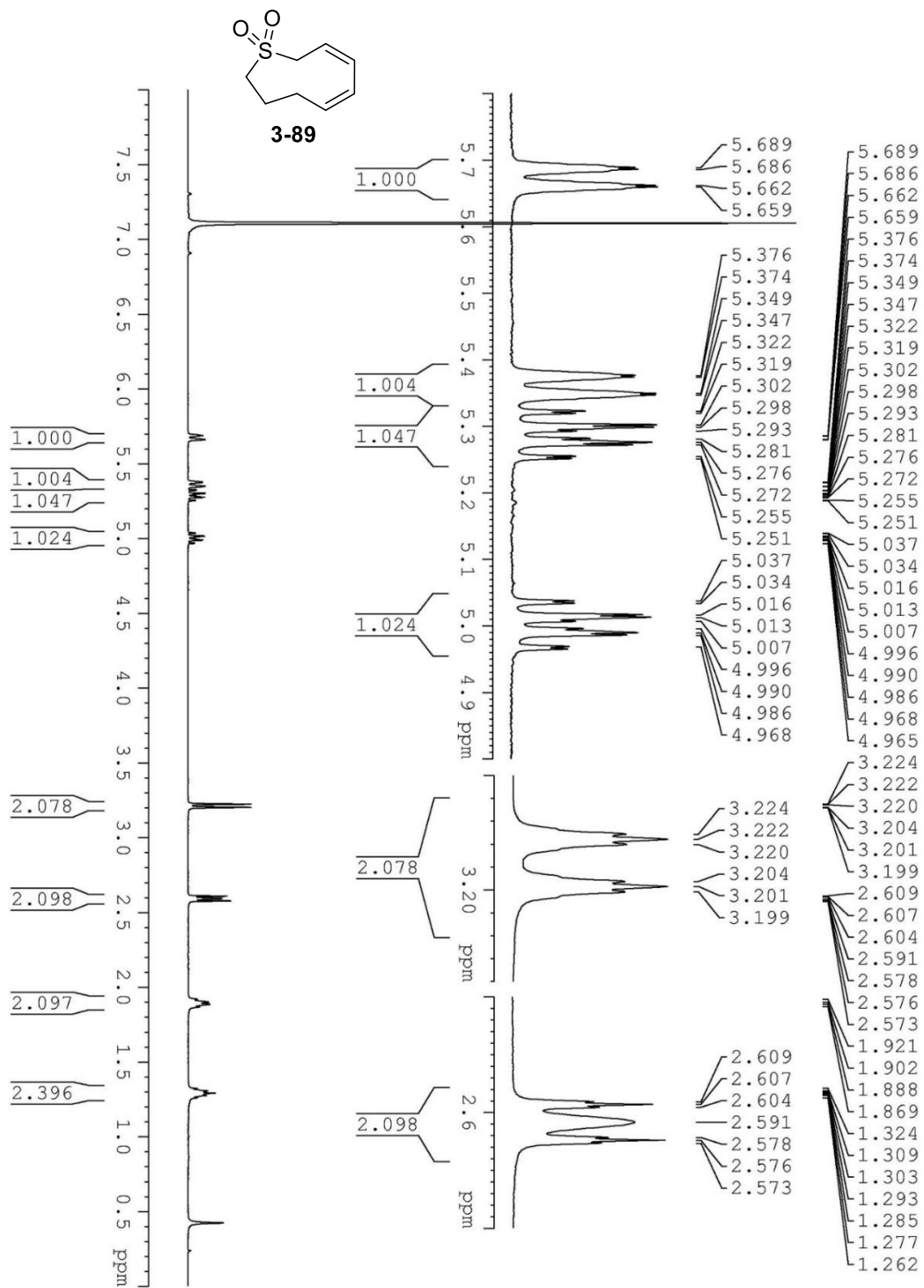


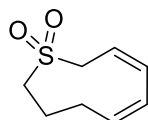


**3-88**  
DEPT-45

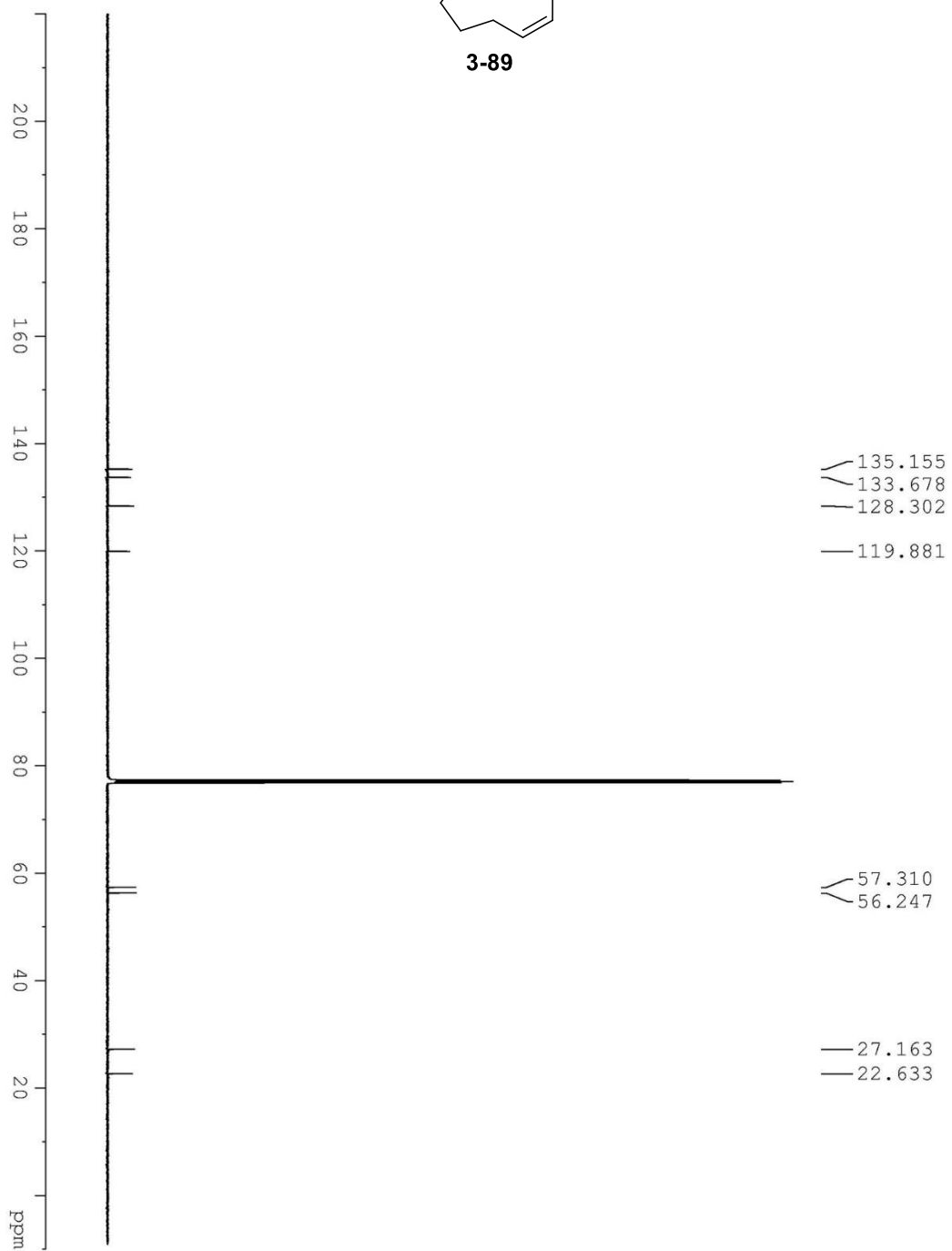




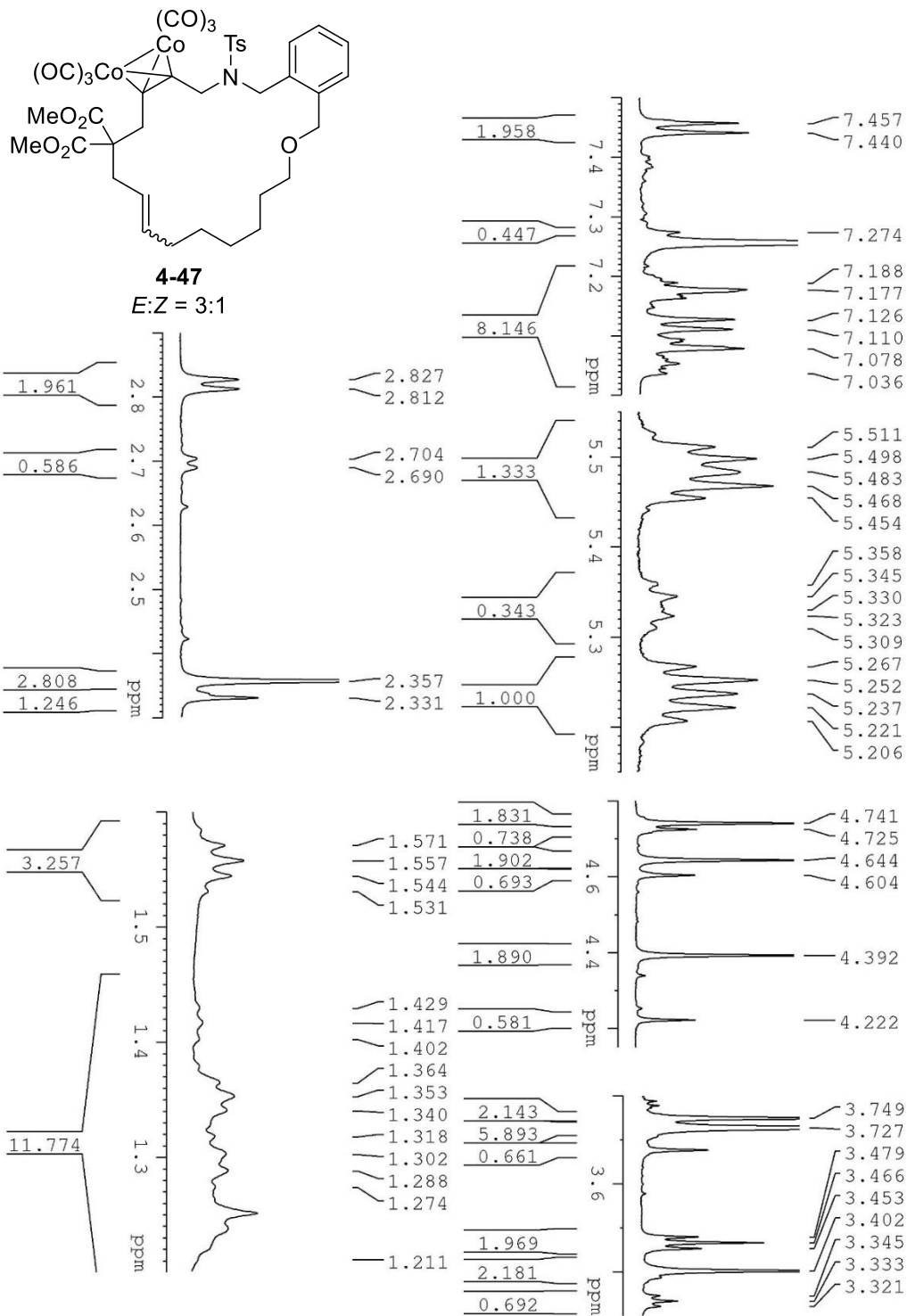


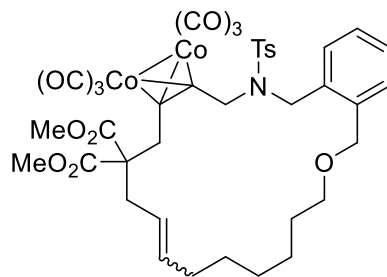


3-89

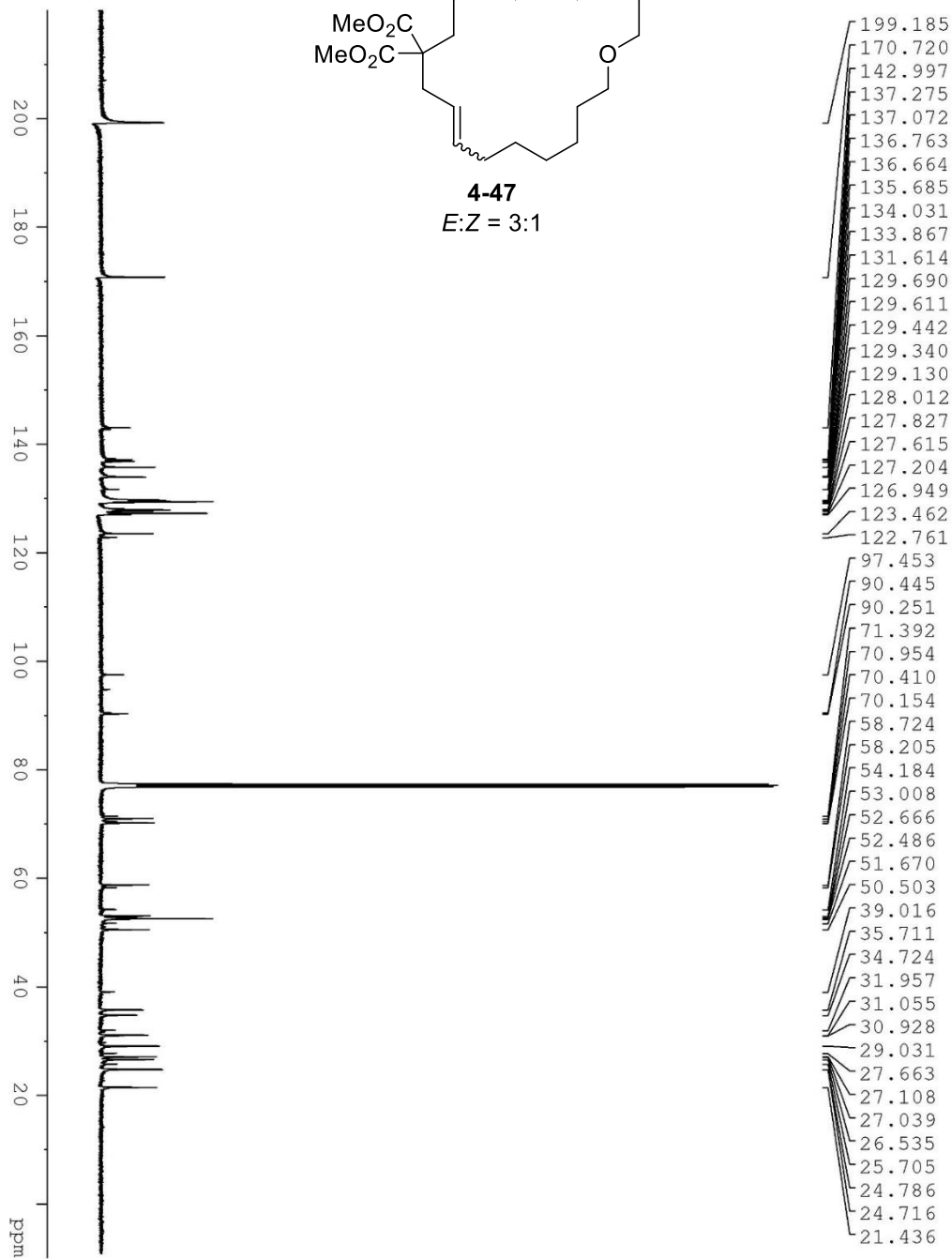


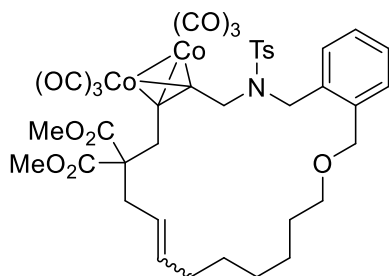
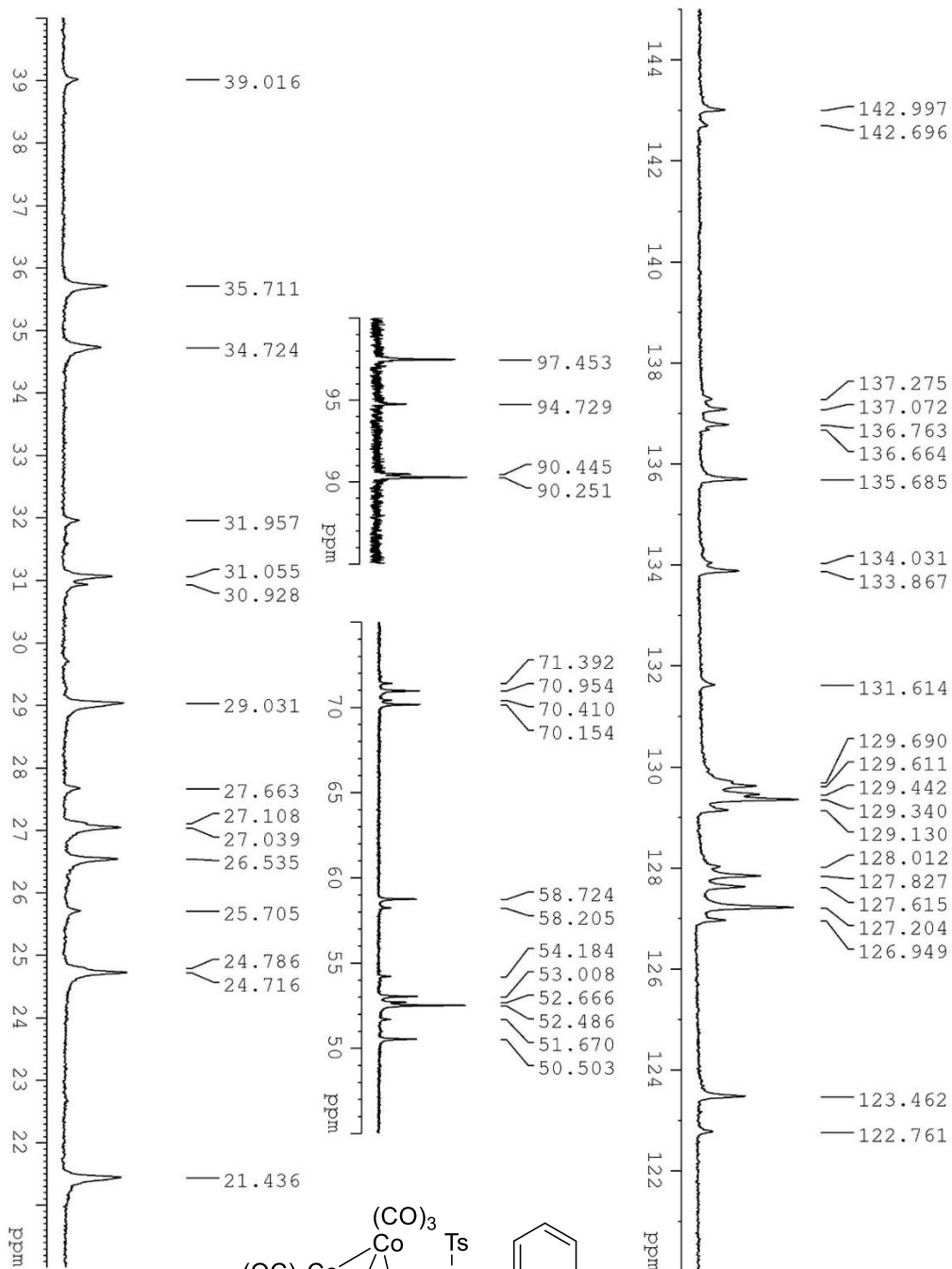


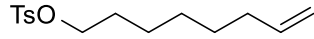




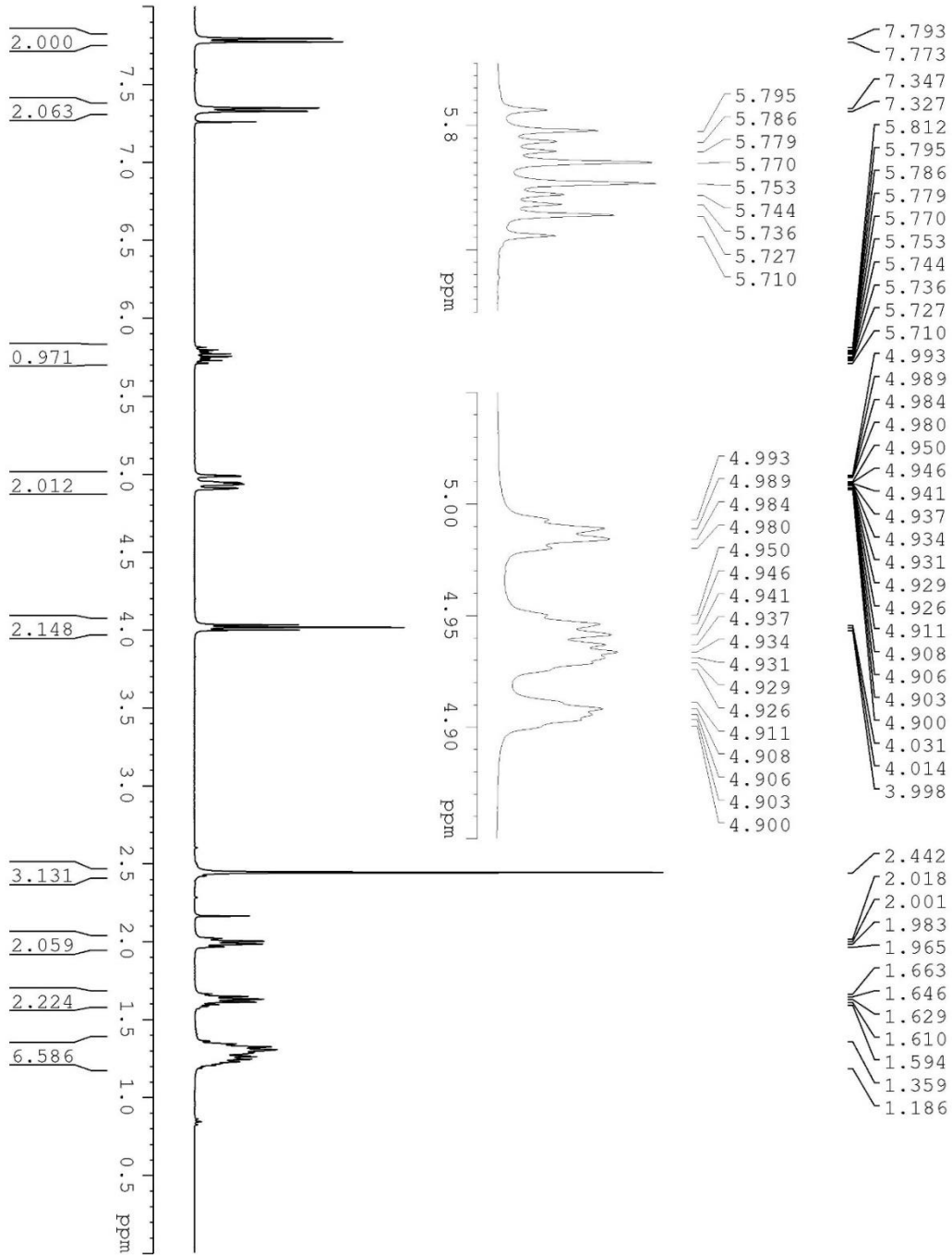
**4-47**  
E:Z = 3:1

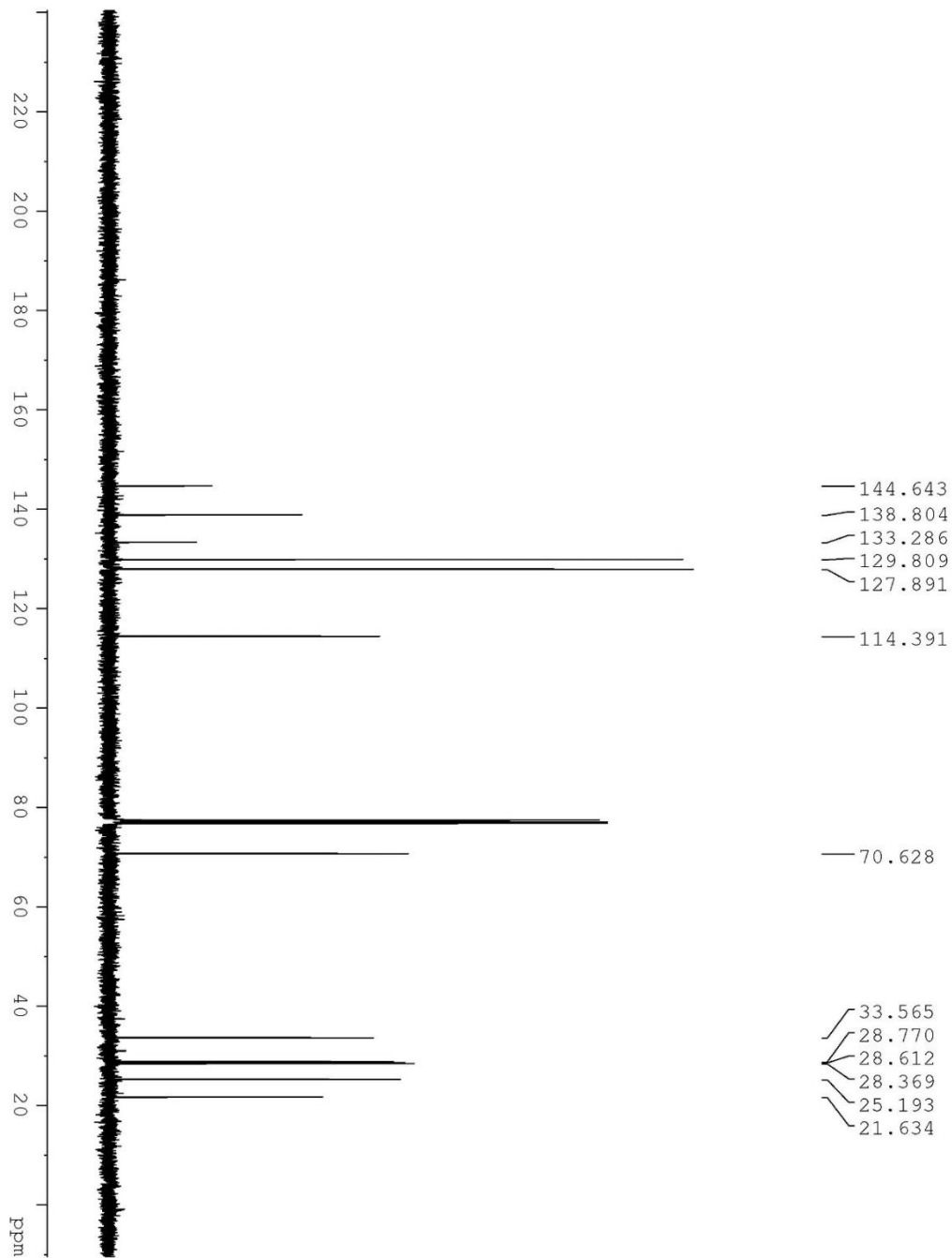
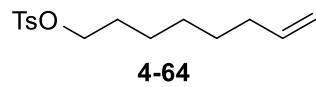




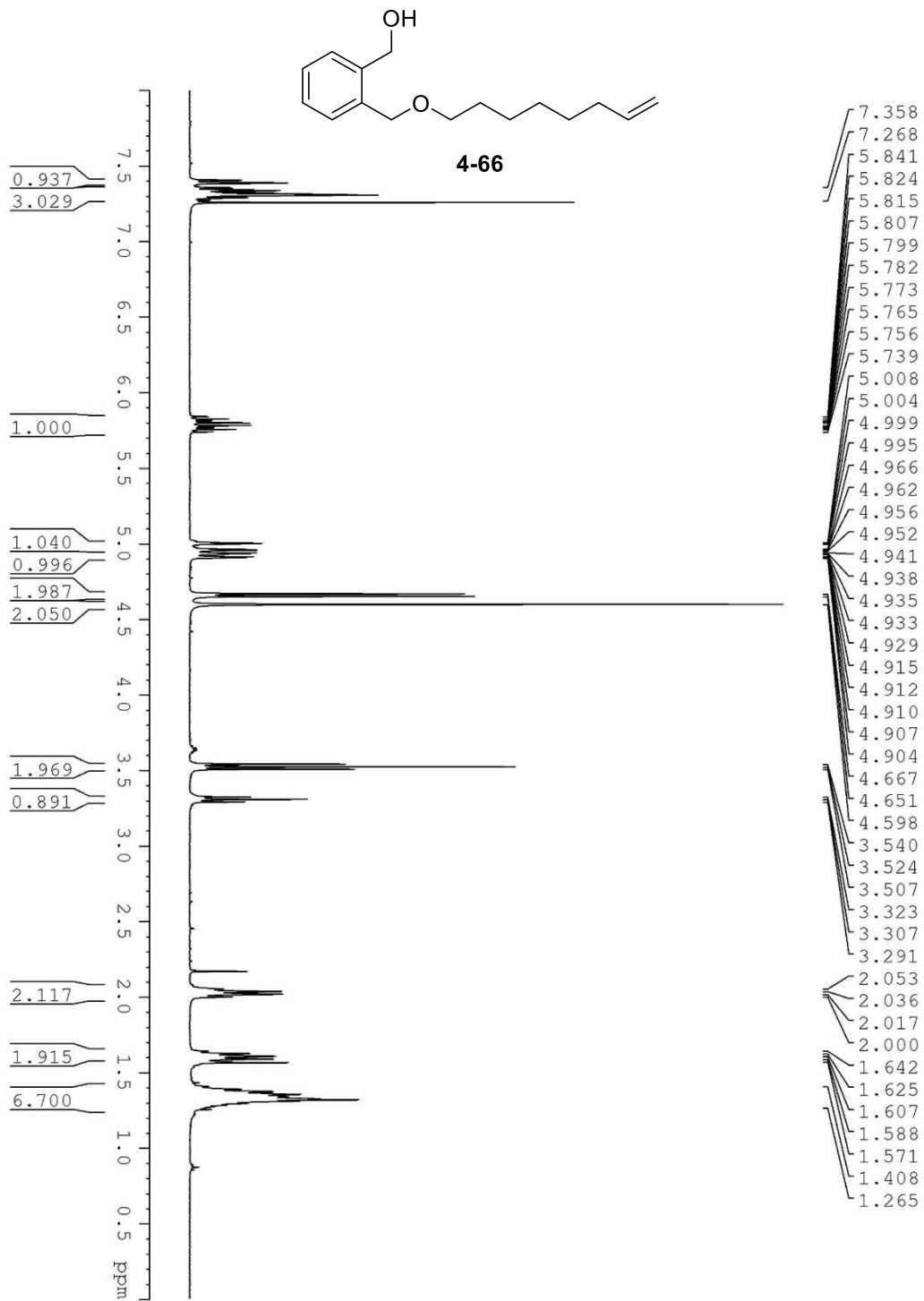


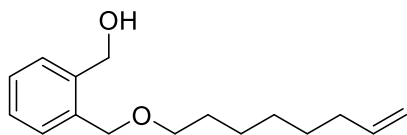
4-64



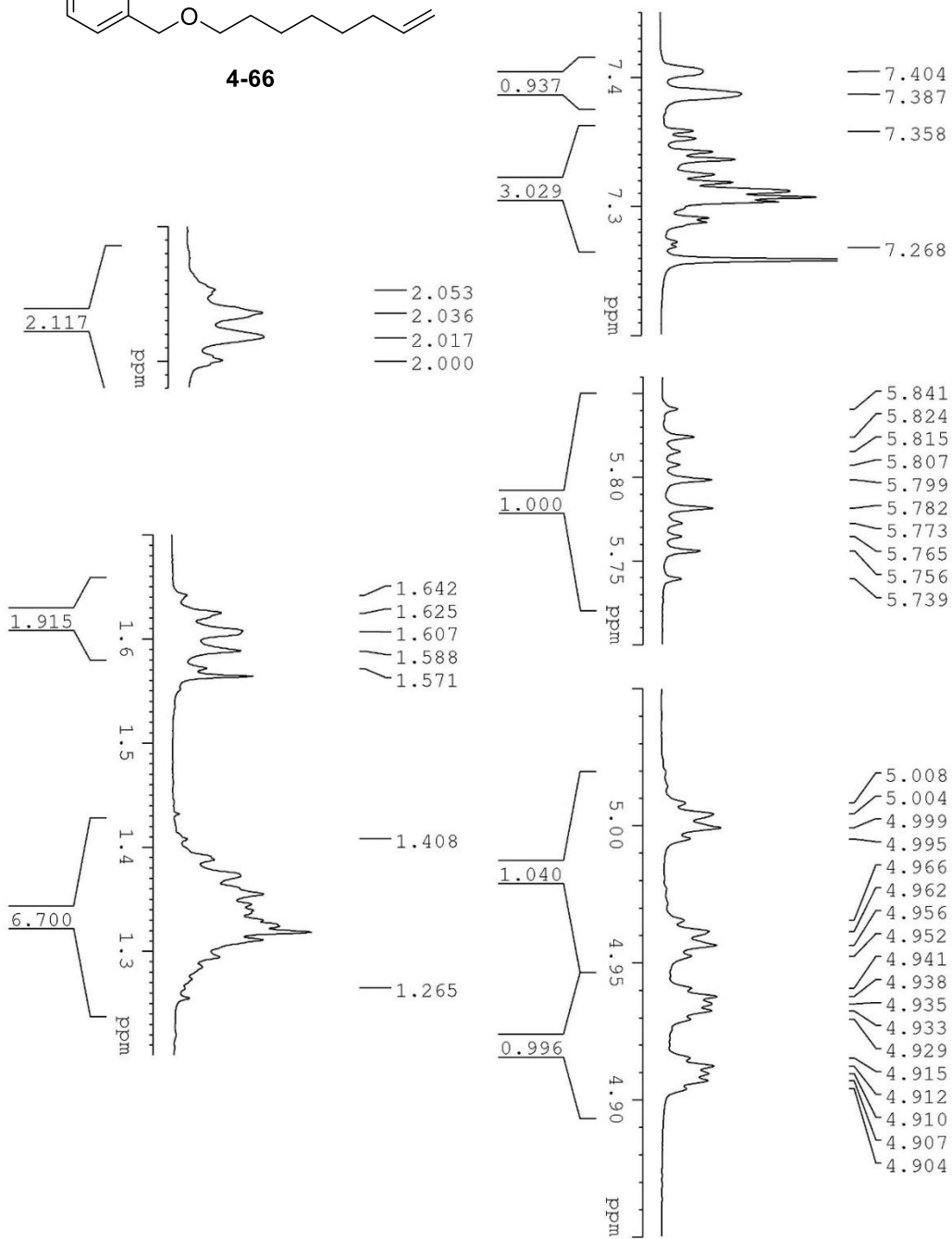


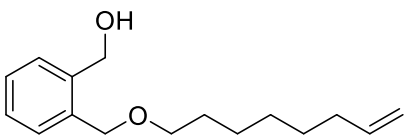




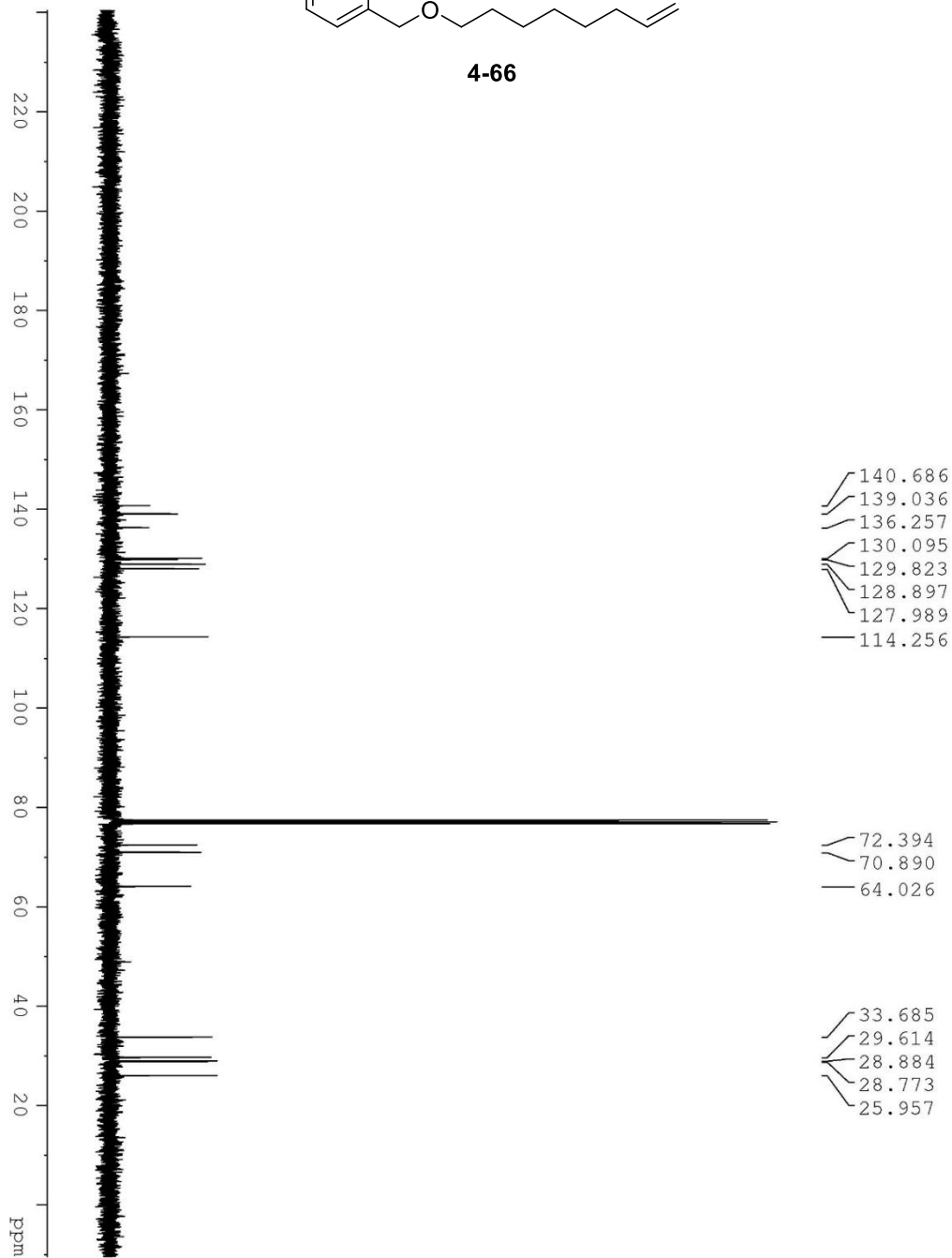


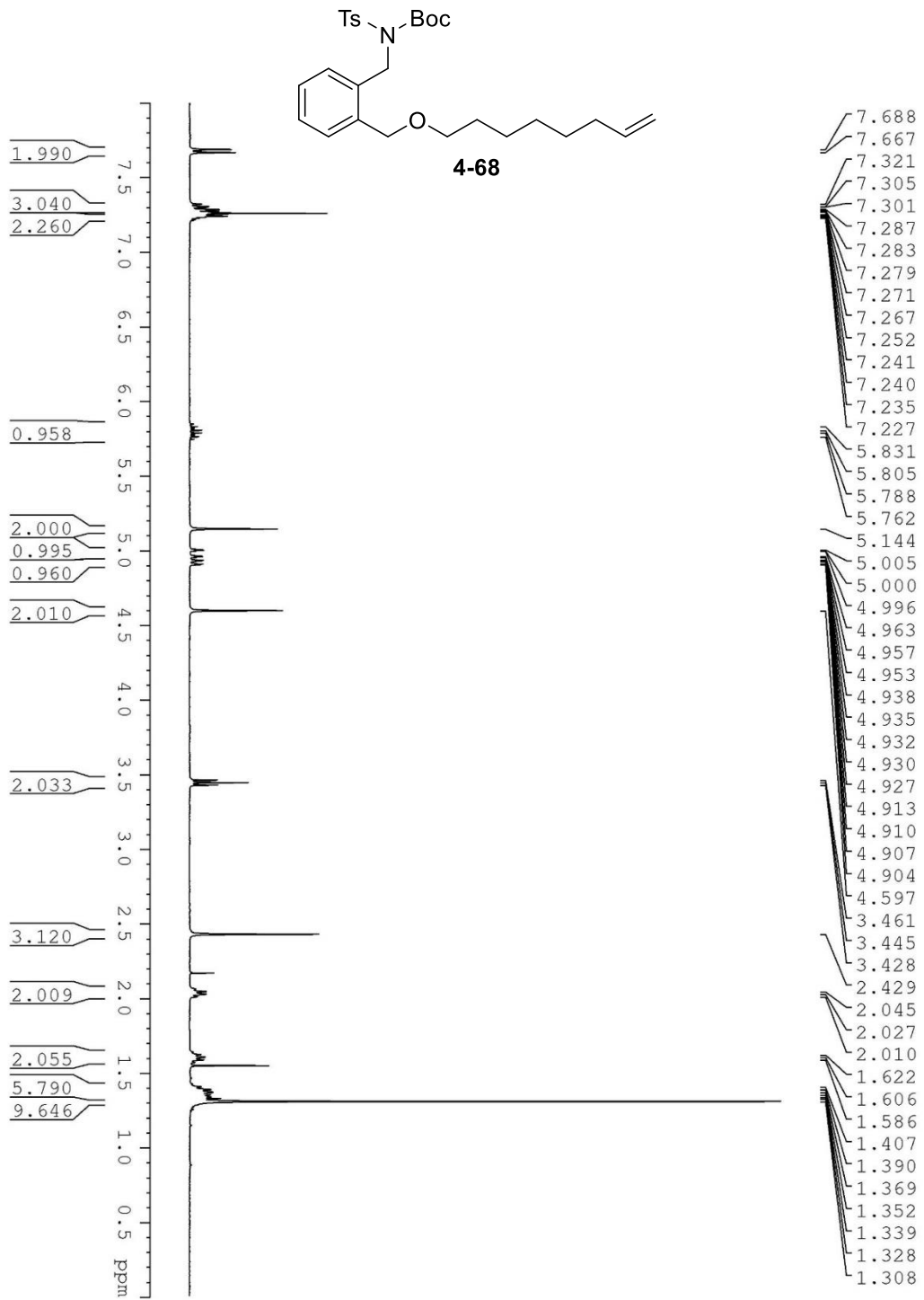
**4-66**

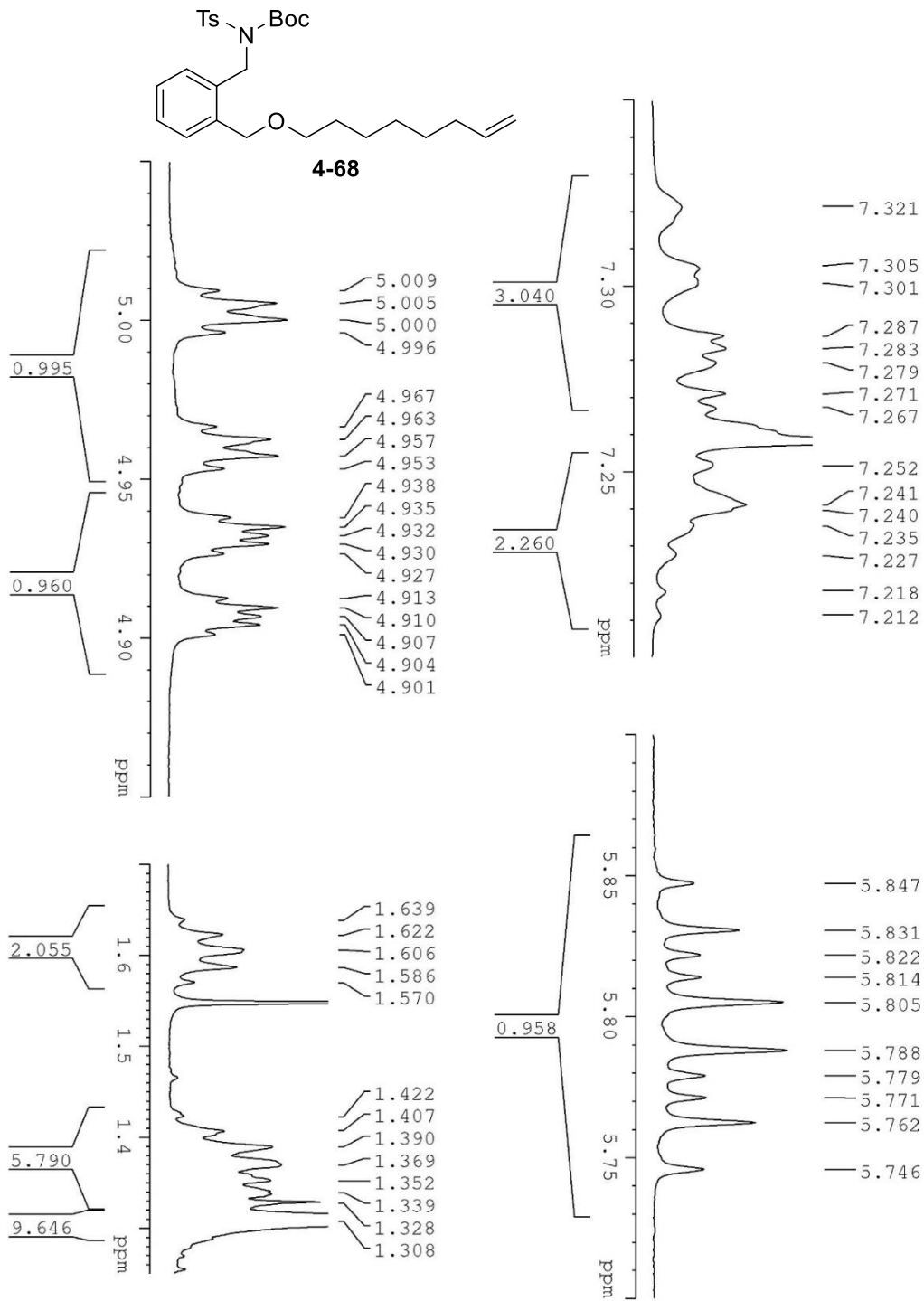


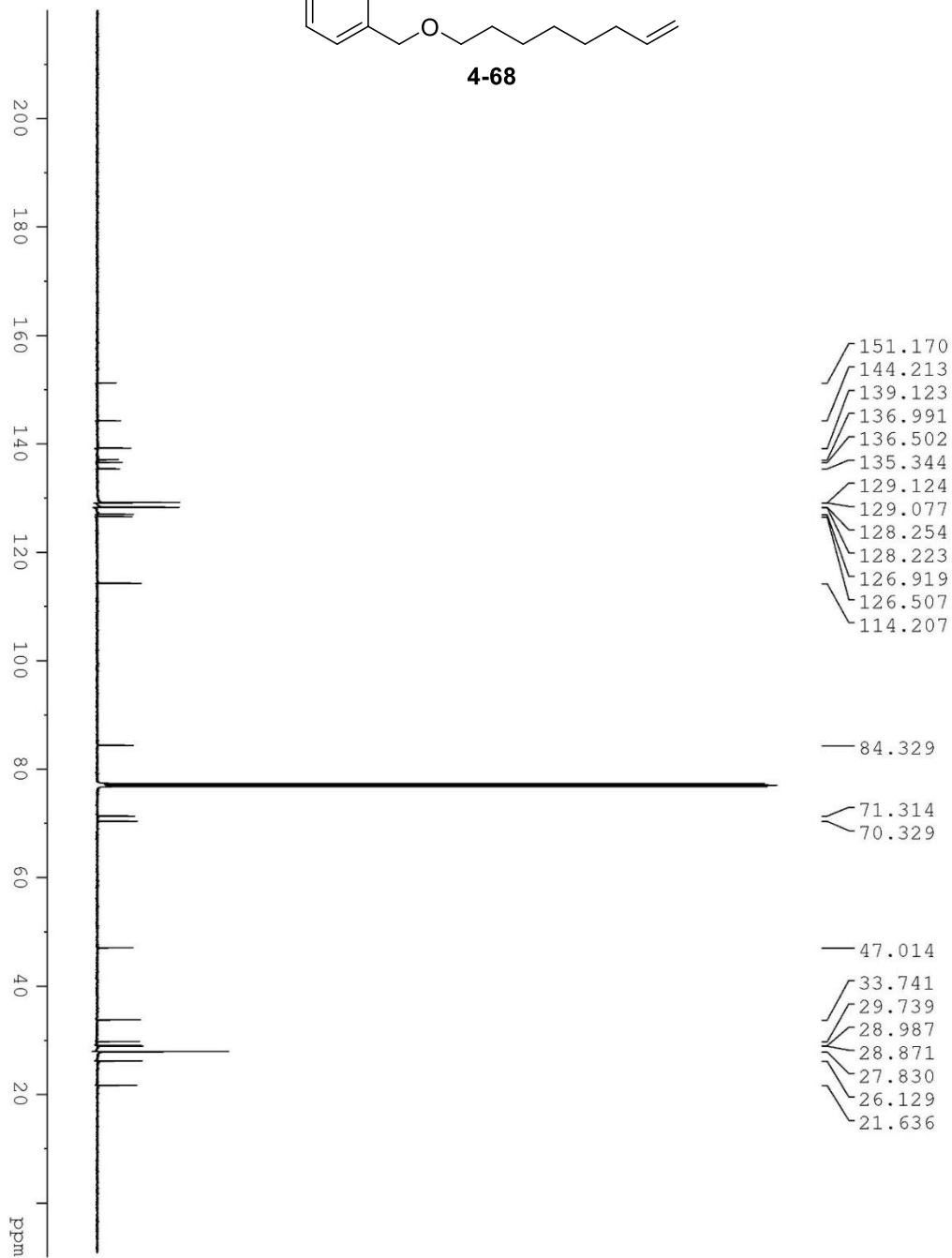
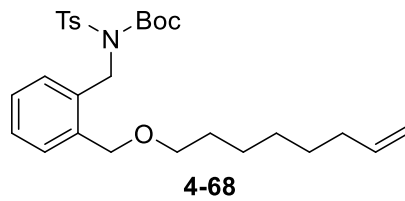


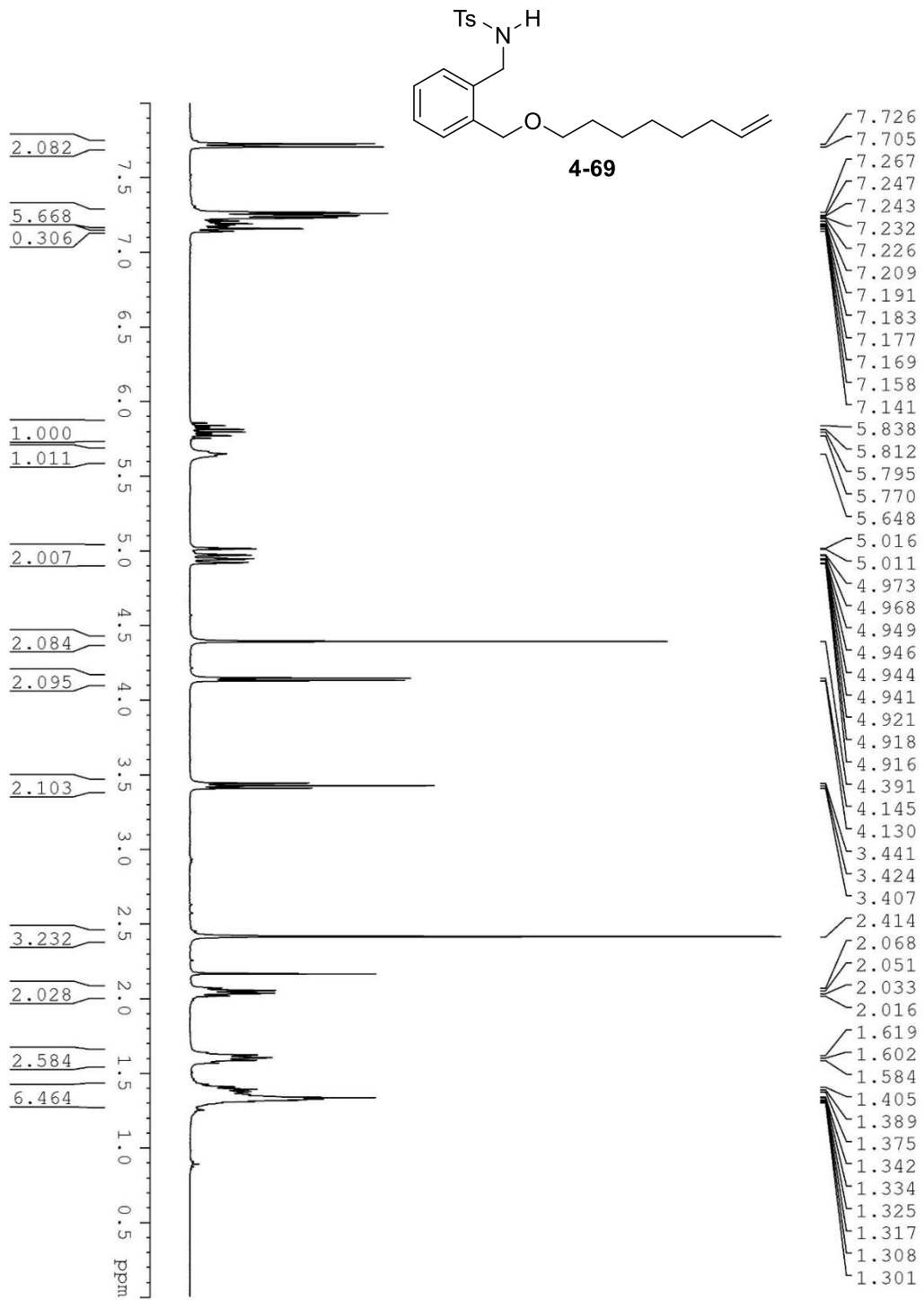
4-66

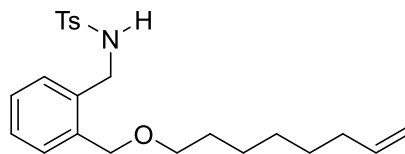




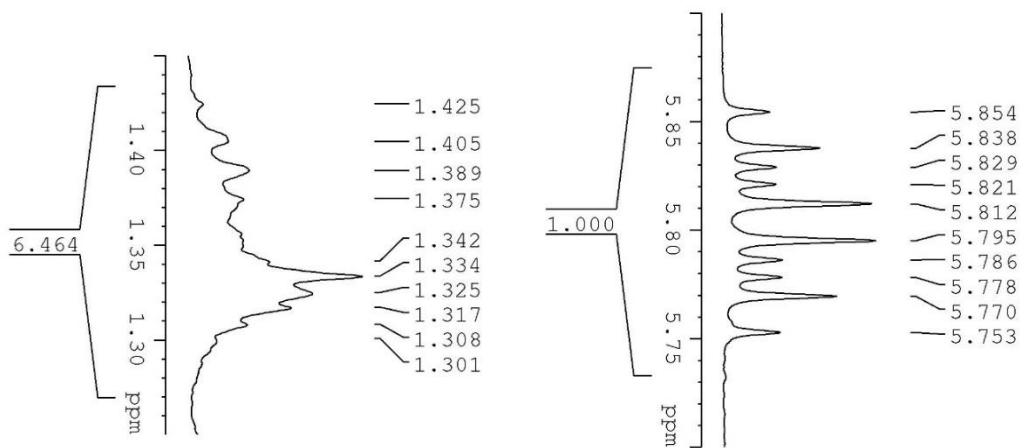
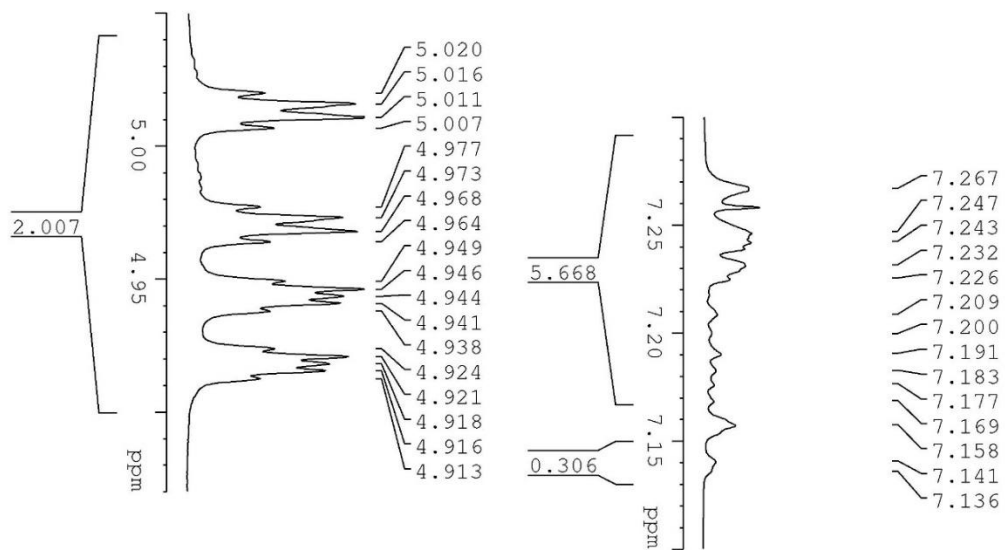




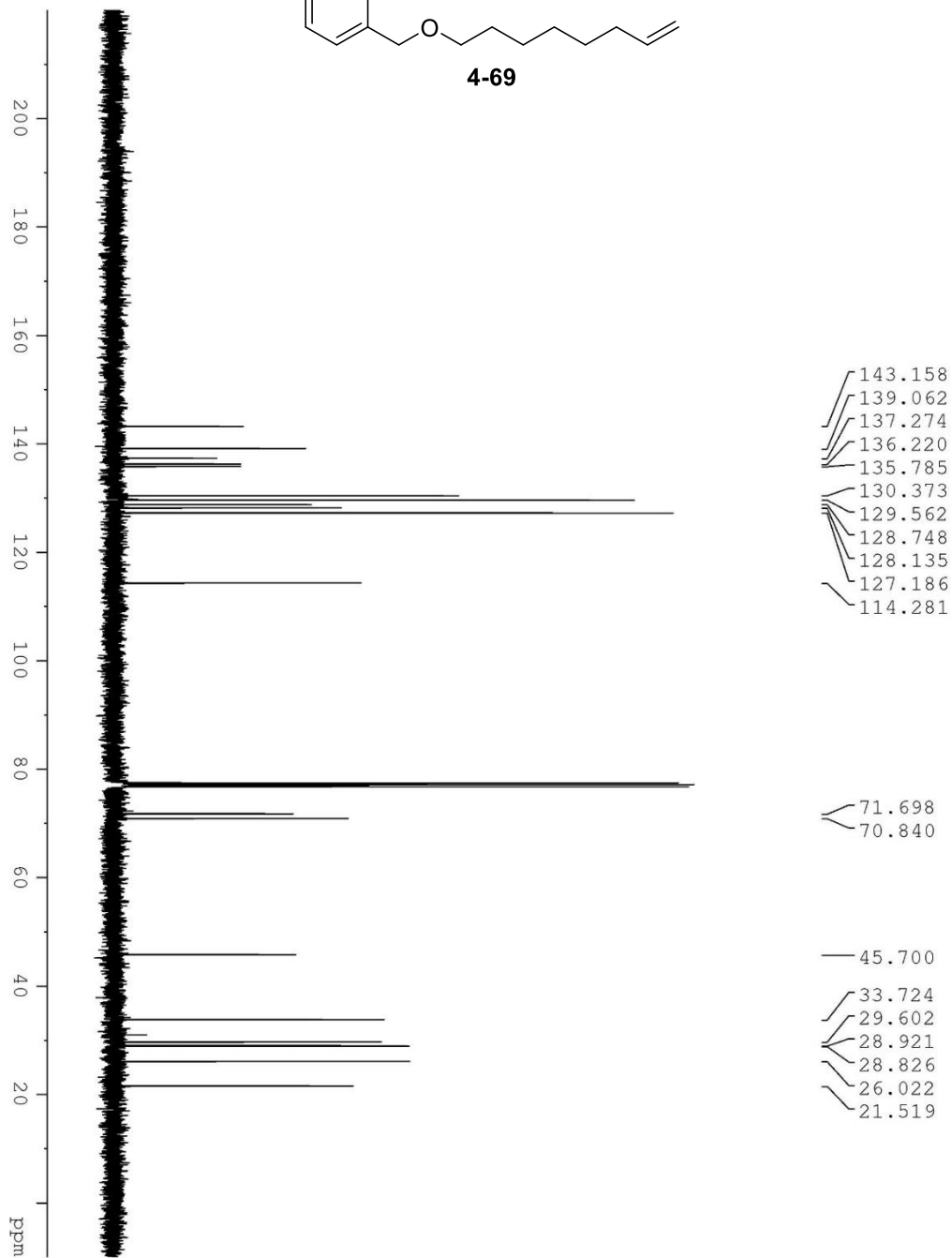
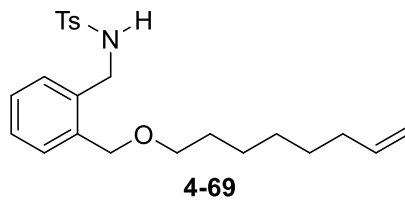


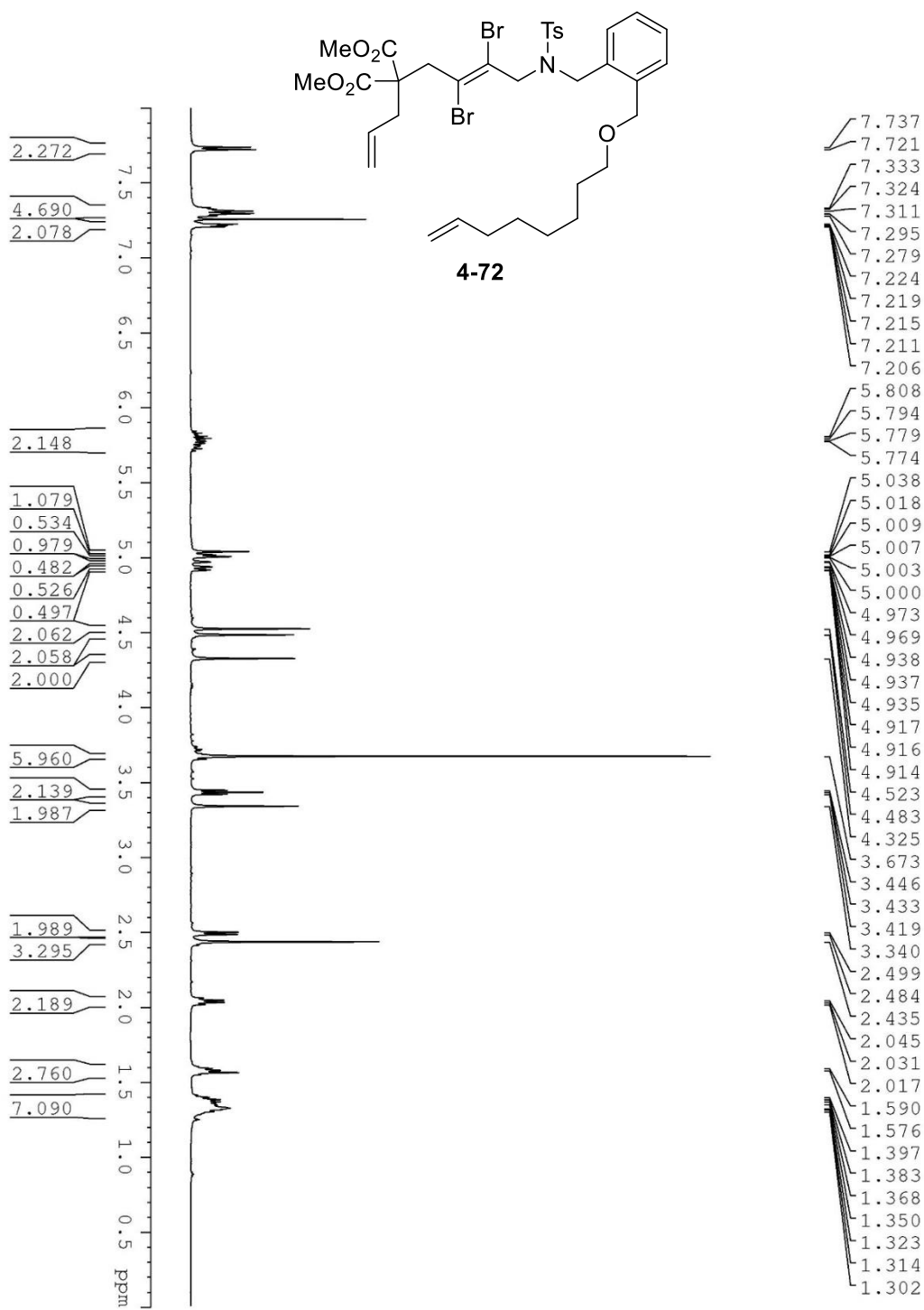


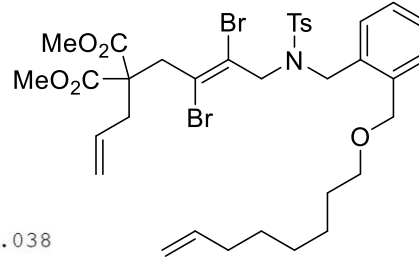
4-69



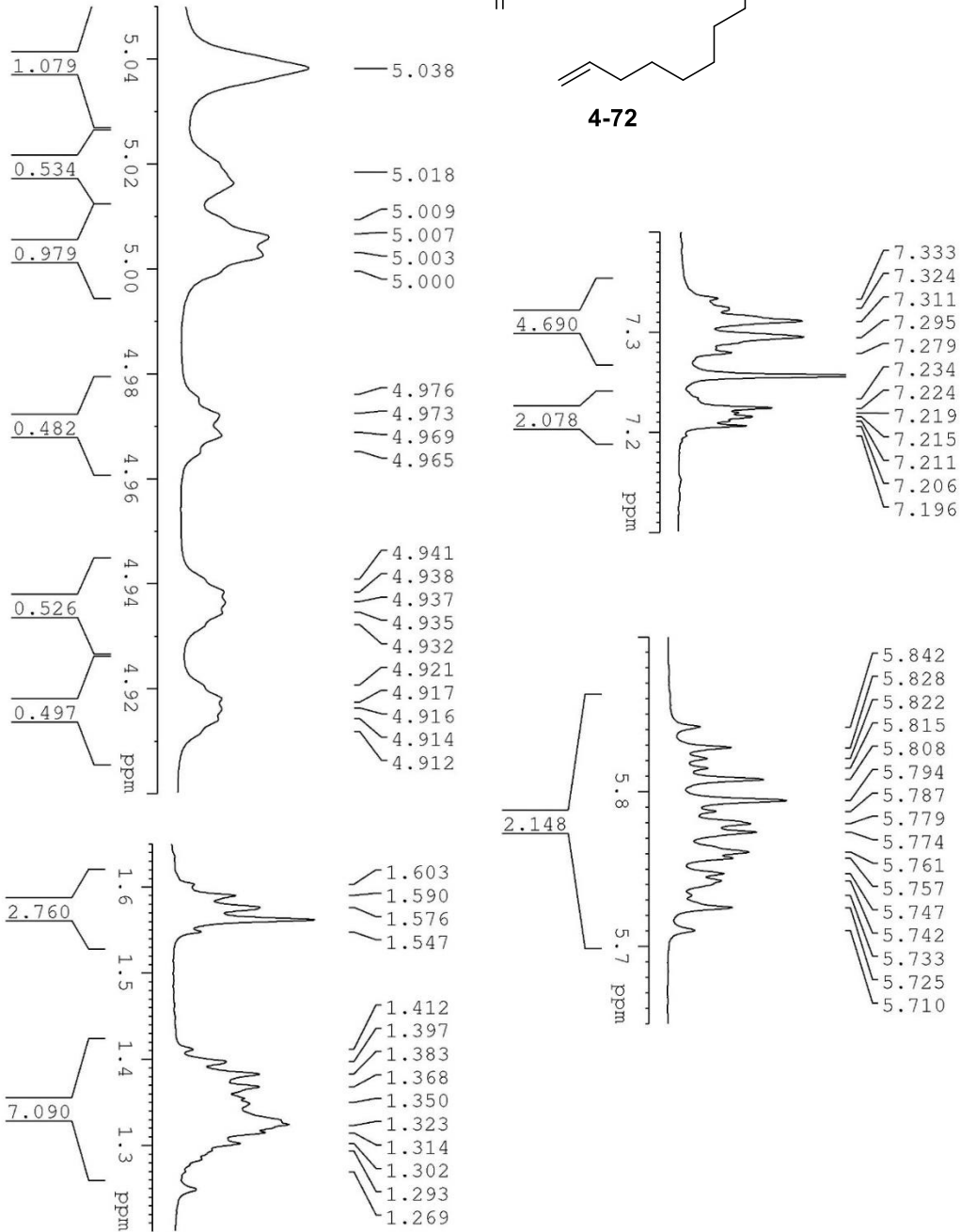


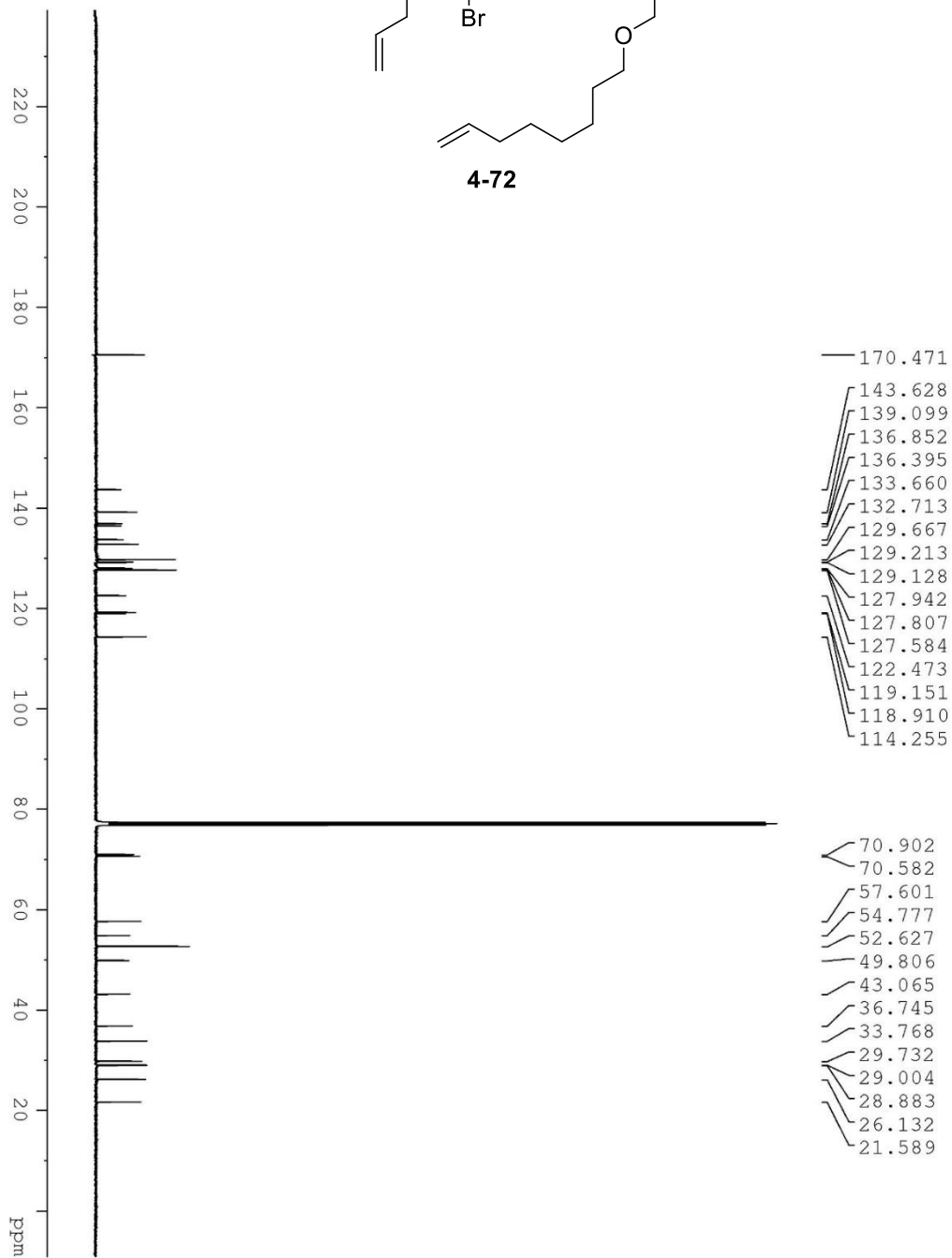
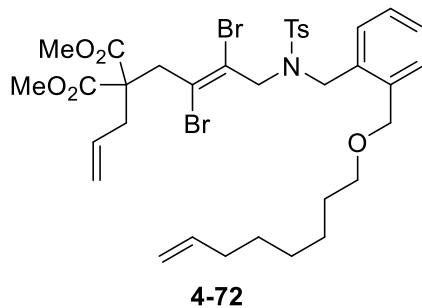


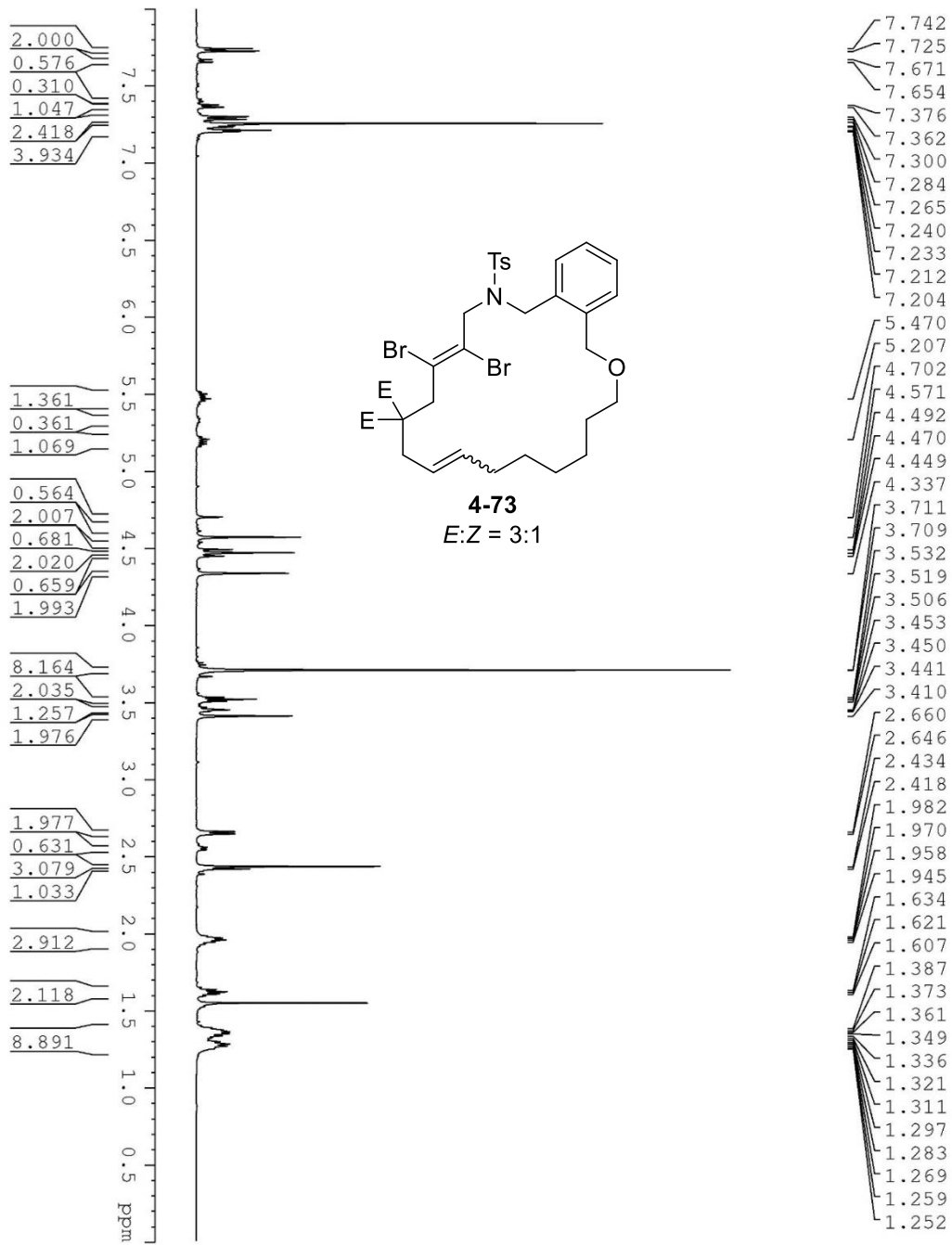


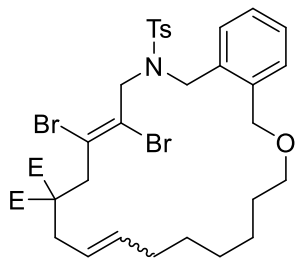


**4-72**



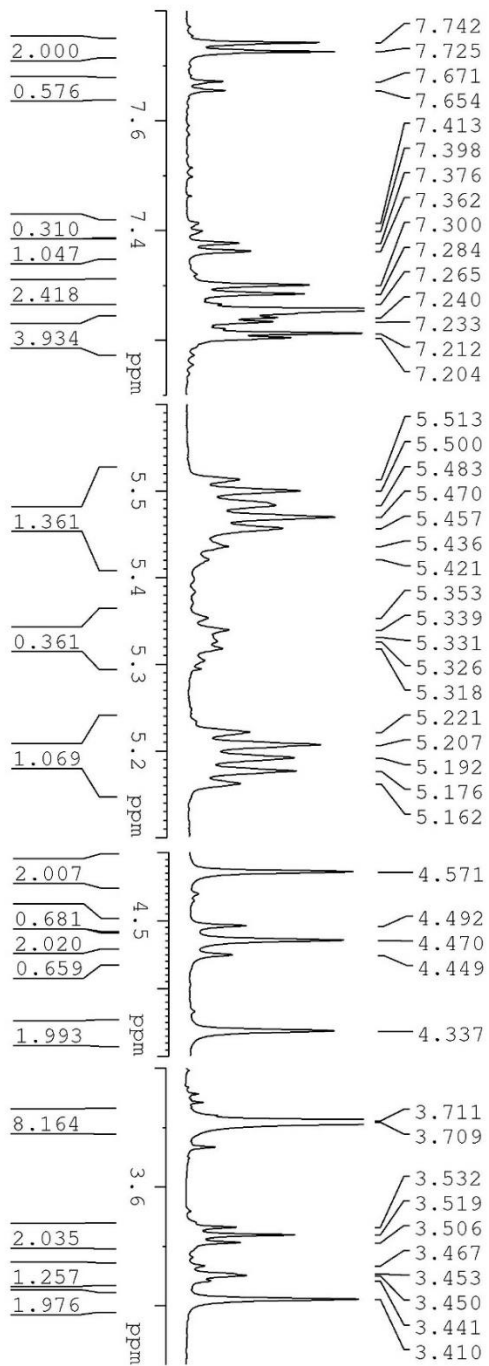
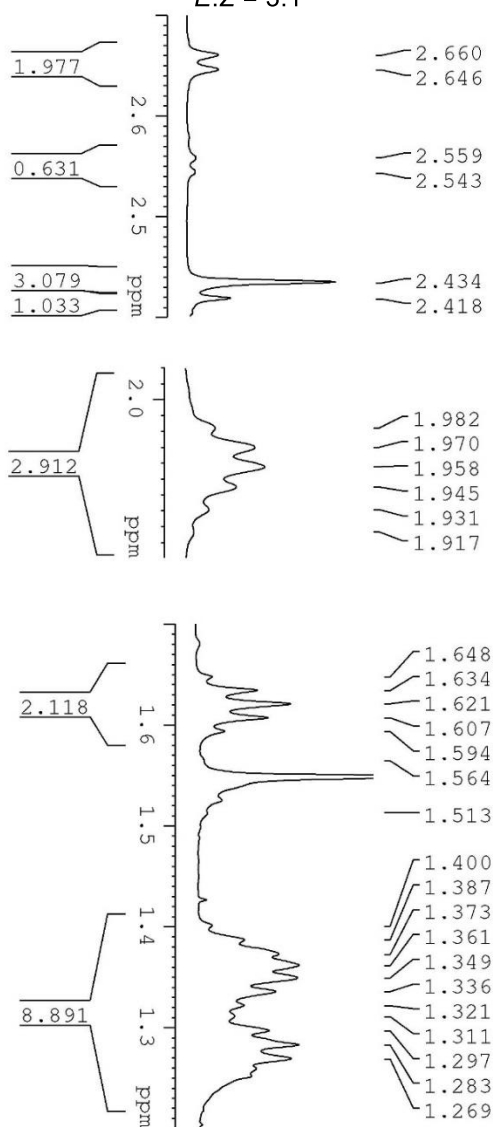


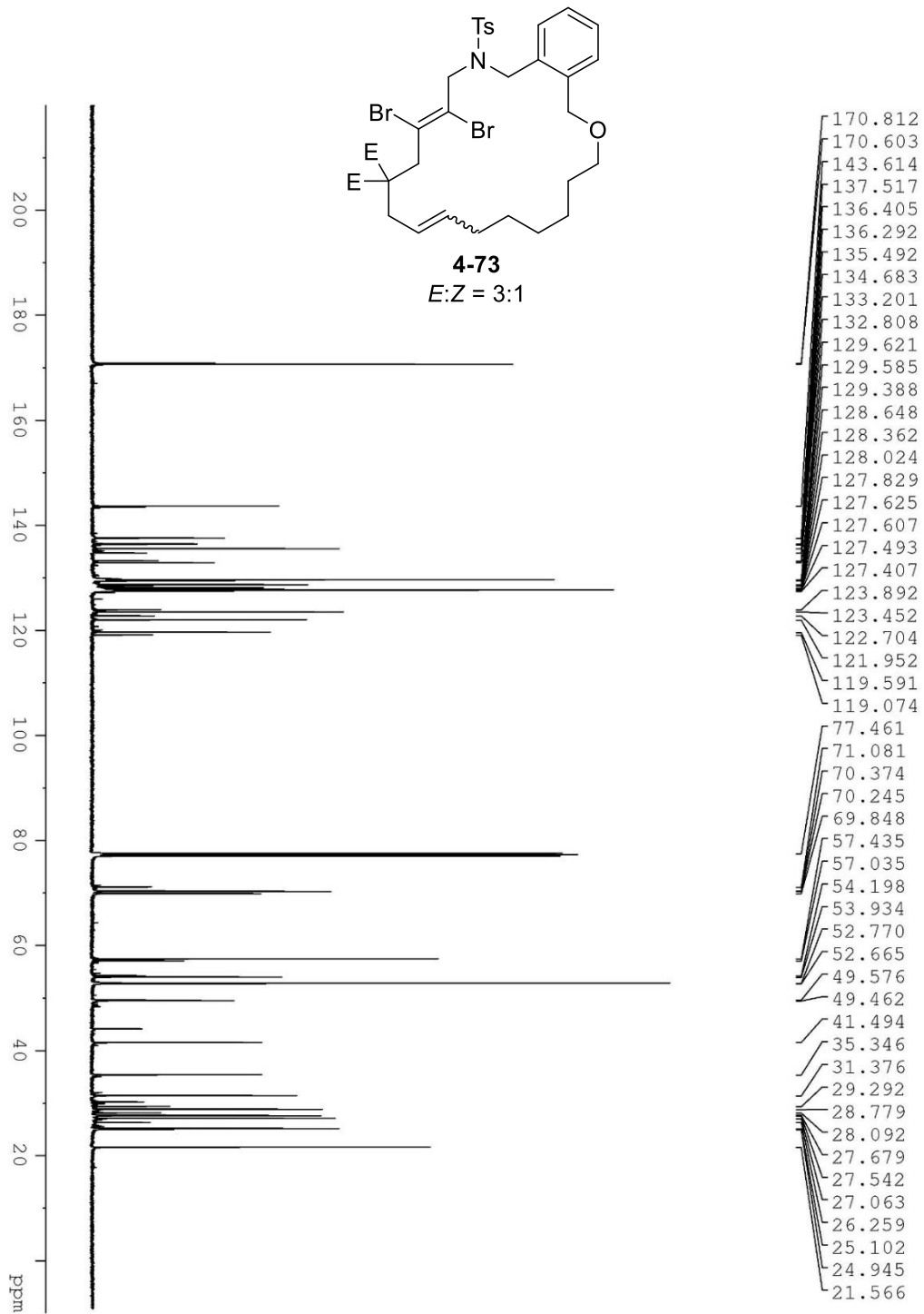


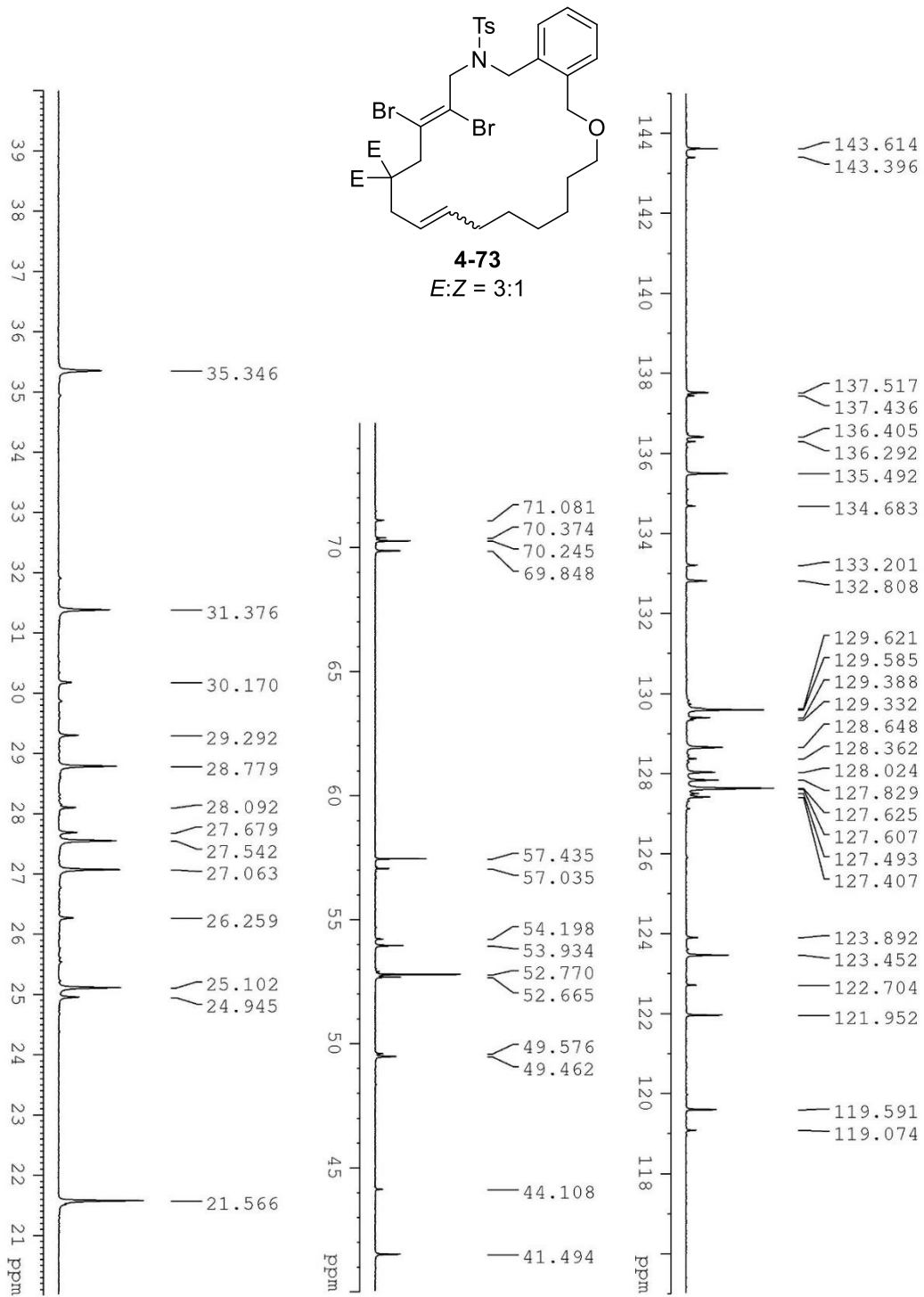


**4-73**

*E:Z* = 3:1

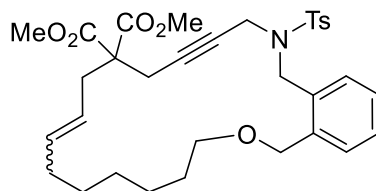
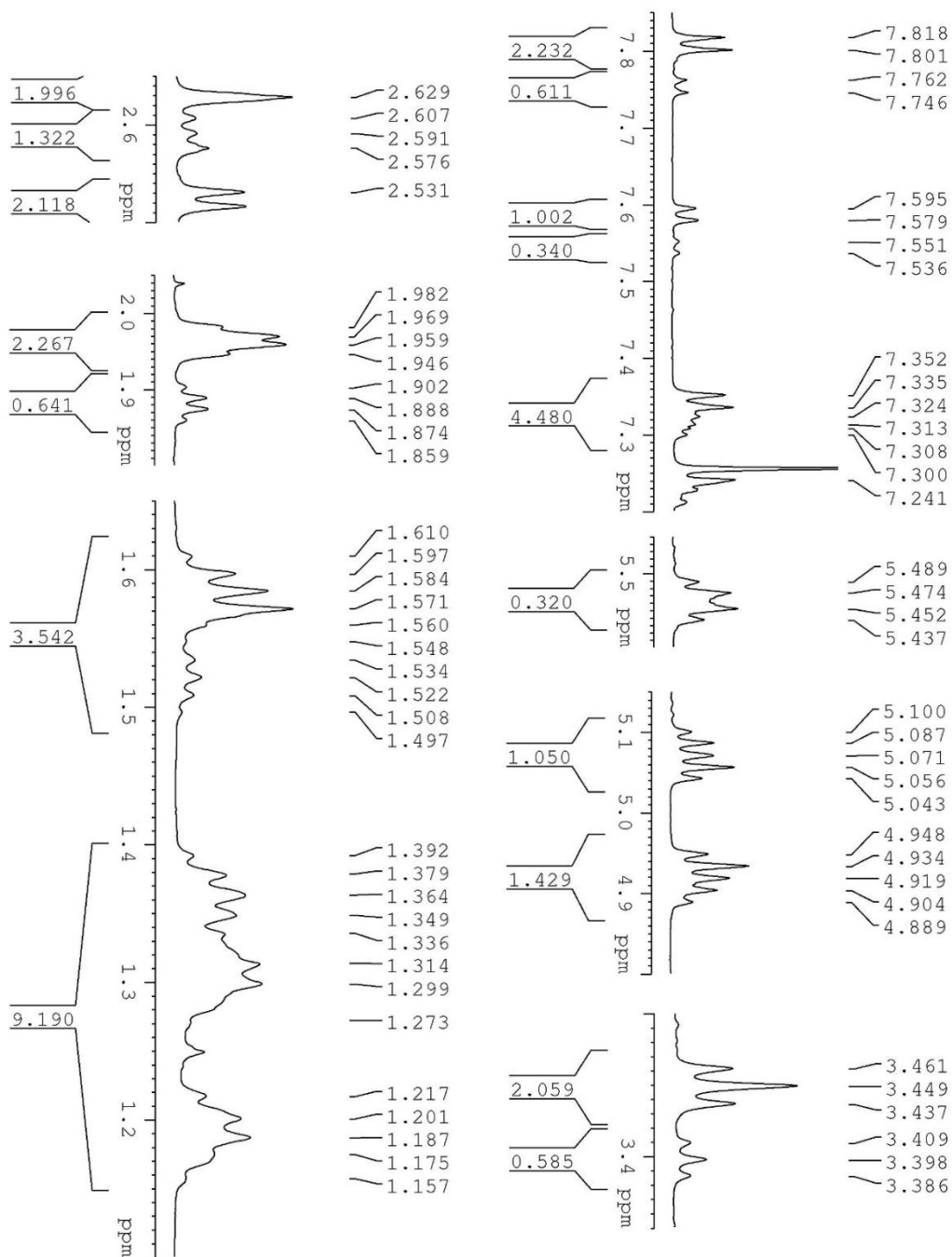




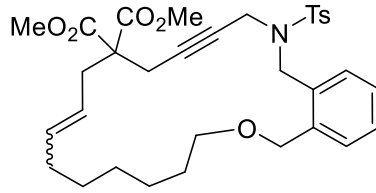




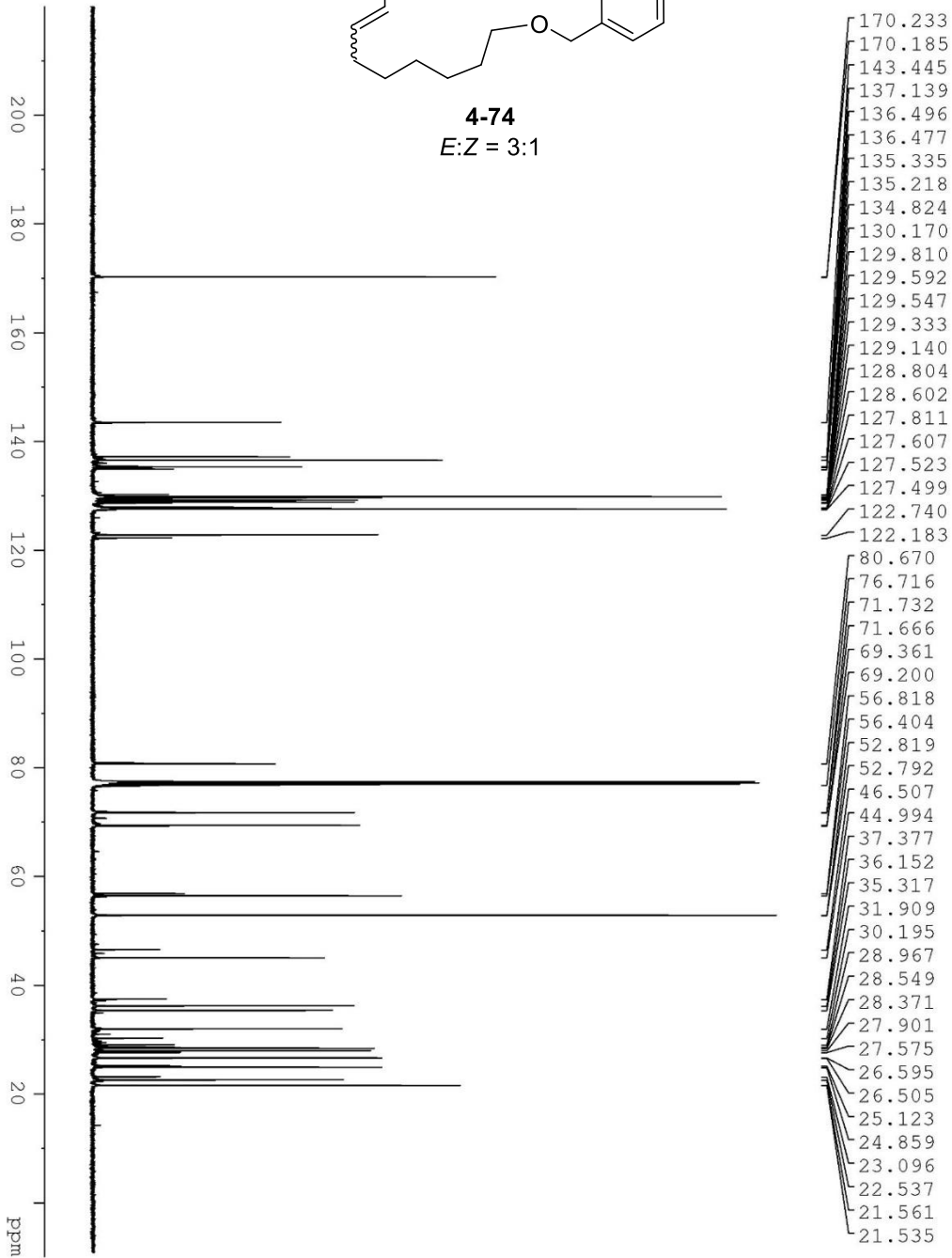




**4-74**  
*E:Z* = 3:1

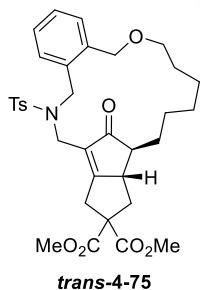
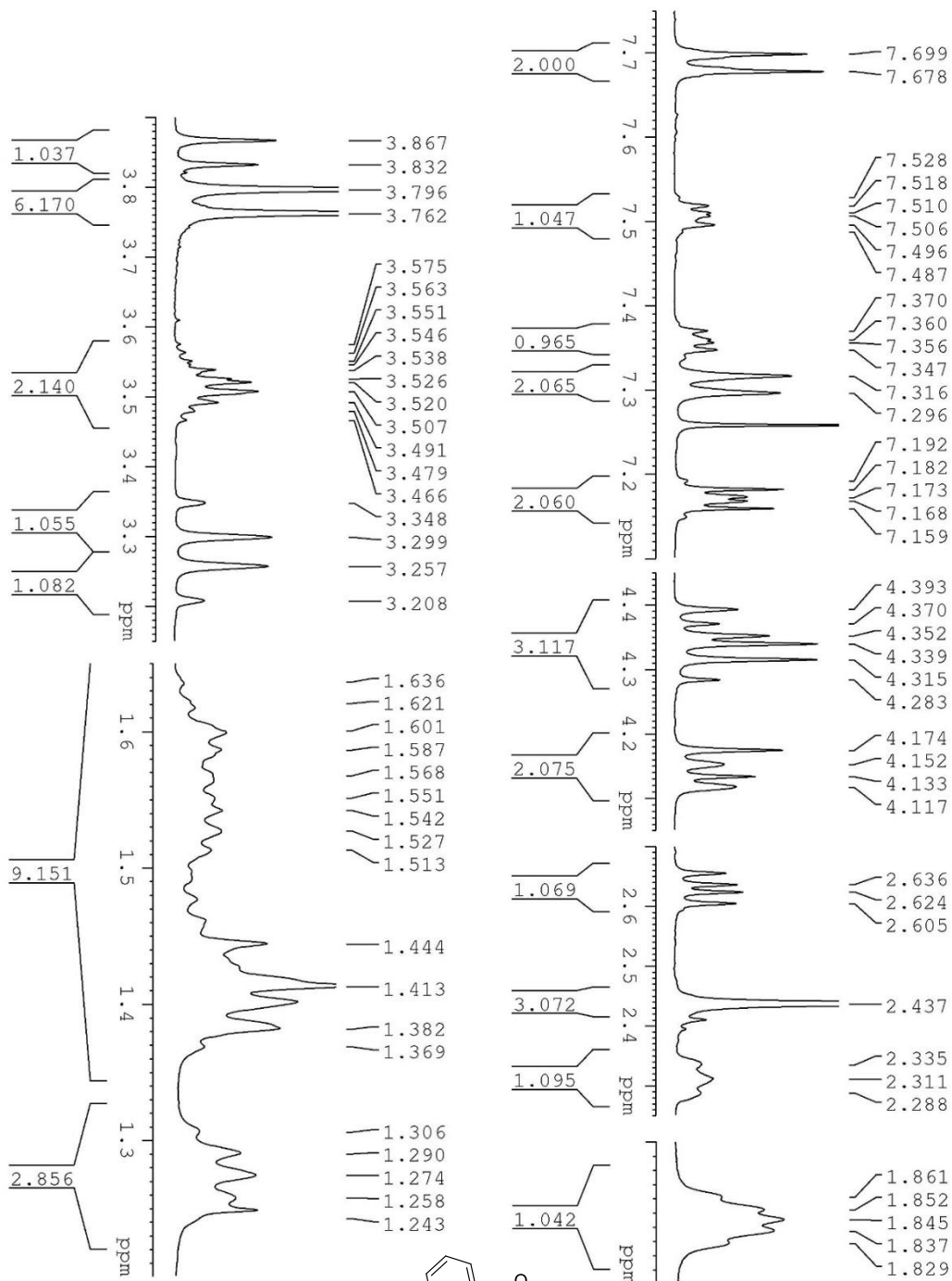


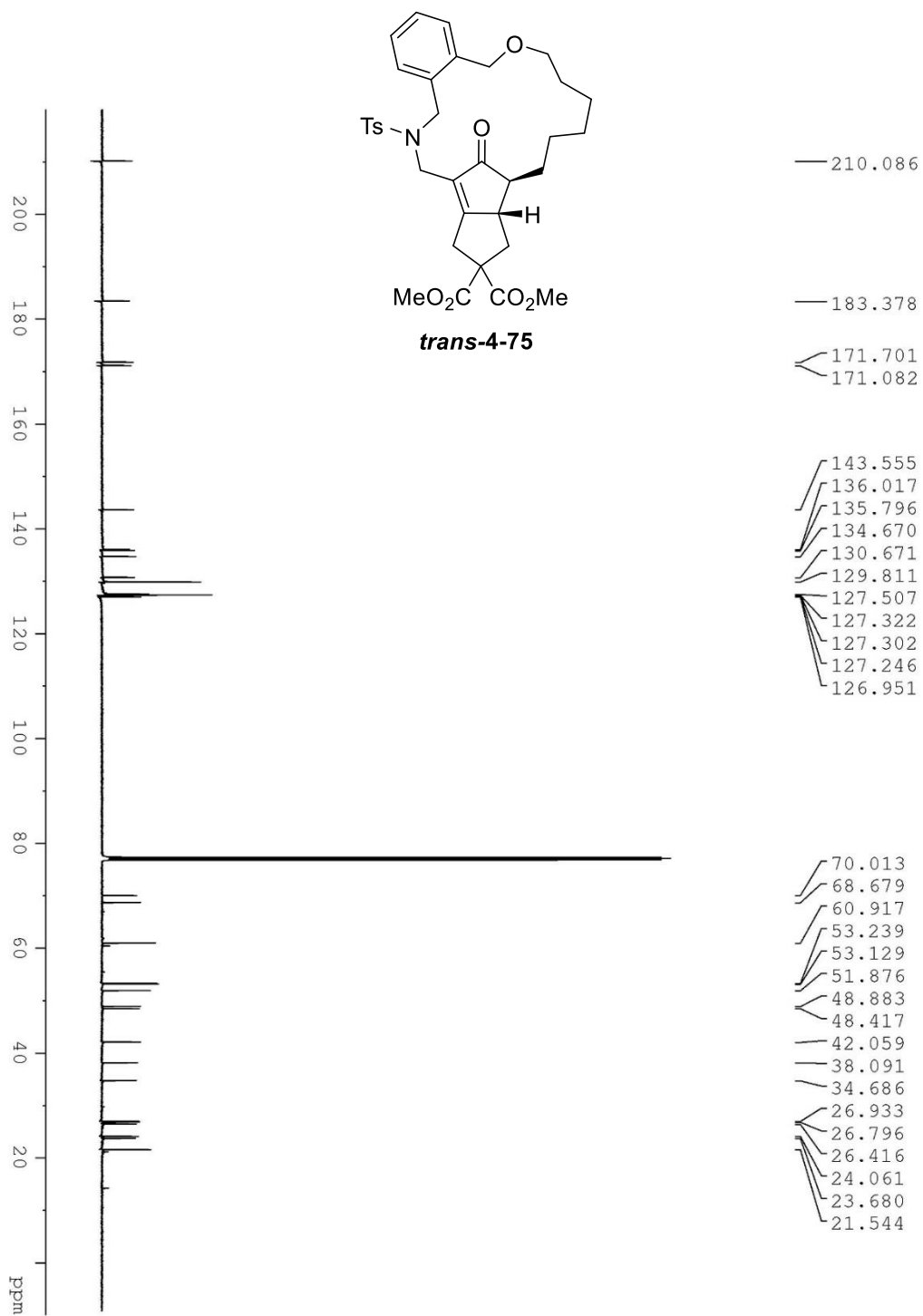
**4-74**  
*E:Z* = 3:1

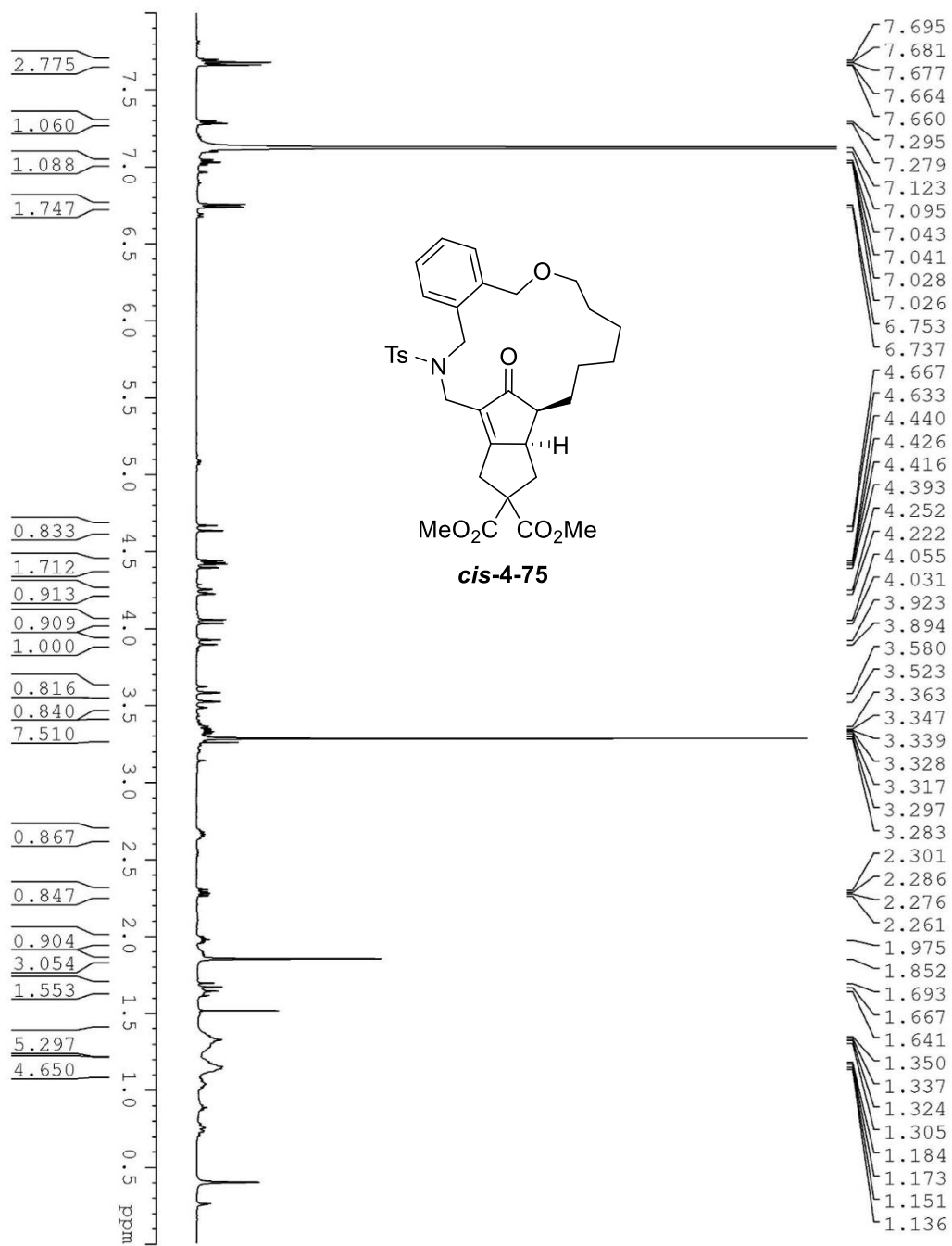




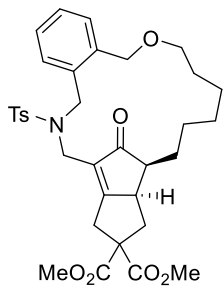
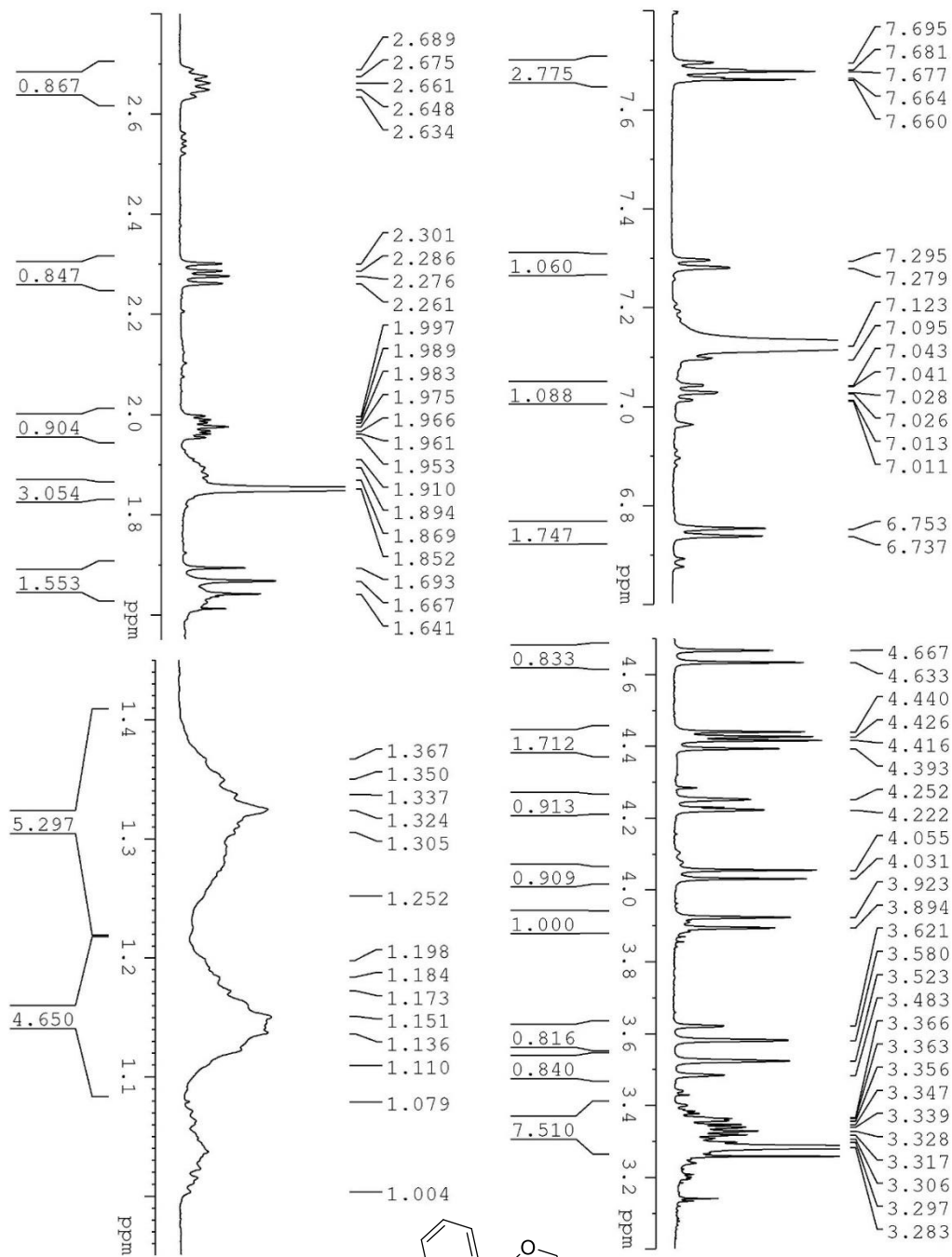




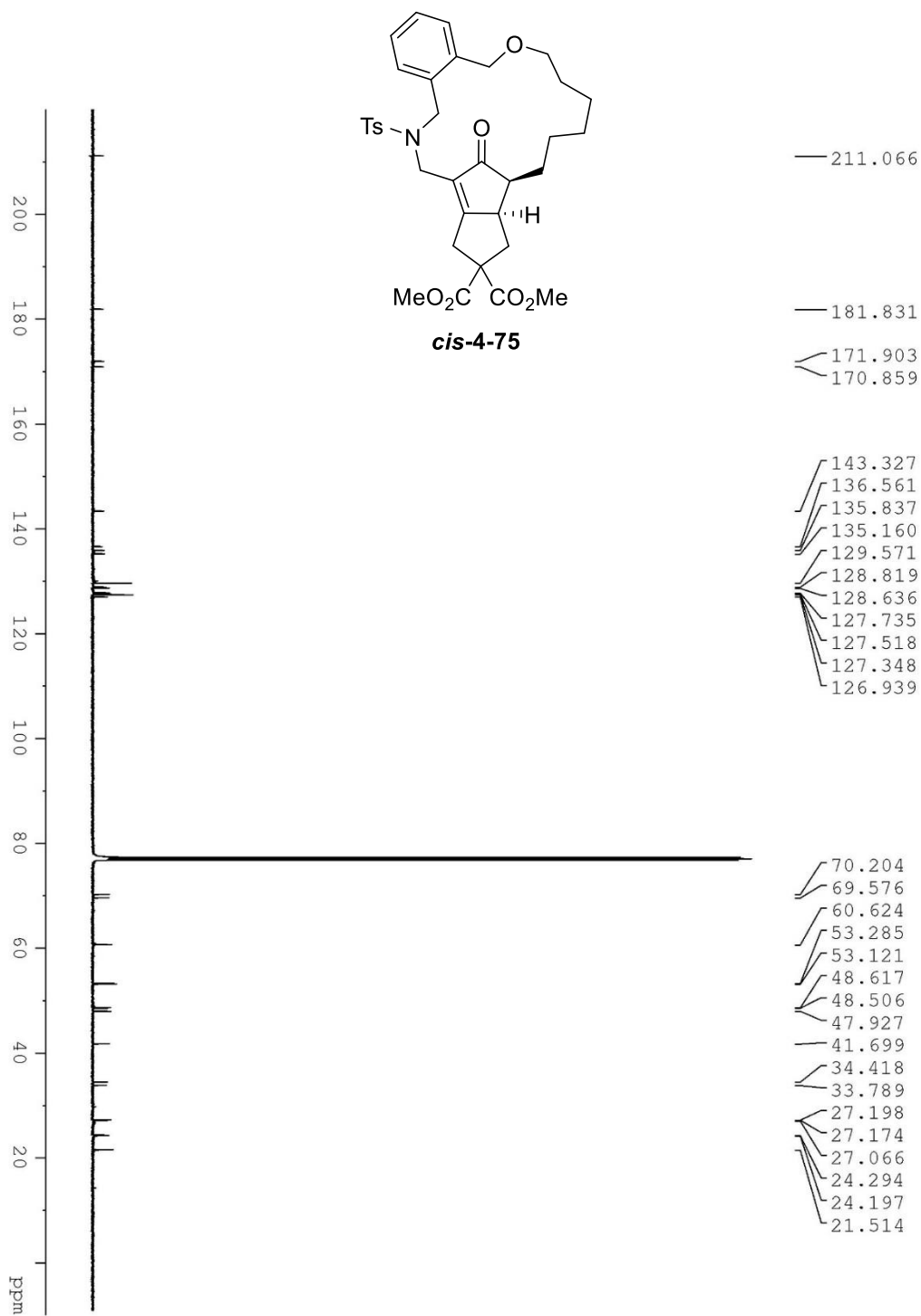


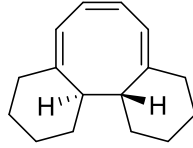




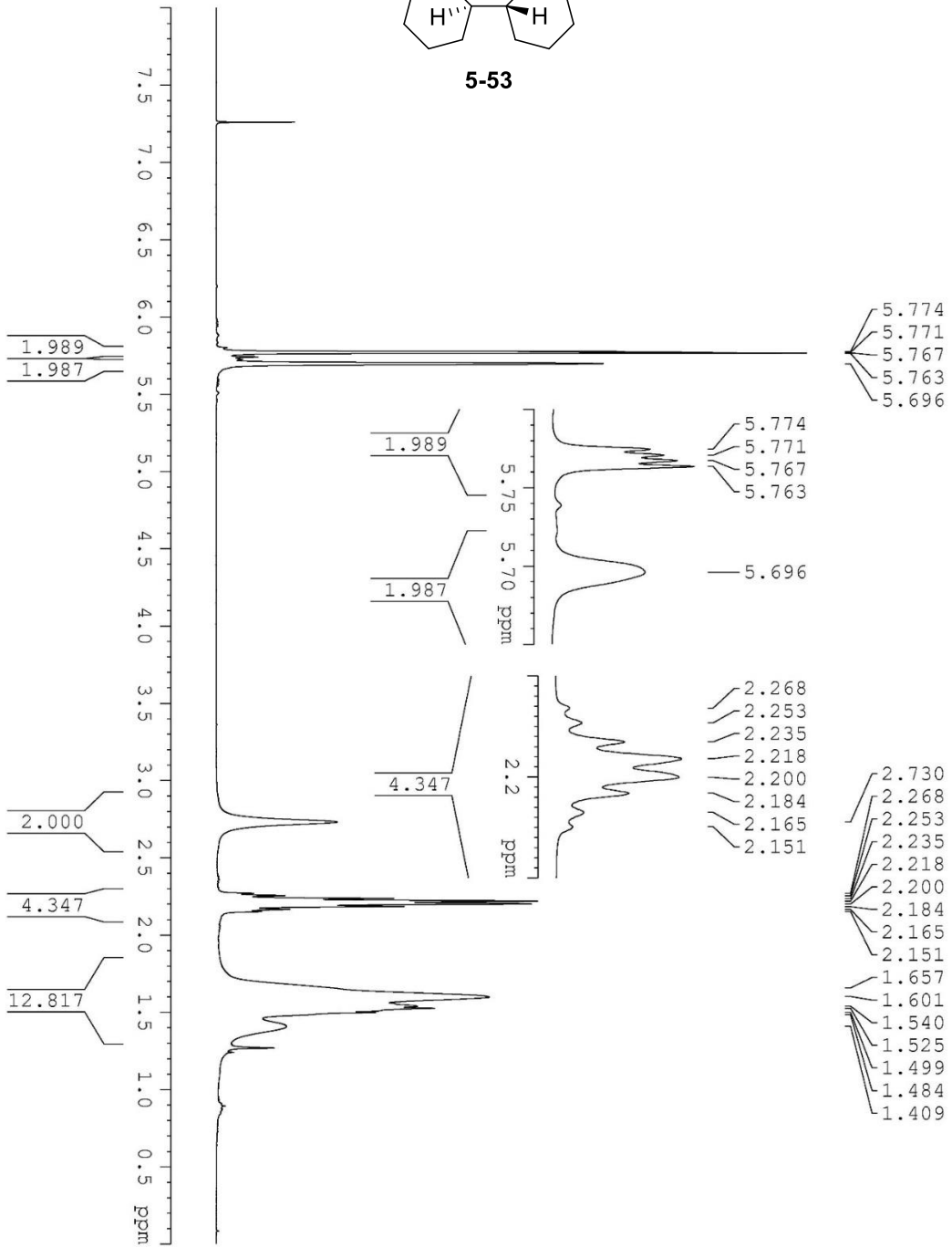


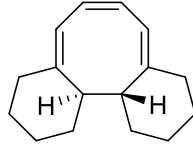
**cis-4-75**



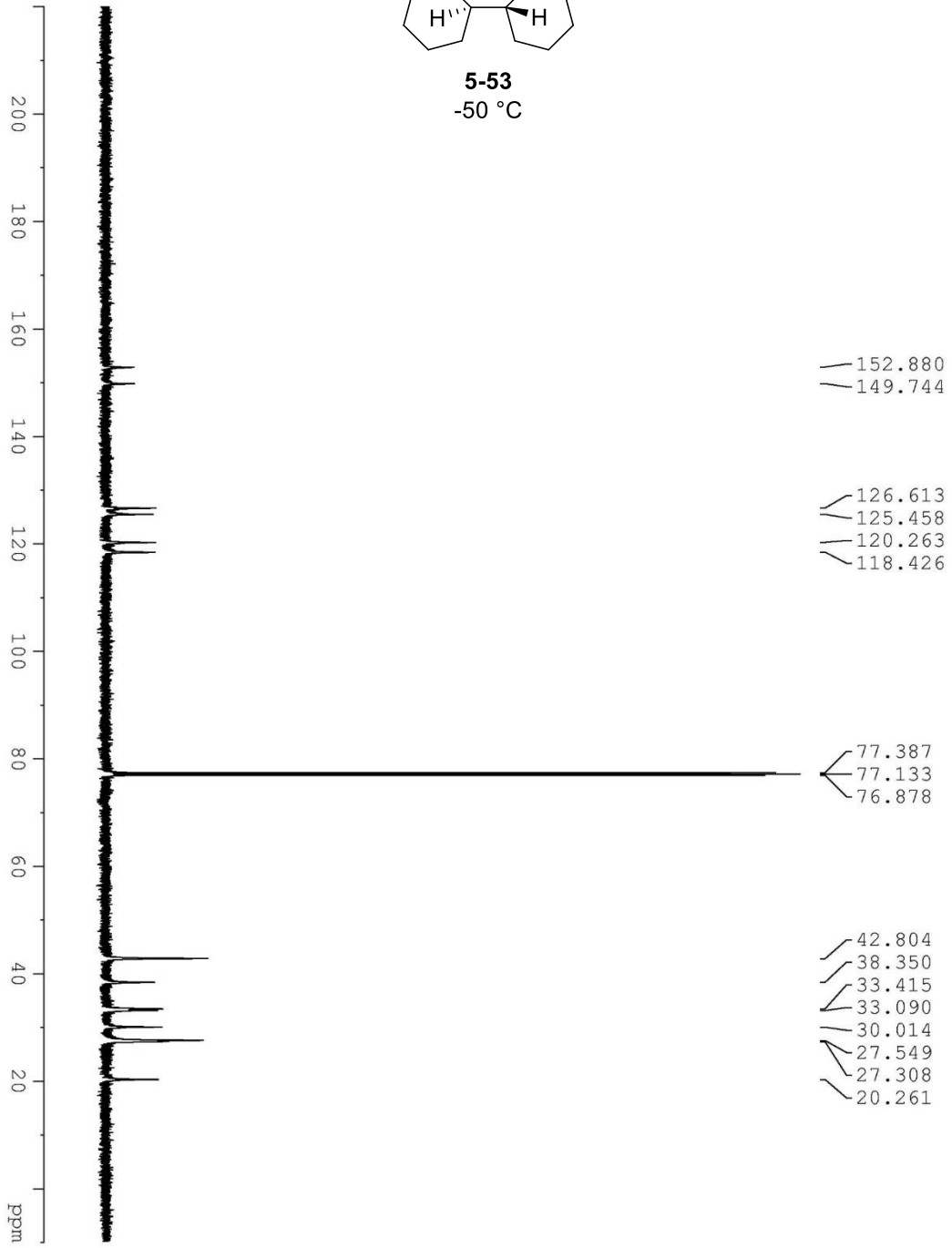


5-53

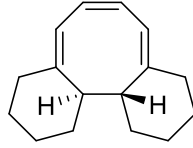




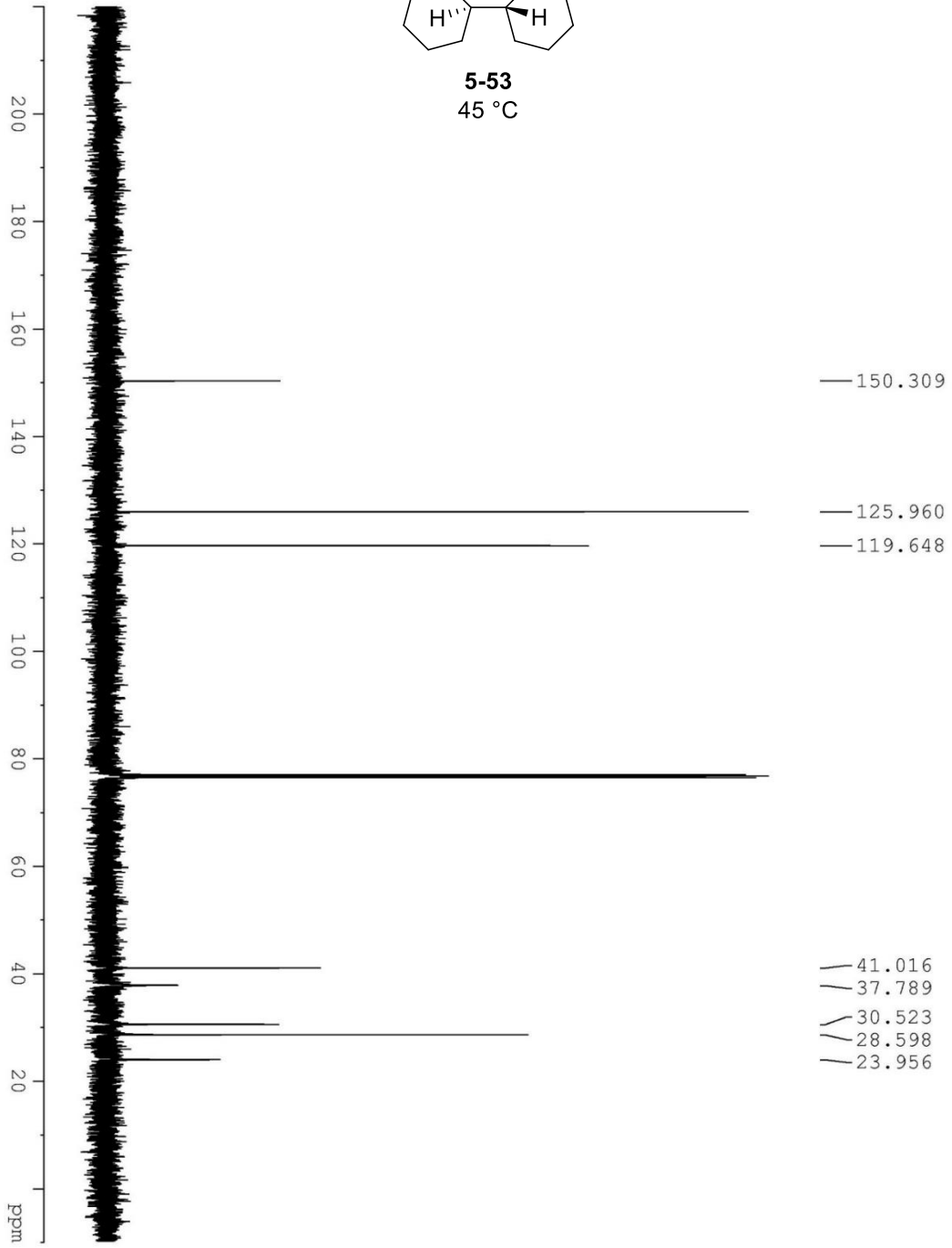
**5-53**  
-50 °C

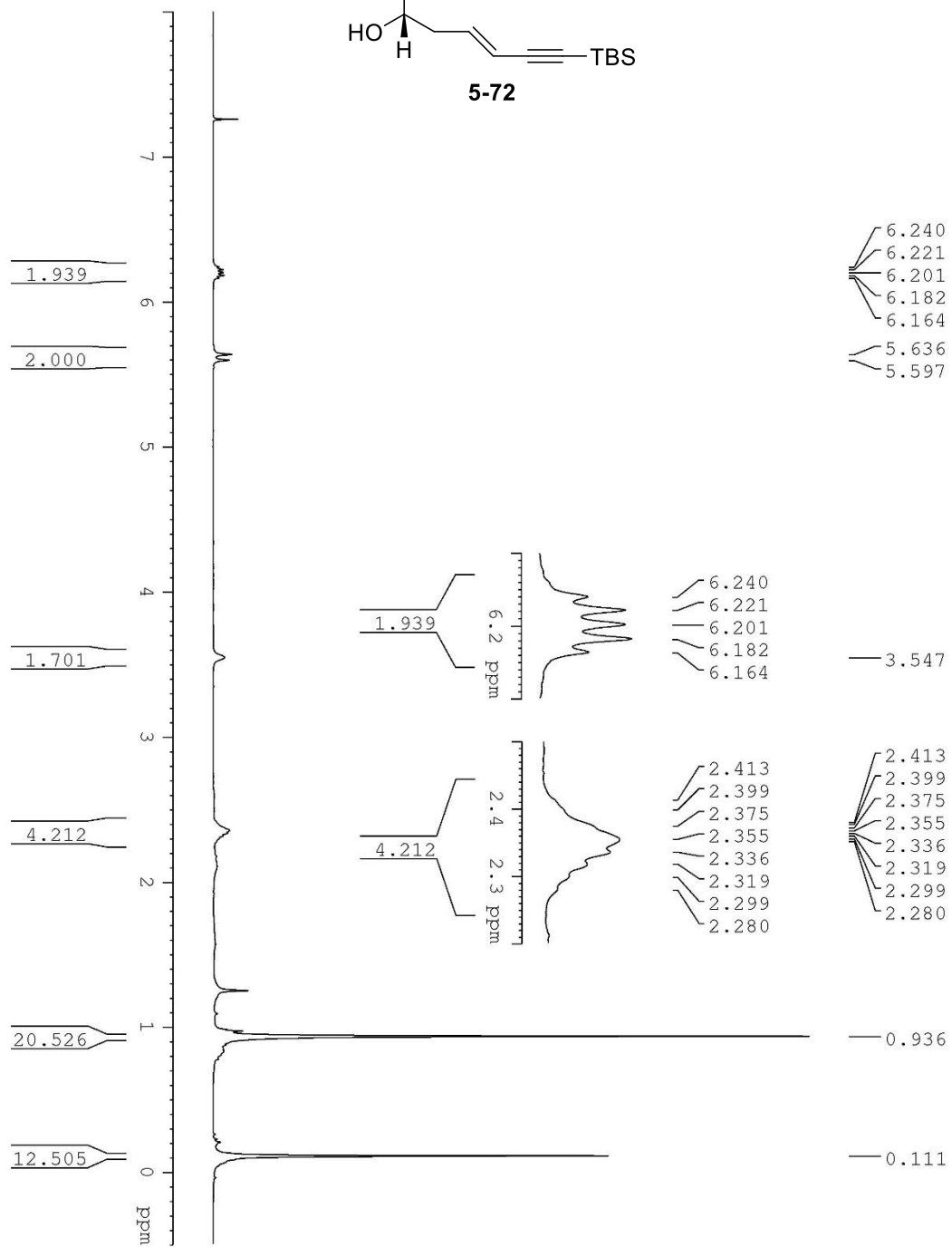
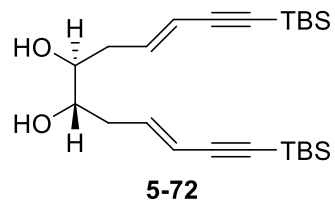






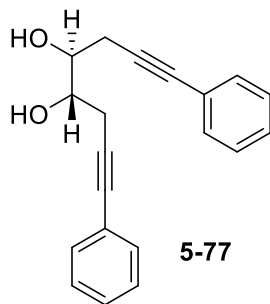
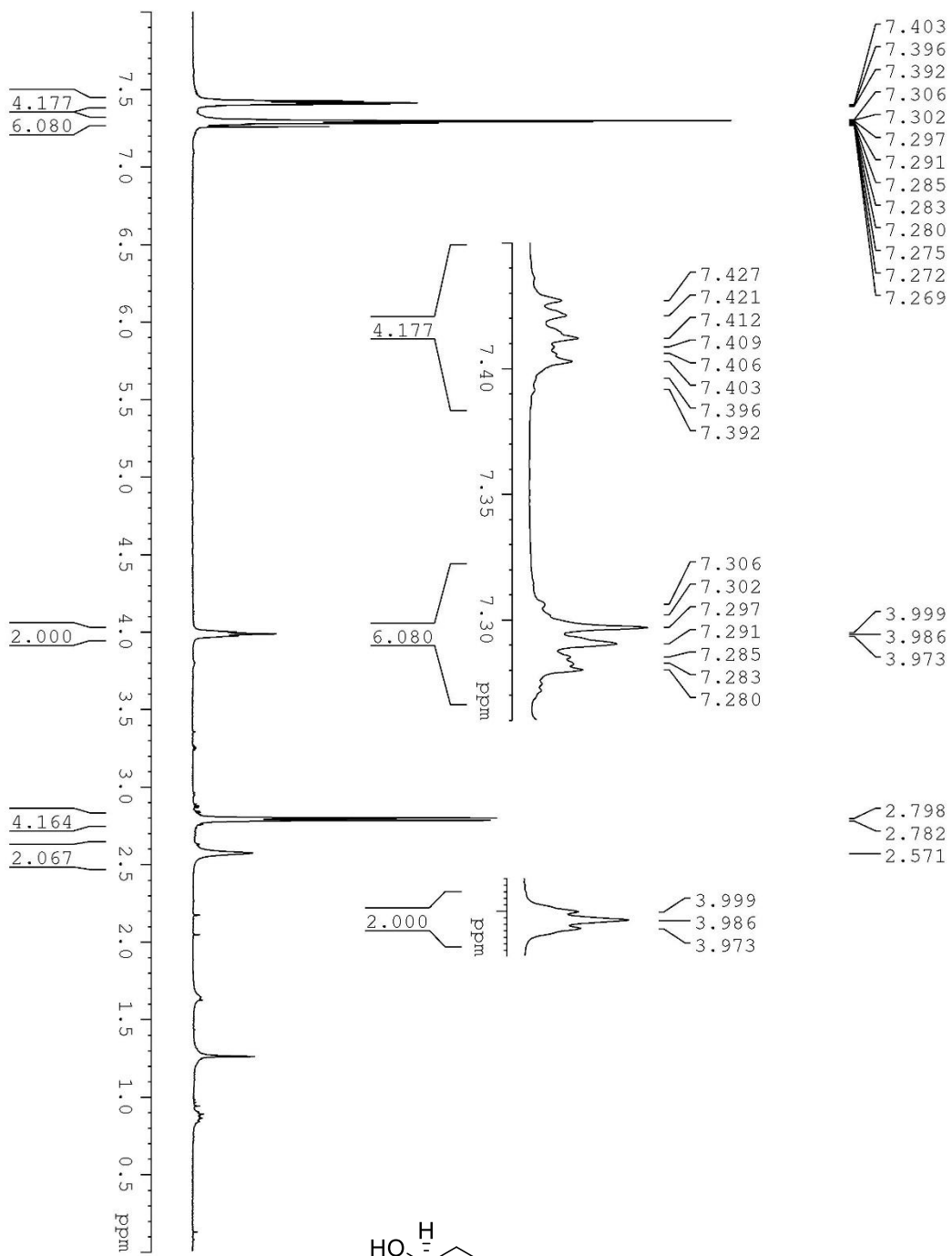
**5-53**  
45 °C

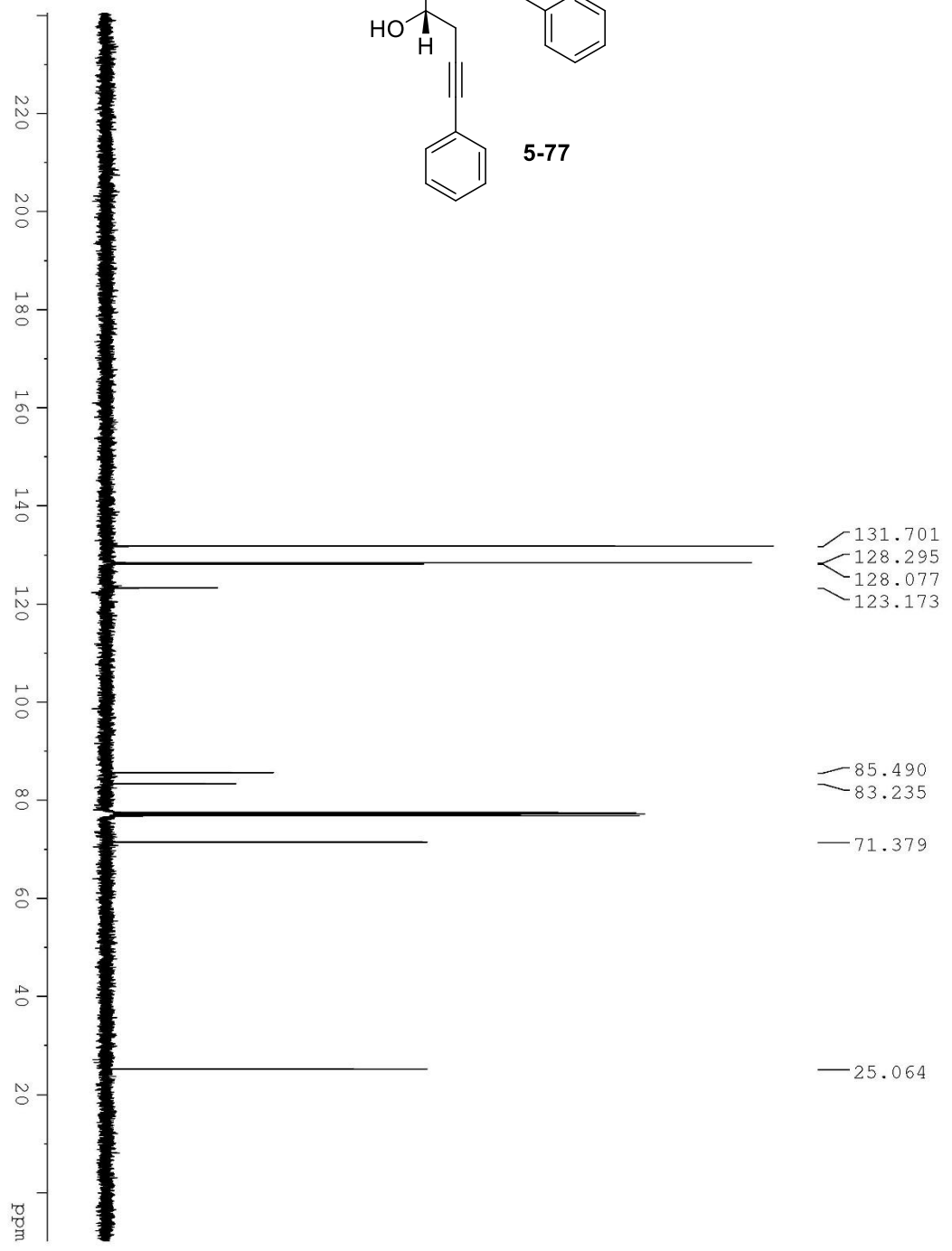
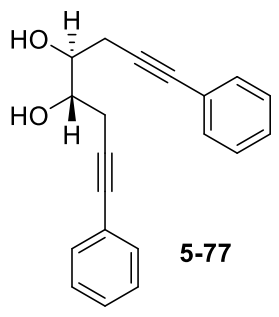


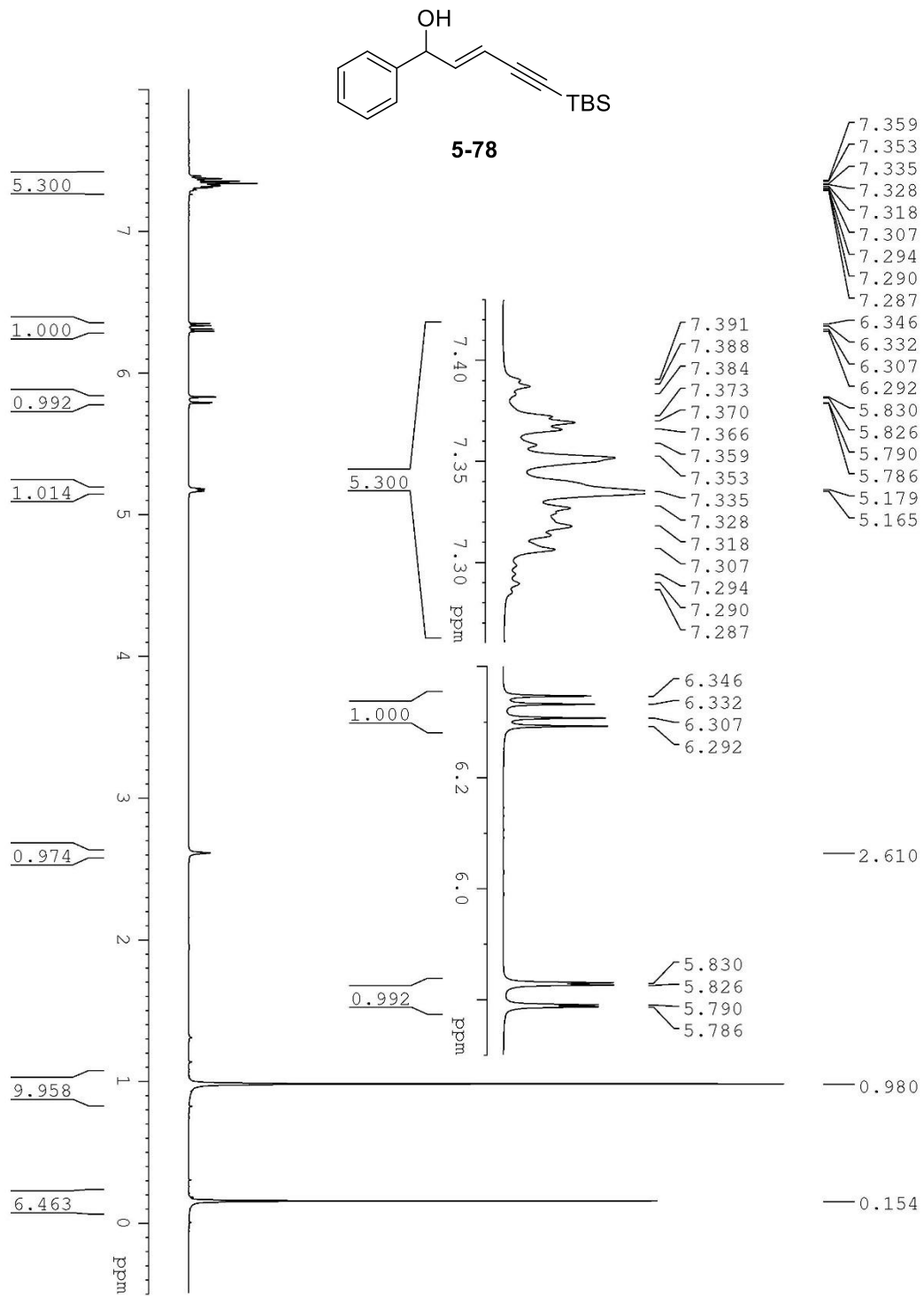


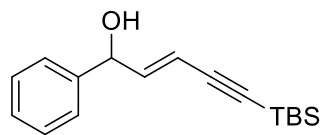




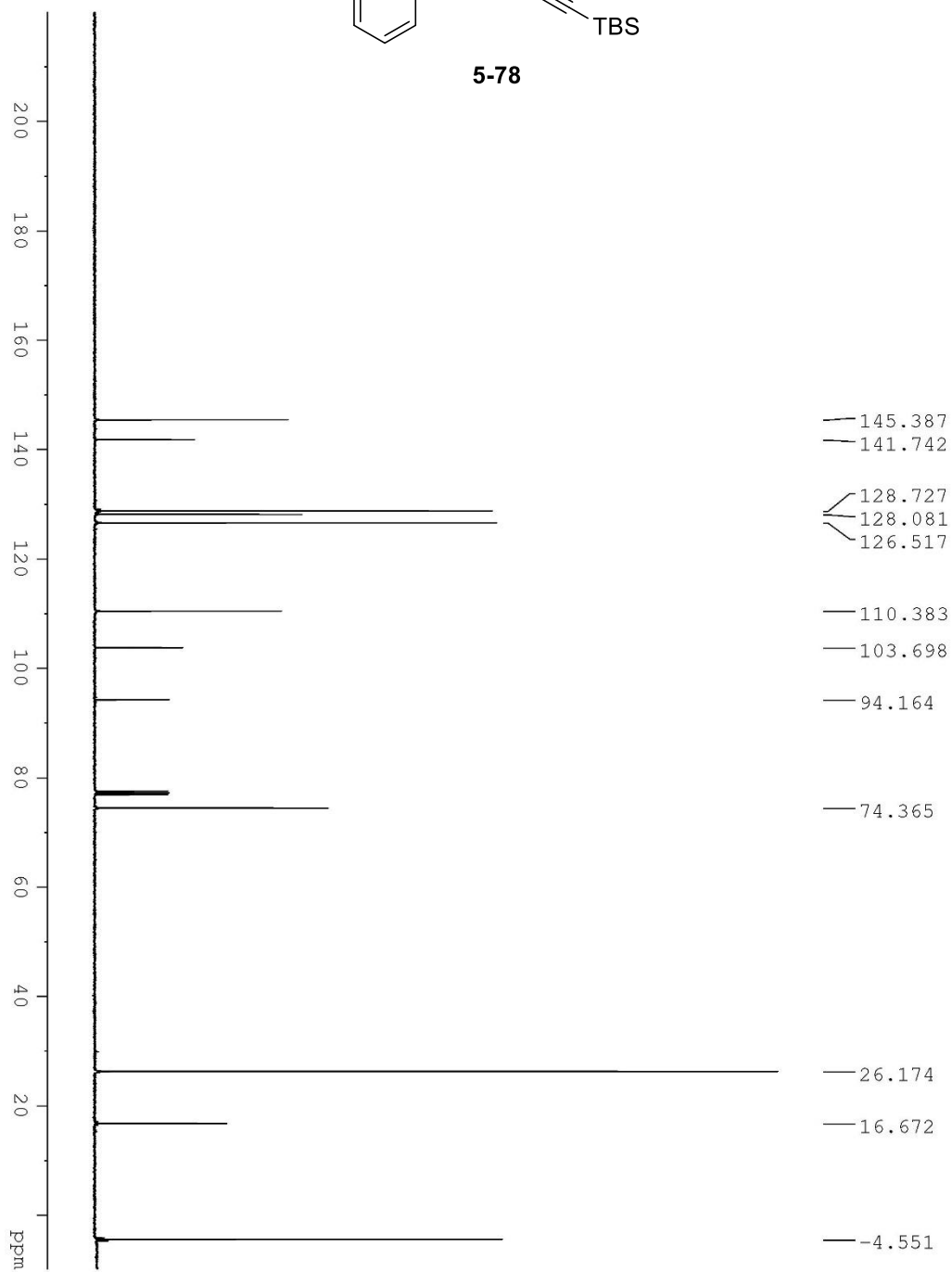






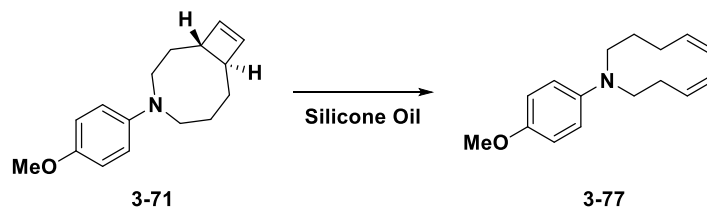


5-78



## Appendix B

### Experimental Kinetic Data



**Scheme A.1** Ring opening reaction for kinetic studies.

**Table A.1.** Kinetic data for conversion of cyclobutene 3-71 to diene 3-77.

T = 185 °C (458 K)		T = 190 °C (463 K)		T = 197 °C (470 K)		T = 218 °C (491 K)	
Time (min)	Percent Conversion	Time (min)	Percent Conversion	Time (min)	Percent Conversion	Time (min)	Percent Conversion
0	0.0%	0	0.0%	0	0.0%	0	0.0%
120	5.1%	120	8.8%	120	11.2%	70	35.9%
240	11.9%	240	13.6%	240	24.3%	110	47.9%
360	15.5%	360	19.7%	360	32.9%	150	60.0%
485	16.7%	480	23.4%	480	42.9%	195	70.0%
600	22.8%	540	25.6%			235	76.1%
						275	81.6%
						315	85.5%

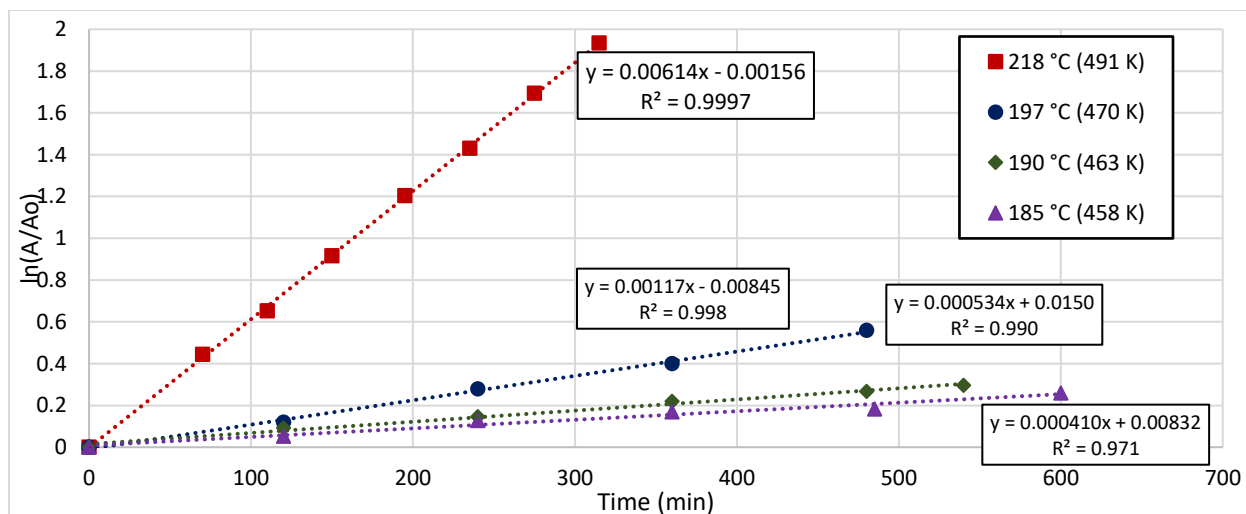


**Figure A.1.** Plot of temperature dependent conversion of cyclobutene 3-71 to diene 3-77 at four temperatures.

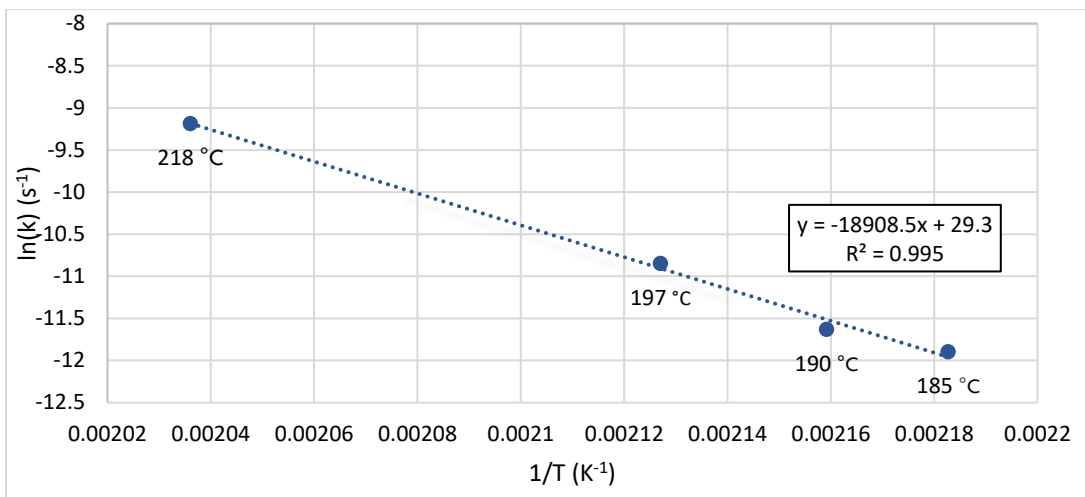


**Figure A.2. Arrhenius plot showing temperature dependent rate constant at four temperatures for thermal ring opening of cyclobutene 3-71 to diene 3-77.**

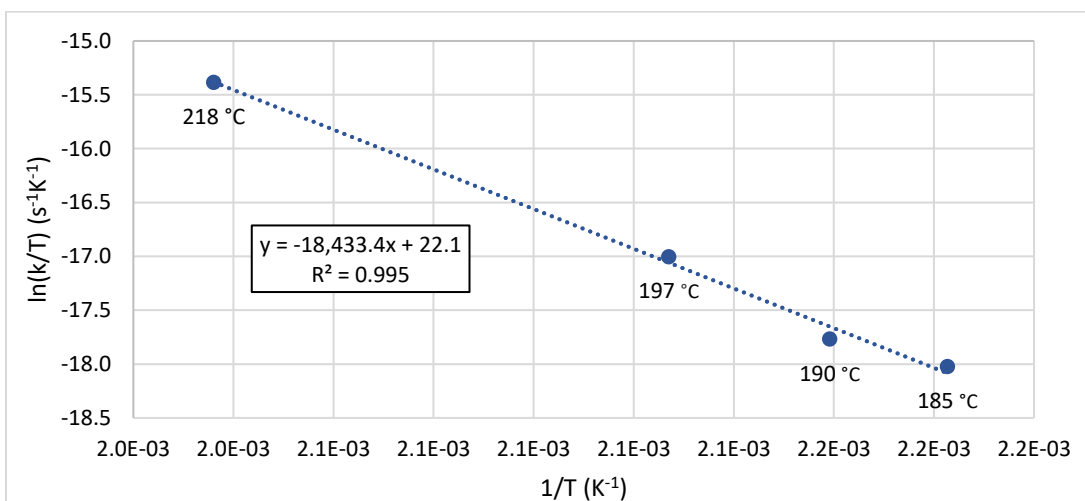


**Figure A.3. Eyring plot showing temperature dependent rate constant at four temperatures for thermal ring opening of cyclobutene 3-71 to diene 3-77.**

## Appendix C

### Computational Data

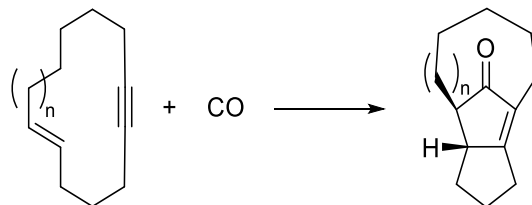


Figure A.4. Computed structures and representative reaction.

Table A.2. Enyne single point energies and zero point energies.

N	Enyne Single Point Energy (hartrees)	Enyne Single Point Energy (kcal/mol)	Enyne Zero-Point Energy (kJ/mol)	Enyne Zero-Point Energy (kcal/mol)
0	-428.636985	-268973.5658	638.22	152.5382409
1	-467.944377	-293639.3081	715.57	171.0253346
2	-507.250188	-318304.0582	791.09	189.0750478
3	-546.554622	-342967.9443	866.78	207.165392
4	-585.855788	-367629.7797	941.68	225.0669216
5	-625.165621	-392297.0537	1017.85	243.2719885

Table A.3. Enyne temperature corrections and Gibbs free energies.

N	Enyne Temperature Correction (kJ/mol)	Enyne Temperature Correction (kcal/mol)	Enyne Gibbs Free Energy (kcal/mol)
0	28.61	6.837954111	-268792.4176
1	31.12	7.437858509	-293437.1627
2	33.68	8.049713193	-318081.3032
3	36.17	8.644837476	-342724.6089
4	38.81	9.27581262	-367365.9028
5	41.18	9.842256214	-392012.6017

**Table A.4. Cyclopentenone single point energies and zero point energies.**

N	Cyclopentenone Single Point Energy (hartrees)	Cyclopentenone Single Point Energy (kcal/mol)	Cyclopentenone Zero-Point Energy (kJ/mol)	Cyclopentenone Zero-Point Energy (kcal/mol)
0	-541.896699	-340045.0557	674.22	161.1424474
1	-581.251085	-364740.2871	751.29	179.5626195
2	-620.587804	-389424.4323	828.23	197.9517208
3	-659.913015	-414101.3561	905.67	216.460325
4	-699.230709	-438773.563	979.1	234.0105163
5	-738.554115	-463449.3541	1054.72	252.08413

**Table A.5. Cyclopentenone temperature corrections and Gibbs free energies.**

N	Cyclopentenone Temperature Correction (kJ/mol)	Cyclopentenone Temperature Correction (kcal/mol)	Cyclopentenone Gibbs Free Energy (kcal/mol)
0	28.51	6.814053537	-339855.4032
1	31.03	7.416347992	-364529.6945
2	33.51	8.009082218	-389192.9706
3	35.77	8.549235182	-413849.1258
4	38.5	9.201720841	-438501.0525
5	41.15	9.835086042	-463156.1200

**Table A.6. Carbon monoxide single point energies and zero point energies.**

Compound	CO Single Point Energy (hartrees)	CO Single Point Energy (kcal/mol)	CO Zero-Point Energy (kJ/mol)	CO Zero-Point Energy (kcal/mol)
A-13	-113.309353	-71102.63879	13.22	3.159655832

**Table A.7. Carbon monoxide temperature corrections and Gibbs free energies.**

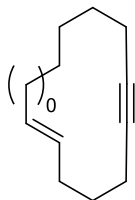
Compound	CO Temperature Correction (kJ/mol)	CO Temperature Correction (kcal/mol)	CO Gibbs Free Energy (kcal/mol)
A-13	8.68	2.07456979	-71090.79914



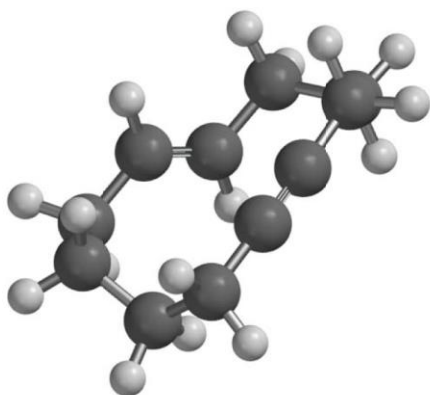
**Table A.8. Gibbs free energies of reaction.**

<b>N</b>	<b>CO Gibbs Free Energy (kcal/mol)</b>	<b>Enyne Gibbs Free Energy (kcal/mol)</b>	<b>Cyclopentenone Gibbs Free Energy (kcal/mol)</b>	<b>Gibbs Free Energy of Reaction (kcal/mol)</b>
0	-71090.79914	-268792.4176	-339855.4032	27.81
1	-71090.79914	-293437.1627	-364529.6945	-1.73
2	-71090.79914	-318081.3032	-389192.9706	-20.87
3	-71090.79914	-342724.6089	-413849.1258	-33.72
4	-71090.79914	-367365.9028	-438501.0525	-44.35
5	-71090.79914	-392012.6017	-463156.12	-52.72

## Computed Coordinates



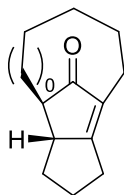
(*E*)-cyclododec-1-en-6-yne  
**A-1**



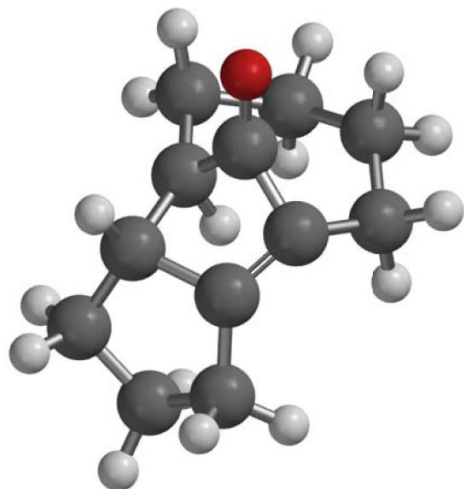
Cartesian Coordinates (Angstroms)				
Atom	X	Y	Z	
1 C C1	1.6142940	-2.0607164	-0.0916664	
2 C C2	0.1681886	-1.8623299	-0.1954774	
3 C C4	0.1910698	1.5559206	-0.4399848	
4 C C5	-0.7588629	1.4675875	0.4930097	
5 C C6	-1.0144870	-1.6112028	-0.2380011	
6 C C8	-2.2300151	1.3022253	0.2158404	
7 C C9	-2.4354011	-1.2560920	-0.2676007	
8 C C10	-2.8201505	-0.0621701	0.6391187	
9 C C11	2.4616385	0.3765017	-0.6022475	
10 C C12	2.3869294	-0.8087053	0.3953269	
11 H H3	2.0208621	-2.3802101	-1.0624927	
12 H H4	1.8192959	-2.8875927	0.6032775	
13 H H7	-2.4247012	1.4603227	-0.8539264	
14 H H8	-2.7881571	2.0850806	0.7508828	
15 H H9	-2.7380061	-1.0274790	-1.3005081	
16 H H10	-3.0355144	-2.1267142	0.0330358	
17 H H11	-3.9153248	0.0156853	0.6285927	

18 H H12	-2.5313012	-0.2880531	1.6737376
19 H H13	3.5133847	0.6661194	-0.7210716
20 H H15	3.4058779	-1.1390265	0.6340449
21 H H16	1.9455022	-0.4748625	1.3424515
22 H H17	-0.4703588	1.4860488	1.5466926
23 H H18	-0.1061445	1.5117382	-1.4905758
24 H H19	2.1273243	0.0505287	-1.5966127
25 C C3	1.6713130	1.6464270	-0.1934860
26 H H2	1.8658168	1.8680134	0.8646458
27 H H5	2.0769275	2.4929554	-0.7670059

Three lowest frequencies (cm-1): 39, 85, 110 (no imaginary frequencies observed)



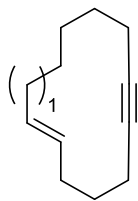
Cyclopentenone **A-2**



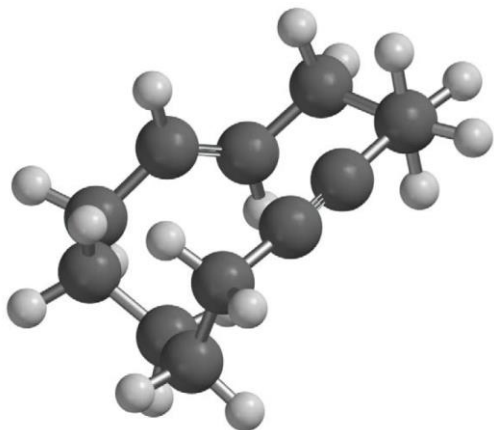
		Cartesian Coordinates (Angstroms)		
Atom		X	Y	Z
1 C	C1	-0.9970510	1.9581358	-0.1067579
2 C	C2	-0.0404589	1.2749930	0.8741589
3 C	C3	-0.8215551	0.1455986	1.4210694
4 C	C4	-0.3923169	-0.9226334	0.4300593
5 C	C5	1.1233575	-0.8419467	1.0102956
6 C	C6	1.1980999	0.7349347	0.7859924
7 O	O1	-1.5620382	0.0252804	2.3723675
8 C	C7	-1.6900063	-1.6417062	0.0481327
9 C	C8	2.2813098	-1.3794009	0.1429845
10 C	C9	2.4029432	1.0707852	-0.0428672
11 C	C10	2.6574852	-0.2376992	-0.8315343
12 H	H1	1.1793327	-1.1941502	2.0441091
13 H	H2	-0.1708275	-0.4512628	-0.5264420
14 C	C11	-2.3579087	-0.4802186	-0.8140465
15 C	C12	-2.3137802	1.0525746	-0.3662707
16 H	H10	3.2685449	1.2995289	0.5966459
17 H	H9	2.2432508	1.9422378	-0.6887020
18 H	H11	2.0054864	-0.2641267	-1.7128994
19 H	H12	3.6888366	-0.3213183	-1.1898729
20 H	H7	2.0205376	-2.3065632	-0.3778766

21 H H8	3.1351204	-1.6057128	0.7941420
22 H H5	-1.5841423	-2.5297744	-0.5847898
23 H H6	-2.2909365	-1.9007134	0.9245161
24 H H13	-1.9064801	-0.5422844	-1.8141794
25 H H14	-3.4249251	-0.7024090	-0.9468644
26 H H16	-2.9381459	1.1583947	0.5256602
27 H H15	-2.8453037	1.5827058	-1.1671940
28 H H4	-1.3879666	2.9169136	0.2539606
29 H H3	-0.4804624	2.1598372	-1.0537970

Three lowest frequencies ( $\text{cm}^{-1}$ ): 110, 125, 171 (no imaginary frequencies observed)



(*E*)-cyclotridec-1-en-6-yne  
A-3

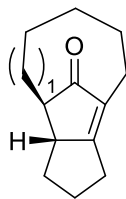


Cartesian Coordinates (Angstroms)

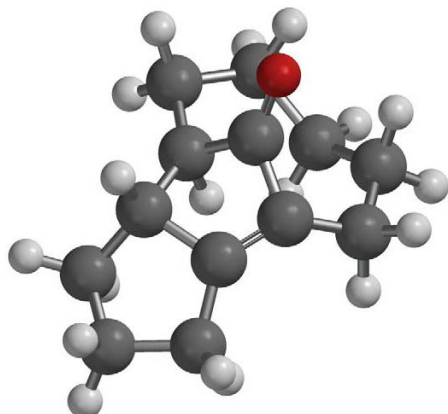
Atom	X	Y	Z
1 C C1	1.1644007	-0.1193747	2.4430302
2 C C2	-0.2293138	-0.1860309	1.9921798
3 C C4	0.2319572	-0.8219527	-1.7154480
4 C C5	-0.8664184	-0.0685912	-1.8131501
5 C C6	-1.3483464	-0.2612561	1.5354861
6 C C7	1.6480549	-0.3378719	-1.8866123
7 C C8	-2.2777296	-0.5266226	-1.5560148
8 C C9	-2.7181596	-0.3836713	1.0278249
9 C C10	-2.9885796	0.1920765	-0.3828310
10 H H1	-0.7598214	0.9802798	-2.1011140
11 H H2	0.1218420	-1.8653238	-1.4111021
12 C C11	2.3579423	-0.1598988	-0.5210910
13 C C12	1.8499702	1.0741216	0.2460997
14 C C13	1.9862152	1.0130956	1.7741111
15 H H3	1.6442071	-1.0878249	2.2449179
16 H H4	1.2040243	0.0125495	3.5330616
17 H H5	2.2149909	-1.0564836	-2.4945588
18 H H6	1.6595934	0.6162188	-2.4309051
19 H H7	-2.2972769	-1.6122733	-1.3882905
20 H H8	-2.8745245	-0.3455672	-2.4626834
21 H H9	-3.0069235	-1.4456158	1.0306286
22 H H10	-3.4037344	0.1103407	1.7313922
23 H H11	-4.0727429	0.1278036	-0.5424632

24 H H12	-2.7360981	1.2601842	-0.3961606
25 H H13	2.1979778	-1.0730990	0.0671735
26 H H14	3.4425274	-0.0843647	-0.6767955
27 H H15	2.3742413	1.9659341	-0.1235727
28 H H16	0.7889056	1.2210428	0.0168872
29 H H17	3.0370697	0.8886381	2.0702086
30 H H18	1.6557492	1.9735372	2.1897917

Three lowest frequencies (cm-1): 46, 102, 109 (no imaginary frequencies observed)



Cyclopentenone **A-4**



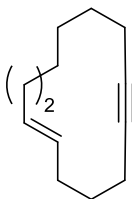
Cartesian Coordinates (Angstroms)

Atom	X	Y	Z
1 C C1	0.6520258	0.1910676	-2.2371602
2 C C2	-0.1137402	-0.6906360	-1.2846373
3 C C3	0.7703715	-1.2066931	-0.2107115
4 C C4	0.2580744	-0.4506170	0.9885409
5 C C5	-1.2175901	-0.9709158	0.8287884
6 C C6	-1.3253545	-0.7057179	-0.7120997
7 O O1	1.6409756	-2.0354965	-0.2544520
8 C C7	1.3856071	-0.2727530	1.9795046
9 C C8	-2.3686210	-0.1138351	1.3687038
10 C C9	-2.6724483	-0.1308750	-1.0535437
11 C C10	-3.4490863	-0.2078064	0.2776667
12 H H1	-1.3266690	-2.0209767	1.1142300
13 H H2	0.0959411	0.5680204	0.6444871
14 C C11	2.5240490	0.4001887	1.1114743
15 C C13	2.0244638	0.6345987	-1.6007797
16 H H3	0.0443733	1.0682030	-2.4808085
17 H H4	0.8931085	-0.3024837	-3.1828294
18 H H5	1.0966847	0.3784318	2.8075948
19 H H6	1.7599977	-1.2111638	2.3909579
20 H H7	-2.0318377	0.9247618	1.4615231
21 H H8	-2.7239958	-0.4393840	2.3472039
22 H H9	-2.5589172	0.9084174	-1.3862806
23 H H10	-3.1678836	-0.6731583	-1.8607874
24 H H11	-4.2100323	0.5682101	0.3698448



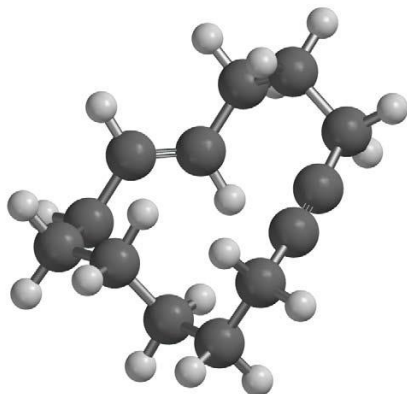
25 H H12	-3.9529235	-1.1760912	0.3488283
26 H H13	3.1001651	1.0532101	1.7710604
27 H H14	3.2067186	-0.3857977	0.7830657
28 H H17	2.7063836	-0.2180272	-1.6550867
29 H H20	2.4207694	1.3818086	-2.2930524
30 C C12	2.1699332	1.2662601	-0.1609061
31 H H16	1.3332680	1.9437857	0.0417605
32 H H18	3.0361891	1.9254645	-0.2620994

Three lowest frequencies (cm-1): 91, 119, 157 (no imaginary frequencies observed)



(*E*)-cyclotetradec-1-en-6-yne

**A-5**

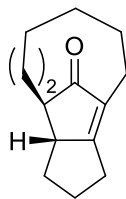


Cartesian Coordinates (Angstroms)

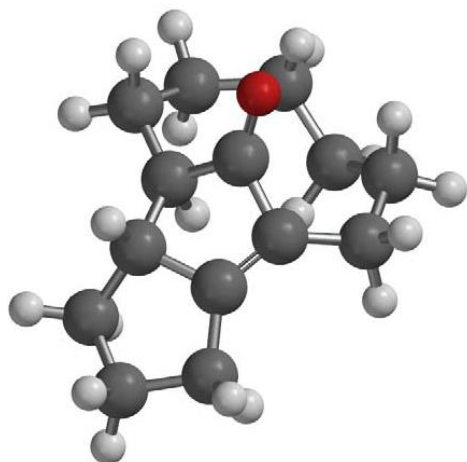
Atom	X	Y	Z
1 C C1	-1.1449202	1.3742026	2.3056089
2 C C2	0.1662167	0.7370894	2.1489811
3 C C4	0.5553815	-0.6801128	-2.0573793
4 C C5	1.2945520	-1.1184904	-1.0330836
5 C C6	1.2542452	0.2410990	1.9572106
6 C C8	2.7664974	-0.8594762	-0.8416593
7 C C9	2.6114163	-0.2515580	1.7039213
8 C C10	3.1532710	0.1109938	0.2966127
9 C C11	-1.8546747	0.2181411	-2.0825191
10 C C12	-2.1818122	-0.1288516	0.4521075
11 C C13	-1.8455118	0.8517566	-0.6808947
12 C C14	-2.3434912	0.5121889	1.8384788
13 H H3	-1.1372419	2.3181216	1.7431731
14 H H4	-1.3014983	1.6554810	3.3562047
15 H H7	3.1919935	-0.4705277	-1.7759235
16 H H8	3.2684406	-1.8209788	-0.6516235
17 H H9	3.2819915	0.1796635	2.4602063
18 H H10	2.6620421	-1.3403826	1.8509570
19 H H11	2.8220071	1.1248452	0.0443777
20 H H12	4.2496120	0.1380887	0.3492095
21 H H13	-2.8745884	-0.1129999	-2.3255752
22 H H15	-3.1104890	-0.6661622	0.2095154
23 H H16	-1.3930653	-0.8865319	0.5184646
24 H H17	-2.5666989	1.6825743	-0.6721966

25 H H18	-0.8574179	1.2900807	-0.4959281
26 H H19	-3.2365461	1.1519714	1.8576476
27 H H20	-2.5144662	-0.2842359	2.5739690
28 H H24	0.8150423	-1.7416395	-0.2762947
29 H H29	-1.5993517	0.9901912	-2.8219693
30 H H14	1.0267929	-0.0508875	-2.8170357
31 C C3	-0.9048725	-0.9893679	-2.2646251
32 H H2	-1.0476770	-1.3774788	-3.2839529
33 H H5	-1.2051791	-1.7968073	-1.5859852

Three lowest frequencies (cm-1): 60, 100, 107 (no imaginary frequencies observed)



Cyclopentenone **A-6**

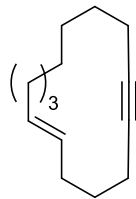


Cartesian Coordinates (Angstroms)

Atom	X	Y	Z
1 C C1	0.9524406	-1.6037364	1.6768487
2 C C2	0.1525359	-0.3518007	1.4469958
3 C C3	0.8420813	0.7457344	0.7200447
4 C C4	-0.1052195	1.0747849	-0.4243150
5 C C5	-1.3853744	1.2204905	0.4715458
6 C C6	-1.1478182	-0.0037727	1.4002557
7 O O1	1.8818755	1.3064323	1.0121509
8 C C7	0.5969433	1.8994916	-1.4906606
9 C C8	-2.7786800	0.9175574	-0.1083000
10 C C9	-2.4565131	-0.6566480	1.7665062
11 C C10	-3.5243365	0.2193566	1.0539139
12 H H1	-1.3912151	2.1744352	1.0167980
13 H H2	-0.3277677	0.1238955	-0.9168425
14 C C11	1.4709051	0.8846193	-2.2989628
15 C C12	1.8112320	-1.4424684	-0.8836941
16 C C13	2.4031503	-0.1339340	-1.5536406
17 C C14	2.1234963	-1.7113041	0.6366811
18 H H3	0.2902485	-2.4764732	1.5994904
19 H H4	1.3957192	-1.6417896	2.6814647
20 H H5	-0.0954828	2.3927787	-2.1835980
21 H H6	1.2236170	2.6722380	-1.0320750
22 H H7	-2.6832879	0.2283095	-0.9588368
23 H H8	-3.3033596	1.8088893	-0.4677037

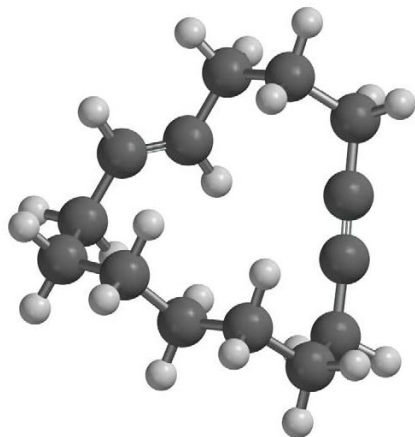
24 H H9	-2.4784353	-1.6942018	1.4024226
25 H H10	-2.6189447	-0.7063201	2.8499724
26 H H11	-4.3853030	-0.3636081	0.7111758
27 H H12	-3.9052489	0.9745611	1.7528984
28 H H13	0.7953031	0.3108436	-2.9519666
29 H H14	2.1161920	1.4610547	-2.9745814
30 H H15	0.7319176	-1.5157672	-1.0577208
31 H H16	2.2321287	-2.2883938	-1.4390537
32 H H17	3.0125134	0.4073342	-0.8248721
33 H H18	3.1042833	-0.4769533	-2.3246980
34 H H19	2.5316743	-2.7243783	0.7346775
35 H H20	2.9187291	-1.0312569	0.9576791

Three lowest frequencies (cm-1): 83, 115, 151 (no imaginary frequencies observed)



(E)-cyclopentadec-1-en-6-yne

**A-7**

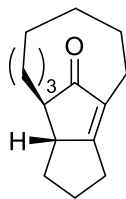


Cartesian Coordinates (Angstroms)

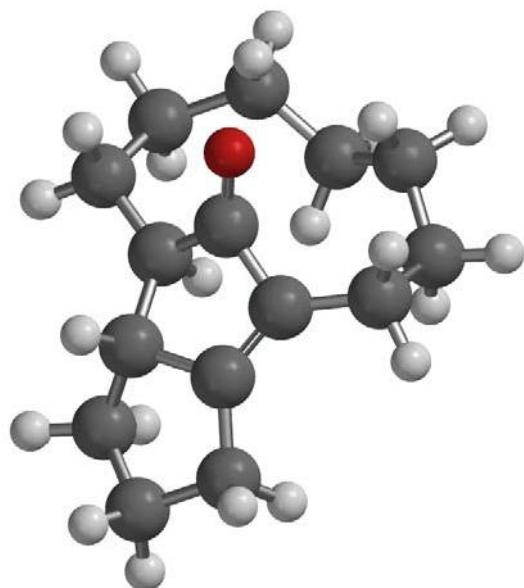
Atom	X	Y	Z
1 C C1	0.3755845	-2.2864943	0.8222421
2 C C3	-1.4467869	1.9935454	0.2857895
3 C C4	-1.8383545	0.7969057	0.7377750
4 C C5	-0.8049239	-2.3327653	0.5548187
5 C C6	-0.2025110	2.7230681	0.7199648
6 C C7	-3.0706028	0.0648868	0.2741567
7 C C8	-2.2283899	-2.4252832	0.2152379
8 C C9	-2.8183877	-1.2174757	-0.5522127
9 H H1	-1.2300658	0.2939545	1.4894467
10 C C10	0.8166234	2.9511292	-0.4229424
11 C C11	1.2671446	1.6755886	-1.1534192
12 C C12	1.9378638	0.6273549	-0.2563319
13 C C13	2.1905792	-0.7016351	-0.9805481
14 C C14	2.7007598	-1.8408044	-0.0840713
15 C C15	1.8016900	-2.1581656	1.1384493
16 H H3	-0.4764125	3.7076345	1.1277639
17 H H4	0.2719955	2.1733218	1.5423476
18 H H5	-3.6772751	0.7445537	-0.3387430
19 H H6	-3.6903714	-0.2041491	1.1436524
20 H H7	-2.3808824	-3.3251166	-0.3975848
21 H H8	-2.8157437	-2.5891721	1.1312976
22 H H9	-2.1728867	-0.9806036	-1.4064128
23 H H10	-3.7834050	-1.5418586	-0.9639540

24 H H11	0.3746497	3.6375161	-1.1591320
25 H H12	1.6909847	3.4723245	-0.0076397
26 H H13	1.9498437	1.9550689	-1.9686505
27 H H14	0.3915016	1.2156667	-1.6304770
28 H H15	2.8815468	1.0248405	0.1480221
29 H H16	1.2873113	0.4366122	0.6039698
30 H H17	1.2507875	-1.0260222	-1.4454689
31 H H18	2.9061850	-0.5499881	-1.8009496
32 H H19	2.8016679	-2.7480299	-0.6933294
33 H H20	3.7043709	-1.6060791	0.2961689
34 H H21	2.1632045	-3.0824169	1.6096205
35 H H22	1.9258354	-1.3720006	1.8956781
36 H H25	-2.0531304	2.4940883	-0.4745345

Three lowest frequencies (cm-1): 43, 87, 95 (no imaginary frequencies observed)



Cyclopentenone **A-8**



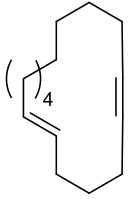
Cartesian Coordinates (Angstroms)

Atom	X	Y	Z
1 C C1	0.9250544	1.0746826	0.5639335
2 C C2	0.0331347	0.0962912	1.2417170
3 C C3	0.1076370	-1.1741099	0.3952048
4 C C4	1.6541266	-1.1865548	0.2053379
5 C C5	1.9167810	0.3253633	0.0446845
6 O O1	-0.5517276	0.2488387	2.2997980
7 C C6	-0.8432887	-2.2613467	0.8775468
8 C C7	2.3040271	-1.7621035	-1.0656099
9 C C8	3.1134658	0.5619827	-0.8429889
10 C C9	3.5546351	-0.8705148	-1.2600665
11 H H1	2.1552793	-1.5876710	1.0993384
12 H H2	-0.2310817	-0.8879665	-0.6067164
13 C C10	-2.2779055	-1.9656016	0.3425037
14 C C11	-2.8958393	-0.5523129	0.5822271
15 C C12	-2.4634721	0.6010335	-0.3906881
16 C C13	-2.1120708	1.9864464	0.2526064
17 C C14	-0.8360262	2.7051507	-0.2893953
18 C C15	0.5001049	2.5097910	0.4974636
19 H H3	-0.5389345	-3.2549529	0.5243831
20 H H4	-0.8496313	-2.2908452	1.9735658

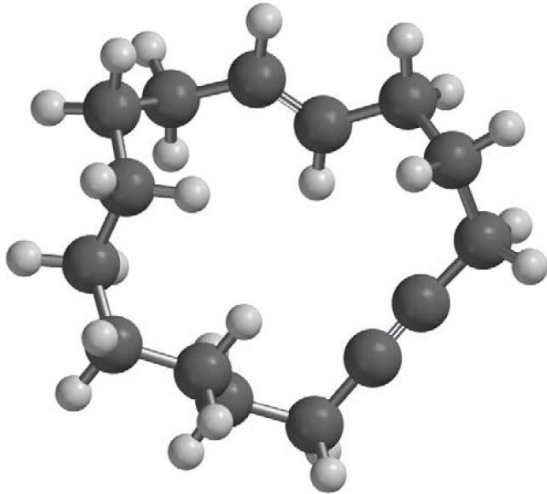


21 H H5	1.6202482	-1.6386048	-1.9167136
22 H H6	2.5522574	-2.8259593	-0.9915308
23 H H7	2.8278568	1.1654622	-1.7150673
24 H H8	3.9175614	1.1103200	-0.3371272
25 H H9	3.9457575	-0.9075279	-2.2818800
26 H H10	4.3563904	-1.2161387	-0.5958069
27 H H11	-2.2903127	-2.1725376	-0.7387059
28 H H12	-2.9542617	-2.7034969	0.7931806
29 H H13	-2.7020982	-0.2587325	1.6170540
30 H H14	-3.9835613	-0.6707924	0.5000429
31 H H15	-1.6237568	0.2758815	-1.0098144
32 H H16	-3.2756611	0.7594493	-1.1109752
33 H H17	-2.9597989	2.6615209	0.0847243
34 H H18	-2.0243466	1.8822877	1.3377931
35 H H19	-0.6729354	2.4215356	-1.3386588
36 H H20	-1.0259358	3.7861667	-0.2977629
37 H H21	1.2759209	3.1326145	0.0361304
38 H H22	0.3524077	2.8829513	1.5202724

Three lowest frequencies (cm-1): 84, 100, 135 (no imaginary frequencies observed)



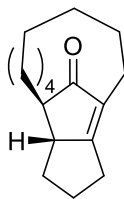
(E)-cyclohexadec-1-en-6-yne  
A-9



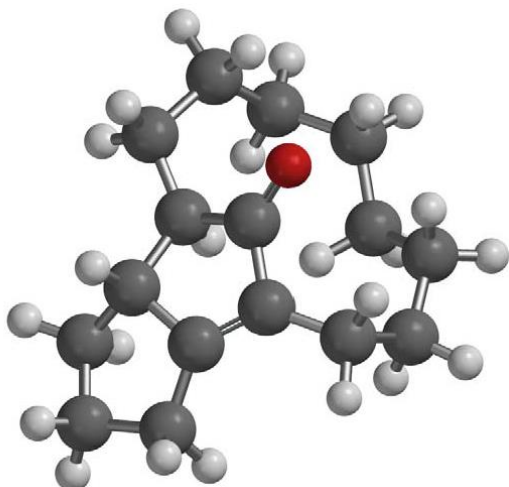
		Cartesian Coordinates (Angstroms)		
Atom		X	Y	Z
-----		-----	-----	-----
1 C	C1	-0.3309173	1.0631838	-2.5746259
2 C	C3	-0.6176326	0.9442322	2.3706895
3 C	C4	-0.7421443	1.7017051	1.2758910
4 C	C5	-0.1070237	2.1109899	-2.0097996
5 C	C6	-1.1485206	-0.4522683	2.5541435
6 C	C7	-0.2193009	3.1102147	1.1639485
7 C	C8	0.2013226	3.4100902	-1.4038437
8 C	C9	0.7904723	3.3757496	0.0266433
9 C	C10	-0.0351358	-1.4989130	2.7909286
10 C	C11	0.8082553	-1.8032542	1.5416918
11 C	C12	0.1097470	-2.7440131	0.5466326
12 C	C13	0.8610865	-2.9258603	-0.7837158
13 C	C14	0.8215592	-1.7100697	-1.7284899
14 C	C15	-0.5600067	-1.4423181	-2.3383244
15 C	C16	-0.6017477	-0.2040338	-3.2607525
16 H	H3	-1.8239933	-0.4646930	3.4227564
17 H	H4	-1.7588800	-0.7363588	1.6868030
18 H	H5	0.2544804	3.3857241	2.1154365
19 H	H6	-1.0654134	3.8046564	1.0334624
20 H	H7	0.9198935	3.9259737	-2.0567075
21 H	H8	-0.7003177	4.0406102	-1.3999621

22 H H9	1.6048998	2.6425131	0.0694278
23 H H10	1.2415479	4.3603163	0.2076670
24 H H11	0.6186215	-1.1342204	3.5954208
25 H H12	-0.4869020	-2.4290782	3.1633976
26 H H13	1.7603496	-2.2613520	1.8441909
27 H H14	1.0661211	-0.8537468	1.0549268
28 H H15	-0.0109567	-3.7263191	1.0249297
29 H H16	-0.9090711	-2.3858139	0.3462521
30 H H17	1.9095899	-3.1741307	-0.5655469
31 H H18	0.4480246	-3.7967435	-1.3127783
32 H H19	1.1601714	-0.8093982	-1.2013117
33 H H20	1.5397012	-1.8725343	-2.5451263
34 H H21	-1.3082333	-1.3096693	-1.5473478
35 H H22	-0.8761909	-2.3154755	-2.9259094
36 H H23	0.1237452	-0.3362980	-4.0771832
37 H H24	-1.5886125	-0.1501521	-3.7414864
38 H H28	-1.2651259	1.3037026	0.4063646
39 H H31	-0.0834629	1.3570524	3.2313069

Three lowest frequencies (cm<sup>-1</sup>): 35, 53, 71 (no imaginary frequencies observed)



Cyclopentenone **A-10**

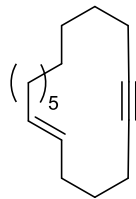


Cartesian Coordinates (Angstroms)

Atom	X	Y	Z
1 C C1	1.4093851	0.7900959	0.1518501
2 C C2	0.5620142	0.0291846	1.1158547
3 C C3	0.1470384	-1.2595061	0.3927550
4 C C4	1.4458239	-1.5441960	-0.4015282
5 C C5	1.9554372	-0.1273312	-0.6695229
6 O O1	0.2824079	0.3669519	2.2540830
7 C C6	-0.5969485	-2.2973586	1.2198808
8 C C7	1.4221355	-2.1500541	-1.8156871
9 C C8	2.7898002	-0.0932587	-1.9255380
10 C C9	2.6858592	-1.5453871	-2.4783121
11 H H1	2.1596323	-2.1032305	0.2244721
12 H H2	-0.5550613	-0.9289164	-0.3827108
13 C C10	-1.9083449	-1.7457640	1.8501584
14 C C11	-2.8299853	-0.8318886	0.9807544
15 C C12	-2.6511397	0.7105830	1.1587206
16 C C13	-1.8988396	1.4762847	0.0375130
17 C C14	-1.1085136	2.7245381	0.5117535
18 C C15	0.1890681	3.0163955	-0.2849923
19 C C16	1.4783599	2.2891636	0.2009581
20 H H3	-0.8363738	-3.1483690	0.5667297
21 H H4	0.0384760	-2.6897619	2.0243652
22 H H5	0.5210164	-1.8117761	-2.3460111

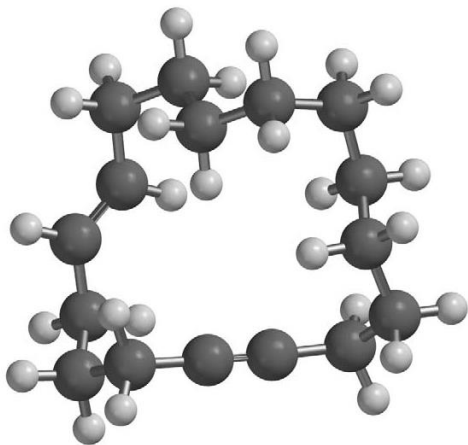
23 H H6	1.4236697	-3.2449784	-1.8305500
24 H H7	2.3824718	0.6395779	-2.6343408
25 H H8	3.8290437	0.2040937	-1.7370118
26 H H9	2.6457192	-1.5763684	-3.5717139
27 H H10	3.5685967	-2.1200474	-2.1721970
28 H H11	-2.4946316	-2.6178715	2.1672644
29 H H12	-1.6513365	-1.1996527	2.7618646
30 H H13	-3.8618315	-1.0774328	1.2594145
31 H H14	-2.7535771	-1.1062261	-0.0821372
32 H H15	-3.6446624	1.1637855	1.2709953
33 H H16	-2.1373258	0.8843705	2.1096957
34 H H17	-1.2081328	0.8057106	-0.4759693
35 H H18	-2.6140075	1.7768878	-0.7410198
36 H H19	-1.7589080	3.6065482	0.4513018
37 H H20	-0.8474425	2.6125111	1.5704129
38 H H21	0.4032665	4.0917510	-0.2303227
39 H H22	0.0263014	2.7939510	-1.3493180
40 H H23	2.3267596	2.6495251	-0.3936101
41 H H24	1.6647794	2.5874660	1.2416953

Three lowest frequencies (cm-1): 63, 87, 102 (no imaginary frequencies observed)



(*E*)-cycloheptadec-1-en-6-yne

**A-11**

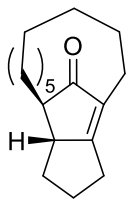


Cartesian Coordinates (Angstroms)

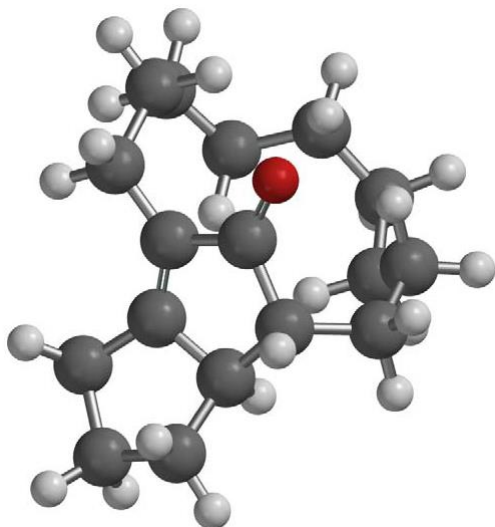
Atom	X	Y	Z
1 C C1	1.2547600	0.4860436	2.0855649
2 C C2	1.9107510	-0.3478247	1.5011716
3 C C3	2.6764646	-1.3656521	0.7762964
4 H H2	3.1055194	-2.0824411	1.4902619
5 H H4	1.9862064	-1.9411225	0.1448028
6 C C4	3.8155198	-0.8063263	-0.1058182
7 H H5	4.2905866	-1.6584339	-0.6112491
8 H H6	4.5817599	-0.3546238	0.5361233
9 C C5	3.3724342	0.2331616	-1.1544297
10 H H3	3.0406272	1.1464660	-0.6458571
11 H H8	4.2603300	0.5065272	-1.7452118
12 C C6	2.2781222	-0.2512859	-2.0689702
13 H H9	2.4465165	-1.2128553	-2.5615563
14 C C7	1.1385025	0.4054922	-2.3040599
15 H H10	0.9840311	1.3670708	-1.8071627
16 C C8	0.4173479	1.4717830	2.7746322
17 H H1	0.1984802	2.3008270	2.0880262
18 H H11	0.9746878	1.9155523	3.6111210
19 C C9	0.0074986	-0.0556885	-3.1836254
20 H H13	0.2207566	-1.0633293	-3.5660428
21 H H14	-0.0657206	0.6026648	-4.0630424
22 C C10	-0.9109970	0.8899985	3.3183293

23 H H12	-0.6779628	0.1958366	4.1358773
24 H H16	-1.4794067	1.7193329	3.7618763
25 C C11	-1.3557243	-0.0439980	-2.4579469
26 H H7	-2.1447963	-0.3158672	-3.1734163
27 H H17	-1.5733749	0.9857465	-2.1417550
28 C C12	-1.7775627	0.1604640	2.2791907
29 H H19	-2.6836711	-0.2058925	2.7831876
30 H H20	-1.2346929	-0.7282815	1.9353186
31 C C13	-1.4105329	-0.9844164	-1.2461327
32 H H18	-0.6002846	-0.7243734	-0.5538623
33 H H21	-1.1940293	-2.0075869	-1.5876114
34 C C14	-2.1850769	1.0176966	1.0720195
35 H H15	-2.6260436	1.9593363	1.4322310
36 H H24	-1.2876523	1.3001714	0.5061960
37 C C15	-2.7512973	-0.9975028	-0.4915937
38 H H22	-3.5452707	-1.3427752	-1.1696757
39 H H26	-2.6901321	-1.7518156	0.3045782
40 C C16	-3.1942932	0.3460082	0.1220766
41 H H25	-3.4358792	1.0525025	-0.6839288
42 H H28	-4.1365008	0.1794109	0.6640670

Three lowest frequencies (cm<sup>-1</sup>): 35, 56, 76 (no imaginary frequencies observed)



Cyclopentenone **A-12**



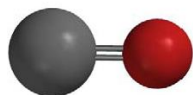
Cartesian Coordinates (Angstroms)

Atom	X	Y	Z
1 C C1	-0.7373338	-3.5835507	1.4022937
2 H H2	-1.4271465	-4.4176447	1.5631282
3 H H4	0.2779970	-3.9880308	1.4875686
4 C C2	-0.9261288	-2.9208540	-0.0021593
5 H H1	-1.8732689	-3.2061086	-0.4749451
6 H H5	-0.1300916	-3.2181496	-0.6974176
7 C C3	-0.9310613	-2.4439821	2.4390440
8 H H3	-1.9989783	-2.2954517	2.6489630
9 H H8	-0.4307042	-2.6536678	3.3904763
10 C C4	-0.3700115	-1.2131749	1.6983783
11 H H9	0.7269581	-1.3034482	1.6951952
12 C C5	-0.8980877	-1.4460477	0.3011468
13 C C6	-1.4203333	-0.3462254	-0.2786820
14 C C7	-0.7914366	0.2280714	2.0462274
15 C C8	-1.4140661	0.7491876	0.7278838
16 O O1	-1.8793389	1.8679412	0.5709048
17 C C16	-2.0650900	-0.1855885	-1.6284815
18 H H26	-2.0613788	-1.1484186	-2.1566896
19 C C17	0.2951331	1.1760246	2.6280561
20 H H14	-0.2153469	1.9411241	3.2245156
21 H H22	0.9121877	0.6024530	3.3344714



22 C C18	-1.4604415	0.9122547	-2.5423791
23 H H25	-1.4175536	1.8488170	-1.9771060
24 H H27	-2.1842724	1.0826437	-3.3504221
25 C C19	-0.1023362	0.6036929	-3.2046068
26 H H24	0.0730859	1.3667231	-3.9769734
27 H H28	-0.1861192	-0.3523722	-3.7426076
28 C C20	1.1871491	1.9166055	1.6106538
29 H H30	1.7987275	2.6428558	2.1641707
30 H H31	0.5294404	2.5118648	0.9698135
31 C C21	2.1221026	1.0515654	0.7429391
32 H H32	2.9941448	0.7519810	1.3406258
33 C C22	1.1350324	0.5444551	-2.2880020
34 H H29	0.9728419	-0.2186344	-1.5198992
35 H H35	1.9913856	0.1945718	-2.8828240
36 H H39	-1.6142491	0.1852285	2.7738469
37 H H45	-3.1186836	0.0819449	-1.4656747
38 H H47	1.6242500	0.1205417	0.4557101
39 C C9	1.5119550	1.8839172	-1.6310385
40 H H6	0.6183800	2.3557915	-1.2046831
41 H H7	1.8647627	2.5711109	-2.4131096
42 C C10	2.5963444	1.7619634	-0.5409177
43 H H11	2.9620006	2.7654401	-0.2804930
44 H H12	3.4595801	1.2225788	-0.9569010

Three lowest frequencies (cm<sup>-1</sup>): 45, 62, 85 (no imaginary frequencies observed)



Carbon monoxide (**A-13**)

		Cartesian Coordinates (Angstroms)		
Atom		X	Y	Z
1	O O1	0.0000000	0.0000000	0.5689782
2	C C1	0.0000000	0.0000000	-0.5689782

Lowest frequency (cm-1): 2210 (no imaginary frequencies observed)